MODERN APPROACHES IN SOLID EARTH SCIENCES

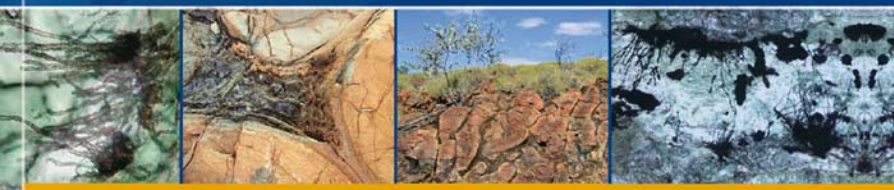

Y. Dilek · H. Furnes · K. Muehlenbachs (Eds.)

Links Between Geological Processes, Microbial Activities & Evolution of Life

Microbes and Geology

Springer

Links Between Geological Processes, Microbial Activities & Evolution of Life

Modern Approaches in Solid Earth Sciences

VOLUME 4

Series Editors

Y. Dilek, *Department of Geology, Miami University, Oxford, OH, U.S.A.*
B.L.N. Kennett, *Research School of Earth Sciences, The Australian National University, Canberra, Australia*
M.J.R. Wortel, *Faculty of Geosciences, Utrecht University, The Netherlands*

For other titles published in this series, go to
www.springer.com/series/7377

Links Between Geological Processes, Microbial Activities & Evolution of Life

Microbes and Geology

Editors

Yildirim Dilek
Department of Geology, Miami University, Oxford, OH, USA

Harald Furnes
Department of Earth Science, University of Bergen, Norway

and

Karlis Muehlenbachs
Department of Earth and Atmospheric Sciences, University of Alberta, Edmonton, AB, Canada

Springer

Dr. Yildirim Dilek
Miami University
Dept. Geology
114 Shideler Hall
Oxford OH 45056
USA
dileky@muohio.edu

Dr. Karlis Muehlenbachs
University of Alberta
Dept. Earth & Atmospheric
Sciences, 1-26 Earth Sciences Bldg.
Edmonton AB T6G 2E3
Canada
Karlis.Muehlenbachs@ualberta.ca

Dr. Harald Furnes
University of Bergen
Dept. Earth Science
Allegaten 41
5007 Bergen
Norway
harald.furnes@geo.uib.no

ISBN: 978-1-4020-8305-1 e-ISBN: 978-1-4020-8306-8

Responsible Series Editors: Y. Dilek and M.J.R. Wortel

Library of Congress Control Number: 2008926909

© 2008 Springer Science+Business Media B.V.

All rights reserved chapter “Evaporite microbial films, mats, microbialites, and stromatolites” by Robin L. Brigmon

No part of this work may be reproduced, stored in a retrieval system, or transmitted in any form or by any means, electronic, mechanical, photocopying, microfilming, recording or otherwise, without written permission from the Publisher, with the exception of any material supplied specifically for the purpose of being entered and executed on a computer system, for exclusive use by the purchaser of the work.

Cover illustration: Upper images reproduced with kind permission of Hubert Staudigel, lower images from Neil Banerjee. Both of these colleagues are the co-authors of the paper by Harald Furnes et al. (Chapter 1) in the book.

Printed on acid-free paper

9 8 7 6 5 4 3 2 1

springer.com

Preface

Geobiology is a rapidly growing and truly interdisciplinary field at the interface between earth and life sciences, and mainstream research in geobiology involves microbes and microbial activities at all scales in different geological environments through time in Earth's history. This research and its findings have strong implications for the evolution of life on the Earth and potentially in other planets. Microbial activities influence water-rock interaction processes and chemical transport between the major geochemical reservoirs, and the formation and transformation of minerals and rocks. On the other hand, geological processes and geochemical controls influence the microbial ecology in extreme environments. Our understanding of these links has been advancing at a fast pace in recent years. The discovery of life in extreme environments and its systematic studies have peaked during the past several decades, and new scientific programs (i.e. Deep Science Initiative) have been initiated in order to maximize international collaboration on most important scientific problems pertaining to underground research and subsurface microbial life. The deep subsurface biosphere may constitute nearly one third of the Earth's biomass, and subsurface microbial communities are major contributors to nutrient cycling through the environment.

We now know that microbes have played important roles as geological agents in mineral growth and dissolution, rock and mineral weathering and alteration, mobilization of metals in metal sulphides, metabolism of hydrocarbons and transformation of organic carbon in sediments for fossil fuel formation, cycling of elements in the global ocean, fractionation of stable isotopes facilitating rock and mineral diagenesis, porosity generation in deep-subsurface, timing of fossil appearance in Earth history, bio-remediation, and emergence of the aerobic biosphere in deep time (i.e. Archaean – Proterozoic transition). How biological activity influences geological processes and what role these processes have played in the geological evolution of the Earth through time still remain fundamental questions. How do we recognize ancient microbial activities in the rock record and what analytical methods do we use to document and to better understand the evolution of life? Can we detect the existence of microbial life in deep time by studying Archaean rocks? Microbial systems in extreme environments and in the deep biosphere may be analogous to potential life on other planetary bodies and hence may be used to investigate the possibilities of extraterrestrial life.

This book is a result of a successful Pardee Keynote Symposium held at the Geological Society of America Annual Meeting in Philadelphia (October 2006) and is intended to explore these questions and the mode and nature of links between geological processes and microbial activities for the origin and evolution of life on the Earth and possibly on other planets. It fills a particular niche in geobiology by focusing on the significance of geology and geological processes for controlling the physical conditions and characteristics of diverse habitats, in which different microorganisms thrive, the geochemical processes that these microorganisms catalyze, and the implications of microbial activities as recorded in the rocks and modern geological environments for the evolution of life. The chapters in the book are primarily concerned with the geological, biological, and geochemical processes that affect habitable environments for microbial communities in extreme conditions (i.e. oceanic crust in deep subseafloor, saline lakes, methane-rich ocean waters, deep sea sediments) and the textural, biological, and fossil evidence that microbes and microbial activities leave behind in the rock record. As such, the book is aimed at documenting some of the best examples (but not all) of links between the geological processes and microbial activities, rather than providing discussions on microbial ecology and microbial physiology, microbiological characterization, and microbial biochemistry. We do not attempt in this book to cover all aspects and examples of geobiology since that would require numerous, diverse contributions from a much larger scientific community. The book is intended for students (upper level undergraduate and graduate students) and researchers in the academia and industry who are interested in exploring the geological record of the biosphere in deep and extreme environments.

The chapters in the book are organized to provide new observations and data as well as presenting a state-of-the art overview on the topics ranging from microbial existence and related processes in the uppermost igneous layer of modern and ancient oceanic crust and deep sea sediments to cyanobacteria – produced stromatolites; microbial communities and their geological artefacts in saline lakes at high altitudes (i.e. Tibetan Plateau) and below sea-level (i.e. Dead Sea), in dry deserts (i.e. Atacama Desert in Chile, Antarctica, the Arctic and western China), and in the deep continental subsurface where high temperature, high pressure and high radiation conditions prevail; and, in ocean waters that have high rates of anaerobic oxidation of methane gas (i.e. The Black Sea). The last chapter presents a critical assessment of a widely discussed "volcanic winter to snowball Earth" hypothesis that holds extensive explosive volcanism around ~635 million years ago responsible for Neoproterozoic climate change in the Earth's history. Solid Earth geological processes, such as subduction and associated magmatism, and the interplay between surficial and atmospheric processes (i.e. glaciation) appear to have played a major role in this event during the Precambrian, and are likely to happen again to affect climate and life in the geological future. We hope that this book will serve as an exciting, contemporary guide to the geobiological literature.

We thank the contributors to this book for their time and effort, and express our gratitude to a large number of scientists who provided valuable reviews of the chapters in it. We are grateful to the Geological Society of America and its International

Division for providing us with funds to organize the 2006 Pardee Keynote Symposium and to support travel expenses of the invited speakers. We are particularly indebted to Petra D. van Steenbergen, Senior Publishing Editor at Springer, for her enthusiastic support and motivation throughout the preparation of this book and to Cynthia de Jonge at Springer – Geosciences for her invaluable assistance in formatting and preparing the book for final publication.

December 2007 Y. Dilek, H. Furnes, and K. Muehlenbachs
Editors

Acknowledgements

We wish to thank the following colleagues for their timely and thorough reviews of the manuscripts that greatly improved the content of the book and helped us maintain high scientific standards. We gratefully acknowledge their efforts.

Miriam Andres, Chevron Energy Technology Center, San Ramon – CA, USA

Wolfgang Bach, University of Bremen, Germany

Neil Banerjee, University of Western Ontario, Canada

Maarten de Wit, University of Cape Town, South Africa

Yildirim Dilek, Miami University, USA

Hailiang Dong, Miami University, USA

Katerina J. Edwards, University of Southern California, USA

Kai Finster, University of Aarhus, Denmark

Martin Fisk, Oregon State University, USA

Harald Furnes, University of Bergen, Norway

Jens Herrle, University of Alberta, Canada

Nils Holm, Stockholm University, Sweden

Ingo Klaucke, IFM-Geomar, Leibniz Institute for Marine Sciences, Kiel, Germany

Paul Knauth, Arizona State University, Tempe, USA

Kurt Konhauser, University of Alberta, Canada

Ian G. Macintyre, Natural History Museum, Smithsonian Institute, USA

Nicola McLoughlin, University of Bergen, Norway

Melani R. Mormile, University of Missouri – Rolla, USA

John Mylroie, Mississippi State University, USA

Karlis Muehlanbachs, University of Alberta, Canada

Eugene A. Shinn, University of South Florida, USA

Mark Skidmore, Montana State University, Bozeman, USA

Andreas Teske, University of North Carolina – Chapel Hill, USA

Volker Thiel, Universitaet Goettingen, Germany
Tamas Torok, Lawrence Berkeley National Laboratory, USA
Marta Torres, Oregon State University, USA
Tina Treude, University of Southern California, USA
David Wacey, University of Oxford, U.K.

Contents

Oceanic Pillow Lavas and Hyaloclastites as Habitats for Microbial Life Through Time – A Review 1
Harald Furnes, Nicola McLoughlin, Karlis Muehlenbachs, Neil Banerjee, Hubert Staudigel, Yildirim Dilek, Maarten de Wit, Martin Van Kranendonk, and Peter Schiffman

Microbial Colonization of Various Habitable Niches During Alteration of Oceanic Crust 69
Magnus Ivarsson and Nils G. Holm

Ambient Inclusion Trails: Their Recognition, Age Range and Applicability to Early Life on Earth 113
David Wacey, Matt Kilburn, Crispin Stoakes, Hugh Aggleton and Martin Brasier

Spatial Distribution of the Subseafloo Life: Diversity and Biogeography . 135
Fumio Inagaki and Satoshi Nakagawa

Analysis of Deep Subsurface Microbial Communities by Functional Genes and Genomics 159
Andreas Teske and Jennifer F. Biddle

Diversity of Bahamian Microbialite Substrates 177
Robert N. Ginsburg and Noah J. Planavsky

Evaporite Microbial Films, Mats, Microbialites and Stromatolites 197
Robin L. Brigmon, Penny Morris and Garriet Smith

Microbial Life in Extreme Environments: Linking Geological and Microbiological Processes 237
Hailiang Dong

Marine Methane Biogeochemistry of the Black Sea: A Review 281
Thomas Pape, Martin Blumenberg, Richard Seifert, Gerhard Bohrmann and Walter Michaelis

From Volcanic Winter to Snowball Earth: An Alternative Explanation for Neoproterozoic Biosphere Stress 313
Robert J. Stern, D. Avigad, N. Miller and M. Beyth

Index 339

Contributors

Hugh Aggleton
Department of Earth Sciences, University of Oxford, Parks Road, Oxford OX1 3PR, UK, hugh.aggletan@jesus.ox.ac.uk

D. Avigad
Institute of Earth Sciences, Hebrew University of Jerusalem, Jerusalem 95501, Israel, avigad@vms.huji.ac.il

Neil Banerjee
Department of Earth Sciences, University of Western Ontario, London, Ontario, Canada N6A 5B7, neil.banerjee@uwo.ca

M. Beyth
Geological Survey of Israel, Malkhei Yisrael St. 30, Jerusalem 95501, Israel, mbeyyth@gsi.gov.il

Jennifer F. Biddle
University of North Carolina at Chapel Hill, Department of Marine Sciences, 351 Chapman Hall, CB 3300, Chapel Hill, North Carolina 27599 USA, jfbiddle@email.unc.edu

Martin Blumenberg
Institute of Biogeochemistry and Marine Chemistry, University of Hamburg, Bundesstrasse 55, D-20146 Hamburg, Germany, martin.blumenberg@zmaw.de

Gerhard Bohrmann
Research Center Ocean Margins, University of Bremen, Klagenfurter Strasse, D-28334 Bremen, Germany, gbathrmann@uni-bremen.de

Martin Brasier
Department of Earth Sciences, University of Oxford, Parks Road, Oxford OX1 3PR, UK, Martin.Brasier@earth.ox.ac.uk

Robin L. Brigmon
Savannah River National Laboratory, Building 999W Aiken, SC 29808, USA, Tel 803-819-8405, r03.brigmon@srnl.doe.gov

Maarten de Wit
AEON and Department of Geological Sciences, University of Cape Town, Rondebosch 7701, South Africa, maarten.De.Wit@uct.ac.za

Yildirim Dilek
Miami University, Department of Geology,114 Shideler Hall Oxford, OH 45056, USA, dileky@muohio.edu

Hailiang Dong
Department of Geology, Miami University, Oxford, OH 45056, USA, Tel: 513-529-2517, Fax: 513-529-1542, dongh@muohio.edu

Harald Furnes
Department of Earth Science & Centre for Geobiology, University of Bergen, Allegaten 41, 5007 Bergen, Norway, Tel: +47 55 583530, Fax: +47 55 583660, Harald.Furnes@geo.uib.no

Robert N. Ginsburg
University of Miami, Comparative Sedimentology Laboratory, Rosenstiel School of Marine and Atmospheric Sciences, 4600 Rickenbacker Causeway, Miami Fl, 33149, rginsburg@rsmas.miami.edu

Nils.G. Holm
Department of Geology and Geochemistry, Stockholm University, Sweden, Frescativägen 8, S-106 91 Stockholm, Sweden, nils.holm@geo.su.se

Fumio Inagaki
Geomicrobiology Group, Kochi Institute for Core Sample Research, Japan Agency for Marine-Earth Science and Technology (JAMSTEC), Monobe B200, Nankoku, Kochi 783-8502, Japan, inagaki@jamstec.go.jp; Subground Animalcule Retrieval (SUGAR) Program, Extremobiosphere Research Center, JAMSTEC, Natsushima-cho 2-15, Yokosuka 237-0061, Japan, inagaki@jamstec.go.jp

Magnus Ivarsson
Department of Geology and Geochemistry, Stockholm University, Sweden, Frescativägen 8, S-106 91 Stockholm, Sweden, magnus.ivarsson@geo.su.se

Matt Kilburn
Department of Materials, University of Oxford, Parks Road, Oxford OX1 3PH, UK and Centre for Microscopy and Microanalysis, University of Western Australia, 35 Stirling Highway, Crawley 6009, WA, Australia, mkilburn@cyllene.uwa.edu.au

Nicola McLoughlin
Department of Earth Science & Center for Geobiology, University of Bergan, Allegaten 41, 5007 Bergan, Norway, Nicola.NcLoughlin@geo.uib.no

Walter Michaelis
Institute of Biogeochemistry and Marine Chemistry, University of Hamburg, Bundesstrasse 55, D-20146 Hamburg, Germany, walter.michaelis@zmaw.de

N. Miller
Geosciences Department, U Texas at Dallas, Richardson TX 75083-0688 USA, Now at Department of Geological Sciences and Engineering, University of Missouri at Rolla, □ Rolla, MO 65409-0140 □, nmiller@mail.utexac.edu

Penny Morris
Department of Natural Science, University of Houston, 1 Main Street, Houston, TX 77002, penny.morris_smith1@jsc.nasa.gov

Karlis Muehlenbachs
University of Alberta, Department of Earth & Atmospheric Sciences Edmonton AB T6G 2E3 1-26 Earth Sciences Building, Canada, Karlis.Muelenbachs@ualberta.ca

Satoshi Nakagawa
Subground Animalcule Retrieval (SUGAR) Program, Extremobiosphere Research Center, JAMSTEC, Natsushima-cho 2-15, Yokosuka 237-0061, Japan, nakagawas@jamstec.go.jp

Thomas Pape
Research Center Ocean Margins, University of Bremen, Klagenfurter Strasse, D-28334 Bremen, Germany, Tel.: +49 4212183918; Fax: +49 4212188664, tpape@uni-bremen.de

Noah J. Planavsky
University of Miami, Comparative Sedimentology Laboratory, Rosenstiel School of Marine and Atmospheric Sciences, 4600 Rickenbacker Causeway, Miami Fl, 33149; University of California, Riverside, Department of Earth Sciences, 900 University Avenue, Riverside Ca, 92521, planavsky@gmail.com

Peter Schiffman
Department of Geology, University of California, Davis, One Shields Avenue, Davis, California 95616-8605, USA, PSCHIFFMAN@UCDAVIS.EDU

Richard Seifert
Institute of Biogeochemistry and Marine Chemistry, University of Hamburg, Bundesstrasse 55, D-20146 Hamburg, Germany, richard.seifert@zmaw.de

Garriet Smith
University South Carolina Aiken, 471 University Parkway, Aiken, SC 29801, smithres@aiken.sc.edu

Hubert Staudigel
Scripps Institution of Oceanography, University of California, La Jolla, CA 92093-0225, USA, hstaudigel@ucsd.edu

Robert J. Stern
Geosciences Dept., U Texas at Dallas, Richardson TX 75083-0688 USA, 972-883-2442 (O) 972-883-2537 (F), rjstern@utdallas.edu

Crispin Stoakes
C.A Stoakes and Associates Pty Ltd, 3185 Victoria Road, Hovea 6071, WA, Australia, stoakesca@optusnet.com.au

Andreas Teske
University of North Carolina at Chapel Hill, Department of Marine Sciences, 351 Chapman Hall, CB 3300 Chapel Hill, North Carolina 27599, USA, Phone: 919.843.2463, Fax: 919.962.1254, teske@email.unc.edu

Martin Van Kranendonk
Geological Survey of Western Australia, 100 Plain Street, East Perth, Western Australia 6004, Australia, martin.vankranendonk@doir.wa.goc.au

David Wacey
Department of Earth Sciences, University of Oxford, Parks Road, Oxford OX1 3PR, UK, davidwa@earth.ox.ac.uk

Oceanic Pillow Lavas and Hyaloclastites as Habitats for Microbial Life Through Time – A Review

Harald Furnes, Nicola McLoughlin, Karlis Muehlenbachs, Neil Banerjee, Hubert Staudigel, Yildirim Dilek, Maarten de Wit, Martin Van Kranendonk, and Peter Schiffman

Abstract This chapter summarizes research undertaken over the past 15 years upon the microbial alteration of originally glassy basaltic rocks from submarine environments. We report textural, chemical and isotopic results from the youngest to the oldest *in-situ* oceanic crust and compare these to data obtained from ophiolite and greenstone belts dating back to c. 3.8 Ga. Petrographic descriptions of the granular and tubular microbial alteration textures found in (meta)-volcanic glasses from pillow lavas and volcanic breccias are provided and contrasted with textures produced by abiotic alteration (palagonitization). The geological setting in particular the degree of deformation and metamorphism experienced by each study site is documented in outcrop photographs, geological maps and stratigraphic columns (where possible). In addition, X-ray mapping evidence and carbon isotopic data that are consistent with a biogenic origin for these alteration textures is explained and a model for their formation is presented. Lastly, the petrographic observations and direct radiometric dating techniques that have been used to establish the antiquity and syngenicity of these microbial alteration textures are reviewed.

The combined dataset presented herein suggests that the microbial alteration of volcanic glass extends back to some of the earliest preserved seafloor crustal fragments. We use observations collected from well preserved, *in-situ* oceanic crust as a guide to interpreting comparable mineralized micro-textures from the ancient seafloor. It emerges that textural evidence is best preserved in undeformed to little-deformed, low grade, meta-volcanic rocks, and that chemical tracers, in particular the $\delta^{13}C_{carb}$ signatures, are more robust and can survive relatively strong deformation and metamorphic conditions. Drawing together all of this data we propose a tentative model for microbial life in the Archean sub-seafloor. Overall, it is argued

H. Furnes
Department of Earth Science & Centre for Geobiology, University of Bergen, Allegt. 41, 5007 Bergen, Norway
e-mail: Harald.Furnes@geo.uib.no

Y. Dilek et al. (eds.), *Links Between Geological Processes, Microbial Activities & Evolution of Life*, © Springer Science+Business Media B.V. 2008

that bioalteration textures in (meta)-volcanic glasses provide a valuable tracer of the deep oceanic biosphere, which constitutes one of the largest and least explored portions of the modern, and especially the ancient, biosphere.

1 Introduction

Microbial activity has until recently only been sought largely in (meta)-sedimentary rocks and environments. It is now, however, realized that microbial life can also colonise volcanic rocks within the Earth's crust to considerable depths, where carbon and energy sources are available and where physical conditions do not inhibit life (e.g., Lovley and Chapelle 1995; Pedersen 1997; Pedersen et al. 1997; Amend and Teske 2005; Schippers et al. 2005). During the last decade, it has also been demonstrated that the upper volcanic part of the *in situ* oceanic crust is a habitat for microbial life (e.g., Thorseth et al. 1992; Thorseth et al. 1995a; Furnes et al. 1996; Fisk et al. 1998; Torsvik et al. 1998; Furnes and Staudigel 1999; Furnes et al. 1999, 2001a, b; Thorseth et al. 2001, 2003; Banerjee and Muehlenbachs 2003; Fisk et al. 2003; Staudigel and Furnes 2004; Staudigel et al. 2004). The *in-situ* oceanic crust however, only extends back to approximately 170 Ma, with the oldest oceanic crust being found in the western Pacific Ocean. Evidence of microbial activity in older oceanic volcanic rocks must be sought in fragments of ancient oceanic crust preserved in ophiolites and greenstone belts. Reliable evidence for microbial life has been found in several ophiolites ranging in age from Cretaceous to Paleoproterozoic (Furnes et al. 2001c, 2002a, 2005), and putative evidence of microbial life has been described from Mesoarchean pillow lavas of the Barberton greenstone belt, South Africa (Furnes et al. 2004; Banerjee et al. 2006) and the Pilbara Craton, Western Australia (Staudigel et al. 2006; Banerjee et al. 2007).

In this chapter, we summarize the various accounts of microbial alteration that span the youngest, *in-situ* oceanic crust to the oldest greenstone belts and present new data pertaining to these findings. In particular, we provide in one manuscript a compilation of lithological logs from the *in-situ* oceanic crust where microbial alteration has been found, along with geological maps, stratigraphic sections and outcrop photographs of all of the ophiolites and greenstone belt examples studied to enable direct comparisons to be made. Previous reviews have largely treated evidence of microbial alteration from the *in situ* oceanic crust (e.g., Fisk et al. 1998; Furnes et al. 2001b) and ophiolites (e.g. Furnes and Muehlenbachs 2003) separately; or largely focussed on a single line of evidence such as textural information (e.g., Furnes et al. 2007a). This manuscript extends the study of Staudigel et al. (2006) to document in detail, the main lines of evidence that have been presented to support microbial alteration in volcanic glass from 11 drill cores from the *in-situ* oceanic crust; 5 ophiolite examples and 4 greenstone belts (Fig. 4). In addition to the review of all relevant aspects covered below, we present new textural and carbon isotope data from several of the investigated ophiolites and greenstone belts that is consistent with bioalteration.

2 Biogenicity and Antiquity – Criteria Used for Establishing Bioalteration

Alteration of basaltic glass in modern pillow lavas and hyaloclastites results from two fundamentally different processes – abiotic and biotic alteration. Abiotic alteration results in the formation of the long-recognized, but enigmatic, material termed *palagonite*. The more recently-recognized biotic alteration involves etching of the glass by rock dwelling (endolithic) microbes creating textures that can be regarded as ichnofossils. These two alteration processes may be contemporaneously active within the temperature limit of life. In a number of recent papers the abiotic and biotic alteration processes have been discussed at length. Below we will only briefly comment on abiotic alteration and focus instead upon the biotic processes of alteration. We present biogenicity and antiquity criteria developed to assess these structures, as well as a refined version of recent models proposed to explain the bioalteration of basaltic glass (Staudigel et al. 2006; Furnes et al. 2007a; McLoughlin et al. 2008). In addition, we briefly review what is currently known about the microorganisms that are thought to be responsible for the bioerosion of volcanic glass.

2.1 Abiotic Alteration

The aqueous alteration of basaltic glass produces a pale yellow to dark brown material referred to as palagonite. Palagonitization has traditionally been regarded as a purely physico-chemical phenomenon and is a complex and continuous aging process involving incongruent and congruent dissolution accompanied by precipitation, hydration and pronounced chemical exchange that occurs at low to high-temperatures (e.g., Thorseth et al. 1991; Stroncik and Schmincke 2001; Walton and Schiffman 2003; Walton et al. 2005). The resulting palagonite occurs around the rims of glass shards and as banded material on either side of fractures with a relatively smooth interface between the fresh and altered glass. Palagonite can be divided into two types: (1) early stage amorphous gel-palagonite that matures to form, (2) fibro-palagonite which consists of clays, zeolites and iron-oxy-hydroxides (Peacock 1926).

2.2 Biotic Alteration

Over recent years mounting evidence has been collected to support the biological mediation of processes involved in the alteration of volcanic glass. One of the earliest reports of the biological etching of glass is the description of surface pitting on church window-pane glass in the vicinity of growing lichens (Mellor 1922; see also Krumbein et al. 1991 for review). Bioerosion of natural glasses was reported somewhat later with the finding of surface grooves on glass shards from Miocene

tephra that were likened to those produced by fungi which bore into carbonate grains (Ross and Fisher 1986). This scenario was confirmed with the observation of bacteria within surface pitting textures on sub-glacial volcanic breccias from Iceland, which lead Thorseth et al. (1992) to propose that the microbes locally modify the pH and thereby accelerate glass dissolution. A range of biochemical mechanisms are employed by microorganisms to dissolve volcanic glass and are thought to include secretion of organic acids, production of siderophores and complexing agents that help to complex metal ions, particularly Al whilst modifying the pH to promote silica glass dissolution (Paul and Zaman 1978). The initial stages of glass pitting have been experimentally investigated by Thorseth et al. (1995b), and Staudigel et al. (1995,1998), who confirmed that volcanic and synthetic glasses inoculated with microbes develop etch pits and surface alteration rinds under laboratory conditions.

Numerous studies have followed to document the widespread occurrence of microbial bioerosion textures in volcanic glass from Ocean Drilling Program (ODP) and Deep Sea Drilling Project (DSDP) drill cores from *in-situ* oceanic crust (e.g., Thorseth et al. 1995a; Furnes et al. 1996; Fisk et al. 1998; Furnes et al. 2001a, b; Thorseth et al. 2001, 2003; Banerjee and Muehlenbachs 2003). Distinct textural, elemental and isotopic signatures are produced by these microbial alteration processes and are reviewed below. As a preface to the individual studies it is first informative to draw together and explain the various lines of evidence and the key observations used to distinguish such bioalteration textures from the products of abiotic palagonitization (see also McLoughlin et al. 2007).

2.2.1 Textures

The bioalteration of volcanic glass produces two principal types of textures that have been termed *granular* and *tubular* textures (Furnes and Staudigel 1999). These are markedly different from the regularly banded alteration rinds that result from abiotic palagonitization (Fig. 1A), and we regard these textures as our prime evidence for the bioalteration of basaltic glass. A model for the textural development of such bioerosion traces is given in Fig. 1. The top line shows abiogenic alteration which results in the production of banded palagonite around glass fragments and along the margins of fractures, with a relatively smooth interface between the fresh and altered glass. This should be contrasted with the granular and tubular ichnofossils shown in the lower lines of the figure which are formed by microorganisms carried by circulating fluids into fractures in the rock. These microbial consortia progressively etch the fresh glass, generating more abundant tubes and granular aggregates around fractures and creating an increasingly ramified alteration front between the fresh and altered glass. In Fig. 1, this is schematically shown from left to right across the diagram and illustrated by the back-scatter electron (BSE) images of real examples. The granular alteration textures consist of micron-sized spherical cavities filled with amorphous to very fine-grained phyllosilicate phases. At the initial stage of bioalteration the granular textures appear as isolated spherical bodies along fractures in the glass (Fig. 1B, stage t_1). With progression of bioalteration these become more

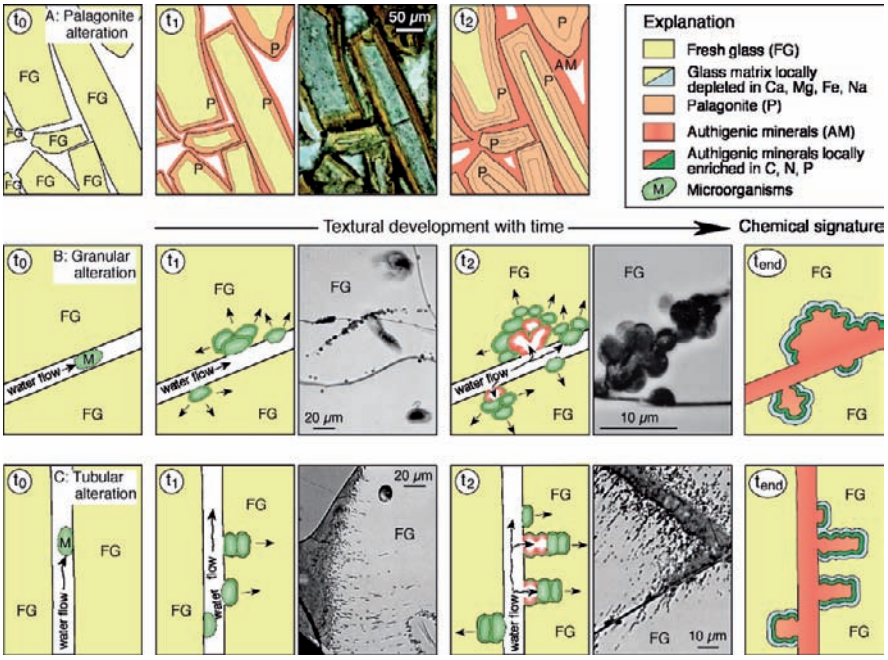

Fig. 1 Schematic diagram showing the generation of alteration textures in fresh volcanic glass (FG) from initial time (t_0) to the final time (t_{end}), accompanied by back scattered electron and thin section images of real examples. The *top line* (**A**) shows abiotic palagonite alteration which produces banded palagonite rims and authigenic minerals around glass fragments. The *middle line* (**B**) shows the growth of granular type textures from isolated spheres in the early stages (t_1) to dense granular aggregates (t_2). The *lower line* (**C**) shows the growth of tubular type from incipient short tubes at stage (t_1) to longer tubes at (t_2). The *right* hand column in (**B**) and (**C**) shows the resulting compositional signatures that are found when these bioalteration textures are infilled by authigenic mineral phases

numerous and coalesce into aggregates that form irregular bands which protrude into the fresh glass along fractures (Fig. 1B, stage t_2). The tubular alteration textures (Fig. 1C) are also concentrated along surfaces in volcanic glass where water once permeated, and become longer and form denser aggregates with progressive alteration.

During the formation of both morphologies of microbially-driven glass dissolution, the total surface area of fresh glass available progressively increases. Staudigel et al. (2004) calculated that the surface area of fresh glass would increase by factors of 2.4 and 200 during the formation of tubular and granular morphotypes, respectively. In contrast, abiotic alteration causes the surface area of fresh glass to progressively decrease, acting as a negative feedback that inhibits further alteration. As long as seawater is accessible to the fresh glass, alteration, whether biotic or abiotic, will continue until all of the fresh glass is altered. With time, the bioalteration textures are filled with authigenic phases and alteration will proceed at a much slower rate until, seawater no longer has access to the fresh glass and alteration will

stop. The final column in Fig. 1 shows the chemical signatures that are preserved, including enrichment in C, N and P along the margins of the bioerosion traces, and depletion in Mg, Fe, Ca, and Na in the surrounding modified glass (discussed further in Section 5, below). We stress that this is a schematic diagram and that the distribution of bioalteration textures will differ in fractures of varying geometries under different fluid flow regimes in and around vesicles and as authigenic minerals precipitate and thereby modify the diffusion processes. Further real examples of bioalteration textures from *in-situ* oceanic crust are described in Section 4.1 and Figs. 23 and 24; from ophiolites in Section 4.2 and Fig. 25; and from greenstone belts in Section 4.3 and Fig. 26.

2.2.2 Syngenicity and Antiquity

To establish the syngenicity of bioalteration textures and exclude an origin from modern endolithic organisms relies in the first instance upon relative age relationships observed by optical microscopy. In volcanic glasses and hyaloclastites (i.e., brecciated volcanic glass), it is therefore necessary to check the distribution of bioalteration textures in pillow margins or glass fragments with respect to fractures that may have acted as conduits for younger fluids and, possibly, also for microbes. In ancient metamorphic samples, the originally hollow bioalteration textures are now filled by secondary minerals (e.g., quartz, chlorite, titanite) and have been overgrown by metamorphic minerals (e.g., Figs. 26 and 27). In such cases, the metamorphic age of the overgrowing mineral gives a minimum age constraint for the bioalteration of the rock, as for example in the case of the $\sim$3.5 Ga bio-etching of the pillow lavas of the Barberton greenstone belt, South Africa (Furnes et al. 2004; Banerjee et al. 2006). This may not always be a trivial task and in some cases it is not possible to confidently establish the timing of bioalteration. However, direct radiometric U-Pb dating of titanite that is commonly found to fill the bioalteration textures, is sometimes possible and has been done for tubular alteration textures in hyaloclastites of the 3350 Ma Euro Basalt of the Kelly Group (Pilbara Craton, Western Australia), yielding a minimum age estimate for bioalteration of $2921 +/- 110$ Ma (Banerjee et al. 2007); this study is discussed in more detail in Section 7.4, below.

2.2.3 Geochemistry

The localised concentration of biologically significant elements in and around volcanic bioalteration textures offers support for the biogenicity of these textures. X-ray element mapping in the vicinity of bioalteration textures (e.g., Furnes et al. 2001b; Banerjee and Muehlenbachs 2003; also Section 5 below and Figs. 28–30), has shown that the tubular and granular textures are commonly lined with carbon. Importantly, these elevated levels of carbon are not associated with enrichments of elements such as calcium, iron, or magnesium that commonly form carbonates. Instead, the source of the carbon is likely residual organic matter (Torsvik et al. 1998). Element maps of bioalteration textures also commonly show enrichments and/or uneven distributions of K, Fe, P, N, and S. For example, Alt and Mata (2000) used

TEM to study nano- to micro- sized alteration textures in 6 Ma-old basaltic glasses and proposed an incongruent dissolution process with significant losses of Mg, Fe, Ca and Na, accompanied by slight loss of Al and Mn and a substantial increase in K due to the circulation of >100 fracture volumes of seawater. Intriguingly, their data lead them to highlight the possible contribution of nano-sized organisms in the bioalteration processes. In another study, Storrie-Lombardi and Fisk (2004) investigated the local chemical composition of biotically and abiotically altered 0.5–170 Ma-old volcanic glasses by electron microprobe and showed through principal component analysis that the alteration products of biotic and abiotic alteration are distinct. In brief, the clays produced by biotic alteration had higher Fe and K contents, whereas abiotic alteration produced clays with higher Mg values. Further geochemical work, applying methods like those just described may help to distinguish between biotic and abiotic alteration structures.

Fresh volcanic glass is scarce throughout the rock record (e.g., Shervais and Hanan 1989), and the oldest reported occurrence is of Mesoproterozoic (ca. 1.1 Ga) age (Palmer et al. 1988). Textural evidence for bioalteration in ophiolites and greenstone belts is therefore more unlikely and of diminishing quality with increasing geological age and thus geochemical fingerprints in the form of elevated levels of biologically important elements provide useful substantiating evidence. These geochemical signatures from *in-situ* oceanic crust, ophiolites and greenstone belts are described and discussed in further detail in Section 5 below.

2.2.4 Stable Carbon Isotope Signatures

Systematic shifts in the carbon isotope values measured from disseminated carbonate in the glassy rims and crystalline cores of pillow basalts have been taken to support the operation of bioalteration processes (e.g., Furnes et al. 2001a). These carbon isotope patterns can also give clues as to the putative microbial metabolisms that may be involved. Typical pillow basalts contain less than 1 wt.% of disseminated carbonate and the $\delta^{13}C_{carb}$ values obtained from fresh unaltered basalts yield values similar to mantle CO_2 between $-5‰$ to $-7‰$ (Alt et al. 1996; Hoefs 1997). These contrast with $\delta^{13}C_{carb}$ values of marine carbonate of $0‰$ and provide the reference frame for the interpretation of $\delta^{13}C_{carb}$ values obtained from volcanic glass (see Fig. 2). The microbial oxidation of organic matter produces ^{12}C-enriched CO_2, which may subsequently be precipitated in carbonate depleted in $^{13}C(-\delta^{13}C)$, as shown by the left hand arrow on Fig. 2. Positive $\delta^{13}C_{carbonate}$ values on the other hand, can result from the lithotrophic utilization of CO_2 by methanogenic Archaea. These microorganisms produce methane from H_2 and CO_2 preferentially producing ^{12}C-enriched methane and leaving the remaining CO_2 enriched in ^{13}C, which will be recorded in any precipitated carbonate as shown by the right hand arrow on Fig. 2. The existence of the latter archaeal processes is supported by the discovery of diagenetic dolomite with $\delta^{13}C$ as high as $+14‰$ in sediments from DSDP Hole 479 (Gulf of California), suggesting a biogenic CO_2 reservoir related to active methanogenesis (Kelts and McKenzie 1982). Compiled $\delta^{13}C_{carbonate}$ data from the *in-situ* ocean crust, ophiolites and greenstone belts of different metamorphic grades is presented

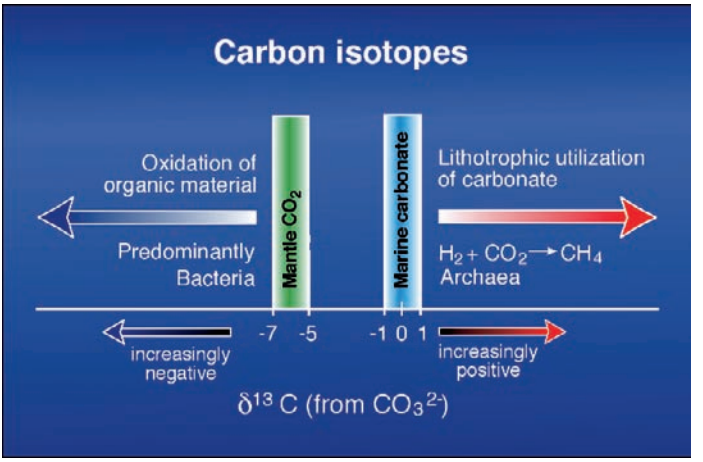

Fig. 2 Diagram summarizing the interpretation of $\delta^{13}C$ values measured on disseminated carbonates from pillow lavas. For reference the $\delta^{13}C$ values of mantle CO_2 and marine carbonates are plotted. The oxidation of organic matter in pillow rims by bacteria is argued to shift the $\delta^{13}C_{carb}$ to progressively more negative values, as low as −25‰ (see for example Fig. 31B). Whereas the lithotrophic utilization of carbonate in pillow rims by archaea shifts the $\delta^{13}C_{carb}$ to more positive values as high as +3.9‰ (see for example Figs. 30 and 31). In contrast, carbonate measured from pillow cores yields a mantle value and carbonate from amygdales gives a marine value. Actual $\delta^{13}C_{carbonate}$ data from pillow lavas are plotted in Figs. 31, 32 and 33

and discussed in detail below (see Section 6 and Figs. 30–32). In summary, it is found that values obtained from pillow interiors are bracketed between primary mantle CO_2 values and those expected from marine carbonates whereas those measured from pillow rims and hyaloclastites display a significantly greater range in $\delta^{13}C_{carbonate}$ values that is consistent with microbial activity. In addition, it has been suggested that variations in the structure and lithology of the oceanic crust may influence the colonizing microbes and resultant carbon isotope signatures (Furnes et al. 2006 and Section 7.3, below).

2.2.5 DNA-Analyses and Microfossil Remains

Nucleic acids derived from bacterial and archaeal DNA are commonly localized within recent bioalteration textures in pillow lavas of young, *in-situ* oceanic crust (Thorseth et al. 1995a, 2001; Giovannoni et al. 1996; Torsvik et al. 1998). The application of DAPI (4, 6 diamino-phenyl-indole) dye which binds to nucleic-acids, along with fluorescent oligonucleotide probes that target bacterial and archaeal RNA has revealed that biological material is concentrated at the ramified interface between fresh and altered glass (e.g., Giovannoni et al. 1996; Torsvik et al. 1998, Fig. 2; Banerjee and Muehlenbachs 2003, Fig. 14; Walton and Schiffman 2003, Fig. 8). For example, staining of volcanic glass samples from the Costa Rica Rift (Fig. 3) show that the most concentrated biological material occurs at the interface of fresh and altered glass, especially in the tips of tubular structures and that the

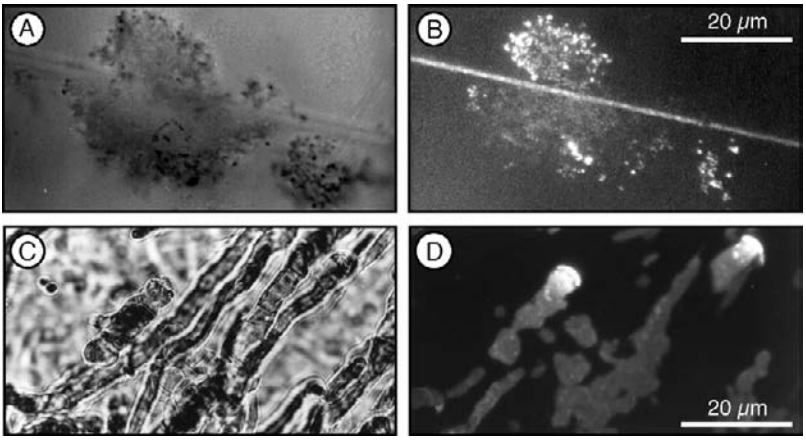

Fig. 3 (**A**) Transmitted light image of the granular bioalteration type; (**B**) epiflourescence image of the same sample showing that the biological material is concentrated along the edges of the granular alteration and within the fracture; (**C**) transmitted light image of the tubular bioalteration type; (**D**) epiflourescence image of the same sample showing that the biological material is concentrated at the ends of the tubes. Both samples (**A** and **C**) are from hole 148-896A-11R-1, 73-73 cm from the Costa Rica Rift (Furnes et al. 1996). The epiflourescent images were obtained using a Nikon Microphot microscope with excitation at 365 nm and emission at 420 nm on samples stained with 10 g/mL DAPI

biogenic material decreases in concentration towards the centre of fractures (Furnes et al. 1996; Giovannoni et al. 1996). We find it appropriate to mention that the application of DAPI may result in ambiguities since some clay minerals may autofluoresce. To ascertain the extent of autofluoresence, Giovannoni et al. (1996) used three different DNA-binding dyes (Hoechst 33342, PO-PRO-3, and Syto 11), which all supported the conclusions of Thorseth et al. (1995a) and Furnes et al. (1996) that microorganisms were present at the glass-alteration interface. Genetic material is not stable over geological lengths of time and so this type of data is not found in ophiolites and greenstone belts. The finding of DNA from *in-situ* oceanic crust that is 122 million-years-old has lead to the suggestion that viable microorganisms may still be active within these bioalteration textures long after eruption of the lavas (Banerjee and Muehlenbachs 2003).

Partially fossilized, mineral encrusted microbial cells have also been observed by scanning electron microscopy (SEM) on the surface of altered glasses from *in-situ* oceanic crust, with morphologies that included filamentous, coccoid, oval, rod and stalked forms (e.g., Thorseth et al. 2001). Moreover, these forms commonly occur in, or near, etch marks in the glass that exhibit forms and sizes resembling the attached microbes, suggesting that it was the microbes that were responsible for the formation of the etch marks (e.g., Thorseth et al. 2003). Within microtubules in volcanic glass fragments from the Ontong Java Plateau, delicate hollow and filled filaments attached to the tube walls have been observed (e.g., Banerjee and Muehlenbachs 2003, Figs. 5–9), along with spherical bodies and thin films

interpreted to represent desiccated biofilms (e.g., Banerjee and Muehlenbachs 2003, Figs. 5–9).

2.2.6 Microbiological Constraints

A consortium of microorganisms that includes heterotrophs and chemolithoautotrophs is thought to be involved in the bioalteration of volcanic glass. Heterotrophs use organic carbon delivered by circulating seawater as a carbon source and chemolithoautotrophs use oxidized compounds principally O_2 and NO_3^- derived from circulating seawater as electron acceptors within the modern sub-seafloor along with Fe(II) and Mn(II) in volcanic glass as electron donors (Edwards et al. 2005). The energetically viable reactions that are possible in these environments and their energy yields are given in Table 1 of Edwards et al. (2005). Under anaerobic conditions hydrogen consuming reactions can support appreciable biomass production and this H_2 may have been supplied by abiotic sources especially on the early earth. In addition, the microbial consortia may derive key nutrients especially phosphorus from the glass, which is found only in low concentration in typically nutrient poor, sub-seafloor conditions.

The suggestion that Mn oxidation is a potentially important chemolithoautotrophic metabolism involved in the bioerosion process is supported by the isolation of diverse manganese oxidizing bacteria from basaltic seamounts where they enhance the rate of Mn oxidation (e.g., Templeton et al. 2005). The possibility that these microbial consortia may also employ iron oxidation is consistent with the resemblance of bacterial moulds found on volcanic glass fragments to the branched and twisted filaments of the Fe-oxidizing bacteria *Gallionella* (e.g., Thorseth et al. 2001, 2003). Moreover it has recently been discovered that a group of bacteria distantly related to the heterotrophic organisms *Marinobacter sp*. and *Hyphomonas sp*. are also capable of chemolithoautrophic growth and employ Fe-oxidation at around pH 7 on substrates including basaltic glass (Edwards et al. 2003). Isolation of a new anaerobic, thermophilic facultative chemolithoautotrophic bacterium from a terrestrial hot spring that is capable of Fe (III) reduction using molecular H as the only energy source and CO_2 as a carbon source (Zavarzina et al. 2007), is also relevant to mention in this connection (see Section 7.3).

Culture independent molecular profiling studies have found that basaltic glass is colonized by microorganisms that are distinct from those found in both deep seawater and seafloor sediments. For example, indigenous microbial sequences obtained from basaltic glass samples dredged from the Arctic seafloor ranging in age from 1 Ma to 20 Ma were found to be affiliated with eight main phylogenetic groups of bacteria and a single marine Crenarchaeota group (Lysnes et al. 2004). Although it is not possible to confidently infer the metabolisms of uncultured microorganisms from molecular phylogenetic relationships, this study did find sequences that were related to known Fe and S metabolizing bacteria and methanogenic archea. Furthermore, it is reported that autotrophic microbes tend to dominate the early colonizing communities and that heterotrophic microbes are more abundant in older,

more altered samples (Thorseth et al. 2001; Santelli et al. 2006). In other words, it appears that prokaryotic microbial consortia, which include microorganisms that employ Fe and Mn oxidation, are plausible candidates for the bioerosion of basaltic glass and that these are associated with a heterotrophic community. There are even reports of eukaryotes from within the oceanic crust, with the finding of microbial remains argued to be marine, cryptoendolithic fungi in carbonate filled amygdales from Eocene Pacific seafloor basalts (Schumann et al. 2004).

Efforts to generate bioalteration textures in laboratory experiments using natural inoculums and various glass substrates have generated useful insights, although each with their own limitations. This work was motivated in part by etch pits found in Icelandic hyaloclastites that show "growth rings", which were taken to suggest that they might develop into tubular shaped alteration structures (Thorseth et al. 1992), although no such extended tubular morphologies have yet to be produced in the laboratory. These early studies involved basaltic glass inoculated with microbes taken from the submarine Surtsey volcano that were cultivated in 1% glucose solution at room temperatures for one year and produced etch pits and alteration rinds (Thorseth et al. 1995b). Monitoring of these experiments over time suggested that the microbes corrode the volcanic glass first via congruent dissolution, followed by incongruent dissolution and it was hypothesized that these involved the secretion of organic acids and metal complexing agents by the microbes (Thorseth et al. 1995b). The limitation of this work was the use of a nutrient rich media that is not comparable to sub-seafloor conditions. Another experimental approach was utilized by Staudigel et al. (1998) who constructed flow through experiments with basaltic glass that was continuously flushed with a natural seawater microbial population and monitored both chemically and isotopically for periods of up to 583 days. These biologically mediated experiments produced twice the mass of authigenic phases compared to the abiotic controls and caused particularly marked Sr exchange. Again, however, these experiments are not directly analogous to sub-seafloor conditions because surface seawater inoculums were used.

Thus, in summary it appears that heterotrophic bacteria, along with chemolithoautotrophs which utilize Fe and Mn oxidation, are responsible for the bioalteration of volcanic glass. However, the full diversity of microorganisms involved is yet to be fully documented, and the conditions under which tubular alteration structures are formed are yet to be replicated in the laboratory.

3 Material Investigated

We have investigated pillow lava and hyaloclastite samples from a large number of DSDP/ODP sites from the *in-situ* (modern) oceanic crust spanning the youngest to the oldest oceanic basins (0–170 Ma). The search for bioalteration has been extended into fragments of ancient oceanic crust preserved in ophiolites of different ages (Section 3.2) and Proterozoic to Archean greenstone belts (Section 3.3). All of

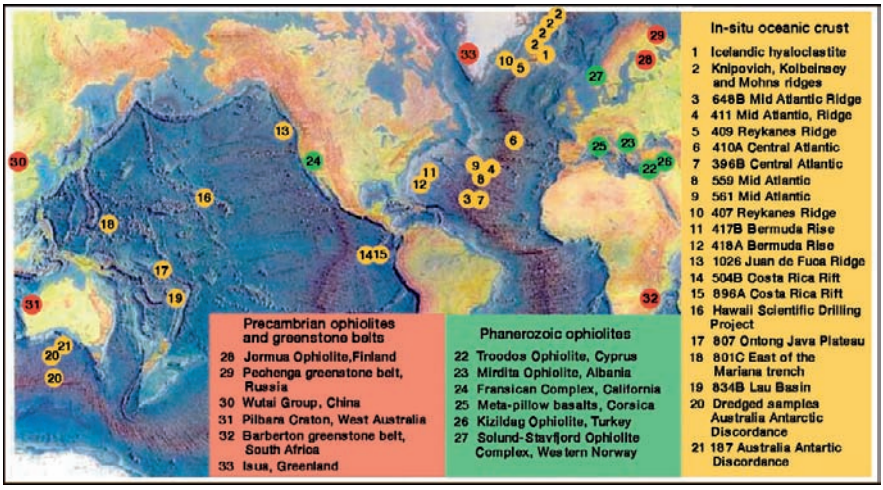

Fig. 4 Map showing the distribution of bioalteration textures documented to date in volcanic glass: examples from *in situ* oceanic basins are shown by *yellow circles*; from fragments of oceanic crust preserved in Phanerozoic ophiolites by *green circles*; and from Precambrian ophiolites and greenstone belts by *red circles*. References for each locality: (1) Thorseth et al. 1991; (2) Thorseth et al. 2001; (3) and (4) Furnes et al. 2001b, Lysnes et al. 2004; (5) Furnes et al. 2001b and Staudigel et al. 2004; (6) H. Furnes et al. 2001b; (7) Furnes et al. 2001b; (8) and (9) Fisk et al. 1998; (10) Staudigel and Furnes 2004; (11) Furnes et al. 2001b; (12) Staudigel and Furnes 2004; (13) Fisk et al. 2000; (14) Furnes et al. 1999; (15) Torsvik et al. 1998; (16) Walton and Schiffman 2003; (17) Banerjee and Muehlenbachs 2003; (18) Fisk et al. 1999; (19) Furnes et al. 2001a,b; (20) and (21) Thorseth et al. 2003; (22) Furnes et al. 2001b; (23) Furnes and Muehlenbachs 2003; (24) herein and K Muehlenbachs, unpub; (25) and (26) herein; (27) Furnes et al. 2002a; (28) Furnes et al. 2005; (29) herein; (30) herein; (31) Banerjee et al. 2007; (32) Furnes et al. 2004; Banerjee et al. 2006; (33) herein

the material discussed in this review are located on the world map shown in (Fig. 4) and plotted on the geological timescale shown in Fig. 36.

3.1 Modern Oceanic Crust (Atlantic, Costa Rica, Lau Basin)

The material from the modern oceanic crust has been collected from DSDP/ODP cores from the Atlantic Ocean, Lau Basin, Costa Rica Rift and the Ontong Java Plateau. The basaltic glass from the Atlantic (Fig. 5) forms the bulk of the investigated samples and was collected from eight drill sites (Holes 407, 409, 410A, 411, 417D, 418A, 396B and 634B). Holes 417D and 418A were drilled during DSDP Legs 51, 52 and 53, and have been described by Robinson et al. (1979). Holes 407, 409, 410A and 411, are situated in the north-central Atlantic Ocean and at the Reykjanes Ridge (Fig. 4), and were drilled during DSDP Leg 49 described by Luydendyk et al. (1978). Holes 396B and 648B are located in the central Atlantic Ocean and were drilled during DSDP Leg 46 and ODP Legs 106/109, described

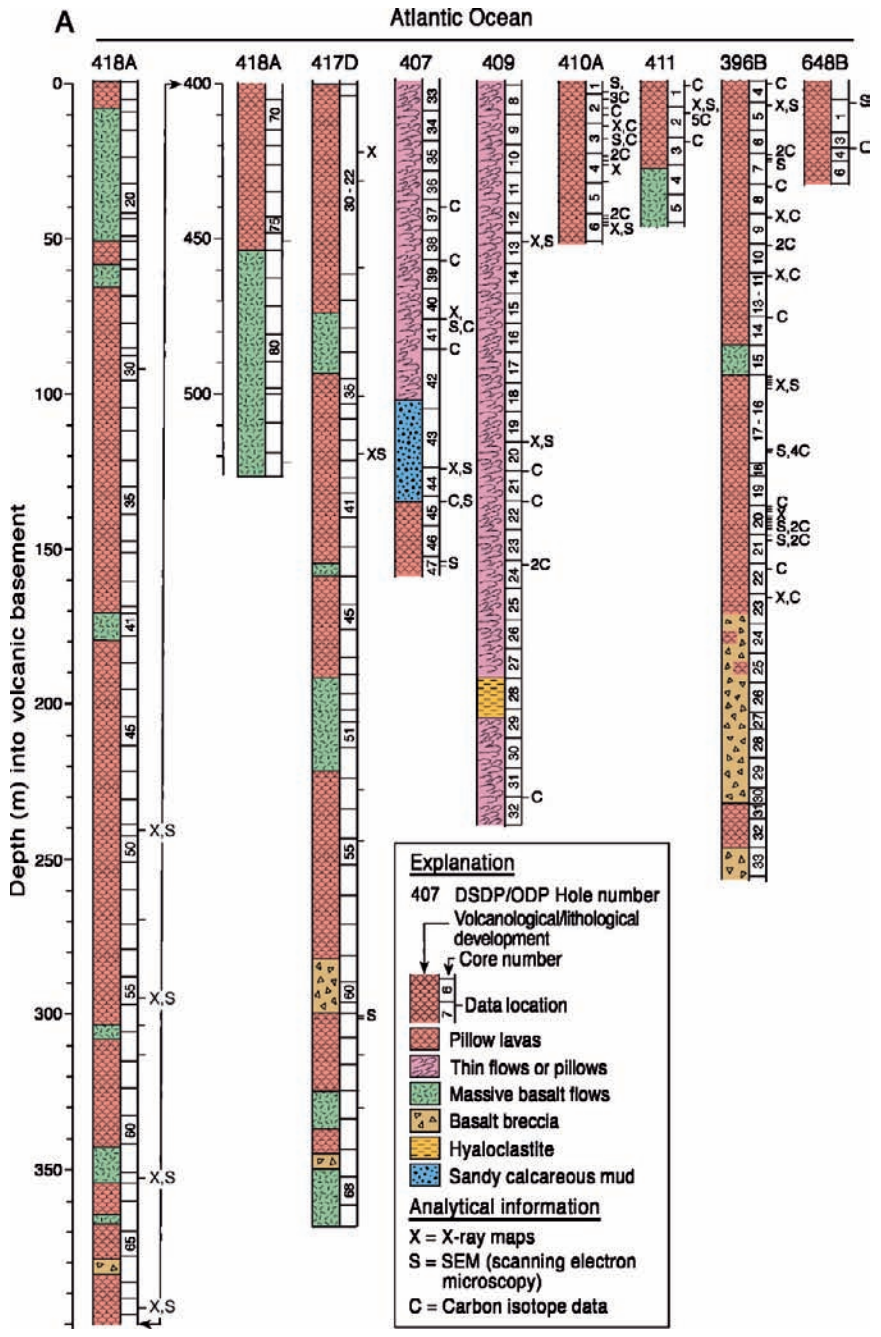

Fig. 5 *Continued*

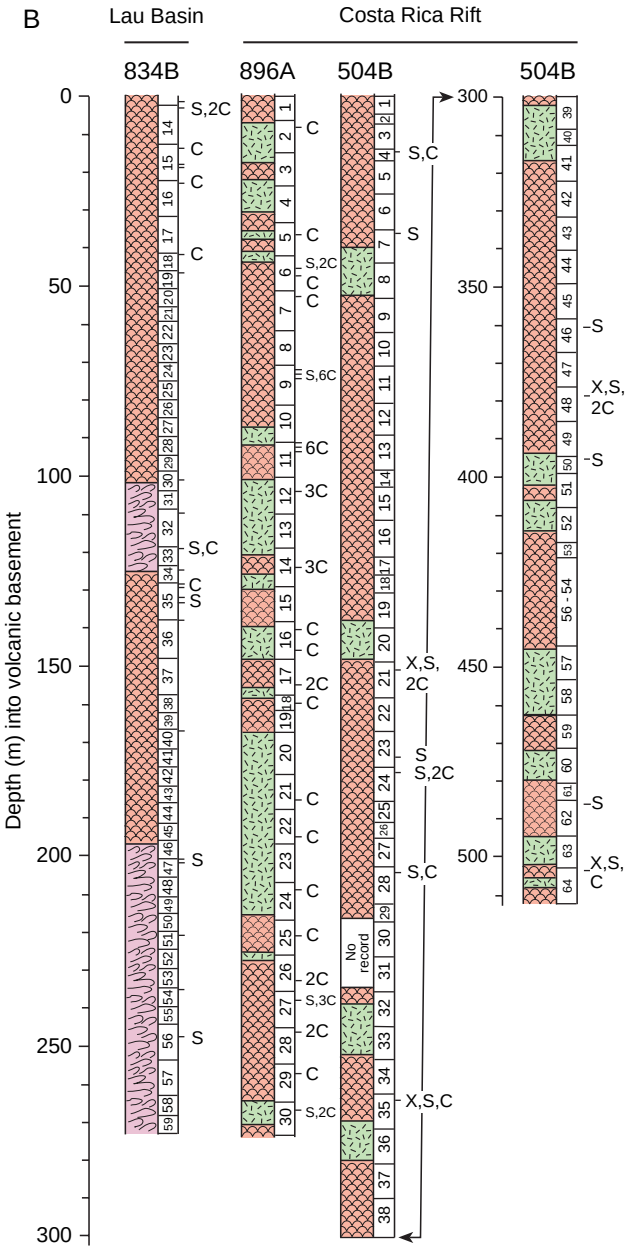

Fig. 5 Compilation of DSDP and ODP holes from the Atlantic Ocean (holes 418A, 417D, 407, 409, 410A, 411, 396B and 648B), the Lau Basin (hole 834A) and Costa Rica Rift (holes 896A and 504B) showing the lithological variations with depth into the volcanic basement. Heights at which bioalteration textures have been studied using scanning electron microscopy (SEM), X-ray mapping (X) and carbon isotopes (C) are shown along with the numbers of samples collected

in Dmitriev et al. (1978) and Detrick et al. (1988) respectively. Pillow lava is the dominant lithology of the ocean crust drilled at these sites, and varies in age from Quaternary to Early Cretaceous. The depth of penetration into the volcanic basement at these drill sites ranges from 33.3 m to 555 m, and the core recovery ranges from 15% in the youngest (648B) to 72% in the oldest (417D) crust (see Furnes et al. 2001a).

The samples investigated from the Lau Basin are from ODP Hole 834B (Fig. 5) described by Parson et al. (1992). The age of the ocean crust is Late Miocene, the depth of penetration into the volcanic basement is 272 m, and the core recovery is 28%. The basalts are composed entirely of pillow lavas and/or thin sheet flows.

The samples from the Costa Rica Rift are from DSDP/ODP Holes 504B and 896A (Fig. 5) described by Alt et al. (1993). Hole 504B is located about 200 km south of the Costa Rica Rift spreading centre and penetrates 550 m of volcanic basement that consists of approximately 75% pillow lavas and 25% massive lavas. Hole 896A (cored during Leg 148) is a re-occupation of Hole 678 (cored during Leg 111), where the palaeontological age of the basal sediment is 5.8–6.4 Ma which is consistent with the ages of the basal sediments of Hole 504B (5.9 Ma) (Alt et al. 1993). The penetration into the basement here was 273.9 m and the volcanic sequence was composed of approximately 60% pillow lava and 40% massive flows (Alt et al. 1993). The core recovery rate was 22% and 27% for Holes 504B and 896A, respectively.

3.2 Ophiolites

The ophiolites from which we present data range in age from Cretaceous to middle Proterozoic. The degree of lithological preservation in these investigated ophiolites varies from a complete Penrose-type ophiolite stratigraphy to dismembered parts of such sequences. We present the detailed volcanic stratigraphy for five of the most complete ophiolites examined in this study (Fig. 6). The degree of deformation varies from undeformed to highly deformed and the metamorphic grade from zeolite to blueschist facies metamorphism. The pillow lavas from the Cretaceous Troodos (Fig. 7A) and Kizildag (Fig. 7B) ophiolites, the Jurassic Mirdita (Fig. 7C) ophiolite, and a Jurassic Californian Coast Range ophiolite fragment (Fig. 7D) are all undeformed, whereas those from the Upper Ordovician Solund-Stavfjord ophiolite (Fig. 8A,B) and the middle Proterozoic Jormua ophiolite (Fig. 8C) vary from little- to highly-deformed. A blueschist pillow breccia from Corsica is shown in Fig. 9A alongside blueschist grade pillow lavas from the Franciscan complex of California in Fig. 9B,C.

3.2.1 Troodos

The Cretaceous Troodos ophiolite of Cyprus (Fig. 10) contains all the components of a Penrose-type complete ophiolite (harzburgite, overlain by layered cumulates, high-level gabbros and trondhjemites, a sheeted dike complex and mafic extrusive rocks) and represents one of the most thoroughly investigated terrestrial fragments

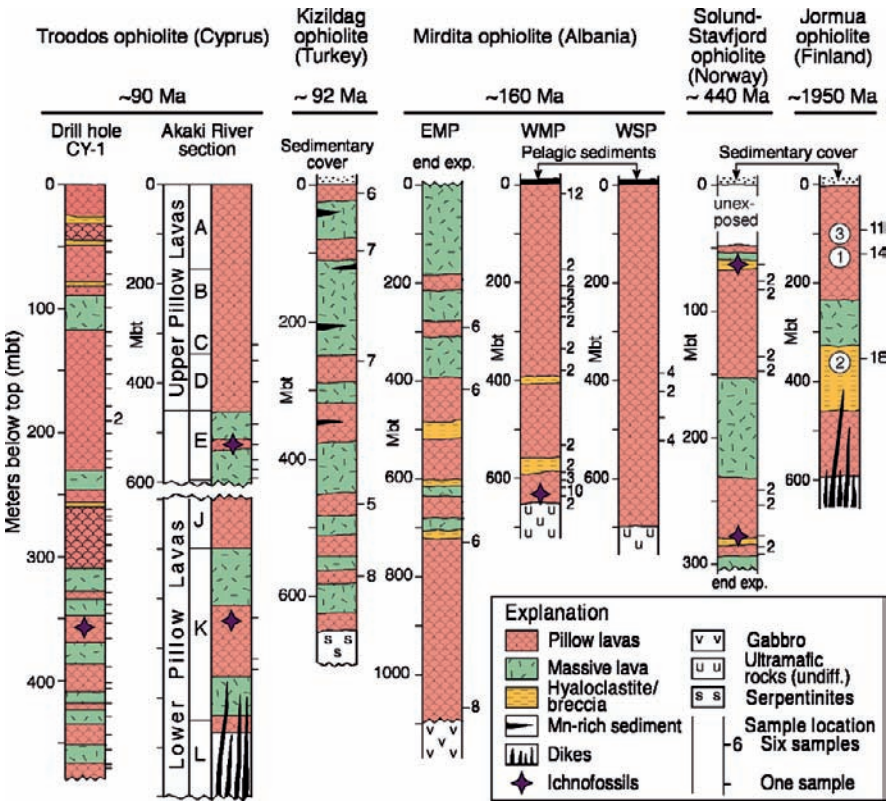

Fig. 6 Compilation of stratigraphic sections measured through the ~90 Ma Troodos ophiolite of Cyprus from drill hole CY-1 and the Akaki River (see also Fig. 10); the ~92 Ma Kizildağ ophiolite of Turkey (see also Fig. 11); the ~160 Ma Mirdita ophiolite of Albania at three sites EMP (eastern main profile), WMP (western main profile) and WSP (western sub-profile) (see also Fig. 12); the ~440 Ma Solund-Stavfjord ophiolite (SSOC) of Norway (see also Fig. 15); and the ~1950 Ma Jormua ophiolite of Finland (see also Fig. 16). The heights at which bioalteration textures or so called ichnofossils have been found are shown by a red star along with the number and positions of samples collected

of ancient oceanic crust (e.g., Panayiotou 1980; Malpas et al. 1990). More than half of the volcanic rocks are pillow lavas, and the remainder are breccias associated with pillow lavas and sheet flows (Schmincke and Bednarz 1990). Samples were taken from various well-exposed parts of the volcanic sequence, also from the drill core CY-1, and from the Akaki River section (boxed area of Fig. 10; for further details see Fig. 1 in Furnes et al. 2001c).

3.2.2 Kizildag

The Cretaceous (~92 Ma) Kizildag ophiolite complex (KOC) in southern Turkey (Fig. 11) occurs in the same Neo-Tethyan ophiolite belt as the Troodos ophiolite,

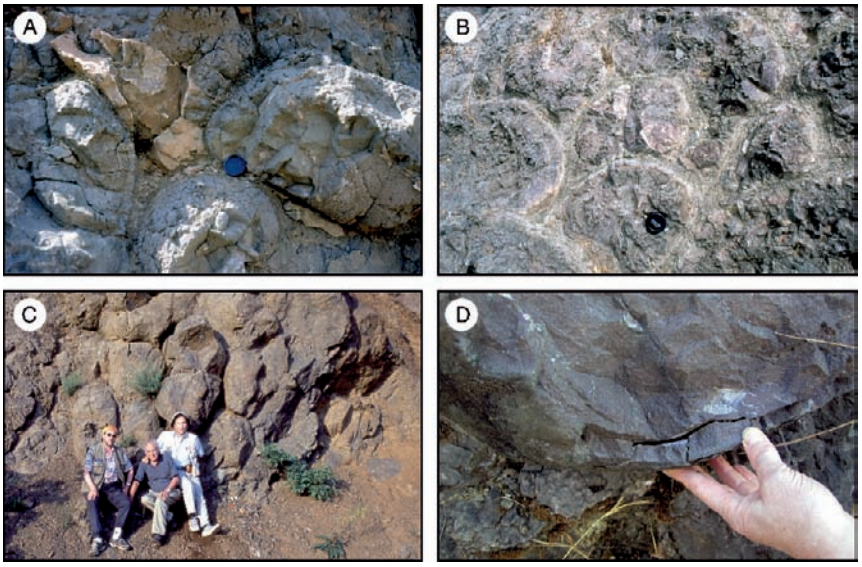

Fig. 7 Outcrop photographs of pillow lavas from: (**A**) the Troodos ophiolite of Cyprus; (**B**) the Kizildag ophiolite of Turkey showing pale *grey*, glassy pillow rims; (**C**) rounded pillows of the Mirdita ophiolite of Albania; and (**D**) the Nicasio Reservoir in California showing the collection of a pillow rim sample. For scale the camera lens cap is 5 cm across

and also displays a complete Penrose pseudostratigraphy. The Kizildag ophiolite rests tectonically on the northwest edge of the Arabian platform and is overlain by Campanian-Maastrichtian clastic sediments. The crustal units of the ophiolite are exposed in a NE-trending, topographically and structurally well-defined graben system, which has been argued to represent a fossilized oceanic spreading axis (Dilek et al. 1998). Based on its internal structure and crustal architecture, the KOC has been interpreted as a slow to intermediate rate spreading axis (Dilek et al. 1998). The extrusive rocks of the KOC form a 300 to 700-m-thick sequences of massive and pillowed lavas intercalated with hyaloclastites, metaliferous umber, and pelagic limestone layers. In addition, there are boninitic lavas which are ~4 Ma younger than the main extrusive sequence. The location of the measured section illustrated in Fig. 6 which was sampled for bioalteration textures is shown on the map in Fig. 11.

3.2.3 Mirdita

The Jurassic (160 Ma) Mirdita ophiolite complex (MOC) in Albania occupies a NNE-SSW-trending corridor within the Dinaride-Hellenide mountain belt of the Alpine-Himalayan orogenic system (Fig. 12). The MOC has been subdivided into western (WMOC) and eastern (EMOC) type complexes based on the rock types and their geochemical characteristics (e.g., Shallo 1995; Dilek et al. 2007). The

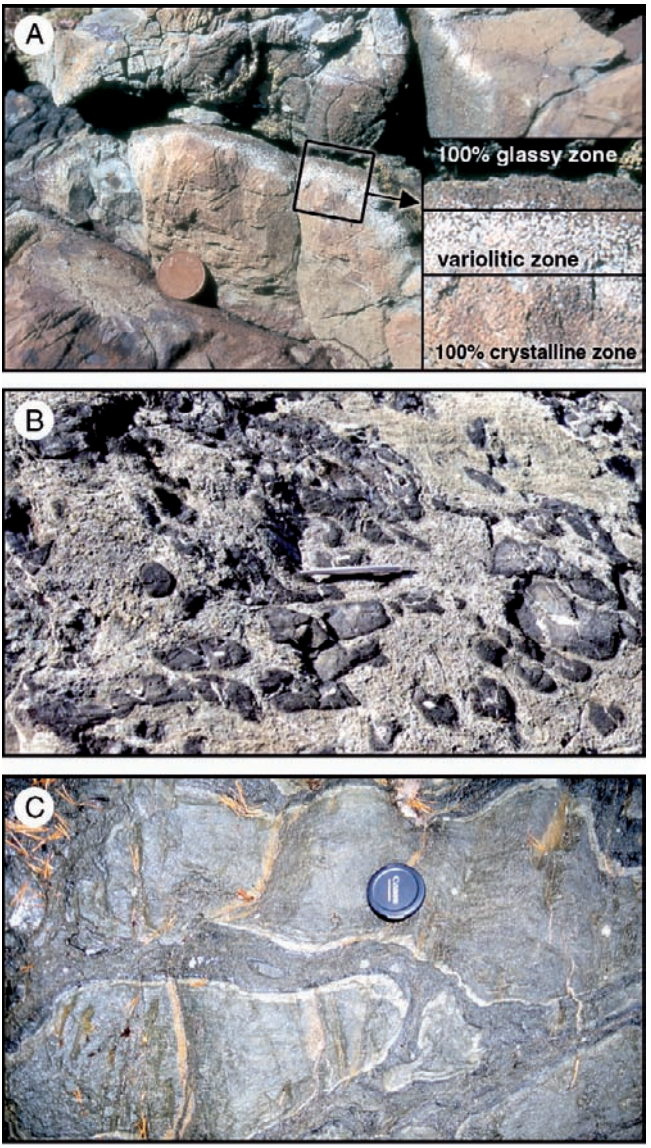

Fig. 8 Outcrop photographs of: (**A**) pillow lavas from the SSOC ophiolite of Norway with an enlarged view of the variolitic zone that occurs around a centimeter inwards of the glassy pillow rim; (**B**) a hyaloclastite breccia also from the SSOC; (**C**) flattened pillow lavas from the upper greenschist grade Jormua ophiolite of Finland. For scale the camera lens cap is 5 cm across

ca. 6-km-thick WMOC contains ~700 m of volcanic rocks composed mainly of MORB-type pillow basalts (Shallo 1995; Bebien et al. 1998), which rest directly on gabbros or mantle lherzolites and/or harzburgites. A well-developed sheeted dike complex is absent within the WMOC, though locally dike swarms and numerous

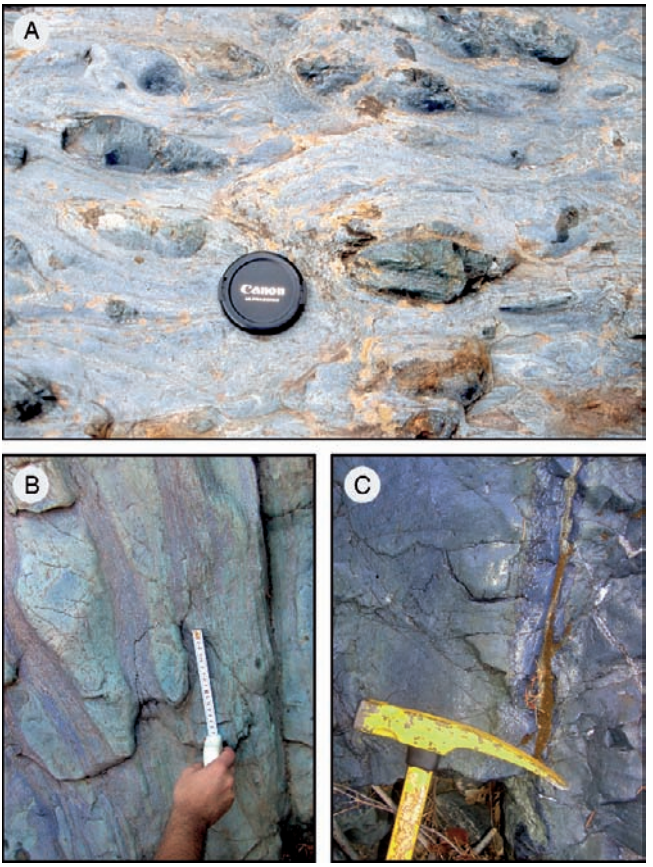

Fig. 9 Outcrop photographs of pillow breccias and pillow lavas from: (**A**) the blueschist grade metabasites of Corsica; (**B**) flattened, blueschist grade pillows from Ward Creek (California) with "streaky" pillow rims; (**C**) glassy pillow rim also from Ward Creek with the variolitic zone (white spots in distinctive blue zone) still visible

single dikes crosscut the peridotites and the lavas. The ca. 10-km-thick EMOC contains a ~1.1 km thick heterogeneous extrusive sequence consisting of pillowed basalts and basaltic andesite, with massive flows of andesite, dacite, and rhyolite; also sheeted dike swarms composed of the above-mentioned lava compositions and boninites. The EMOC is intruded by numerous small to large diorite bodies. There is no apparent tectonic break between the western- and eastern-type sequences of the MOC and recent studies by Nicolas et al. (1999) have ascribed the contrast between the WMOC and EMOC to successive episodes of magmatic and amagmatic spreading in a slow-spreading environment. Samples were collected from pillow lava rinds from both the WMOC and the EMOC. The profiles from which samples have been collected are shown in Fig. 12.

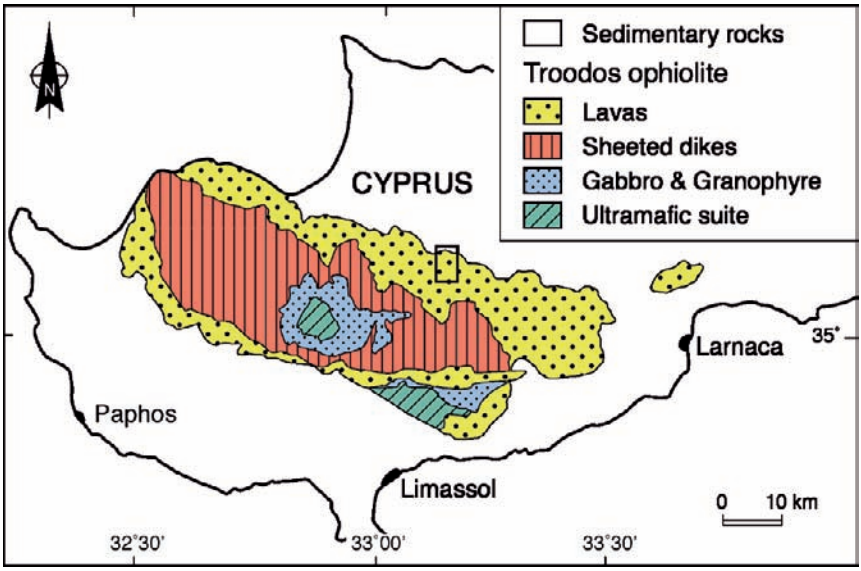

Fig. 10 Schematic geological map of the ~90 Ma Troodos ophiolite in Cyprus. The location of the Akaki River section and drill core CY-1 (shown in Fig. 6) is shown by the boxed area within the lava section. Map is modified from Furnes et al. (2001c)

3.2.4 California: Nicasio Reservoir and Ward Creek

In California, fragments of Jurassic-aged oceanic crust are exposed both in coherent sequences within the California Coast Range Ophiolite (CCRO), as well as in tectonic blocks within the Franciscan Complex. Submarine lavas in the CCRO were recrystallized under zeolite, prehnite-pumpellyite, and greenschist facies conditions during ocean-floor metamorphism (Schiffman et al. 1984, 1991; Evarts and Schiffman 1983). Submarine lavas within the Franciscan Complex were metamorphosed in a subduction zone setting and exhibit zeolite, blueschist- and eclogite-facies metamorphism (Wakabayashi 1999; Swanson and Schiffman 1979). Samples were collected from two pillow lava locations the Nicasio Reservoir and the Ward Creek of low- and high-grade metamorphism, respectively, both are within the Central Belt of the Franciscan Complex (Fig. 13).

The Nicasio Reservoir pillow lava pile is over 1 km thick and associated with a structural horizon that is intermediate within the Franciscan Complex (Wakabayashi 1992). The pillows are undeformed and their mineral composition includes albitized plagioclase phenocrysts, in a matrix of chlorite, pumpellyite, and laumonite. The metamorphic grade is thus of zeolite to prehnite pumpellyite facies (Swanson and Schiffman 1979). This pillow lava pile is considered to represent part of a seamount that became incorporated into the Franciscan subduction complex in late Mesozoic/early Cenozoic time (Cloos 1990).

The Ward Creek pillow lavas form part of a complex association of tectonic blocks of metabasaltic rocks, serpentinites, metagreywackes and glaucophane-bearing rocks

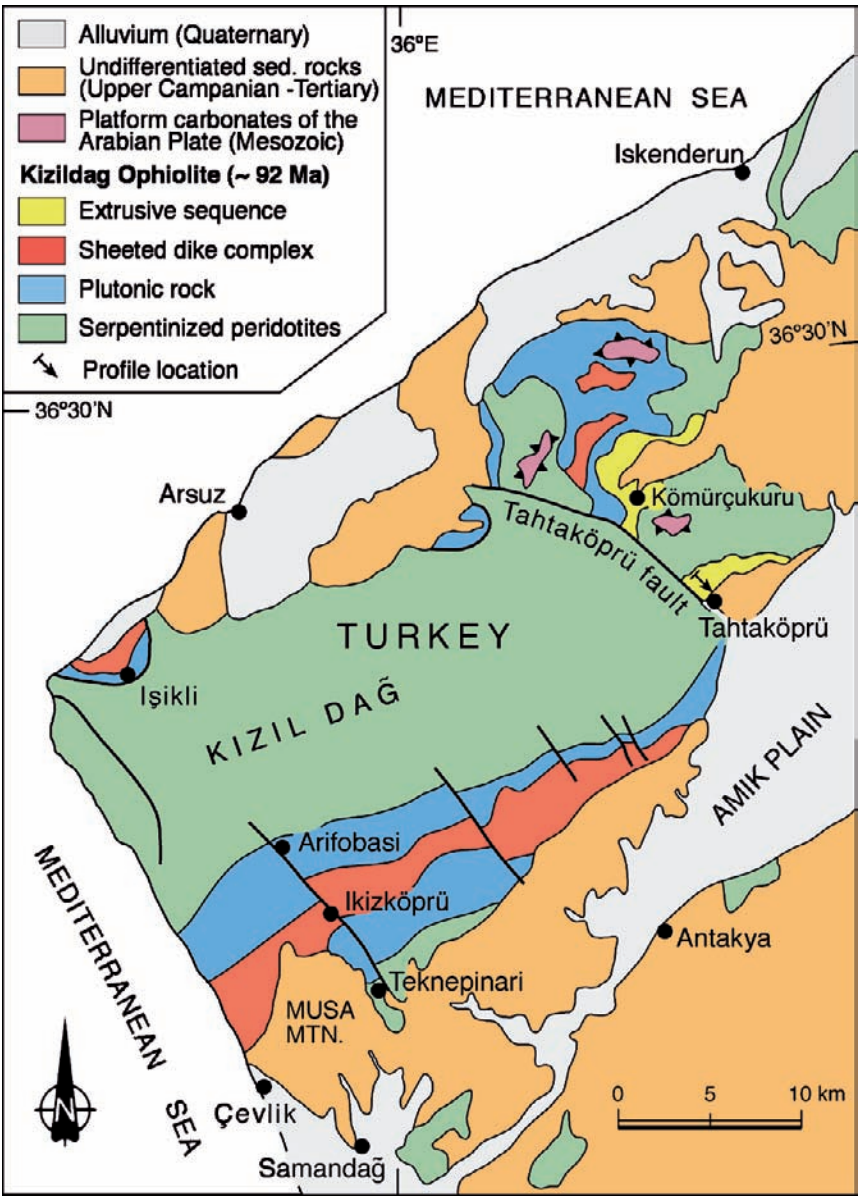

Fig. 11 Schematic geological map of the ~92 Ma Kizildağ ophiolite in Turkey showing the location of the measured section given in Fig. 6. Map is modified from Dilek and Thy (1998)

that were described by Coleman and Lee (1963). These high-pressure low temperature metamorphic rocks preserve various metamorphic grades such as lawsonite-, pumpellyite-, and epidote-zones (Maruyama and Liou 1988). In the lawsonite and pumpellyite zones pillow structures and primary igneous textures are well-preserved,

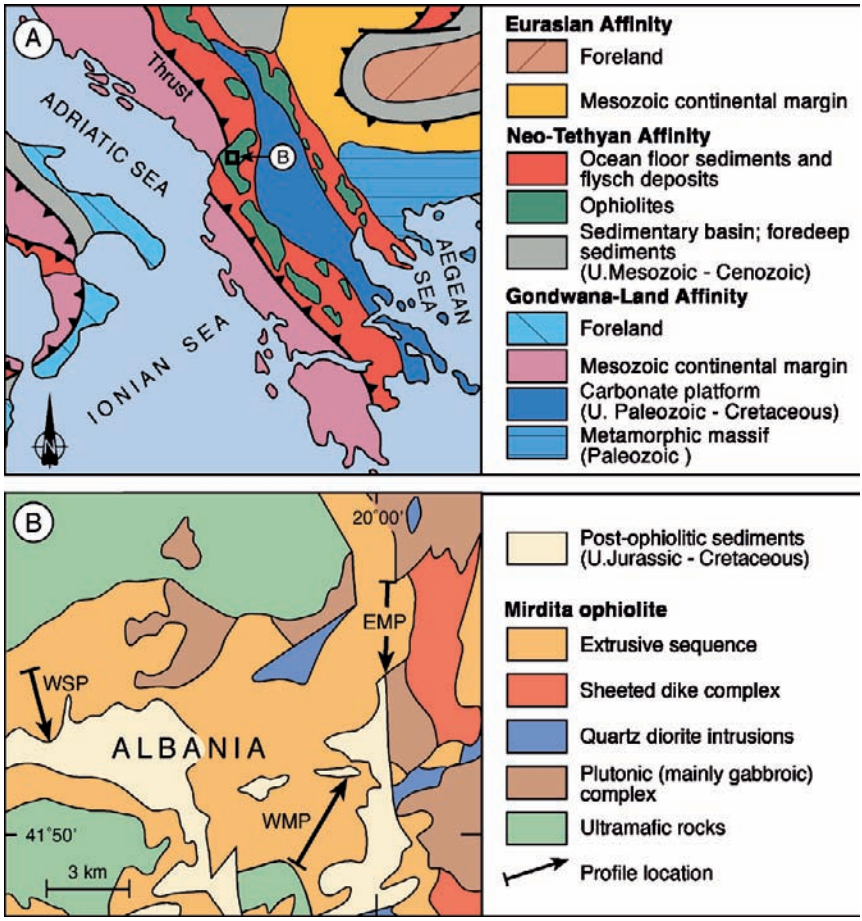

Fig. 12 (**A**) regional geological map of Albania and adjacent countries; (**B**) enlarged geological map of part of the ~160 Ma Mirdita ophiolite in Albania showing the location of the measured sections WSP (western sub-profile), WMP (western main profile) and EMP (eastern main profile) shown in Fig. 6. Map is modified from Dilek et al. (2007)

whereas in the epidote-zone the metabasalts which contain glaucophane and red garnet (~ 290°C, 6.5–9 Kb) are more strongly deformed, their primary igneous textures are largely obliterated, although pillow structures can still be discerned (Fig. 9B,C).

3.2.5 Corsica

Ophiolitic rocks and associated sedimentary rocks (Fig. 14) that represent the remnants of the former Mesozoic Ligurian Tethys Ocean are found in the north/northeastern part of Corsica (Lemoine et al. 1987). These ophiolitic units occur in nappe sheets emplaced during the Alpine orogeny (Ohnenstetter et al. 1976) and

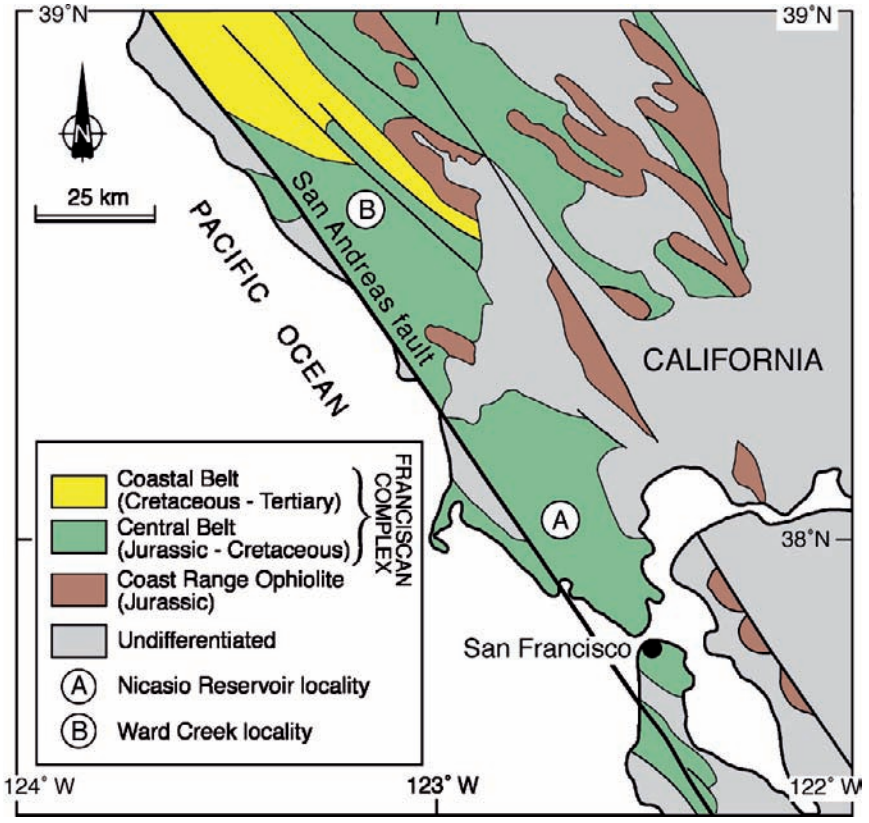

Fig. 13 Schematic geological map of north western California showing the Franciscan Complex sampled at the zeolite grade Nicasio Reservoir (**A**) and the blueschist grade Ward Creek (**B**) localities. Map is modified from Coleman (2000) and Ingersoll (2000)

experienced high pressure low temperature blueschist metamorphism with relics of eclogites (Ohnenstetter et al. 1976; Dal Piaz and Zirpoli, 1979; Fournier et al. 1991). The blueschist-facies pillow lavas and pillow breccias (Fig. 9A) have been subject to pressure of at least 11 kbar (Fournier et al. 1991). Sampling locations are shown in Fig. 14.

3.2.6 Solund-Stavfjord

The Late Ordovician (443 +/ − 3 Ma) Solund-Stavfjord ophiolite complex (SSOC) in the western Norwegian Caledonides (Fig. 15) displays a well-preserved, ca. 800-m-thick volcanic sequence of basaltic pillow lavas and pillow breccias (Fig. 8A,B), sheet flows and volcanic breccias, a ca. 1000-m- thick sheeted dike complex and minor amounts of high-level gabbro (Furnes et al. 2001d, and references therein). These volcanic rocks experienced pervasive lower greenschist facies

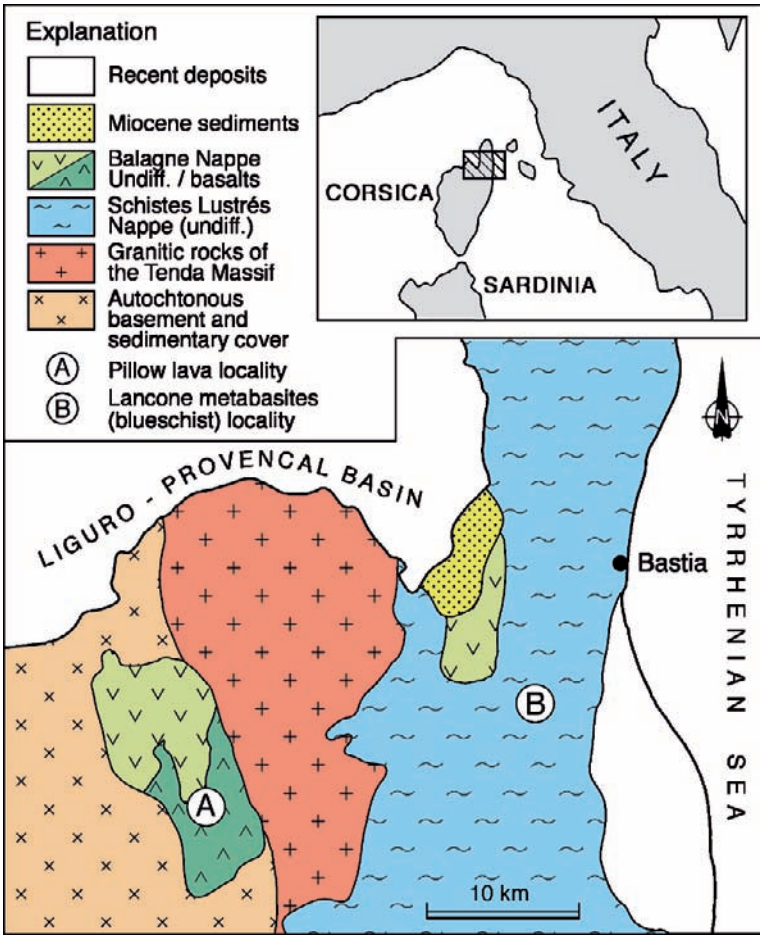

Fig. 14 Schematic geological map of the Mediterranean Island of Corsica showing the Jurassic pillow basalt locality (**A**) and the blueschist metabasite locality (**B**) also illustrated in Fig. 9A. Map is modified from Daniel et al. (1996)

metamorphism (chlorite, actinolite and epidote form the principal minerals). The extent to which the volcanic rocks were deformed varies significantly depending on their position in major folds (Furnes et al. 2001d).

3.2.7 Jormua

The Jormua ophiolite complex (JOC) is located in central northern Finland (Fig. 16) and contains all of the principal components of a Penrose-type ophiolite, i.e. pillow lavas and volcanic breccias, a sheeted dike complex, plutonic rocks, and mantle peridotites (Kontinen 1987). The age of the complex has been determined as 1.95 Ga (Peltonen et al. 1996). The volcanic sequence consists of pillow lavas, pillow

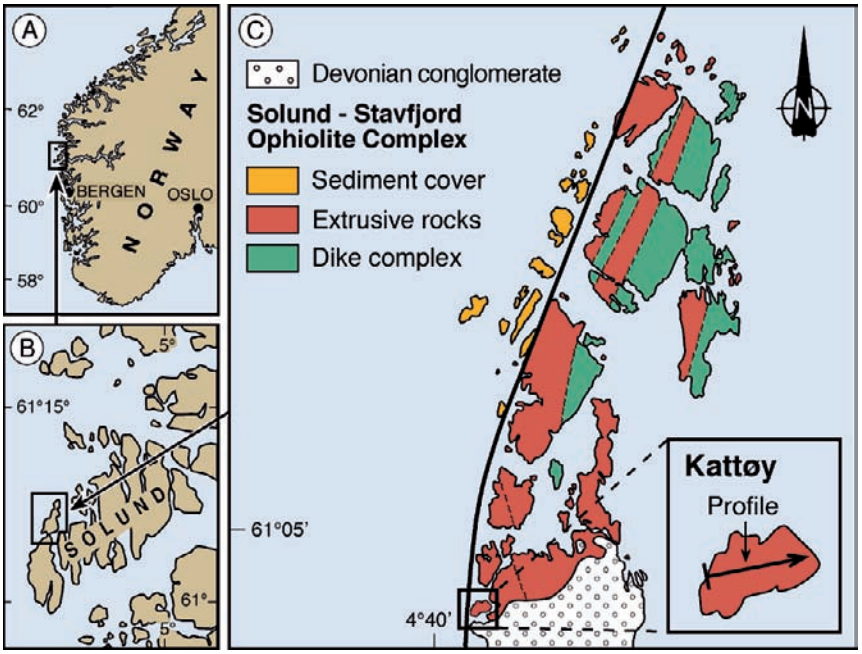

Fig. 15 Regional map of the ~440 Ma Solund-Stavfjord Ophiolite Complex (SSOC) of Norway (**A** and **B**), with an enlarged map (**C**) showing a schematic geological map and the location of the measured profile given in Fig. 6 from the extrusive rocks of Kattøy which contain bioalteration textures. Map is modified from Furnes et al. (2002a)

breccias and hyaloclastites (Fig. 8C) and its thickness appears to be at least 500 m. The volcanic rocks and the sheeted dikes experienced lower amphibolite-facies metamorphism, as evidenced by the mineral assembly composed of pale-green amphibolite, oligoclase-andesine plagioclase, epidote and chlorite (Kontinen 1987). The volcanic rocks also display a pronounced foliation.

3.3 Greenstone Belts

Greenstone belts are deformed sequences of Archean and Proterozoic rocks comprising meta-volcanic rocks and intercalated metasedimentary rocks that are preserved between granitoid complexes. Greenstone belts that were sampled for bioalteration studies include the Barberton greenstone belt of South Africa, the Pilbara Supergroup of Western Australia and the Pechenga greenstone belt of Russia (Fig. 17), ranging in age from Middle Proterozoic to MesoArchean. In addition restricted sampling has been undertaken in the PaleoArchean Isua supracrustal belt of Greenland, and in the NeoArchean Wutai, China (N. McLoughlin et al., unpub. data), and Abitibi greenstone belt, Canada (N. Banerjee et al. unpub. data). The

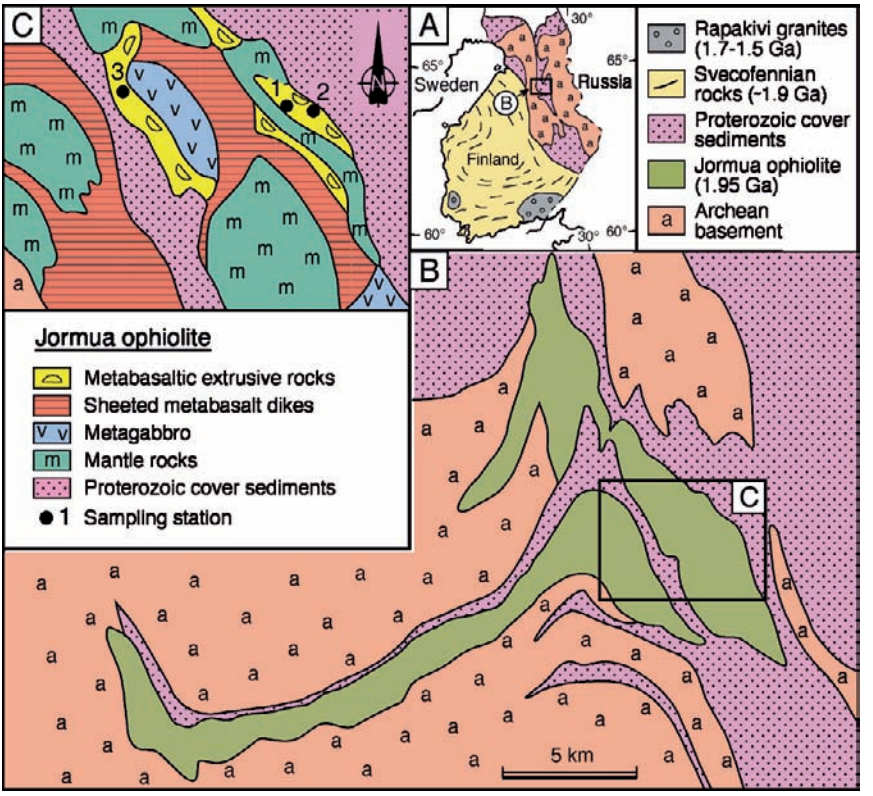

Fig. 16 (**A**) regional geological map of northern Finland and Russia showing the location of the ~1.95 Ga Jormua ophiolite; (**B**) enlarged geological map, and (**C**) showing the location of sampling stations 1–3 in the metabasaltic extrusive rocks shown in the composite section in Fig. 6. Map is modified from Furnes et al. (2005)

preservation of pillow lavas is remarkably good at all of these sites (see Fig. 18) and an overview of their stratigraphy is given below.

3.3.1 Isua Supracrustal Belt, West Greenland

The Paleoarchaean Isua supracrustal belt (ISB) is situated in southwest Greenland and contains metabasalts (amphibolite), metagabbros and ultramafic rocks that are associated with metapelites, cherts, banded iron formation (BIF) and felsic rocks (e.g., Nutman 1986; Rosing et al. 1996). The rocks are in general strongly deformed and metamorphosed to amphibolite facies. Primary features are scarce and their protoliths are a matter of debate, but undisputable (ocelli bearing) pillow lavas have been found within the metabasalts (Komiya et al. 1999; Myers 2001). A whole rock Sm-Nd isochron (amphibolite-grade meta-basaltic pillows and metagabbro) defines an age of 3777 +/− 44 Ma (Boyet et al. 2003). Komiya et al. (1999)

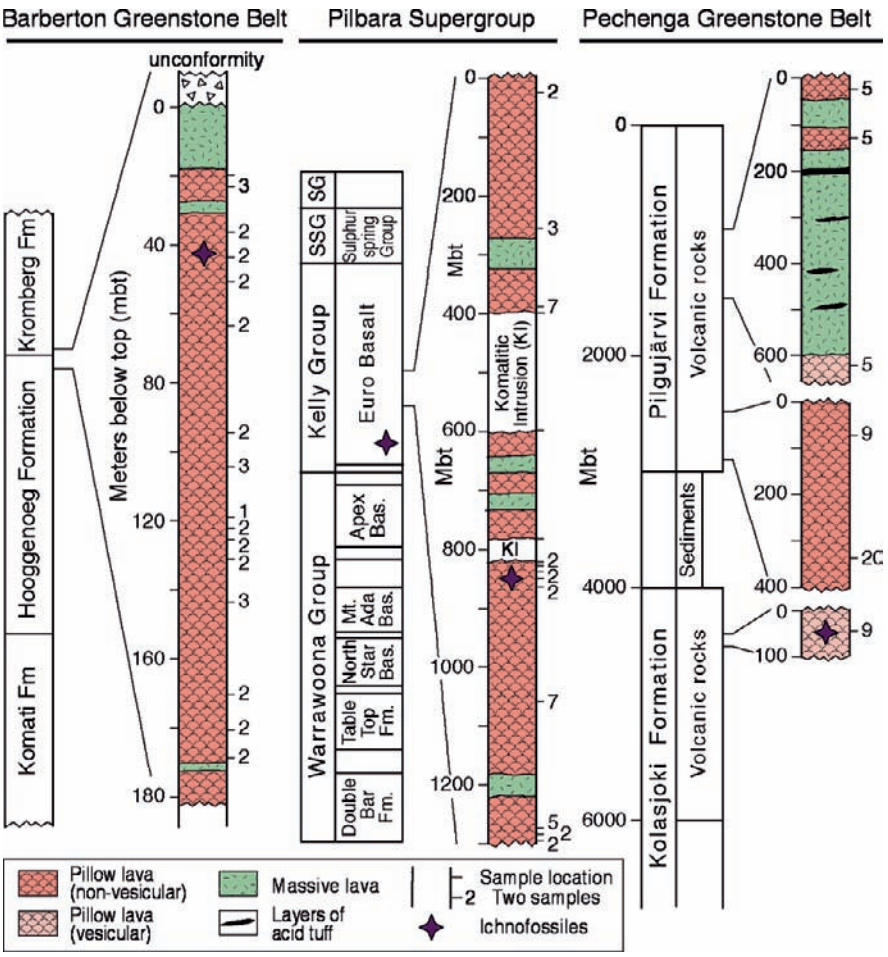

Fig. 17 Compilation of stratigraphic sections measured from the ~3.5 Ga upper Hooggenoeg and lower Kromberg Formations of the Barberton greenstone belt of South Africa (see also Fig. 19) (modified from de Wit et al. 1987); the ~3.4 Ga Euro Basalt of the Kelly Group of the Pilbara Supergroup of Western Australia (see also Fig. 20) (modified from Van Kranendonk 2006. Note that the unlabelled boxes represent acid volcanics and cherts); and volcanic rocks from the ~2.0 Ga Pilgujärvi and Kolasjoki Formations of the Pechenga greenstone belt Russia (see also Fig. 21) (modified from Melezhik et al. 2007). The bioalteration localities from the *upper part* of the Hooggenoeg Formation and the *lower part* of the Euro Basalt (indicated within the box) are from Furnes et al. (2004) and Banerjee et al. (2007), respectively. The bioalteration localities from the middle part of the Euro Basalt and from the upper part of the Kolasjoki Formation are unpublished

suggested that this oceanic-like crust may have been emplaced within an accretionary wedge around 3.7 Ga and Furnes et al. (2007b) reported the occurrence of a sheeted dike complex suggesting the presence of a c. 3.8 Ga ophiolite in the Isua supracrustal belt.

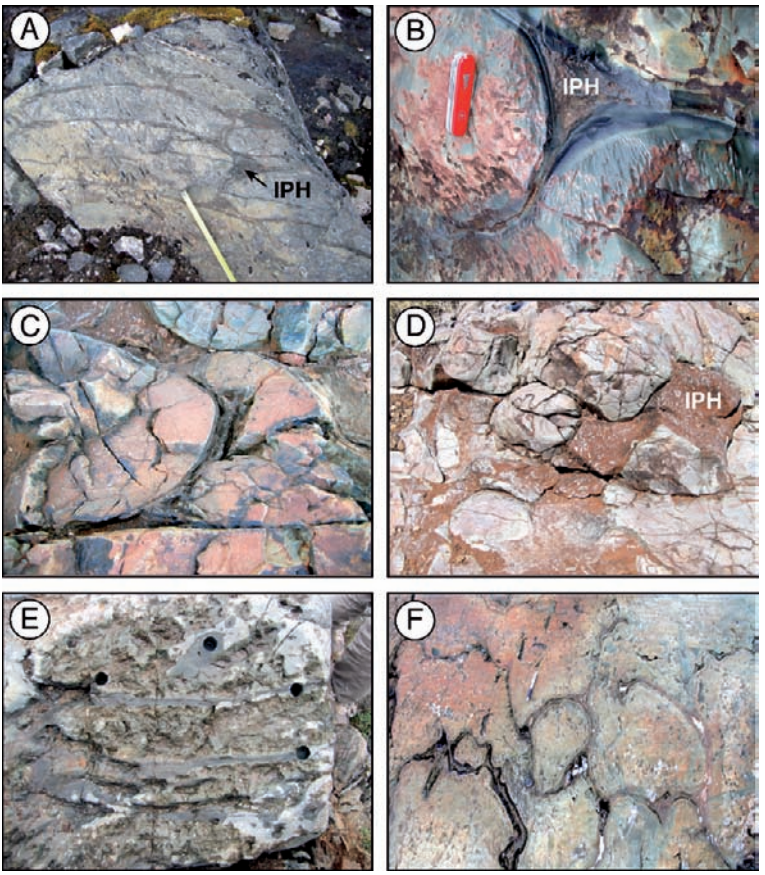

Fig. 18 Outcrop photographs of: (**A**) deformed pillow lavas exhibiting chilled margins (dark selvages) and pockets of inter-pillow hyaloclastite (IPH) from the ~3.8 Ga Isua supracrustal belt, West Greenland; (**B**) pillow lavas from the ~3.5 Hooggenoeg Formation of the Barberton greenstone belt in South Africa with dark glassy rims and a pocket of interpillow hyaloclastite (see also Fig. 19); (**C**) pillow lavas from the ~3.4 Ga Euro Basalt of the Pilbara Craton, Western Australia (see also Fig. 20); (**D**) carbonate altered pillow lavas from the ~3.4 Ga Euro Basalt of the Pilbara Craton, Western Australia displaying large pockets of inter-pillow hyaloclastite; (**E**) flattened pillow lavas from the ~2.5 Ga Wutai Group of the North China Craton, showing well preserved pillow rims that have been sampled by micro-drilling; (**F**) pillow lavas from the ~2.0 Ga Pechenga greenstone belt of the Kola Peninsula, Russia

3.3.2 Barberton Greenstone Belt, South Africa

The Mesoarchean Barberton greenstone belt, South Africa (Fig. 19) contains some of the world's oldest and best-preserved pillow lavas (de Wit et al. 1987; Brandl and de Wit 1997). The magmatic sequence comprises 5–6 km of predominantly basaltic and komatiitic extrusive (pillow lavas, minor hyaloclastite breccias and sheet flows) of the Theespruit, Komati, Hooggenoeg, and Kromberg Formations of the ca. 3.52–3.35 Ga Onverwacht Group, and subordinate intrusive rocks. This igneous

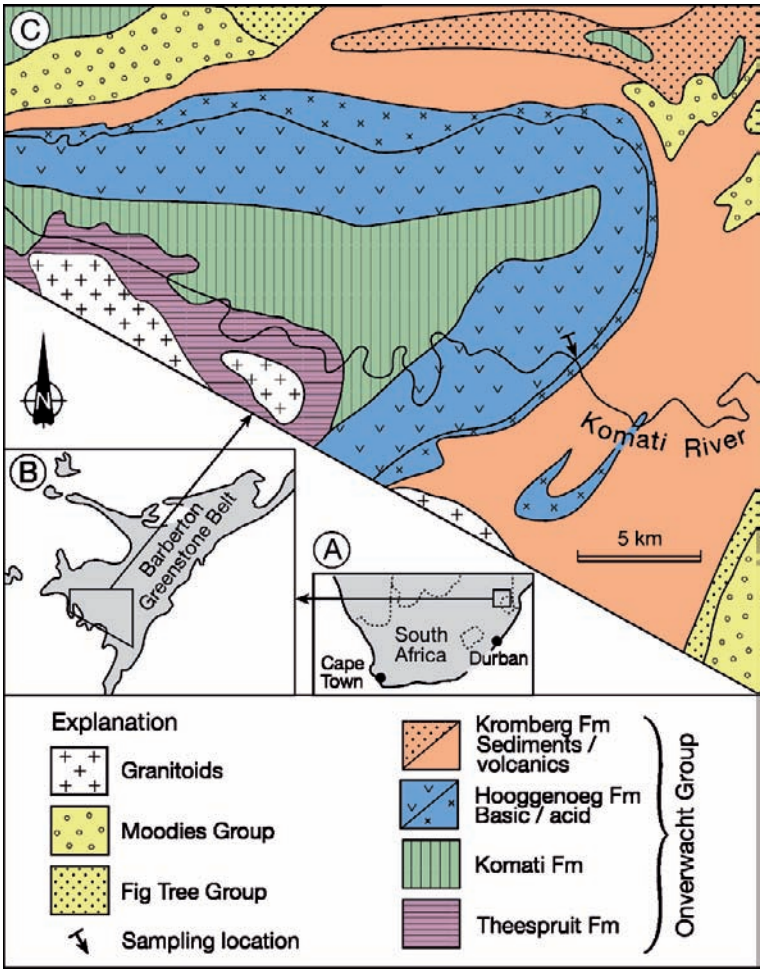

Fig. 19 (**A**) Regional map showing the location of the Barberton greenstone belt in South Africa, enlarged in (**B**) with a simplified geological map of the Onverwatch antiform shown in (**C**) giving the location of the measured section through the Hooggenoeg Fm and sample sites shown in Fig. 17. Map is modified from de Wit et al. (1987)

sequence is intercalated with chert layers and is overlain by cherts, banded iron formations (BIF) and shales. The Onverwacht Group has been interpreted by some workers to represent a fragment of Archean oceanic crust, termed the Jamestown Ophiolite Complex (de Wit et al. 1987; de Wit 2004), that developed in a successor subduction environment at between approximately 3480–3220 Ma (Armstrong et al. 1990; de Ronde and de Wit 1994). Moving upwards from the middle to the upper part of the Onverwacht Group the metamorphic grade decreases from greenschist to prehnite-pumpellyite facies. Stratigraphically downward into the Theespruit Formation, there is a rapid increase in the metamorphic grade to lower amphibolite facies (de Ronde and de Wit 1994).

3.3.3 Pilbara Craton, Western Australia

The Pilbara Craton, Western Australia (Fig. 20) contains some of the best preserved geological record of the early Earth (Van Kranendonk and Pirajno 2004; Van Kranendonk et al. 2002, 2004, 2007). The ancient nucleus of the craton is preserved in the East Pilbara Terrane, which contains a 20-km-thick succession of low-grade metamorphic, dominantly volcanic supracrustal rocks of the Pilbara Supergroup that were deposited in four autochthonous groups from 3.52–3.165 Ga (Van Kranendonk 2006; Van Kranendonk et al. 2007). These include, from base to top, the 3.52–3.43 Ga Warrawoona Group, the 3.42–3.31 Ga Kelly Group, the 3.27–3.23 Ga Sulphur Springs Group, and the 3.23–3.165 Ga Soanesville Group. Pillows and interpillow hyaloclastites were collected from the Dresser Formation

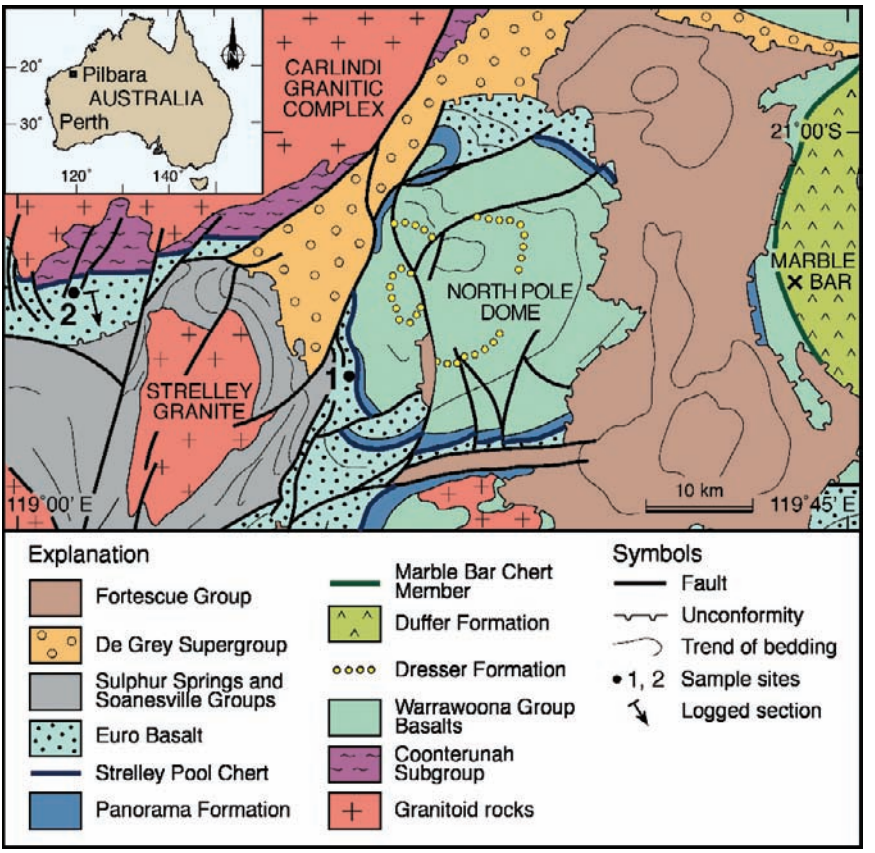

Fig. 20 Simplified geological map of the Pilbara region of Western Australia showing the location of sample sites 1 and 2 where bioalteration has been identified within the Euro Basalt of the Kelly Group and the location of the section measured at site 2 that is illustrated in Fig. 17. Map is modified from Van Kranendonk (2006)

and Apex Basalt of the Warrawoona Group and the Euro Basalt of the Kelly Group. To date, bioalteration textures have only been found in the Euro Basalt (Fig. 20).

3.3.4 Wutai Group, North China Craton

In the Eastern Block of the North China Craton, oceanic pillow lavas form part of the Wutai Group (Fig. 21) which consists of late Archean to Paleoproterozoic granitoid rocks and metamorphosed volcanic and sedimentary rocks (Zhou et al. 1998; Zhao et al. 2001). Traditionally, the Wutai Group has been considered a typical greenstone belt (Zhai et al. 1985; Kröner et al. 2001) and zircon ages for the complex range in age from 2.52 Ga to 2.57 Ga (Kröner et al. 2001). Deformed, yet well-preserved pillow lavas occur in the Baizhiyan Formation of the Middle Wutai Group. They are

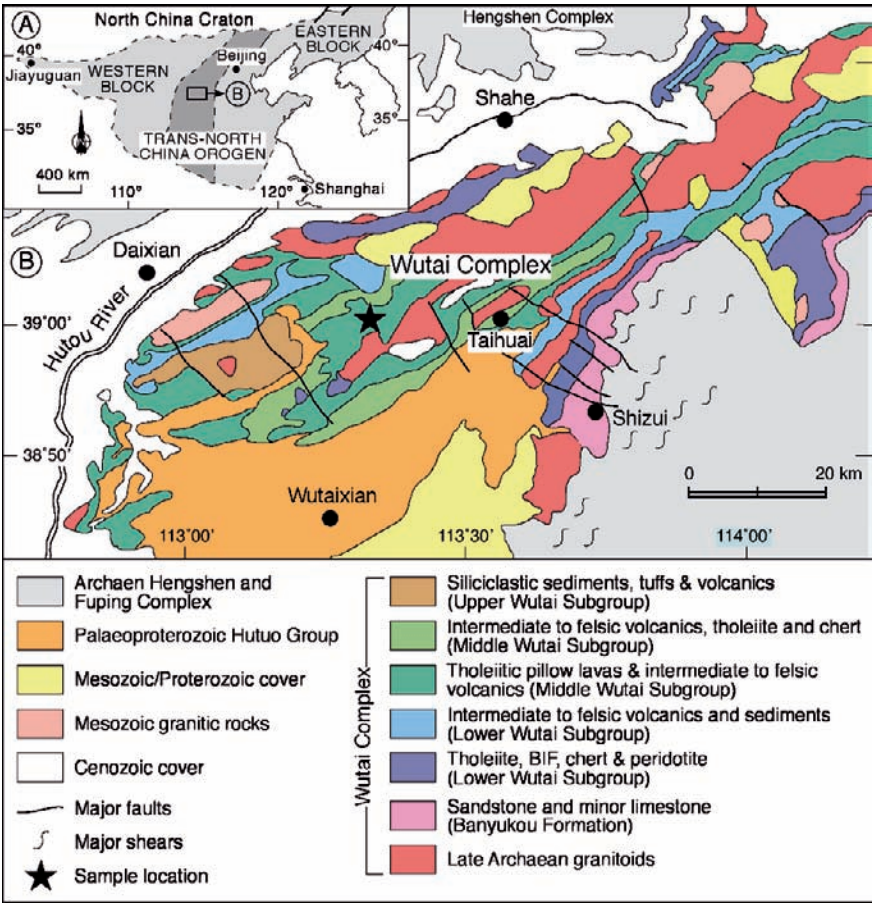

Fig. 21 Geological map of the North China Craton, and the Wutai Complex within the Trans-North China Orogen. Pillow lavas sampling (shown by star) was undertaken within the greenschist facies tholeiites of the Middle Wutai Subgroup. Map is modified from Zhao et al. (2001)

delineated by 1–2 cm wide epidote-rich rims that surround a core of fine-grained material composed chiefly of chlorite, carbonate, albite and epidote. A variety of mafic and felsic lavas and tuffs are associated with the pillow lavas, ranging in composition from MORB-like basalts to calc-alkaline andesites and rhyolites (Kröner et al. 2001).

3.3.5 Pechenga Greenstone Belt, Kola Peninsula, Russia

The Paleoproterozoic Pechenga greenstone belt (Fig. 22) is in the Russian part of the Fennoscandian Shield situated in the Kola Peninsula (Melezhik and Sturt 1994). The > 10-km-thick Northern Pechenga Group is composed of four sedimentary-volcanic cycles whose evolution spans more than 400 Ma of Earth history with a total thickness of more than 10 km. Although the rocks have experienced polyphase metamorphism ranging from prehnite-pumpellyite to upper amphibolite grades, their sedimentary and volcanic features are locally well preserved.

The most voluminous of the volcanic units is the 3-km-thick uppermost Pilgujärvi Volcanic Formation. The bulk of the Pilgujärvi volcanic rocks are submarine

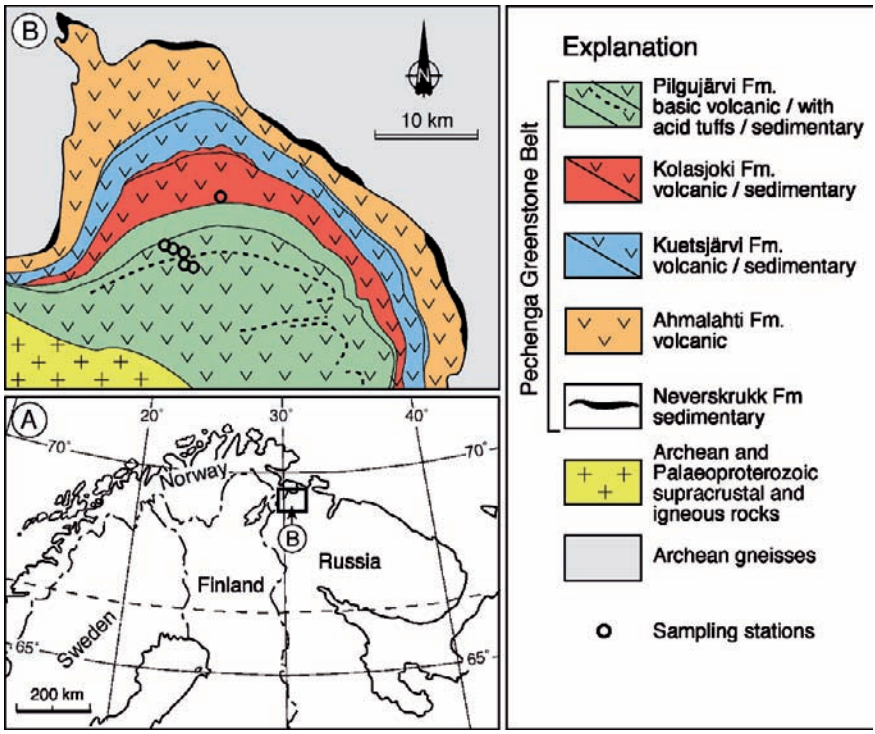

Fig. 22 (**A**) regional location map of the Pechenga greenstone belt of the Kola Peninsula, Russia; (**B**) simplified geological map showing sampling sites for bioalteration studies in volcanic horizons of the Pilgujärvi and Kolasjoki Formations. Map is modified from Melezhik and Sturt (1994)

tholeiitic basalts occurring as massive and pillowed lavas and hyaloclastites. An acid tuffaceous unit with a thickness of a few tens of meters occurs in the middle part of the formation (Fig. 22). U-Pb, Sm-Nd and Rb-Sr systems have yielded ages of ca. 1980 Ma for ferropicritic and tholeiitic metavolcanites and genetically related intrusive rocks from the Pilgujärvi Volcanic Formation (Hanski et al. 1990; Balashov 1996; Smolkin et al. 2003). A similar U-Pb zircon age (1970 ± 5 Ma; Hanski et al. 1990) has also been obtained for a thin felsic unit.

4 Bioalteration Textures in Pillow Lava and Hyaloclastite

Textures that we ascribe to microbial dissolution of originally glassy pillow lava rims and hyaloclastites have been found in sequences ranging in age from recent to 3.5 Ga. In this section, we document some of the most characteristic bio-generated textures from *in-situ* oceanic crust, ophiolites and greenstone belts.

4.1 Modern Oceanic Crust

Granular bioalteration (Fig. 23) does not generally display symmetrical arrangement on the opposite sides of fractures along which it develops with a variable thickness and distribution. Thus, we can distinguish the bands and aggregates of granular alteration from the more symmetric alteration produced by abiotic palagonitization (e.g., Fig. 1 lines A and B). Locally, banded abiotic palagonite can be found in the centre of a fracture with granular or tubular textures occupying the outermost interface with the fresh glass (e.g., Fig. 23D). Less commonly, granular and tubular textures can be seen on the opposite sides of the same fracture (e.g., Fig. 23F). The diameter of the granules, regardless of age, location, as well as depth into the crust, varies from 0.1 μm to 1.4 μm, with the most common size around 0.4 μm (Furnes et al. 2007a).

The tubular bioalteration textures are most typically unbranched, straight and/or curved (Fig. 23A,B,C,F and Fig. 24) although rare, branched examples also occur (e.g., Fig. 23H,I). With progressive bioalteration they develop from small, isolated individuals into dense bundles of long, numerous tubes originating from fractures in the glass (Fig. 23C). Individual tubes may show segmentation and localized swellings (e.g., Fig. 24E,F). In some cases the tubes propagate perpendicular to the alteration front (e.g., Fig. 23F), although random orientations are also common (Fig. 24C). Rare tube alignment, independent from the orientation of the fracture in which the tubes are rooted is attributed to tube-propagation controlled by strain-orientation in the glass (Furnes et al. 2001b). In samples that contain vesicles and or varioles the tubes can be seen to have grown radially outwards into the fresh glass (e.g., Fig. 23B). Tubular structures have also been observed to exploit concentric stress fractures that have developed around phenocrysts (e.g., Furnes et al. 2007a). The tubular bioalteration textures are substantially larger than the granular textures, and there is only a minor overlap in their size distributions (Furnes et al. 2007a).

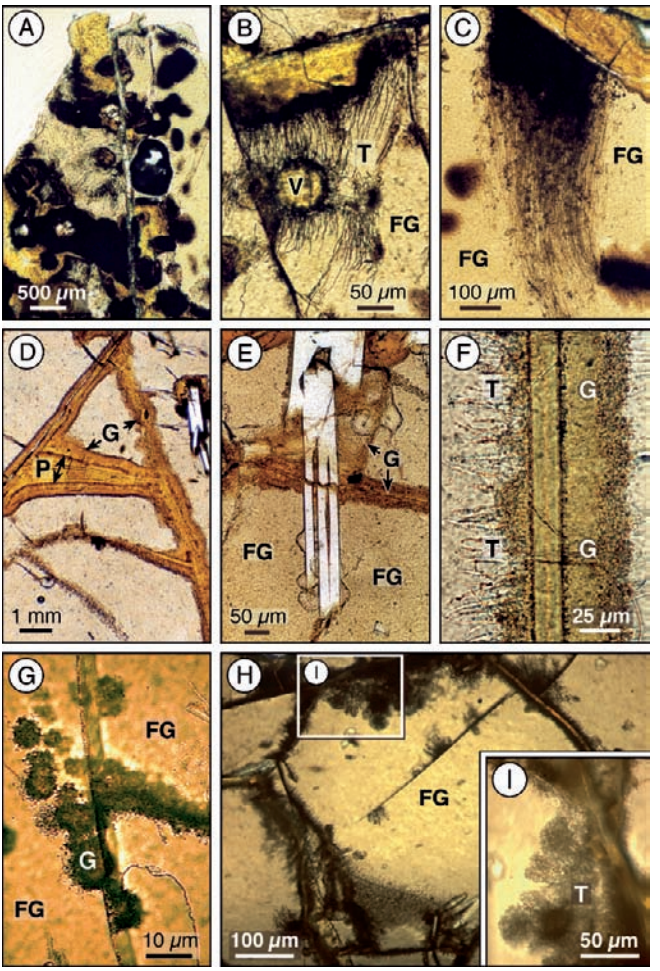

Fig. 23 Transmitted light photomicrographs of microbial alteration textures in volcanic glass from in situ oceanic crust. (**A**) Portion of pillow basalt thin section showing pale-cream glass, *yellow* palagonite alteration, tubular alteration textures enlarged in (**B**) and *dark brown* circular, varioles or quench textures. (B) Enlarged view showing tubular alteration (T) in fresh volcanic glass (FG) radiating from fractures and around a vesicle (V). (**C**) A dense cluster of tubes growing from a palagonite filled fracture in the top of the image. (**D**) Banded palagonite alteration (P) at the centre of fractures in volcanic glass with granular alteration (G) on the outer margins. (**E**) Granular alteration along a fracture in volcanic glass which is interrupted by a large plagioclase phenocryst. (**F**) Fracture in volcanic glass with tubular alteration on the left hand side and granular alteration on the right hand side of the same fracture. (**G**) Granular alteration along intersecting fractures in volcanic glass accompanied by circular clusters of granular alteration in the nearby glass. (**H**) Branched tubes radiating from a network of fractures in a volcanic glass. (**I**) enlarged view showing the dendritic branching. Samples: (**A** and **B**) Hole 396B thin Section 43; (**C**) Hole 418A thin Section 2; (**D**) Hole 418A thin Section 12; (**E**) Hole 418A thin Section 12; (**F**) Hole 896A thin Section 23; (**G**) Hole 396B thin Section 28; (**H** and **I**) Hole 396B thin Section 38; (**I**)

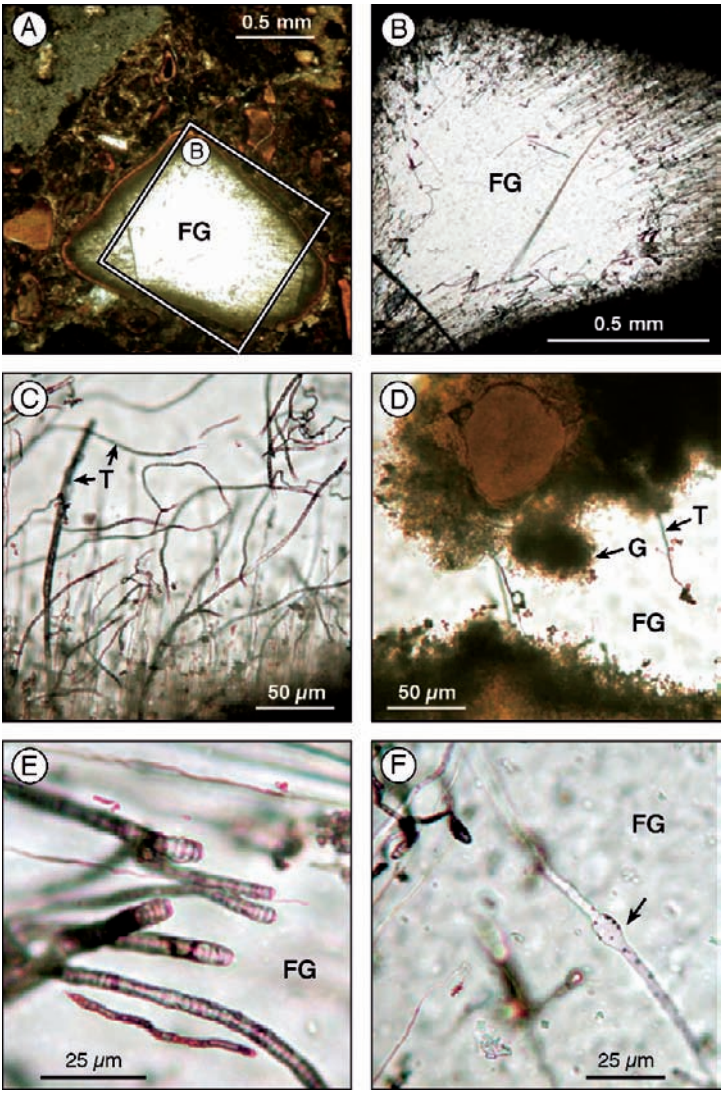

Fig. 24 Transmitted light photomicrographs of microbial alteration textures in volcanic glass fragments in a vitric tuff from the Ontong Java Plateau: (**A**) A glass grain with tubular bioalteration textures radiating inwards from the margin, rimmed by red-brown clay and in a volcaniclastic matrix comprising altered glass and lithic fragments cemented by clay and zeolites. (**B**) Enlarged view showing the tubular alteration textures radiating inwards. (**C**) Assemblage of unbranched tubular (T) structures extending from a granular alteration boundary. (**D**) Granular (G) and tubular alteration textures extending from the clay alteration boundary into fresh glass. (**E**) Tubular structures with dark walls and segmented appearance. (**F**) Hollow tubular structure with swelling (arrowed)

Their diameters range from ~0.5 μm to 6 μm with an average diameter of 1.4 μm (Furnes et al. 2007a). The lengths of the tubes are highly variable, from a few microns up to several hundred microns (Furnes et al. 2007a).

4.2 Ophiolites

Bioalteration textures in pillow lavas and or hyaloclasties from the Troodos, Mirdita and Solund-Stavfjord ophiolite complexes are shown in Fig. 25. In the Troodos ophiolite abundant fresh glass is still present and both granular and tubular textures (Fig. 25A–C) are found at all stratigraphic levels within the lava sequence. These textures occur at the boundary between fresh and altered glass (Fig. 25B). The most common type is the isolated and/or persistent zones consisting of coalesced spherical bodies about 1–3 μm in diameter. Although the alteration is most commonly asymmetrically arranged around cracks, it can also, sometimes be symmetric. In close association with the patches of coalesced spherical bodies are abundant, unbranched mainly straight but also curved tubes that may attain lengths of up to 100 μm (Fig. 25A–C). Spectacular examples of spiral shaped tubes are found, both single helical tubes and forms with a simple central tubular shaft around which is coiled an outer spiralled tube, analogous to a "pogo stick"(Fig. 25C). Another tubular form may reach lengths of up to 500 μm, diameters up to 20 μm and show well-defined segmentation with 5–10 μm spacing and sometimes a terminal swelling. These are generally seen to be closely associated with vesicles, with one end terminating at a vesicle wall (Fig. 25A). These bioalteration textures may be hollow, especially many of the tubular examples or filled with very fine-grained phyllosilicate phase.

The Mirdita ophiolite contains both granular and tubular bioalteration textures preserved in volcanic glass and also zeolites (Fig. 25D–F). Granular alteration textures occur as asymmetric bands along palagonite filled fractures (Fig. 25D) and as cluster in the adjacent glass (Fig. 25F). Simple unbranched tubes, locally with complex twisted shapes are also found (Fig. 25E) both in the fresh glass and in zeolites. These structures are mineralized by titanite.

The Solund-Stavfjord ophiolite contains lower greenschist grade meta-volcanic glass now composed predominantly of chlorite (Fig. 25G,H). This contains band of titanite with tubular projections that are interpreted as mineralized zones of tubular bioalteration.

4.3 Greenstone Belts

In the originally glassy, chilled rim of pillow lavas and associated interpillow hyaloclatites from Barberton, Pilbara, Pechenga and Wutai greenstone belts (Fig. 17) we have found titanite filled tubes, interpreted as mineralized microbial alteration textures (Fig. 26A–D) restricted to localized horizons in the thick volcanic sequences

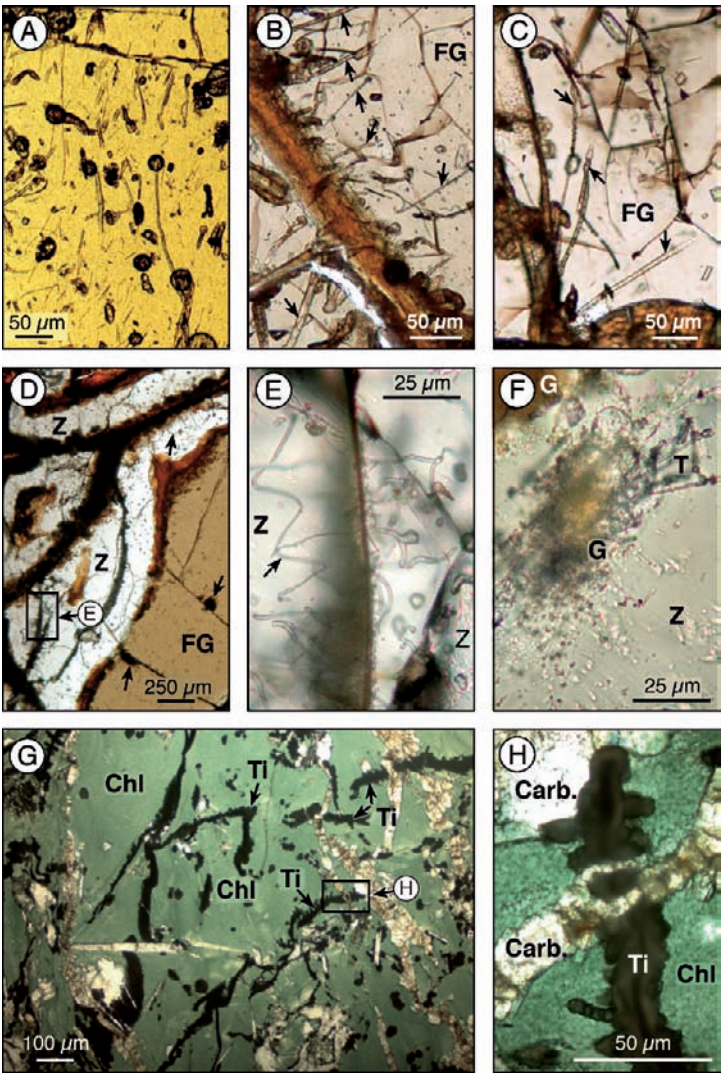

Fig. 25 Transmitted light photomicrographs of microbial alteration textures in (meta) volcanic glass from selected ophiolites. (**A**) Image of volcanic glass from the Troodos ophiolite contains hollow tubular alteration textures aligned largely north-south in this image and large, dark circular vesicles. (**B**) Palagonite filled fractures around the rims of a volcanic glass fragments containing tubular alteration textures arrowed, also from the Troodos ophiolite. (**C**) Alteration textures in volcanic glass from the Troodos ophiolite show a central tube with an outer spiral (arrowed). (**D**) Volcanic glass (FG) from the Mirdita ophiolite with zeolite (Z) and brown palagonite filled fractures. (**E**) Enlarged view showing tubular bioalteration textures preserved in zeolites. (**F**) Cluster of granular (**G**) alteration textures and a few tubes (T) also from the Mirdita ophiolite. (G) Image of meta-volcanic glass from the Solund-Stavfjord ophiolite, matrix is now largely composed of chlorite and contains bands of titanite with tubular projections. (**H**) Enlarged and rotated view of a titanite band with tubular projections on the margins

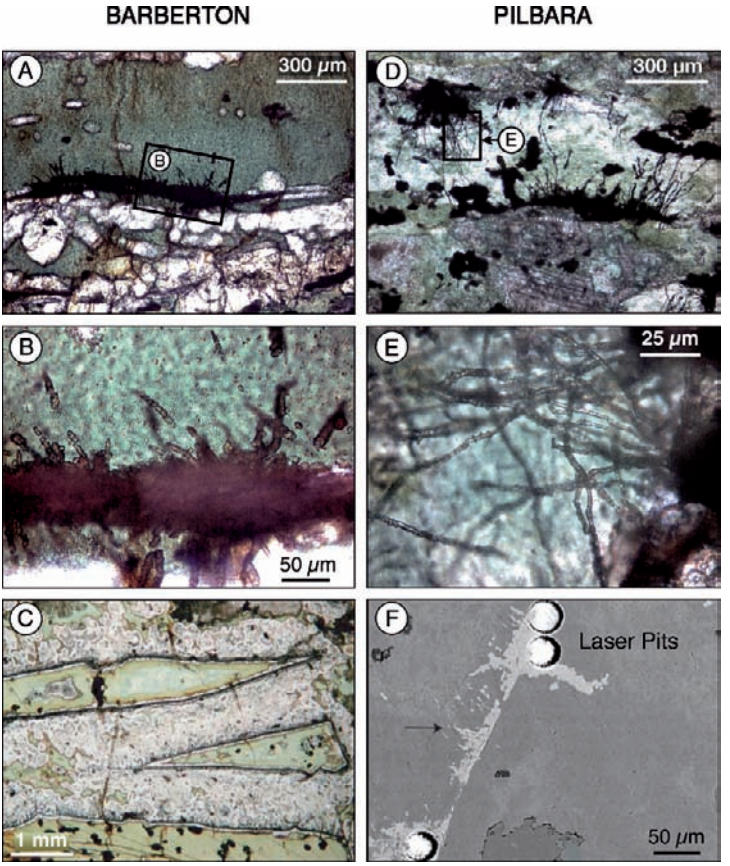

Fig. 26 Tubular bioaltextures in interpillow hyaloclastites from the Hooggenoeg Formation of the Barberton greenstone belt, South Africa (*left* hand column) and interpillow hyaloclastites from the Euro Basalt of the Pilbara Supergroup, Western Australia (*right* hand column). (**A**) The black zone across the middle part of the picture is composed of titanite which infills the tubes and these are rooted upon a healed boundary between the originally glassy fragments. The fine grained green mineral is chlorite, and the white, stubby mineral grains below the titanite zone are epidote crystals. The boxed area is enlarged in (**B**) which shows the segmented nature of the tubules and the overgrowth of metamorphic chlorite. (**C**) Image of a meta-volcanic interpillow hyaloclastite in which the original glass shards are completely replaced by chlorite, quartz, and epidote and the interstitial spaces are filled with quartz and calcite. There is very little evidence of deformation and the original "jigsaw-fit" breccia textures are still preserved. The dark, spherical spots within the fragments (particularly the lower fragment) are variolitic textures (originally pyroxene needles crystallized around a plagioclase nucleii). (**D**) From the Pilbara shows black zones of titanite along the healed boundary between originally glassy fragments and on which the tubular structures are rooted. The fine grained green mineral is chlorite, and the white to light brownish mineral is calcite. The boxed area is enlarged in (**E**) which shows the segmented nature of the intertwined tubules. (**F**) Is a back scatter electron image showing the size and location of laser pits in the "root zone" of titanite tubes used for U/Pb radiometric dating. The titanite is light grey and the chlorite and quartz form the darker areas

(Furnes et al. 2004; Banerjee et al. 2006, 2007; Staudigel et al. 2006). The tubular textures (Fig. 26A,B,D–F) are by far the most common, and are observed to extend away from healed fractures and/or grain boundaries along which seawater may once have flowed. Some of these tubular structures exhibit segmentation into sub-spherical bodies (Fig. 26B,E). Putative granular textures (from the Barberton greenstone belt) have also been observed (Banerjee et al. 2006, Fig. 6), may have originated along fractures in the originally glassy fragments, or grain margins of shards in interpillow hyaloclastites (Fig. 26C). The widths of the tubular structures vary between 1–9 μm, and their lengths up to 200 μm (Furnes et al. 2007a). The tubes are filled predominantly with titanite (Fig. 27), but quartz and chlorite is also commonly observed.

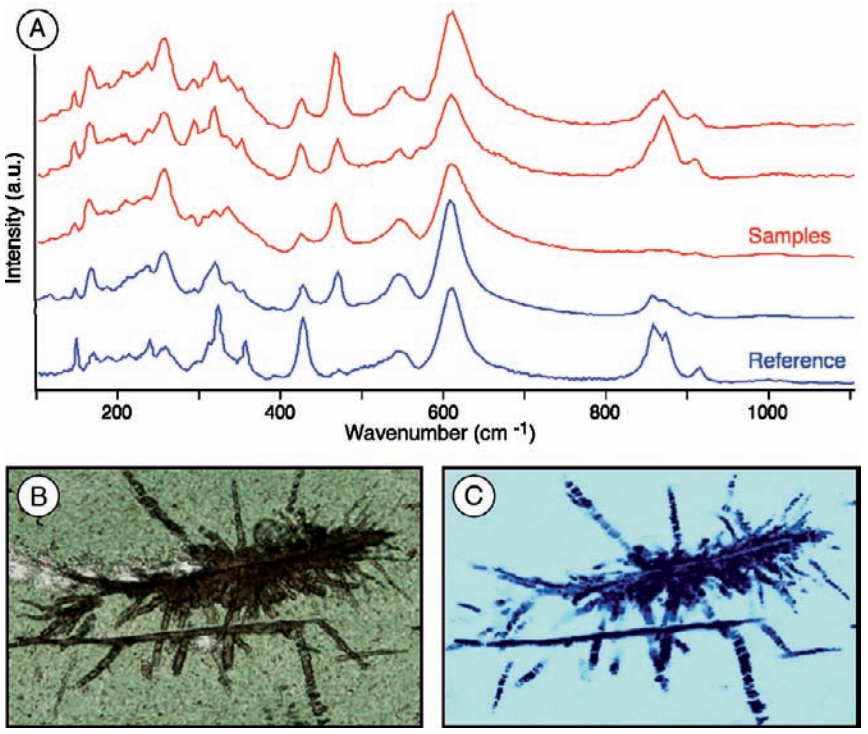

Fig. 27 (**A**) Raman spectra plotted as wavenumber (cm^{-1}) against intensity (in arbitrary units) of a mineral phase shown in red that infills bioalteration textures in meta-volcanic glass and is comparable to the reference spectra obtained from the mineral titanite ($CaTiSiO_4$ shown in *blue*); (**B**) petrographic image of these bioalteration textures in meta-volcanic glass now composed of chlorite from the ~3.4 Ga Barberton greenstone belt of South Africa (cf. Fig. 25); (**C**) a Raman intensity map of the same area showing the titanite infilled cluster of radiating tubes which are septate due to thin divisions created by chlorite overgrowths from the meta-volcanic matrix. (This Raman map was collected by L. Nasdala using a laser excitation of 632.8 nm (8 mW) and 1.5 μm steps, across an area 310 by 190 steps.)

4.4 What Controls the Development of Bioalteration Textures?

Above we have demonstrated that bioalteration textures are found in basaltic glass from *in-situ* oceanic crust, ophiolites and greenstone belts (Figs. 23–26), ranging in age from ~0 Ma to 3500 Ma. To date we do not know what controls the variation in size and morphology of the microbial alteration textures. It is conceivable that comparable microbial consortia in volcanic glass may produce differently shaped bioalteration textures under varying environmental conditions. For illustration, consider microbial colonies grown on agar plates the morphologies of which are controlled by the physics of nutrient diffusion, such that dendritically-branched colonies form when nutrient concentrations are low, as opposed to compact, concentrically zoned colonies when nutrient concentrations are high (e.g., Matsushita et al. 2004). Analogously, microorganisms in volcanic glass may be capable of producing tubular or granular bioalteration morphologies under varying nutrient or substrate conditions. We highlight, therefore, the absence of a one-to-one relationship between the morphologies of bioalteration textures and the dominant microorganism in the constructing microbial consortia.

5 Geochemical Signatures

Supporting evidence for a microbial origin of the textures described herein is provided by X-ray mapping of several elements, particularly carbon. A large number of glassy or originally glassy samples of pillow margins and hyaloclastites from *in-situ* oceanic crust, ophiolites and greenstone belts have been studied. In many cases where SEM imaging found bio-alteration textures, these were associated with elevated concentrations of carbon and possibly also nitrogen and sometimes phosphorus. These X-ray maps were collected using an electron microprobe on iridium-coated thin sections that were prepared using Al-grinding powders to prevent carbon contamination during thin section grinding and polishing. Carbon was routinely measured on two spectrometers and full details of the analytical methods developed are given in Banerjee et al. (2006).

The observed enrichments in carbon are generally highly restricted to the margins of the microbial alteration textures and diminish sharply away from these areas. Elevated levels of carbon have been found in samples of varying age and metamorphic grade and the intensity of the carbon signal gives a qualitative indication of the amount of carbon present. N/C ratios of marine bacteria have been reported to range from 0.07 to 0.35 (Fagerbakke et al. 1996) and these are comparable to samples containing bioalteration textures from Site 896A at the Costa Rica Rift most of which showed N/C values between 0.08 and 0.25 (Torsvik et al. 1998). Due to the mobility of carbon and nitrogen however, both at surface and subsurface conditions, it is quite probable that carbon and particularly nitrogen are lost in differing proportions from microbial alteration textures during burial and later metamorphism. For this reason, no further attempt to quantitatively determine N/C ratios has been undertaken.

Our interpretation is that both carbon and nitrogen are concentrated from seawater by microbial activity within the oceanic crust. We hypothesize that as microbes etch volcanic glass, multiply and die their organic remains are left within the alteration textures produced. These are then incorporated along the margins of the textures during mineralization by clays and iron-oxyhydroxides in the recent oceanic crust and or by titanite in greenstone belts samples. At the nanometer scale the distribution of carbon bearing phases is more complex as revealed by a recent study that used focussed ion beam milling to obtain a wafer from across a tubular bioalteration structure (Benzerara et al. 2007). STXM (scanning transmission X-ray microscopy) and EELS (energy electron loss spectroscopy) found that some of the C is contained in a carbonate phase and some in an organic carbon phase that possibly contains a carbonyl group, with further high resolution sampling required to fully characterize the nm distribution. Concerning phosphorus, which is also sometimes concentrated at the margins of bioalteration structures it is uncertain if microorganisms are able to extract P from the glass. Phosphorus is present in volcanic glass and deep seawater in only very low concentrations and it seems likely that the elevated concentrations associated with microbial alteration textures are due to sequestration by living cells (Torsvik et al. 1998).

Element maps of calcium, magnesium, iron, aluminium, sodium, potassium, silicon, sulphur, chlorine, and titanium were also routinely measured and can be highly informative depending on the phases which mineralize the bioalteration textures (clays, iron oxy-hydroxides, quartz) and the host rock (silicate glass or a metamorphic assemblage that may include chlorite, quartz and carbonate). It is noteworthy that maps of Ca, Mg and Fe do not show enrichments that correlate with carbon highs and this eliminates inorganic carbonates as the source of the carbon linings on the bioalteration textures. Likewise, maps of Cl were used to exclude epoxy as the source of carbon. Maps showing a common enrichment of sodium, potassium and magnesium along fracture planes from which bioalteration radiates, can also be a useful tracer of fluid circulation.

5.1 Modern Oceanic Crust

Figure 28 shows a SEM image and a series of element maps of a region of granular alteration on both sides of a fracture in volcanic glassy material from the central Atlantic Ocean. The zones of granular alteration show slight enrichment in carbon, nitrogen and phosphorus. Carbon also shows bright spots in the outermost parts of the granular textures. Calcium and magnesium are, on the other hand, strongly depleted within the alteration zone. It is important to note that the carbon enrichments do not correlate with any enrichment in Ca, eliminating calcium carbonate as a carbon bearing phase, and hence the carbon is regarded as organic. This feature has repeatedly been shown in a number of papers (e.g., Furnes et al. 2001b; Furnes and Muehlenbachs 2003; Staudigel and Furnes 2004; Staudigel et al. 2004). In particular the enrichments in carbon, nitrogen and phosphorus are very supportive of a

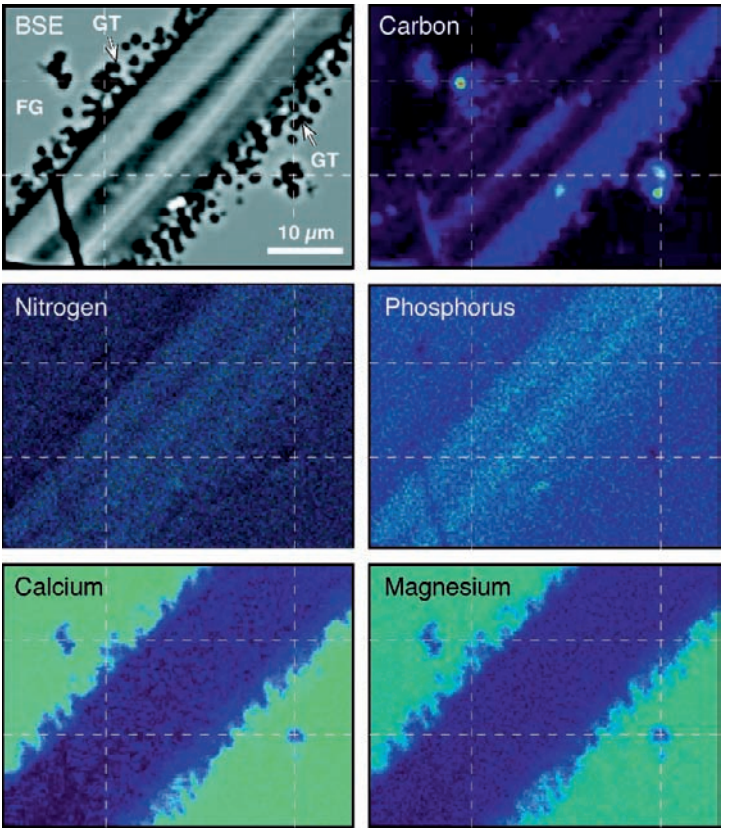

Fig. 28 Back scatter electron image of granular bioalteration on either side of a fracture in volcanic glass from *in-situ* oceanic crust with accompanying X-ray maps showing the distribution of carbon, nitrogen, phosphorus, calcium, and magnesium. Relative concentration scale (from lowest to highest): *black-blue-green-yellow-red*. Sample from Hole 46-396B-5R-2, 36-46 cm from the Atlantic Ocean. FG = fresh glass; GT = granular texture. Vertical and horizontal lines have been drawn on the X-ray maps to aid comparison

microbial involvement in the granular alteration but it does not prove that these cavities are actually made by these microbes. A large number of altered glass rims from the in-situ oceanic crust have been X-ray mapped, and in nearly all, particularly in samples from the younger part of the crust, elevated concentrations of carbon occur.

5.2 Ophiolites

Among the X-ray mapped samples from ophiolites, those from the Troodos ophiolite have provided some of the best results. Figure 29 shows a SEM image along with carbon, nitrogen, phosphorus, calcium and magnesium maps of altered glass

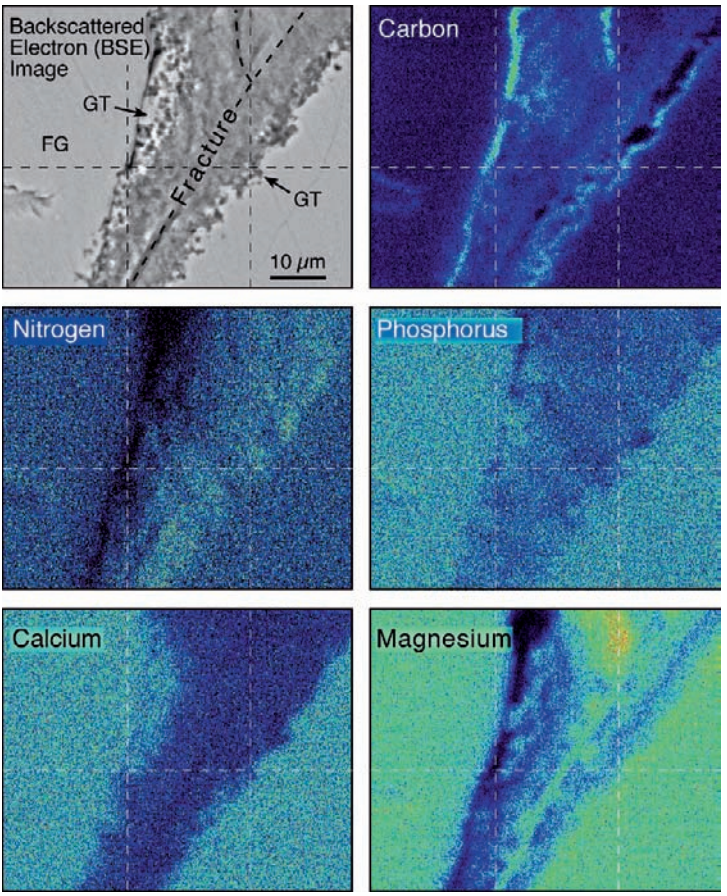

Fig. 29 Back scatter electron image of granular bioalteration fronts along a NE-SW trending fracture (Y shaped, bifurcates in the *top right* of the image) in volcanic glass from the ~90 Ma Troodos ophiolite with accompanying X-ray maps of C, N, P, Ca and Mg distribution. C and N are both enriched along the margins (N only along the right margin; an instrumental artifact due to the position of the spectrometer) of the granular alteration band, although they do not exactly correlate, whereas P shows no enrichment in this example relative to the glass. Calcium is depleted in the granular bioalteration band confirming the absence of carbonate. Magnesium is also in general depleted along the fresh glass/alteration interface, but is concentrated at the centre of the fracture, showing the presence of different authigneic materials within the alteration zone. Relative concentration scale (from lowest to highest): *black-blue-green-yellow-red*. Sample CYP-99-14A is from the Akaki valley. FG = fresh glass; GT = granular texture. Vertical and horizontal lines have been drawn on the X-ray maps to aid comparison

developed adjacent to a fracture. Enrichment in carbon, and to some extent, nitrogen can be seen clearly in these images. Phosphorus, however, is depleted, and this is opposite to what we observe in much younger sample from the *in-situ* oceanic crust (Fig. 28). Calcium and magnesium are also depleted, thereby excluding carbonate as the source of the carbon.

5.3 Greenstone Belts

Along the margins of the tubular structures in hyaloclastites from both the Barberton and Pilbara Archean greenstones, X-ray mapping reveals in some cases elevated concentrations of carbon and, to a lesser extent, nitrogen and phosphorus (Fig. 30).

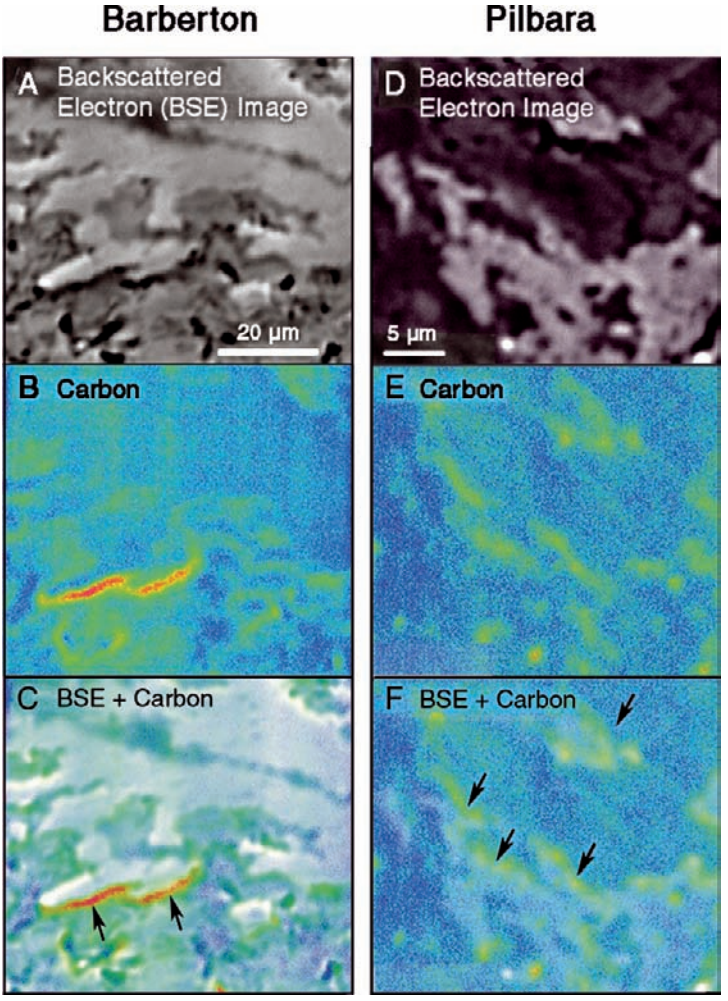

Fig. 30 Back scatter electron (BSE) image of titanite infilled tubular bioalteration textures from the ~3.5 Ga volcanics of the Barberton greenstone belt (*left* hand column) and ~3.4 Ga pillow lavas from the Pilbara Supergroup (*right* hand column) accompanying X-ray maps show the enrichments in carbon (measured using two detectors at different orientations) along the margins of the tubes; highlighted by arrows on the combined BSE and carbon maps in the lower part of the figure. Relative concentration scale (from lowest to highest): *black-blue-green-yellow-red*. Sample 29-BG-03 from the Barberton and 74-PG-04 from the Pilbara. Additional X-ray maps of further elements along with optical images of the studied areas are given in Furnes et al. (2004) and Banerjee et al. (2006) for the Barberton examples and Banerjee et al. (2007) for the Pilbara example

These enrichments are highly restricted to the immediate area of the titanite tubes while quickly diminish away from these areas. Calcium, iron, and magnesium maps (not shown here), from the same region, show opposite trends compared to carbon, again confirming that carbon is not bound in carbonate (see GSA Data Repository Fig. DR1, Banerjee et al. 2007).

6 Carbon Isotope Signatures

A large number of samples of glassy and crystalline samples of pillow lavas from *in-situ* oceanic crust and core-rim pairs from ophiolites and greenstone belts have been analysed for $\delta^{13}C$ measured on disseminated carbonate and the results have been compiled in Fig. 31. We refer the reader back to Section 2.2.4 and Fig. 2 for an explanation of how this data is interpreted. This data is obtained by measurements of the CO_2 liberated by phosphoric acid dissolution of whole rock powders dissolved in 100% phosphoric acid details of the analytical method used are given in Furnes et al. (2001a) and all results are quoted relative to the PDB standard.

The compiled $\delta^{13}C$ (‰) versus wt.% carbonate results from in-situ oceanic crust and ophiolites/greenstone belts, are shown in Fig. 31A,B respectively. In both cases there is a marked shift in the $\delta^{13}C_{carb}$ values of the glassy pillow rim samples towards more negative values than for the crystalline pillow core samples. If we take the $\delta^{13}C_{carb}$ value of -7‰ as the lower limit for magmatic values, the percentages of crystalline (pillow core) and glassy (pillow rim) samples from the *in-situ* oceanic crust that exhibit $\delta^{13}C_{carb}$ values lower than -7‰, are $\sim$ 14% and 52%, respectively. We take this as support for microbial activity within the glassy pillow rim samples for which there is supporting textural evidence; whereas, the crystalline pillow core samples which lack bioalteration textures predominantly show $\delta^{13}C_{carb}$ values between mantle CO_2 (-7‰) and marine carbonate ($0 +/ - 1$‰) values.

The pillow lavas of the ophiolites and greenstone belts (Fig. 31B) show values broadly comparable with those seen for *in-situ* oceanic crust; i.e. the percentages of crystalline and glassy samples that define $\delta^{13}C_{carb}$ values lower than -7‰, are $\sim$ 15% and 35%, respectively. Fig. 32 shows all our $\delta^{13}C_{carb}$ of pillow lavas from ophiolites and greenstones, plotted against weight percent carbonate and we have further sub-divided these data into Archean, Proterozoic and Phanerozoic samples (Fig. 36) in order to compare the similarities and differences between the three plots. In fact, for the pillow lavas from all these sequences we see that the originally glassy margins generally display lower $\delta^{13}C_{carb}$ values than the crystalline interiors. In some samples, however, the glassy margins display the highest $\delta^{13}C_{carb}$ values ($> +1$), a phenomenon particularly demonstrated by the Archean samples (Fig. 32A). In general, the $\delta^{13}C_{carb}$ values of pillow margins show a considerably wider range than the crystalline interiors that are generally bracketed between 0 and -7‰ (Fig. 32).

In order to explore the extent to which the characteristic $\delta^{13}C_{carb}$ values of rims and interior of pillow lavas retain their original values during progressive metamorphism, we have split the samples from ophiolites and greenstone belts

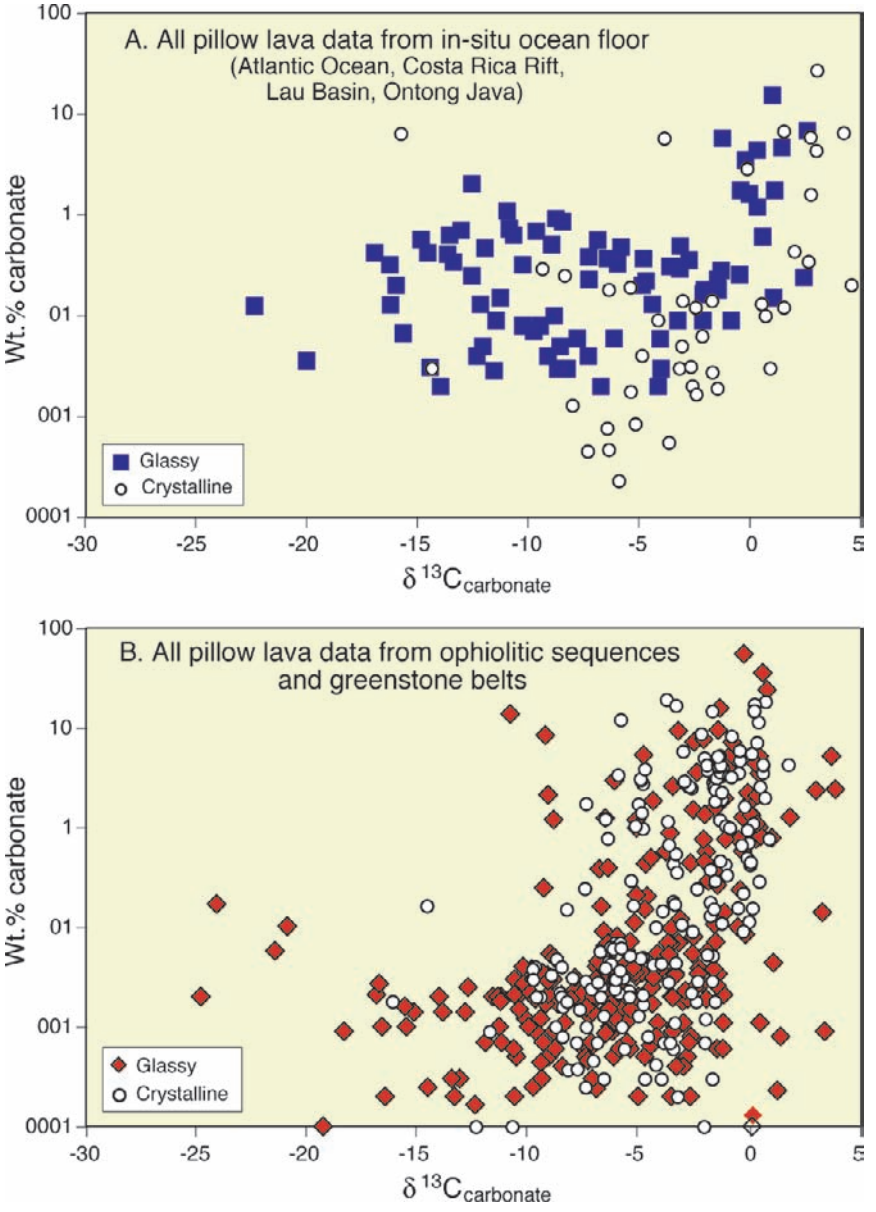

Fig. 31 Plots of $\delta^{13}C_{carbonate}$ versus weight percent carbonate from: (**A**) all measured pillow lavas from *in-situ* oceanic crust; (**B**) all measured ophiolites and greenstone belts. Data from glassy pillow rims are shown by filled symbols and these are more negatively fractionated relative to the samples from the crystalline pillow interiors shown by hollow symbols (cf. Fig. 2)

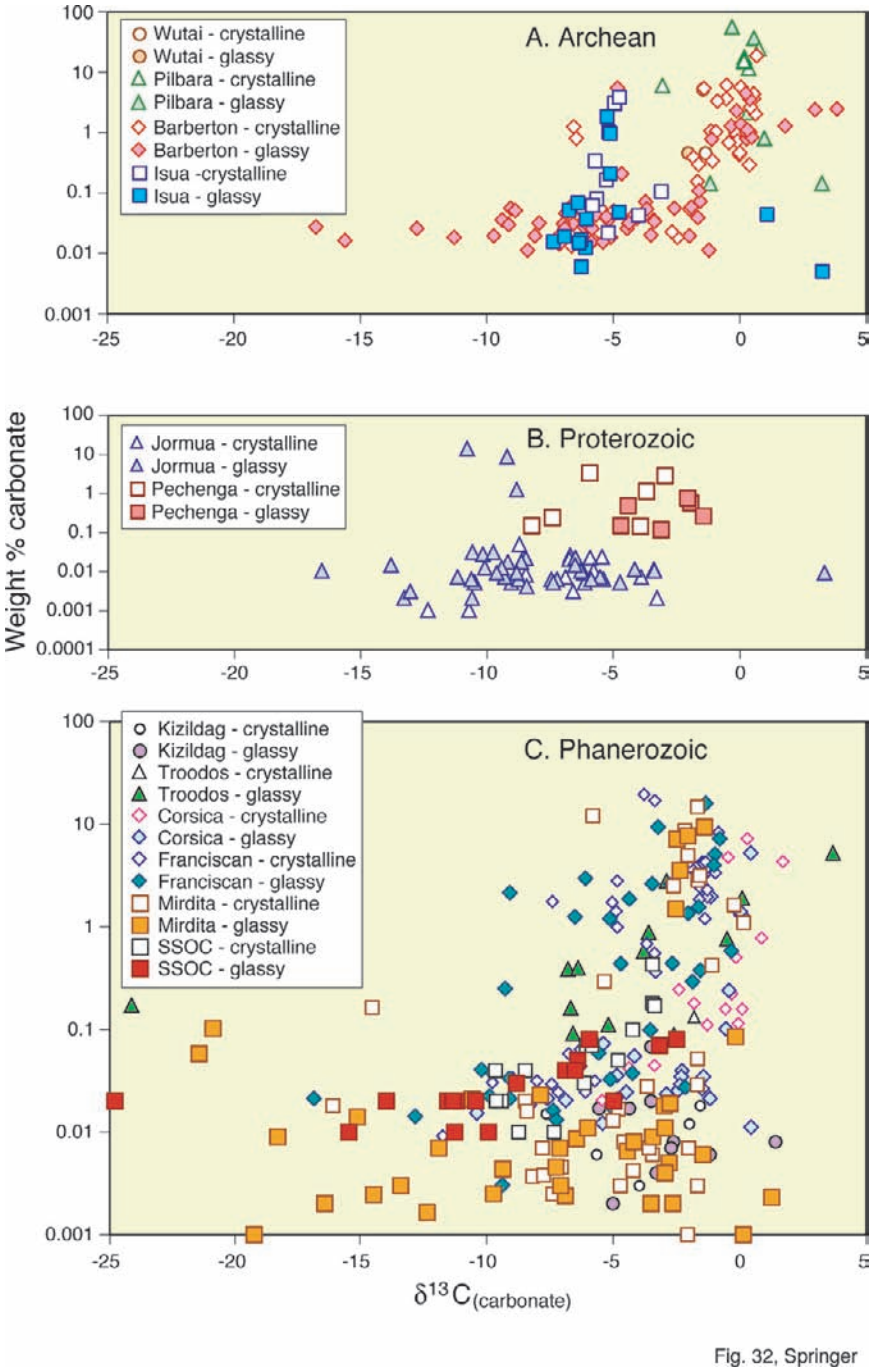

Fig. 32 Plots of $\delta^{13}C_{carbanoate}$ versus weight percent carbonate of crystalline interiors and glassy rims of pillows from Archean, Proterozoic and Phanerozoic ophiolites and greenstone belts

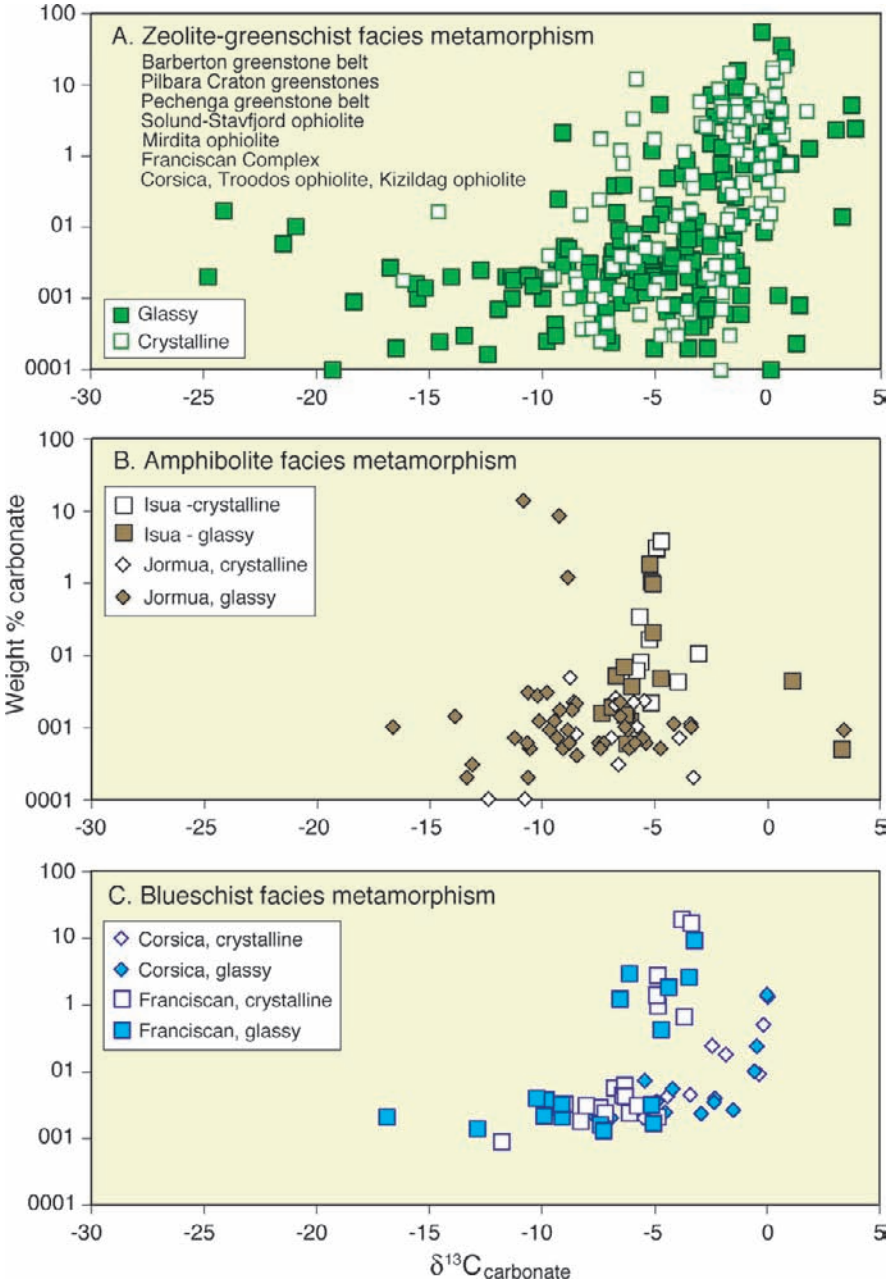

Fig. 33 Plots of $\delta^{13}C_{carbanoate}$ versus weight percent carbonate sub-divided by metamorphic grade: (**A**) zeolite to greenschist facies metamorphism; (**B**) amphibolite facies metamorphism; (**C**) blueschist facies metamorphism. Data from glassy pillow rims are shown by filled symbols and these are more negatively fractionated than the samples from the crystalline pillow interiors shown by hollow symbols (cf. Fig. 2)

according to their metamorphic grade, i.e. zeolite-greenschist-, amphibolite- and blueschist-facies metamorphism (Fig. 33). The majority of the samples have been collected from zeolite-greenschist metamorphic pillows, and the glassy samples show a considerably wider range in the $\delta^{13}C_{carb}$ values than their crystalline counterparts (Fig. 33A). This also applies to the samples that have suffered amphibolite facies metamorphism (Fig. 33B). Even some of the blueschist samples from the Franciscan glassy samples show very low $\delta^{13}C_{carb}$ values, whereas the majority of the crystalline samples are bracketed between 0 and $-7‰$ (Fig. 33C). It thus appears that the $\delta^{13}C_{carb}$ values from metamorphosed pillow margins largely retain their pre-metamorphic values, and that they are comparable with those from non-metamorphic *in-situ* oceanic crust, in spite of even high-grade metamorphism. We emphasize, however, that the glassy blueschist samples from Corsica do not show the low $\delta^{13}C_{carb}$ values. More data is needed to substantiate whether blueschist facies rocks, or even higher metamorphic grade rocks, can still preserve the original carbon isotope signatures. It is interesting in this context to mention that carbon isotope values ($\delta^{13}C$) of some diamonds from majoritic garnet-bearing host eclogites are attributed to an organic source material within subducting oceanic crust (Tappert et al. 2005). These findings support our suggestion that the Franciscan blueschist pillow rims exhibit isotopic values consistent with microbial alteration (Fig. 33C).

7 Significanc of Microbial Alteration as a Biomarker

The biogenic textures described above, the associated element distributions (in particular carbon enrichments) and $\delta^{13}C_{carb}$ values documented from meta-volcanic glass back to the Mesoarchean have far reaching implications for the nature and extent of microbial processes. In this section, we discuss some of these aspects in light of our present knowledge.

7.1 Mapping the Oceanic Biosphere

Granular and tubular bioalteration textures are easily observed by ordinary light microscopy upon samples of *in situ* oceanic crust where fresh glass is still present. This is because the dark, commonly mineral-filled structures appear in strong contrast to the light yellowish-brown, isotropic glass (Figs. 23, 24). This makes it possible to identify and quantitatively estimate the extent of bioalteration as a function of depth by reinvestigating DSDP and ODP cores. The only study of this kind to date is that of Furnes and Staudigel (1999), which documented the relative proportions of granular and tubular bioalteration types in basaltic glass as a function of depth (to $\sim$500 m) and temperature in the oceanic crust. In this study, the percentage bioalteration was estimated visually from geological thin sections. The data have been compiled from oceanic crustal sections collected at Sites 417 and 418 of the 110 Ma Western Atlantic, and at Sites 504B and 896A of the 5.9 Ma Costa Rica Rift. This compilation

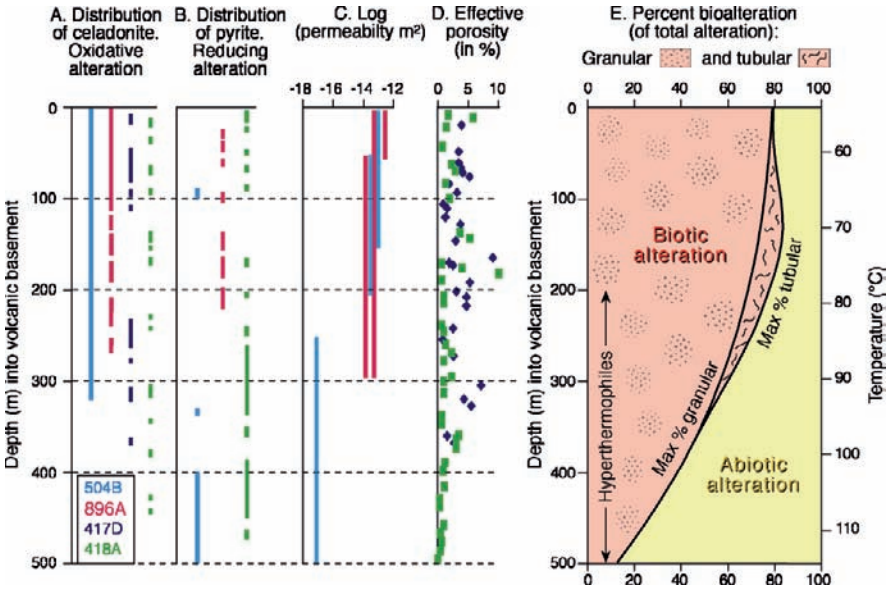

Fig. 34 Down-hole data to show the controls on the distribution of bioalteration textures with depth in the oceanic crust. The data are mainly from holes 396B, 407, 409, 410A, 417D, 418A in the Atlantic Ocean, holes 504B and 896A from the Costa Rica Rift in the Pacific Ocean, and hole 834B in the Lau Basin (for further information, see Fig. 5). (**A**) shows the occurrence of celadonite which is an indicator of oxidative alteration; (**B**) shows the occurrence of pyrite which is an indicator of reducing conditions; (**C**) shows permeability down-hole; (**D**) shows effective porosity determined by comparing air-dried and water-saturated sample weights; (**E**) shows estimates of the relative percentages of granular alteration textures (*pink* dots); tubular alteration (*pink* lines); and abiotic alteration (*yellow*) calculated from thin section observations and redrawn from Furnes et al. (2001b) and Staudigel et al. (2006)

illustrated in Fig. 34 shows that the granular type is by far the most abundant and can be found at all depths into the volcanic basement where the presence of fresh glass allows bioalteration to be traced down to ~550 m. At the surface, as well as below ~350 m into the volcanic basement, the tubular textures are absent or very rare. In the upper ~350 m of the crust the granular alteration type is dominant, being most abundant in the upper 200 m at temperatures below ~ 80°C, and decreasing steadily in abundance to become subordinate at temperatures of ~ 115°C near the currently known, upper temperature limits of hyperthermophilic life. The tubular alteration textures, meanwhile, constitute only a minor fraction, at most ~ 20% of the total alteration and show a clear maximum at ~120–130 m depth corresponding to temperatures of ~ 70°C. (These percentage bioalteration estimates are likely to be an underestimate however, because ambiguous textures were regarded as abiotic in these estimates and glass hydration processes may also have obscured some textures.)

The abundance of bioalteration with depth at Sites 504B and 417/418 increases with permeability and also the presence of mineral phases such as celadonite which

is indicative of relatively oxygenated waters (e.g., Furnes and Staudigel 1999; Furnes et al. 2001b). It is noteworthy that both the 5.9 Ma Costa Rica Rift and the 110 Ma Western Atlantic oceanic sections show similar maxima in the amount of bioalteration as a percentage of the total alteration, despite their very different ages (see Fig. 11 of Furnes et al. 2001b). This suggests that a substantial portion of the bioalteration happens very early and that the net bioalteration pattern is established within ~6 Ma. (It should be appreciated that most drill holes in the oceanic crust have recoveries that can be as low as 20% or less). In broad terms this is consistent with the theoretical estimates of microbial biomass production over time from oxidative alteration and hydrolysis within the upper oceanic crust as it migrates away from an oceanic spreading center (cf., Bach and Edwards 2003). However, as long as fresh glass is present and seawater circulation persists, the bioalteration processes are likely to continue. There exists a wealth of drill core samples of pillow lavas from the *in situ* oceanic crust that are yet to be systematically investigated in this manner for evidence of bioalteration.

7.2 The Oceanic Crust as a Bioreactor

Microbial seafloor alteration has a profound effect on chemical exchange between the oceans and the oceanic crust across the full range of seafloor environments, including: high temperature mid-oceanic ridge hydrothermal systems, low temperature off-axis settings and oceanic hot spots (e.g., Staudigel et al. 1998; Staudigel and Furnes 2004). Microbial communities in the oceanic crust may be mobilized and expelled into the overlying water column during diking events that involve massive expulsion of low temperature hydrothermal effluents into the water column (e.g., Delaney et al. 1998). These bring the microbial biomass into the oceans where they may provide a food source for higher trophic levels. In the converse direction, the subduction of bioaltered oceanic crust deep into the Earth's mantle provides a relatively little-explored geochemical connection between the Earth's biosphere and mantle. The existence of this pathway is supported by the finding of very deep asthenospheric micro-diamonds that have low $\delta^{13}C$ signatures suggestive of a biogenic origin (e.g., Tappert et al. 2005). Taken together these processes comprise an oceanic crustal "bioreactor", changes in the extent and activity of which have profound implications for the evolution of seawater chemistry, and for the composition of the oceanic crust and mantle through geological time. At present relatively little is known about the connections between bioaltered oceanic crust and the mantle; we therefore, here focus instead on the better understood interactions between the oceanic crustal bioreactor and seawater chemistry.

Experimental investigations (e.g., Staudigel et al. 1998) have revealed profound differences between biotic and abiotic seafloor alteration processes. Glass alteration experiments involving surface seawater microbial populations have shown that microbial activity enhances chemical exchange in water-rock reactions, especially for Sr, and results in higher rates of authigenic mineral production along with increased uptake of Ca relative to sterile controls (Staudigel et al. 1998, 2004). Abiotic

alteration, in contrast, results in pronounced uptake of Mg and effective removal of Si (Staudigel et al. 2004). Biotic experiments with a natural seawater microbial inoculum at temperatures up to 100°C have also shown significant mobility of K, Rb, Cs, Li, B, U, Th, Pb, and strongly temperature dependent U-Pb fractionation (Staudigel et al. 1998). Although further experiments are needed to explore the biotic and abiotic controls of these processes, to the first order these findings confirm that microbes have a pronounced effect on element fluxes and mobility during glass alteration in the oceanic crust. Moreover, these differences in chemical redistribution patterns between biotic and abiotic water-rock interactions confirm that they represent two different modes of seafloor alteration. This implies that the chemical fluxes and consequently the seawater composition in the pre-biotic world may have been radically different from the modern world in which seafloor bioalteration is prevalent. Fluid inclusion analyses of Archean rocks may help to track these changes in seawater chemistry (cf. Foriel et al. 2004)

The total biomass found within the modern oceanic crust and its productivity remain unconstrained. Bach and Edwards (2003) estimated that submarine basalts can provide enough energy to support a primary productivity of about 10^{12}g/a cellular C, which represents an upper limit for chemosynthetic carbon fixation in the oceanic crust, although it is unknown as to what extent the deep biosphere utilizes this energy source. In addition the influx of organic carbon entering the oceanic crust via hydrothermal recharge may provide a further energy source for heterotrophic microbes. A complimentary approach is to estimate the maximum numbers of cells required to produce the density of tubular and granular bioalteration textures observed in the oceanic crust. While this approximates the numbers of cells to within one or two orders of magnitude necessary to create the textures found in a given thin section, these data are difficult to extrapolate into a global inventory of the oceanic crustal biomass because their metabolic rates are unknown. It is also difficult to extrapolate the abundance of fresh glass to an oceanic crustal scale given that oceanic drilling rarely recovers more than 30% core. Thus, at present we can only speculate about the biomass and the primary productivity of the deep ocean crustal bioreactor. Nonetheless, the importance of this microbial community is indisputable when considering the geochemical fluxes between seawater, the ocean crust, and the Earth's mantle.

7.3 Tectonic Control of Bioalteration in Modern and Ancient Oceanic Crust

Bioalteration of glass has been found in many submarine volcanic settings that preserve fresh, or minimally altered, glass from fast- to slow-spreading centres, also oceanic plateaus, ophiolites and greenstone belts of all ages (Figs. 4 and 36). These examples provide markedly different seafloor spreading rates and environments which offer different boundary conditions for bioalteration processes, in particular with respect to the depth of water circulation, density of fracturing and the

lithology of the upper part of the oceanic crust (e.g., Dilek et al. 1998; Fig. 4). Where as intermediate- to fast-spreading ridges (i.e., $\sim$ 6–12 cm/yr) exhibit thick extrusive sections that lack major tectonic disruption (e.g., Sinton and Detrick 1992; Fouquet et al. 1996), slow-spreading ridges (i.e., $<$ 2.5 cm/yr) show deep-seated normal faulting and may expose upper mantle rocks at the seafloor enabling deep circulation of hydrothermal solutions into the lower crust and peridotites (Karson 1998). In such settings the deeper fluid circulation may carry microbes to greater depths where they may utilise H_2 and or CH_4 produced by the serpentinization of ultramafics (e.g., Berndt et al. 1996; Kelley 1996). For example, the production of H_2 and CH_4 as a result of serpentinization of ultramafic rocks is presently occurring in the Zambales ophiolite (Abrajano et al. 1990) and the Lost City ultramafic field (Kelley et al. 2005). These contrasting tectonic styles and alteration regimes found at slow- to fast-spreading centres are shown schematically in Fig. 35A,B, and it seems reasonable to hypothesise that the higher H_2 production found at slow-spreading ridges may favour methanogenic bacteria compared to fast-spreading ridges. These differences may be recorded in the carbon isotopes of disseminated carbonates found in pillow basalts at such different sites.

In order to explore the potential for such differences, Furnes et al. (2006) compared the $\delta^{13}C_{carb}$ variations measured upon bioaltered pillow margins from different oceanic basins. They found substantial overlap in data between basins but distinct ranges in $\delta^{13}C_{carb}$ (Fig. 35). The $\delta^{13}C$ of finely disseminated carbonates from bioaltered, glassy basaltic pillow rims from slow- and intermediate-spreading oceanic crust of the central Atlantic Ocean (CAO) ranges from $-17‰$ to $+3‰$ (PDB), whereas those from the faster-spreading Costa Rica Rift (CRR) define a much narrower range and cluster at lighter values between $-17‰$ and $-7‰$ (Fig. 35C; Furnes et al. 2006). A similar $\delta^{13}C_{carb}$ pattern has been observed in some ophiolites; for example, the Jurassic Mirdita ophiolite in Albania shows a structural architecture similar to that of the slow-spreading CAO crust and a similar range in $\delta^{13}C_{carb}$ values (Fig. 35D). In contrast, the Late Ordovician Solund-Stavfjord Ophiolite Complex (SSOC) in western Norway exhibits structural and geochemical evidence indicative of an intermediate-spreading rate environment and displays $\delta^{13}C_{carb}$ signatures similar to those of the modern CRR oceanic crust (Fig. 35D). While much remains to be done to document systematic differences in $\delta^{13}C_{carb}$ between different ocean basins, the hypothesis that methanogenic bacteria may be a more important component of the bioalteration community at slow-spreading centres appears to be supported by the current data. Ophiolites, in particular, offer much potential for further testing this hypothesis because they provide an opportunity to study ancient fluid transport and alteration regimes in three-dimensional field exposure.

7.4 Bioalteration and the History of Early Life

Microbes that colonize volcanic glass may be among the earliest life forms on Earth. Textural evidence of bioalteration in submarine, originally glassy pillow lava rims

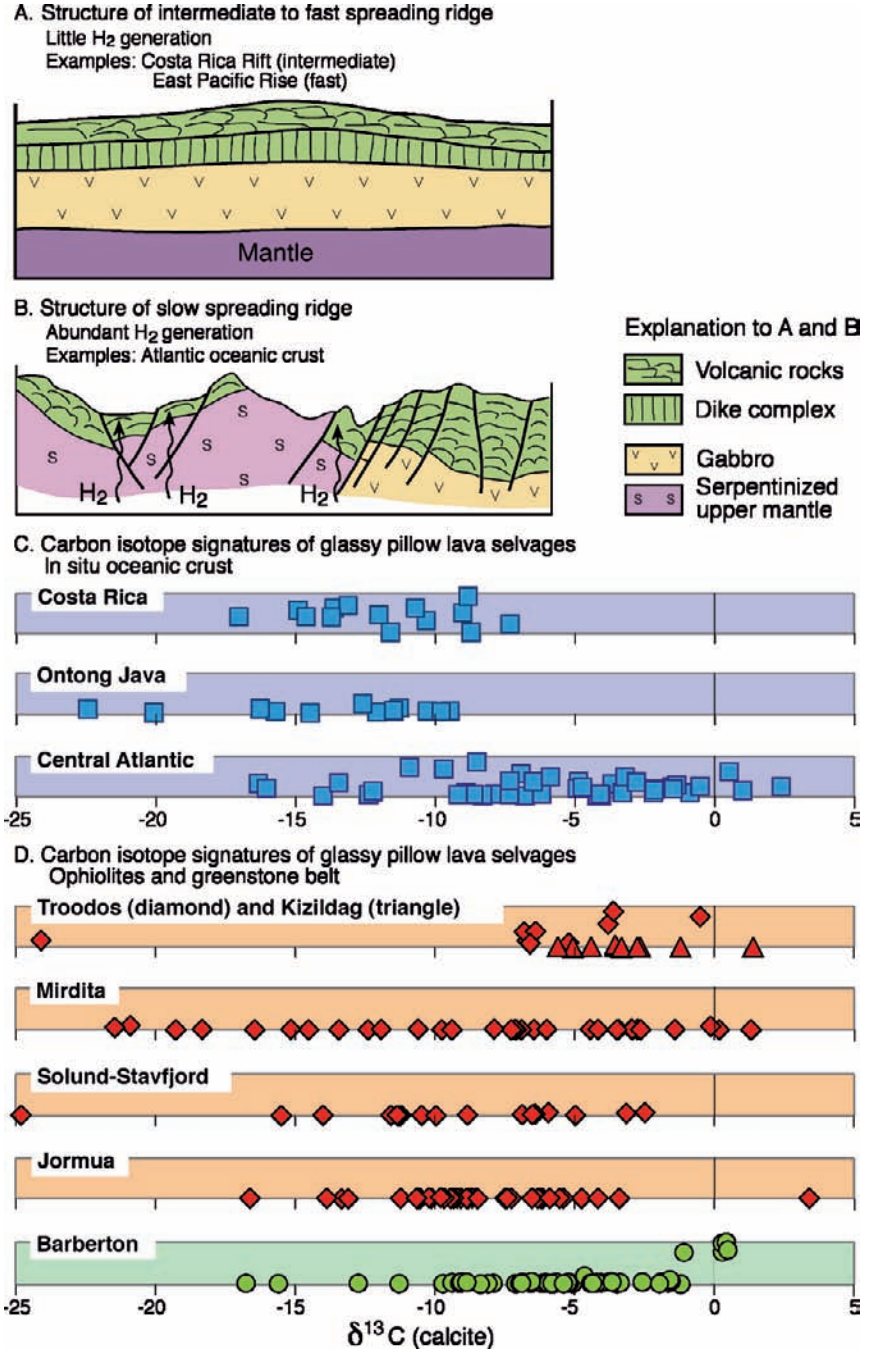
A. Structure of intermediate to fast spreading ridge
Little H_2 generation
Examples: Costa Rica Rift (intermediate)
East Pacific Rise (fast)
Mantle
B. Structure of slow spreading ridge
Abundant H_2 generation
Examples: Atlantic oceanic crust
H_2
H_2
H_2
Explanation to A and B
Volcanic rocks
Dike complex
Gabbro
Serpentinized upper mantle
C. Carbon isotope signatures of glassy pillow lava selvages
In situ oceanic crust
Costa Rica
Ontong Java
Central Atlantic
-25
-20
-15
-10
-5
0
D. Carbon isotope signatures of glassy pillow lava selvages
Ophiolites and greenstone belt
Troodos (diamond) and Kizildag (triangle)
Mirdita
Solund-Stavfjord
Jormua
Barberton
-25
-20
-15
-10
-5
0
$\delta^{13}C$ (calcite)

and hyaloclastites from the 3.3–3.5 Ga Barberton Greenstone Belt of South Africa (BGB) and the Pilbara Supergroup of western Australia (PWA) are reviewed above (Section 4.3, Fig. 26; see also Furnes et al. 2004; Banerjee et al. 2006, 2007). These titanite-filled bioalteration textures also have geochemical signatures (BGB and PWA, Fig. 30) and isotopic data (Fig. 31, BGB) that are suggestive of a biogenic origin. Furthermore, the syngenicity of these structures has been confirmed by direct U-Pb radiometric dating of the PWA examples in addition to the observation that the BGB bioalteration textures are cross-cut by early metamorphic mineral phases (Furnes et al. 2004). This radiometric dating was conducted using a new multicollector-ICP-MS technique for measuring $^{206}Pb/^{238}U$ ratios within titanite from the "root zones" at the centre of tubular clusters (Banerjee et al. 2007; and methodology in Simonetti et al. 2006). A minimum age of 2921 $\pm$ 110 Ma was obtained which is $\sim$ 400 Ma younger than the accepted $\sim$3350 Ma eruptive age of the Euro Basalt pillows, given by a U-Pb zircon age from an interbedded tuff (Nelson 2005). This titanite date corresponds to the age of regional metamorphism related to the last phase of deformation and widespread granite intrusion (the North Pilbara Orogeny) that affected our sample site in the western part of the East Pilbara Terrane at $\sim$2930 Ma (Van Kranendonk et al. 2002, 2007). Since chlorite formation, which occurred around $\sim$2930 Ma, or earlier ($\sim$3.24 Ga; Wijbrans and McDougall 1987), overprints the titanite tubules we therefore interpret this age to represent a minimum estimate for titanite formation. This implies a $<$ 400 Ma post eruptive period during which the bioalteration textures in the Euro Basalt were mineralized; however, it does not exclude the possibility that the textures formed soon after eruption and were mineralized somewhat later. Presently we do not know whether biological processes contribute to the formation of titanite, or in other words, whether it is a biomineral. We draw attention to the fact that titanium can be passively accumulated during microbial etching of glass (e.g. Banerjee and Muehlenbachs 2003), and that Ti-rich nodules have been found in association with microbial alteration of Pleistocene Hawaiian basaltic glass (Walton and Schiffman 2003).

Fig. 35 Schematic diagram summarizing the inferred relationship between tectonism and the development of $\delta^{13}C_{carbonate}$ signatures measured on volcanic glasses from slow and fast spreading ridges: (**A**) shows the typical "layer cake" structure of an intermediate to fast spreading ridge; (**B**) shows the generalized structure of a slow spreading ridge with exposure of serpentinized upper mantle rocks and widespread H_2 generation. In the lower part of the figure, $\delta^{13}C_{carbonate}$ versus weight percent carbonate (range 0–1% on the vertical axis) is plotted for: (**C**) volcanic glasses from in-situ oceanic crust and (**D**) ophiolites and greenstone belts. This reveals that samples from intermediate to fast spreading ridges (e.g. Costa Rica and SSOC) have a narrower range of $\delta^{13}C_{carbonate}$ values typically between $-17‰$ to $-7‰$ which is consistent with the bacterial oxidation of organic matter. Whereas samples from slow spreading ridges (e.g. the Central Atlantic and Mirdita Ophiolite) have a wider range of $\delta^{13}C_{carbonate}$ values which include positive values up to $+4‰$ that are suggestive of the lithotrophic utilization of CO_2 by methanogenic bacteria that may utilize the H_2 generated at slow spreading centers (see also Furnes et al. 2006)

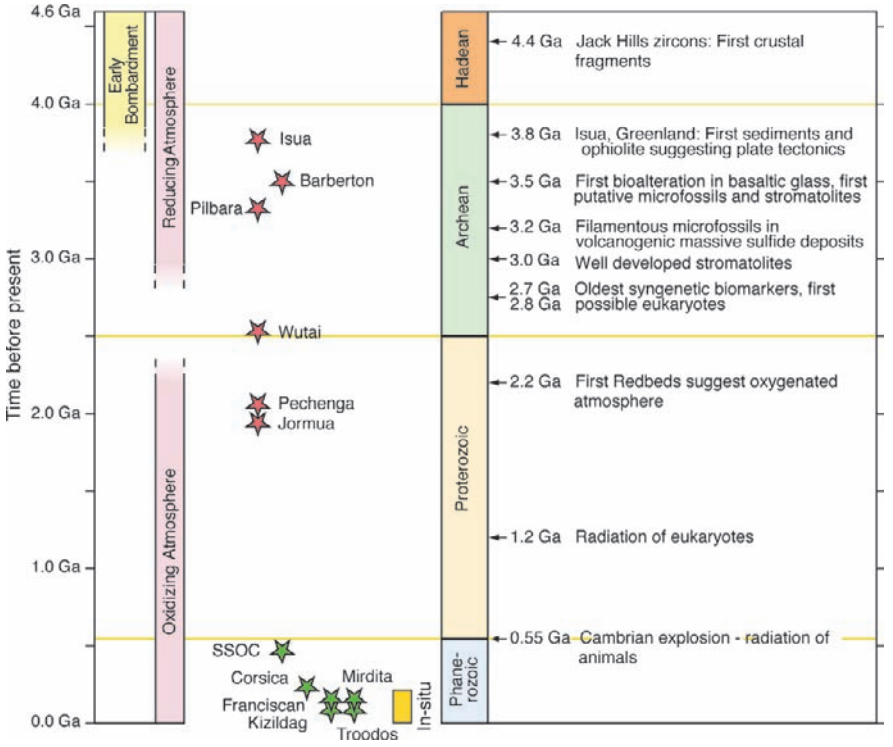

Fig. 36 Geological timeline showing the investigated Precambrian ophiolites and greenstone belts (*red* stars), Phanerozoic ophiolites (*green* stars), and *in-situ* oceanic crust (*yellow* bar), seen in conjunction with a schematic evolution of life (broadly following the review of Nisbet and Sleep 2001). Data from Isua are from Rosing (1999) and Furnes et al. (2007b), and data from Jack Hills are from Wilde et al. (2001)

These findings of Archean bioalteration textures are placed on a geological timeline in Fig. 36 that summarizes the major events in the evolution of the Earth's biosphere. This emphasizes the longevity of bioalteration processes through geological time, stretching from modern *in-situ* oceanic crust, through the Phanerozoic and Proterozoic as sporadically recorded in ophiolites, to the some of the earliest pillow lavas on Earth as preserved in greenstone belts. The Archean mineralized bioalteration traces from Australia and South Africa predate the oldest, previously known euendolithic microfossils described from ~1.7 Ga silicified stromatolites in China (Zhang and Goloubic 1987). Furthermore, this timeline shows that our bioalteration textures fall in the interval at ~3.4–3.8 Ga, when the earliest purported microfossils (e.g., Schopf and Packer 1987; Ueno et al. 2001) and stromatolites (e.g., Walter et al. 1980; Hofmann et al. 1999) have been found and thus meta-volcanic glasses provide a new target lithology that may help to decipher the origins of life in some of these earliest ~3.5 Ga pillow lavas on Earth. Given that volcanic lavas constitute a

volumetrically more significant component of the early Archean greenstone belts than the more traditionally sought chert horizons, they provide abundant opportunities for seeking fossilized evidence of life within the ancient crust (see also Section 7.5).

Considering this possibility, an endolithic mode of life may have been an attractive strategy in the early Archean, conferring many advantages on an early biosphere. Firstly, the oceanic crust may have provided abundant electron donors, principally Fe and Mn, found in basaltic rocks along with electron acceptors for chemolithoautotrophic organisms. Secondly, circulating fluids in the early oceanic crust may have provided carbon for heterotrophic organisms derived either from biotic carbon possibly recycled from the overlying water column, or abiotic carbon derived from alteration of the abundant ultramafic rocks. Lastly, crustal habitats would have provided protection from the elevated UV irradiation, abundant meteoritic and cometary impacts that affected the early Earth.

These submarine volcanic lavas from the Pilbara and Barberton are not however, the world's oldest. The earliest, ~3.8 Ga evidence of purported life on Earth is solely geochemical and based on isotopically light carbon in graphite contained within amphibolite to granulite grade metamorphic rocks in the Isua and Akilia supracrustal complexes of southwest Greenland (Schidlowski 1988, 2001; Mojzsis et al. 1996; Rosing 1999; McKeegan et al. 2007). This evidence is strongly debated (see Moorbath 2005 and references therein) and new light on this discussion may be shed by the investigation of the pillow basalts for bioalteration textures. Work to date has, however, failed to find reliable bioalteration textures in these rocks.

The discovery of bioalteration textures in the Archean begs the question: what role did submarine volcanoes play during the origin of life itself? Previous evidence to support a "hydrothermal cradle for life" comes from purported microfossils and stromatolites in ~3.45 Ga black hydrothermal cherts (e.g., Ueno et al. 2001; Van Kranendonk 2006) and filamentous microfossils in ~3.2 Ga volcanogenic massive sulfide deposits (Rasmussen 2000). Much remains to be done to map and constrain the nature of viable habitats in early volcanic seafloor settings and to explore whether volcanoes were the primary environment where life originated, or a secondary environment where life found shelter and/or co-developed with other settings (see Section 7.5 below).

The possibility of subaqueous basaltic glass alteration on early Mars has also been suggested and might involve both abiotic and biotic processes (e.g., Banerjee et al. 2004). The recent discovery in the Nakhla meteorite of carbonaceous vein filling material with tubular and bleb shaped microstructures that are similar to terrestrial bioalteration textures have renewed interest in these hypotheses (McKay et al. 2006; Gibson et al. 2006). In addition, microtubular weathering channels in olivines and pyroxenes from this same class of meteorite have been recently described by Fisk et al. (2006). Testing of the biogenicity and syngenicity of these meteoritic structures relies heavily on terrestrial comparisons and will undoubtedly help to strengthen the criteria used to establish the veracity of ancient bioalteration textures.

7.5 Tracing Back and Mapping the Pattern of Early Bioalteration

The bioalteration of volcanic glass is among the oldest fossilized evidence for life on Earth, and its textural expressions appear to have remained remarkably conservative through geological time. The question of whether we can see the same pattern of bioalteration in pillow lavas of the ancient oceanic crust as in the young, *in situ* oceanic crust is particularly intriguing. To answer this question we can as yet only provide some provisional data based upon bioalteration textures found in the Hooggenoeg Formation of the Barberton greenstone belt and the Euro Basalt of the Pilbara Craton. We firstly assume that these biotextures must have developed when the ambient temperatures were below $\sim 113^{\circ}$C to permit the existence of life (Stetter et al. 1990). It is unlikely that bioalteration could have occurred continuously throughout the relatively thick Archean volcanic sequences, some of which

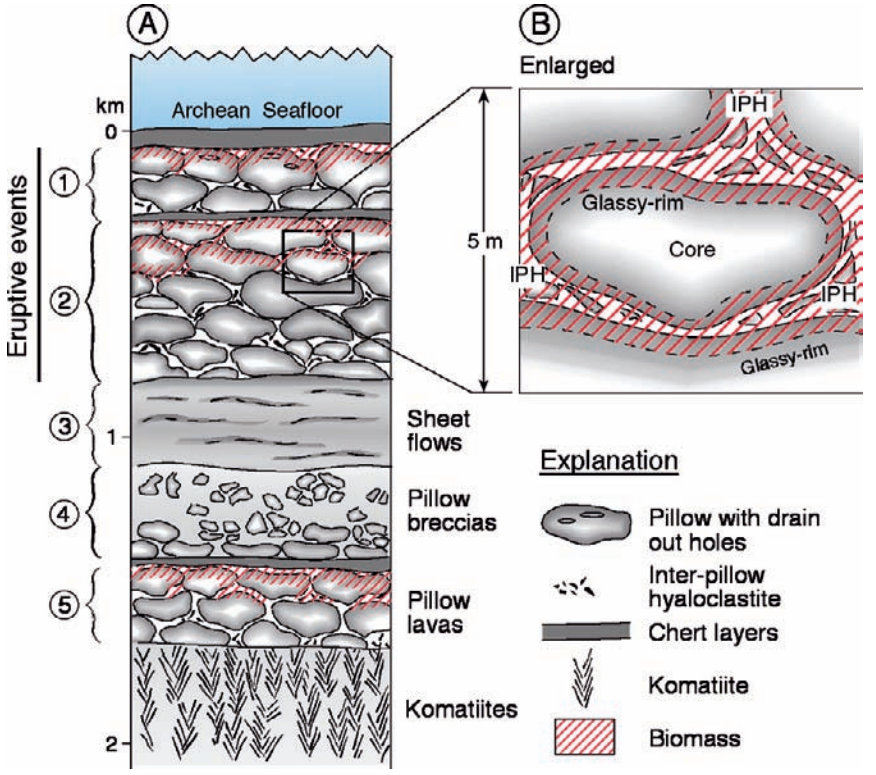

Fig. 37 Model of bioalteration in the Archean seafloor: (**A**) schematic column of a pillow lava pile with interbedded sheet flow produced in 5 eruptive events with interbedded komatiites and seafloor cherts, the biomass shown by red hashes is patchy and concentrated towards the tops of pillow lava eruptive packages; (**B**) enlarged view of a single pillow showing the concentration of endolithic biomass in the glassy pillow rims and inter-pillow hyaloclastites. This model is based upon observation made in the measured Archean greenstone belt sections illustrated in Fig. 17

were probably erupted relatively quickly and buried at temperatures that were too high for life to exist. It is therefore not surprising that examples of bioalteration textures found to date are limited to apparently narrow horizons of these thick submarine lava sequences. For example, the only bioalteration textures found to date in the interpillow hyaloclastite from the Euro Basalt are from the lower part of the 5–8-km-thick basalt succession (Fig. 17). The basal flows of the Euro Basalt are dated at 3350 +/ − 2 Ma, whereas a thin felsic volcaniclastic unit in the upper part of the formation has yielded an age of <3346 Ma (see Fig. 2 in Van Kranendonk 2006), suggesting that most of this very thick volcanic succession was erupted within a few million years, probably exceeding temperature viable for life during much of this time. Similarly, from the 2–3-km-thick succession of submarine basalts (pillow lavas and massive sheet flows) of the Hooggenoeg Formation in the Barberton greenstone belt, bioalteration textures have been found only within restricted pockets of interpillow hyaloclastites in the upper part of the sequence (Fig. 17). Based upon these data, we have constructed a working model for the distribution of biomass in the ancient oceanic crust as shown in Fig. 37 that differs from the more continuous distribution pattern documented from the *in-situ* oceanic crust (Fig. 34).

A further point to consider in this context is the predominance of tubular alteration textures in Archean lavas that contrasts with the alteration textures in *in-situ* oceanic crust, where granular textures are by far the most predominant. Indeed, only rare examples of possible granular textures have been identified along fractures in originally glassy fragments of hyaloclastite from the Archean Hoeggenoeg Formation (see Fig. 6 of Banerjee et al. 2006). The predominance of the tubular over granular alteration textures in Archean lavas may be explained by the masking of the finer, granular textures by titanite mineralization and re-crystallization of the host rock. Conversely, the (early) precipitation of titanite to infill many of the larger tubular textures may have enhanced their preservation by limiting the destructive effects of ongoing re-crystallization of the host rock. In this way, the pattern of Archean oceanic crustal bioalteration might have been modified by taphonomic processes i.e. changes during diagenesis and metamorphism, which may have significantly modified the original distribution pattern of bioalteration.

8 Summary

In this chapter, we have summarized results obtained over the last 15 years which argue that submarine volcanic rocks are and have been for most of Earths history an important habitat for microbial life. To illustrate this conclusion we present data from *in-situ* oceanic crust (0–110 Ma), ophiolites (∼90–1995 Ma) and greenstone belts (∼2000–3800 Ma). During the microbial colonization and simultaneous dissolution of volcanic glass referred to here as *bioalteration*, distinct textural, elemental and isotopic signatures are produced. Two principal types of textures, *granular* and *tubular* are formed. The granular type are individual and coalesced aggregates of spherical bodies usually less than 1 μm in diameter, whereas the tubular type are

long, up to ~200 μm tubes commonly 1–5 μm in diameter. These two textural types are invariably rooted in fractures in the glass and are distinct from the regularly banded alteration rinds produced by abiotic alteration (palagonitization). The bioalteration textures are formed by microbial dissolution or etching that produces pits or holes in the glass which are subsequently infilled by secondary minerals, initially clay minerals and zeolites that are transformed to chlorite, calcite, quartz and titanite during metamorphism. Locally elevated concentration of biologically significant elements, especially carbon, nitrogen, phosphorus and sulphur, are commonly observed within these bioalteration textures and offer significant support for their biogenicity. Further, there is a systematic difference in the $\delta^{13}C$ values of disseminated carbonate between glassy pillow rims and crystalline pillow interiors. The latter are bracketed between primary mantle CO_2 values and those expected from marine carbonates whereas pillow rims and hyaloclastites display a significantly greater range in $\delta^{13}C_{carbonate}$ values that is consistent with microbial activity. Even in the sequences that have experienced amphibolite and blueschist metamorphism this shift in isotope values persists, indicating that this bioalteration signal can survive high grade metamorphism.

The significance of these biosignatures for modern and ancient oceanic crustal processes is summarized below:

- **Mapping the oceanic biosphere**. Conspicuous bioalteration textures visible in thin section have made it possible to quantitatively estimate the extent of bioalteration as a function of depth in the sub-seafloor. This suggests that bioalteration predominates in the upper ~350 m of the glassy volcanic pile of the *in-situ* oceanic crust.
- **The oceanic crust as a bioreactor**. Although little is known about "glass-eating" microbial communities their ecologies and metabolisms, it is known that bioalteration increases the available glass surface area thereby enhancing reaction rates. It is thus likely that microbial activity results in increased exchange of chemical components between seawater and the crust.
- **Tectonic control of bioalteration in modern and ancient oceanic crust**. The carbon isotope signatures ($\delta^{13}C$) of finely disseminated carbonates in bioaltered pillow rims from slow- and fast-spreading oceanic crust differ. This is thought to be related to the liberation of H_2 during serpenitization which is much greater at slow-spreading ridges where it may support the lithotrophic utilization of CO_2 by methanogenic Archaea. This difference in $\delta^{13}C_{carb}$ values appears also to be found in ophiolites of slow versus fast spreading affinities.
- **Bioalteration and history of early life**. Bioalteration textures found in metavolcanic glasses provide a new target for deciphering the origins of life in some of the oldest, well-preserved rocks (~3.5 Ga) on Earth. Titanite mineralized textures in meta-pillow lava rims are comparable to those found in the modern oceanic crust and have a relatively high preservation potential. These structures can be considered amongst the earliest ichnofossils in the fossil record.
- **Tracing back and mapping the pattern of early bioalteration**. In the thick volcanic piles of the Archean greenstone belts that we have studied (Barberton

and Pilbara) the distribution of tubular bioalteration textures is apparently patchy and has been modified by subsequent metamorphism. This contrasts with the *in-situ* oceanic crust in which biotextures can be found continuously throughout.

Acknowledgments We acknowledge the help of many colleagues with the work reviewed herein describing the microbial bioerosion of volcanic glass, including: I.H. Thorseth, T. Torsvik, O. Tumyr, and A. Simonetti. Financial support for this research was provided by the Norwegian Research Council; the National Sciences and Engineering Research Council of Canada; the US National Science Foundation; the Agouron Institute and the National Research Foundation of South Africa. We thank F. Daniel of Nkomazi Wilderness for hospitality and the Mpumalanga Parks Board for access during field work in the Barberton Mountain Land of South Africa. This research used samples and data provided by the Ocean Drilling Program (ODP). ODP was sponsored by the NSF and participating countries under management of Joint Oceanographic Institutions (JOI), Inc. Participation for NB on the ODP Leg 192 was provided by Canada ODP. The Geological Survey of Western Australia, A. Hickman and C. Stoakes are also thanked for assistance with fieldwork in the Pilbara. Torgeir Andersen introduced us to the blueschist pillow lavas in Corsica, and R.C. Erickson assisted us on the classical Ward Creek blueschist locality in California. V. Melezhik and E. Hanski introduced us to the Pechenga greenstone belt (Russia), G. Zhao and P. Robinson to the Wutai area in the North China Craton, and M. Rosing to the Isua supracrustal belt (Greenland). We thank all these persons for their help. We also thank L. Nasdala for permission to publish Raman spectroscopy data shown in Fig. 27. This work has greatly benefited from the constructive review by Wolfgang Bach, Nils Holm and Dave Wacey. J. Ellingsen kindly helped with the illustrations. This paper is published with the permission of the Executive Director of the Geological Survey of Western Australia. This is AEON contribution number 46.

References

Abrajano TA, Sturchio NC, Kennedy BM, Muehlenbachs K, Bohlke JK (1990) Geochemistry of reduced gas related to serpentinization of Zambales ophiolite, Philippines. Appl Geochem 5:625–630

Alt JC, Mata P (2000) On the role of microbes in the alteration of submarine basaltic glass: a TEM study. Earth Planet Sci Lett 181:301–313

Alt JC, Kinoshita H, Stokking LB, et al (1993) Proc. ODP, Init. Repts, 148. (U. S. Government Printing Office), Washington

Alt JC, Laverne C, Vanko DA, Tartarotti P, Teagle DAH, Bach W, Zuleger E, Erzinger J, Honnorez J, Pezard PA, Becker K, Salisbury MH, Wilkens RH (1996) Hydrothermal alteration of a section of upper oceanic crust in the eastern equatorial Pacific: a synthesis of results from site 504 (DSDP Legs 69, 70, and 83, and ODP Legs 111, 137, 140 and 148). In: Alt JC, Kinoshita H, Stokking LB, Michael JP (eds) Proc. ODP, Sci. Results 148, College Station, TX, (Ocean Drilling Program), pp 417–434

Amend JP, Teske A (2005) Expanding frontiers in deep subsurface microbiology. Palaeogeo Palaeoclim Palaeoecol 219:131–55

Armstrong RA, Compston W, de Wit MJ, Williams IS (1990) The stratigraphy of the 3.5–3.2 Ga Barberton Greenstone Belt revisited: a single zircon ion microprobe study. Earth Planet Sci Lett 101:90–106

Bach W, Edwards KJ (2003) Iron and sulphide oxidation within the basaltic ocean crust: implications for chemolithoautotrophic microbial biomass production. Geochim Cosmochim Acta 67:3871–3887

Balashov A (1996) Paleoproterozoic geochronology of the Pechenga-Varzuga structure, Kola Peninsula. Petrology 4:1–22

Banerjee NR, Muehlenbachs K (2003) Tuff Life: bioalteration in volcaniclastic rocks from the Ontong Java Plateau. Gechem Geophys Geosyst 4(4). doi:1029/2002GC000470

Banerjee NR, Furnes H, Muehlenbachs K, Staudigel H, de Wit M (2004) The potential for early life hosted in basaltic glass on Mars. Second Conference on Early Mars: Geologic, hydrologic, and climatic evolution and the implications for life. Jackson Hole, Wyoming, USA

Banerjee NR, Furnes H, Muehlenbachs K, Staudigel H, de Wit MJ (2006) Preservation of microbial biosignatures in 3.5 Ga pillow lavas from the Barberton Greenstone Belt, South Africa. Earth Planet Sci Lett 241:707–722

Banerjee NR, Simonetti A, Furnes H, Staudigel H, Muehlenbachs K, Heaman L, Van Kranendonk MJ (2007) Direct dating of Archean microbial ichnofossils. Geology 35:487–490

Bebien J, Shallo M, Mania K, Gega D (1998) The Shebenik Massif (Albania): a link between MOR- and SSZ-type ophiolites? Ofiliti 23(1):7–15

Benzerara K, Menguy N, Banerjee NR, Tyliszczak T, Brown GE Jr, Guyit F (2007) Alteration of submarine basaltic glass from the Ontong Java Plateau: a STXM and TEM study. Earth Planet Sci Lett 260:187–200

Berndt ME, Allen DE, Seyfried DE Jr (1996) Reduction of CO_2 during serpentinitization of olivine at 300°C and 500 bar. Geology 24:351–354

Boyet M, Blichert-Toft J, Rosing M, Storey M, Telouk P, Albarede F (2003) ^{142}Nd evidence for early Earth differentiation. Earth Planet Sci Lett 214:427–442

Brandl G, de Wit MJ (1997) The Kaapvaal Craton, South Africa. In: de Wit MJ, Ashwal L (eds) Greenstone Belts. Oxford Univ Press, UK, pp 581–607

Cloos M (1990) Nicasio pillow basalts: a fragment of sea-mount accreted during Franciscan subduction, northern California. A.A.P.G., Pacific Section Guidebook No 66:9–16

Coleman RG (2000) Prospecting for ophiolites along the California continental margin. In: Dilek Y, Moores EM, Elthon D, Nicolas A (eds) Ophiolites and Oceanic Crust: New Insights from Field Studies and the Ocean Drilling Program. Geol Soc Am Spec Pap 351:351–364

Coleman RG, Lee DE (1963) Glaucophane-bearing metamorphic rock types of the Cazadeno area, California. J Petrol 4:260–301

Dal Piaz GV, Zirpoli G (1979) Occurrence of eclogite relics in the ophiolitic nappe from Marine d'Albo, Northern Corsica. N Jb Miner Mh 3:118–122

Daniel J-M, Jovilet L, Goffe B, Poinssot C (1996) Crustal-scale strain partitioning: footwall deformation below the Alpine Oligo-Miocene detachment of Corsica. J Struct Geol 18:41–59

Delaney JR, Kelley DS, Lilley MD, Butterfield DA, Baross JA, Wilcock WSD, Embley RW, Summit M (1998) The quantum event of oceanic crustal accretion: impacts of diking at mid-ocean ridges. Science 281:222–230

de Ronde CEJ, de Wit MJ (1994) Tectonic history of the Barberton greenstone belt, South Africa: 490 million years of Archean crustal evolution. Tectonics 13:983–1005

de Wit MJ (2004) Archean greenstone belts do contain fragments of ophiolites. In: Kusky TM (ed) Precambrian Ophiolites and Related Rock. Developments in Precambrian Geology 13 Elsevier, Amsterdam, Holland

de Wit MJ, Hart RA, Hart RJ (1987). The Jamestown Ophiolite Complex, Barberton mountain belt: a section through 3.5 Ga oceanic crust. J Afr Earth Sci 6:681–730

Detrick R, Honnorez J, Bryan WB, Juteau T, et al. (1988) Proc. ODP, Init. Repts, 106/109. (U. S. Government Printing Office), Washington

Dilek Y, Thy P (1998) Structure, petrology, and seafloor spreading tectonics of the Kizildag ophiolite, Turkey. In: Mills RA, Harrison K (eds) Modern ocean floor processes and the geologic record. Geol Soc London Spec Publ 148:43–69

Dilek Y, Moores EM, Furnes H (1998) Structure of modern oceanic crust and ophiolites and implications for faulting and magmatism at oceanic spreading centers. In: Buck R, Karson J, Delaney P, Lagabrielle Y (eds) Faulting and Magmatism at Mid-Ocean Ridges. Geophysical Monograph, American Geophysical Union, Washington, DC 106:216–266

Dilek Y, Furnes H, Shallo M (2007) Suprasubduction zone ophiolite formation along the periphery of Mesozoic Gondwana. Gondwana Res 11:453–475

Dmitriev L, Heirtzler J, et al (1978) Init. Repts. DSDP, 46. (U. S. Government Printing Office), Washington

Edwards KJ, Rogers DR, Wirsen CO, McCollom TM (2003) Isolation and Characterization of Novel Psychrophilic, Neutrophilic, Fe-oxidising, Chemolithoautotrophic α- and γ-Proteobacteria from the Deep Sea. Appl Environ Microbiol 69:2906–2913

Edwards, KJ; Bach W; McCollom TM (2005). Geomicrobiology in oceanography: microbe-mineral interactions at and below the seafloor. Trends in Microbiol 13:449–456

Evarts RC, Schiffman P (1983) Submarine hydrothermal metamorphism of the Del Puerto ophiolite, California. Am J Sci 283:289–340

Fisk MR, Giovannoni SJ, Thorseth IH (1998) The extent of microbial life in the volcanic crust of the ocean basins. Science 281:978–979

Fisk MR, Staudigel H, Smith DC, Haveman SA (1999) Evidence of microbial activity in the oldest ocean crust: EOS 80:F84–85

Fisk MR, Thorseth IH, Urbach E, Giovannoni SJ (2000) Investigation of microorganisms and DNA from surface thermal water and rock from the east flank of the Juan de Fuca Ridge. In: Fisher A, Davis EE, Escutia C (eds) Proc. ODP, Sci. Results 168. College Station, TX (Ocean Drilling Program), 167–174

Fisk MR, Storrie-Lombardi MC, Douglas S, Popa R, McDonald G, Di Meo-Savoie C (2003) Evidence of biological activity in Hawaiian subsurface basalts. Geochem Geophys Geosyst 4(4). doi:10.1029/2003GC000387

Fisk MR, Popa R, Mason OU, Storrie-Lombardie MC, Vicenzi EP (2006) Iron-magnesium silicate bioweathering on Earth (and Mars?). Astrobiology 6(1):48–68

Foriel J, Philippot P, Rey P, Somogyi A, Banks D, Menez B (2004) Biological control of Bl/Br and low sulphate concentration in a 3.5-Gyr-old seawater from North Pole, Western Australia. Earth Planet Sci Lett 228:451–463

Fouquet Y, Knott R, Cambon P, Fallick A, Rickard D, Desbruyeres D (1996) Formation of large sulfide mineral deposits along fast spreading ridges. Example from off-axial deposits at 12°43'N on the East Pacific Rise. Earth Planet Sci Lett 144:147–162

Fournier M, Jovilet L, Goffe B, Dubois R (1991) Alpine Corsica metamotphic core complex. Tectonics 10:1173–1186

Furnes H, Thorseth IH, Tumyr O, Torsvik T, Fisk MR (1996) Microbial activity in the alteration of glass from pillow lavas from Hole 896A. In: Alt JC, Kinoshita H, Stokking LB, Michael PJ (eds) Proceedings of the Ocean Drilling Program, Ocean Drilling Program, College Station, TX Scientific Results 148:191–206

Furnes H, Staudigel H (1999) Biological mediation in ocean crust alteration: how deep is the deep biosphere? Earth Planet Sci Lett 166:97–103

Furnes H, Muehlenbachs K, Tumyr O, Torsvik T, Thorseth IH (1999) Depth of active bio-alteration in the ocean crust: costa Rica Rift (Hole 504B). Terra Nova 11:228–233

Furnes H, Muehlenbachs K, Torsvik T, Thorseth IH, Tumyr O (2001a) Microbial fractionation of carbon isotopes in altered basaltic glass from the Atlantic Ocean, Lau Basin and Costa Rica Rift. Chem Geol 173:313–330

Furnes H, Staudigel H, Thorseth IH, Torsvik T, Muehlenbachs K, Tumyr O (2001b) Bioalteration of basaltic glass in the oceanic crust. Geochem Geophys Geosyst 2(8). doi:10.1029/2000GC000150

Furnes H, Muehlenbachs K, Tumyr O, Torsvik T, Xenophontos C (2001c) Biogenic alteration of volcanic glass from the Troodos ophiolite, Cyprus. J Geol Soc London 158:75–84

Furnes H, Hellevang B, Dilek Y (2001d) Cyclic volcanic stratigraphy in a Late Ordovician marginal basin, west Norwegian Caledonides. Bull Volcanol 63:164–178

Furnes H, Muehlenbachs K, Torsvik T, Tumyr O, Lang S (2002a) Bio-signatures in metabasaltic glass of a Caledonian ophiolite West Norway. Geol Mag 139:601–608

Furnes H., Thorseth IH, Torsvik T, Muehlenbachs K, Staudigel H, Tumyr O (2002b) Identifying bio-interaction with basaltic glass in oceanic crust and implications for estimating the depth of the oceanic biosphere: a review. In: Smellie JL, Chapman MG (eds) Volcano-Ice Interaction on Earth and Mars. Geol Soc London, Spec Publ 202, 407–421

Furnes H, Muehlenbachs K (2003) Bioalteration recorded in ophiolitic pillow lavas. In: Dilek Y, Robinson PT (eds) Ophiolites in Earth's History, vol 218. Geological Society of London Special Publications, pp 415–426

Furnes H, Banerjee NR, Muehlenbachs K, Staudigel H, de Wit MJ (2004) Early life recorded in Archean pillow lavas. Science 304:578–581

Furnes H, Banerjee NR, Muehlenbachs K, Kontinen A (2005) Preservation of biosignatures in metaglassy volcanic rocks from the Jormua ophiolite complex, Finland. Precamb Res 136: 125–137

Furnes H, Dilek Y, Muehlenbachs K, Banerjee NR (2006) Tectonic control of bioalteration in modern and ancient oceanic crust as evidenced by C-isotopes. The Island Arc 15:143–155

Furnes H, Banerjee NR, Staudigel H, Muehlenbachs K, de Wit M, McLoughlin N, Van Kranendonk M (2007a) Bioalteration textures in recent to mesoarchean pillow lavas: a petrographic signature of subsurface life in oceanic igneous rocks. Precamb Res 158:156–176

Furnes H, de Wit M, Staudigel H, Rosing M, Muehlenbachs K (2007b) A vestige of Earth's oldest ophiolite. Science 315:1704–1707

Gibson EK, Clemett SJ, Thomas-Keprta KL, McKay DS, Wentworth SJ, Robert F, Verchovsky AB, Wright IP, Pillinger CT, Rice T, Van Leer B (2006) Observation and analysis of in situ carbonaceous matter in Nakhla: part II (2006). The 37th Lunar and Planetary Science Conference, Houston 2006, abstract 2039

Giovannoni SJ, Fisk MR, Mullins TD, Furnes H (1996) Genetic evidence for endolithic microbial life colonizing basalic glass/seawater interfaces. In: Alt J, Kinoshita H, Stokking LB, Michael PJ (eds) Proceedings of the Ocean Drilling Program, Scientific Results, Ocean Drill. Program, College Station, Texas 148:207–214

Hanski EJ, Huhma H, Smolkin VF, Vaasjoki M (1990) The age of the ferropicritic volcanics and comagmatic intrusions at pechenga, Kola Peninsula, USSR. Geol Soc Finl Bull 62:123–133

Hoefs J (1997) Stable Isotope Geochemistry, Springer, pp 201

Hofmann HJ, Grey K, Hickman AH, Thorpe RI (1999) Origin of 3.45 Ga Coniform Stromatolites in the Warrawoona Group, Western Australia. Bull Geol Soc Am 111:1256–1262

Ingersoll RV (2000) Models for the origin and emplacement of Jurassic ophiolites of northern California. In: Dilek Y, Moores EM, Elthon D, Nicolas A (eds) Ophiolites and Oceanic Crust: new insights from field Studies and the Ocean Drilling Program. Geol Soc Am Spec Pap 351:395–402

Karson JA (1998) Internal structure of oceanic lithosphere: a perspective from tectonic windows. In: Buck R, Karson J, Delaney P, Lagabrielle Y (eds) Faulting and Magmatism at Mid-Ocean Ridges. Geophysical Monograph, 106:177–218. American Geophysical Union, Washington, DC

Kelley DS (1996) Methane-rich fluids in the oceanic crust. J Geophys Res 101:2943–2962

Kelley DS, Karson JA, Früh-Green GL, Yoerger DR, Shank TM, Butterfield DA, Hayes JM, Schenk MO, Olson EJ, Proskurowski G, Jakuba M, Bradley A, Larson B, Ludvig K, Glickson D, Buckman K, Bradley AS, Brazelton WL, Roe K, Elend MJ, Delacour A, Bernasconi SM, Lilley MD, Baross JA, Summons RE, Sylva S (2005) A serpentine-hosted ecosystem: The Lost City hydrothermal field. Science 307:1428–1434

Kelts K, McKenzie JA. (1982) Diagenetic dolomite formation in Quarternary anoxic diatomaceous muds of Deep Sea Drilling Project Leg 64, Gulf of California. Init. Reps. DSDP, 64. (U. S. Government Printing Office), Washington, pp 553–569

Komiya T, Maruyama S, Masusa T, Nohda S, Hayashi M, Okamoto K (1999) Plate tectonics at 3.8-3.7 Ga: Field evidence from the Isua accretionary complex, southern West Greenland. J Geol 107:515–554

Kontinen A (1987) An early Proterozoic ophiolite – The Jormua mafic-ultramafic complex, northeastern Finland. Precamb Res 35:313–341

Kröner A, Zhao GC, Wilde SA, Zhai MG, Passchier CW, Sun M, Guo JH, O'Brian PJ, Walte N (2001) A Late Archaean to Palaeoproterozoic Lower to Upper Crustal Section in the Hengshan-Wutaishan Area of North China. Guidebook for Penrose Conference Field Trip, September 2002. Chinese Academy of Sciences, Beijing, pp 63

Krumbein WE, Urzi CECA, Gehrman C (1991) Biocorrosion and biodeterioration of antique and medieval glass. Geomicrob J 9:139–160
Lemoine M, Tricard P, Boillot G (1987) Ultramafic and gabbroic ocean floor of the Ligurian Tethys (Alps, Corsica, Appennines): In search of a genetic model. Geology 15:622–625
Lovley DR, Chapelle FH (1995) Deep subsurface microbial processes. Rev Geophys 33:365–381
Lysnes K, Thorseth IH, Steinsbu BO, Øvreås L, Torsvik T, Pedersen RB (2004) Microbial community diversity in seafloor basalts from the Arctic spreading ridges. FEMS Microbiol Ecol 50:213–230
Luydendyk BP, Cann JR. et al (1978) Init. Repts. DSDP, 49, Washington (U. S. Government Printing Office)
Malpas J, Moores EM, Panayiotou A, Xenophontos C (1990) Ophiolites: Oceanic Crustal Analogues. Proceeding of the Symposium "Troodos 1987". The Geological Survey Department, Ministry of Agriculture and Natural Resources, Nicosia, Cyprus, pp 733
Maruyama S, Liou JG (1988) Petrology of Franciscan metabasites along jadeite-glaucophane type facies series, Cazadero, California. J Petrol 29:1–37
Matsushita M, Hiramatsu F, Kobayashi N, Ozawa T, Yamazaki Y, Matsuyama T (2004) Colony formation in bacteria: experiments and modelling. Biofilms 1:305–317. doi:10.1017/S1479050505001626
McKay DS, Clemett SJ, Thomas-Keprta KL, Wentworth SJ, Gibson EK, Robert F, Verchovsky AB, Pillinger CT, Rice T, Van Leer B (2006) Observation and analysis of in situ carbonaceous matter in Nakhla: part I. The 37th Lunar and Planetary Science Conference, Houston 2006, abstract 2251
McKeegan KD, Kudryavtsev AB, Schopf JW (2007) Raman and ion microscopic imagery of graphitic inclusions in apatite from older than 3830 Ma Akilia supracrustal rocks, west Greenland. Geology 35(7):591–594
McLoughlin N, Brasier MD, Wacey D, Green OR, Perry RS (2007) On biogenicity criteria for endolithic microborings on early earth and beyond. Astrobiology 7:10–26
McLoughlin N, Furnes H, Banerjee NR, Staudigel H, Muehlenbachs K, de Wit M, Van Kranendonk M (2008) Micro-Bioerosion in Volcanic Glass: extending the Ichnofossil Record to Archean basaltic crust. In: Wisshak M, Tapanila L (eds) Springer Verlag
Melezhik VA, Sturt BA (1994) General geology and evolutionary history of the early Proterozoic Polmak-Pasvik-Pechenga-Imandra/Varzuga-Ust'Ponoy Greenstone Belt in the north-eastern Baltic Shield. Earth Sci Rev 36:205–241
Melezhik VA, Huhma H, Fallick AE, Whitehouse MJ (2007) Temporal constraints on the Paleoproterozoic Lomagundi-Jatuli carbon isotope event. Geology 35(7):655–658
Mellor E (1922) Les lichen vitricole et la déterioration dex vitraux d'église: Thèse de dochert thesis, Sorbonne, Paris
Mojzsis SJ, Arrhenius G, McKeegan KD, Harrison TM, Nutman AP, Friend CRL (1996) Evidence of life on Earth before 3800 million years ago. Nature 384:55–59
Moorbath S (2005) Dating earliest life. Nature 434:155
Myers JS (2001) Protoliths of the 3.8-3.7 Ga Isua greenstone belt, West Greenland. Precamb Res 105:129–141
Nelson DR (2005) GSWA geochronology dataset, In: Compilation of geochronology data, June 2005 update. Western Australia Geological Survey, GSWA 178042
Nicolas A, Boudier F, Meshi A (1999) Slow spreading accretion and mantle denudation in the Mirdita ophiolite (Albania). J Geophys Res 104:15155–1517
Nisbet EG, Sleep NH (2001) The habitat and nature of early life. Nature 409:1083–1090
Nutman AP (1986) The early Archaean to Proterozoic history of the Isukasia area, southern West Greenland. Grønlands Geol Unders Bull 154:80
Ohnenstetter D, Ohnenstetter M, Rocci G (1976) Etude des metamorphismes successife des cumulates ophiolitiques de Corse. Bull Soc Geol France XVIII:115–134
Palmer HC, Tazaki K, Fyfe WS, Zhou Z (1988) Precambrian glass. Geology 16:221–224
Panayiotou A (ed) (1980) Ophiolites. Proceedings of the International ophiolite Symposium, Cyprus 1979. Cyprus Geological Survey Department, pp 781

Parson I, Hawkins J, Allan J, et al. (1992) Proc. ODP, Init. Repts, 135. (U. S. Government Printing Office), Washington

Paul A, Zaman MS (1978) The relative influences of Al_2O_3 and Fe_2O_3 on the chemical durability of silicate glasses at different pH values. J Mat Sci 13:1499–1502

Peacock MA (1926) The petrology of Iceland. Part I, The basic tuffs. Trans Roy Soc Edinburgh 55:51–76

Pedersen K (1997). Microbial life in deep granitic rocks. FEMS Microbiol Rev 20:399–414

Pedersen K, Ekendahl S, Tullborg E-L, Furnes H, Thorseth IH, Tumyr O (1997) Evidence of ancient life at 207 m depth in a granitic aquifer. Geology 25:827–830

Peltonen P, Kontinen A, Huhma H (1996) Petrology and geochemistry of metabasalts from the 1.95 Ga Jormua ophiolite, Northeastern Finland. J Petrol 37:1359–1383

Rasmussen B (2000) Filamentous microfossils in a 3,250-million-year-old volcanogenic massive sulphide deposit. Nature 405:676–679

Robinson PT, Flower MFJ, Swanson DA, Staudigel H (1979) Lithology and eruptive stratigraphy of Cretaceous oceanic crust, western Atlantic Ocean. In: Donelly T, Francheteau J, Bryan W, Robinson P, Flower M, Salisbury M. et al (eds) Init. Repts. DSDP, LI, LII, LIII. (U. S. Government Printing Office), Washington

Rosing MT (1999) ^{13}C-depleted carbon microparticles in >3700-Ma sea-floor sedimentary rocks from West Greenland. Science 283:674–676

Rosing MT, Rose NM, Bridgwater D, Thomsen HS (1996) Earliest part of Earth's stratigraphic record: a reappraisal of the >3.7 Ga Isua (Greenland) supracrustal sequence. Geology 24:43–46

Ross KA, Fisher RV (1986) Biogenic grooving on glass shards. Geology 14:571–573

Santelli CM, Bach W, Edwards KJ (2006). Microorganisms and the weathering of basalt at the seafloor. Geochim Cosmochim Acta 70 (issue 18) A556 (Goldschmidt Conference Abstracts) doi:10.1016/j.gea.2006.06.1027

Schidlowski M (1988) A 3800-million-year isotopic record of life from carbon in sedimentary rocks. Nature 333:313–318

Schidlowski M (2001) Carbon isotopes as biogeochemical recorders of life over 3.8 Ga of Earth history: evolution of a concept. Precamb Res 106:117–134

Schiffman P, Williams AE, Evarts RC (1984) Oxygen isotope evidence for submarine hydrothermal alteration of the Del Puerto ophiolite, California. Earth Planet Sci Lett 70:207–220

Schiffman P, Evarts RCE, Williams AE, Pickthorn WJ (1991) Hydrothermal metamorphism in oceanic crust from the Coast Ranges ophiolite of California:fluid-rock interaction in a rifted island arc. In: Peters TJ., Nicolas A, Coleman RG (eds) Ophiolite Genesis and Evolution of the Oceanic Lithosphere. Kluwer Academic Publishers, Dordrecht, pp 399–425

Schippers A, Neretin LN, Kallmeyer J, Fendelman TG, Cragg BA, Parkes RJ, Jørgensen BB (2005) Prokaryotic cells of the deep sub-seafloor biosphere identified as living bacteria. Nature 433:861–64

Schmincke H-U, Bednarz U (1990) Pillow, sheet flow and breccia flow volcanoes and volcanotectonic hydrothermal cycles in the Extrusive Series of the northeastern Troodos ophiolite (Cyprus). In: Malpas J, Moores EM, Panayiotou A, Xenophontos C (eds) Ophiolites Oceanic Crustal Analogues, Proceedings of the Symposium "Troodos 1987". The Geological Survey Department, Ministry of Agriculture and Natural Resources, Nicosia, Cyprus, pp 185–206

Schopf JW, Packer BM (1987) Early Archean (3.3 Billion to 3.5 Billion-Year-Old) Microfossils from Warrawoona Group, Australia. Science 237:70–73

Schumann G, Manz W, Reitner J, Lustrino M (2004) Ancient Fungal Life in North Pacific Eocene Ocenaic Crust. Geomicrobiol J 21:241–246

Shallo M (1995) Volcanics and sheeted dykes of the Albanian SSZ ophiolite. Buletini i Shkencave Gjeologjike 91:99–118

Shervais JW, Hanan BB (1989) Jurassic volcanic glass from the Stonyford volcanic complex, Franciscan assemblage, northern California Coast Ranges. Geology 17:510–514

Simonetti A, Heaman LM, Chacko T, Banerjee NR (2006) In situ petrographic thin section U–Pb dating of zircon, monazite, and titanite using laser ablation–MC–ICP-MS. Internat J Mass Spectrometry 253:87–97

Sinton JM, Detrick RS (1992) Mid-ocean ridge magma chambers. J Geophys Res 97:197–216
Smolkin VF, Bayanova TB, Fedotov Zh A (2003) Ore-bearing mafic-ultramafic rocks of the Pechenga-Allarechka area, Kola region: isotopic dating. In: Proceedings of the II Russian Conference on Isotope Geochemistry, St. Petersburg, pp 467–470 (in Russian)
Staudigel H, Chastain RA, Yayanos A, Bourcier R (1995) Biologically mediated dissolution of glass. Chem Geol 126:119–135
Staudigel H, Yayanos A, Chastain R, Davies G, Verdurmen EATh, Schiffman P, Bourcier R, De Baar H (1998) Biologically mediated dissolution of volcanic glass in seawater. Earth Planet Sci Lett 164:233–244
Staudigel H, Furnes H (2004) Microbial mediation of oceanic crust alteration. In: Davis E, Elderfield H (eds) Hydrology of the Oceanic Lithosphere. Cambride University Press, pp 608–626
Staudigel H, Furnes H, Kelley K, Plank T, Muehlenbachs K, Tebo B, Yayanos A (2004) The Oceanic Crust as a Bioreactor. In: AGU Monograph 144. Deep Subsurface Biosphere at Mid-Ocean Ridges pp 325–341
Staudigel H, Furnes H, Banerjee NR, Dilek Y, Muehlenbachs K (2006) Microbes and Volcanos: A tale from the Oceans, Ophiolites and Greenstone Belts. GSA Today 16(10). doi:10.1130/GSAT01610A.1
Stetter KO, Fiala G, Huber G, Segerer A (1990) Hypothermophilic microorganisms. FEMS Microbiol Rev 75:117–124
Storrie-Lombardi MC, Fisk MR (2004) Elemental abundance distributions in suboceanic basalt glass: Evidence of biogenic alteration. Geochem Geophys Geosyst 5(10). doi:10.1029/2004GC000755
Stroncik N, Schmincke H-U (2001) Evolution of palagonite: Crystallization, chemical changes, and element budget. Geochem Geophys Geosyst 2(7). doi:10.1029/2000GC000102
Swanson SE, Schiffman P (1979) Textural evolution and metamorphism of pillow basalts from the Franciscan Complex, western Marin County, California. Contrib Mineral Petrol 69: 291–299
Tappert R, Stachel T, Harris JW, Muehlenbachs K, Ludwig T, Brey GP (2005) Subducting oceanic crust: The source of deep diamonds. Geology 33:565–568
Templeton AS, Staudigel H, Tebo BM (2005) Diverse Mn(II)-Oxidizing bacteria isolated from submarine Basalts at Loihi Seamount. J Geomicrobiol 22:127–139
Thorseth IH, Furnes H, Tumyr O (1991) A textural and chemical study of Icelandic palagonite of varied composition and its bearing on the mechanism of the glass-palagonite transformation. Geochim Cosmochim Acta 55:731–749
Thorseth IH, Furnes H, Heldal M (1992) The importance of microbiological activity in the alteration of natural basaltic glass. Geochim Cosmochim Acta 56:845–850
Thorseth IH, Torsvik T, Furnes H, Muehlenbachs K (1995a) Microbes play an important role in the alteration of oceanic crust. Chem Geol 126:137–146
Thorseth IH, Furnes H, Tumyr O (1995b) Textural and chemical effects of bacterial activity on basaltic glass: an experimental approach. Chem Geol 119:139–160
Thorseth IH, Torsvik T, Torsvik V, Daae FL, Pedersen RB, Keldysh-98 Scientific party (2001) Diversity of life in ocean floor basalts. Earth Planet Sci Lett 194:31–37
Thorseth IH, Pedersen RB, Christie DM (2003) Microbial alteration of 0–30-Ma seafloor and sub-seafloor basaltic glasses from the Australian Antarctic Discordance. Earth Planet Sci Lett 215:237–247
Torsvik T, Furnes H, Muehlenbachs K, Thorseth IH, Tumyr O (1998) Evidence for microbial activity at the glass-alteration interface in oceanic basalts. Earth Planet Sci Lett 162:165–176
Ueno Y, Maruyama S, Isozaki Y, Yurimoto H (2001) Early Archean (ca. 3.5 Ga) microfossils and ^{13}C-depleted carbonaceous matter in the North Pole area, Western Australia: Field occurrence and geochemistry, In: Nakashima S, Maruyama S, Brack A, Windley BF (eds) Geochemistry and the origin of life. Universal Academy Press Inc, Tokyo, pp 203–236

Van Kranendonk MJ (2006) Volcanic degassing, hydrothermal circulation and the flourishing of early life on Earth: A review of the evidence from c. 3490-3240 Ma rocks of the Pilbara Supergroup, Pilbara Craton, Western Australia. Earth-Sci Rev 74:197–240

Van Kranendonk MJ, Pirajno F (2004) Geochemistry of metabasalts and hydrothermal alteration zones associated with c. 3.45 Ga chert and barite deposits: implications for the geological setting of the Warrawoona Group, Pilbara craton, Australia. Geochemistry: Exploration Environment Analysis 4:253–278

Van Kranendonk MJ, Hickman AH, Smithies RH, Nelson DN, Pike G (2002) Geology and tectonic evolution of the Archaean North Pilbara terrain, Pilbara Craton, Western Australia. Econ Geol 97(4):695–732

Van Kranendonk MJ, Collins WJ, Hickman A, Pawley MJ (2004) Critical tests of vertical vs. horizontal tectonic models for the Archean East Pilbara Granite-Greenstone Terrane, Pilbara Craton, Western Australia. Precamb Res 131:173–211

Van Kranendonk MJ, Hickman AH, Smithies RH, Champion DC (2007) Review: secular tectonic evolution of Archaean continental crust: interplay between horizontal and vertical processes in the formation of Pilbara Craton, Australia. Terra Nova 19:1–39

Wakabayashi J (1992) Nappes, tectonics of oblique plate convergence, and metamorphic evolution related to 140 million years of continuous subduction, Franciscan Complex, California. J Geol 100:19–40

Wakabayashi J (1999) The Franciscan Complex, San Francisco Bay Area: A record of subduction complex processes. In: Wagner DL, Graham SA (eds) Geologic Field Trips in Northern California. California Division of Mines Special Publication 119:1–21

Walter MR, Buick R, Dunlop JSR (1980) Stromatolites, 3,400–3,500 Myr old from the North Pole area, Western Australia. Nature 284:443–445

Walton AW, Schiffman P (2003) Alteration of hyaloclastites in the HSDP 2 Phase 1 Drill Core 1. Description and paragenesis. Geochem Geophys Geosyst 4(5). Doi: 10.1029/2002GC000368

Walton AW, Schiffman P, Macperson GL (2005) Alteration of hyaloclastites in the HSDP 2 Phase 1 Drill Core: 2. Mass balance of the conversion of sideromelane to palagonite and chabazite. Geochem Geophys Geosyst 6(9). doi: 10.1029/2004GC000903

Wijbrans JR, McDougall I (1987) On the metamorphic history of an Archaean granitoid greenstone terrane, East Pilbara, Western Australia, using the $^{40}Ar/^{39}Ar$ age spectrum technique. Earth Planet Sci Lett 84:226–242

Wilde SA, Valley JW, Peck WH, Graham CM (2001) Evidence from detrital zircons for the existence of continental crust and oceans on the Earth 4.4 Gya ago. Nature 409:175–178

Zavarzina DG, Sokolova TG, Tourova TP, Chernyh NA, Kostrikina NA, and Bonch-Osmolovskaya EA (2007) Thermincola ferriacetica sp nov, a new anaerobic, thermophilic, faculatively chemolithoautotrophic bacterium capable of dissimilatory Fe(III) reduction. Extremophiles 11:1–7

Zhai MG, Yan YH, Lu WJ, Zhou JB (1985) Geochemistry and evolution of the Qingyuan Archean granite-greenstone terrain, N. China. Precamb Res 27:37–62

Zhao G, Wilde SA, Cawood PA, Sun M (2001) Archean blocks and their boundaries in the North China Craton: lithological, geochemical, structural and *P-T* path constraints and tectonic evolution. Precamb Res 107:45–73

Zhang Z, Goloubic S (1987) Endolithic microfossils (cyanophyta) from early Proterozoic Stromatolites, Hebei China. Acta Micropaleontol Sin 4:1–12

Zhou GC, Wilde SA, Cawood PA, Lu LZ (1998) Thermal evolution of the Archean basement rocks from the eastern part of the North China Craton and its bearing on tectonic setting. Int Geol Rev 40:706–721

Microbial Colonization of Various Habitable Niches During Alteration of Oceanic Crust

Magnus Ivarsson and Nils G. Holm

Abstract Tunnel structures in volcanic glass are a world wide phenomenon and known to harbor microorganisms of the deep sub-seafloor biosphere. As alteration and weathering of the ocean crusts proceeds, volcanic glass is altered and devitrified. Palagonitization of volcanic glass results in the secondary phases palagonite, phillipsite and smectite. The alteration and palagonitization result in destruction of microbial habitats. Colonization of new habitable niches is thus forced upon the microorganisms by external forces.

In basalt samples that were drilled and collected during the Ocean Drilling Program (ODP) Leg 197 at the Emperor Seamounts in the Pacific Ocean, fossilized microorganisms are found in various geological niches that cover the whole palagonite process. From tunnel structures in volcanic glass, via fossilized filaments attached onto altered glass and basalt, to fossilized cells and filaments both attached to zeolites (phillipsite) and found in wedge-like cavities between zeolite crystals. The C content (∼10–∼50 wt% C) and the fact that the carbon is not bound to or associated with carbonates suggest that the fossilized microorganisms contain organic carbon. The concentration of C_2H_4 and lipids in the filamentous structures further supports that they contain organic carbon and organic compounds. Bonding to PI, which is a dye that binds to damaged membranes and dead bacteria cells, provides further evidence for a biogenic origin of the microfossils.

The close association between microfossils and iron oxides, the accumulation of iron oxides onto the filaments, the high iron content of the filaments as well as the higher degree of alteration and accumulation of iron at the surface zones where the microfossils are found indicate that the microorganisms were involved in iron oxidizing reactions and that the colonization of new niches clearly was influenced by redox chemistry.

M. Ivarsson
Department of Geology and Geochemistry, Stockholm University, Sweden, Frescativägen 8, S-106 91 Stockholm, Sweden
e-mail: magnus.ivarsson@geo.su.se

Y. Dilek et al. (eds.), *Links Between Geological Processes, Microbial Activities & Evolution of Life*, © Springer Science+Business Media B.V. 2008

The microbial capability to inhabit new niches during alteration of oceanic crust extends the occurrence and opportunities of the deep sub-seafloor biosphere both in time and in space. The results suggest that the sub-seafloor biosphere can sustain during geological processes and that the spatial extension of the biosphere is much larger than was previously known.

1 Introduction

Knowledge about the deep biosphere that lives around hydrothermal vents on the ocean floor has exploded since its discovery in the late 1970s. However, the deep sub-seafloor biosphere, that has been suggested to extend beneath the ocean floor, has been more inaccessible (Edwards et al. 2005). The occurrence of microorganisms in hydrothermal vent waters that disseminates from vent areas on the ocean floors has led to suspicions about a sub-seafloor biosphere (Gold 1992; Deming and Baross 1993), but studying such a biosphere in situ involves serious obstacles. Sampling of the sub-seafloor biosphere requires drilling in ocean crust which obviously disturbs collection of living organisms. Organisms rarely survive such treatment, and the samples that are brought to the surface rarely contain living species. Dead or fossilized microorganisms are normally what researchers have to deal with. Nevertheless, since the early 1990s a rather small but steady stream of reports have established the sub-seafloor biosphere as a viable feature in ocean crusts around the world (Thorseth et al. 1995a, 2001, 2003; Giovannoni et al. 1996; Furnes et al. 1996; Furnes and Staudigel 1999; Fisk et al. 1998).

The deep biosphere has been recognized to consist of lithoautotrophic and chemoautotrophic microorganisms. Such organisms use chemical energy stored in minerals or in compounds dissolved in the hydrothermal fluids as an energy source (Thorseth et al. 1995a, 2001, 2003). It is most likely that the sub-seafloor biosphere consists of lithoautotrophs as well and that they are endolithic in the sense that they live within minerals and rocks. The most accessible elements and compounds for such organisms in hydrothermal settings are H_2, H_2S, S, CO, CH_4, Mn^{2+} and Fe^{2+} and electron acceptors could be CO_2, SO_4 or O_2. Usually, endolithic lithoautotrophs occupy habitats at the interface between two environments with divergent redox chemistry. In sub-seafloor settings microbes have been found mostly associated with highly reduced volcanic glass. In contact with oxidized seawater, volcanic glass is out of chemical equilibrium, and redox reactions exploitable for microorganisms can occur. The reactions are relatively slow at low temperatures, and the microorganisms can catalyze the reactions and gain metabolic energy in the process. Thus, microorganisms found in these environments are associated with mineral surfaces, either attached onto them or incorporated within them. Volcanic glass has been recognized as the most accessible material that microorganisms are associated with (Thorseth et al. 1995a, 2001, 2003; Giovannoni et al. 1996; Furnes et al. 1996; Furnes and Staudigel 1999; Fisk et al. 1998). Biomediated tunnel structures that serve as microhabitats for microorganisms have been found to be a world wide phenomenon in volcanic glass in ocean crust. The microbial activity in volcanic glass

accelerates the weathering and alteration of the oceanic crust contemporaneous with the inorganic weathering and alteration (Thorseth et al. 1995a, b; Alt and Mata 2000; Furnes et al. 2001). Both the organic and the inorganic alteration of basaltic glass, also called palagonitization, lead to hydration, oxidation and alteration of the volcanic glass and thus also destruction of the microorganisms habitats. Recently, microorganisms have been found associated with the secondary minerals zeolites in sub-seafloor environments (Thorseth et al. 2003). Zeolites represent a secondary product of the alteration of the volcanic glass, which indicates that microbes are able to colonize new habitats as the alteration of the volcanic glass proceeds. In this paper we will review the current literature regarding the sub-seafloor biosphere and together with new data present a relationship between microorganisms and on-going sub-seafloor geochemistry.

2 Microbial Niches in Sub-seafloo Environments

Microorganisms interact with their environment in a variety of ways that leave various biosignatures. Such biosignatures can consist of, for example, biominerals, cellular fossils, trace fossils (burrows, tunnels), fractionation of stable isotopes as well as organic molecules like hydrocarbons, fatty acids or nucleic acids. In sub-seafloor hydrothermal environments a variety of biosignatures has been found which indicates microbial activity. Mostly, such bioactivity appears to be associated with volcanic glass. Some observations have been made where the microbes are associated with secondary minerals like altered basalt (Thorseth et al. 2001, 2003) and zeolites (Thorseth et al. 2003). The following is an overview of the different niches where microbes are found and the various ways in which they occur and behave in these different environments.

2.1 Tunnel Structures in Volcanic Glass

Microbial weathering of volcanic glass occurs at glass surfaces that are in contact with water, usually along fractures and veins in basaltic rock (Fisk et al. 1998, 2003; Furnes and Staudigel 1999; Furnes et al. 2001, 2004; Storrie-Lombardi and Fisk 2004). A common feature of such weathering is tunnel structures, also called galleries, which emerge perpendicularly from the glass surface and inward into the glass. These tunnel structures can vary in size from 1–10 μm in diameter and 5–100 μm in length. The tunnels have an undulating appearance and can occur in abundance. These structures have been interpreted as trace fossils meaning that they do not represent true fossilized microorganisms (Furnes et al. 2004; Banerjee et al. 2005).

Tunnel structures have been associated with a variety of organic material. Cell-like bodies have been found in them, and concentrations of nucleic acids, C, N and P have been detected (Thorseth et al. 1995a; Furnes et al. 1996, 2001;

Giovannoni et al. 1996; Torsvik et al. 1998; Fisk et al. 2003, 2006). Even DNA of novel microorganisms has been extracted from rocks that contain similar tunnel-like galleries (Fisk et al. 2003).

Laboratory experiments have shown that microorganisms attached to a surface of volcanic glass form depressions due to biomediated dissolution of the glass (Thorseth et al. 1992, 1995b). It has also been shown that microbes form grooves in glass that exceed 10 μm in length and 0.5 μm in width (Staudigel et al. 1995). Tunnel structures longer than that have not been produced in biotic laboratory experiments. On the other hand, such tunnel structures have not been produced in abiotic laboratory experiments either. A distinct difference has been demonstrated between abiotic weathering of volcanic glass and weathering of volcanic glass that involves and is stimulated by microbial activity (Staudigel et al. 2006, 2004, 1995; Thorseth et al. 1995a; Fisk et al. 1998; Furnes et al. 2001). Abiotic weathering results in unembayed, smooth alteration fronts that affect the whole glass surface. This results in parallel alteration fronts with respect to the glass fragment. Microbially mediated alteration results in completely different textures because it is dominated by the formation of local cavities that enter the glass from exterior surfaces in granular-appearing agglomerations or tunnel-like morphologies. Such textures in volcanic glass have been acknowledged as reliable signs of microbial activity and work as textural biomarkers (Staudigel et al. 2006; Fisk et al. 1998; Furnes et al. 2001).

Tunnel structures have been recognized as a world wide phenomenon, both in recent as well as in ancient oceanic crust. In fact, the oldest traces of life are represented by gallery structures found in pillow lavas from the ~3.5 Ga old Barberton Greenstone Belt (BGB), South Africa (Furnes et al. 2004; Banerjee et al. 2005). Galleries have also been found in olivines and pyroxenes from Hawaiian basalts and dunites as well as in Martian meteorites (Fisk et al. 2006). Thus, it is possible to conclude that tunnel and gallery structures in volcanic glass and basalts are recognized as a global niche for microbial life and has existed as long as life has been known on Earth.

2.2 Surfaces of Volcanic Glass and Altered Basalt

In contrast to tunnel structures in volcanic glass that are trace fossils, true fossilized microorganisms have been found attached to mineral surfaces like volcanic glass. Coccoids and rod-shaped cells as well as star-shaped, branched and twisted filaments have been found attached onto surfaces of volcanic glass, altered glass or basalt minerals (Al-Hanbali et al. 2001; Al-Hanbali and Holm 2002; Thorseth et al. 2001, 2003; Ivarsson 2006). Basaltic rocks usually have a zone of glass toward veins and fractures due to rapid cooling of the outermost parts. When this zone is in contact with water that circulates in the veins, the glass becomes altered. Microbes can be found attached onto this zone or incorporated in the zone. Usually, depressions in the mineral surfaces are found associated with the presence of

microorganisms. Such depressions are probably a result of bio-mediated dissolution of the mineral surfaces.

The microfossils are usually associated with iron/manganese-oxides/oxyhydr oxides in their close vicinity or directly deposited onto their cell surfaces. They can sometimes be found with a thick iron/manganese crust on them.

2.3 Surfaces of Secondary Minerals Like Zeolites

Encrusted and fossilized microbes have also been found attached onto zeolites (phillipsites), which are a secondary alteration product of basalt (Thorseth et al. 2003). Just like the occurrence of microorganisms on surfaces of volcanic glass, microbes attached onto zeolites appear to produce depressions on the mineral surface. The encrusted microorganisms contain Fe and Mn indicating that the microorganisms are involved in iron or/and manganese oxidation reactions. Both Fe and Mn could probably serve as energy sources for the microbes.

3 Alteration of the Ocean Floor Basalts – Palagonitization

Palagonitization, a concept that is frequently used but still relatively poorly understood, is usually defined as a low-temperature ($< 250^{\circ}$C) process during which fresh basaltic glass is hydrated and altered by seawater. The end result of the palagonitization is called palagonite as well as secondary minerals like zeolites and smectites. Palagonite is a term used very differently by various authors but it usually refers to a yellow-orange, amorphous material that appears isotropic or very nearly so in plane polarized light. Peacock (1926) was the first to perform a comprehensive petrographic study of palagonite and he distinguished two major varieties: gel-palagonite and fibro-palagonite. Gel-palagonite was described as a yellow, transparent, isotropic, clear, commonly concentrically banded material and fibro-palagonite as a yellow-brown, translucent, slightly anisotropic, slightly to strongly birefringent, fibrous, lath-like, or granular material. Fibro-palagonite has later been identified as smectite or poorly crystallized smectite and the term is therefore seldom used today (Zhou et al. 1992). Stroncik and Schmincke (2001) recommend that the term fibro-palagonite not to be used and that what has previously been called gel-palagonite should simply be called palagonite henceforth.

The mineralogical nature of palagonite is still poorly defined. Hay and Iijima (1968) proposed that palagonite is composed of montmorillonite and mixed-layer mica montmorillonite. Furnes (1984) suggested that palagonite consists of kaolinite, illite, mixed-layer clay minerals or zeolites. According to Honnorez (1981) palagonite is a mixture of altered, hydrated and oxidized glass with authigenic minerals (clays and zeolites). Palagonite has also been suggested to consist of some smectite variety and minor amounts of zeolites and oxides (Daux et al. 1994; Eggleton and Keller 1982; Staudigel and Hart 1983; Zhou et al. 1992). Since the final product

of palagonitization is a mix of palagonite and secondary phases it can be quite hard to distinguish specific minerals and phases. Usually, alteration rinds develop concentric to the glass surface reflecting different stages in the alteration process and different phases. An ideal cross-section of a glass shard that not is completely palagonitized should therefore consist from the center outward of (1) a fresh glass core, (2) palagonite, (3) smectite and (4) zeolites. This is, however, seldom the case. Different rinds representing various stages in the palagonitization occur as well as intermediate stages between different phases like palagonite and smectite. Honnorez (1981) went further and suggested that the term palagonite should be abandoned while retaining the term palagonitization to describe the alteration of glass.

In this paper we will follow Stroncik and Schmincke (2001) and use the term palagonite defined as the gel-like, amorphous, yellowish material that replaces glass. The term palagonitization will be used as the process in which glass is altered to palagonite.

Honnorez (1978) divided the palagonitization process into three different stages: initial, mature and final stage. The stages are distinguished by the presence or absence of glass or secondary minerals. The major secondary mineralization products of palagonitization are the zeolite species phillipsite and the clay species smectite. The three stages are defined as follows:

(1) **The initial stage** is characterized by the presence and abundance of unaltered basaltic glass. Occurrence of altered glass is rare and replacement of secondary minerals is absent at this point. Spaces between the glass shards, however, are filled with authigenic minerals.
(2) **The mature stage** is characterized by the alteration of all fresh glass. The residual glass begins to be replaced in situ by phillipsite and smectite. Altered glass is thus associated with both inter- and intragranular authigenic minerals.
(3) **The fina stage** of palagonitization is characterized by the almost complete alteration of the glass. The final material consists of an aggregate of authigenic minerals where inter- and intragranular phases cannot be distinguished from each other since the contours of the parent glassy granules have been obliterated. At this stage, the residual glass has been replaced almost completely by secondary minerals.

The three stages of the palagonitization process can be explained by the following two major reactions:

(a) Fresh glass + seawater → palagonite + intergranular authigenic minerals.
(b) Palagonite + sea water → intragranular authigenic minerals.

Walton et al. 2005 partly support this interpretation of the palagonitization process with some exceptions. They had the opportunity to study each stage of alteration in The Hawaii Scientific Drilling Project 2 Phase 1 Drill Core, since each step was separated vertically. The initial material in their samples is sideromelane, a variety of basalt glass that contains few quench crystals and appears transparent and light colored in thin section. The zone of palagonite formation in their samples

most closely matches the initial stage as defined by Honnorez (1978) with the exception that not only are pores filled with secondary minerals but the margins of glass shards are altered to palagonite and lined with smectite. Another difference is also that chabazite is the final product. The alteration follows the mineral progression described by Honnorez (1978) with smectite and phillipsite but end with chabazite. The zone of smectitic alteration in their samples resembles the mature stage of Honnorez (1978) with the exception that the grain replacing material is primarily smectite and titaniferous spherules, not zeolite. Another difference is that smectite alteration predates formation of characteristic features of the zone of palagonitic alteration, rather than following them. Phillipsite form in a late stage of alteration but chabazite is the final product. The basic reaction is summarized as follows:

sideromelane + components from pore waters
= palagonite + chabazite + components to pore waters

Walton and Schiffman (2003, 2005) concluded that the alteration was the result of at least four different processes: dissolution, biological attack producing reddened smectitic grain replacements, a (presumably abiotic) process producing green smectitic grain replacements, and the formation of palagonite.

The geochemical processes behind the palagonite formation are not fully understood, and different calculation methods related to element mobility have been proposed (Furnes and El-Anbaawy 1980; Staudigel and Hart 1983; Furnes 1984; Jercinovic et al. 1990; Walton and Schiffman 2005). In general, during the palagonitization process, Mg, Ca, K, P, Ba, Si, Al and Na are leached out of the glass and Fe and Ti are accumulated in the palagonite. The elements leached from the volcanic glass are precipitated as intergranular authigenic phillipsite and smectite, the two major secondary products of palagonitization. In the total rock K, Na, Mg are enriched and Ca is lost while Si, Ti, Al and Fe are unchanged except for the passive effects of other elements being enriched or depleted. This shows that a redistribution of most elements occurs during the process. The enrichment of K, Na and Mg is probably due to seawater contribution, and loss of Ca is probably due to Ca release to the seawater. The secondary products, phillipsite and smectite, probably work as traps for seawater K, Na and Mg.

The element distribution in the palagonite shows high local variability and uneven redistribution of the elements relative to the parental glass. In many cases, rinds with different chemical composition and texture are developed in the same glass shard due to different processes involving leaching and precipitation of elements at different stages of the palagonitization. The processes behind the dissolution and hydration of the original glass have been explained both by congruent dissolution (Crovisier et al. 1987) and by selective and partial dissolution (Berger et al. 1987). The most basic process for destruction of the volcanic glass is the dissolution of the Si-Al network, which requires high pH:s that exceed pH 8.

Thorseth and co-workers (1991) proposed a different evolutionary model that included several stages. The first step in the alteration process represents an incipient incongruent dissolution of the glass characterized by extensive loss of Ti, Fe, Mn, Mg and Na. Ca is the second most depleted element and Al the third.

Si becomes passively enriched during this stage. In the second step the residual material dissolves congruently producing a porous residue. To achieve extensive loss and to keep Fe, Al and Ti in solution the pH of the solution needs to be low, less than pH 3. In the final stages Si is dissolved which requires high pH and which leads to a high degree of destruction of the network and a high porosity of the material. At such high pH Fe, Ti and Al have low solubility and precipitate as hydroxides outside the leached zone in the pores. These different stages result in a zoning of the palagonite with different chemical composition and varied texture and porosity.

The model by Thorseth and co-workers (1991, 1992) requires pH variations from acidic to alkaline on a microscale (a few μm). Establishment of such local microenvironments with divergent pH conditions is difficult in a system with only circulating fluids. However, Thorseth et al. (1991) identified bacteria associated with the palagonite and the weathering pit-textures of glass and suggested a relationship between the palagonitization and bacterial activity. They proposed that the bacteria are able to create microenvironments with very local variations in pH. Depending on which bacterium is present the pH can be either low or high. At high pH the glass Si-Al network would suffer strong dissolution, and at low pH elements like Fe, Ti and Al would be kept in dissolution and removed from the local area. Laboratory experiments and further field observations have confirmed that microbial activity plays an important role in the alteration of volcanic glass and oceanic crust (e.g. Thorseth et al. 1992, 1995a, b; Torsvik et al. 1998; Staudigel et al. 1995; Walton and Schiffman 2003).

4 ODP Leg 197, Emperor Seamounts

During ODP Leg 197 three seamounts belonging to the Emperor Seamounts were drilled, Detroit, Nintoku and Koko Seamounts (Fig. 1). Emperor Seamounts is the oldest and northernmost part of the Emperor-Hawaiian volcanic hotspot track in the Pacific Ocean. During this leg four sites were drilled: Sites 1203 and 1204 on the summit of Detroit Seamount, Site 1205 on Nintoku Seamount and Site 1206 on Koko Seamount. The greatest depth was 954 m below seafloor (mbsf) and was drilled at Site 1204 (Tarduno et al. 2002). During this cruise fractured and veined basaltic rocks were collected to study the occurrence and abundance of sub-seafloor microorganisms. Table 1–4 is an overview of the samples used in this study.

The basalts collected during ODP Leg 197 are altered in varying degree and all three stages of palagonitization are represented in the samples. Volcanic glass occurs, both unaltered and altered as well as palagonite and the zeolite species phillipsite. Veins in less altered samples contain minor zeolites and are usually filled with carbonates. As the degree of alteration increases in the samples, the abundance of zeolites increases and the abundance of vein filling carbonates decreases. In the most altered parts, the veins are only filled with zeolites and almost completely lack carbonates. Such samples represent the final stage of palagonitization according to

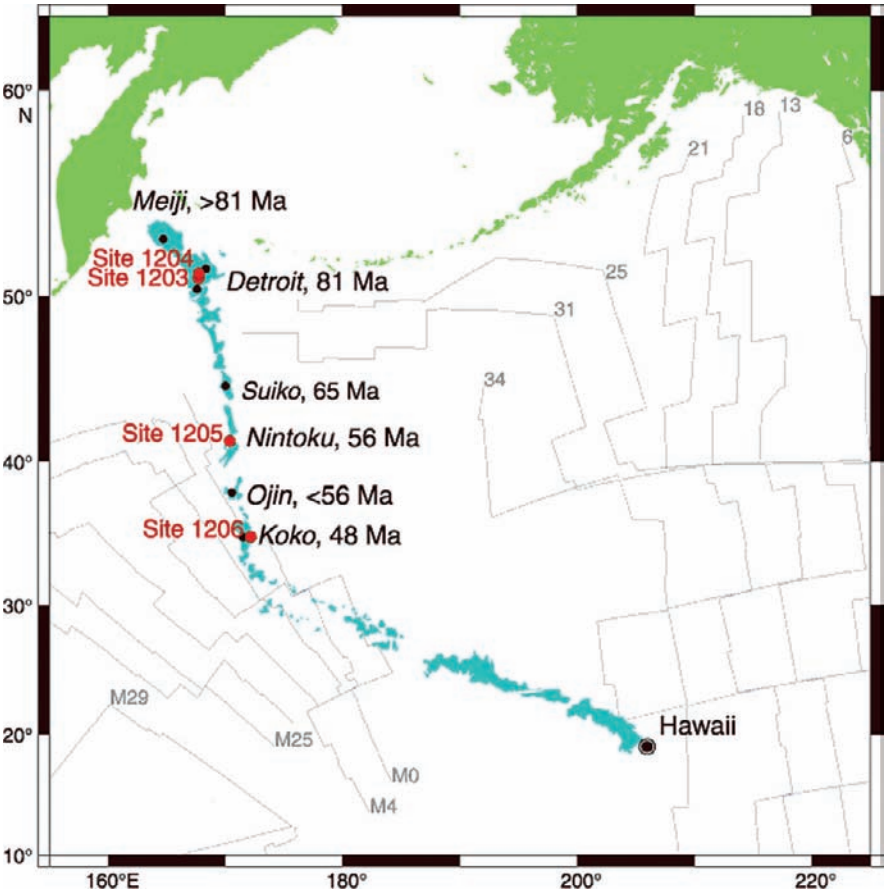

Fig. 1 Map showing the Emperor-Hawaiian hotspot chain with ages of the specific seamounts in black and the individual sites in red. From ODP

Honnorez (1978). Table 5 shows the general chemical composition of the minerals of interest in this study.

The different stages of alteration and palagonitization were studied to observe differences in the occurrence of microorganisms with regard to abundance, morphology and association with mineral surfaces. A variety of filamentous structures was discovered associated with different mineral surfaces and degree of alteration. Globular cell-like structures were also observed in a few samples. Sections 4.2–4.5 sum up the mineralogical niches where microfossils were found.

To establish a biogenic origin of these structures different methods like ESEM (Environmental Scanning Electron Microscope), EDS (Energy Dispersive Spectrometry), ToF-SIMS (Time of Flight Secondary Ion Mass Spectrometry) and PI (Propidium Iodide) staining were used as described in Section 4.1.

Table 1 Sample log for site 1203

Core, section, interval (cm)	Depth (mbsf)	Lava lobe	Methods	Vein minerals	Microfossil structures
1203A-18R-2, 72	466.02	Lobe interior	Microscopy, ESEM	Calcite, goethite	Sheaths, segmented filaments, globules
1203A-30R-1, 63	570.43	Lobe margin	Microscopy, ESEM, XRD	Calcite, phillipsite	Galleries, sheaths, segmented filaments, twisted filaments
1203A-36R-1, 37	618.70	Lobe margin	Microscopy, ESEM	Calcite	Segmented filaments
1203A-36R-2, 130	620.17	Lobe interior	Microscopy, XRD	Calcite	
1203A-41R-5, 0	671.85	Lobe base	Microscopy, ESEM	Calcite, phillipsite, goethite	Galleries, sheaths
1203A-42R-2, 125	678.25	Lobe interior	Microscopy, ESEM	Calcite, phillipsite	Sheaths
1203A-46R-6, 13	719.9	Lobe margin	Microscopy, XRD	Calcite, phillipsite, analcime	
1203A-49R-6, 22	739.13	Lobe interior	Microscopy, ESEM	Calcite, phillipsite	Sheaths
1203A-52R-2, 57	762.87	Lobe interior	Microscopy	Calcite	
1203A-52R-3, 40	764.14	Lobe interior	Microscopy	Goethite, calcite	
1203A-55R-5, 37	797.46	Lobe boundary	Microscopy, ESEM, XRD	Calcite, goethite	Sheaths
1203A-57R-3, 103	812.93	Lobe base	Microscopy, ESEM, ToF-SIMS	Calcite	Branched filaments, sheaths
1203A-65R-3, 40	878.90	Lobe interior	Microscopy, ESEM, XRD	Calcite, phillipsite, goethite	Sheaths, segmented filaments

4.1 Samples and Methods

Samples were selected with the aim of being as representative as possible and to cover as much variation among the samples as possible. Various parameters were considered during the selection process like depth, mineralogy, alteration, vein abundance, vein size and representation of all three seamounts. Since the study is focused on veins, samples containing veins were chosen over samples that lack veins. Thirteen samples from site 1203, six samples from site 1204, twelve samples

Table 2 Sample log for site 1204

Core, section, interval (cm)	Depth (mbsf)	Lava lobe	Methods	Vein minerals	Microfossil structures
1204A-7R-2, 30	821.25	Lobe interior	Microscopy	Calcite	
1204A-7R-4, 10	823.92	Lobe interior	Microscopy, ESEM, XRD	Calcite, Goethite, phillipsite	Segmented filaments, globules
1204B-2R-4, 115	824.95	Lobe interior	Microscopy, ESEM, fluorescence	Calcite, phillipsite	Globules
1204B-12R-1, 24	906.54	Sparsely veined diabase	Microscopy, ESEM	Calcite, goethite, phillipsite	Galleries, sheaths, segmented filaments
1204B-16R-1, 41	935.61	Hyaloclastite breccia	Microscopy, XRD	Phillipsite, garronite	
1204B-16R-1, 145	936.65	Hyaloclastite breccia	Microscopy	Phillipsite, calcite	

Table 3 Sample log for site 1205

Core, section, interval (cm)	Depth (mbsf)	Lava lobe	Methods	Vein minerals	Microfossil structures
1205A-5R-2, 60	34.48	Clast conglomerate	Microscopy, ESEM	Phillipsite, aragonite	Segmented filaments
1205A-6R-2, 53	44.33	Massive	Microscopy, ESEM	Aragonite	Galleries, amorphous filaments
1205A-14R-3, 82	84.82	Massive	Microscopy, XRD	Aragonite	
1205A-19R-4, 48	114.53	Sparsely veined	Microscopy, ESEM	Aragonite	Segmented filaments
1205A-21R-2, 2	130.69	Massive	Microscopy	Aragonite	
1205A-27R-3, 94	181.02	Sparsely veined	Microscopy, XRD	Phillipsite	
1205A-30R-1, 18	206.28	Massive	Microscopy, XRD	Aragonite, chabazite	
1205A-36R-1, 23	254.53	Massive	Microscopy, Raman, ESEM	Gypsum	Sheaths, segmented filaments
1205A-36R-2, 104	256.14	Lobe interior	Microscopy, ESEM, XRD	Chabazite, aragonite	
1205A-36R-7, 108	263.17	Massive	Microscopy	Aragonite, phillipsite	
1205A-42R-1, 117	293.97	Highly veined	Microscopy, XRD	Aragonite, chabazite	
1205A-42R-2, 48	294.78	Sparsely veined	Microscopy, XRD	Aragonite	

Table 4 Sample log for site 1206

Core, section, interval (cm)	Depth (mbsf)	Lava lobe	Methods	Vein minerals	Microfossil structures
1206A-5R-1, 114	76.24	Hyaloclastite	Microscopy, ESEM	Aragonite	Branched filaments
1206A-15R-2, 119	130.89	No information/massive	Microscopy, XRD	Aragonite	
1206-16R-3, 67	136.66	No information/highly vesicular	Microscopy, XRD, ESEM	Aragonite, goethite	Segmented filaments
1206A-17R-1, 33	143.13	Lobe boundary	Microscopy	Aragonite, phillipsite	
1206A-18R-1, 104	153.44	Lobe interior	Microscopy, ESEM	Aragonite, phillipsite	Sheaths
1206A-21R-5, 95	178.68	Lobe base	Microscopy, fluorescence	Aragonite, phillipsite	Globules
1206A-24R-4, 123	198.36	Lobe interior	Microscopy, ESEM	Aragonite, phillipsite	Sheaths
1206A-26R-3, 39	213.42	Lobe boundary	Microscopy, XRD	Aragonite, phillipsite	
1206A-29R-3, 16	232.63	Lobe interior	Microscopy, XRD	Aragonite, phillipsite	
1206A-30R-2, 7	240.77	Lobe base	Microscopy, ESEM, Fluorescence	Aragonite, phillipsite	Sheaths, globules
1206A-37R-3, 72	295.13	Lobe interior	Microscopy, ESEM, ToF-SIMS, fluorescence	Aragonite	Sheaths, segmented filaments, globules
1206A-40R-1, 38	306.88	Lobe interior	Microscopy	Aragonite	
1206A-40R-3, 21	309.32	No information/highly vesicular	Microscopy, XRD	Phillipsite	

from site 1205 and thirteen samples from site 1206 were chosen. The samples were prepared as doubly polished thin sections due to their advantages in microfossil studies over ordinary thin sections (Ivarsson 2006). Properties like greater thickness ($\sim$150–200 μm) and the possibility to view the samples from both sides result in advantages such as better visibility, better light conditions and an increased three-dimensional view compared to ordinary thin sections. These are essential tools in the study of morphology, microfossil assemblages and association with the substrate that the microfossils are attached to. Samples with different mineralogy and from different depths were selected to get an overview of the main occurrence of putative fossilized microorganisms and, if possible, to observe any variations in occurrence, types or habitats. The mineralogy of the veins was studied to determine

Table 5 Table showing EDS data for the minerals discussed in this paper. The data is given in wt%

Elements	Volcanic glass (1203A-30R-1, 63)	Altered basalt (1203A-65R-3, 40)	Altered basalt (1206A-24R-4, 123)	Calcite (1204A-7R-4, 10)	Phillipsite (1204A-7R-4, 10)	Fe-Oxide (1204B-12R-1, 24)	Fe-oxide deposited on a filament (1204B-12R-1, 24)
C	–	–	–	7.89	–	–	25.42
O	35.60	40.17	41.99	46.66	51.17	47.08	18.28
Na	–	2.45	3.00	–	4.48	–	–
Mg	0.75	6.81	4.92	–	–	–	3.76
Al	6.25	6.83	9.05	–	10.99	2.08	5.73
Si	37.59	26.91	24.52	–	28.97	3.20	16.01
K	4.52	–	–	–	4.39	–	3.52
Ca	4.73	8.66	7.27	45.45	–	–	–
Ti	–	–	1.06	–	–	–	–
Fe	10.55	8.17	8.20	–	–	47.64	27.28
Total	100.00	100.00	100.00	100.00	100.00	100.00	100.00

what material the microfossils are embedded in. The degree of alteration of the host rock as well as the vein filling minerals was studied to know where it would be easiest to detect unaffected microfossils. Higher degree of alteration can result in less preserved microfossils.

In some samples with high abundance of filament-like structures, two thin sections were prepared for different analytical methods. ToF-SIMS, for example, cannot be performed on samples that have been used in ESEM because the electron beam in ESEM dissociates adsorbed molecules on the sample surface. This effect can result in a disturbed surface monolayer. During the preparation of the thin sections precautions were taken to limit the risk of contamination as much as possible. Water was used both during the sawing and polishing and the samples were not heated. Epoxy was used during the preparation process.

The thin sections were not treated with chemicals before ToF-SIMS and ESEM analyses due to the risk of dissolving organic material in the filaments. They were only kept in boxes and exposed to the atmosphere as little as possible. They were also never touched with ungloved hands and only handled with forceps made of stainless steel. Efforts were made to avoid introduction of extraneous fluorescent particles (e.g. threads or dust).

Minerals were identified by a combination of microscopy, Raman spectrometry and ESEM. Fossilized microorganisms were studied by a combination of microscopy, ESEM and ToF-SIMS.

The ESEM analyses were performed using a Philips XL 30 ESEM-FEG which is a field emission microscope. EDS analyses were performed using a Philips EDAX (Energy Dispersive Analysis of X-rays) instrument. The samples were subjected to a pressure of 0.5 torr and the accelerating voltage was 20 kV. The EDS analyses were performed by standardless quantification. The point detection of the EDS instrument on subjects in the size range of the fossilized filaments, which never are less than 1 μ, is very precise and the measurements are not mixed with the surrounding minerals. The element mapping was performed during a period of 12 h.

The Raman microprobe measurements were performed using a HORIBA JOBIN YVON LabRam-HR equipped with an OLYMPUS BX41 optical microscope and Si-based charge-coupled device (CCD) detector. Spectra were excited with the He-Ne 632.8 nm line and a 514.5 nm line of an argon ion laser. The laser power was decreased to 0.7 mW (measured at the sample surface) to exclude potential local upheating effects due to heavy light absorption. The wavenumber accuracy was $\pm$ 0.5 cm^{-1}, and the spectral resolution was about 0.8 cm^{-1}.

The ToF-SIMS analyses were performed using a ToF-SIMS IV (ION-TOF GmbH Germany), equipped with Bi_n^+ and C_{60}^+ cluster ion sources. All analyses were done using keV Bi_3^+ primary ions.

The fluorescence microscopy was performed using an OLYMPUS Vanox epifluorescence microscope, and the samples were stained with Propidium Iodide (PI). PI is a dye that binds to cells with damaged membranes and indicates dead bacteria and traces of DNA (Tobin et al. 1999). The disadvantage of using PI is that its potential to bind with minerals has not been systematically studied. However, the

thin sections were examined with fluorescent microscopy before staining to determine that no native fluorescence occurred in the regions of interest.

Each thin section was rinsed with 70% ethanol for 30 min before staining. The thin sections were then stained with PI (1.0 mg/mL solution in water) and exposed to the dye for 30–60 min. After exposure to PI the thin sections were rinsed repeatedly by phosphate buffered saline solution before they were studied under fluorescent microscope. To be able to penetrate cavities and fractures in the minerals the samples were pressurized in cycles between 1.5 and 0.3 torr in ESEM. By this method the PI stain was forced into zeolite fractures. Thin sections were also treated with HCl in some cases to dissolve the calcite and more easily reach the fossilized microorganisms. However, the microfossils were not entirely exposed. The purpose of the HCl treatment was to produce cracks and fractures in the thin sections that the dye could use to penetrate down to the microfossils. All steps of preparation took place before staining. The samples that were treated with HCl were also pressurized in cycles during washing to remove unbound stain.

4.2 Tunnel Structures in Volcanic Glass

Thin, threadlike tunnels with an undulating appearance were found in the basaltic glass (Fig. 2A and B). These tunnel-like textures extend perpendicularly to the vein walls, from the glass surface and inwards into the glass. They occur in abundance and usually extend in both directions from the vein boundaries, giving the veins a "hairy" appearance. The tunnels are between 2 and 5 μm thick and can vary in length from ~20 to ~200 μm. Most commonly they are somewhere between 100 and 200 μm in length. They are characterized by subdivided internal textures that in several cases make the tunnels look as though they consist of individual segments (Fig. 2B). Most tunnels end with an almost round and much thicker part compared to the rest of the tunnels.

EDS analyses show that the C content in the galleries range between ~10 and ~40 wt% C (Table 6) and element mapping shows that the C is not bound in carbonates (Fig. 3A). Minor amounts of Al, Mg, Si, Na, K, Ti and Fe also occur, probably as traces from the host rock.

4.3 Fossilized Filaments Attached to Altered Basalt and Altered Volcanic Glass

In contrast to the tunnel-like textures that extend into the volcanic glass, fossilized filament-like structures attached to the volcanic glass are found in several samples (Fig. 4). These filament-like microstructures are usually attached with one end to the volcanic glass of the vein walls and with the rest of the filament embedded in the secondary vein filling minerals like calcite, aragonite or gypsum. Some filament features are attached with both ends to the volcanic glass. Usually, the filament

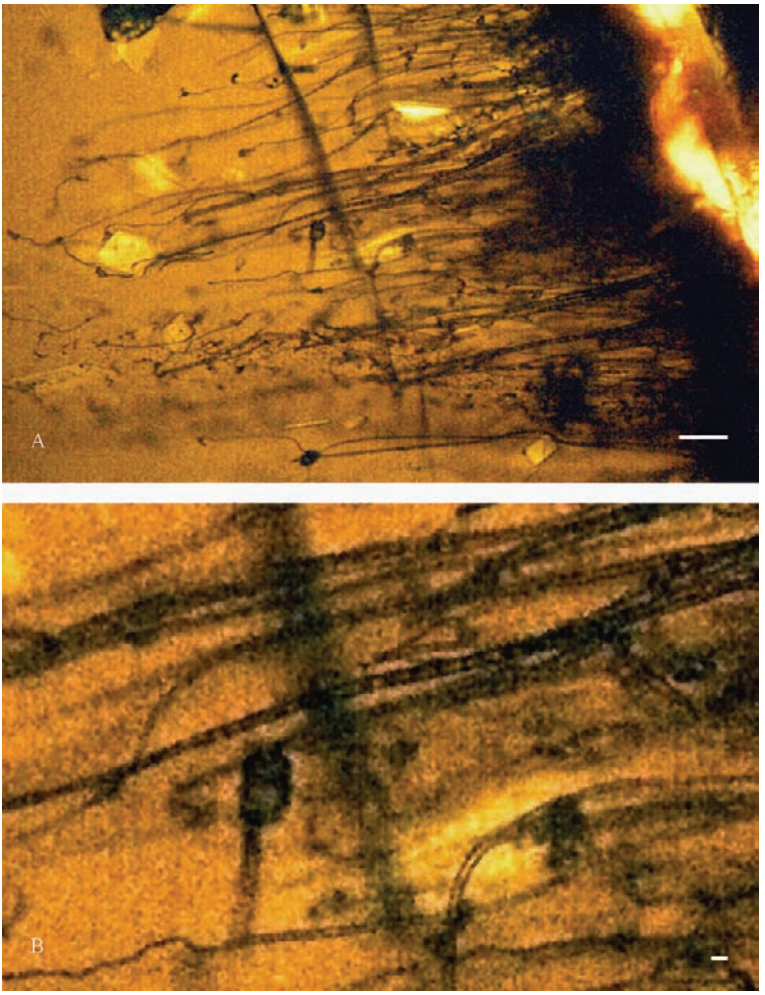

Fig. 2 Microphotographs obtained with transmission light microscope showing tunnel structures in volcanic glass from sample1203A-30R-1, 63. **Picture A** show several tunnel structures emerging perpendicular from a vein and into volcanic glass. **Picture B** is a close up showing the segmented internal structure of the tunnels. The scale bar in picture A is 10 μm and in picture B 1 μm

structures have a "worm-like", smoothly curved appearance and are ~10–100 μm long and ~2–10 μm thick.

The filamentous microstructures vary greatly both in appearance and size. They were divided into five different types according to morphology: sheaths, segmented filaments, amorphous filaments, twisted filaments and branched filaments. Sheaths are made up of hollow, tube-like filamentous structures that resemble one thinner tube inserted into a thicker one (Fig. 4A). This type is typically attached to volcanic glass at both ends as opposed to the other classes which are attached only at one

Table 6 Table of EDS data showing the chemical composition of tunnel-structures, filaments attached to both altered basalt and phillipsites, globules attached on phillipsite and biofilm occurring on the surfaces of som phillipsites. The data is given in wt%

Elements	Tunnel-structure in glass (1203A-30R-1, 63)	Tunnel structure in glass (1205A-6R-2, 53)	Filament, sheath (1206A-18R-1, 104)	Filament, segmented (1204B-12R-1, 24)	Filament, amorphous (1205A-6R-2, 53)	Filament, twisted (1203A-30R-1, 63)	Filament branched (1203A-57R-3, 40)	Filament attached to zeolite (1206A-37R-3, 72)	Globule (1206A-37R-3, 72)	Globule (1206A-30R-2, 7)	Biofilm (1206A-30R-2, 7)
C	12.03	36.13	50.42	40.95	9.53	24.70	51.39	41.28	42.46	50.42	59.08
O	41.38	30.63	18.28	23.68	34.86	33.60	23.09	15.68	21.21	18.28	24.08
Na	1.64	1.09	0.44	0.71	–	1.03	–	–	–	–	–
Mg	4.67	3.28	3.76	0.79	1.44	2.37	4.74	8.36	2.12	3.76	–
Al	7.93	5.75	5.73	1.12	1.84	3.74	1.72	1.47	2.65	5.73	–
Si	21.60	17.04	16.01	2.58	4.45	16.75	8.32	20.33	16.17	16.01	–
K	1.37	0.99	1.71	–	–	2.54	–	0.89	3.98	3.52	–
Ca	–	–	1.37	1.39	1.84	–	3.49	–	–	–	16.84
Cl	–	0.66	–	0.77	0.54	–	–	–	–	–	–
Ti	2.54	–	–	0.69	1.09	–	–	–	–	–	–
Fe	6.84	4.42	2.28	27.32	44.42	15.28	7.26	11.99	11.41	2.28	–
Total	100.00	100.00	100.00	100.00	100.00	100.00	100.00	100.00	100.00	100.00	100.00

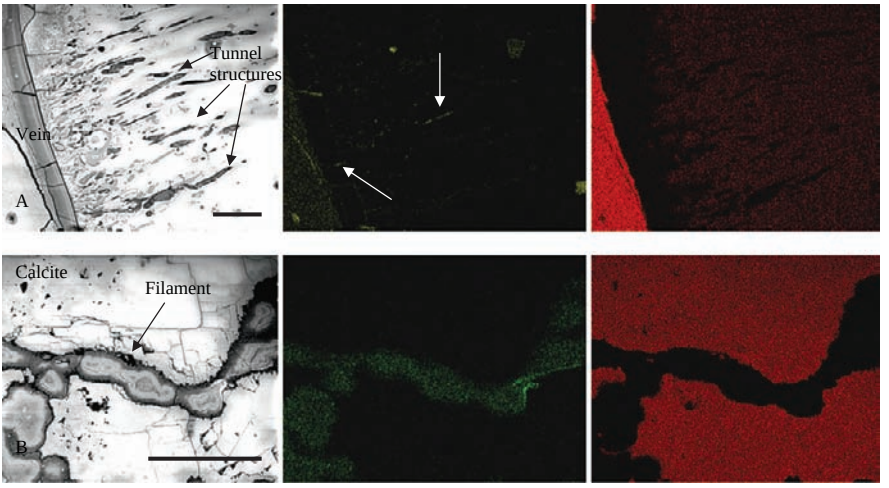

Fig. 3 Element mapping by EDS. ESEM microphotograph to the left, carbon distribution in the middle (*green*) and calcium distribution to the right (*red*). **A**: (1203A-30R-1, 63) Tunnel structures in volcanic glass. To the left in the picture is a vein filled with calcite or clay from which the tunnels are emerging. White arrows indicate carbon enriched in tunnel structures. **B**: (1203A-57R-3, 103) Filament in calcite. Scale bars are 5 μm

end. This is also the most common kind. Segmented filaments resemble the previous type but lack the consistent tube shape. Instead, they consist of individual segments making up a long filament (Fig. 4B). This seems to divide the filament in individual divisions or segments that are connected to each other. Amorphous filaments are microstructures with no visual inner texture (Fig. 4C). The only characteristic feature is a thicker, spherical end at the top of the filament like a bean on a stalk. Twisted filaments are the least common type. It only occurs in one single sample (Fig. 4D). It resembles the first two types in shape but lacks the tube-like outline as well as the segments. Instead, the filaments are twisted in a screw-like fashion. Branched filaments consist of a group of filamentous structures that branch off from each other creating a complicated network. These filaments are abundant where they occur and occupy considerable space. In some samples they fill a whole vesicle or parts of veins (Fig. 4E).

All the filament-like structures occur together in accumulations and very seldom as single features (Fig. 4F). Commonly they occur in thin veins, a couple of mm thick, inside volcanic lobes where veins are sparse. In brecciated, heavily altered samples where veins are wider and much more common, the filaments are absent. The filament-like structures are also closely associated to globular Fe-oxyhydroxides. In some samples, iron-oxides are attached or assimilated onto the filaments (Fig. 5A and B).

The filamentous structures are all relatively similar in chemical composition and dominated by carbon and iron contents. The carbon content varies between different filaments from ∼10 wt% to ∼50 wt% (Table 6). The iron content is also highly

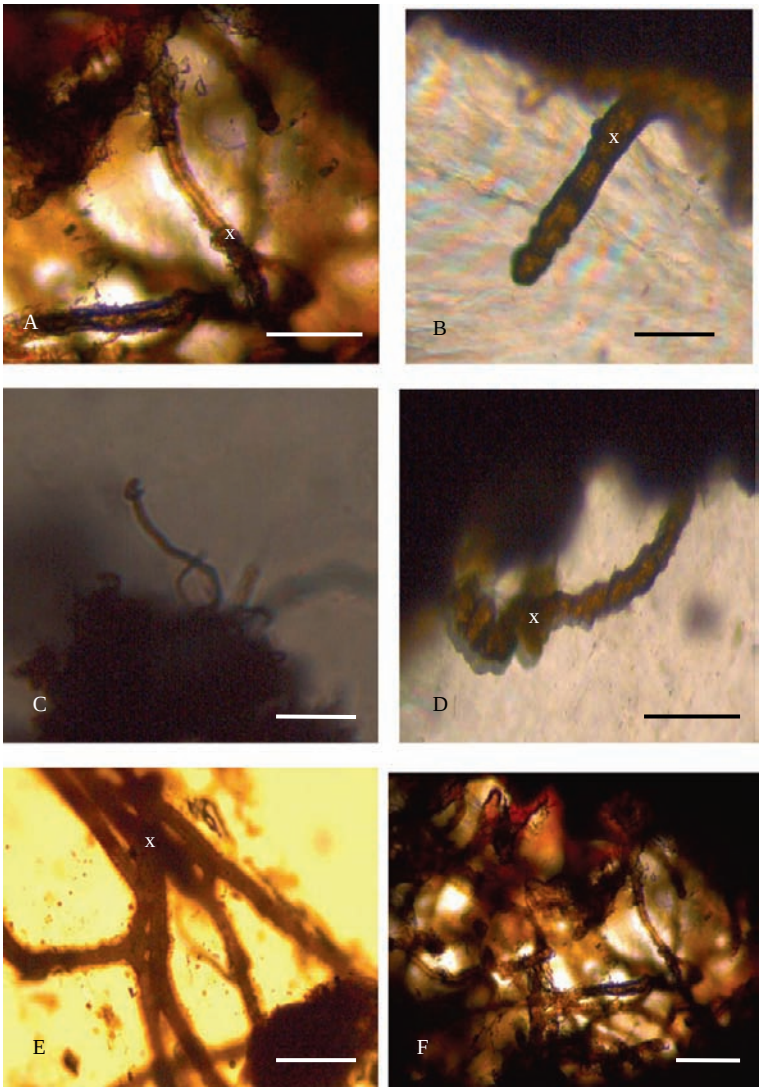

Fig. 4 Microphotographs obtained with transmission light microscope showing the different types of fossilized filaments according to morphology. **A**: sheaths (1206A-18R-1, 104), **B**: segmented filament (1204B-12R-1, 24), **C**: amorphous filament (1205A-6R-2, 53), **D**: twisted filament (1203A-30R-1, 63), **E**: branched filaments (1203A-57R-3, 40) and **F**: Colony of microfossils (1206A-18R-1, 104). The light mineral in which the filaments are embedded is calcite/aragonite and the dark material that they are attached to is basalt/altered basalt. Scale bars in A-E are 5 μm, F are 10 μm. X marks the analysis point. In C the X is removed because it blocks the view of the morphology. However, the analysis was performed on the top of the filament

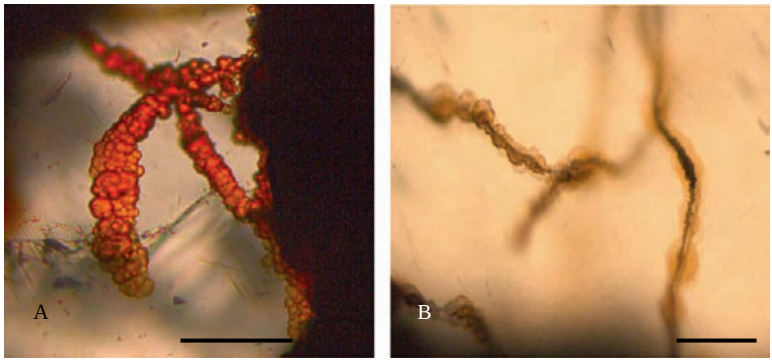

Fig. 5 Microphotograph showing Fe-oxyhydroxides deposited onto filamentous structures. **A**: (1204B-12R-1, 24) In **B** (1203A-49R-6, 22) it is possible to see the original filament in the middle and globular Fe-oxides precipitated on the surfaces. Table 1 show the chemical composition of the Fe-oxides on the filamentous structure. Scale bars are 10 μm

varied with contents from only a couple of weight percent to up to ~50 wt%. There are also variations in elements like Si, Al and Mg between a couple of wt% up to ~20 wt% as well as minor variations of a couple of wt% in Ca, K, Cl and Ti. Element mapping demonstrate that the C is not bound in carbonates (Fig. 3B).

Figure 6 shows ion images for C_2H_4, Fe and PO_3 from the ToF-SIMS analysis performed on sample 1206 37R3, in which these signals are concentrated at the spot where a filament structure reaches the surface. The corresponding spectra from this spot (Fig. 7) show a distinct signal from a molecule with mass 783.6 u (atomic mass unit), appearing as protonated/deprotonated molecular ions at 784.6 and 782.6 u, respectively. The peak patterns for these signals are similar to that typically seen for lipids. We have, however, not yet been able to identify the molecule in question.

4.4 Fossilized Globules and Filaments Attached onto Zeolite Surfaces

Small, globular microstructures, ~1–2 μm in size, are found attached to zeolite surfaces and embedded in calcite (Fig. 8). These features appear in abundance and have a reddish appearance under the microscope. They can sometimes cover the whole outer surface of a border of fan-shaped phillipsites and give it a red color. In microscopy the globules appear to be connected by a thin film that goes along the surface of the phillipsites (Fig. 8C). It usually appears as if the film is attached to the zeolite surface and that the globules are concentrated within this film. The globule itself is, thus, not always attached to the zeolite surface but incorporated in the film that is attached to the mineral surface.

The chemical composition of the globules is rather uniform, but it is worth noting the carbon content of the globules that ranges between ~10 and 50 wt% (Table 6) compared to ordinary globular iron-oxides that contain no C at all (Table 5). The

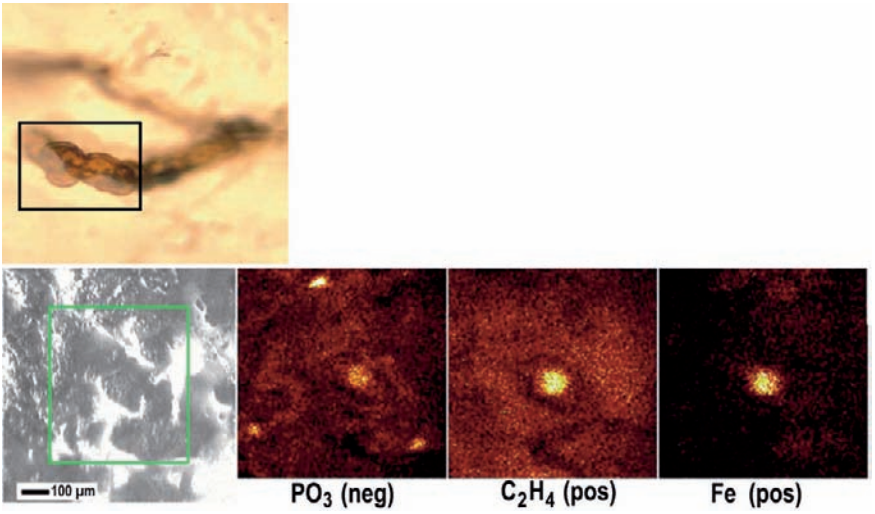

Fig. 6 ToF-SIMS video microscope image of analysed area (*green rectangle*) on sample 37R3, and the corresponding secondary ion images (field of view = 500 × 500 µm) for PO_3- (diagnostic ion for phosphates), $C_2H_4^+$ (fragment ion from organic molecules), and Fe. The negative ion images is slightly misaligned with respect to the positive ion images, but comparison with the overall structure of the images shows that the three depicted substances are co-localized in the middle of structure indicated in the video image. The square in top picture shows the surficial part of the filament

globules further have an iron content between ~3 and 20 wt%. Fluorescence microscopy showed that PI binds to the globules (Fig. 8D).

Ordinary iron-oxides found throughout the samples show features that differ from the globules found on the zeolite surfaces. The iron oxides occur most frequently associated with altered basalt and rarely with zeolites. The iron oxides occur in accumulations of several hundred globules and seldom as single features. They contain no C at all and do not bind to PI.

The chemical composition of the film found on zeolite surfaces is characterized by a carbon content of ~50 wt% C. The area where this film appears is at the border between the phillipsite and the calcite, and it is therefore highly influenced by the calcite. This is shown by a varying content of calcium. However, the carbon content is always much higher than the calcium content in comparison to the calcite where it is the other way around. In some cases PI binds to the film.

In rare cases filament-like structures associated with the zeolites occur (Fig. 9). These fossilized filament-like structures are usually attached to the zeolite surfaces with one end and stretches out into the vein where they are embedded in the calcite. In some cases the filament-like structures reach from one side of a vein to the opposite side where they are attached with their second end to the zeolites. The filament structures appear to originate from cracks and wedge-like cavities in the zeolites (Fig. 9C). The filaments are relatively long, ~100–200 µm in length, ~5 µm thick,

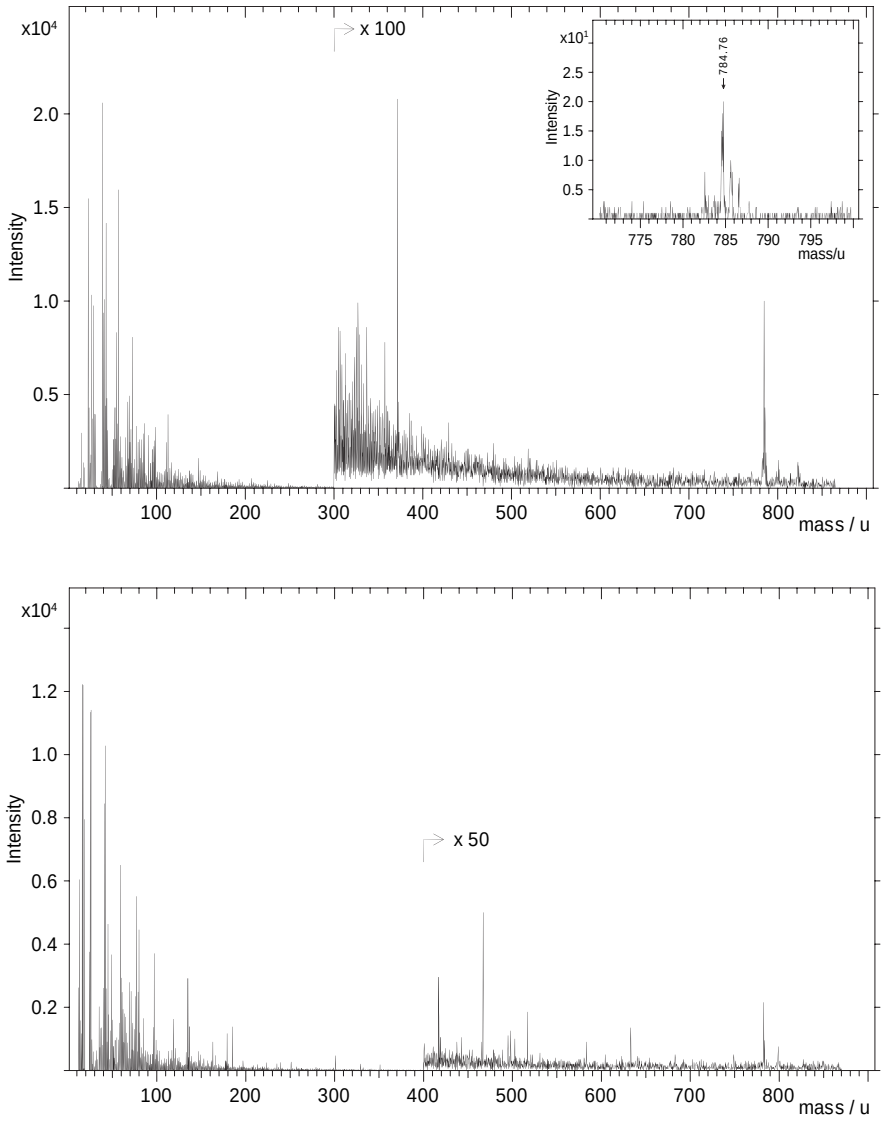

Fig. 7 Positive (*upper panel*) and negative (*lower panel*) secondary ion mass spectra from sample 37R3. The spectra were extracted from the area showing high Fe and C_2H_4 signals intensities in the ion images in Fig. 6. The peak cluster at 784 u (inset, upper panel) shows a pattern that is typical of lipids

and have an undulating appearance. It is possible to distinguish a segmentation of the filament-like structures and they are, just like the globules, reddish in appearance.

The chemical composition of the filament-like structures is very similar to the chemical composition of the globules. It is interesting to note the carbon content that is ∼40 wt% C (Table 6). PI binds to surficial parts of the filaments (Fig. 9D).

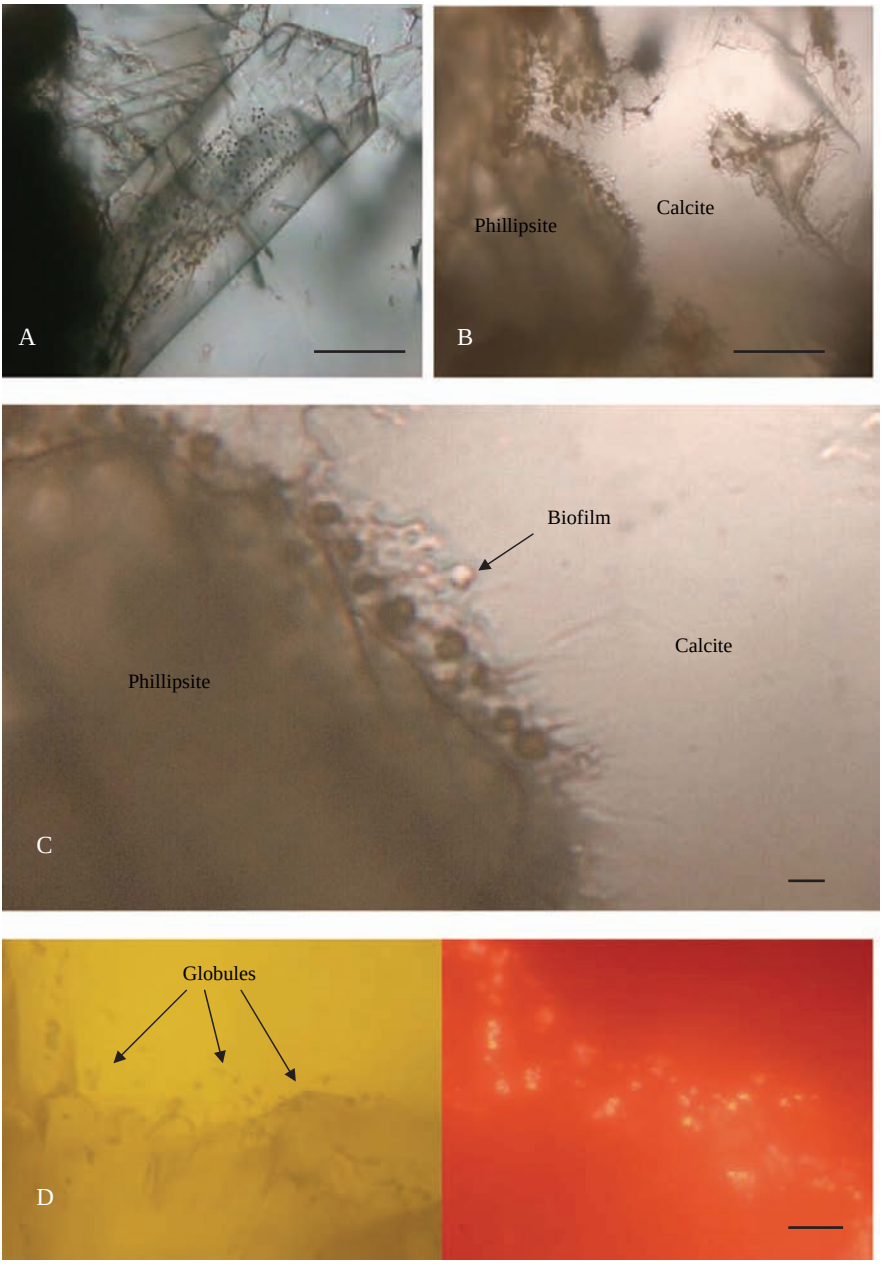

Fig. 8 Microphotographs obtained with light microscope showing the general occurrence of globular micro-structures associated with phillipsite surfaces. **A**: (1204B-2R-4, 115). In **B** (1206A-37R-3, 72) it is possible to see the biofilm along the phillipsite surface. **C**: (1206A-37R-3, 72) Close-up of the globules and the biofilm in which the globules are concentrated. **D**: (1206A-21R-5, 95) Fluorescence. Globules associated with the phillipsite surface and concentrated in a biofilm. Pictures on the left side show prior to staining with PI. Pictures on the right hand show after staining with PI and with fluorescence. Scale bar in A: 50 μm, in B and D: 10 μm and in C: 1 μm

Furthermore, the presence of globules and filamentous structures on phillipsite surfaces are accompanied with a marked increase in weathering of the zeolite surfaces (Fig. 10A). Where globules are present the mineral surface is characterized by circular holes and depressions, ~1 μm in diameter. Phillipsites lacking globules have a smoother surface without cavities. They can, however, have a thin alteration zone parallel to the mineral surface (Fig. 10B).

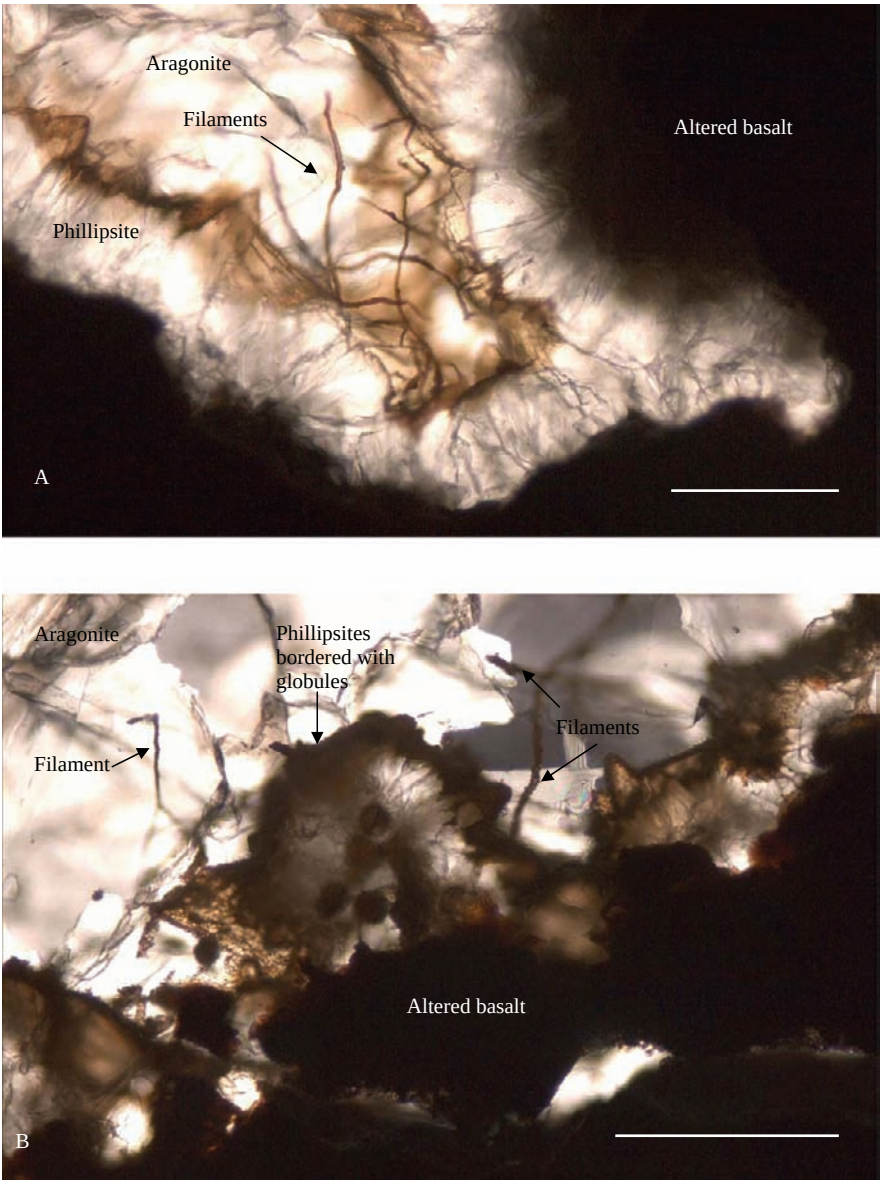

Fig. 9 (continued)

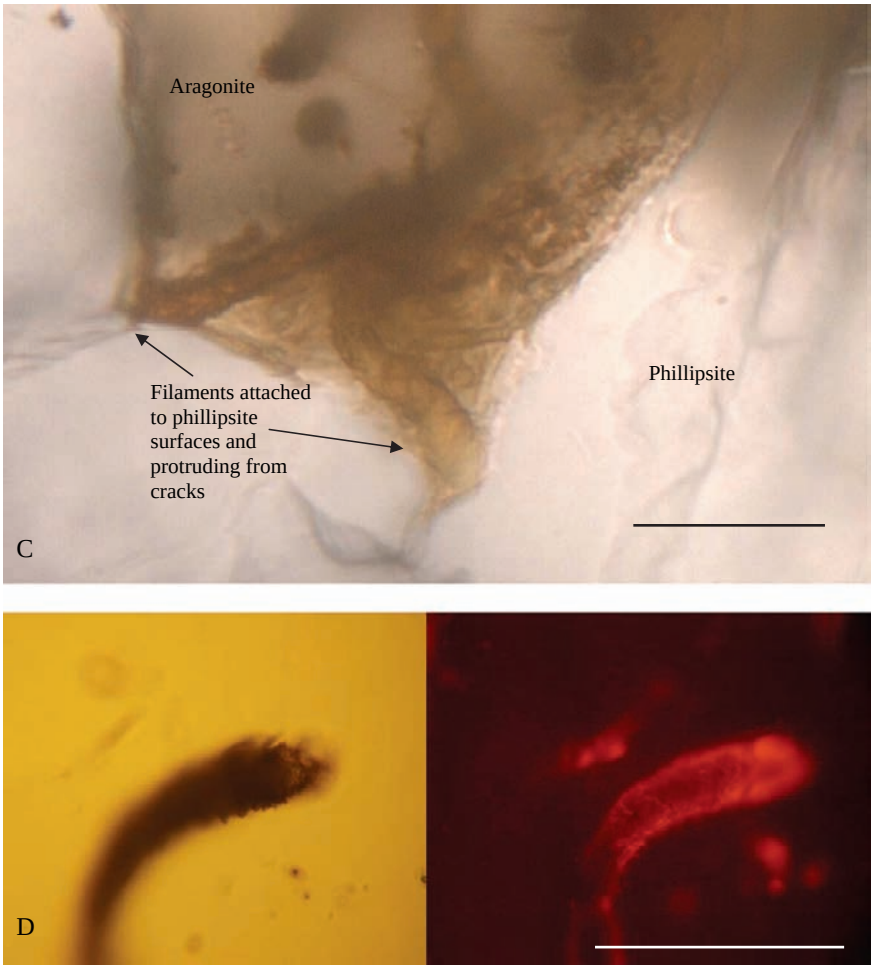

Fig. 9 (1206A-37R-3, 72). **A–C**: Pictures showing fossilized filaments attached to phillipsite surfaces. In A it is possible to see how some filaments stretch from one vein side to the other. **C**: Close up on the base of the filaments attached to phillipsite surfaces. Note how they appear to originate from cavities and fractures. **D**: Fluorescence. Left picture show prior to staining with PI and right picture show after staining with PI and with fluorescence. Scale bars in A and B: 100 μm. Scale bar in C: 10 μm. Scale bar in D: 5 μm

4.5 Fossilized Globules in Zeolite Cavities

Phillipsite crystals can appear as single crystals along the vein walls or in minor assemblages of single crystals. However, in more altered zones these single crystals cluster to fan-shaped or rosette-like assemblages with several hundred individual crystals together (Fig. 11A). In the center of such an assemblage the crystals appear to be rather massive and intergrown, and it is difficult to single out one individual

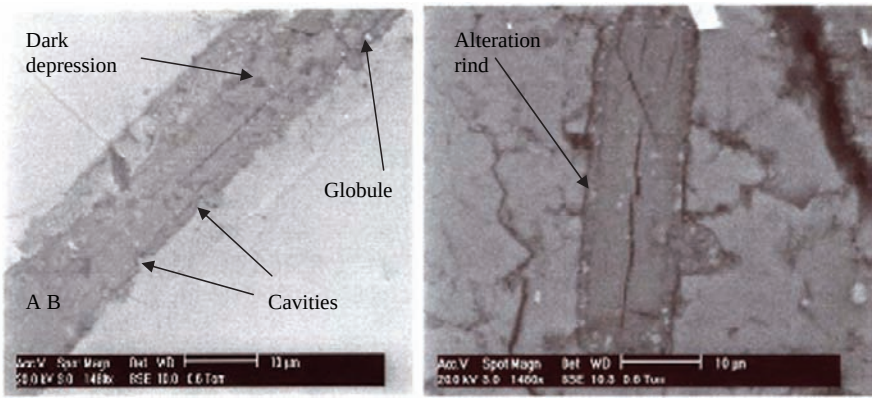

Fig. 10 (1204B-2R-4, 115) ESEM pictures showing the different degree of weathering due to presence of globular structures on the surfaces. **A** show a highly weathered phillipsite crystal with a surface deformed by depressions and cavitities (dark patches). The white dots are globules still attached to the surface. **B** show a phillipsite crystal that has not been subject of microbial weathering. The rind parallel to the mineral surface is an alteration zone, most likely abitocally produced

crystal. Farther out in the assemblages, however, the crystals separate from each other and at the outer limit each single crystal points out as a needle, giving a thorny appearance to the whole "phillipsite rosette". In between these crystals wedge-shaped cavities occur. These wedges have an orifice width of ~2–7 μm and become less wide toward the bottom of the cavity. The length of the wedges varies but is usually about ~10 μm. The wedges are sometimes empty but more often filled or partly filled with minerals. In some cases these wedges are filled with the overall vein mineral that usually is calcite or aragonite, but in many cases they are filled with iron oxides. These iron oxides were identified by Raman spectrometry to consist of both goethite and hematite (Fig. 12). A characteristic feature of these iron minerals is that they have a globular nucleus in the middle (Fig. 11). These globules resemble those found attached onto the zeolite surfaces. Usually the globules occur as single features in the bottom of the wedges or attached on one side of the inner walls, surrounded by an iron phase. The abundance of these sorts of features varies but in many cases every second cavity is partly filled with some iron oxides containing a globular structure. Phillipsites containing a considerable amount of iron oxides have a red-yellowish appearance visual to the eye. The globules found in wedges do, just like the globules attached on the phillipsite surfaces, bind to PI (Fig. 11C).

4.6 Alteration Zones

Most surfaces of altered glass and basalt are characterized by parallel alteration rims towards the veins (Fig. 13). These alteration rims reflect different alteration processes in the basalt where various elements either are leached or precipitated at different intervals. The elements Si, Al, Na, Mg, K, Ti, Ca and Fe vary with

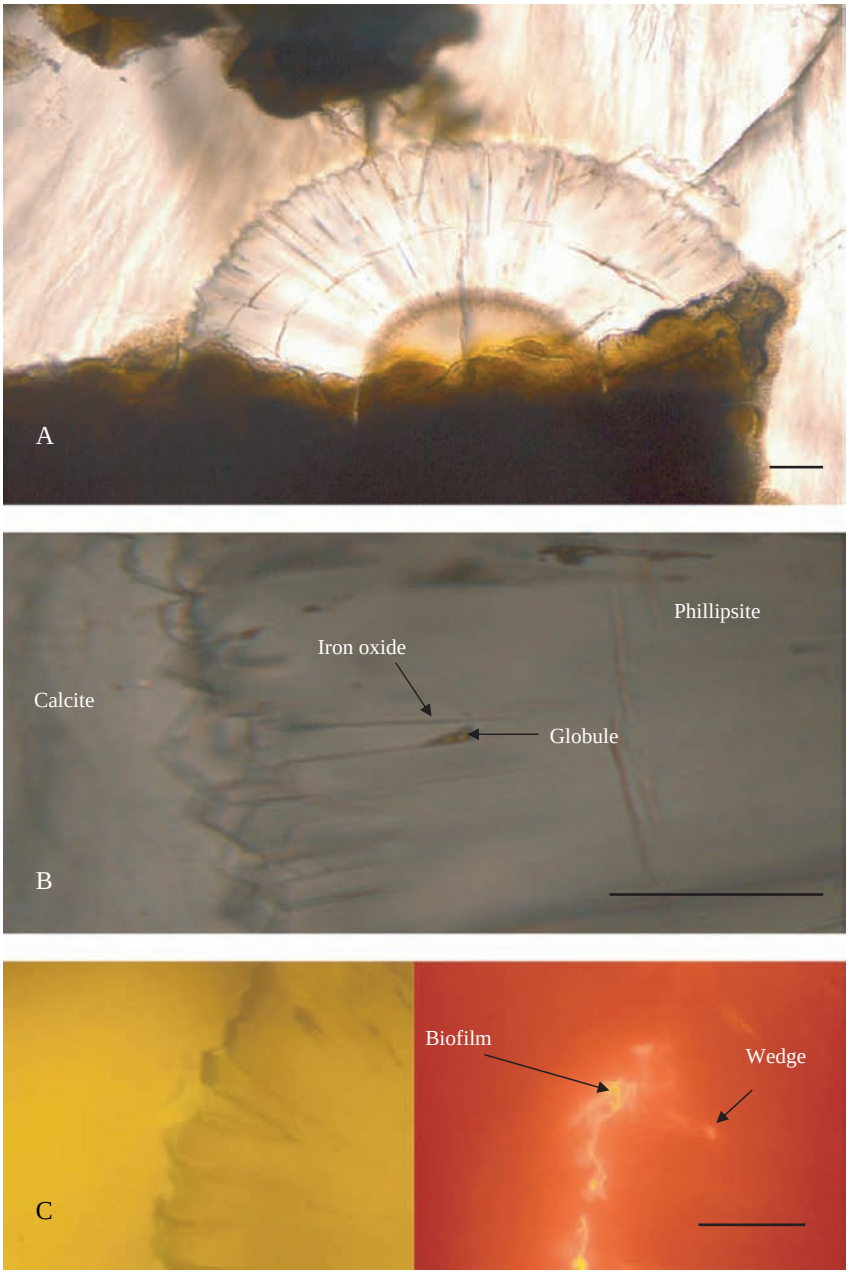

Fig. 11 Microphotographs of zeolites obtained with light microscope. **A** (1206A-21R-5, 95): Fan-shaped phillipsite assemblage. **B** (1206A-21R-5, 95): Wedge-shaped cavities in phillipsite with globules and iron oxides. Note how the globules and iron oxides are concentrated to the bottom of the wedges. **C** (1206A-21R-5, 95): Fluorescence. Pictures on the left side show prior to staining with PI. Pictures on the right hand show after staining with PI and with fluorescence. Globules both on the surface and in the wedge. Note how the film along the zeolite surface fluoresce as well. Scale bars: 10 μm

respect to each other in between these zones. Surfaces onto which filamentous structures are attached differ in composition compared to structures where no filamentous structures are attached (Table 7). At surfaces where filaments are attached, the concentration of the elements Si, Al and Na decrease toward the veins and Mg increases toward the veins. The elements K, Ca and Ti do not show any strong trend.

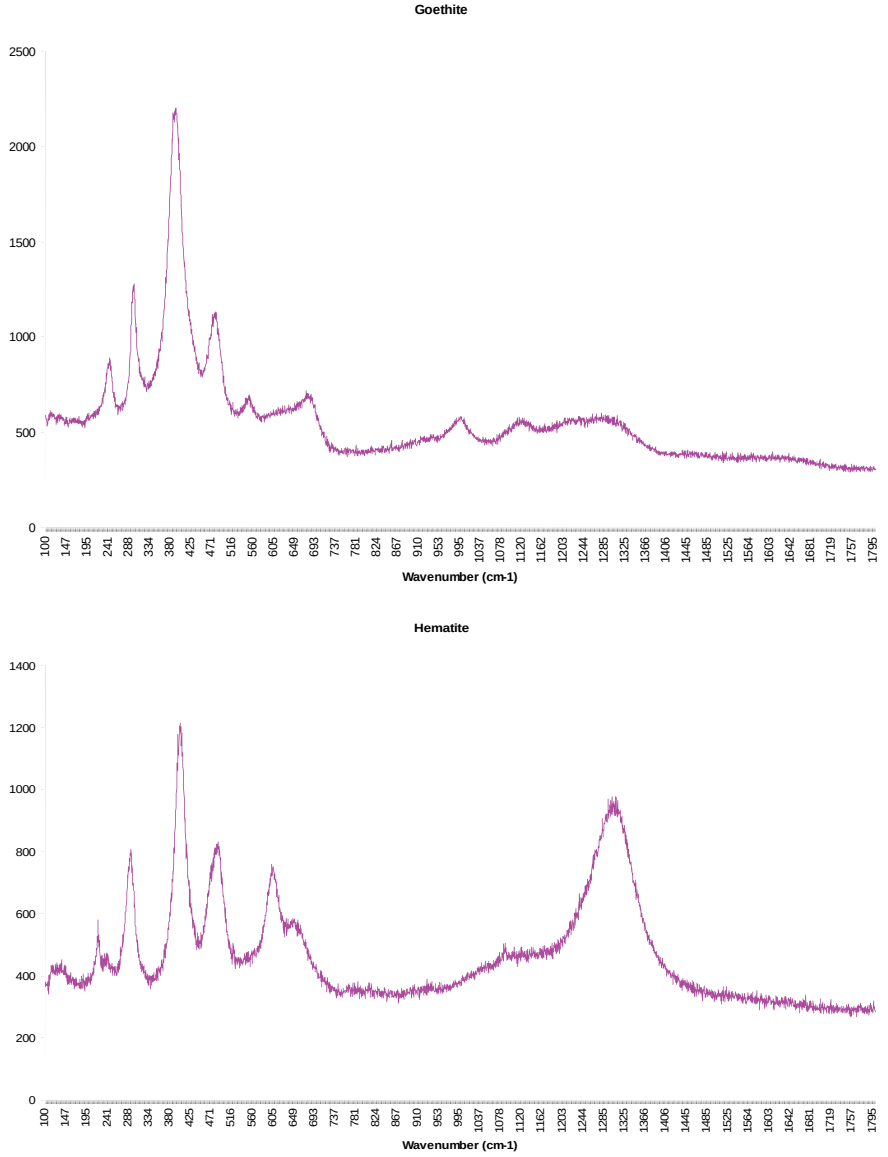

Fig. 12 (continued)

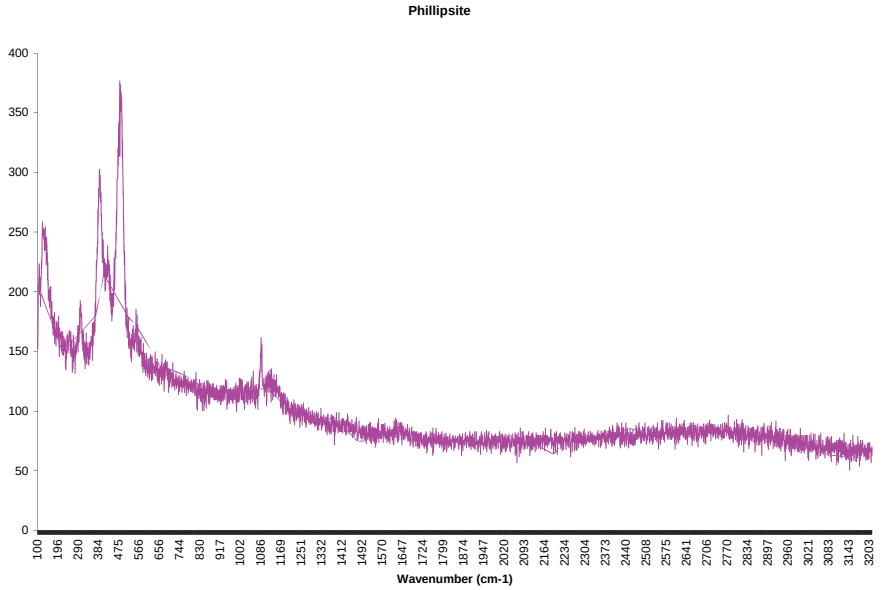

Fig. 12 Raman spectra of goethite and hematite from mineral inclusions in wedge-shaped cavities in phillipsites as well as a spectra of the host mineral, phillipsite. Raman spectra obtained from sample 1206A-21R-5, 95

Fe, however, is highly enriched toward the outer zones as well as Mn occasionally. Fe and Mn show, in some samples, very distinct zones where either one is enriched or totally depleted. They seldom occur in the same zone together.

At the surfaces where no filaments are attached, Fe is more or less unaffected and shows no distinct enrichment toward the outer zones. In many cases Fe shows the opposite behavior and decreases toward the vein margins. Similar trends are found for the other elements as well, with either small changes toward the veins or the opposite behavior compared to the zones where filaments are attached.

5 Discussion

5.1 Biogenicity of the Structures

The tunnel structures found in the samples of volcanic glass from ODP Leg 197 closely resemble structures found by e.g. Fisk et al. (1998, 2003), Furnes and Staudigel (1999), Furnes et al. (2001, 2004), Storrie-Lombardi and Fisk (2004). The structures in those reports have been interpreted as results of microbial activity and recognized as reliable textural biomarkers in volcanic glass (Staudigel et al. 2006; Fisk et al. 1998; Furnes et al. 2001, 2004). The C content ranging between ~10 and

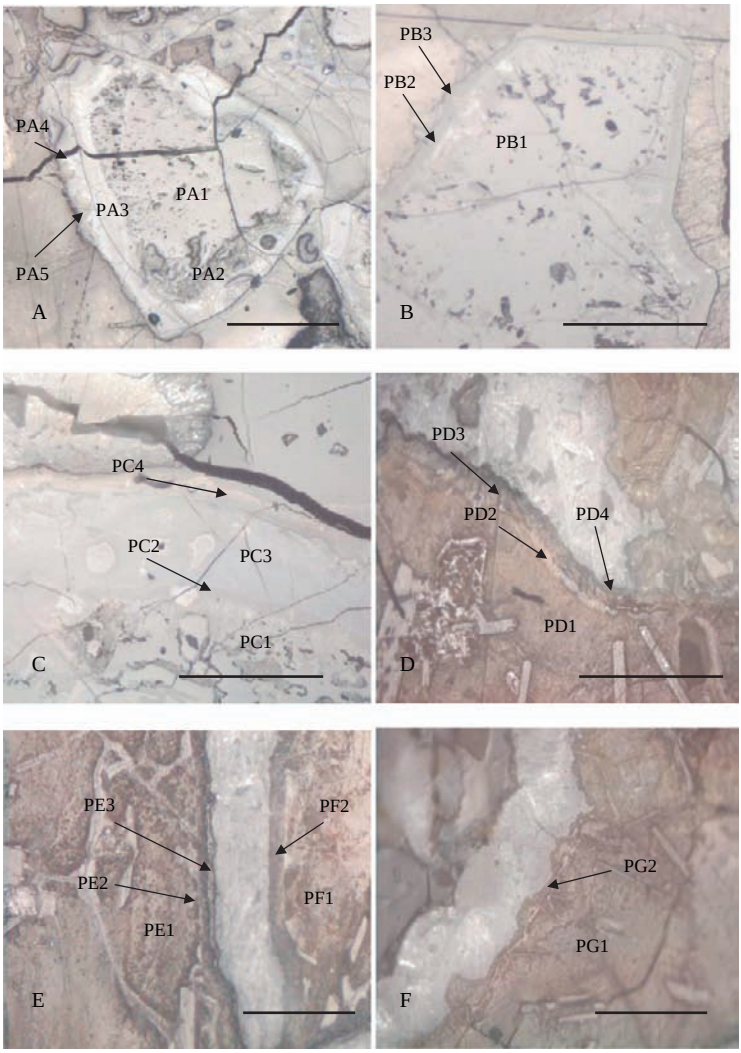

Fig. 13 Microphotograph obtained with plane-polarized light microscopy showing profiles along alteration rinds in glass shards. The profiles start in the unaltered center of the glass shards and progress outwards. Figure A, B and C represent surfaces with attached filaments. Figure D, E and F represent surfaces without attached filaments. EDS data for the rinds are given in Table 3. **A** and **B**: 1203A-30R-1, 63. **C**: 1203A-41R-5, 0. **D**: 1204B-16R-1, 41. **E** and **F**: 1204B-16R-1, 145Scale bars are 50 μm except in C in which the scale bar is 10 μm

Table 7A Alteration zones associated with microfossils. PA, PB and PC represent profiles beginning within a glass shard and going outwards to the veins, crossing different zones (Fig. 13 A, B, C). The data is given in wt%A

O	40.32	40.38	32.97	30.54	43.19	35.37	39.15	40.96	47.13	50.06	42.02	43.79
C	4.59	4.46	11.16	13.03	10.95	11.18	9.17	6.57	5.70	5.96	4.70	4.16
Na	5.26	1.29	1.11	1.33	0.40	5.74	1.41	–	4.37	–	0.85	–
Mg	1.00	1.50	1.40	1.30	1.16	–	1.95	1.49	–	2.85	2.81	2.36
Al	7.54	2.79	2.77	2.92	2.38	12.08	4.33	3.06	10.86	7.09	11.18	8.20
Si	23.19	6.78	5.84	6.47	5.92	25.87	16.40	6.97	27.15	14.38	25.33	25.80
K	0.56	–	–	–	–	–	1.50	–	4.79	1.14	3.85	3.86
Ca	5.20	3.44	4.32	5.25	7.27	6.95	6.16	7.46	–	1.82	–	–
Ti	1.54	–	2.60	2.56	–	–	1.25	3.23	–	–	–	–
Mn	–	–	–	–	–	–	–	–	–	16.71	–	–
Fe	10.80	39.36	37.83	36.60	28.73	2.92	18.68	30.26	–	–	9.27	11.83
Total	100.00	100.00	100.00	100.00	100.00	100.00	100.00	100.00	100.00	100.00	100.00	100.00

Table 7B Alteration zones associated with surfaces lacking filamentous structures (Fig. 13 D, E, F). The data is given in wt%B

	PD1	PD2	PD3	PD4	PE1	PE2	PE3	PF1	PF2	PG1	PG2
O	43.43	41.02	43.46	40.72	40.78	44.71	44.61	45.45	47.41	44.68	46.78
C	–	–	–	–	–	–	–	4.51	5.14	4.56	4.09
Na	5.43	1.96	1.77	2.79	1.16	2.20	2.93	1.81	1.73	1.58	1.72
Mg	–	4.92	4.45	4.94	6.13	4.53	5.00	7.76	3.82	7.54	4.07
Al	17.88	9.01	9.47	9.08	8.02	9.36	8.99	6.16	11.14	6.20	11.62
Si	23.76	24.92	26.37	24.80	22.94	27.77	23.72	22.17	24.57	20.60	25.27
K	–	–	3.13	–	1.15	2.98	–	1.69	2.26	1.23	2.31
Ca	8.62	7.48	1.37	7.77	7.60	–	6.79	–	–	–	–
Ti	–	1.35	–	1.26	1.18	–	1.07	0.53	–	3.71	–
Fe	0.88	9.34	9.98	8.64	11.04	8.45	6.88	9.91	3.93	9.89	4.14
Total	100.00	100.00	100.00	100.00	100.00	100.00	100.00	100.00	100.00	100.00	100.00

∼40 wt% C and the fact that the carbon is not bound to or associated with carbonates suggests that the tunnel structures presented in this paper contain organic carbon.

Observations of filamentous microbial structures or putative microfossils from sub-seafloor environments are on the contrary rare. Filamentous microorganisms have previously been found attached to volcanic glass or altered basalt from the ocean floor (Thorseth et al. 2001, 2003) and filamentous microorganisms as well as filamentous structures interpreted as biogenic in origin have been found in Fe- and Mn-deposits associated with hydrothermal vents (Boyd and Scott 2001; Edwards et al. 2004, 2003; Emerson and Moyer 2002). Filamentous structures associated with iron oxides observed in vent fluids have been suggested to originate from sub-seafloor environments and to have been transported to the ocean floors by hydrothermal fluids (Kennedy et al. 2003). Putative filamentous microfossils have also been found in ancient hydrothermal deposits (Rasmussen 2000; Little et al. 2004).

The filament structures found in our samples bear a close resemblance morphologically to some of the microbial filaments and putative fossilized microorganisms described in the reports mentioned above. Morphological structures like a twisted stalk, segmented filaments and tubular-like sheaths are common features of such microbial filaments (Emerson et al. 2002; Kennedy et al. 2003; Little et al. 2004; Edwards et al. 2004).

The carbon contents (between ∼10 wt% and ∼50 wt%) and the concentration of carbon in the filament structures compared to calcium, which is depleted in the filament structures, show that the carbon is not bound in the carbonates. The concentration of C_2H_4 and lipids in the filamentous structures and their binding to PI show that they contain organic carbon, organic compounds and that they most likely are biogenic in origin. Lipids are excellent biomarkers, and ToF-SIMS has previously been reported to be a very good tool for the identification of biomarkers (Steele et al. 2001; Toporski and Steele 2004; Thiel et al. 2007). PI has been shown to bind to cells with damaged membranes and indicates dead bacteria and traces of DNA (Tobin et al. 1999).

Globular iron oxides are found throughout the samples of Leg 197 and are a characteristic part of the vein mineralogy. Such iron oxides are described in the Initial Reports of the ODP Leg 197 and belong to the alteration assemblages (Tarduno et al. 2002). However, the globules associated with the zeolite surfaces vary in several ways from ordinary iron oxides. Iron oxides seldom occur as single features but, more commonly, assemble in clusters of several hundred iron globules. The globules found on the zeolite surfaces occur one to one, almost lined up along the surfaces. They never occur in assemblages but are concentrated in the film as single features. Another difference is that they almost exclusively are associated with the zeolites where the filaments are attached. However, the most striking difference is the chemical content. Iron oxides are almost exclusively made up of iron and oxygen with minor traces of silica, aluminum and magnesium. The iron oxides contain no carbon at all even though they occur in calcite, and traces of carbon from the calcite could be suspected to interfere with the EDS analyses. The globules associated with the zeolite surfaces, on the other hand, contain high amounts of carbon and less iron, even though iron is an important constituent in those as well.

The globules associated with zeolites also bind to the pigment PI which ordinary oxides do not. The enrichment of K further suggests that organic remnants are still present in the globules (Staudigel et al. 2004; Furnes and Staudigel 1999; Thorseth et al. 1995a).

The globules associated with zeolites probably represent fossilized microbial cells, considering the differences from ordinary iron oxides, the carbon content and the binding to PI. Fossilized or encrusted cell-like microorganisms have previously been found in ocean-floor basalts (Thorseth et al. 2001, 2003) and in ancient hydrothermal deposits (Westall et al. 2000). Thorseth et al. (2003) even found encrusted cell-like structures attached to phillipsite surfaces that they interpreted as former microorganisms. The cell-like structures in our samples have probably been attached to the zeolite surfaces or attached via a biofilm to the surfaces. The film that covers the mineral surfaces and concentrates the microbial cells is most likely a microbially formed biofilm considering the C content and binding of PI. The cell-like structures Thorseth et al. (2003) found attached to phillipsite surfaces in samples from the Australian Antarctic Discordance (AAD) were, however, attached directly onto the mineral surfaces and did not involve a biofilm.

The globules found in the wedge-shaped cavities in the phillipsites are most likely biogenic in origin as well, considering the close relationship with the other globules and the binding of PI. It is probable that the wedges act as protective micro environments where microorganisms can thrive. The bacterial cells are well protected from a harsh environment in the bottom of these wedges, and the fact that filaments originate and protrude from these cavities indicates that they serve as viable micro environments for microbial life.

The fossilized microorganisms in our samples are interpreted to have lived in the open spaces of the veins while the veins still were circulated by fluids. There, the microorganisms were anchored to volcanic glass, altered basalt and zeolites in the vein walls and lived in the circulating fluids. As soon as the veins were filled with carbonates precipitating from the fluids, the microorganisms were entrapped and preserved within these mineral phases. The formation of the minerals and the embedding of the microorganisms were a relatively quick event considering the high grade of preservation of the structures (morphology, high carbon content and occurrence of lipids).

5.2 Microbial Colonization of New Habitats During Alteration of the Ocean Crust

The variety of habitable niches in the samples from ODP Leg 197 covers all stages of palagonitization, from the initial stage represented by tunnel structures in fresh glass via the mature stage represented by attached filaments on altered glass and basalt to the final stage where microbes are both attached on and found in cavities in zeolites. Following is a summary of the different micro-environments/habitats found in the samples from ODP Leg 197:

1. Tunnel structures (galleries) in volcanic glass.
2. Fossilized microorganisms attached to surfaces of altered volcanic glass and basalt.
3. Fossilized microorganisms attached to zeolite (phillipsite) surfaces.
4. Fossilized microorganisms in wedge-shaped cavities in between phillipsite crystals.

It is interesting to note how the association with the substrate varies with the degree of alteration. In fresh glass the microorganisms almost exclusively live within tunnel structures in the material. As soon as the volcanic glass is slightly altered and an alteration front is produced at the outer zone of the glass surfaces, the microorganisms are attached onto the surfaces instead. When the alteration proceeds resulting in zeolite formation the microorganisms are still attached on the surfaces, but as the zeolite formation increases, and larger accumulations of zeolites are formed, the microorganisms colonize wedge-like cavities in the zeolites as well.

Several different types of inhabiting behaviors occur. To distinguish between the different types some terms have to be introduced. Normally for microorganisms that live within minerals or rocks, the term endoliths is used and would be applicable in this case as well because all these microfossils are found within cracks and fissures in the rocks. However, there is a need to specify their behavior even more because some microbes are found attached onto mineral surfaces in veins and some in tunnels or cavities within the minerals. The latter circumstance is also in some cases a result of microbial activity which needs to be specified. Usually in the literature endoliths are divided into euendoliths, cryptoendoliths and chasmoendoliths according to their relationship to the substrate (Golubic et al. 1981; Ehrlich 1996; McLoughlin et al. 2007). Euendoliths are microorganisms that actively bore in rocks and create microtubular cavities. Cryptoendoliths are microorganisms that invade preexistent pores in rocks where they cause alteration of the rock in the area that they inhabit. Chasmoendoliths are microorganisms that invade preexistent cracks without altering the rock. In the case of the samples of the ODP Leg 197, the tunnel structures in glass would be a result of euendoliths. It is most likely, based on previous reports (Staudigel et al. 2006; Fisk et al. 1998; Furnes et al. 2001), that the microorganisms are completely responsible for the tunnel structures and therefore would be boring microbes. In contrast, the globules found in wedge-like cavities in between phillipsite crystals occupy already existing cavities and have not been observed to cause alteration of the mineral and would therefore be termed chasmoendoliths. The iron oxides that they are associated with probably do not originate in the minerals themselves but rather represent dissolved iron from fluids penetrating the cavities and scavenged by the microbes. The filaments and globules found attached onto mineral surfaces in veins occupy already existing spaces but appear to be involved in the alteration of the minerals. Therefore they are termed cryptoendoliths. The filaments attached onto volcanic glass, basalts and altered glass or basalt are involved in the oxidation of the substrate and probably mediate the alteration processes. The globules found attached onto phillipsites are clearly involved in the weathering and dissolution of the minerals. Phillipsites associated with globules are much more

Table 8 Table showing the different stages of palagonitization vs. microbial association with the mineral and microbial morphology

Degree of palagonitization:	Initial stage	Mature stage	Final stage
Mineralogy and alteration	Fresh glass	Palagonite & zeolites	Zeolites & minor traces of palagonite
Microbial association with the substrate	Euendolithic	Cryptoendolithic	Cryptoendolithic and chasmoendolithic
Microbial morphology	Cells	Filaments	Cells and filaments

weathered than phillipsites that lack attached globules. Table 8 summarizes the different behavior types with the different stages of alteration.

Another feature that vary with the different microenvironments is the variations in morphology. The tunnel structures in fresh glass are, most likely, dominated by single cellular structures. No filamentous microfossils are observed in these samples, but previous reports of similar structures have been associated with bacterial cells (Thorseth et al. 1995a; Furnes et al. 1996, 2001). Attached microorganisms on altered basalt and glass, on the other hand, appear to be dominated by filament structures. The zeolites appear to be dominated by globules, both attached on the surfaces as well as in the cavities, but in rare cases filaments occur, usually protruding from a wedge-like cavity or a crack in the mineral. It appears as if different types of morphology are more frequent than others in certain microenvironments. Globules, for example, appear to dominate the euendoliths and chasmoendoliths that are found in narrow fissures while filaments dominate the cryptoendoliths attached onto surfaces in wider veins. Whether it is the same species that evolves as the external environment changes or if different species replace each other is difficult to determine. Thorseth et al. (1995b) observed that the morphology of microorganisms attached to volcanic glass changes over time from cells to stalks and filaments and they interpreted it as different species that dominated each other during specific periods of time and also were responsible for leaching of different elements. Microorganisms are known to adopt various modes of life at different stages in their life cycle or in response to a changing external environment (De los Ríos et al. 2005). At this point, however, it is impossible to conclude anything regarding microbial adaptation but only establish the various niches microorganisms are found in and the different modes of life that appear to be characteristic for each inhabitable niche.

5.3 Element Accumulation and Possible Energy Sources

An attempt to discuss or draw some conclusions regarding what elements the microorganisms once used as energy sources can be rather speculative and risky. However, it is commonly accepted that elements involved in the metabolism of the microorganisms are accumulated in their cells, cell walls or deposited onto the microbes (Ehrlich 1996). Microorganisms and microfossils found in seafloor

environments usually are encrusted with iron oxides (Thorseth et al. 2001, 2003). This encrustment usually contains minor amounts of other elements like Si, Al, Mg, Na, Ti and Mn, but Fe and Mn are the only elements with redox potential useful for microbes. Since reduced iron is abundant in such environments, for example in volcanic glass and unweathered basalt minerals like olivine and pyroxene, it is available for microorganisms to oxidize. Thus iron is, most likely, the most accessible element for microorganisms. Several studies on microbes collected around hydrothermal vents on the ocean floors and cultivated in laboratories support this and suggest that iron is an important energy source in these environments (Edwards et al. 2003, 2004; Emerson and Moyer 2002). Manganese oxidation has been proposed as well due to enrichment of Mn in encrustations (Thorseth et al. 2003). However, manganese oxidation has not yet been proven in autotrophy, only in heterotrophy which is not likely in sub-seafloor environments.

5.4 Redox Driven Colonization of New Niches

The iron content of the filaments, the close association with iron oxides and the deposition of iron oxides onto the surfaces of the filaments of the samples from ODP Leg 197 indicate that the microorganisms were involved in iron oxidizing reactions. For the microorganisms living in the tunnel structures in the volcanic glass, iron is an obvious energy source since glass contains reduced iron. By inhabiting such phases the microorganisms can mediate iron oxidation and gain metabolic energy from it. The filaments found attached to altered glass and basalt have also clearly inhabited environments where redox reactions were favored. Table 7B shows that the microfossils are strongly associated with surfaces where iron has been highly accumulated in the outer alteration zones. It is difficult to assess whether this is due to the microbial activity or if the microbes just select areas that contain high amounts of reduced iron so the conditions for iron oxidation are favorable. Rogers and Bennett (2004) showed that microorganisms preferentially colonize and weather silicates that contain the limiting nutrients P and Fe, while leaving similar non-nutrient silicates uncolonized and unweathered. The close association between microfossils and iron oxides, the accumulation of iron oxides onto the filaments, the high iron content of the filaments as well as the higher degree of alteration and accumulation of iron at the surface zones where the microfossils are found indicate that the microorganisms in our samples were involved in the alteration and oxidation reactions and probably mediated such processes.

The microfossils found associated with zeolites are a bit harder to explain. They have, most likely, been involved in iron-oxidation reactions but the source of iron is not entirely clear. The phillipsites do not contain iron in their stoichiometric formula. That leaves two alternatives, one is that they use dissolved iron from the hydrothermal fluids and the second is that their activity leads to dissolution of the zeolite mineral and that iron trapped within the zeolitic framework is released and scavenged by the microbes. Zeolites are known as good adsorbers of almost everything from

organic compounds via gases to metals. Iron is known to be adsorbed in zeolites (Sheta et al. 2003) and since the zeolites that are associated with microfossils are more weathered than zeolites not associated with microfossils, it is possible that iron is released during the microbial activity. This indicates that iron is an important energy source for microorganisms in these environments. However, that does not exclude these other elements or compounds as energy sources. Compounds like H_2 or CH_4, which do not accumulate as easy as iron in the microfossil encrustations, could also have been used (Sposito et al. 1999).

The various habitats where microfossils are found, except the zeolites, all represent microenvironments with high redox potential. It appears as if the microbes prefer such habitats and that the selection and colonization of new habitats are influenced by redox chemistry.

5.5 Implications for the Deep Sub-seafloo Biosphere

As the ocean-floor basalts weather and are being subject to alteration processes, the conditions for the deep biosphere change and there is a need for organisms to inhabit new environments. Volcanic glass has previously been shown to harbor microbial communities (Fisk et al. 1998, 2003; Storrie-Lombardi and Fisk 2004; Furnes et al. 1996, 2001). As the alteration of the oceanic crust proceeds, the volcanic glass becomes palagonitisized and uninhabitable. The microbes either die or are forced to inhabit other habitable niches. It is evident, considering the results from ODP Leg 197, that the microbial activity in sub-seafloor environments is not only restricted to volcanic glass. The fact that microbial activity involves altered basalt and zeolites as well extends the occurrence of a deep sub-seafloor biosphere both in time and in space. The alteration of oceanic crust is a process that continuous long after the volcanically active period of time has ended. Results of the ODP Leg 201 reveal that fresh seawater is still channeled, 40 Ma or more after the formation of the basement, into deep-sea sediments from the rocks underneath (D'Hondt et al. 2003). This shows that the sub-seafloor basalts are circulated during a time period of millions of years. Since microorganisms can sustain as long as fluids are present in the rocks and inhabit new niches during ocean floor alteration, this indicates that a deep sub-seafloor biosphere can sustain for a very long time. Furthermore, phillipsites are the most common zeolite mineral in volcanic rocks of the oceanic crust and the major result of the sub-seafloor palagonitization (Honnorez 1978). Thus, microbial activity in phillipsites would be a common feature in the oceanic crust elsewhere and a global phenomenon. This would increase the potential volume of habitable areas for microorganisms and extend their spatial existence in sub-seafloor environments. It would further extend the oceanic crust as a bioreactor dramatically (Staudigel et al. 2004).

The same forces that destroy the old habitats of the microbes create new opportunities and offer new habitable environments for them. It is as if geochemical processes support the prolongation of a deep sub-seafloor biosphere. On the other

hand, microbial activity mediates and enhances the weathering of the ocean crust and is as responsible as abiotic processes for the destruction of old habitats and creation of new ones (Thorseth et al. 1992, 1995a, b).

6 Summary

The alteration and weathering of ocean-floor basalts, also termed palagonitization, is a process where fresh volcanic glass and basalts are hydrated and leached and finally degraded to a residue called palagonite. While palagonite is the major end product of palagonitization, the zeolite species phillipsite and the clay smectite are the secondary products. The palagonitization process is divided into three major stages: initial, mature and final stages, distinguished by the presence or absence of glass or secondary minerals. The general trend is that the amount of fresh glass decreases and the amount of palagonite and secondary minerals increases toward the final stage.

Microorganisms of the deep sub-seafloor biosphere are known to thrive in tunnel structures within fresh glass. As the weathering and alteration of the oceanic crust proceeds, the habitats of the microorganisms are destroyed and the microorganisms need to inhabit new habitats and environments with different conditions.

In samples consisting of drilled ocean-floor basalts from the ODP Leg 197, fossilized microorganisms have been found associated with all three stages of palagonitization. The microfossils range from bored tunnel structures in volcanic glass, via filaments of different morphologies attached onto altered glass and basalt, to globules (cells) and filaments both attached onto phillipsites and found within wedge-like cavities in between phillipsite crystals.

The biogenicity of the fossilized microorganisms is supported by a C content (~10–~50 wt% C) and by the fact that the carbon is not bound to or associated with carbonates. Furthermore, the concentration of C_2H_4 and lipids in the filamentous structures show that they contain organic carbon and organic compounds. Binding to PI, which is a dye that binds to damaged membranes and dead bacteria cells, provide further evidence that they most likely are biogenic in origin.

The characteristic content of iron, close association of iron oxides and deposition of iron onto the fossilized microorganisms indicate that the microbes were involved in iron oxidation reactions and that iron probably served as an energy source for the metabolism of the microorganisms.

In the first stages (volcanic glass and altered basalt) it is evident that the colonization of new niches is redox driven. Both volcanic glass and unweathered basalt minerals contain high amounts of reduced iron from which microbes can gain energy by mediating oxidation. The zeolites, on the other hand, are not obvious sources of iron. They contain no iron in their crystal structure. However, it is possible that the zeolites adsorbed iron or other reduced elements or compounds like CH_4 or H_2 within their framework which the microbes scavenge during microbial weathering of the minerals. It is also possible that the microbes have used dissolved iron in the fluids as a source.

Microbial colonization of new niches during ocean-floor alteration and palagonitization extends the occurrence and opportunities for a deep sub-seafloor biosphere both in time and space. The wide range of different mineralogical habitats opens up new possibilities for a sub-seafloor biosphere that probably inhabit much larger volumes of the world's ocean crusts than was previously known. It further shows that the deep sub-seafloor biosphere can sustain over geological time as the alteration processes continue.

Acknowledgments We would like to thank following people for contributions to this work: Jukka Lausmaa at the Swedish National Testing and Research Institute, Borås, Sweden, for the ToF-SIMS analysis. Marianne Ahlbom and Kjell Wannäs at the Department of Geology and Geochemistry at Stockholm University for the ESEM and EDS analysis. Lutz Nasdala at the Institute of Geosciences – Mineralogy at Johannes Gutenberg University, Mainz, Germany for the Raman spectroscopy analysis. Kjell Helge at Minoprep AB for the preparation of doubly polished thin sections. Anna Neubeck at the Department of Geology and Geochemistry at Stockholm University for processing of pictures. Hildred Crill for correcting the English. This work has been funded by the Swedish Research Council, the Swedish National Space Board and the Stockholm Marine Research Center.

References

Al-Hanbali HS, Holm NG (2002) Evidence for fossilized subsurface microbial communities at the TAG hydrothermal mound. Geomicrobiol J 19:429–438

Al-Hanbali HS, Sowerby SJ, Holm NG (2001) Biogenicity of silicified microbes from a hydrothermal system: relevance to the search for evidence of life on earth and other planets. Earth Planet Sci Lett 191:213–218

Alt JC, Mata P (2000) On the role of microbes in the alteration of submarine basaltic glass: a TEM study. Earth Planet Sci Lett 181:301–313

Banerjee NR, Furnes H, Muehlenbachs K, Staudigel H, de Wit M (2005) Preservation of ~3.4–3.5 Ga microbial biomarkers in pillow lavas and hyaloclastites from the Barberton Greenstone Belt, South Africa. Earth Planet Sci Lett 241:707–722

Berger G, Schott J, Loubet M (1987) Fundamental processes controlling the first stage of alteration of a basalt glass by seawater: an experimental study between 200 and 320°C. Earth Planet Sci Lett 84:431–445

Boyd TD, Scott SD (2001) Microbial and hydrothermal aspects of ferric oxyhydroxides and ferrosic hydroxides: the example of Franklin Seamount, Western Woodlark Basin, Papua New Guinea. Geochem Trans 7

Crovisier JL, Honnorez J, Eberhart JP (1987) Dissolution of basaltic glass in seawater: Mechanism and rate. Geochim Cosmochim Acta 51:2977–2990

Daux V, Crovisier JL, Hemond C, Petit JC (1994) Geochemical evolution of basaltic rocks subjected to weathering: fate of the major elements, rare earth elements, and thorium. Geochim Cosmochim Acta 58:4941–4954

De los Ríos A, Sancho LG, Wierzchos J, Ascaso C (2005) Endolithic growth of two *Lecidea* lichens in granite from continental Antarctica detected by molecular and microscopy techniques. New Phytol 165:181–190

Deming JW, Baross JA (1993) Deep-sea smokers: windows to a subsurface biosphere? Geochim Cosmochim Acta 57:3219–3230

D'Hondt SL, Jørgensen BB, Miller DJ (2003) Proc ODP, Init Repts 201

Edwards KJ, Rogers DR, Wirsen CO, McCollom TM (2003) Isolation and characterization of novel psychrophilic, neutrophilic, Fe-oxidizing, chemolithoautotrophic α- and γ-*Proteobacteria* from the deep sea. Appl Environ Microbiol 69:2906–2913

Edwards KJ, Bach W, McCollom T, Rogers DR (2004) Neutrophilic iron-oxidizing bacteria in the ocean: Their habitats, diversity, and roles in mineral deposition, rock alteration, and biomass production in the deep-sea. Geomicrobiol J 21:393–404

Edwards KJ, Bach W, McCollom T (2005) Geomicrobiology in oceanography: microbe-mineral interactions at and below the seafloor. TRENDS in Microbiol 13:449–456

Eggleton RA, Keller J (1982) The palagonitization of limburgite glass – a TEM study. N Jb Min 7:321–336

Ehrlich HL (1996) Geomicrobiology, third edition, revised and expanded. Marcel Dekker, New York, pp 719

Emerson D, Moyer CL (2002) Neutrophilic Fe-oxidizing bacteria are abundant at the Loihi Seamount hydrothermal vents and play a major role in Fe oxide deposition. Appl Environ Microbiol. 68:3085–3093

Fisk MR, Giovannoni SJ, Thorseth IH (1998) Alteration of oceanic volcanic glass: textural evidence of microbial activity. Science 281:978–980

Fisk MR, Storrie-Lombardi MC, Douglas S, Popa R, McDonald G, Di Meo-Savoie C (2003) Evidence of biological activity in Hawaiian subsurface basalts. Geochem Geophys Geosyst 4:1103, doi:10.1029/2002GC000387

Fisk MR, Popa R, Mason OU, Storrie-Lombardi MC, Vicenzi EP (2006) Iron-magnesium silicate bioweathering on Earth (and Mars?). Astrobiology 6:48–68

Furnes H (1984) Chemical changes during progressive subaerial palagonitization of a subglacial ilivine tholeiite hyaloclastite: A microprobe study. Chem Geol 43:271–285

Furnes H, El-Anbaawy MIH (1980) Chemical changes and authigenic mineral formation during palagonitization of a basanite hyaloclastite, Gran Canaria, Canary Islands. Neues Jahrb Mineral Abh 139:279–302

Furnes H, Staudigel H (1999) Biological mediation in ocean crust alteration: how deep is the deep biosphere? Earth Planet Sci Lett 166:97–103

Furnes H, Thorseth IH, Tumyr O, Torsvik T, Fisk R (1996) Microbial activity in the alteration of glass from pillow lavas from hole 896A. Proc ODP, Scientific Results 148:191–206

Furnes H, Muehlenbachs K, Tumyr O, Torsvik T, Xenophontos C (2001) Biogenic alteration of volcanic glass from the Troodos ophiolite, Cyprus. J Geol Soc, London, 158:75–84

Furnes H, Banerjee NR, Muehlenbachs K, Staudigel H, de Wit M (2004) Early life recorded in Archean pillow lavas. Science 304:578–581

Giovannoni SJ, Fisk MR, Mullins TD, Furnes H (1996) Genetic evidence for endolithic microbial life colonizing basaltic glass-seawater interfaces. Proc ODP, Scientific Results 148:207–214

Gold T (1992) The deep, hot biosphere. Proc Natl Acad Sci 89:6045–6049

Golubic S, Friedmann I, Schneider J (1981) The lithobiontic ecological niche, with special reference to microorganisms. J Sediment Petrol 51:475–478

Hay RL, Iijima A (1968) Nature and origin of palagonite tuffs of the Honolulu Group on Oahu, Hawaii. Geol Soc Am Mem 116:338–376

Honnorez J (1978) Generation of phillipsites by palagonitization of basaltic glass in sea water and the origin of K-rich deep-sea sediments. Natural Zeolites, Occurrence, Properties, Use. Pergamon Press, London

Honnorez J (1981) The aging of the oceanic lithosphere. In: Emiliani C (ed) The oceanic lithosphere. John Wiley, New York, pp 525–587

Ivarsson M (2006) Advantages of doubly polished thin sections for the study of microfossils in volcanic rock. Geochem. Trans. 7:5.

Jercinovic MJ, Keil K, Smith MR, Schmitt RA (1990) Alteration of basaltic glasses from north-central British Columbia, Canada. Geochim. Cosmochim. Acta 54:2679–2696.

Kennedy CB, Scott SD, Ferris FG (2003) Ultrastructure and potential sub-seafloor evidence of bacteriogenic iron oxides from Axial Volcano, Juan de Fuca Ridge, northeast Pacific Ocean. FEMS Microbiol. Ecol. 43:247–254.

Little CTS, Glynn SE, Mills RA (2004) Four-hundred-and-ninety-million-year record of bacteriogenic iron oxide precipitation at sea-floor hydrothermal vents. Geomicrobiol. J. 21:415–429.

McLoughlin N, Brasier MD, Wacey D, Green OR, Perry RS (2007) On biogenicity criteria for endolithic microborings on early Earth and beyond. Astrobiology 7:10–26.

Peacock MA (1926) The petrology of Iceland, Part 1, The basic tuffs. R. Soc. Edinb Trans. 55:53–76.

Rasmussen B (2000) Filamentous microfossils in a 3,235-million-year-old volcanogenic massive sulphide deposit. Nature 405:676–679.

Rogers JR, Bennett PC (2004) Mineral stimulation of subsurface microorganisms: release of limiting nutrients from silicates. Chem. Geol. 203:91–108

Sheta AS, Falatah AM, Al-Sewailem MS, Khaled EM, Sallam ASH (2003) Sorption characteristics of zinc and iron by natural zeolite and bentonite. Microporous Mesoporous Mater 61:127–136

Sposito G, Skipper NT, Sutton R, Park SH, Soper AK, Greathouse JA (1999) Surface geochemistry of the clay minerals. Proc Natl Acad Sci USA 96:3358–3364

Staudigel H, Hart ST (1983) Alteration of basaltic glass: Mechanism and significance for the oceanic crust-seawater budget. Geochim Cosmochim Acta 47:337–350

Staudigel H, Chastain RA, Yayanos A, Bourcier W (1995) Biologically mediated dissolution of glass. Chem Geol 126:147–154

Staudigel H, Tebo B, Yayanos A, Furnes H, Kelley K, Plank T, Muehlenbachs K (2004) The oceanic crust as a bioreactor. The Subseafloor Biosphere at Mid-Ocean Ridges. In: Wilcock WSD, DeLong EF, Kelley DS, Baross JA, Cary SC (eds) Geophysical monograph 144:325–241

Staudigel H, Furnes H, Banerjee NR, Dilek Y, Muehlenbachs K (2006) Microbes and volcanoes: a tale from the oceans, ophiolites, and greenstone belts. GSA Today 16:4–10

Steele A, Toporski JKW, Avci R, Guidry S, McKay DS (2001) Time of flight secondary ion mass spectrometry (ToFSIMS) of a number of hopanoids. Org Geochem 32:905–911

Storrie-Lombardi MC, Fisk MR (2004) Elemental abundance distributions in sub-oceanic basalt glass: evidence of biogenic alteration. Geochem Geophys Geosyst 5:10

Tarduno JA, Duncan RA, Scholl DW (2002) Proc ODP, Init Repts 197:1–92

Stroncik NA, Schmincke H-U (2001) Evolution of palagonite: Crystallization, chemical changes, and element budget. Geochem Geophys Geosyst 2:7

Tarduno JA, Duncan RA, Scholl DW (2002) Leg 197 summary. Proc ODP, Init Repts 197:1–92

Thiel V, Toporski J, Schumann G, Sjövall P, Lausmaa J (2007) Analysis of archaeal core ether lipids using Time of Flight-Secondary Ion Mass Spectrometry (ToF-SIMS): exploring a new prospect for the study of biomarkers in geobiology. Geobiology 5:75–83

Thorseth IH, Furnes H, Tumyr O (1991) A textural and chemical study of Icelandic palagonite of varied composition and its bearing on the mechanism of the glass-palagonite transformation. Geochim Cosmochim Acta 55:731–749

Thorseth IH, Furnes H, Heldal M (1992) The importance of microbiological activity in the alteration of natural basaltic glass. Geochim Cosmochim Acta 56:845–850

Thorseth IH, Torsvik T, Furnes H, Muehlenbachs K (1995a) Microbes play an important role in the alteration of oceanic crust. Chem Geol 126:137–146

Thorseth IH, Furnes H, Tumyr O (1995b) Textural and chemical effects of bacterial activity on basaltic glass: an experimental approach. Chem Geol 119:139–160

Thorseth IH, Torsvik T, Torsvik V, Daae FL, Pedersen RB, Keldysh-98 Scientific Party (2001) Diversity of life in ocean floor basalt. Earth Planet Sci Lett 194:31–37

Thorseth IH, Pedersen RB, Christie DM (2003) Microbial alteration of 0-30-Ma seafloor and sub-seafloor basaltic glass from the Australian Antarctic Discordance. Earth Planet Sci Lett 215:237–247

Tobin KJ, Onstott TC, DeFlaun MF, Colwell FS, Fredrickson J (1999). In situ imaging of microorganisms in geologic material. J Microbiol Met 37:201–213

Toporski J, and Steele A (2004) Characterization of purified biomarker compounds using time of flight-secondary ion mass spectrometry (ToF-SIMS). Org. Geochem 35:793–811

Torsvik T, Furnes H, Muehlenbachs K, Thorseth IH, Tumyr O (1998) Evidence for microbial activity at the glass-alteration interface in oceanic basalts. Earth Planet Sci Lett 162:165–176

Walton AW, Schiffman P (2003) Alteration of hyaloclastites in the HSDP 2 Phase 1 Drill Core 1. Description and paragenesis. Geochem Geophys Geosyst 4:5

Walton AW, Schiffman P, Macpherson, GL (2005) Alteration of hyaloclastites in the HSDP 2 Phase 1 Drill Core: 2. Mass balance of the conversion of sideromelane to palagonite and chabazite. Geochem Geophys Geosyst 6:9

Westall F, Steele A, Toporski J, Walsh M, Allen C, Guidry S, McKay D, Gibson E, Chafetz H (2000) Polymeric substances and biofilms as biomarkers in terrestrial material: implications for extraterrestrial samples. J Geophys Res 105:24511–24527

Zhou ZH, Fyfe WS, Tazaki K, Vandergaast SJ (1992) The structural characteristics of palagonite from DSDP Site-335. Can Mineral 30:75–81

Ambient Inclusion Trails: Their Recognition, Age Range and Applicability to Early Life on Earth

David Wacey, Matt Kilburn, Crispin Stoakes, Hugh Aggleton and Martin Brasier

Abstract Ambient inclusion trails (AITs) are a distinct class of microtubular structure, first reported almost half a century ago from Precambrian rocks. Classification of a structure as an AIT implies formation by means of migration of a mineral crystal through a lithified substrate. Historically, AITs have been problematical in two ways. Firstly, they have caused confusion in studies of early life because they are similar, morphologically, to both filamentous microfossils and microborings made by endolithic bacteria. Secondly, their formation mechanism has not been rigorously studied, so there has been much debate about whether AITs are purely an inorganic phenomena or whether a biological component is necessary.

In this paper we review all reported examples of AITs, documenting the criteria necessary for their recognition, their taphonomic preservation in the rock record, their differentiation from modern contamination, and recent advances made in the Pilbara Craton of Western Australia which appear to support a biogenic formation mechanism for at least some AITs. We also report what we believe are the youngest examples of AITs in Phanerozoic rocks. These come from the Middle Devonian of Northern Scotland. Their excellent preservation within phosphatic fish scales not only gives further insights into AIT formation, it extends their known range forward by almost 200 Ma. Clearly, AITs were not just a Precambrian phenomenon.

1 Introduction: Recognizing AITs

Microtubular structures are a relatively rare but intriguing component of the rock record. Such structures are of particular interest in Archean rocks because they might provide clues to the former existence of primitive life. Ambient inclusion trails (AITs) are one particular type of microtubular structure, thought to form when small metal-rich inclusions, usually pyrite, are propelled through a lithified substrate such as chert (cf. Tyler and Barghoorn 1963; Knoll and Barghoorn 1974).

D. Wacey
Department of Earth Sciences, University of Oxford, Parks Road, Oxford OX1 3PR, UK
e-mail: davidwa@earth.ox.ac.uk

Y. Dilek et al. (eds.), *Links Between Geological Processes, Microbial Activities & Evolution of Life*, © Springer Science+Business Media B.V. 2008

This process leaves behind a hollow tubular trail, which may remain empty or be infilled by secondary mineral phases.

The ability to differentiate between a microtubular trail left by a migrating crystal and morphologically-similar features, such as filamentous microfossils and endolithic microborings, is of vital importance. Confusion of AITs with such structures has been both widespread and detrimental to studies of early life (see examples below). Using previously published work and our new examples of AITs, we are able to propose nine criteria for the recognition of AITs in petrographic thin section. These are summarised in Fig. 1, beginning with the most diagnostic.

Although AITs rarely exhibit all of these features, they should be relatively easy to identify when well preserved. It is strange therefore, that only a few examples have been documented in the literature (see below). We suggest that far more examples are embedded in the literature as supposed 'fossils', 'microborings' or even 'predatorial borings' and that diagenesis and mineral replacement in poorly preserved examples has precluded the correct identification of numerous other examples. The discovery of new occurrences of well preserved AITs is clearly essential if we are to advance our understanding of their mechanisms of formation.

2 History of AITS

The first report of AITs came from the 1900 Ma Gunflint Formation of Ontario and the ~2000 Ma Biwabik Formation of Minnesota (Tyler and Barghoorn 1963). Here, pyrite crystals have been propelled through carbonaceous black cherts, leaving clear trails behind that were subsequently infilled with either quartz or carbonate. The carbonate trails range in size from less than 1 μm to around 10 μm in diameter, and up to 100 μm in length (Fig. 2a, b). They have diverse morphologies from straight to curved, to spiral, to rather irregular, and have a complete lack of any preferred orientation. The quartz filled trails are larger, up to 1.4 mm in diameter and almost 3 mm in length, and tend to be less morphologically diverse (Fig. 2c). In both cases the diameter of the trail is always equal to the diameter of the pyrite crystal, and the profile of the distal end of the trail is a direct image of the pyrite-trail interface (cf. Fig. 1a). Occasionally, magnetite can also be propelled, for example in the Ironwood Iron Formation from the Precambrian of Michigan (Tyler and Barghoorn 1963). Here magnetite grains of around 30 μm diameter, have been propelled through a ferruginous chert matrix for distances of up to 1 mm. These trails are filled with chlorite, which has been interpreted as a replacement of carbonate. The structures were originally thought to form due to the forces induced by the crystallisation of the quartz or carbonate 'appendages', but this explanation left several questions unanswered and was later abandoned in favour of a second explanation involving possible biological mediation (see below).

The oldest reported AITs come from the ~3500 Ma Warrawoona Group of Western Australia, first described by Awramik and his co-workers (1983). These trails are around 2–5 μm in diameter and several tens of microns in length, are filled with microcrystalline silica, and have hematite crystals (presumed to be pseudomorphs

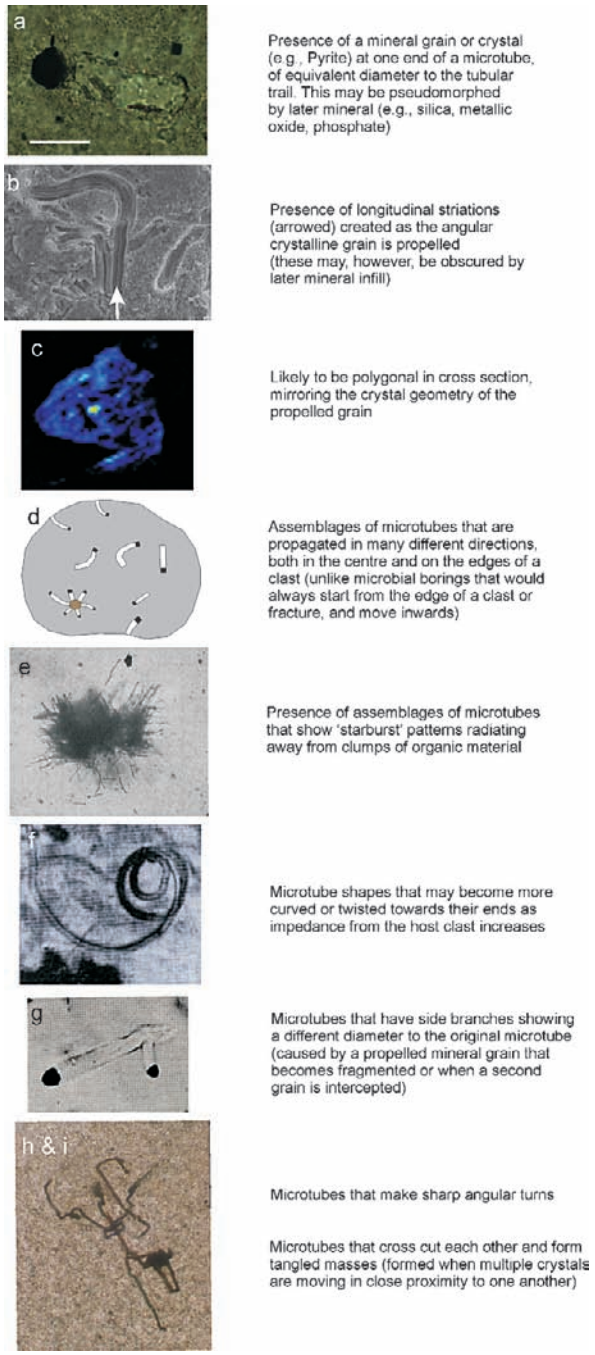

Fig. 1 Criteria to identify ambient inclusion trails in thin section. Images from Tyler and Barghoorn 1963, Knoll and Barghoorn 1974, Xiao and Knoll 1999, Wacey et al. 2007, and courtesy of Maia Schweizer

after pyrite) at their terminations (Fig. 2d). Interestingly, they occur in rocks which were once claimed to host some of the earliest evidence of life on Earth, in the form of filamentous 'microfossils' (Awramik et al. 1983; Awramik 1992) but later considered doubtful (Buick 1984, 1990; Schopf 1993).

Knoll and Barghoorn (1974) describe AITs from the ~2700 Ma Fortescue Group of Western Australia. These structures are an order of magnitude smaller than those mentioned above, with diameters of 0.5–0.8 μm and lengths of up to 60 μm. The trails often radiate randomly from a central locus, forming 'starbursts' (Figs. 1e, 2e), although single trails also exist. These AITs typically contain terminal pyrite crystals and are infilled with carbonate. The importance of this report, however, lies in the explanation advanced for their formation. Knoll and Barghoorn suggest that AITs from the Fortescue Group, as well as those previously described from the Gunflint, Biwabik and Ironwood Formations, were formed by pressure solution. This could have been initiated by gas evolution from decaying organic (possibly biological) matter attached to the pyrite crystals. This proposed formation mechanism is especially significant because AITs are found in some of the most

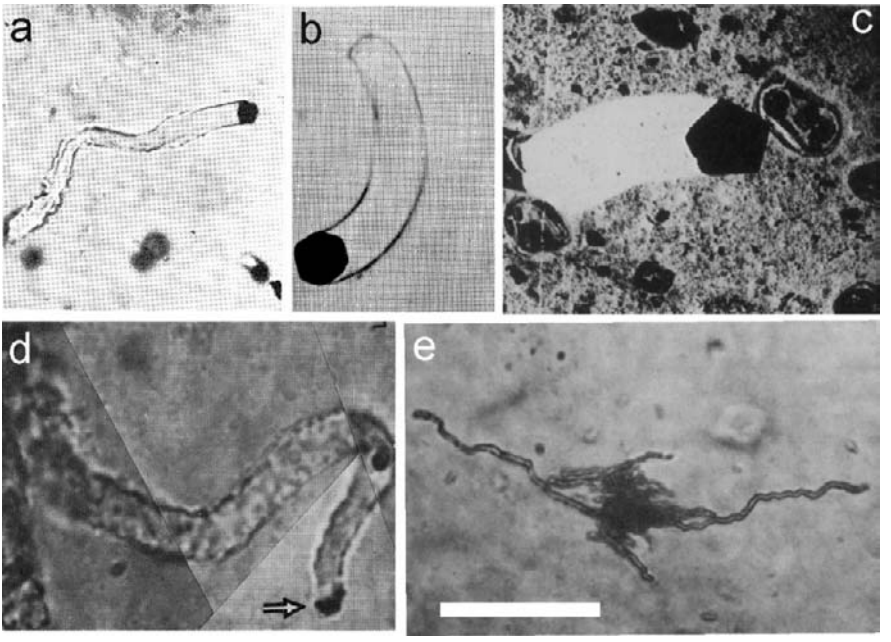

Fig. 2 AIT occurrences reported from the literature. (**a**) and (**b**) Pyrite with sinuous and gently curved carbonate filled trails from the ~ 2000 Ma Biwabik Iron Formation, Minnesota (from Tyler and Barghoorn 1963); (**c**) Large pyrite with quartz filled trail from the 1900 Ma Gunflint Iron Formation, Canada (from Knoll and Barghoorn 1974); (**d**) Silica filled AIT from the ~3500 Ma Warrawoona Group, Western Australia. Arrow indicates partly degraded terminal crystal (from Awramik et al. 1983); (**e**) Cluster of AIT around clot of organic matter from the ~ 2700 Ma Fortescue Group, Western Australia (from Knoll and Barghoorn 1974); Scale bar is about 40 μm for (**a**); 20 μm for (**b**); 70 μm for (**c**); 10 μm for (**d**); 50 μm for (**e**)

ancient rocks where the presence of life is still hotly debated (e.g., Schopf 1993, 2006; Brasier et al. 2002, 2005, 2006 and see below).

In younger parts of the geological record, other reports of AITs come from phosphorites of the ~570 Ma Doushantou Formation of China (Zhang 1984; Xiao and Knoll 1999). These trails are 10–80 μm in diameter and up to 1 mm in length, commonly twisted and coiled (Fig. 3). 'Starburst' varieties are common, as are tubes that entangle and cross cut one another. Many of these AITs have remained empty so that characteristic continuous longitudinal striae can readily be seen along the walls (Figs. 1b, 3a, b, d). A spectacularly preserved AIT has also been discovered

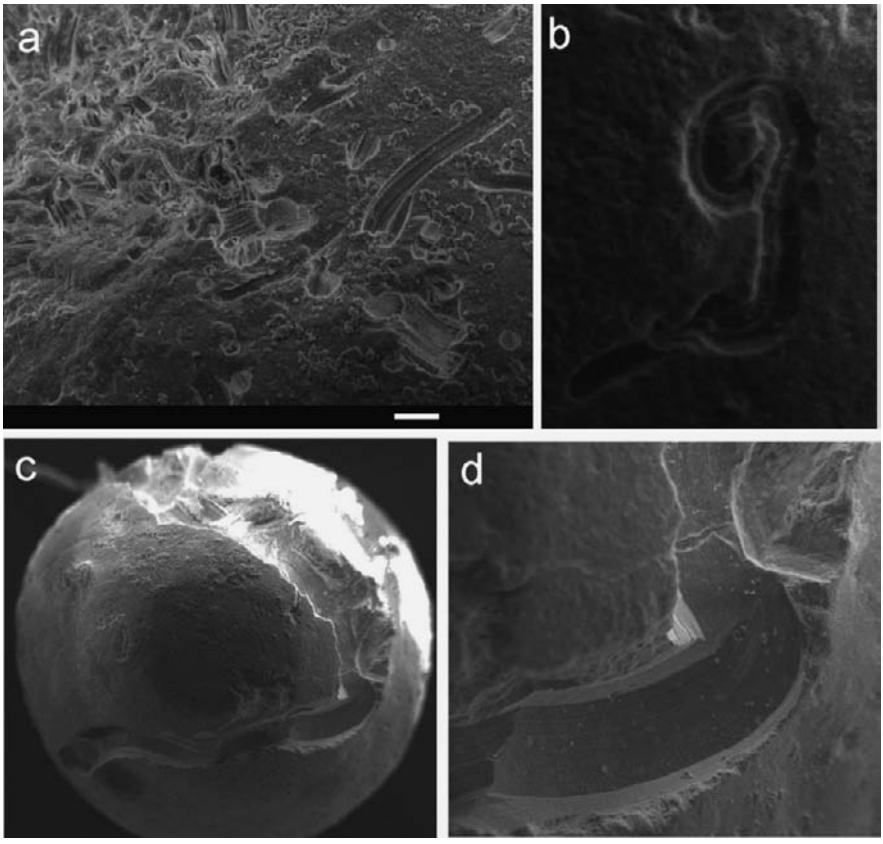

Fig. 3 AITs from the ~ 570 Ma Doushantou Formation, China, similar to those reported by Xiao and Knoll (1999). (**a**) Multiple short AITs (*top left*) and several longer AITs (*bottom right*) moving in various directions on the surface of an isolated fossilised 'embryo'; (**b**) Single AIT exhibiting a looped 'g' shape and prominent longitudinal striations; **c** Large AIT in fossilised 'embryo'; (**d**) Close up of the sharp bend in c, showing fine longitudinal striations caused by the propelled pyrite crystal. Scale bar is 20 μm for (**a**); 10 μm for (**b**); 50 μm for (**c**); 20 μm for (**d**). Photos courtesy of Maia Schweizer

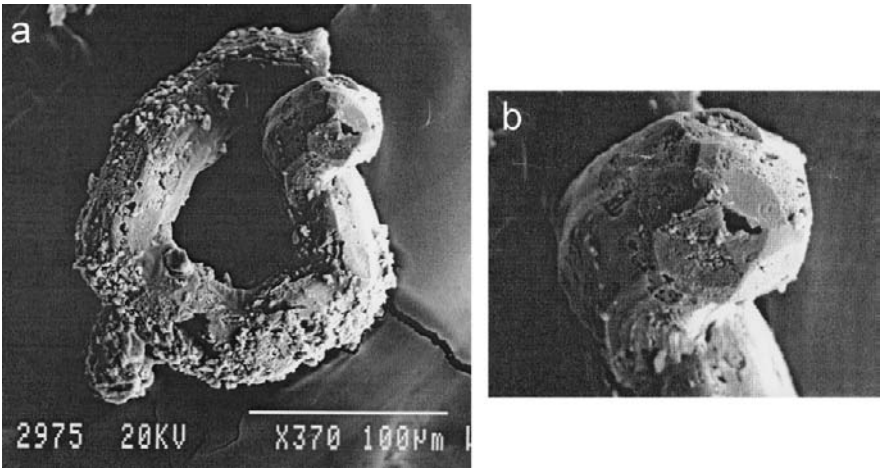

Fig. 4 (**a**) Large coiled phosphate-filled AIT isolated from the lower Cambrian Soltanieh Formation of Iran, exhibiting an angular termination and longitudinal striations. (**b**) Enlargement of the terminal face showing the phosphate pseudomorph of a pyrite dodecahedron

by us in the lower Cambrian Soltanieh Formation of Iran where the terminal pyrite crystal is pseudomorphed by phosphate (Fig. 4).

As well as these *bona fide* reports of AITs, there are several examples in which AITs have been confused with other types of structures. Microtubular structures from Archean Soudan cherts (Gruner 1923, 1925), for example, were originally

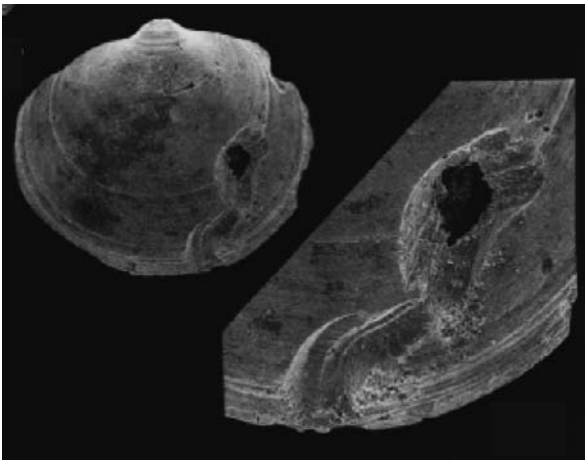

Fig. 5 Putative AIT from a Cambrian brachiopod shell (from Conway Morris and Bengtson 1994). Right hand image is enlargement of the AIT from the left hand image to show longitudinal striations caused by the propelled crystal. This was mistakenly interpreted as a predatory boring by Conway Morris and Bengtson (1994) but reinterpreted as an AIT by Xiao and Knoll (1999). Brachiopod is $\sim$ 1.5 mm in diameter

classified as blue green algae, while an occurrence of 'predatory microborings' in Cambrian brachiopod shells (Fig. 5; Conway Morris and Bengtson 1994) are suggested to be AITs based upon the clearly visible longitudinal striations according to Xiao and Knoll (1999). The AITs described above from the Doushantou phosphorite were originally interpreted as animal trace fossils (Dong et al. 1984) and some of those in the Warrawoona chert may have been misinterpreted as filamentous microfossils according to Awramik et al. (1983). The Khubsugal phosphorite of latest Ediacarian age in Mongolia (see Zhegallo et al. 2000, fig. 32) contains similar controversial structures, and Grey (1986) describes microtubular structures from the ~1100 Ma Discovery Chert of Western Australia, concluding that many of these are also more likely AITs than microfossils.

3 Recent Investigations in the Pilbara

3.1 Geological Setting

The Pilbara craton of Western Australia contains some of the most ancient and best preserved supracrustal rocks on Earth. The oldest part of the craton is the East Pilbara granite-greenstone terrane (Fig. 6) which consists of ~3655–2850 Ma granitoid bodies, and almost contemporaneous ~3515–3100 Ma volcanic and minor sedimentary rocks (Pilbara Supergroup). The latter are now preserved as low-grade meta-volcanics and meta-sediments in several greenstone belts (Van Kranendonk 2006). The stratigraphy of the Pilbara Supergroup has been refined quite significantly over the last few years. Here we use the latest nomenclature published by the Geological Survey of Western Australia (Van Kranendonk 2006, 2007). The Pilbara Supergroup contains four unconformity bound stratigraphic intervals (groups) – the ~3530–3430 Ma Warrawoona Group, ~3420–3300 Ma Kelly Group, ~3270–3230 Ma Sulphur Springs Group and the ~3230–3170 Ma Soansville Group. Each of the four groups were deposited on top of one another and consistently dip away from the domal granitoids. Dips gradually decrease with time suggesting deposition took place as thickening wedges adjacent to the growing granitoid diapirs (e.g., Van Kranendonk et al. 2002).

Microtubular structures have recently been found in each of the three oldest groups, specifically from the 3460 Ma 'Apex chert'of the Warrawoona Group; the ~3420 Ma 'Strelley Pool sandstone' of the Kelly Group; and a ~3240 Ma chert from the uppermost Kangaroo Caves Formation of the Sulphur Springs Group (Fig. 4, localities 1, 2 and 4; see Wacey et al. 2007). Microtubes in the Strelley Pool sandstone (Fig. 7) are by far the most common.

3.2 Recognition of AITs by Auto-Montage

Auto-Montage is a sophisticated image acquisition and processing software package, and has proved an ideal tool in the examination of microtubular structures

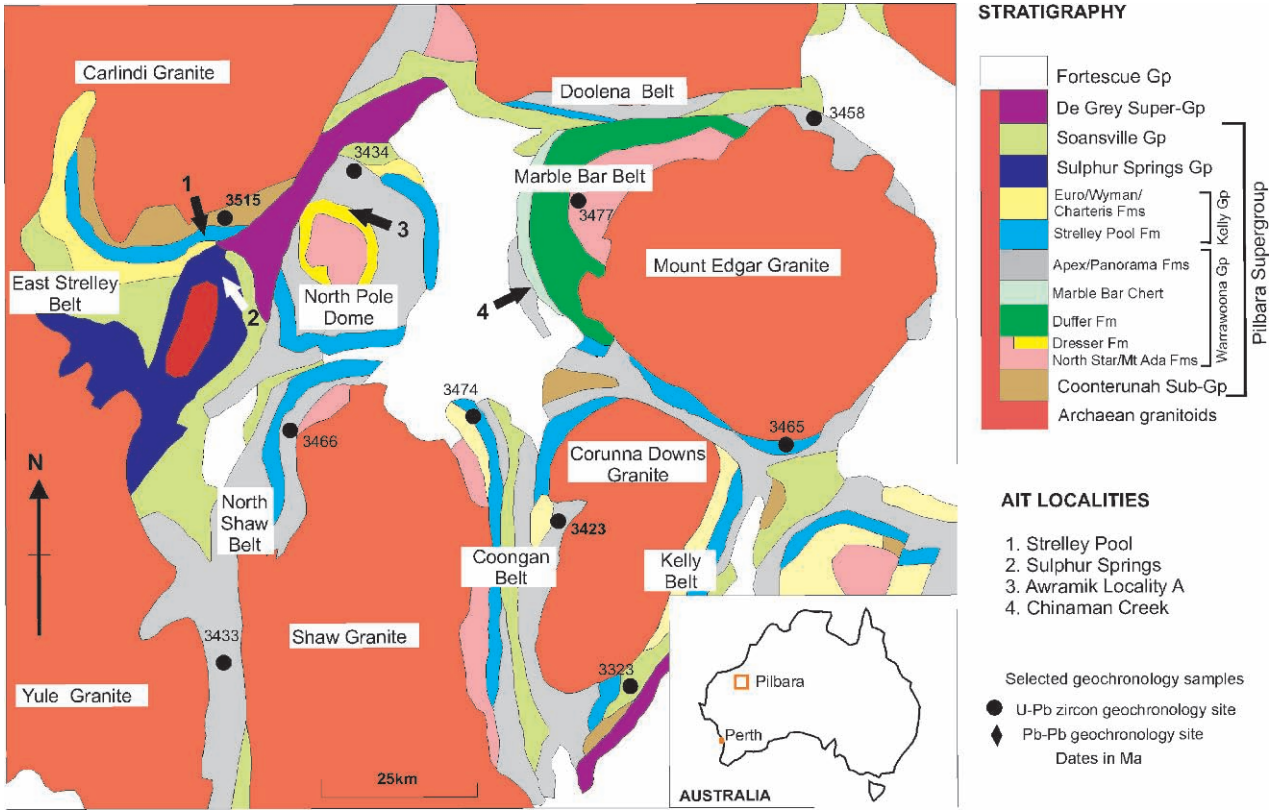

Fig. 6 Regional geological map of the East Pilbara Granite-Greenstone Terrane, showing the three localities of AITs recently described by our group, plus the Awramik et al. (1983) locality (modified from Van Kranendonk et al. 2001 and Wacey et al. 2006)

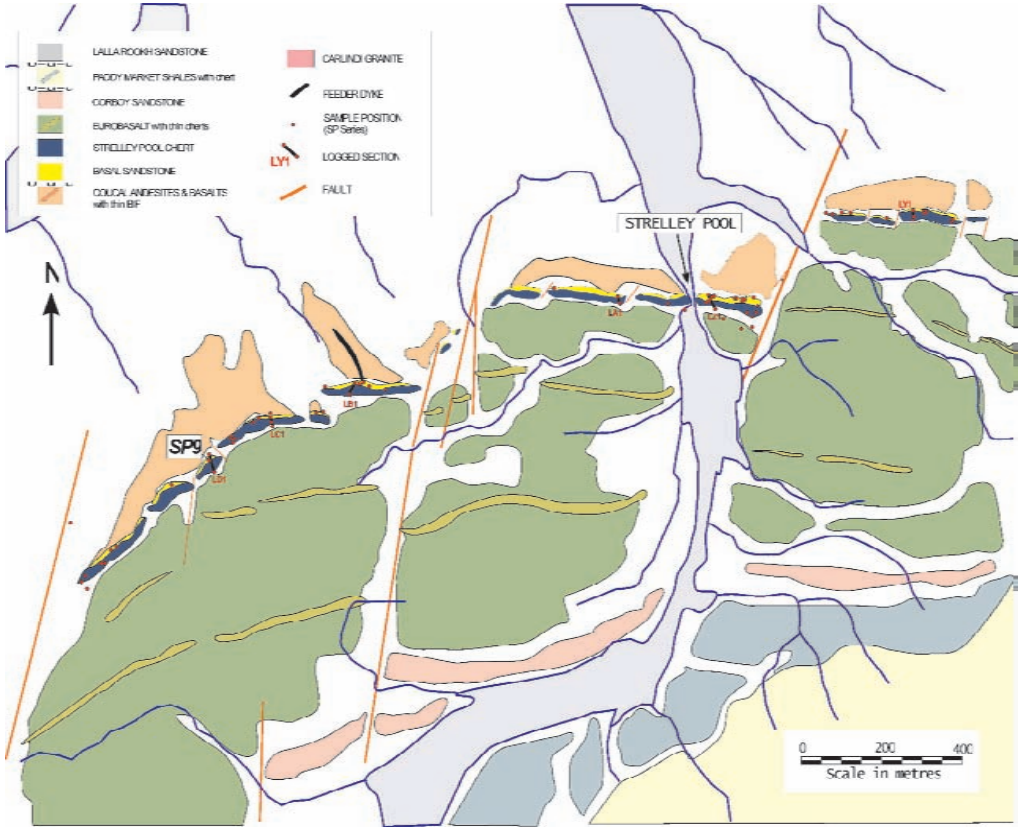

Fig. 7 A new and refined geological map of the Strelley Pool region, East Pilbara, showing locality (SP9) of AIT bearing samples within the basal sandstone unit

within standard and non-standard thin sections (Brasier et al. 2002, 2005). The software allows the capture, processing and combination of multiple source images obtained at different focal planes within the thin section. Processing algorithms enable the most sharply focussed areas of each source image to be combined into a single well-focused 'montaged' image. This rendering facility is ideal for obtaining high-resolution images of 3-D microscopic structures aligned obliquely to the z-axis within a slide. It is similar to the established technique of manual montage, in which images of a microstructure are collected by optical photomicrography and then manually spliced in the darkroom or laboratory. It differs, however, in that selected focal planes from the 'montaged' image can also be displayed on the screen or print. Depth maps, confidence maps and 3-D images can also be generated from the series of 2-D source images. An example of the extra information obtained from two Strelley Pool sandstone AITs using *Auto-Montage* is shown in Fig. 8.

Table 1 summarises the characteristics of microtubular structures from the Apex chert, Kangaroo Caves chert and Strelley Pool sandstone reported by Wacey et al. (2007) using the *Auto-Montage* technique. It can be seen that the microtubes have a large size range from 1–100 μm in diameter and ~10–300 μm in length. They also have a variety of infilling mineral phases with silica the most common, followed by phosphate, chlorite, jarosite and iron oxide. Nevertheless, each of the separate occurrences of microtubes exhibit sufficient features to enable their unambiguous identification as AITs.

The Apex chert microtubes (Figs. 1h–i, 9d) have sharp turns, angular terminations and cross-cutting relationships. They occur in close proximity to pyrite and are found away from obvious conduits for younger endolithic activity. Many of the Strelley Pool examples (Figs. 1c, 8, 10, 11) have terminal pyrite crystals, propagate in multiple directions (often from the centre of grains), have polygonal cross sections, and show branching and cross cutting. The Kangaroo Caves microtubes (Fig. 9a–c) also have terminal pyrite crystals, longitudinal striations, polygonal cross sections, and are seen to propagate in several directions with starburst patterns, side branches and cross cutting tangles.

Of particular note in the Kangaroo Caves examples is that only a small proportion of the pyrite crystals present have formed AITs. All pyrite crystals that are less than 15 μm or more than 100 μm in diameter appear to have remained stationary (e.g., some in Fig. 9a). It is also notable that the chert is quite 'clean', with limited amounts of organic matter present. This suggests that, in this substrate at least, there was a maximum size, above which impedance of the chert was too great to allow for mobilisation. The very small pyrite crystals, on the other hand may not have had enough organic matter attached to them to effect movement.

The location of the Strelley Pool examples (Fig. 7) is particularly pertinent for studies of early life because the sandstone lies stratigraphically directly beneath a laminated chert member of the Strelley Pool Formation. It exposes stromatolite-like structures claimed to be of biogenic origin (e.g. Allwood et al. 2006).

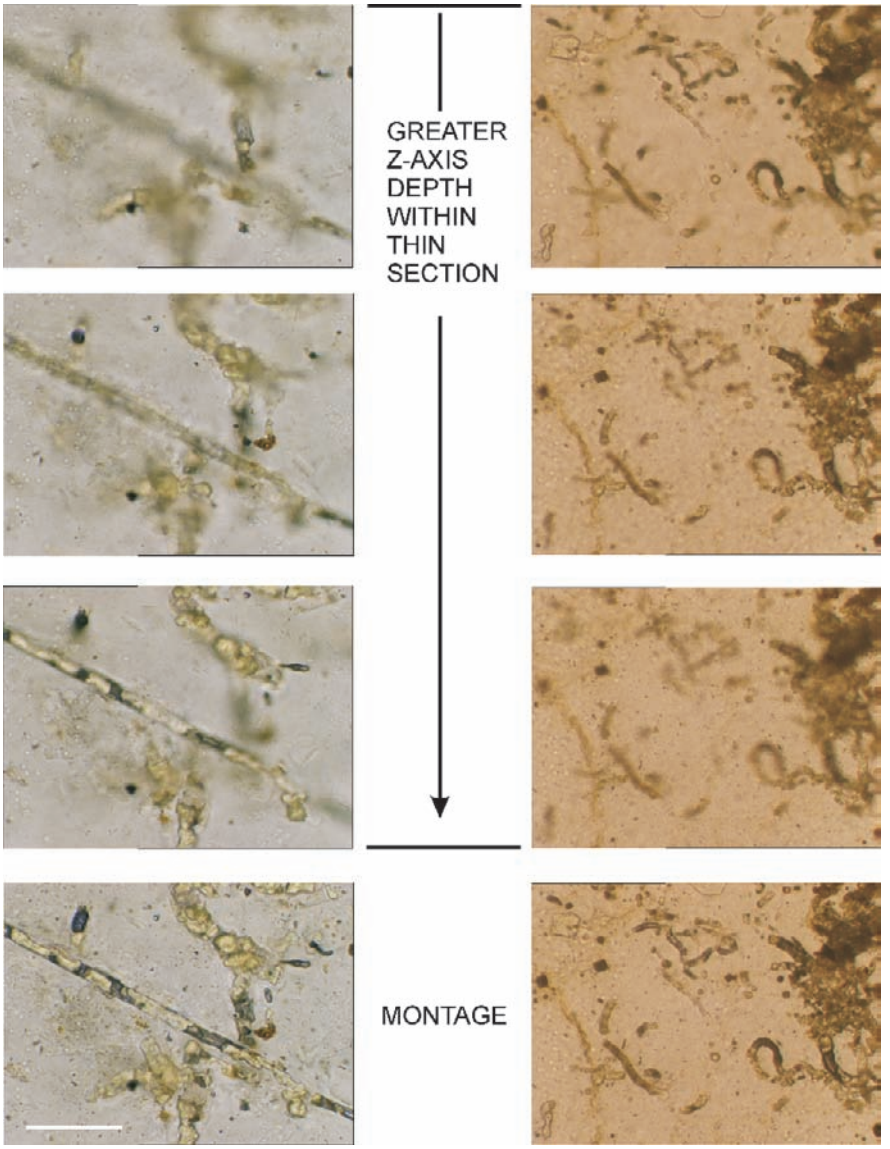

Fig. 8 Images of two areas of AITs from the ~3420 Ma Strelley Pool sandstone, using the *Auto-montage* technique. The three upper images in each column are sourced from different focal planes within the thin section. The bottom image in each column uses the most sharply focused areas of each source image to build up an accurate and 'in focus' montage of the AITs and surrounding features. Scale bar is 50 μm for the left column and about 75 μm for the right column

Table 1 Characteristic features of ~3460–3240 Ma AITs from the Pilbara Craton of Western Australia: √ = feature is present; – = feature is not observed

	Apex Chert (~3460 Ma)	Strelley Pool sst (~3420 Ma)	Kangaroo Caves chert (~3240 Ma)
Host lithology	Carbonaceous stratiform chert	Detrital chert grains in sandstone	Stratiform grey chert
Size range	1–4 μm diameter; ~10–100 μm long	1–15 μm diameter; up to 300 μm long	15–100 μm diameter; up to 100 μm long
Terminal mineral grain	Rare (Iron oxide)	√ (Pyrite)	√ (Pyrite)
Infilling mineral	Iron phosphate, iron oxide	Silica, iron phosphate, aluminium phosphate, jarosite	Chlorite, silica
Longitudinal striations	–	–	√
Polygonal cross sections	–	√	√
Multiple propagation directions	√	√	√
Starburst patterns	√	√	√
Impedance from host grain	–	√	–
Side branches	√	√	√
Angular turns	√	–	–
Cross cut one another	√	√	√
Figures herein	1h, 1i, 9d	1a, 1c, 8, 10, 11	9a, 9b, 9c

3.3 Clues to AIT Formation Mechanism from NanoSIMS

Nano-scale secondary ion mass spectroscopy (NanoSIMS) is a relatively new technique to palaeobiology. It enables both elemental mapping and isotopic analysis at extremely high spatial resolution (~50 nm lateral resolution for some elements).

Wacey et al. (2007) used NanoSIMS to geochemically map AITs from the centre of microcrystalline quartz grains within the Strelley Pool sandstone (Locality 1, Fig. 6). They found correlated enrichments in carbon and nitrogen near the margins of several AITs (Fig. 11d; see also Wacey et al. 2007, Fig. 4). Because these enrichments did not correlate with either calcium, magnesium or oxygen, the elemental patterns were used to argue for an organic rather than carbonate source for the carbon within the AITs (e.g. Fig. 11a–c). Furthermore, *in situ* NanoSIMS carbon isotope measurements of $\delta^{13}C = -27 \pm 3\%$, combined with enrichments of P, S, Co, Ni, and Zn in and around this carbonaceous material, were used to support the argument that the organic material was biological in origin (Wacey et al. 2007).

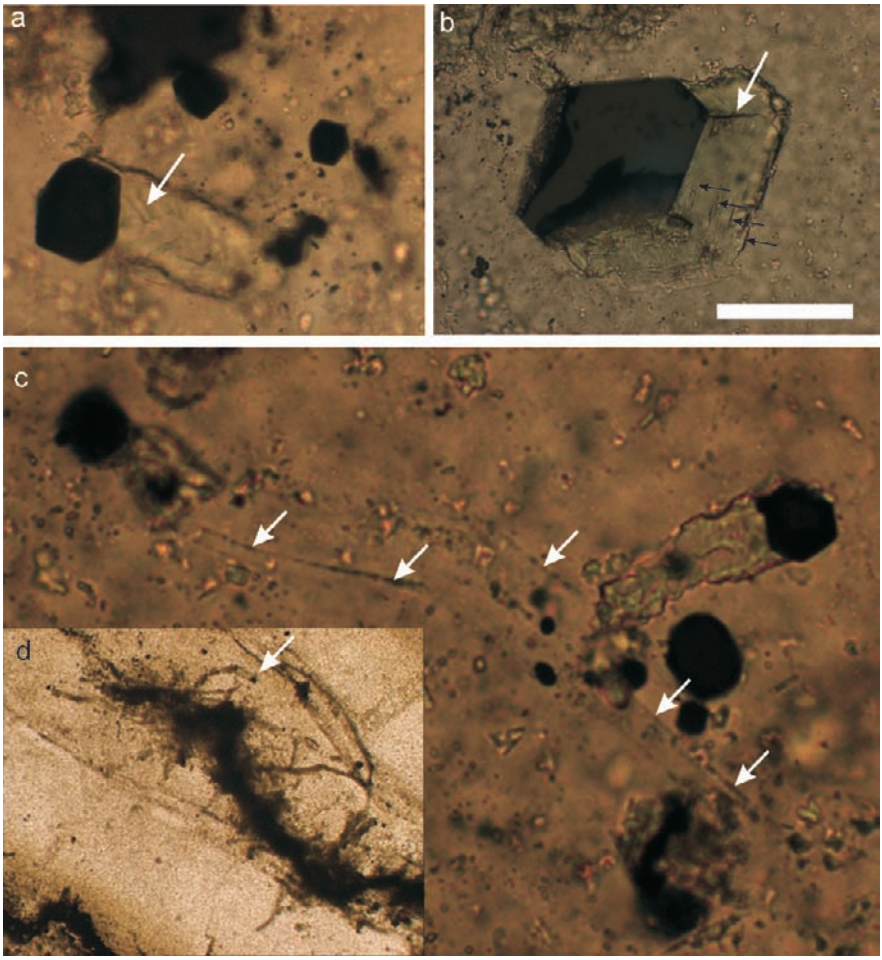

Fig. 9 AITs from Kangaroo Caves chert (**a**–**c**) and Apex chert (**d**). (**a**) Single chlorite-filled AIT in chert. Note terminal pyrite grain, dark margins to the microtube, and faint striations at an angle to the edge of the tube (*arrowed*). Note also that other pyrite grains within the field of view have remained stationary; (**b**) A large pyrite grain that has moved only a short distance through the chert substrate. There appears to be some degradation of the leading edge of the pyrite crystal. Both longitudinal striations (*white arrow*) and faint lines of residual material (*small black arrows*) are visible. The latter may indicate a stepwise movement of the crystal through the silica substrate; (**c**) Small chlorite-filled AIT (*top right*) and long, microquartz-filled AIT (*running from bottom right to top left*) with fine longitudinal striations and accumulations of organic material (*arrowed*); (**d**) Several AITs in starburst pattern moving away from a clump of organic material in chert. Terminal pyrite crystal is arrowed in a long curved AIT. Scale bar is 40 μm for (**a** and **c**); 70 μm for (**b**); 100 μm for (**d**) ((**b**) is from Wacey et al. 2007)

Further NanoSIMS analyses away from the AITs detected enrichments in carbon and nitrogen associated with pyrite grains sealed within the centres of these detrital sandstone grains (e.g. Fig. 12). This helps to rule out modern contamination as a source of the biological material in the AITs.

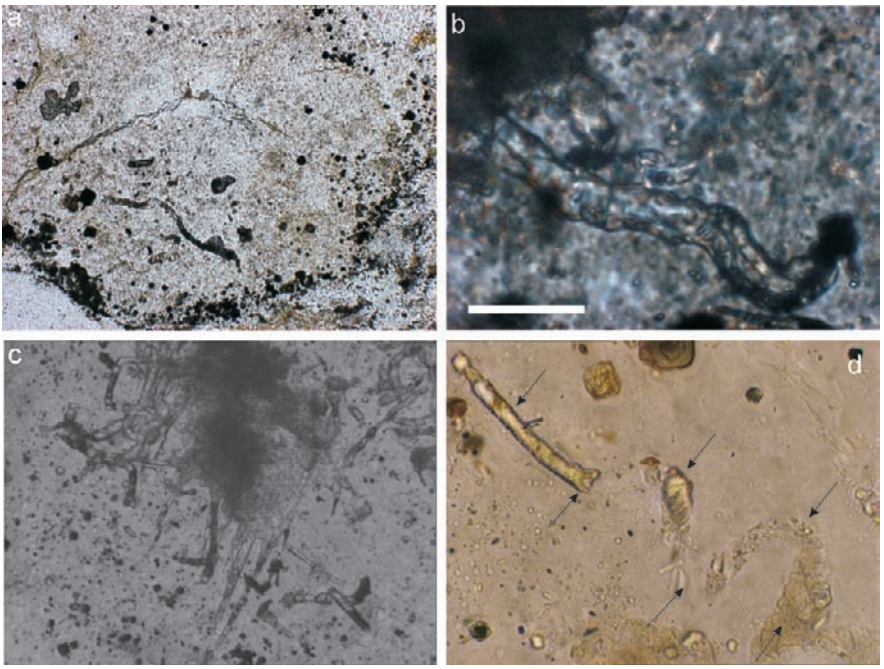

Fig. 10 AITs from Strelley Pool. (**a**) Typical AIT-containing clast, with concentrations of pyrite and organic material; (**b**) Silica-filled AIT with pyrite crystal propelled away from clot of organic matter (*movement top left to bottom right*); (**c**) Cluster of AITs that cross cut one another and are associated with clumps of organic matter; (**d**) Helical AIT (*defined by arrows*) now partly filled with jarosite. Note cubic terminal crystal of jarosite pseudomorphing pyrite (*top left*). Scale bar is 100 μm for (**a**); 15 μm for (**b** and **d**); 50 μm for (**c**)

4 New AITs from Devonian Fish Scales

4.1 Geological Setting

New examples of AITs come from the ~390 Ma Achanarras Limestone of the Middle Old Red Sandstone in northern Scotland. The specimens were collected from a fish bed within Achanarras Quarry, about 20 km south of Thurso in north-east Scotland. Here, the Achanarras Limestone is about 3.6 m thick and consists of alternating 1–2 mm microcrystalline carbonate with clastic laminae representing annual rhythms in a stratified lake (Trewin 1986). These are subdivided by further fine (<0.1 mm) laminae rich in algal material. The fish bed in the quarry is 1.95 m thick and is composed of triplets of carbonate, clastic and organic materials on the mm scale. The whole sequence is estimated to have been deposited in about 4000 years, formed as a deep water deposit when Lake Orcadie was at or near its greatest aerial extent (Trewin 1986). The fish beds within the Achanarras Limestone represent catastrophic events such as salinity crises, storms stirring up toxic bottom waters, or shock mixing of cold deep waters with warmer surface waters (Dineley

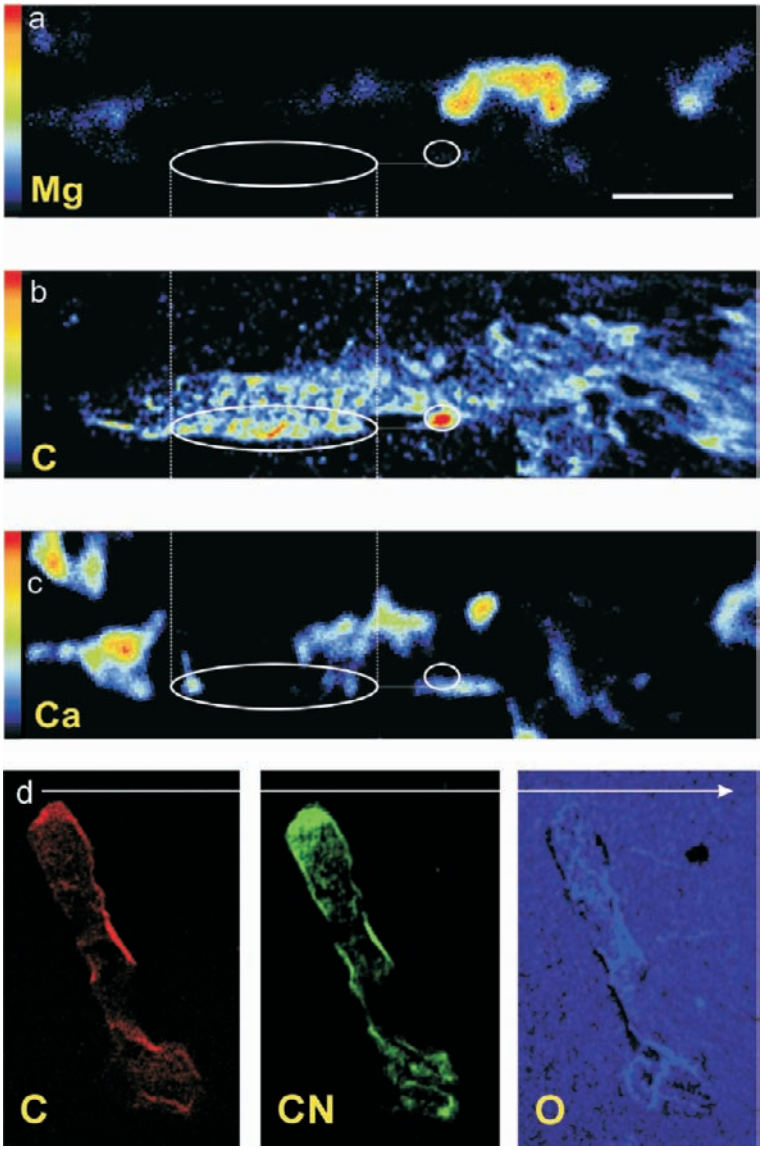

Fig. 11 NanoSIMS ion images of AITs from the Strelley Pool sandstone. (**a**–**c**) are from one AIT, (**d**) is from a different AIT. (**a**–**c**) These show the distribution of magnesium, carbon and calcium within an AIT (two elliptical areas are highlighted in white for inter-image comparison). Note the complete lack of correlation between these elements which is evidence of an organic rather than carbonate source for the carbon; (**d**) Enrichments of carbon and nitrogen within the AIT, especially along the outer margins. This enrichment shows an approximate inverse correlation with oxygen and provides evidence of a biological component to AIT formation. Scale bar is 20 μm and chemical symbols are in yellow (modified from Wacey et al. 2007)

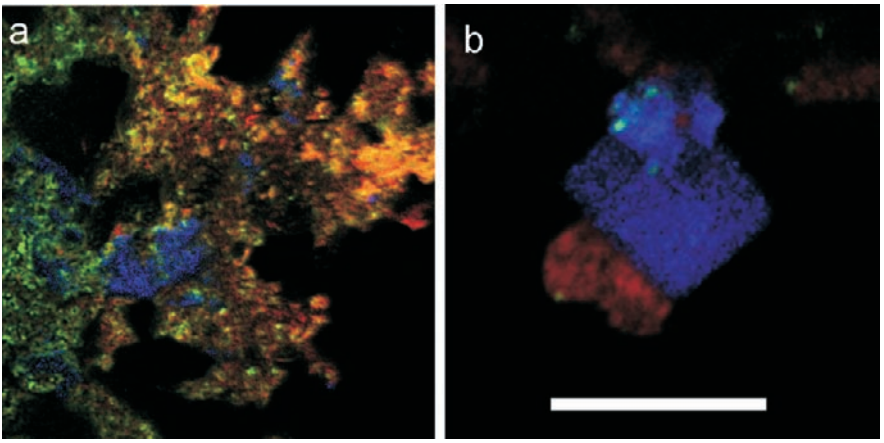

Fig. 12 NanoSIMS ion images of pyrite (*blue*) associated with carbon (*red*) and nitrogen (*green*) in areas separate from those containing AITs within the Strelley Pool sandstone. (**a**) Pyrite surrounded by organic material. Equal enrichment of carbon and nitrogen results in an orange colour; (**b**) Cube of pyrite with small lump of carbonaceous material attached. Scale bar is 15 μm for (**a**); 2 μm for (**b**)

and Metcalf 1999), which killed schools of fish. The dead fish then settled into a stagnant anoxic mud deposit on the bottom of the lake, where preservation of bones, scales and even fins took place.

The AITs occur in well preserved phosphatic scales of the early lungfish *Dipterus valenciennesi* (Aggleton 2007) (Fig. 13), one of 16 species of fish found in Achanarras Quarry.

Fig. 13 *Dipterus valenciennesi* from Achanarras Quarry. AIT are found in phosphatic scales from a less complete specimen. Specimen is ~20 cm long

4.2 Description

AITs are numerous (over 100 in a single thin section) and range in diameter from 5–12 μm, with most about 10 μm. They can be up to 150 μm in length and of diverse morphologies, from gently curved and twisted (Fig. 14a) to looped (Fig. 14b, arrowed). Terminal pyrite crystals are preserved in the shorter AITs, but only parts of pyrite crystals are preserved in longer AITs (compare Fig. 14e to Fig. 14c, d and f),

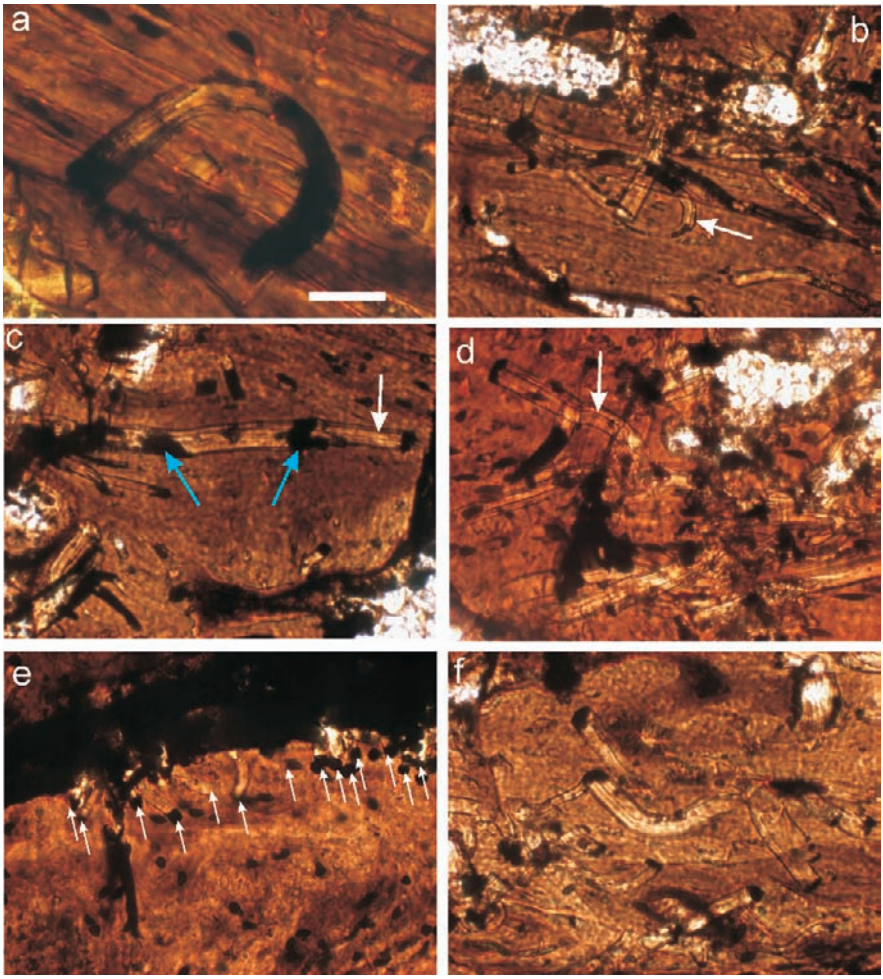

Fig. 14 AITs from middle Devonian fish scales. (**a**) Single, planispirally curved AIT with build up of dark organic material along the walls; (**b**) Several curved AITs, the arrowed example is looped; (**c**) Cluster of AITs on left side of image, with one long example showing longitudinal striations (*white arrow*), clumps of organic material (*blue arrows*) and part of a terminal crystal (*far right*); (**d**) Cluster of AITs associated with organic material. Striations are preserved in arrowed example; (**e**) Numerous short AITs (*white arrows*) propagating from pyrite rich area at edge of the fish scale; (**f**) Two long S-shaped AITs (*centre of image*) with partially degraded terminal crystal and dark organic rich margins. Scale bar is 20 μm

implying that the pyrite crystals were degraded as they were propelled. Longitudinal striations are often seen (white arrows on Fig. 14c and d), and small accumulations of organic material occur both along the microtube edges and in clumps within the microtube (blue arrows in Fig. 14c). The AITs preferentially occur in areas of those fish scales which have a concentration of organic matter and pyrite crystals.

Importantly, we observe that where pyrite crystals are numerous, the AITs are relatively short in length (~25 μm; arrowed in Fig. 14e), but where the crystals are more isolated, the AITs can be up to 150 μm long (Fig. 14f). This relationship implies that when there were several pyrite crystals clustered together, there was only sufficient decaying organic material associated with each one to propel each a short distance.

5 Taphonomic Preservation of AITs

In the forgoing sections we have shown that AITs can form in quite different taphonomic settings. We also find they can be variously preserved together with pyrite, silica, chlorite, ferrous phosphate, aluminium phosphate, jarosite and iron oxides, and associated with biological signals (Wacey et al. 2007). These observations now allow us to identify a series of key stages in their formation and their subsequent diagenetic history (Fig. 15).

The following model builds upon the hypothesis first put forward by Knoll and Barghoorn (1974): that propulsion results from 'pressure solution initiated by gas evolution from organic material attached to the pyrite'. Although recent geochemical evidence is consistent with this hypothesis, experimental justification of its truth is still required.

Stage one of our model began with deposition of a sediment that was rich in iron sulphide and organic matter. In the case of the Strelley Pool sandstone, this involved detrital chert grains deposited in a low oxygen environment (Wacey et al. 2006). A

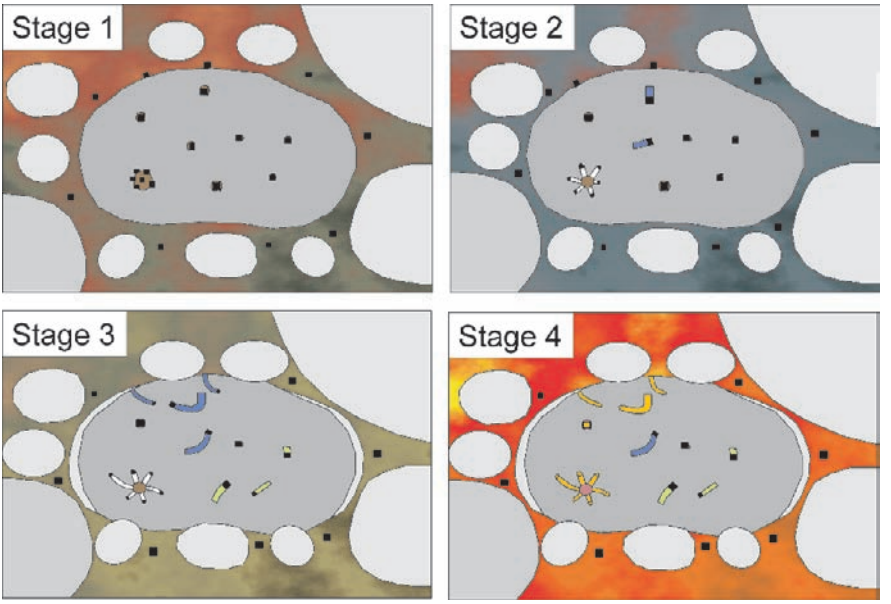

Fig. 15 A proposed model for AIT formation and subsequent taphonomic preservation (see text for details)

low oxygen environment was required, at least locally, so that pyrite was not oxidised and broken down. In some cases this environment may also have aided extensive pyrite formation by sulphate-reducing bacteria. An impermeable host lithology and early lithification also appears to have been necessary so that gas from decaying organic matter was trapped within an impermeable substrate, enabling fluid pressure to build up.

During stage two, compaction and heating during shallow burial caused the degassing of some of the decomposing organic material that was attached to pyrite grains (cf. Knoll and Barghoorn 1974). This build up of fluid pressure was probably insufficient to drive pyrite movement unaided. We here propose that fluid pressure was accompanied by dissolution of the silica substrate, facilitated by localised changes in pH brought about by microbial communities (cf. Brehm et al. 2005). These combined factors then allowed the pyrite grains to move short distances through the silica. Similar processes can be envisaged for a phosphate substrate. At this stage the microtubes may have remained hollow or been infilled with ferrous phosphate minerals that may likewise have been biologically mediated.

During stage three, further heating and/or burial associated with the prehnite-pumpellyite facies regional metamorphism (e.g., Van Kranendonk 2000) propelled more pyrite grains for yet greater distances through the medium. Fluid pressures may have been great enough at this stage to propel further pyrite crystals from the matrix into microcrystalline grains (e.g. Strelley Pool) or into fish scales (e.g. Achanarras). Under suitable conditions of fluid flow and permeability, chlorite could have precipitated within the AITs at this stage (e.g. Kangaroo Caves). Only a small degree of metamorphic heating is needed for sufficient degassing of organic matter to occur. Intense metamorphism would overprint the original mineralogy and textures so that identification of AITs would be near to impossible.

Stage 4 is envisaged as substantially more recent and sees overprinting of much of the original AIT mineralogy. In the case studied in detail by Wacey et al. (2007) from Strelley Pool, this is particularly common near the edges of grains. Here, both pyrite and phosphate phases are replaced by jarosite and various iron oxides, presumably during uplift and weathering in a modern, oxygen rich environment. The centre of some of these altered grains clearly remained out of contact with these later oxygenated fluids, as shown by the localised preservation of pyrite, ferrous phosphate and grey black carbonaceous material.

In some samples, a later Stage (4b) is evident (Fig. 16a–c), in the form of further microtubular structures which may be mistaken for AITs. These show no substratum preference; they may be found both in megaquartz (Fig. 16c) and chert grains, in the sandstone matrix, and crossing grain boundaries (Fig. 16b). They are typically brown to red in colour, carbon rich and filled with iron oxides. Only found clustered around the weathered margins of rock chips and thin sections (e.g., dotted area of Fig. 16a), they show few or none of the characteristic features of AIT. These microtubes are here interpreted as modern endolithic contaminants, most likely fungal hyphae (cf. Sterflinger 2000). Thus, for the best taphonomic preservation, protection is needed from modern weathering, which obliterates the original mineralogy and makes AIT identification more difficult.

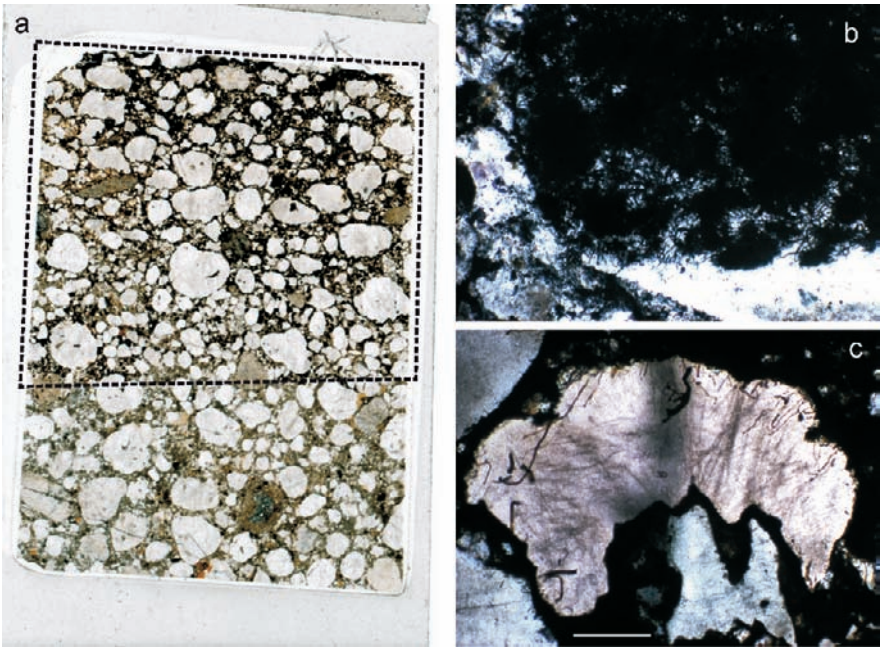

Fig. 16 Modern endolithic contamination in the Strelley Pool sandstone. (**a**) Thin section taken from the weathered outer zone of the sandstone. A red to dark-brown weathering zone extends approximately 20 mm into the thin section (*boxed area*); (**b**) A large clump of microtubular structures cutting across grain boundaries, found near the top of the boxed area in (**a**); (**c**) Iron oxide filled microtubes penetrating a corroded megaquartz grain, again from the top of the boxed area in (**a**). Thin section is ~40 mm long; scale bar is ~100 μm

6 Conclusions

This summary of AIT occurrences, in particular recent work in the Pilbara of Western Australia (Brasier et al. 2006; Wacey et al. 2006, 2007) documenting the metre- to nano-scale context of the Strelley Pool AITs suggests that such microstructures are indeed worthy of consideration as potential biomarkers in Archean rocks.

Our report of AITs from Devonian fish scales represents the youngest occurrence of such structures in the Phanerozoic rock record and shows that suitable conditions for AIT formation and preservation continued well beyond the Precambrian, at least within anoxic lacustrine environments. The better preservation of these more modern examples gives further clues about AIT formation. The size and distribution of these AITs clearly demonstrate the importance of both pyrite density and the associated volume of decaying organic matter in their formation. The enhanced degradation of the propelled pyrite during Devonian microtube formation appears to be the main difference between this and Precambrian examples.

It is now necessary to further test a mechanism of AIT formation that involves biological gaseous propulsion and dissolution. This will require laboratory

experiments using pyrite grains, a variety of substrates, and a range of modelled geological conditions, combined with detailed geochemical and isotopic studies on Phanerozoic AITs, such as the Devonian examples reported here.

Acknowledgments We thank the Geological Survey of Western Australia for assistance with field work, in particular Arthur Hickman, Martin Van Kranendonk and Kath Grey; Norman Charnley and Owen Green for laboratory support; Nicola McLoughlin for insightful discussions; and NERC and The Royal Society for financial support.

References

Aggleton H (2007) The preservation and analytical potential of the early tetrapod, *Acanthostega gunnari*. Unpublished Masters project, University of Oxford

Allwood AC, Walter MR, Kamber BS, Marshall CP, Burch IW (2006) Stromatolite reef from the Early Archaean era of Australia. Nature 441:714–718

Awramik SM (1992) The oldest records of photosynthesis. Photosyn Res 33:75–89

Awramik SM, Schopf JW, Walter MR (1983) Filamentous fossil bacteria from the Archean of Western Australia. Precambrian Res 20:357–374

Brasier MD, Green OR, Jephcoat AP, Kleppe AK, Van Kranendonk MJ, Lindsay JF, Steele A, Grassineau NV (2002) Questioning the evidence for Earth's oldest fossils. Nature 416:76–81

Brasier MD, Green OR, Lindsay JF, McLoughlin N, Steele A, Stoakes C (2005) Critical testing of Earth's oldest putative fossil assemblage from the ~3.5 Ga Apex chert, Chinaman Creek Western Australia. Precambrian Res 140:55–102

Brasier MD, McLoughlin N, Green OR, Wacey D (2006) A fresh look at the fossil evidence for early Archaean cellular life. Philos Trans R Soc Lond B Biol Sci 361:887–902

Brehm U, Gorbushina A, Mottershead D (2005) The role of microorganisms and biofilms in the breakdown and dissolution of quartz and glass. Palaeogeogr Palaeoclimatol Palaeoecol 219:117–129

Buick R (1984) Carbonaceous filaments from North Pole, Western Australia: are they fossil bacteria in Archaean stromatolites? Precambrian Res 24:157–172

Buick R (1990) Microfossil recognition in Archaean rocks: an appraisal of spheroids and filaments from 3500 M.Y old chert-barite at North Pole, Western Australia. Palaios 5:441–459

Conway Morris S, Bengtson S (1994) Cambrian predators: possible evidence from boreholes. J Palaeontol 68:1–23

Dineley DL, Metcalf SJ (1999) Fossil fishes of Great Britain. Geol Conserv Rev Ser, Joint Nature Conservation Committee. 16:675pp

Dong Y, Ji Q, Wang S (1984) The discovery of microscopic trace fossils in the Sinian Doushantou Formation in southwestern China. Sci Geol Sin 1984:346–347

Grey K (1986) Problematic microstructures in the Proterozoic Discovery Chert, Bangemall Group, Western Australia. Ambient grains or microfossils. West Aus Geol Surv Rec ISSN 0508-4741

Gruner JW (1923) Algae, believed to be Archean. J Geol 31:146–148

Gruner JW (1925) Discovery of life in the Archean. J Geol 33:151–152

Knoll AH, Barghoorn ES (1974) Ambient pyrite in Precambrian chert: new evidence and a theory. Proc Natl Acad Sci USA 71:2329–2331

Schopf JW (1993) Microfossils of the early Archaean Apex chert: new evidence for the antiquity of life. Science 260:640–646

Schopf JW (2006) Fossil evidence of Archean life. Philos Trans R Soc Lond B Biol Sci 361:869–886

Sterflinger K (2000) Fungi as geologic agents. Geomicrobiol J 17:97–124

Trewin NH (1986) Palaeoecology and sedimentology of the Achanarras fish bed of the Middle Old Red Sandstone, Scotland. Trans R Soc Edinb Earth Sci 77:21–46

Tyler SA, Barghoorn ES (1963) Ambient pyrite grains in Precambrian cherts. Am J Sci 261: 424–432

Van Kranendonk MJ (2000) Geology of the North Shaw 1:100,000 sheet. West Aus Geol Surv Rec Perth

Van Kranendonk MJ (2006) Volcanic degassing, hydrothermal circulation and the flourishing of early life on Earth: a review of the evidence from c. 3490–3240 Ma rocks of the Pilbara Supergroup, Pilbara Craton, Western Australia. Earth Sci Rev 74:197–240

Van Kranendonk MJ, Hickman AH, Williams IR, Nijman W (2001) Archean geology of the East Pilbara granite-greenstone terrane, Western Australia – a field guide. West Aus Geol Surv Rec 9:134p

Van Kranendonk MJ, Hickman AH, Smithies RH, Nelson DR (2002) Geology and tectonic evolution of the Archean North Pilbara Terrain, Pilbara Craton, Western Australia. Econ Geol 97:695–732

Van Kranendonk MJ, Smithies RH, Hickman AH, Champion DC (2007) Review: secular tectonic evolution of Archean continental crust: interplay between horizontal and vertical processes in the formation of the Pilbara Craton, Australia. Terra Nova 19:1–38

Wacey D, McLoughlin N, Green OR, Parnell J, Stoakes CA, Brasier MD (2006) The ~3.4 billion-year-old Strelley Pool Sandstone: a new window into early life on Earth. Int. J. Astrobiol 5: 333–342

Wacey D, Kilburn M, McLoughlin N, Parnell J, Stoakes CA, Grovenor CRM, Brasier MD (2007) Use of NanoSIMS in the search for early life on Earth: ambient inclusion trails in a c.3400 Ma sandstone, J Geol Soc London 165: 43–53

Xiao S, Knoll AH (1999) Fossil preservation in the Neoproterozoic Doushantuo phosphorite Lagerstätte, South China. Lethaia 32:219–240

Zhang Z (1984) Appendaged pyrite in the Sinian of South China. Kexue Tongbao 29:368–371

Zhegallo EA, Rozanov AY, Ushatinskaya GT, Hoover RB, Gerasimenko LM, Ragozina AL (2000) Atlas of microorganisms from ancient phosphorites of Khubsugal (Mongolia), NASA, TP209901, 167pp

Permissions: Permission has been granted for the reproduction of Tyler and Barghoorn 1963 (their plate 1 – figures 2 and 6, plate 3 – figure 2); Knoll and Barghoorn 1974 (their figures 1c, 2a, 2b); Awramik et al. 1983 (their figure 2f); Conway Morris and Bengtson 1994 (their figures 6.9 and 6.10; Xiao and Knoll 1999 (their figure 8e).

Spatial Distribution of the Subseafloo Life: Diversity and Biogeography

Fumio Inagaki and Satoshi Nakagawa

Abstract Marine subsurface sediments that cover more than two-thirds of the Earth harbor remarkable numbers of microbial cells. Subseafloor microbial activities may affect global biogeochemical cycles; however, our knowledge of the deep-subseafloor biosphere remains very limited. Recent molecular ecological studies have shown that subseafloor microbial communities are predominantly composed of yet -uncultivated, -uncharacterized bacteria and archaea with great phylogenetic diversity. Some phylogenetic groups are commonly detected in global marine sediments regardless of location and depth, and environmental factors such as sedimentological, geochemical, and geophysical characteristics probably control their activities, biomass, and community structures. This chapter reviews emerging patterns of microbial diversity in deeply buried marine sediments and discusses the potential ecological roles and distribution of microbial communities.

1 Introduction

Initial microbiological studies of marine subsurface sediments recovered by the Ocean Drilling Program (ODP) and the Integrated Ocean Drilling Program (IODP) have demonstrated that over 10^5 microbial cells cm^{-3} are consistently present in sediments down to the depth of 800 m below the seafloor (mbsf) (Parkes et al. 1994, 2000). Microbial cell densities generally decrease with increasing sediment depth, indicating a correlation with the amount of consumable organic matter as nutrients buried in the sediment from the overlying ocean. Despite their abundance, diagenetic models of porewater chemical constituents as well as radiotracer incubation experiments indicate that the metabolic activities of subseafloor microbes are extraordinarily low in general and decrease from coastal or continental margin environments towards central oceanic basins (D'Hondt et al. 2002).

F. Inagaki
Geomicrobiology Group, Kochi Institute for Core Sample Research, Japan Agency for Marine-Earth Science and Technology (JAMSTEC), Monobe B200, Nankoku, Kochi 783-8502, Japan; Subground Animalcule Retrieval (SUGAR) Program, Extremobiosphere Research Center, JAMSTEC, Natsushima-cho 2-15, Yokosuka 237-0061, Japan
e-mail: inagaki@jamstec.go.jp

Y. Dilek et al. (eds.), *Links Between Geological Processes, Microbial Activities & Evolution of Life*, © Springer Science+Business Media B.V. 2008

ODP Leg 201 was the first deep-drilling expedition dedicated to microbiological and biogeochemical research on the deep-subseafloor biosphere in the eastern tropical Pacific and Peru Margin (D'Hondt et al. 2004). Based on previous geochemical studies, the eastern equatorial Pacific was selected as an organic matter-poor, low microbial-activity site; the continental shelf off Peru, however, contains large amounts of organic matter buried by the Peruvian upwelling system, and high microbial activities in deeply buried marine sediments were expected. During the Leg 201 expedition, a variety of potential carbon sources and electron donors to and acceptors for indigenous microbes were quantified. The chemical profiles demonstrated that microbial activities in the Peru Margin sites were greater than those in open Pacific sites as expected, which was consistent with shore-based tracer experiments such as the measurement of sulfate reduction rates (D'Hondt et al. 2004; Parkes et al. 2005). At ODP Site 1229 in the Peru Margin, cell abundance specifically proliferated in a sulfate-methane transition zone at 90 mbsf, and sulfate reduction rates were also significantly increased near the surface level (Parkes et al. 2005). These observations suggest that microbial cells are ubiquitous in marine subsurface environments as a 'silent majority' in general but, in certain high-energy-flux habitats or at geochemical interfaces, the microbial population and activity are stimulated.

Since a large biomass has been observed globally even in low-energy-flux and geologically old subseafloor habitats, it was questioned whether the cells are alive and well, growing slowly, simply surviving, preserved as dormant cells or spores, or even all dead. Catalyzed reporter deposition-fluorescence in situ hybridization (CARD-FISH) is a highly sensitive technique to identify the presence of intracellular RNA that is rapidly degraded enzymatically after cell death (Davis et al. 1986). Schippers et al. (2005) first used CARD-FISH with domain Bacteria- and Archaea-specific probes to demonstrate that a large fraction of the subseafloor biomass is potentially alive, even in very old ($\sim$16 Ma) and deep ($>$400 m) sediments. Using the same technique, Mauclaire et al. (2004) reported that the population of Archaea increased with depth and that Deltaproteobacteria were detected throughout the core collected from the Peru Margin. These observations consistently suggest, on one hand, that a large population of subseafloor microbes is not dead but potentially alive; and on the other hand, that the abundance and physiological status of populations undetectable using CARD-FISH remain uncertain.

A standard approach to evaluate microbial diversity is the sequencing of 16S rRNA gene fragments amplified by the polymerase chain reaction (PCR) using a specific primer set for the domains Bacteria and Archaea. The PCR product is usually inserted into a high copy-number plasmid vector, and then cloned using *Escherichia coli*. In most cases, the entire fragment of representative clones, which are selected by 93–97% similarity cutoff short sequences (approximately 500 bp) or fingerprinting methods such as restriction fragment length polymorphism (RFLP), is determined. Although this protocol only allows the detection of PCR-amplifiable, major microbial components, it is a powerful tool to obtain initial insights into the microbial diversity in nature including the deep subseafloor.

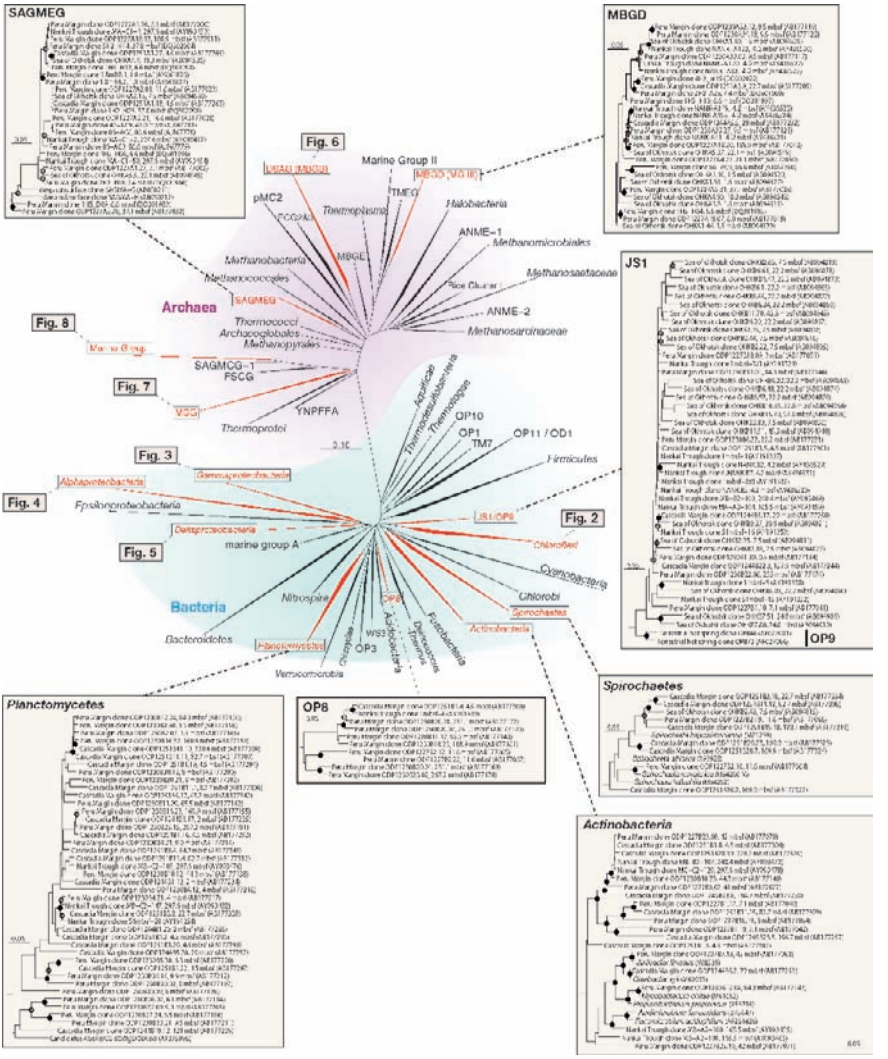

Fig. 1 16S rRNA-based tree showing the major phyla of Archaea and Bacteria. Red triangles represent branches with cultured or uncultured microorganisms frequently discovered in deep-subseafloor sediments. Several subtrees are shown in expanded boxes. GenBank/DDBJ/EMBL accession numbers are shown in parentheses. The scale bar represents the expected number of changes per nucleotide position. Sequence data were analyzed with ARB software package (Ludwig et al. 2004) and PAUP* 4.0b10 (Swofford 2000). Distances were estimated with the Jukes-Cantor correction. Unambiguously aligned positions (390 bases) were used. Bootstrap analyses with 100 trial replications were used to obtain confidence estimates for the tree topologies. Branch points conserved with bootstrap values of $> 75\%$ (*solid circles*) and with bootstrap values of $> 50\%$ (*open circles*) are indicated

Along with methodological progress in DNA extraction and contamination assays, DNA sequences from verifiable deep subseafloor materials have accumulated. During ODP Leg 201 (Peru Margin) and Leg 204 (Cascadia Margin off Oregon), over 3,000 clone sequences of bacterial and archaeal 16S rRNA genes from high-resolution depth samples were investigated (Sørensen et al. 2004; Parkes et al. 2005; Inagaki et al. 2006a; Webster et al. 2006). The communities of 'metabolically active' Archaea were also investigated using the reverse-transcribed PCR technique (Biddle et al. 2006b; Sørensen and Teske 2006). Compiling these molecular data from deep-subseafloor microbes, we note some trends in their distribution, that is, some microbes are widely distributed in marine sediments while others are not (Fig. 1). Here we reconstruct the phylogenetic trees of the Bacteria and Archaea domains as a catalogue of the diversity of deep-subseafloor microbes and review the general trends in their diversity and distribution. We focus on bacterial and archaeal phyla frequently detected in deep-subseafloor environments.

2 Diversity of Deep-Subseafloo Bacteria

Bacterial 16S rRNA sequences from deep-subseafloor habitats suggest that the community compositions are highly diverse and differ from those in the overlying surface world such as terrestrial and oceanic environments. Although the DNA extraction protocol and PCR conditions vary slightly in each laboratory, multiple molecular studies of subseafloor bacterial communities have provided consistent results. We compile here these sequences from deep-subseafloor microbial habitats into the same phylogenetic trees and describe the phylogenetic characteristics at the phylum level.

2.1 Chloroflex

The phylum Chloroflexi has been alternatively called Green Non-sulfur Bacteria (GNS). A number of phylotypes has been detected from surface and subsurface (hemi-)pelagic clay and silt deposits. At ODP Site 1176 in the Nankai Trough (Leg 190) and Sites 1227 and 1229 in the Peru Margin (Leg 201), 50–80% of clones were affiliated with Chloroflexi (Kormas et al. 2003; Inagaki et al. 2006a; Webster et al. 2006). Chloroflexi was also predominantly detected in clone libraries from hemi-pelagic clay layers of the Sea of Okhotsk core (Inagaki et al. 2003) and methane hydrate-associated sediments in the Nankai Trough (Reed et al. 2002) and the Gulf of Mexico (Mills et al. 2005). The predominance of Chloroflexi was also reported using a community fingerprinting method of denaturing gradient gel electrophoresis (DGGE) from the Mediterranean Sea sapropel layers (Coolen et al. 2002) and the tidal flat subseafloor sediments in the Wadden Sea (Wilms et al. 2006).

The phylum Chloroflexi is currently divided into five classes: Anaerolineae (cluster I), 'Dehalococcoidetes' (cluster II), Chloroflexi (cluster III), uncultured cluster IV (SAR202 cluster), and Thermomicrobia (Sekiguchi et al. 2003; Hugenholtz and Stackebrandt 2004; Morris et al. 2004; Yamada et al. 2006). The members of Chloroflexi from the deep marine subsurface are mainly affiliated with 'Dehalococcoidetes' (Fig. 2). The representative bacterium within this class, *Dehalococcoides ethenogenes*, is a facultatively hydrogenotrophic and heterotrophic anaerobe that uses chlorinated compounds as electron acceptors (Maymo-Gatell et al. 1997). Although it is unknown whether the deep-subseafloor, Dehalococcoides, relatives have physiology similar to *D. ethenogenes*, the dechlorination pathway would be a good candidate because available electron acceptors are very limited in deep-subsurface environments. Members of other subphyla of Chloroflexi have been retrieved less frequently from deep marine sediments, which makes sense because the cultivated representative genera *Chloroflexus, Chloronema, Heliothrix, Oscillochloris*, and *Herpetosiphon* are either phototrophic or chemoheterotrophic bacteria isolated from terrestrial environments (Garrity and Holt 2001). Several clones of the class 'Anaerolineae' have been reported from deep-subseafloor environments. Within the class 'Anaerolineae,' the two genera *Anaerolinea* and *Levilinea* were isolated from anaerobic granular sludge, representing thermophilic and mesophilic filamentous heterotrophs, respectively (Yamada et al. 2006). Their growth was stimulated significantly upon co-culture with hydrogenotrophic methanogens (Yamada et al. 2006), suggesting the occurrence of similar microbial interactions in subseafloor environments (Inagaki et al. 2006a). The uncultured cluster IV involves environmental clone sequences retrieved from various environments. Because of the absence of isolates within this class, their physiology is unexpectable. The class Thermomicrobia was recently reclassified from the phylum Actinobacteria to Chloroflexi (Hugenholtz and Stackebrandt 2004), and no relatives have been detected from deep-subseafloor environments.

2.2 Candidate Division JS1

This phylogenetic group involves a large number of environmental clone sequences from shallow to deep marine sediments (Fig. 1). JS1 bacteria were formerly classified as relatives of the candidate division OP9 (e.g., Teske et al. 2002; Inagaki et al. 2003). However, since the phylogenetic position of the OP9 sequences, which were originally derived from the Obsidian Pool hot spring in Yellowstone National Park (Hugenholtz et al. 1998), are distinct from the marine environmental sequences (Fig. 1) and the OP9-associated cluster was found for the first time in Japan Trench sediment (Rochelle et al. 1994), the cluster of marine environmental clones has been reclassified as the candidate division JS1 (Webster et al. 2004). Although JS1 bacteria are distributed in global marine sediments, previous surveys suggested that they preferentially inhabit methane- and/or hydrocarbon-rich deep marine sediments on the continental margins such as in the Nankai Trough (Reed et al. 2002;

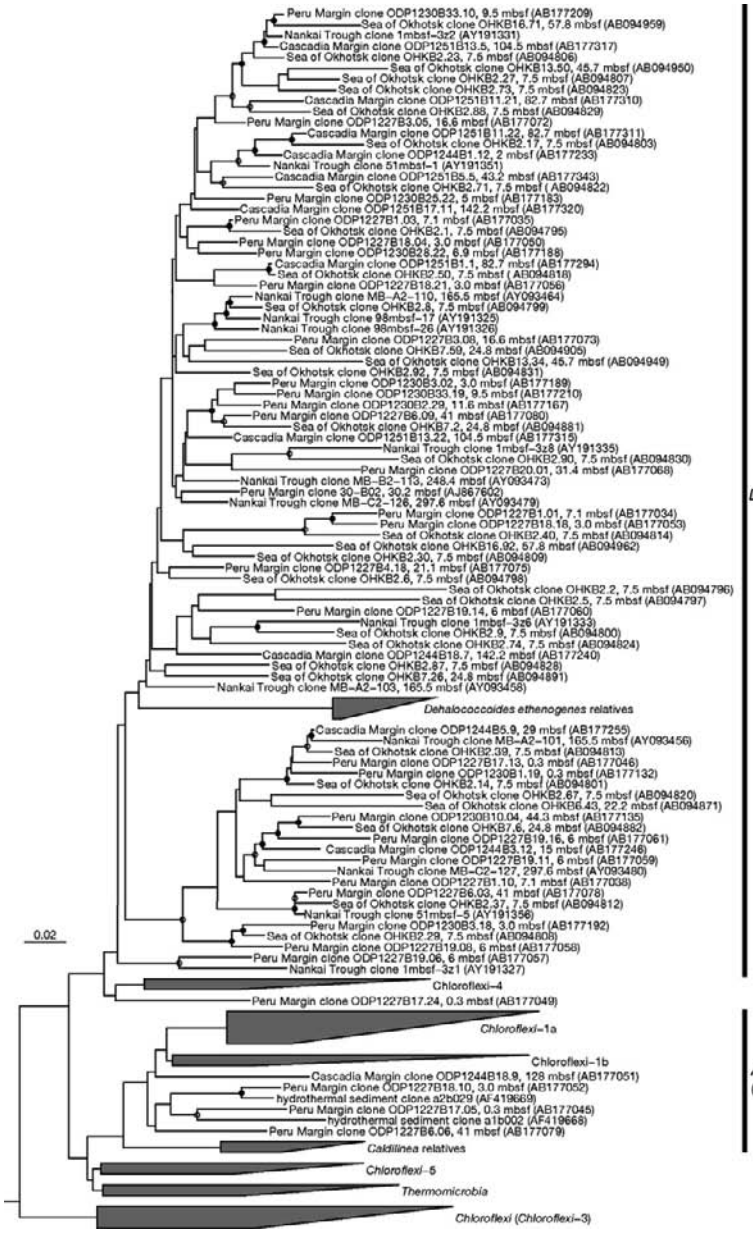

Fig. 2 Phylogenetic tree of Chloroflexi based on 16S rRNA gene sequences. The size of triangles is proportional to the number of sequences analyzed. See the legend to Fig. 1 for details

Newberry et al. 2004), Sea of Okhotsk (Inagaki et al. 2003), Cascadia Margin (Inagaki et al. 2006a), and Peru Margin (Parkes et al. 2005; Inagaki et al. 2006a; Webster et al. 2006; Fry et al. 2006). Given the predominance of JS1 bacteria in methane-rich marine sediments, their ecological roles in carbon cycling are thought to be important.

2.3 Proteobacteria

Members of the phylum Proteobacteria are widely distributed in the surface world on Earth. Proteobacteria are sometimes predominant even in the subsurface, as shown by both cultivation and culture-independent molecular analyses. The phylum Proteobacteria includes remarkably diverse isolates of chemolithoautotrophs, heterotrophs, and mixotrophs and is classified into five subphyla (Alpha-, Beta-, Gamma-, Delta- and Epsilonproteobacteria). It is widely recognized among microbiologists that Proteobacteria play important roles in biogeochemical cycles in marine environments such as sulfate reduction by Deltaproteobacteria, sulfur oxidation by Gamma- and Epsilonproteobacteria, aerobic methane oxidation by Alpha- and Gammaproteobacteria, and consumption of buried organic matter or dissolved inorganic carbon by heterotrophic or chemolithotrophic members.

2.3.1 Gammaproteobacteria

In deep-subseafloor sediments, the most frequently detected and cultivated Proteobacteria are members of the subphylum Gammaproteobacteria. In a 58-m giant piston core from the Sea of Okhotsk, *Gammaproteobacteria* were predominantly detected in volcanic ash layers, whereas Proteobacteria were relatively minor in pelagic clays (Inagaki et al. 2003). Within the Gammaproteobacteria, most clone sequences are closely related to known isolates such as the genera *Halomonas, Psychrobacter, Photobacterium, Shewanella, Moritella, Colwellia, Oceanospirillum, and Methylophaga* (Figs. 3 and 4). The most frequently detected phylotypes were *Halomonas* relatives. The predominance of Gammaproteobacteria in marine sediments was also observed at the south hydrate ridge of the Cascadia Margin.

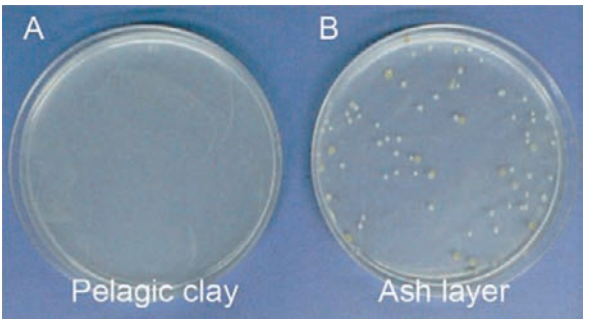

Fig. 3 Bacterial colonies from (**A**) pelagic clay and (**B**) volcanic ash samples in 58 m sediment core from the Sea of Okhotsk (Inagaki et al. 2003). Sizable populations of facultatively anaerobic heterotrophs could be retrieved only from volcanic ash layers

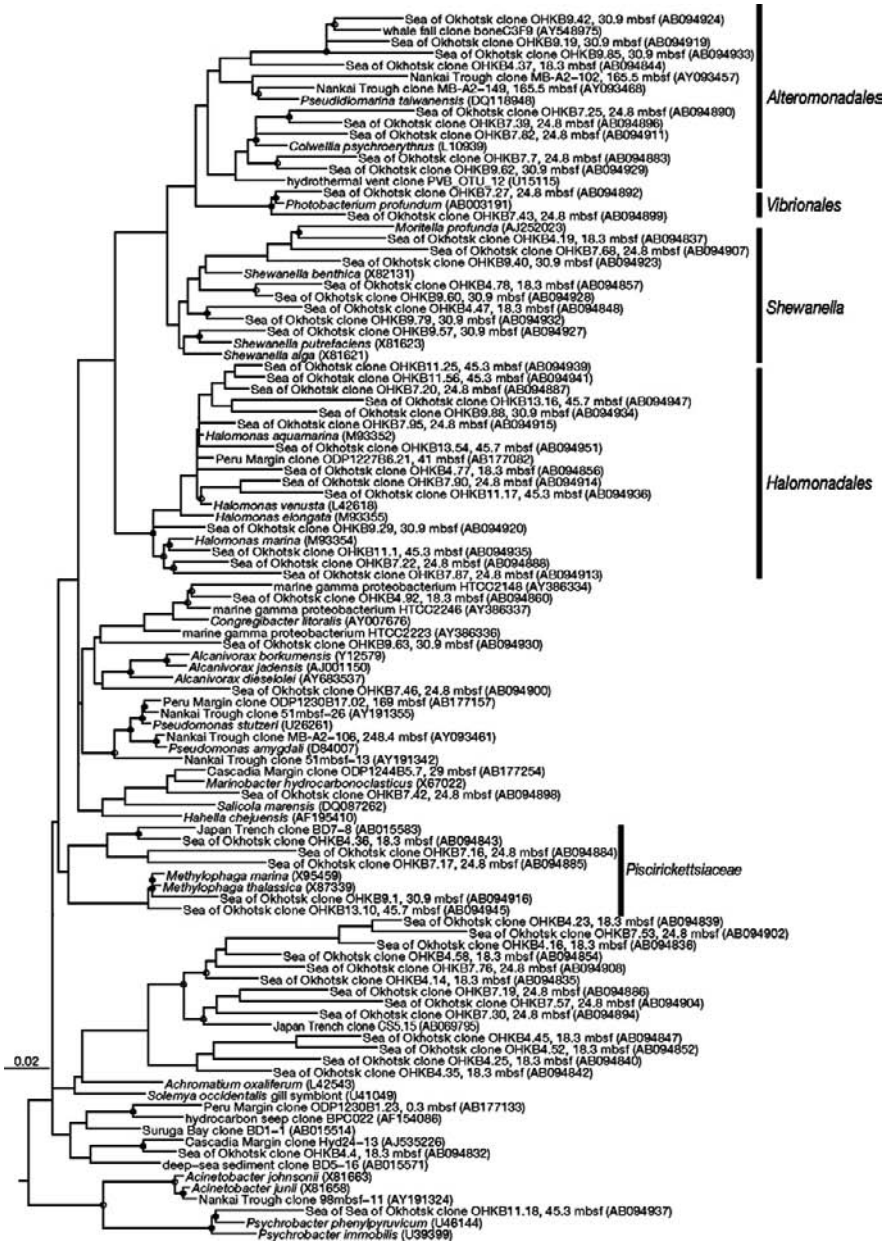

Fig. 4 Phylogenetic tree of Gammaproteobacteria based on 16S rRNA gene sequences. See the legend to Fig. 1 for details

All 16S rRNA gene sequences in a clone library at 204 mbsf were closely related to *Marinobacter aquaeolei* (96.1% similarity to the representative clone sequence), although the lithological feature has not been determined (Inagaki et al. 2003). At ODP Site 1229 in the Peru Margin, DGGE and clone library analyses showed the presence of other Gammaproteobacteria, including the genera *Stenotrophomonas* and *Serratia* (Fry et al. 2006; Webster et al. 2006). Most isolates of these genera are facultatively anaerobic heterotrophs, and some isolates are halophilic or piezophilic (pressure-loving or -tolerant) bacteria. Among these *Gammaproteobacteria* from deep-subseafloor environments, of particular interest are methanotroph relatives exclusively detected in several ash layers (Inagaki et al. 2003) (Fig. 4). It is hard to believe that aerobic methanotrophs detected from ash layers utilize oxygen in situ. However, the typical physiotype of methanotrophs as a 'microbial tracer' may indicate the potential reconstruction of aquatic subseafloor niches that may contain methane and some available electron acceptors.

The predominance of Gammaproteobacteria was also supported by the colony-forming unit (CFU) cultivation assay. The CFUs of *Halomonas* and *Psychrobacter* relatives on agar plates showed good agreement with their clonal frequencies. Since the CFU values of Gammaproteobacteria reach 10^4–10^5 colonies cm^{-3}, they are most likely alive in deep-subseafloor environments and may require sufficient pore spaces for their habitat and/or for high porewater flux via volcanic ash or sandy layers. At ODP Site 1230 in the Peru Margin, members of the genera *Halomonas*, *Marinobacter*, *Shewanella*, *Photobacterium*, and *Vibrio* were also isolated from the deep sediments (D'Hondt et al. 2004; Biddle et al. 2006b), although the analysis of 16S rRNA gene clone libraries indicated that these members were minorities (Inagaki et al. 2006a).

2.3.2 Alphaproteobacteria

Although Alphaproteobacteria are generally rarely recovered from deep-subseafloor environments, a sizeable number of alpha-proteobacterial clones were detected in clone library or DGGE analysis of bacterial 16S rRNA genes. The detected sequences were related to known isolates such as *Sulfitobacter*, *Octadecabacter*, and *Sphingomonas* from the Sea of Okhotsk (Inagaki et al. 2003), *Bradyrhizobium*, *Pedomicrobium* and *Sphingomonas* from the Peru Margin and the Cascadia Margin (Inagaki et al. 2006a), and *Caulobacter* (Webster et al. 2006) (Fig. 5). *Sulfitobacter* spp. were frequently isolated from ash layers of the Sea of Okhotsk (Inagaki et al. 2003). In the sapropel-containing core from the eastern Mediterranean Sea, although culture-independent molecular studies indicated the dominance of Chloroflexi (Coolen et al. 2002), *Rhizobium radiobacter* was found to be the most predominantly isolated bacterium (Suss et al. 2004). Suss et al. (2006) also found using quantitative PCR that *R. radiobacter* accounted for 0.001–5.1% of total cells in the sediments. During ODP Leg 201, *R. radiobacter* relatives were representative isolates from the eastern equatorial Pacific and Peru Margin and at ODP Sites 1227 and 1230, which were organic matter-rich, high-microbial-activity sites with and without methane hydrates, respectively (D'Hondt et al. 2004). The information

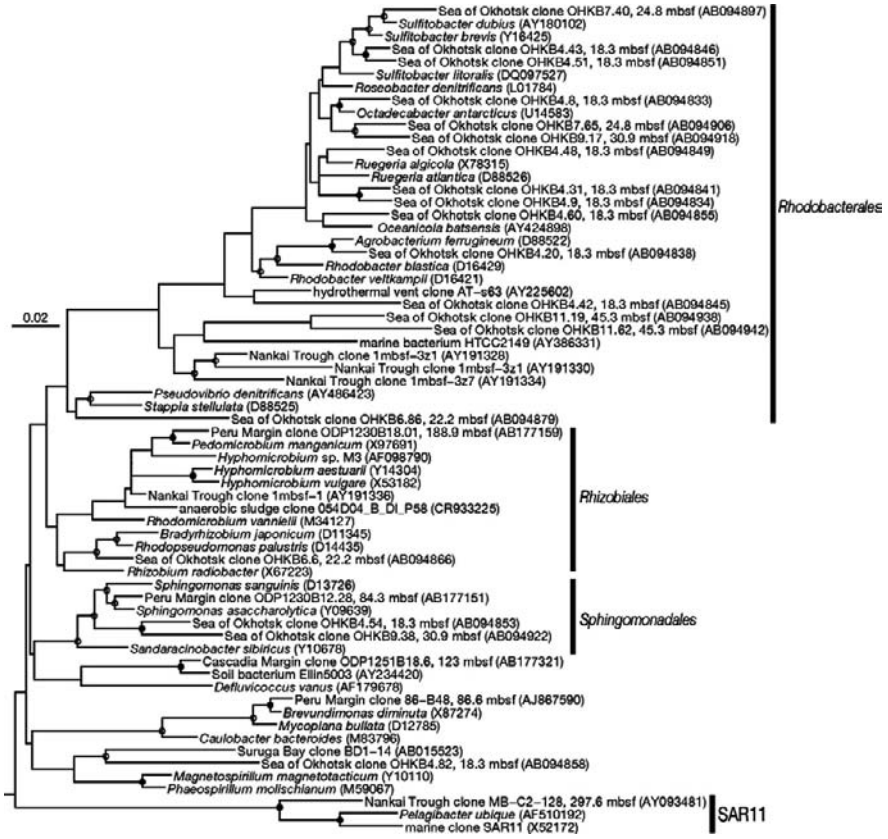

Fig. 5 Phylogenetic tree of Alphaproteobacteria based on 16S rRNA gene sequences. See the legend to Fig. 1 for details

described above suggests that sizable numbers of Alphaproteobacteria are present in continental margin marine sediments and their community compositions vary geographically.

2.3.3 Deltaproteobacteria

The anaerobic respiration of the members of Deltaproteobacteria may significantly contribute to sulfur and carbon cycling in the deep marine subsurface. During ODP Leg 128, the sulfate reducer *Desulfovibrio profundus* was isolated from deep sediments (80 and 500 m) at ODP Site 798 in the Japan Sea (Bale et al. 1997). Also, sulfate-reducing bacteria (SRB) within Deltaproteobacteria play an important role in the anaerobic oxidation of methane (AOM) in methane-seep sediments on the seafloor. In most cases, a consortium composed of methanotrophic Archaea and SRB within Deltaproteobacteria is responsible for AOM (e.g., Boetius et al. 2000;

Knittel et al. 2005). However, very little is known about which organisms are responsible for AOM in deep marine sediments.

In deep-subseafloor environments, molecular ecological surveys revealed that a variety of Deltaproteobacteria are occasionally detected throughout the cores examined, regardless of the presence of sulfate in porewater. The frequently detected Deltaproteobacteria from a variety of deep marine sediments such as the Sea of Okhotsk, Peru Margin, and Cascadia Margin (Inagaki et al. 2003, 2006a) were related to *Desulfobacterium anilini* and *Desulfomonile* spp. (Fig. 6). *D. anillini* can degrade a variety of aryl compounds completely to CO_2 and NH_3 with sulfate as an electron acceptor (Schnell et al. 1989). *Desulfononile* species can utilize aromatic chloride compounds as electron acceptors (e.g., Mohn and Tiedje 1992). From an organic-rich methane hydrate site off Peru, a few Deltaproteobacteria were related

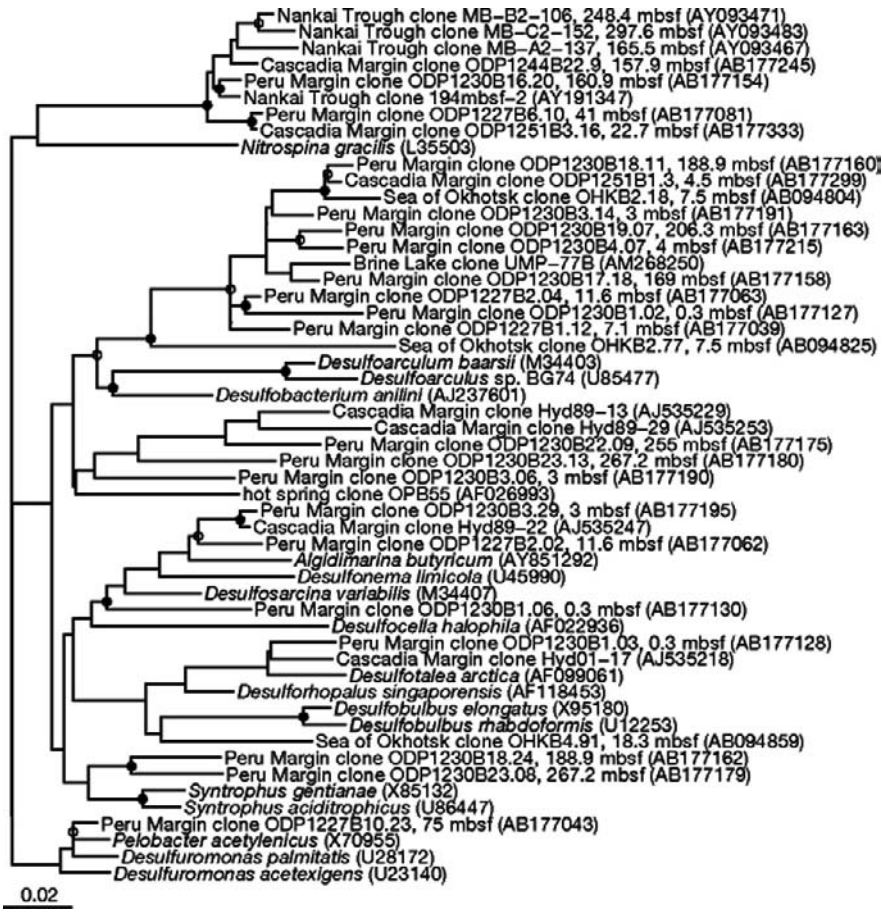

Fig. 6 Phylogenetic tree of Deltaproteobacteria based on 16S rRNA gene sequences. See the legend to Fig. 1 for details

to *Syntrophus buswellii* (Fig. 6). *S. buswellii* can also degrade aromatic compounds such as benzoate, 3-phenylpropionate, and crotonate to acetate, CO_2, and hydrogen (Auburger and Winter 1996). Since deeply buried marine sediments, especially on the continental margins, contain high concentrations of humic acid substrates after the biological degradation of organic matter in surface sediments, the organic matter available as energy sources is very limited in deep marine sediments. Therefore, it is reasonable to assume that these Deltaproteobacteria can grow on aromatic compounds coupled with sulfate reduction. In addition, the growth of *S. buswellii* is stimulated during co-culture with hydrogenotrophic methanogens (Auburger and Winter 1996). Dechlorination under the control of a low hydrogen concentration for the syntrophic growth of Deltaproteobacteria and Chloroflexi members may be a fairly common feature of microbial ecosystems in energy-starved deep-subseafloor environments.

2.4 Other Deep-Subseafloo Bacteria

Diverse bacteria within other phylogenetic groups have been detected from deep-marine sediments. In organic-rich and/or methane hydrate-bearing deep marine sediments, Planctomycetes are also detected as predominant bacteria (Fig. 1) (Reed et al. 2002; Inagaki et al. 2003, 2006a). The sequences detected are highly diverse and distantly related to isolates such as the genera *Planctomyces* and *Pirellula* as well as the members of anaerobic ammonia-oxidizing (anammox) bacteria. Small numbers of Actinobacteria, Bacteroidetes, Flavobacteria, Firmicutes, Chlamydia, Spirochaetes, Deferribacteres, candidate divisions OP1, OP3, OP8, OP10, OP11, WS1, and WS3, and several unknown phylogroups were found in deep sediments and accounted for small percentages of the total (Inagaki et al. 2006a) (Fig. 1). Most of these phylogroups represent uncultivated and physiologically uncharacterized assemblages.

3 Diversity of the Deep-Subseafloo Archaea

A variety of archaeal phylotypes have been collected from deep-subseafloor environments. Phylogenetic analysis revealed that most subseafloor Archaea are affiliated with clusters consisting only of uncultivated environmental clone sequences. Thus the physiological and metabolic characteristics of Archaea in marine sediments remain largely unknown. Nevertheless, Archaea are obviously important at least for the methane cycle in the subseafloor because both the production and consumption of methane may be attributed to methane-producing (methanogens) and methane-consuming (methanotrophs) Archaea, respectively. Here, we describe the major groups of subseafloor Archaea detected and the biogeography of their preferential subseafloor habitats based on the results of 16S rRNA gene sequencing.

3.1 Deep-Sea Archaeal Group

The members of the deep-sea archaeal group (DSAG) (Takai and Horikoshi 1999), of which a cluster is designated marine benthic group-B (MBG-B) (Vetriani et al. 1999), are phylogenetically diverse, globally distributed and most frequently detected in methane hydrate-associated sediments from offshore continental margins. The DSAG sequences were originally reported from hydrothermal vent sites. DSAG-dominated archaeal communities have been reported from gassy hemipelagic clay layers in the Sea of Okhotsk (Inagaki et al. 2003), methane hydrate-bearing deep marine sediments in the Nankai Trough (Reed et al. 2002), Peru Margin ODP Site 1230 (Inagaki et al. 2006a) and Cascadia Margin ODP Sites 1244 and 1251 (Inagaki et al. 2006a) (Fig. 7). In these sediment samples, DSAG Archaea are generally detected in the relatively shallow subsurface (0–100 mbsf). In addition, DSAG Archaea were obtained less frequently from a variety of seafloor sediments, i.e., Atlantic deep-sea sediments (Vetriani et al. 1999), methane-seep sediments of the Cascadia Margin (Knittel et al. 2005) and the Kuroshima Knoll (Inagaki

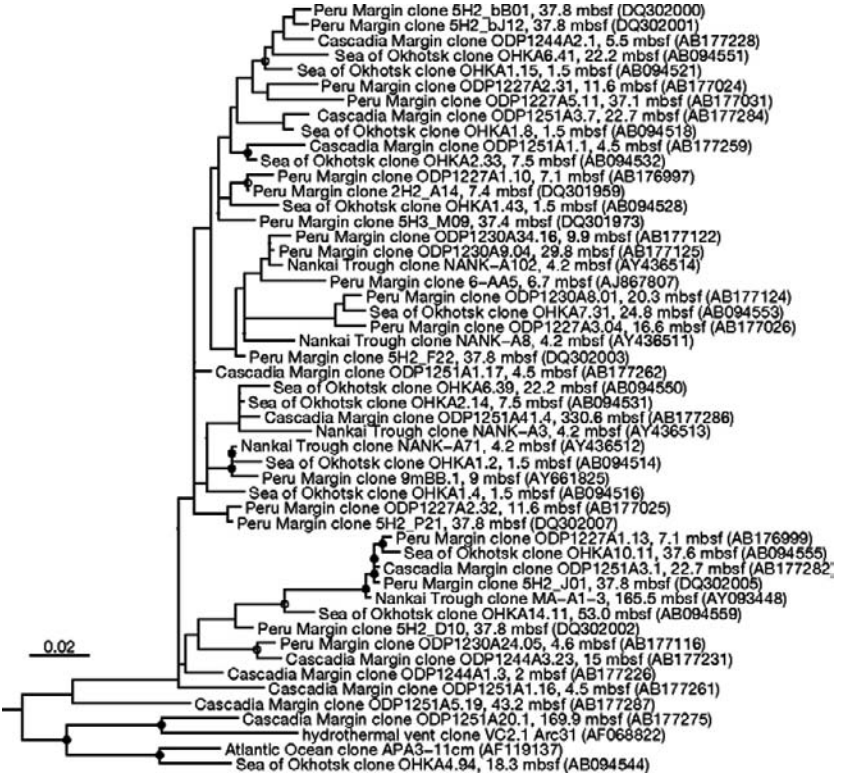

Fig. 7 Phylogenetic tree of the deep-sea archaeal group (DSAG) based on 16S rRNA gene sequences. See the legend to Fig. 1 for details

et al. 2004), and hydrothermal deposits (or sediments) of the Izu-Ogasawara Arc (Takai and Horikoshi 1999) and the Guaymas Basin (Teske et al. 2002). However, DSAG have not been detected (or only a few sequences have been detected) from the sapropel layers of the eastern Mediterranean Sea (Coolen et al. 2002), ODP Site 1176 in the Nankai Trough Forearc Basin (Kormas et al. 2003), volcanic ash layers in the Sea of Okhotsk core (Inagaki et al. 2003), ODP Sites 1227 (Inagaki et al. 2006a) and 1229 (Parkes et al. 2005; Webster et al. 2006) from the Peru Margin, and the liquid CO_2-bearing hydrothermal sediments at the Yonaguni Knoll of the southern Okinawa Trough (Inagaki et al. 2006b). Although the DSAG were relatively minor components at ODP Site 1227 off Peru in the DNA-based molecular study, DSAG-dominated archaeal community structures were observed at the sulfate-methane transition zone in an RNA-based study (Sørensen and Teske 2006). Taking the results of these molecular surveys together, the DSAG Archaea appear to inhabit anoxic methane- and/or organic-rich clay sediments preferentially and may actively contribute to the carbon cycle in deep subseafloor environments.

3.2 South African Gold Mine Euryarchaeotic Group

The phylotypes of the South African Gold Mine Euryarchaeotic Group (SAGMEG) were originally reported from deep fissure waters in a South African gold mine (Takai et al. 2001). SAGMEG phylotypes were also reported as a minor component from the microbial mat samples in borehole hot water in a Japanese epithermal gold mine (Nunoura et al. 2005). Since the 16S rRNA gene sequences have relatively high G + C content and the fissure waters are derived from the deep hot aquifer, SAGMEG Archaea were hypothesized to be thermophiles (Takai et al. 2001). However, SAGMEG have recently been retrieved from cold deep-marine sediments such as sapropel from the eastern Mediterranean Sea (Coolen et al. 2002), Nankai Trough Forearc (Reed et al. 2002), volcanic ash layers of the Sea of Okhotsk core (Inagaki et al. 2003), ODP Sites 1227 (Inagaki et al. 2006a; Sørensen and Teske 2006) and 1229 (Parkes et al. 2005; Webster et al. 2006) of the Peru Margin, and ODP Sites 1245 and 1251 on the South Hydrate Ridge of the Cascadia Margin (Inagaki et al. 2006a) (Fig. 1). These observations suggest that SAGMEG Archaea globally inhabit the marine and terrestrial subsurface and may consist of both mesophiles and thermophiles. However, their nutrient and energy metabolism, morphology, lifetime and adaptation to the subsurface environments remain largely unknown.

3.3 Miscellaneous Crenarchaeotic Group

Within the Crenarchaeota, remarkably diverse sequences from a variety of natural environments are affiliated with a huge cluster designated the miscellaneous Crenarchaeotic group (MCG). MCG consists of a number of environmental sequences

from various natural environments, such as soil, seawater, sludge, compost, hot springs, hydrothermal areas, deep gold mines, marine surface sediments, and deep marine sediments (Fig. 8). Some phylotypes are reported to be the most frequently detected in deep subseafloor environments, i.e., OHKA4.47 (accession no. AB094540) comprised 79/299 archaeal clones obtained from ash layers of the Sea of Okhotsk core (Inagaki et al. 2003) (Fig. 8).

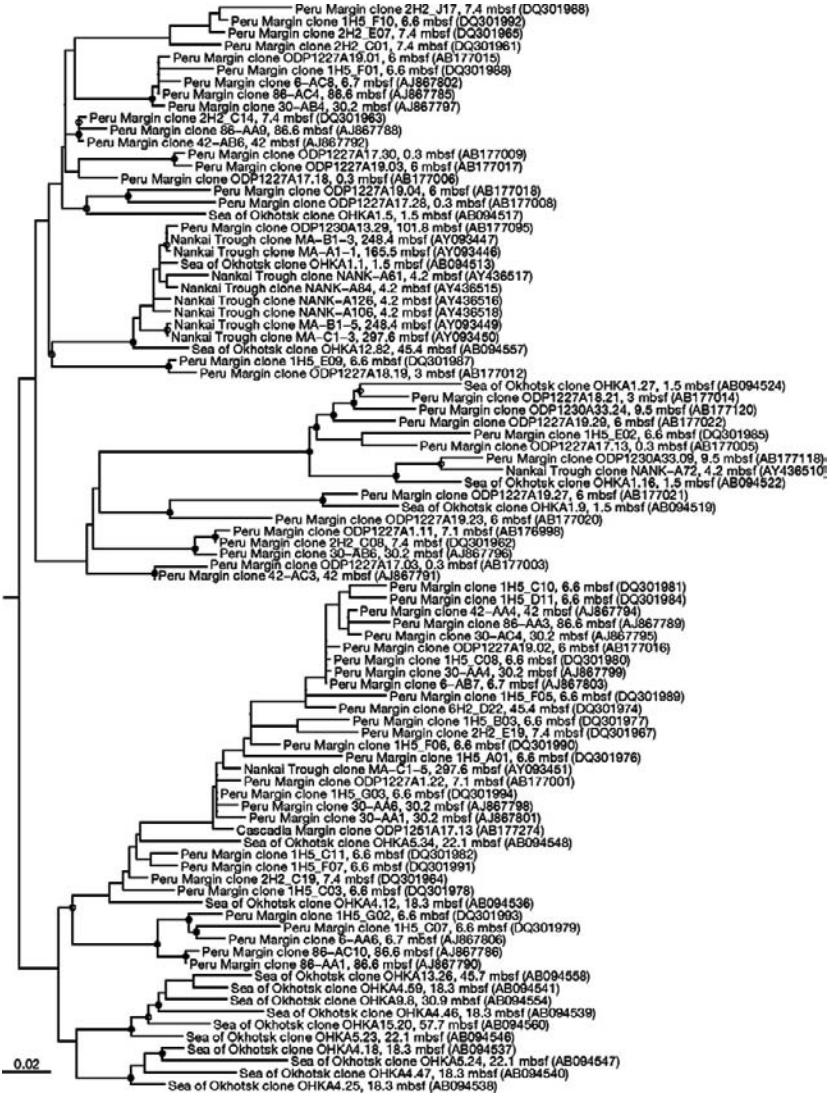

Fig. 8 Phylogenetic tree of the miscellaneous crenarchaeotic group (MCG) based on 16S rRNA gene sequences. See the legend to Fig. 1 for details

Although almost nothing except the phylogeny is known about the MCG Archaea, the environmental clone surveys imply that their preferential habitat is the deep-subseafloor environment. In the Sea of Okhotsk sediment core, MCG Archaea were predominantly detected from the volcanic ash layers, while DSAG members dominated in pelagic clay horizons (Inagaki et al. 2003). Even in the methane hydrate-bearing core sediments, in which generally DSAG sequences are predominantly detected if the hydrates form in sandy layers, MCG dominated clone libraries (i.e., Reed et al. 2002; Inagaki et al. 2006a unpublished data). In addition, MCG sequences have often been detected with members of SAGMEG (Inagaki et al. 2003, 2006a; Parkes et al. 2005; Webster et al. 2006; Sørensen and Teske 2006), indicating that both archaeal groups have a widespread habitable zone in the terrestrial and marine subsurface around the continental margins and may prefer porous or aquatic habitats in subsurface environments.

3.4 Methanogens and Methane-Consuming Archaea

Since approximately 500–2,500 Gt of total methane carbon are stored as hydrate or free gas in the continental margin sediments (Milkov 2004) and vast amounts of stored methane are considered biological products (Kvenvolden 1995), methanogenic Archaea are of particular interest in studies of subseafloor microbial communities. Despite the ample geochemical evidence for biogenic methane production, as indicated by high C1/C2 ratios, highly ^{13}C-depleted stable carbon isotopic compositions (less than $-60‰$), and methanogenesis activity measurements using radiotracer methods (e.g., Parkes et al. 2005), methanogens are rarely found in deep-subseafloor environments.

From the deep subseafloor, *Methanoculleus submarines* was the first isolate from methane hydrate-bearing sediments in the Nankai Trough at 247 mbsf, which requires acetate as a carbon source and hydrogen or formate as an energy source (Mikucki et al. 2003). A few strains of the hydrogenotrophic chemolithoautotrophic methanogen *Methanococcus aeolicus* were also isolated from the same sediment sample (Kendall et al. 2006).

The presence of putative mesophilic methanogens in some deep-subseafloor environments was also confirmed in culture-independent molecular studies. During ODP Leg 146 at the Cascadia Margin, the 16S rRNA gene sequences related to the genera *Methanosarcina* and *Methanobrevibacter* were detected from methane hydrate-bearing sediments at four depths of 9, 198, 222, and 234 mbsf using a methanogen-specific PCR primer set (Marchesi et al. 2001). During ODP Leg 204 at the Cascadia Margin, sequences related to *Methaonosarcina acetivorans* and *Methanoculleus palmolei* were detected from hydrate-bearing sediments at 22.7 and 43.2 mbsf using general archaeal primers (Inagaki et al. 2006a). Furthermore, a functional gene of the methanogenesis pathway, the methyl-co-enzyme-M reductase a-subunit gene (*mcrA*), was retrieved from the Nankai Trough (Newberry et al. 2004) and Peru Margin (Parkes et al. 2005; Inagaki et al. 2006a) sediments.

These molecular results consistently suggest that mesophilic methanogens are indeed distributed in methane-rich deep marine sediments on the continental margins. However, any causative relationships of the occurrence of these populations to the mechanism of methane hydrate formation remain elusive.

Recent studies of methane- or hydrocarbon-seep microbial communities have revealed that the members of anaerobic methane-oxidizing (ANME) Archaea play a major role in AOM in marine sediments (e.g., Boetius et al. 2000; Orphan et al. 2001; Inagaki et al. 2004; Knittel et al. 2005). The reaction of AOM requires sulfate as an electron acceptor and a consortium composed of ANME Archaea and sulfate-reducing bacteria is responsible for AOM. Despite the molecular detection of putative sulfate reducers within Deltaproteobacteria, the 16S rRNA and *mcrA* gene sequences of ANME archaea have been rarely detected from deep marine sediments. Only two clones belonging to the ANME-1 cluster were detected from the Sea of Okhotsk core at 14.7 mbsf (OHKA3.36: accession no. AB094534); however, geochemical data on sulfate and methane concentrations have not been determined (Inagaki et al. 2003). The components, population size, and functioning of AOM communities in deep-subseafloor environments is currently largely unknown.

3.5 Other Deep-Subseafloo Archaea

In addition to the predominant archaeal groups described above, a number of minor archaeal phylotypes within other groups or clusters have been detected from recently explored deep-subseafloor environments. The clone library data include sequences within the MBG-D (alternatively designated marine group III), marine crenarchaeota group I (marine group I), and several unclassified phylotypes (Fig. 1). The MBG-D belongs to the Thermoplasmatales and has frequently been retrieved from methane-seep or methane-rich environments associated with AOM (e.g., Orphan et al. 2001; Girguis et al. 2003; Inagaki et al. 2004). Therefore, the ecological role of MBG-D Archaea may be important for understanding biologically mediated hydrocarbon flows in deep-subseafloor environments. At the ODP methane hydrate Site 1230 off Peru, members of marine group I were detected as predominant Archaea from hydrate-bearing deep marine sediments (Inagaki et al. 2006a). Members of marine group I are widely distributed in oceanic environments. Marine group I members detected from Site 1230 were highly diverse and affiliated mainly with the γ-subclass of the marine group I cluster (Massana et al. 1997) (Fig. 9). Recently, one marine group I member, *Nitrosopumilus maritimus*, has successfully been isolated and found to be a chemolithoautotrophic ammonia-oxidizing archaeon (Könneke et al. 2005). Metagenomic analyses of marine Crenarchaeota have revealed that the widespread presence of diverse archaeal ammonia monooxigenase alpha-subunit (*amoA*) genes in seawater and suboxic sediments (Francis et al. 2005; Hallam et al. 2006). These cultivation and molecular studies are also necessary to understand physiological characteristics of the deep subseafloor Crenarchaeota.

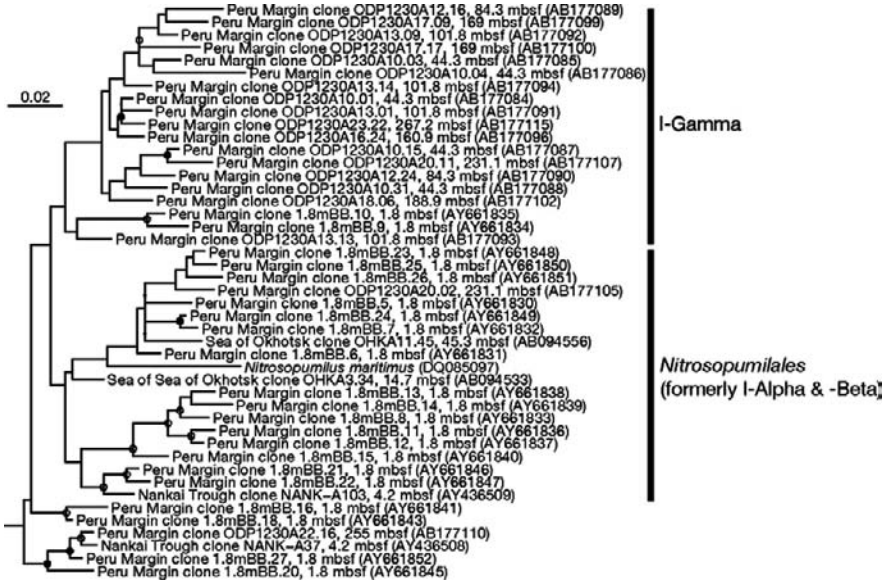

Fig. 9 Phylogenetic tree of marine group I (MGI) based on 16S rRNA gene sequences. See the legend to Fig. 1 for details

4 Discussion

Despite the successful detection of diverse and previously unknown microbial components from the deep-subseafloor environments, their growth characteristics as well as ecological impacts are largely unknown. The 16S rRNA gene sequence data have significantly expanded our knowledge of community composition and structure in distinctive subseafloor environments and they are useful for the development of future cultivation trials and molecular ecological studies like CARD-FISH. However, it must be noted that clone library methods using PCR may have significant biases. First, our recent study of DNA extraction from deep-marine sediments has indicated that a large fraction of microbial cells are highly resistant to enzymatic and/or SDS extraction, suggesting that subseafloor microbial communities may be more diverse than thought and we have not grasped the true microbial community structures (Inagaki et al. unpublished results). Even if the environmental intracellular DNA is completely extracted, since our knowledge of the conserved sequences for constructing PCR primers or probes is originally based on the sequence of known isolates from the surface world, there are no guarantees that previously unknown microbes code the same sequences in their genome applicable for PCR and other molecular techniques (Teske and Sørensen, 2008). Therefore, as the next step, we must pay more attention to bias issues in cell detection, biomolecular extraction (e.g., DNA, RNA, lipids), and molecular studies; otherwise we may not receive the true view of natural subseafloor life.

Based on the development of culture-independent molecular or biogeochemical approaches, we may address the question 'How is phylogenetic composition based on the 16S rRNA gene sequence linked to biogeochemical function?' One recent demonstration of this involved FISH-secondary ion mass spectrometry (FISH-SIMS). Using this technique, Biddle and colleagues revealed that archaeal cells in sulfate-methane transition zones are fueled by buried organic matter (Biddle et al. 2006a). Although the phylogenetic positions of the heterotrophs remain unknown, those results provided the first information on a physiological characteristic of deep subseafloor microbes without cultivation. Based on the 16S rRNA gene data, similar or more advanced single phylotype-targeted isotopic and/or genomic approaches using flowcytometry and NanoSIMS will be applicable to achieve a better understanding of the uncultivated subseafloor microbial components (Eek et al. 2007; Podar et al. 2007; Kuypers and Jørgensen, 2007).

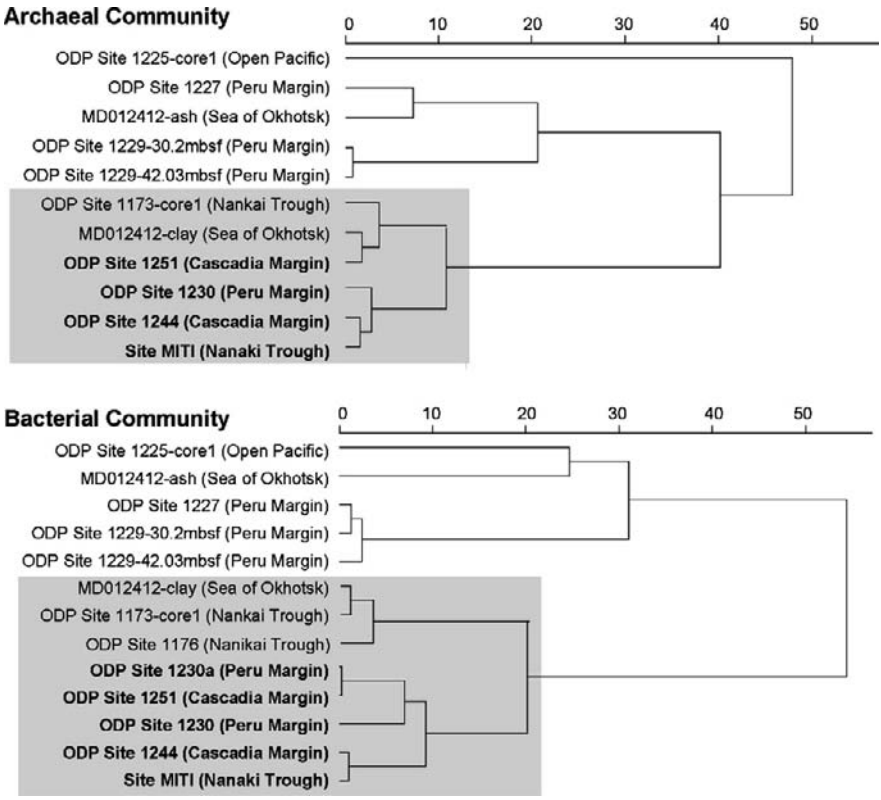

Fig. 10 Cluster analysis of archaeal and bacterial community compositions based on clonal frequencies of 16S rRNA gene phylotypes from various deep subseafloor sediments. Gray boxes and bold characters indicate the sampling sites where methane hydrates are believed to exist by seismic surveys and are visually confirmed, respectively. The communities inhabiting methane hydrate-bearing sediments are distinguishable from those in non-hydrate fields (Inagaki et al. 2006a)

To understand the biogeographical distribution of microbial life in deep-subseafloor environments, we need more opportunities to collect deep samples for microbiological research. Access to the lithosphere like basaltic environments for microbiology is difficult, but the deployment of borehole observatories, referred to as circulation obviation retrofit kits (CORKs), at hydrologically active sites may provide one solution, allowing microbes transferred from deep subseafloor to be collected as many times/as long as necessary (Cowen et al. 2003; Huber et al. 2006; Nakagawa et al. 2006). Either on the local or the global scale, environmental conditions seem to control microbial diversity and community structure. The results of previous molecular surveys of subseafloor microbial diversity suggested that microbial communities inhabiting sediments in methane hydrate areas are significantly different from those in non-hydrate areas on the Pacific continental margins (Inagaki et al. 2006a) (Fig. 10). In addition, there are some obvious tendencies in the preferential habitats of subseafloor microbes, like DSAG and MCG described above, indicating that biogeographical distribution may occur in association with sedimentological, geohydrological, and geological settings. Further microbiological surveys in deep-subseafloor environments will clarify on the global and local scale how deep microorganisms can live and survive, how they are distributed or adapt to their environment, and how biogeographical distribution affects the evolution of subseafloor life on our planet.

5 Conclusions

Culture-independent molecular ecological surveys of deep-subseafloor environments have revealed the presence of highly diverse, previously uncultivated microbial communities. Since most subseafloor microbial components are phylogenetically distinct from known isolates from the overlying surface world, their physiological and metabolic characteristics remain largely unknown. Nevertheless, the geochemical characteristics of deep marine environments indicate that subseafloor microbial communities play important roles in subseafloor biogeochemical cycles and that their occurrence and activities are closely associated with environmental settings such as substrate and energy transportation via geohydrological flows and tectonic movements. In conclusion, the deep-subseafloor biosphere is another world containing unknown microbial communities, and further multidisciplinary studies of their function, metabolic flux, geographical distribution, living strategies, and evolution will be necessary for future research on deep-subseafloor environments.

References

Auburger G, Winter J (1996) Activation and degradation of benzoate, 3-phenylpropionate and crotonate by *Syntrophus buswellii* strain GA. Evidence for electron-transport phosphorylation during crotonate respiration. Appl Environ Microbiol 44:807–815

Bale SJ, Goodman K, Rochelle PA, Marchesi JR, Weightman AJ, Parkes RJ (1997) *Desulfovibrio profundus* sp. nov., a novel barophilic sulfate-reducing bacterium from deep sediment layers in the Japan Sea. Int J Syst Bacteriol 47:515–521

Biddle JF, Lipp JS, Lever, MA, Lloyd KG, Sørensen KB, Anderson R, Fredricks HF, Elvert M, Kelly TJ, Schrag DP, Sogin ML, Brenchley JE, Teske A, House CH, Hinrichs K-U (2006a) Heterotrophic Archaea dominate sedimentary subsurface ecosystems off Peru. Proc Natl Acad Sci USA 103:3846–3851

Biddle JF, House CH, Brenchley JE (2006b) Microbial stratification in deeply buried marine sediment reflects changes in sulfate/methane profiles. Geobiology 3:287–295

Boetius A, Ravenschlag K, Schubert CJ, Rickert D, Widdel F, Gieseke A, Amann R, Jørgensen BB, Witte U, Pfannkuche O (2000) A marine microbial consortium apparently mediating anaerobic oxidation of methane. Nature 407:623–626

Coolen MJL, Cypionka H, Sass AM, Sass H, Overmann J (2002) Ongoing modification of Mediterranean Pleistocene sapropels mediated by prokaryotes. Science 296:2407–2410

Cowen JP, Giovannoni SJ, Kenig F, Johnson HP, Butterfield D, Rappe MS, Hutnak M, Lam P (2003) Fluids from aging ocean crust that support microbial life. Science 299:120–123

Davis BD, Luger SM, Tai PC (1986) Role of ribosome degradation in the death of starved *Escherichia coli* cells. J Bacteriol 166:439–445

D'Hondt S, Rutherford S, Spivack AJ (2002) Metabolic activity of subsurface life in deep-sea sediments. Science 295:2067–2070

D'Hondt S, Jørgensen BB, Miller DJ, Batzke A, Blake R, Cragg BA, Cypionka H, Dickens GR, Ferdelman T, Hinrichs K-U, Holm NG, Mitterer R, Spivack A, Wang G, Bekins B, Engelen B, Ford K, Gettemy G, Rutherford SD, Sass H, Skilbeck CG, Aiello IW, Guerin G, House C, Inagaki F, Meister P, Naehr T, Niitsuma S, Parkes RJ, Schippers A, Smith DC, Teske A, Wiegel J, Padilla CN, Acosta JLS (2004) Distributions of metabolic activities in deep subseafloor sediments. Science 306:2216–2221

Eek KM, Sessions AL, Lies DP (2007) Carbon-isotopic analysis of microbial cells sorted by flow cytometry. Geobiology 5:85–95

Francis CA, Roberts KJ, Beman JM, Santoro AE, Oakley BB (2005) Ubiquity and diversity of ammonia-oxidizing archaea in water columns and sediments of the ocean. Proc Natl Acad Sci USA 102:14683–14688

Fry JC, Webster G, Cragg BA, Weightman AJ, Parkes RJ (2006) Analysis of DGGE profiles to explore the relationship between prokaryotic community composition and biogeochemical processes in deep subseafloor sediments from the Peru Margin. FEMS Microbiol Ecol 58:86–98

Garrity GM, Holt, JG (2001) Phylum BVI. *Chloroflexi* phy. nov. In: Boone DR, Castenholz RW, Garrity GM (eds) Bergey's manual of systematic bacteriology, 2nd edn. vol 1 (The Archaea and the deeply branching and phototrophic Bacteria). Springer, New York, p 427

Girguis PR, Orphan VJ, Hallam SJ, DeLong EF (2003) Growth and methane oxidation rates of anaerobic methanotrophic archaea in a continuous-flow bioreactor. Appl Environ Microbiol 69:5472–5482

Hallam SJ, Konstantinidis KT, Putnam N, Schleper C, Watanabe Y, Sugahara J, Preston C, de la Torre J, Richardson PM, DeLong EF (2006) Genomic analysis of the uncultivated marine crenarchaeote *Cenarchaeum symbiosum*. Proc Natl Acad Sci USA 103:18296–18301

Huber JA, Johnson HP, Butterfield DA, Baross JA (2006) Microbial life in ridge flank crustal fluids. Environ Microbiol 8:88–99

Hugenholtz P, Pitulle C, Hershberger KL, Pace NR (1998) Novel division level bacterial diversity in a Yellowstone hot spring. J Bacteriol 180:366–376

Hugenholtz P, Stackebrandt E (2004) Reclassification of *Sphaerobacter thermophilus* from the subclass *Sphaerobacteridae* in the phylum *Actinobacteria* to the class *Thermomicrobia* (emended description) in the phylum *Chloroflexi* (emended description). Int J Syst Evol Microbiol 54:2049–2051

Inagaki F, Suzuki M, Takai K, Oida H, Sakamoto T, Aoki K, Nealson KH, Horikoshi K (2003) Microbial communities associated with geological horizons in coastal subseafloor sediments from the Sea of Okhotsk. Appl Environ Microbiol 69:7224–7235

Inagaki F, Tsunogai U, Suzuki M, Kosaka A, Machiyama H, Takai K, Nunoura T, Nealson KH, Horikoshi K (2004) Characterization of C1-metabolizing prokaryotic communities in methane seep habitats at the Kuroshima Knoll, Southern Ryukyu Arc, by analyzing *pmoA*, *mmoX*, *mxaF*, *mcrA*, and 16S rRNA genes. Appl Environ Microbiol 70:7445–7455

Inagaki F, Nunoura T, Nakagawa S, Teske A, Lever M, Lauer A, Suzuki M, Takai K, Delwiche M, Colwell FS, Nealson KH, Horikoshi K, D'Hondt S, Jørgensen BB (2006a) Biogeochemical distribution and diversity of microbes in methane hydrate-bearing deep marine sediments on the Pacific Ocean margin. Proc Natl Acad Sci USA 103:2815–2820

Inagaki F, Kuypers MM M, Tsunogai U, Ishibashi J, Nakamura K, Treude T, Ohkubo S, Nakaseama M, Gena K, Chiba H, Hirayama H, Nunoura T, Takai K, Jørgensen BB, Horikoshi K, Boetius A (2006b) Microbial community in a sediment-hosted CO_2 lake of the southern Okinawa Trough hydrothermal system. Proc Natl Acad Sci USA 103:14164–14169

Kendall MM, Liu Y, Sieprawska-Lupa M, Stetter KO, Whitman WB, Boone DR (2006) *Methanococcus aeolicus* sp. nov., a mesophilic methanogenic archaeon from shallow and deep marine sediments. Int J Syst Evol Microbiol 56:1525–1529

Knittel K, Lösekann T, Boetius A, Kort R, Amann R (2005) Diversity and distribution of methanotrophic archaea at cold seeps. Appl Environ Microbiol 71:467–479

Könneke M, Bernhard AE, de la Torre JR, Walker CB, Waterbury JB, Stahl DA (2005) Isolation of an autotrophic ammonia-oxidizing marine archaeon. Nature 437:543–546

Kormas KA, Smith DC, Edgcomb V, Teske A (2003) Molecular analysis of deep subsurface microbial communities in Nankai Trough sediments (ODP Leg 190, Site 1176). FEMS Microbiol Ecol 45:115–125

Kuypers MM, Jørgensen BB (2007) The future of single-cell environmental microbiology. Environ Mirobiol 9:6–7

Kvenvolden KA (1995) A review of the geochemistry of methane in natural gas hydrate. Org Geochem 23:997–1008

Ludwig W, Strunk O, Westram R, 29 other authors (2004) ARB: a software environment for sequence data. Nucleic Acids Res 32:1363–1371

Marchesi JR, Weightman AJ, Cragg BA, Parkes RJ, Fry JC (2001) Methanogen and bacterial diversity and distribution in deep gas hydrate sediments from the Cascadia Margin as revealed by 16S rRNA molecular analysis. FEMS Microbiol Ecol 34:221–228

Massana R, Murray AE, Preston CM, DeLong EF (1997) Vertical distribution and phylogenetic characterization of marine planktonic archaea in the Santa Barbara Channel. Appl Environ Microbiol 63:50–56

Mauclaire L, Zepp K, Meister P, Mckenzie J (2004) Direct in situ detection of cells in deep-sea sediment cores from the Peru Margin (ODP Leg 201, Site 1229). Geobiology 2: 217–223

Maymo-Gatell X, Chien Y-T, Gossett JM, Zinder SH (1997) Isolation of a bacterium that reductively dechlorinates tetrachloroethene to ethene. Science 276:1568–1571

Mikucki JA, Liu Y, Delwiche M, Colwell FS, Boone DR (2003) Isolation of a methanogen from deep marine sediments that contain methane hydrates, and description of *Methanoculleus submarines* sp. nov. Appl Environ Microbiol 69:3311–3316

Milkov AV (2004) Global estimates of hydrate-bound gas in marine sediments: how much is really out there? Earth-Sci Rev 66:183–197

Mills HJ, Martinez RJ, Story S, Sobecky PA (2005) Characterization of microbial community structure in Gulf of Mexico gas hydrates: comparative analysis of DNA- and RNA-derived clone libraries. Appl Environ Microbiol 71:3235–3247

Mohn WW, Tiedje JM (1992) Microbial reductive dehalogenation. Microbiol Rev 56:482–507

Morris RM, Rappe MS, Urbach E, Connon SA, Giovannoni SJ (2004) Prevalence of the *Chloroflexi*-related SAR202 bacterioplankton cluster throughout the mesopelagic zone and deep ocean. Appl Environ Microbiol 70:2836–2842

Nakagawa S, Inagaki F, Suzuki Y, Steinsbu BO, Lever MA, Takai K, Engelen B, Sako Y, Wheat CG, Horikoshi K (2006) Microbial community in black rust exposed to hot ridge flank crustal fluids. Appl Environ Microbiol 72:6789–6799

Newberry CJ, Webster G, Cragg BA, Parkes RJ, Weightman AJ, Fry JC (2004) Diversity of prokaryotes and methanogenesis in deep subsurface sediments from the Nankai Trough, Ocean Drilling Program Leg 190. Environ Microbiol 6:274–287

Nunoura T, Hirayama H, Takami H, Oida H, Nishi S, Shimamura S, Suzuki Y, Inagaki F, Takai K, Nealson KH, Horikoshi K (2005) Genetic and functional properties of uncultivated thermophilic crenarchaeotes from a subsurface gold mine as revealed by analysis of genome fragments. Environ Microbiol 7:1967–1984

Orphan VJ, Hinrichs K-U, Ussler W III, Paull CK, Taylor LT, Sylva SP, Hayes JM, DeLong EF (2001) Comparative analysis of methane-oxidizing archaea and sulfate-reducing bacteria in anoxic marine sediments. Appl Environ Microbiol 67:1922–1934

Parkes RJ, Cragg BA, Bale SJ, Getllff JM, Goodman K, Rochele PA, Fry JC, Weightman AJ, Harvey SM (1994) Deep bacterial biosphere in Pacific ocean sediments. Nature 371: 410–413

Parkes RJ, Cragg BA, Wellsbury P (2000) Recent studies on bacterial populations and processes in subseafloor sediments: a review. Hydrogeol J 8:11–28

Parkes RJ, Webster G., Cragg BA, Weightman AJ, Newberry CJ, Ferdelman TG, Kallmeyer J, Jørgensen BB, Aiello IW, Fry JC (2005) Deep sub-seafloor prokaryotes stimulated at interfaces over geological time. Nature 436:390–394

Podar M, Abulencia CB, Walcher M, Hutchison D, Zengler K, Garcia JA, Holland T, Cotton D, Hauser L, Keller M (2007) Targeted access to the genomes of low-abundance organisms in complex microbial communities. Appl Environ Microbiol 73:3205–3214

Reed DW, Fujita Y, Delwiche ME, Blackwelder DB, Sheridan PP, Uchida T, Colwell FS (2002) Microbial communities from methane hydrate-bearing deep marine sediment in a forearc basin. Appl Environ Microbiol 68:3759–3770

Rochelle PA, Cragg BA, Fry JC, Parkes RJ, Weightman AJ (1994) Effect of sample handling on estimation of bacteria diversity in marine sediments by 16S rRNA gene sequence diversity. FEMS Microbiol Ecol 15:215–226

Schippers A, Neretin LN, Kallmeyer J, Ferdelman TG, Cragg BA, Parkes RJ, Jørgensen BB (2005) Prokaryotic cells of the deep sub-seafloor biosphere identified as living bacteria. Nature 433:861–864

Schnell S, Bak F, Pfenning N (1989) Anaerobic degradation of aniline and dihydroxybenzenes by newly isolated sulfate-reducing bacteria and description of *Desulfobacterium anilini*. Arch Microbiol 152:556–563

Sekiguchi Y, Yamada T, Hanada S, Ohashi A, Harada H, Kamagata Y (2003) *Anaerolinea thermophila* gen. nov., sp. nov., and *Caldilinea aerophila* gen. nov., sp. nov., novel filamentous thermophiles that represent a previously uncultured lineage of the domain Bacteria at the subphylum level. Int J Syst Evol Microbiol 53:1843–1851

Sørensen KB, Lauer A, Teske A (2004) Archaeal phylotypes in a metal-rich and low-activity deep subsurface sediment of the Peru Basin, ODP Leg 201, Site 1231. Geobiology 2:151–161

Sørensen KB, Teske A (2006) Stratified communities of active archaea in deep marine subsurface sediments. Appl Environ Microbiol 72:4596–4603

Suss J, Engelen B, Cypionka H, Sass H (2004) Quantitative analysis of bacterial communities from Mediterranean sapropels based on cultivation-dependent methods. FEMS Microbiol Ecol 51:109–121

Suss J, Schubert K, Sass H, Cypionka H, Overmann J, Engelen B (2006) Widespread distribution and high abundance of *Rhizobium radiobacter* within Mediterranean subsurface sediments. Environ Microbiol 8:1753–1763

Swofford DL (2000) PAUP*. Phylogenetic analysis using parsimony (and other methods), version 4. Sinauer Associates, Sunderland, MA

Takai K, Horikoshi K (1999) Genetic diversity of Archaea in deep-sea hydrothermal vent environments. Genetics 152:1285–1297

Takai K, Moser DP, DeFlaun M, Onstott TC, Fredrickson JK (2001) Archaeal diversity in waters from deep South African gold mines. Appl Environ Microbiol 67:5750–5760

Teske A, Hinrichs K-U, Edgcomb V, Gomez A de V, Kysela D, Sylva SP, Sogin ML, Jannasch HW (2002) Microbial diversity of hydrothermal sediments in the Guaymas Basin: evidence for anaerobic methanotrophic communities. Appl Environ Microbiol 68:1994–2007

Teske A, Sørensen KB (2008). Uncultured Archaea in deep marine subsurface sediments: have we caught them all? The ISME Journal 2:3–18

Vetriani C, Jannasch HW, MacGregor BJ, Stahl DA, Reysenbach AL (1999) Population structure and phylogenetic characterization of marine benthic Archaea in deep-sea sediments. Appl Environ Microbiol 65:4375–4384

Webster G, Parkes RJ, Fry JC, Weightman AJ (2004) Widespread occurrence of a novel division of bacteria identified by 16S rRNA gene sequences originally found in deep marine sediments. Appl Environ Microbiol 70:5708–5713

Webster G, Parkes RJ, Cragg BA, Newberry CJ, Weightman AJ, Fry JC (2006) Prokaryotic community composition and biogeochemical processes in deep subseafloor sediments from the Peru Margin. FEMS Microbiol Ecol 58:65–85

Wilms R, Kopke B, Sass H, Chang TS, Cypionka H, Engelen B (2006) Deep biosphere-related bacteria within the subsurface of tidal flat sediments. Environ Microbiol 8:709–719

Yamada T, Sekiguchi Y, Hanada S, Imachi H, Ohashi A, Harada H, Kamagata Y (2006) *Anaerolinea thermolimosa* sp. nov., *Levilinea saccharolytica* gen. nov., sp. nov. and *Leptolinea tardivitalis* gen. nov., sp. nov., novel filamentous anaerobes, and description of the new classes *Anaerolineae* classis nov. and *Caldilineae* classis nov. in the bacterial phylum *Chloroflexi*. Int J Syst Evol Microbiol 56:1331–1340

Analysis of Deep Subsurface Microbial Communities by Functional Genes and Genomics

Andreas Teske and Jennifer F. Biddle

1 Introduction: Molecular and Cultivation Surveys of Marine Deep Subsurface Sediments

Marine sediments cover more than two-thirds of the Earth's surface and microbial cells and prokaryotic activity in these sediments appear to be widespread. Direct counts of intact cells provide evidence of prokaryotic populations in sediments as deep as 800 m below the seafloor (Parkes et al. 2000). Prokaryotic activity, in the form of sulfate reduction and/or methanogenesis, occurs in sediments throughout the world's oceans (D'Hondt et al. 2002). The prokaryotes of marine subsurfacesediments may constitute a major portion of Earth's prokaryotic biomass and total living biomass (Parkes et al. 2000; Whitman et al. 1998), however, fundamental aspects of this subseafloor ecosystem are poorly known. What is the phylogenetic composition of prokaryotic communities in the marine sedimentary subsurface? What are their functional genes and the metabolic activities that allow these prokaryotes to grow and to persist in their subsurface habitat?

The deep marine subsurface biosphere, its composition and activity, is a now a major research field at the interface of geology, geochemistry and microbiology (Amend and Teske 2005; Jørgensen and D'Hondt 2006). Over the last few years, gene-based analyses of microbial community composition and function in deep subsurface sediments have uncovered a previously unknown subsurface biosphere of novel archaea and bacteria with cosmopolitan occurrence patterns (Biddle et al. 2006; Coolen et al. 2002; Fry et al. 2006; Inagaki et al. 2003, 2006; Inagaki et al., this volume; Kormas et al. 2003; Newberry et al. 2004; Parkes et al. 2005; Reed et al. 2002; Schippers et al. 2005; Schippers and Neretin 2006; Sørensen and Teske 2006; Sørensen et al. 2004; Teske 2006; Webster et al. 2003; 2004; 2006; Wilms 2006a, b). In contrast to the highly diverse subsurface populations that have been detected by molecular, gene-based approaches, cultured

A. Teske
University of North Carolina at Chapel Hill, Department of Marine Sciences, 351 Chapman Hall, CB 3300, Chapel Hill, North Carolina 27599, USA
e-mail: teske@email.unc.edu

Y. Dilek et al. (eds.), *Links Between Geological Processes, Microbial Activities & Evolution of Life*, © Springer Science+Business Media B.V. 2008

isolates from subsurface sediments are mostly limited to a handful of phylogenetic lineages: heterotrophic, psychrophilic or mesophilic members of the Proteobacteria, the Cytophaga-Flavobacterium phylum, the Actinobacteria and the Firmicutes (Biddle et al. 2005a, b; D'Hondt et al. 2004; Köpke et al. 2005; Lee et al. 2005; Süss et al. 2004, 2006; Toffin et al. 2004a, b; Toffin et al. 2005). Thus, the divergent outcomes of molecular and cultivation-based analyses imply that only a small selection of the actual bacterial and archaeal diversity in deep subsurface sediments is currently being cultured; attempts to close the "cultivation gap" require a battery of labor-intensive, innovative cultivation approaches, which remain a poor match for the diversity of microbial habitats and niches in Nature. Organic-rich marine sapropels and coastal sediments of intertidal mud flats are the only major exceptions where cultivations have captured a quantitatively significant segment of the natural bacterial population (Köpke et al. 2005; Süss et al. 2004, 2006).

2 The Functional Gene Approach

As a consequence of this situation, understanding the physiology and function of microbial communities in different environments is left behind and eclipsed by rapid progress in rRNA microbial diversity mapping on the scale of entire ecosystems (Von Mering et al. 2007). The biogeochemical function and physiological properties of subsurface communities are to some extent reflected in biogeographical occurrence patterns (Inagaki et al. 2006), vertical stratification within geochemical gradients (Sørensen and Teske 2006), or correlations with geochemical habitat characteristics (Fry et al. 2006). However, these approaches allow only indirect inferences. A widely used molecular strategy to directly link genotype and phenotype, and to reconnect microbial diversity studies to microbial function, is the functional gene approach. Here, the target of molecular detection is a functional gene, coding for an enzyme or an enzyme subunit that is essential and characteristic for a specific metabolic pathway, and for the bacteria and archaea of this metabolic type (Wagner et al. 2005; Friedrich 2005). In most cases, the detection technique is a PCR assay of actual or alleged specificity; in combination with reverse transcription of the target gene mRNA, the expression of the target gene can be detected via RT-PCR (Neretin et al. 2003). DNA-based PCR detection of the target gene, as well as messenger RNA-based detection of its expression, can be quantified (Bustin 2000; Stults et al. 2001; Suzuki et al. 2000). By focusing on a specific physiological and functional group of microorganisms, the functional gene approach is highly selective and detects relatively rare "minority populations" of bacteria and archaea that are easily overlooked by more general assays, such as rRNA sequencing. As a prerequisite, the functional gene of choice has to be sufficiently conserved in order to carry meaningful phylogenetic information; its link to the evolutionary lineage of its host cell should not be obscured by frequent and/or unknown gene transfer events. Gene transfer events are accounted for by comparisons of rRNA and multiple functional gene phylogenies within the same functional group; the sulfate-reducing

prokaryotes provide an instructive example (Wagner et al. 1998; Friedrich 2002; Klein et al. 2002; Zverlov et al. 2005). In such well-documented cases, the complexity and database size of functional gene phylogenies is catching up with the rRNA framework, significantly broadening the molecular tool kit for high-resolution microbial diversity surveys and enabling evolutionary studies on the origin of specific microbial functions and metabolic pathways (Stahl et al. 2002; Dhillon et al. 2005a). The caveat must be added that functional gene phylogenies have sprouted multiple branches without cultured representatives, similar to the rRNA tree of life. An uncultured bacterium or archaeon is supposed to have the specific physiological trait encoded by the gene, even if comparisons to cultured isolates are not yet possible (for example, Dhillon et al. 2003); however, this assumption is only valid as long as the gene product remains without structurally and functionally significant changes and retains its specific function (for an interesting case study, see Laue et al. 2001).

3 Functional Gene Analyses in Deep Subsurface Sediments

The functional gene approach opens new avenues of research for subsurface microbiology. Since most studied deep marine subsurface sediments are from organic-rich margin environments, the predominant microbial processes in the anaerobic degradation of buried organic biomass at these sites are sulfate reduction, methanogenesis, and sulfate-dependent anaerobic methane oxidation, as evidenced by the conspicuous geochemical gradients of sulfate and methane that delineate these processes and allow calculations of process rates in addition to direct rate measurements (D'Hondt et al. 2002, 2004). Consequently, most functional key gene surveys of deep subsurface sediments have targeted the gene for dissimilatory sulfite reductase alpha and beta subunit (*dsrAB*), an essential gene of microbial sulfite and sulfate reduction (Wagner et al. 1998; Klein et al. 2001; Zverlov et al. 2005) and the gene for methyl-coenzyme M reductase alpha subunit (*mcrA*), the key gene of methanogenesis and anaerobic methane oxidation (Springer et al. 1995; Luton et al. 2002; Hallam et al. 2003, 2004). However, in organic-poor sediments, microbial respiration with oxygen, nitrate or metals consumes the available biomass; sulfate reduction and methanogenesis rates remain minimal or undetectable (D'Hondt et al. 2004). A functional gene study in Northwest Pacific surficial sediment layers, where nitrate respiration is a preferred process, successfully detected nitrate reductase genes (Braker et al. 2000, 2001). More organic-poor sediments need to be examined to determine the extent and phylogeny of these metabolisms in the subsurface.

Sample availability, low nucleic acid content, and challenges to PCR sensitivity are probably the most important reasons why only a few deep, and mostly margin, subsurface sediments have been examined in detail, in contrast to numerous functional gene surveys of surficial marine sediments (examples in Bidle et al. 1999; Bahr et al. 2005; Kondo et al. 2004; Dhillon et al. 2003, 2005b) and increasing studies of shallow subsurface coastal sediments in the 1–5 m depth range (Thomsen et al. 2001; Wilms et al. 2007). At present, deep subsurface sediments in the Peru

Margin and in Nankai Trough (in the depth range of up to 300 m below sediment surface) represent the best case studies for PCR, cloning and sequencing of functional genes of sulfate reduction, methanogenesis and anaerobic methane oxidation in the deep marine subsurface (Parkes et al. 2005; Newberry et al. 2004; Inagaki et al. 2006; Webster et al. 2006; Lever and Teske 2007).

3.1 Sulfate Reduction Genes

Although sulfur isotope fraction data and sulfate reduction rate measurements clearly indicate active sulfate reduction in deep subsurface sediments of the Peru Margin (Böttcher et al. 2006; Parkes et al. 2005), functional gene detection of sulfate-reducing prokaryotes has been challenging. At a single depth horizon of ODP Site 1228 (48 mbsf), *dsrA* gene fragments could be amplified (Webster et al. 2006), and were related to *dsrAB* sequences of an uncultured branch of sulfate-reducing bacteria (group IV) previously seen in the Guaymas Basin (Dhillon et al. 2003), in methane seeps in the Gulf of Mexico (Lloyd et al. 2006), in New England salt marsh sediment (Bahr et al. 2005), and surficial sediment cores from the Eastern Pacific continental margin (Liu et al. 2003). No *dsrA* gene fragments were detectable at the nearby ODP Site 1229 on the Peru Margin (Webster et al. 2006). A quantitative PCR analysis of the Peru Margin ODP Site 1227 detected *dsrA* genes in patchy distribution in the sediment column, unrelated to methane-sulfate gradients (Schippers and Neretin 2006); however, the *dsrA* gene fragments were not sequenced and the identify of the sulfate reducers is therefore not known. All Peru Margin studies used a primer pair that amplified a very short fragment (ca. 180 nucleotides) of the *dsrA* gene (Kondo et al. 2004); previous attempts to amplify *dsrA* and *dsrAB* genes with published primer pairs targeting longer fragments remained unsuccessful (Webster et al. 2006; Lloyd and Teske, unpublished results). Possibly, the population density of sulfate-reducing prokaryotes in the Peru Margin sediments is too low to allow reliable detection by DNA extraction and PCR (Parkes et al. 2005).

3.2 Methanogenesis Genes

Currently, the key gene of methanogenesis and anaerobic methane oxidation, *mcrA*, provides the most comprehensive functional gene dataset for marine subsurface sediments (Fig. 1). The emerging diversity of *mcrA* genes in the deep subsurface and in relevant analog habitats (near-surface sediments supplied with subsurface-derived substrates) allows an initial assessment of subsurface methanogens in the context of habitat characteristics and substrate availability.

The *mcrA* phylotypes that have been recovered from deep subsurface sediments are affiliated to cultured genera and families of methanogens (Fig. 1). For example, the *mcrA* phylotypes in organic-rich sediments of the Peru Margin (ODP Site 1229) were closely related to members of the methanogenic genera *Methanobrevibacter*

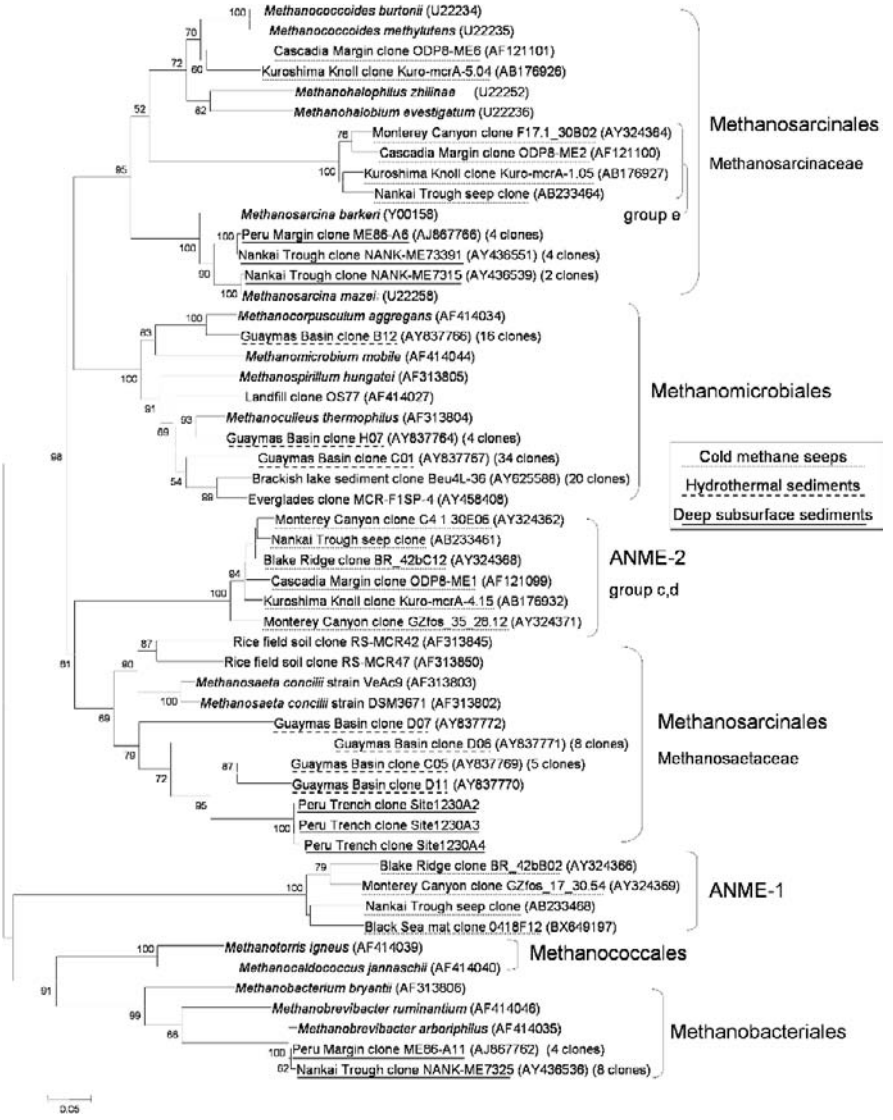

Fig. 1 Phylogenetic tree based on nucleotide sequences of methyl-coenzyme M reductase alpha subunit *(mcrA)* genes. Sequences were retrieved from the GenBank database and aligned by ClustalW (Thompson et al. 1994). Tree was constructed using neighbor-joining analysis by MEGA software (Kumar et al. 2004) based on 718 nucleotides. Bootstrap values are based on 1,000 replicates, values are shown for branches with more than 50% bootstrap support. The Methanosarcinaceae, the Methanosaetaceae, the Methanomicrobiales and the ANME-2 lineage (Group c, d) are each well-supported, mutually exclusive lineages (89–100% bootstrap support). In agreement with published analyses (Hallam et al. 2003), hierarchical branching patterns within the root of these four lineages are not well supported (<70%); together they form a strongly supported cluster (98%) that excludes the ANME-1 group, the Methanococcales and the Methanobacteriales. The *mcrA* lineages c, d and 2 are based on Hallam et al. (2003). The methanogen taxonomy follows Bergey's Manual of Systematic Bacteriology (Garrity and Holt 2001)

and *Methanosarcina* (Parkes et al. 2005; Webster et al. 2006); the same phylogenetic affiliation was found for *mcrA* phylotypes from the Western Pacific in the Nankai Trough offshore Japan (Site 1173; Newberry et al. 2004). *Methanosarcina* species use acetate, methylated compounds, and H_2/CO_2 as substrates of methanogenesis (Boone and Mah 2001); *Methanobrevibacter* species use H_2 and occasionally formate as methanogenic substrates (Miller 2001). These substrates are available in deep subsurface sediments, albeit in low concentrations. Acetate and formate porewater concentrations in the sediment column of the Peru Margin were quite similar to each other, both in the 1–4 uM range (higher in methane/sulfate interfaces; Shipboard Scientific Party 2003a, b). Potential methanogenesis rates using formate and acetate as methanogenic substrates were detectable at Site 1229, these rates reached maximally 15 pmol methane cm^{-3} d^{-1} in the sediment column (Parkes et al. 2005). In contrast, *mcrA* phylotypes from the sediment column of the Peru Trench (ODP Site 1230; D'Hondt et al. 2004) formed a sister group to the genus *Methanosaeta* (Inagaki et al. 2006). *Methanosaeta* species grow strictly by acetoclastic methanogenesis (Patel 2001). Acetate concentrations in the Peru Trench sediments are in the 50–200 μM range, which is 50 times higher than in Peru Margin sediments; formate concentrations are in the 5–20 μM range (Shipboard Scientific Party 2003c). The higher acetate concentrations in the Peru Trench sediments would be consistent with the occurrence of acetate-dependent, acetoclastic methanogens in this subsurface habitat.

4 Methanogens in Marine Sedimentary Habitats

Comparisons of deep subsurface *mcrA* phylotypes with their counterparts from shallow marine and estuarine sediments reveal interesting differences as well as common denominators in community structure and habitat characteristics. Diverse marine habitats have been studied by *mcrA* surveys: organic rich sediments and peat in a brackish estuary (Banning et al. 2005); cold methane seep sediments in organic-rich continental margin sediments (Hallam et al. 2003, 2004; Inagaki et al. 2004; Nunuora et al. 2006); sediments covering methane hydrates (Bidle et al. 1999); and hydrothermal sediments of Guaymas Basin, characterized by geothermal alteration of buried organic matter (Dhillon et al. 2005b). Selected *mcrA* phylotypes from these and other marine environments are included in the phylogenetic tree (Fig. 1).

The Guaymas Basin is a particularly interesting analog to deep subsurface sediments. Biomass is buried in the thick sediment layers, and is hydrothermally altered to organic substrates (petroleum compounds, aromatics, alkanes) that are usually encountered in deep, hot oil fields and other geothermal subsurface environments (Didyk and Simoneit 1989). These substrates are transported back into the upper sediment column and towards the sediment-water interface, where they sustain complex benthic microbial communities (Pearson et al. 2005) and create a spatially compressed sequence of anaerobic microbial processes and communities near the

sediment surface, which elsewhere extend over tens and hundreds of vertical meters within the deep marine sedimentary subsurface (D'Hondt et al. 2002, 2004). Thus, Guaymas Basin provides a natural laboratory for investigation of a dominant deep marine subsurface process, microbial utilization of thermally matured buried carbon (Wellsbury et al. 1997), in a near-surface location. Interestingly, some methanogen populations reflect this similarity. Several Guaymas *mcrA* phylotypes form a sister group to *Methanosaeta* spp. within the Methanosarcinales; at the same time, they are the closest known relatives of the *Methanosaeta*-related Peru Trench phylotypes from ODP Site 1230 (Inagaki et al. 2006) (Fig. 1). These uncultured *Methanosaeta*-related methanogens occur in surficial Guaymas sediments that are abundantly supplied with low-molecular weight organic acids, originating from thermal degradation of buried biomass; for example, acetate occurs in concentrations up to 0.2 mM within the upper 11 cm, and reaches 0.9 mM at 15 cm depth (Dhillon et al. 2005b). Thus, the *Methanosaeta*-related methanogens in Guaymas Basin and in the Peru Trench appear to reflect a shared habitat characteristic, high concentrations of organic acids, in particular the methanogenic key substrate acetate. In both cases, the organic acids are most likely derived from subsurface degradation of buried complex organic substrates (Pearson et al. 2005; Heuer et al. 2006).

Other Guaymas Basin *mcrA* phylotypes were members of the Methanomicrobiales; within this group, they were phylogenetically intertwined with *mcrA* clones from an estuarine brackish water lake (Banning et al. 2005) (Fig. 1). At present, no deep subsurface *mcrA* phylotypes are known within the Methanomicrobiales, which commonly depend on H_2/CO_2 as methanogenic substrates. However, the Methanomicrobiales cannot be discounted as potential subsurface methanogens; the Methanomicrobiales increased with depth in shallow (4 m deep) marine subsurface sediments in the Skagerrak, as indicated by combined 16S rRNA-based clone libraries, T-RFLP profiles and H_2/CO_2 methanogenesis rates (Parkes et al. 2007).

One of the current minor enigmas of deep subsurface microbiology is the difficulty to detect anaerobic methane-oxidizing archaea in deep methane-sulfate interfaces. Population densities and activities of these anaerobic methane oxidizers, the basis of their detection, appear to be depth-related; anaerobic methane oxidizers are easily detected at methane/sulfate interfaces in the shallow marine subsurface on a scale of 1–4 m (for example, Parkes et al. 2007) but remain elusive in deep subsurface sediments where methane-sulfate gradients extend over tens of meters. The methane-sulfate interfaces of the conspicuous subsurface methane-sulfate gradients in Peru Margin sediments were repeatedly checked for methane-oxidizing archaeal populations that are the microbial catalysts of this process; however, 16S rRNA and *mcrA* gene analyses have not detected any of the known, sulfate-dependent archaeal methane oxidizers of the ANME-1, ANME-2 and ANME-3 groups (Boetius et al. 2000; Orphan et al. 2001, 2002; Niemann 2006). Published *mcrA* sequences from deep subsurface methane-sulfate interfaces fall within the Methanobacteriales and the Methanosarcinales (Parkes et al. 2005; Newberry et al. 2004) and are distinct from the ANME-1 and ANME-2-affiliated *mcrA* phylotypes that are consistently found at methane seeps (Hallam et al. 2003, 2004; Inagaki et al. 2004; Nunuora et al. 2006) (Fig. 1). Molecular surveys based on 16S rRNA show uncultured, active

archaeal lineages (Biddle et al. 2006; Sørensen et al. 2006). The conspicuous absence of *mcrA* genes of anaerobic methane oxidizers at deep subsurface methane-sulfate interfaces could be explained in two ways that are not mutually exclusive: Other archaeal groups mediate anaerobic methane oxidation, possibly via a "dissimilatory" methane oxidation process that derives energy without incorporating methane-derived carbon into archaeal cell biomass (Biddle et al. 2006). Also, classical methane-oxidizing archaea could occur at deep subsurface methane-sulfate interfaces, but are hard to detect due to low cell density or mismatched PCR primers (Lever and Teske 2007).

5 Genomic Approaches

While studies of PCR-amplified functional genes can provide an overview of potential metabolisms in an environment, it is limited in that it does not examine complete metabolic pathways and excludes genes that may be more divergent than those used for primer design. In recent years, the approach of examining the genetic potential of an environment has shifted to that of metagenomics. In this method, all genes of an environment are examined, regardless of their function. It is a viable method for discovering new genes (Krause et al. 2006), for examining the entire assemblage of metabolic pathways contained in an environment (Tyson et al. 2004), and for reconstructing specific pathways that are characteristic for a microbial habitat (Hallam et al. 2004). Metagenomics can currently be performed via two different methods: the traditional approach of Sanger-based shotgun sequencing (Venter et al. 2004), or the newer method of pyrosequencing (Edwards et al. 2006). Advantages of pyrosequencing are its lower cost and ability to sequence low amounts of DNA without processing through *Escherichia coli*. A disadvantage is that results from pyrosequencing are obtained in short fragments. However, the advantage of the low input DNA for pyrosequencing makes it extremely applicable to the deeply buried biosphere.

The metagenome of subsurface sediment was recently obtained by pyrosequencing (Biddle 2006; Biddle et al. 2008). Over 60 million basepairs of sequence was retrieved from sediments at 1, 16, 32 and 50 mbsf from ODP Site 1229 on the Peru Margin. The short sequences retrieved by pyrosequencing were compared to two publicly available databases, the GenBank non-redundant (nr) and the protein family (pfam) databases (Finn et al. 2006; Altschul et al. 1997; Biddle et al. 2008). The top match was used to identify the most likely gene annotation and this was used to sort sequence reads into functional gene classes based on gene ontology categories. Sequences that were sorted as genes involved in a methanogenic pathway, based on protein family identity, were counted at each depth (Fig. 2; Panel B). Based on the geochemistry at Site 1229, it is expected that methanogenic microorganisms would increase at depth, mirroring the increase in observed methane at between 40 and 90 mbsf (Fig. 2; Panel A) (more detailed geochemistry is available from D'Hondt et al. 2003).

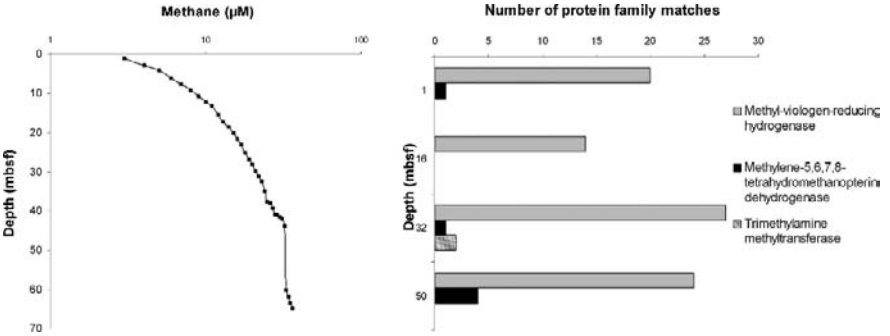

Fig. 2 *Panel A*: Methane concentrations at ODP Site 1229 on the Peru Margin, 1–65 mbsf, data from D'Hondt et al. (2003). *Panel B*: numbers of sequenced reads annotated as belonging in a methanogenic pathway, based on gene ontology categories, from the pyrosequenced metagenome of sediments at 1, 16, 32 and 50 mbsf at ODP Site 1229. Data were reanalyzed from Biddle (2006)

The most frequently detected genes code for methyl-viologen-reducing hydrogenase. This type of hydrogenase may be involved at multiple steps in methanogenesis, but it should be noted that it is also involved in other anaerobic metabolic processes. As such, it does not vary greatly with depth as it may not be a direct indicator of a methanogen (Fig. 2; Panel B). Also, the trimethylamine methyltransferase genes detected at 32 mbsf are not solely methanogenic enzymes if identified only at the level of protein family. A gene that is a more specific indicator of methanogenesis at the protein family level is that which encodes methylene-5,6,7,8-tetrahydromethanopterin dehydrogenase. This enzyme is essential for the conversion of methenyl-H_4MPT to methylene-H_4MPT, a step catalyzed by the reduction of F_{420}. This gene was detected in increasing levels at greater depths (Table 1) with the most abundant detection (four 100 bp read matches) at 50 mbsf, where there is a peak of methane gas in the sediment column (Fig. 2; Panel A). Although no *mcrA* genes were detected, the increase of a methanogenic gene at the peak of methane

Table 1 Detailed analysis of Methylene-5,6,7,8-tetrahydromethanopterin dehydrogenase annotations

Depth detected	Identity of most similar BLAST match	nr bit score	nr Evalue	Pfam Evalue
1	*Methanothermobacter thermautotrophicus* str. Delta H	50.1	3.0×10^{-05}	1.8×10^{-06}
32	*Methanospirillum hungatei* JF-1	54.3	2.0×10^{-06}	5.6×10^{-13}
50	*Methanoculleus marisnigri* JR1	42.4	7.0×10^{-03}	6.1×10^{-06}
50	*Archaeoglobus fulgidus* DSM 4304	55.1	1.0×10^{-06}	6.2×10^{-10}
50	*Methanocaldococcus jannaschii* DSM 2661	38.9	7.1×10^{-02}	2.3×10^{-05}
50	*Methanothermobacter thermautotrophicus* str. Delta H	48.1	1.0×10^{-04}	6.8×10^{-08}

gas gives confidence that with continued sequencing, representatives of *mcrA* may be uncovered.

Although the short sequences provided by pyrosequencing (average 100 bp per read) may not yield reliable phylogenetic information for general metabolic genes, such as ABC transporters, it is interesting to look at the relationship of the methanogen-specific methylene-5,6,7,8-H_4MPT dehydrogenases detected in the metagenome (Table 1). As with the previously discussed *mcrA* clones, the sequences are most homologous to multiple groups of methanogens and archaea. The Methanomicrobiales, Methanobacteriales and Methanococcales are represented. Additionally, *Archaeoglobus fulgidus* is the most similar match for a sequence from 50 mbsf. This is not unexpected as we might expect the subsurface methanogens to be divergent from surface groups (Inagaki et al. 2006) and the cultured *Archaeoglobus* has the methanogenic pathway except for *mcrA* (Klenk et al. 1997). There has been no detection of genes similar to *Methanosarcina*, despite the detection of that group by PCR studies (Parkes et al. 2005).

This first examination of the marine subsurface metagenome yielded only two genes for sulfate reduction. At Site 1229, sulfate reduction is expected to be abundant at 1, 16 and 32 mbsf, however by the *dsrA* genes have proved difficult to find by PCR (discussed in Section 3.1; Webster et al. 2006). At 1 mbsf metagenome, a gene was detected that had similarity to a beta-subunit of sulfite reductase from *Moorella thermoacetica* (NP_393526). At 16 mbsf, a gene was found that was similar to the alpha subunit of dissimilatory sulfite reductase from an uncultured sulfate-reducing bacterium in the Eastern Mediterranean Sea (AY590556). No sulfite reductases or other marker genes for sulfate reduction were detected in the metagenome from 32 or 50 mbsf. To our knowledge this is the first report of a *dsr* gene at ODP Site 1229. While subsurface sulfate reducing microorganisms may just be minority populations (Parkes et al. 2005), sulfate reduction is such a widespread metabolism in the global marine subsurface that more genes are expected to be detected by both metagenomic and PCR based studies. At this point, it is unknown whether they evade our detection or perhaps are divergent from the pelagic genes and simply lie undiscovered.

6 Outlook

Linking diversity to function requires improved DNA/RNA recovery for metagenomic sequencing and gene expression analyses; it will require targeted molecular, physiological and geochemical studies of specific groups and lineages of subsurface bacteria and archaea, and – last but not least – innovative cultivations that yield representative deep subsurface bacteria and archaea for direct physiology and genetic studies. DNA recovery can be improved with a new approach, multiple strand displacement amplification (MDA) using ϕ29 DNA polymerase, which generates copies of PCR templates while replacing previously generated copy strand that has been left in place by its closest ϕ29 DNA polymerase neighbor; the result is a branched amplification where the template strand is copied multiple times simultaneously, in an isothermal DNA amplification step (Hutchinson et al. 2005; reviewed

in Zhang et al. 2006). The procedure is applicable to deep subsurface sediments, as it generates microgram amounts of amplified DNA from extracted DNA-poor sediment samples (Abulencia et al. 2006), or even from a single cell (Raghunathan et al. 2005). Initial tests with amplifications of mixed pure cultures and amplified serial dilutions showed potential amplification biases; however, the phylogenetic spectrum of non-amplified and amplified environmental DNA turned out to be similar; the bacterial phyla that are represented in the native DNA are also found in the amplified DNA (Abulencia et al. 2006). Although amplification biases have to be taken into account, genomic surveys and functional gene studies, for example using microarray technology, will become feasible for microbial communities in DNA- and biomass-limited samples (Wu et al. 2006). Particularly, novel bacteria and archaea that lack natural reservoirs where they occur in high densities, could be enriched using small-scale culture enrichments and physical cell separation and sorting (Kalyuzhnaya et al. 2006). Thus, a much greater proportion of the microbial world would be in reach for genomic and functional gene analyses; the recently postulated "Rare Biosphere" would become accessible (Sogin et al. 2006).

New combinations of geochemical and molecular methods can identify specific, active microbial populations even in the absence of cultivations. For example, Micro-FISH experiments can couple CARD-FISH identification of individual cells with substrate uptake and utilization patterns (Teira et al. 2004). Fluorescent-In-situ-hybridization Secondary-Ion-Mass-spectroscopy (FISH-SIMS) allows stable carbon isotopic analysis of individual microbial cells stained with FISH probes (Orphan et al. 2001). Structural and C-isotopic analysis of prokaryotic biomarker lipids (Sturt et al. 2004) combined with C-isotopic analysis of individual cells by FISH-SIMS (Orphan et al. 2001) and with cloning and sequencing of reverse-transcribed rRNA (Inagaki et al. 2002) can identify active microbial populations and their stable-carbon isotopic signatures in parallel. This strategy has been successfully applied for archaeal communities in deeply buried methane-sulfate interfaces at Peru Margin ODP Sites 1227, 1229 and 1230 (Biddle et al. 2006). In these organic-rich sediments, the active archaeal community was shown to assimilate buried organic carbon of photosynthetic origin, but not DIC or methane (Biddle et al. 2006). As a next step, this analysis can be performed for selected phylogenetic groups of active subsurface bacteria and archaea that dominate the deep subsurface, using group-specific probes.

Cultivation techniques for difficult-to-culture bacteria and archaea, in particular oligotrophic strains, have started to reveal their potential for subsurface microbiology. Serial dilution approaches and oligotrophic natural media (unamended seawater, unamended sediment) are already widely used in marine microbiology (Connon and Giovannoni 2002; Bruns et al. 2003a, b; Kaeberlein et al. 2002; Süss et al. 2004), leading to the isolation of new phyla and dominant marine pelagic bacteria (Rappé et al. 2002; Cho et al. 2004). An essential and often overlooked aspect of oligotrophic cultivations is the technical challenge of detecting low-density growth, for example in the terminal steps of dilution series or in batch cultures of bacteria that do not grow in high densities. Improved cell staining with more sensitive nucleic acid stains allows the reliable quantification of prokaryotic cells in low-density

solution (Martens-Habbema and Sass 2006). A related issue is the observation that microbial colonies growing on solid media and filters do not always develop into the traditional, large colonies that are visible with the unaided eye; growth and division of a single cell may proceed only for a few divisions and produce microcolonies that require detection by microscopy (Højberg et al. 1997; Kaeberlein et al. 2002). Such experimental constraints and caveats will most likely apply to the cultivation of deep subsurface bacteria and archaea, considering their nutrient- and energy-depleted habitat and their physiological adaptations to a life as microbial starvation artists. The cultivation of slow-growing, low-density bacteria and archaea from the deep subsurface will have positive feedback effects on functional gene and genomics studies; newly cultured members of largely uncultured lineages or phyla will serve as benchmark species and strains to explore their physiological capabilities, genomic potential, and environmental relevance.

Acknowledgments Andreas Teske was supported by the NASA Astrobiology Institutes "Environmental genomes" (NCC 2-1054), "Subsurface biospheres" (NCC 2-1275), and by the Ocean Drilling Program. Jennifer Biddle was supported by the NASA Astrobiology Institute "Evolution of a habitable planet" and by a NASA Postdoctoral Program fellowship administered through the Oak Ridge Associated Universities.

References

Abulencia CB, Wyborski DL, Garcia JA, Podar M, Chen W, Chang SH, Chang HW, Watson, D, Brodie EL, Hazen TC, Keller M (2006). Environmental whole-genome amplification to access microbial populations in contaminated sediments. Appl Environ Microbiol 72:3291–3301

Altschul SF, Madden TL, Schäffer AA, Zhang J, Zhang Z, Miller W, Lipman DJ (1997) Gapped BLAST and PSI-BLAST: a new generation of protein database search programs. Nucleic Acids Res 25:3389–3402

Amend JP, Teske A (2005) Expanding frontiers in deep subsurface microbiology. Palaeogeogr Palaeoclimatol Palaeoecol 219:131–155

Bahr M, Crump BC, Klepac-Ceraj V, Teske A, Sogin ML, Hobbie JE (2005) Molecular characterization of sulfate-reducing bacteria in a New England salt marsh. Environ Microbiol 7: 1175–1185

Banning N, Brock F, Fry JC, Parkes RJ, Hornibrook ERC, Weightman AJ (2005) Investigation of the methanogen population structure and activity in a brackish lake sediment. Environ Microbiol 7:947–960

Biddle JF (2006) Microbial populations and processes in deeply buried marine sediments. PhD thesis, Pennsylvania State University

Biddle JF, Fitz-Gibbon S, Schuster S, Brenchley JE, House CH (2008) Metagenomic signatures of the Peru Margin subseafloor biosphere. Proc Natl Acad Sci USA, in press

Biddle JF, House CH, Brenchley JE (2005a) Enrichment and cultivation of microorganisms from sediment from the slope of the Peru Trench (ODP site 1230). In: Jørgensen, BB, D'Hondt, SL, Miller, DJ (eds) Proc. ODP, Sci. Results, 201 [Online]. Available from World Wide Web: <http://www-odp.tamu.edu/ publications201_SR/107107.htm> [Cited 2007-04-25]

Biddle JF, House CH, Brenchley JE (2005b) Microbial stratification in deeply-buried marine sediment reflects changes in sulfate/methane profiles. Geobiology 3:287–295

Biddle JF, Lipp JS, Lever MA, Lloyd KG, Sørensen KB, Anderson R, Fredricks HF, Elvert M, Kelly TJ, Schrag DP, Sogin ML, Brenchley JE, Teske A, House CH, Hinrichs KU (2006)

Heterotrophic Archaea dominate sedimentary subsurface ecosystems off Peru. Proc Natl Acad Sci USA 103:3846–3851

Bidle KA, Kastner M, Bartlett DH (1999) A phylogenetic analysis of microbial communities associated with methane hydrate containing marine fluids and sediments in the Cascadia Margin (ODP Site 892B). FEMS Microbiol Lett 177:101–108

Boetius A, Ravenschlag K, Schubert C, Rickert D, Widdel F, Gieseke A, Amann R, Jørgensen BB, Witte U, Pfannkuche O (2000) A marine microbial consortium apparently mediating anaerobic oxidation of methane. Nature 407:623–626

Boone DR, Mah RA. (2001) Genus I. *Methanosarcina*. In: Boone DR, Castenholz, RW (eds) Bergey's manual of systematic bacteriology. 2nd Edition. Volume 1. The Archaea and the deeply branching and phototrophic bacteria. New York: Springer, New York, pp 269–276

Böttcher ME, Ferdelman TG, Jørgensen BB, Blake RE, Surkov AV, Claypool GE (2006) Sulfur isotope fractionation by the deep biosphere within sediments of the eastern equatorial Pacific and Peru Margin. In: Jørgensen BB, D'Hondt SL, Miller DJ (eds) Proc ODP, Sci Results, 201 [Online]. Available from World Wide Web: <http://www-odp.tamu.edu/publications/201_SR/109/109.htm>.[Cited 2006-06-25]

Braker G, Zhou J, Wu L, Devol AH, Tiedje JM (2000) Nitrite reductase genes (*nirK* and *nirS*) as functional markers to investigate diversity of denitrifying bacteria in Pacific Northwest marine sediment communities. Appl Environ Microbiol 66:2096–2104

Braker G, Ayala-del-Río HL, Devol AH, Fesefeldt A, Tiedje JM (2001) Community structure of denitrifiers, bacteria, and archaea along redox gradients in Pacific Northwest marine sediments by terminal restriction fragment length polymorphism analysis of amplified ntrite reductase (*nirS*) and 16S rRNA genes. Appl Environ Microbiol 67:1893–1901

Bruns A, Hoffelner H, Overmann J (2003a) A novel approach for high throughput cultivation assays and the isolation of planktonic bacteria. FEMS Microbiol Ecol 45:161–171

Bruns A, Nübel U, Cypionka H, Overmann J (2003b) Effect of signal compounds and incubation conditions on the culturability of freshwater bacterioplankton. Appl Environ Microbiol 69:1980–1989

Bustin SA (2000) Absolute quantification of mRNA using real-time reverse transcription polymerase chain reaction assays. J Mol Endocrinol 25:169–193

Cho JC, Vergin KL, Morris RM, Giovannoni SJ (2004). *Lentisphaera araneosa* gen. nov., sp. nov, a transparent exopolymer producing marine bacterium, and the description of a novel bacterial phylum, Lentisphaerae. Environ Microbiol 6:611–621

Connon SA, Giovannoni SJ (2002) High-throughput methods for culturing micro-organisms in very-low-nutrient media yield diverse new marine isolates. Appl Environ Microbiol 68: 3878–3885

Coolen MJL, Cypionka H, Sass AM, Sass H, Overmann J (2002) Ongoing modification of Mediterranean sapropels mediated by prokaryotes. Science 296:2407–2410

Dhillon A, Teske A, Dillon J, Stahl DA, Sogin ML (2003) Molecular characterization of sulfate-reducing bacteria in the Guaymas Basin. Appl Environ Microbiol 69:2765–2772

Dhillon A, Goswami S, Riley M, Teske A, Sogin ML (2005a). Domain evolution and functional diversification of sulfite reductases. Astrobiology 5:18–29

Dhillon A, Lever MA, Lloyd KG, Albert DB, Sogin ML, Teske A (2005b) Methanogen Diversity Evidenced by Molecular Characterization of Methyl Coenzyme M Reductase A (*mcr*A) Genes in Hydrothermal Sediments of the Guaymas Basin. Appl Environ Microbiol 71:4592–4601

D'Hondt SL, Jørgensen BB, Miller DJ, and the Shipboard Scientific Party (2003) Proceedings of the ocean drilling program, Initial Reports 201 [CD-ROM]. Available from: Ocean Drilling Program, Texas A&M University, College Station TX 77845-9547, USA

D'Hondt S, Jørgensen BB, Miller DJ, Batzke A, Blake R, Cragg BA, Cypionka H, Dickens GR, Ferdelman T, Hinrichs KU, Holm NG, Mitterer R, Spivack A, Wang G, Bekins B, Engelen B, Ford K, Gettemy G, Rutherford SD, Sass H, Skilbeck CG, Aiello IW, Guèrin G, House C, Inagaki F, Meister P, Naehr T, Niitsuma S, Parkes RJ, Schippers A, Smith DC, Teske A, Wiegel J, Padilla CN, Acosta JLS (2004) Distributions of microbial activities in deep subseafloor sediments. Science 306:2216–2221

Didyk BM, Simoneit BR (1989) Hydrothermal oil of Guaymas Basin and implications for petroleum formation mechanisms. Nature 342:65–69

Edwards RA, Rodriguez-Brito B, Wegley L, Haynes M, Breitbart M, Peterson D, Saar M, Alexander S, Alexander EC, Rohwer F (2006) Using pyrosequencing to shed light on deep mine microbial ecology under extreme hydrogeologic conditions. BMC Genomics 7:57

Finn RD, Mistry J, Schuster-Bockler B, Griffiths-Jones S, Hollich V, Lassmann T, Moxon S, Marshall M, Khanna A, Durbin R, Eddy SR, Sonnhammer ELL, Bateman A (2006) Pfam: clans, web tools and services. Nucleic Acids Res. 34:D247–D251

Friedrich MW (2002) Phylogenetic analysis reveals multiple lateral transfers of adenosine-5′-phosphosulfate reductase genes among sulfate-reducing microorganisms. J Bacteriol 184: 278–289

Friedrich MW (2005) Methyl-coenzyme M reductase genes: unique functional markers for methanogenic and anaerobic methane-oxidizing archaea. Methods Enzymol 397:428–442

Fry JC, Webster G, Cragg BA, Weightman AJ, Parkes JR (2006) Analysis of DGGE profiles to explore the relationship between prokaryotic community composition and biogeochemical processes in deep sub-seafloor sediments from the Peru Margin. FEMS Microbiol Ecol 58:86–98

Garrity GM, Holt JG (2001) The roadmap to the manual. In: Boone RD, Casteholz RW (eds) Bergey's manual of systematic bacteriology. Volume 1: the Archaea and the deeply branching and phototrophic bacteria. Springer; New York, Berlin, Heidelberg, pp 119–166

Hallam SJ, Girguis PR, Preston CM, Richardson PM, DeLong EF (2003) Identification of methyl coenzyme M reductase A (*mcrA*) genes associated with methane-oxidizing archaea. Appl Environ Microbiol 69:5483–5491

Hallam SJ, Putman N, Preston CM, Detter JC, Rokhsar D, Richardson PNM, DeLong EF (2004) Reverse methanogenesis: testing the hypothesis with environmental genomics. Science 305:1457–1462

Højberg O, Binnerup SJ, Sørensen J (1997) Growth of silicone-immobolized bacteria on polycarbonate membrane filters, a technique to study microcolony formation under anaerobic conditions. Appl Environ Microbiol 63:2920–2924

Hutchinson CA, Smith HO, Pfannkoch C, Venter JC (2005) Cell-free cloning using ϕ 29 DNA polymerase. Proc Natl Acad USA 102:17332–17336

Inagaki F, Suzuki M, Takai K, Oida H, Sakamoto T, Aoki K, Nealson KH, Horikoshi K (2003) Microbial communities associated with geological horizons in coastal subseafloor sediments from the Sea of Okhotsk. Appl Environ Microbiol 69:7224–7235

Inagaki F, Tsunogai U, Suzuki M, Kosaka A, Machiyama H, Takai K, Nunoura T, Nealson K, Horikoshi K (2004) Characterization of C1-metabolizing prokaryotic communities in methane seep habitats at the Kuroshima Knoll, Southern Ryukyu Arc, by analyzing *pmoA, mmoX, mxaF, mcrA*, and 16S rRNA genes. Appl Environ Microbiol 70:7445–7455

Inagaki F, Nunoura T, Nakagawa S, Teske A, Lever MA, Lauer A, Suzuki M, Takai K, Delwiche M, Colwell FS, Nealson KH, Horikoshi K, D'Hondt SL, Jørgensen BB (2006) Biogeographical distribution and diversity of microbes in methane hydrate-bearing deep marine sediments on the Pacific Ocean Margin. Proc Natl Acad Sci USA 103:2815–2820

Jørgensen BB, D'Hondt SL (2006) A starving majority deep beneath the seafloor. Science 314:932–934

Kaeberlein T, Lewis K, Epstein SS (2002) Isolating "uncultivable" microorganisms in pure culture in a simulated natural environment. Science 296:1127–1129

Kalyuzhnaya MG, Zabinsky R, Bowerman S, Baker DR, Lidstrom ME, Chistoserdova L (2006) Fluorescence in situ hybridization-flow cytometry-cell sorting-based method for separation and enrichment of type I and type II methanotroph populations. Appl Environ Microbiol 72: 4293–4301

Klein M, Friedrich M, Roger AJ, Hugenholtz P, Fishbain S, Abicht H, Blackall LL, Stahl DA, Wagner M (2001) Multiple lateral transfers of dissimilatory sulfite reductase genes between major lineages of sulfate-reducing prokaryotes. J Bacteriol 183:6028–6035

Klenk HP, Clayton RA, Tomb JF, White O, et al (1997) The complete genome sequence of the hyperthermophilic, sulphate-reducing archaeon *Archaeoglobus fulgidus*. Nature 390:364–370

Kondo R, Nedwell DB, Purdy KJ, de Queiroz Silva S (2004) Detection and enumeration of sulphate-reducing bacteria in estuarine sediments by competitive PCR. Geomicrobiol 21:145–157

Köpke B, Wilms R, Engelen B, Cypionka H, Sass H (2005) Microbial diversity in coastal subsurface sediments: a cultivation approach using various electron acceptors and substrate gradients. Appl Environ Microbiol 71:7819–7830

Kormas AK, Smith DC, Edgcomb V, Teske A (2003) Molecular analysis of deep subsurface microbial communities in Nankai Trough sediments (ODP Leg 190, Site 1176). FEMS Microbiol Ecol 45:115–125

Krause L, Diaz NN, Bartels D, Edwards RA, Puhler A, Rohwer F, Meyer F, Stoye J (2006) Finding novel genes in bacterial communities isolated from the environment. Bioinformatics 22: 281–289

Kumar S, Tamura K, Nei M (2004) MEGA3: integrated software for molecular evolutionary genetics analysis and sequence alignment. Brief Bioinform 5:150–163

Laue H, Friedrich MW, Ruff J, Cook A (2001) Dissimilatory sulfite reductase (desulfoviridin) of the taurine-degrading, non-sulfdate-reducing bacterium *Bilophila wadsworthia* RZATAU contains a fused dsrB-dsrD subunit. J Bacteriol 183:1717–1733

Lee Y, Wagner I, Brice ME, Kevbrin VV, Mills G, Romanek CS, Wiegel J (2005) *Thermosediminibacter oceani* gen. nov., sp. nov. and *Thermosediminibacter litoriperuensis* sp. nov., new anaerobic thermophilic bacteria isolated from Peru Margin. Extremophiles 9:375–383

Lever M, Teske A (2007) Vertical distribution of methanogens and active Archaea in subsurface sediments of the Peru Trench as evaluated from functional genes and 16S rRNA profiles. Abstract at 2007 ASLO Meeting, Santa Fe, NM.

Liu X, Bagwell CE, Wu L, Devol AH, Zhou J (2003) Molecular diversity of sulfate-reducing bacteria from two different continental margin habitats. Appl Environ Microbiol 69:6073–6081

Lloyd KG, Lapham L, Teske A (2006) An anaerobic methane-oxidizing community of ANME-1 Archaea in hypersaline Gulf of Mexico sediments. Appl Environ Microbiol 72:7218–7230

Luton PE, Wayne JM, Sharp RJ, Riley PW (2002) The *mcrA* gene as an alternative to 16S rRNA in the phylogenetic analysis of methanogen populations in landfill. Microbiology 148:3521–3530

Martens-Habbena W, Sass H (2006) Sensitive determination of microbial growth by nucleuic acid staining in aqueous suspension. Appl Environ Microbiol 72:87–95

Miller TL (2001) Genus II. *Methanobrevibacter*. In: Boone DR, Castenholz R. (eds) Bergey's Manual of Systematic Bacteriology. 2nd Edition. Volume 1. The Archaea and the deeply branching and phototrophic bacteria. New York: Springer, New York, pp 219–226

Neretin LN, Schippers A, Pernthaler A, Hamann K, Amann R, Jørgensen BB (2003) Quantification of dissimilatory (bi)sulphite reductase gene expression in *Desulfo-bacterium autotrophicum* using real-time RT-PCR. Environ Microbiol 5:660-671

Newberry CJ, Webster G, Weightman AJ, Fry JC (2004) Diversity of prokaryotes and methanogenesis in deep subsurface sediments from the Nankai Trough, Ocean Drilling Program Leg 190. Environ Microbiol 6:274–287

Niemann H, Lösekann T, de Beer D, Elvert M, Nadalig T, Knittel K, Amann R, Sauter EJ, Schlüter M, Klages M, Foucher JP, Boetius A (2006) Novel microbial communities of the Haakon Mosby mud volcano and their role as a methane sink. Nature 443:854–858

Nunoura T, Oida H, Toki T, Ashi J, Takai K, Horikoshu K (2006) Quantification of *mcrA* by quantitative fluorescent PCR in sediments from methane seep of the Nankai Trough. FEMS Microbiol Ecol 57:149–157

Orphan VJ, House CH, Hinrichs KU, McKeegan KD, DeLong EF (2001) Methane-consuming archaea revealed by directly coupled isotopic and phylogenetic analysis. Science 293:484–487

Orphan VJ, House CH, Hinrichs KU, McKeegan KD, DeLong EF (2002) Multiple groups mediate methane oxidation in anoxic cold seep sediments. Proc Natl Acad Sci USA 99: 7663–7668

Parkes RJ, Cragg BA, Wellsbury P (2000) Recent studies on bacterial populations and processes in subseafloor sediments: a review. Hydrogeology J. 8:11–28

Parkes RJ, Webster G, Cragg BA, Weightman AJ, Newberry CJ, Ferdelman TG, Kallmeyer J, Jørgensen BB, Aiello IW, Fry JC (2005) Deep sub-seafloor prokaryotes stimulated at interfaces over geological time. Nature 436:390–394

Parkes RJ, Cragg BA, Banning N, Brock F, Webster G, Fry JC, Hornibrook E, Pancost RD, Kelly S, Knab N, Jørgensen BB, Rinna J, Weightman AJ (2007) Biogeochemistry and biodiversity of methane cycling in subsurface marine sediments (Skagerrak, Denmark). Environ Microbiol 9:1146–1161

Patel GB (2001) Genus I. *Methanosaeta*. In: Boone DR, Castenholz RW (eds) Bergey's manual of systematic bacteriology. 2nd Edition. Volume 1. The Archaea and the deeply branching and phototrophic bacteria. New York: Springer, New York, pp 289–294

Pearson A, Seewald JS, Eglinton TI (2005) Bacterial incorporation of relict carbon in the hydrothermal environment of Guaymas Basin. Geochim Cosmochim Acta 69:5477–5486

Raghunathan A, Ferguson HR, Bornarth CJ, Song W, Driscoll M, Lasken RS (2005) Genomic amplification from a single bacterium. Appl Environ Microbiol 71:3342–3347

Rappé MS, Connon SA, Vergin KL, Giovannoni SJ (2002) Cultivation of the ubiquitous SAR11 marine bacterioplankton clade. Nature 418:630–633

Reed DW, Fujita Y, Delwiche ME, Blackwelder DB, Sheridan PP, Uchida T, Colwell FS (2002) Microbial communities from methane hydrate-bearing deep marine sediments in a forearc basin. Appl Environ Microbiol 68:3759–3770

Schippers A, Neretin LN (2006) Quantification of microbial communities in near-surface and deeply buried marine sediments on the Peru continental margin using real-time PCR. Environ Microbiol 8:1251–1260

Schippers A, Neretin LN, Kallmeyer J, Ferdelman TG, Cragg BA, Parkes JR, Jørgensen BB (2005) Prokaryotic cells of the deep sub-seafloor biosphere identified as living bacteria. Nature 433:861–864

Shipboard Scientific Party (2003a) Site 1228. In: D'Hondt SL, Jørgensen BB, Miller DJ, et al (eds) Proceedings of the ocean drilling program, Initial reports 201. Ocean Drilling Program, Texas &M University, College Station, Tex. [CD-ROM], pp 1–72

Shipboard Scientific Party (2003b) Site 1229. In: D'Hondt SL, Jørgensen BB, Miller DJ, et al (eds) Proceedings of the ocean drilling program, Initial reports 201. Ocean Drilling Program, Texas &M University, College Station, Tex. [CD-ROM], pp 1–78

Shipboard Scientific Party (2003c) Site 1230. In: D'Hondt SL, Jørgensen BB, Miller DJ, et al (eds) Proceedings of the Ocean Drilling Program, Initial reports 201. Ocean Drilling Program, Texas &M University, College Station, Tex. [CD-ROM], pp 1–107

Sogin ML, Morrison HG, Huber JA, Welch DM, Huse SM, Neal PR, JArrieta JM, Herndl GJ (2006) Microbial diversity in the deep sea and the under explored "rare biosphere". Proc Natl Acad Sci USA 103:12115–12120

Sørensen KB, Teske A (2006) Stratified communities of active archaea in deep marine subsurface sediments. Appl Environ Microbiol 72:4596–4603

Sørensen KB, Lauer A, Teske A (2004) Archaeal phylotypes in a metal-rich, low-activity deep subsurface sediment of the Peru Basin, ODP Leg 201, Site 1231. Geobiology 2:151–161

Springer E, Sachs MS, Woese CR, Boone DR (1995) Partial gene sequences for the alpha-subunit of methyl-coenzyme M reductase (MCR1) as a phylogenetic tool for the family Methanosarcinaceae. Int J Syst Bacteriol 45:554–559

Stahl DA, Fishbain S, Klein M, Baker BJ, Wagner W (2002) Origins and diversification of sulfate-respiring microorganisms. Antonie Van Leeuwenhoek 81:189–195

Stults JR, Snoeyenbos-West O, Methe B, Lovley DR, Chandler DP (2001) Application of the 5′ fluorogenic exonuclease assay (TaqMan) for quantitative ribosomal DNA and rRNA analysis in sediments. Appl Environ Microbiol 67:2781–2789

Süss J, Engelen B, Cypionka H, Sass H (2004) Quantitative analysis of bacterial communities from Mediterranean sapropels based on cultivation-dependent methods. FEMS Microbiol Ecol 51:109–121

Süss J, Schubert K, Sass H, Cypionka H, Overmann J, Engelen B (2006) Widespread distribution and high abundance of *Rhizobium radiobacter* within Mediterranean subsurface sediments. Environ Microbiol 8:1753–1763

Suzuki MT, Taylor LT, DeLong EF (2000) Quantitative analysis of small-subunit rRNA genes in mixed microbial populations via 5′-nuclease assays. Appl Environ Microbiol 66: 4605–4614

Teira E, Reinthaler T, Pernthaler A, Pernthaler J, Herndl GJ (2004) Combining catalyzed reporter deposition-fluorescence in situ hybridization and microautoradiography to detect substrate utilization by bacteria and archaea in the deep ocean. Appl Environ Microbiol 70:4411–4414

Teske A (2006) Microbial communities of deep marine subsurface sediments: molecular and cultivation surveys. Geomicrobiol J 23:357–368

Thomsen TR, Finster K, Ramsing NB (2001) Biogeochemical and molecular signatures of anaerobic methane oxidation in a marine sediment. Appl Environ Microbiol 67:1646–1656

Thompson JD, Higgins DG, Gibson TJ (1994) CLUSTAL W: improving the sensitivity of progressive multiple sequence alignments through sequence weighting, position specific gap penalties and weight matrix choice. Nucl Acids Res 22:4673–4680

Toffin L, Bidault A, Pignet P, Tindall BJ, Slobodkin A, Kato C, Prieur D (2004a) *Shewanella profunda* sp. nov., isolated from deep marine sediment of the Nankai Trough. Int J Syst Evol Microbiol 54:1943–1949

Toffin L, Webster G, Weightman AJ, Fry JC, Prieur D (2004b) Molecular monitoring of culturable bacteria from deep-sea sediment of the Nankai Trough, Leg 190 Ocean Drilling Program. FEMS Microbiol Ecol 48:357–367

Toffin L, Zink K, Kato C, Pignet P, Bidault A, Bienvenu N, Birrien JL, Prieur D (2005) *Marinilactobacillus piezotolerans* sp. nov., a novel marine lactic acid bacterium isolated from deep subseafloor sediment of the Nankai Trough. Int J Syst Evol Microbiol 55:345–351

Tyson GW, Chapman J, Hugenholtz P, Allen EE, Ram RJ, Richardson PM, Solovyev VV, Rubin EM, Rokhsar DS, Banfield JF (2004) Community structure and metabolism through reconstruction of microbial genomes from the environment. Nature 428:37–43

Venter JC, Remington K, Heidelberg JF, Halpern AL, Rusch D, Eisen JA, Wu D, Paulsen I, Nelson K, Nelson W, Fouts DE, Levy S, Knap AH, Lomas MW, Nealson K, White O, Peterson J, Hoffman J, Parsons R, Baden-Tillson H, Pfannkoch C, Rogers Y-H, Hamilton SO (2004) Environmental genome shotgun sequencing of the sargasso sea. Science 304:66–74

Von Mering C, Hugenholtz P, Raes J, Tringe SG, Doerks T, Jensen LJ, Ward N, Bork P (2007) Quantitative phylogenetic assessment of microbial communities in diverse environments. Science 315:1126–1130

Wagner M, Roger AJ, Flax JL, Brusseau GA, Stahl DA (1998) Phylogeny of dissimilatory sulfite reductases supports an early origin of sulfate respiration. J Bacteriol 180:2975–2982

Wagner M, Loy A, Klein M, Lee N, Ramsing NB, Stahl DA, Friedrich MW (2005) Functional marker genes for identification of sulfate-reducing prokaryotes. Environ Microbiol Meth Enzymol 397:469–489

Webster G, Newberry CJ, Fry JC, Weightman AJ (2003) Assessment of bacterial community structure in the deep sub-seafloor biosphere by 16S rDNA-based techniques: a cautionary tale. J Microbiol Meth 55:155–164

Webster G, Parkes RJ, JFry JC, Weightman AJ (2004) Widespread occurrence of a novel division of bacteria identified by 16S rRNA gene sequences originally found in deep marine sediments. Appl Environ Microbiol 70:5708–5713

Webster G, Parkes RJ, Cragg BA, Newberry CJ, Weightman AJ, Fry JC (2006) Prokaryotic community composition and biogeochemical processes in deep subseafloor sediments from the Peru margin. FEMS Microbiol Ecol 58:65–85

Wellsbury P, Goodman K, Barth T, Cragg BA, Barnes SP, Parkes RJ (1997) Deep bacterial biosphere fuelled by increasing organic matter availability during burial and reheating. Nature 388:573–576

Whitman WB, Coleman DC, Wiebe WJ (1998) Prokaryotes: the unseen majority. Proc Natl Acad Sci USA 95:6578–6583

Wilms R, Köpke B, Sass H, Chang TS, Cypionka H, Engelen B (2006a) Deep biosphere-related bacteria within the subsurface of tidal flat sediments. Environ Microbiol 8: 709–719

Wilms R, Sass H, Köpke B, Koster H, Cypionka H, Engelen B (2006b) Specific bacterial, archaeal, and eukaryotic communities in tidal-flat sediments along a vertical profile of several meters. Appl Environ Microbiol 72:2756–2764

Wilms R, Sass H, Köpke B, Cypionka H, Engelen B (2007) Methane and sulfate profiles within the subsurface of a tidal flat are reflected by the distribution of sulfate-reducing bacteria and methanogenic archaea. FEMS Microbiol Ecol 59:611–621

Wu L, Liu X, Schadt CW, Zhou J (2006) Microarray-based analysis of subnanogram quantities of microbial community DNAs by using whole community genome amplification. Appl Environ Microbiol 72:4931–4941

Zhang K, Martiny AC, Reppas NB, Barry KW, Malek J, Chisholm S, Church GM (2006) Sequencing genomes from single cells by polymerase cloning. Nat Biotechnol 24:680–686

Zverlov V, Klein M, Lucker S, Friedrich MW, Kellermann J, Stahl DA, Loy A, Wagner M (2005) Lateral gene transfer of dissimilatory (bi)sulfite reductase revisited. J Bacteriol 187:2203–2208

Diversity of Bahamian Microbialite Substrates

Robert N. Ginsburg and Noah J. Planavsky

Abstract Stromatolites, laminated columnar and branched structures of limestone and dolomite, are the only macroscopic evidence of life for the first few billion years of earth history. These organo-sedimentary structures are a prominent constituent of Precambrian carbonate successions and occur sporadically throughout the Phanerozoic. They are hosts for metallic ores and serve as reservoir rocks for hydrocarbons. Still living Bahamian columnar forms that are counterparts of ancient microbialites (stromatolitic and thrombolitic) provide a special opportunity to examine if their substrates played a role in determining the occurrences and patterns of these remarkable structures. The cyanobacterial builders of Bahamian stromatolites can colonize almost all substrates except mobile sands. The development of columnar structures with significant relief however, requires either a hard or firm substrate. From published reports on substrates and our own observations we recognize two families of substrates: inherited, consisting of pre-existing rock surfaces and renewable, including all substrates that can develop repeatedly during accumulation. Inherited substrates in the Bahamas include Pleistocene limestone with or without palimpsest encrustations of caliche or paleosol. Renewable substrates in the marine environment include syndepositional hardgrouds, large skeletons of corals and mollusks, encrustations of coralline algae or vermetid gastropods, and firm grounds of fine-grained carbonate sediment. Recognizing the key roles of renewable substrates in determining the occurrences and age variations of modern Bahamian specimens emphasizes the need for increased attention to the foundations of microbialites in future studies.

1 Introduction

Stromatolites are laminated, lithified columnar, branched, and hemispheroidal structures that accrete from a single point (Semikhatov et al. 1979). They are a major component of carbonate platforms in the Precambrian and sporadically throughout

R.N. Ginsburg
University of Miami, Comparative Sedimentology Laboratory, Rosenstiel School of Marine and Atmospheric Sciences, 4600 Rickenbacker Causeway, Miami Fl, 33149
e-mail: rginsburg@rsmas.miami.edu

Y. Dilek et al. (eds.), *Links Between Geological Processes, Microbial Activities & Evolution of Life*, © Springer Science+Business Media B.V. 2008

Fig. 1 Example of classic Precambrian stromatolites, Pethei Group, Great Slave Lake, NWT, Canada. The large slumped slab shows the columnar growth form (in plan view) and the characteristic convex-upward laminations (in cross sectional view). Photo Paul Hoffman

the Phanerozoic (Fig. 1). Stromatolites form through the dynamic interactions of a microbial community, geochemical reactions, and local sedimentation. Cyanobacteria are the predominant element of benthic communities forming nearly all modern stromatolites and were most probably also the builders of the majority of their fossil counterparts.

The cyanobacterial builders of stromatolites are ever-present on the earth's surface: hot springs, polar ice, terrestrial environments, fresh and hypersaline waters, and are likely some of the most abundant life forms in the oceans (Waterbury et al. 1979). When many species of cyanobacteria encounter a stable substrate, they attach, multiply and spread to form a benthic community. Cyanobacterially-dominated benthic microbial communities are complex associations of photosynthetic and heterotrophic bacteria (Monty 1976; Papineau et al. 2005). Transforming a prostrate microbial mat into a microbialite rising above the surroundings requires building materials. Luckily, two sources have long been available. One is sediment trapped and firmly bound by the agile bacteria. The other building material, which is predominate in early Precambrian stromatolites, is calcium carbonate precipitated like plaster on or within the microbial mat. This carbonate precipitation in many extant stromatolites is triggered by the metabolic activities of the benthic microbial community, a topic that has been extensively studied. Within the benthic microbial community, cyanobacterial photosynthesis can locally lower the carbon dioxide concentration, which raises the pH and induces carbonate precipitation. Organic matter remineralization, predominately through sulfate reduction, can also promote carbonate precipitation (For recent reviews see Andres et al. 2006; Arp et al. 1999, 2003; Visscher et al. 2000; Visscher et al. 1998). Whichever of these two building

materials is used, the formation of single lamina must be repeated to build a structure rising above its surroundings. This repetition can be caused by cyanobacteria motility, recolonization of the growth surface, variation in the types of benthic communities, or periodicity in the accretion linked to a dynamic environment (Monty 1976; Reid et al. 2000). The end result of repeated laminae of sediment or precipitated carbonate are structures composed of convex-upward laminations—stromatolites (Fig. 1).

2 Discovery and Significance of Holocene Stromatolites

When stromatolites were first discovered, late 19th and early 20th century, paleontologists and sedimentary geologists were baffled by these non-skeletal laminated domes and columns. There was longstanding debate if these layered structures they were animal, plant or purely mineral.

One of the early breakthroughs in understanding the origins of stromatolites came in the 1930s when an adventurous young Englishman named Maurice Black traversed the shallow lakes and swamps of Andros Island, Bahamas by canoe. His paper (Black 1933) described how self-replicating cyanobacterial mats alternating with periodic deposition of sediment could produce unlithified laminated structures resembling ancient stromatolites.

The discovery of well-lithified marine stromatolites, first in a hyper-saline lagoon in Shark Bay in Western Australia (Fig. 2) (Logan 1961; Playford and Cockbain

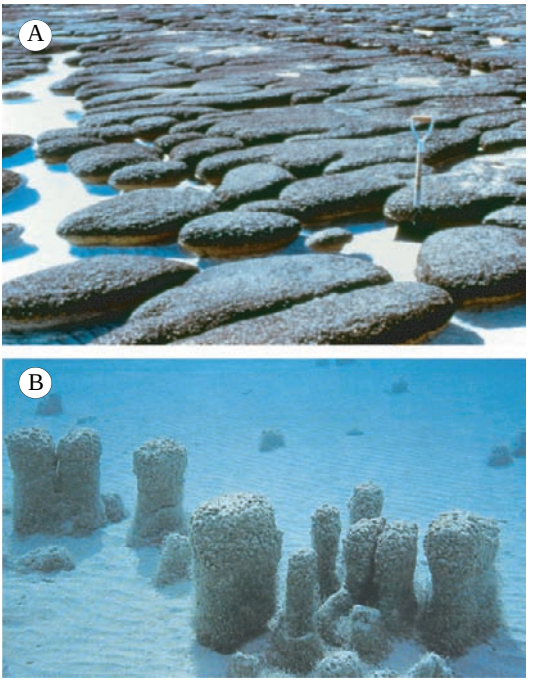

Fig. 2 Shark Bay stromatolites, Western Australia. (**A**) Exposed, wave-trained and elongated stromatolites. Photograph B. Logan. (**B**) Subtidal columnar stromatolites of variable heights. The tallest stromatolites in photo are 40 cm. Photograph P. Playford

1976) and more recently in tidal channels of the Bahamas (Dill et al. 1986; Dravis 1983; Reid et al. 1995)(Fig. 3), inspired seminal research on microbial carbonates. For example, detailed research on intertidal stromatolites in the Bahamas added novel concepts about stromatolite laminae formation (Andres, Sumner, Reid and Swart 2006; Browne et al. 2000; Macintyre et al. 2000; Reid et al. 2000; Visscher et al. 2000).

The Bahamian stromatolites are of special relevance to interpreting fossil examples. They develop in subtidal settings of up to 10 m deep in waters of oceanic salinities (35–37 ppt) (Dill et al. 1986). The Bahamian stromatolites, therefore, form

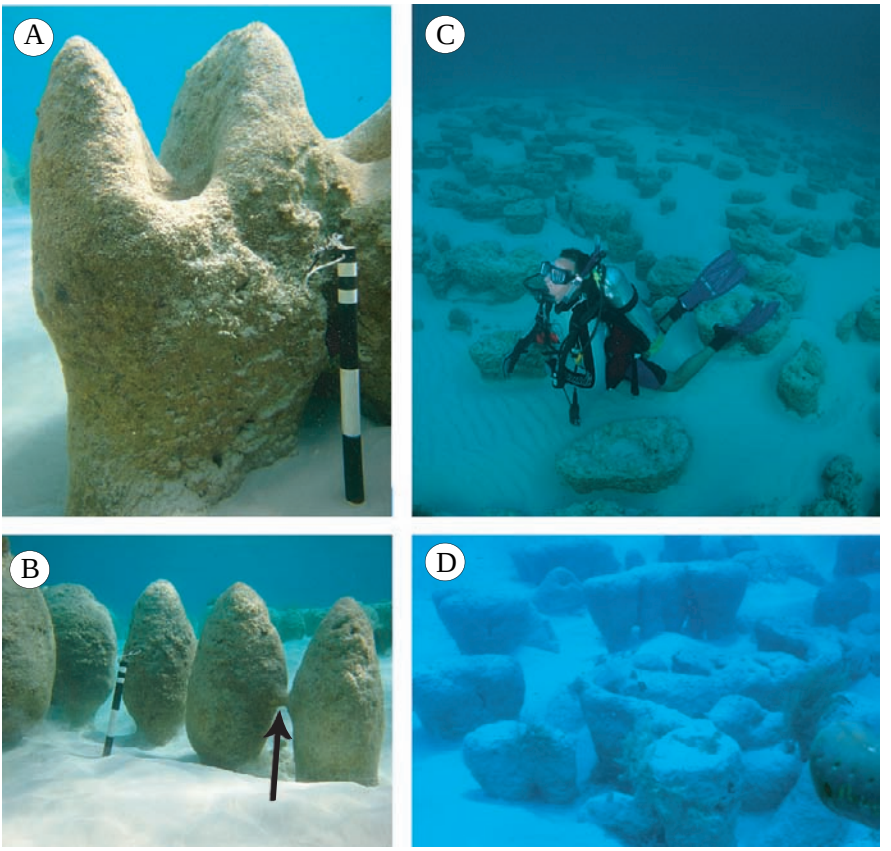

Fig. 3 Underwater views of diverse morphologies of Bahamian microbialites. (**A**) Microbialite with two conical projections—either branched or two ovoids fused by cemented sand when buried. Bock Cay, depth ∼ 4 m. Scale divisions 2 and 10 cm. (**B**) A row of ovoid microbialites with two bridged by cemented sand (arrow). Scale divisions 2 and 10 cm. (**C**) Underwater view of Adderly Channel floor, depth ∼ 5 m, with abundant mostly individual microbialites. (**D**) A varied cluster of microbialites in Adderly Channel, ∼ 6 m deep, The three specimens at top are fused together; so are the two at lower left partly buried in sand. The central microbialite appears to be compound

in a sedimentological setting that can be more directly related to the marine fossil examples than other modern analogues, such as the relatively common modern lacustrine stromatolites. Further, the Bahamian stromatolites are morphologically variable (Fig. 3) and occur as columns up to two meters tall, characteristics common in Precambrian, but rare in most modern stromatolites.

The most extensive and well-cemented Bahamian stromatolites are found in the tidal channels of the Exuma Islands, notably in Adderly Channel (Figs. 4 and 5). Lithified stromatolites also occur in the intertidal zone of these islands (Fig. 4). We have recently discovered stromatolites in the large apron of ooid shoals around the Tongue of the Ocean (Fig. 4). For unknown reasons they have not been detected on ooid shoals in the Western Bahamas or on Little Bahama Bank. The Bahamian microbial structures were initially described as stromatolites (Dill et al. 1986; Dravis 1983; Reid et al. 1995). Some of these specimens lack laminations but have clotted fabrics and have been termed thrombolites (Browne et al. 2000; Dill 1991; Feldman and McKenzie 1998). Additionally, both lithified and unlithified laminated microbial structures are widespread in peritidal sediments, especially on the extensive tidal flats of Andros Island (Fig. 4) (Monty 1976). These varied settings provide a special opportunity to consider two key elements of stromatolite construction: the variety of substrates and the supply of building materials. We are fortunate that our predecessors' research on these elements and their physical environment provides a thorough foundation of information and analysis. Our research over two field seasons provides significant additional data.

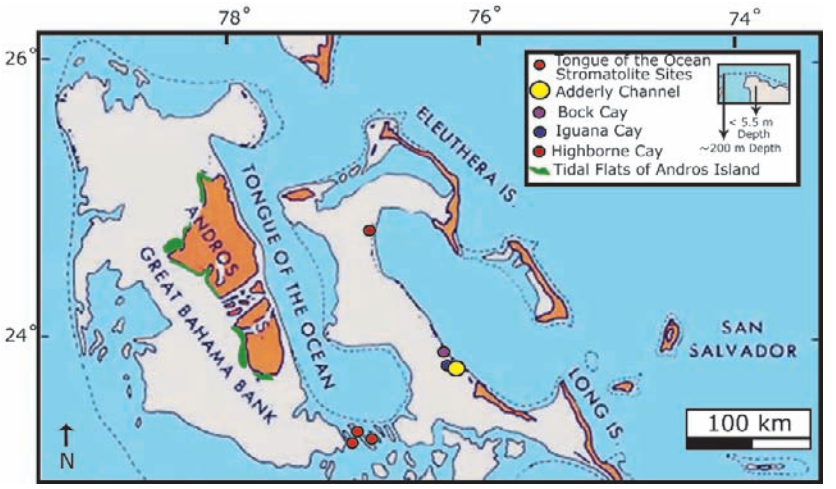

Fig. 4 Map of examined Bahamian stromatolites and peritidal microbial mats localities. The stromatolites are all occur on the shallow banks between sand wavers at depths of <10 m. Several stromatolites localities are in the tidal channels along a thin string of Pleistocene island, the Exumas. Modified from map by Chris Kendall

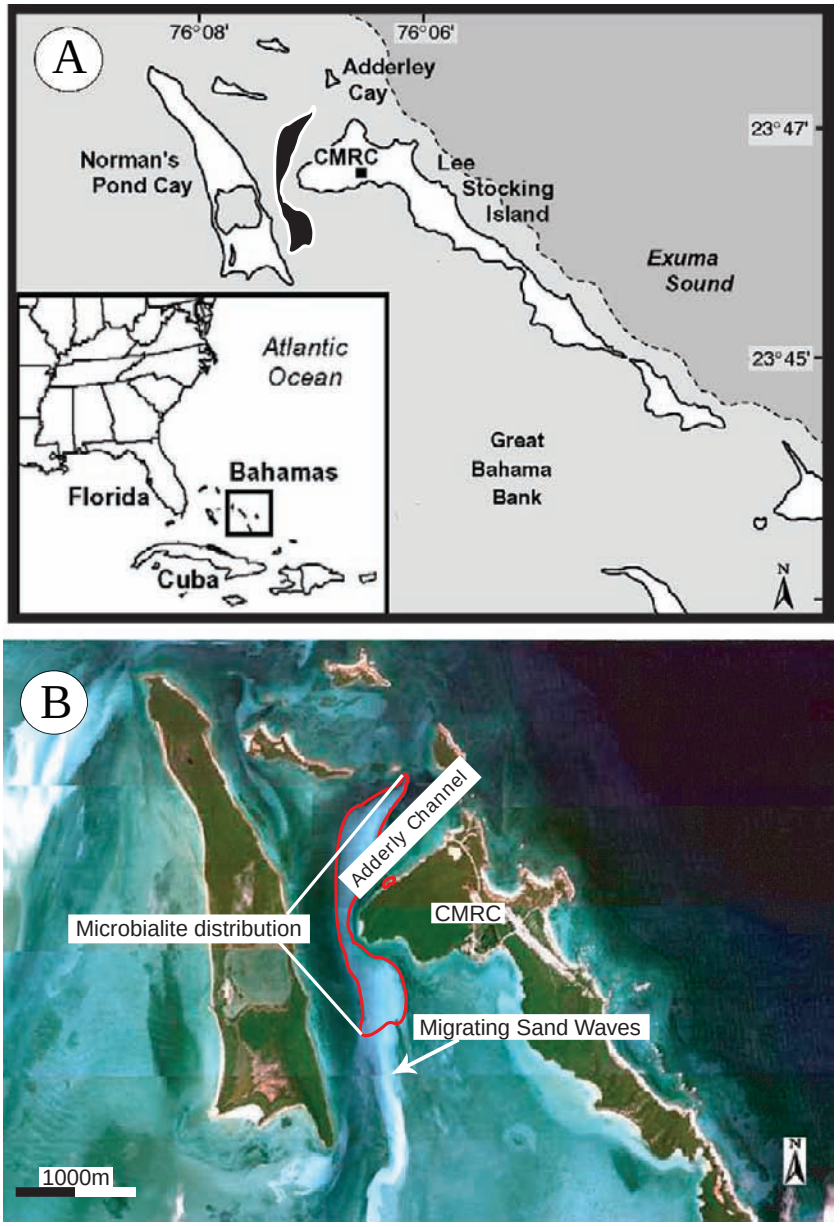

Fig. 5 (**A**) Detail of the depositional setting of Adderly Channel near Lee Stocking area, Exuma Islands. The blackened area outlines a sand bar in the Adderly tidal channel, the site of imaged and studied microbialites substrates. Modified from (Hu and Burdige 2007). (**B**) Aerial photograph of Adderly Channel showing the mid-channel sand bar and extent of microbialites. The sand bar varies from 5–7 m below sea level, and it is ornamented by sand waves up to ~2 m high oriented at high angles to the bar trend. The sand waves are moved by the twice-daily tidal currents and periodically cover and uncover the microbialites. CRMC is the Caribbean Marine Research Center

3 Types of Holocene Substrates

We found two main classes of substrates, those that are pre-existing rock surfaces, here termed (1) inherited, and those that are developed repeatedly by sedimentary processes, here termed (2) renewable substrates.

3.1 Inherited Substrates

There have been detailed descriptions of inherited substrates of Holocene stromatolites. From his extensive observations of the Adderly Channel stromatolites Dill [1991] concluded that the stromatolites grew on "... either rubble hard-ground or caliche-encrusted paleosol." The paleosol overlies Pleistocene coral heads whose partial dissolution is usually considered evidence of subaerial exposure. Shapiro and others described four short diamond cores of the substrate of an area of stromatolites near Iguana Key less than a few kilometers from Adderly Channel. The stromatolites developed either on Pleistocene eolianite with rhizomorphs or early Holocene coral skeletons. In addition to these known examples, our diamond coring in Adderly Channel in 2006 recovered well-cemented limestone with features characteristic of subaerial exposure of Pleistocene limestone (for example blackened surfaces and black pebbles (Pierson and Shinn 1983)) below four different areas of stromatolites.

3.2 Renewable Substrates

We found stromatolites growing on several previously undocumented types of substrates that can form syndepositional. These renewable substrates include submarine hardgrounds, large mollusk shells, conglomerates composed of intraclasts, and firmgrounds.

3.3 Submarine Hardgrounds

Submarine hardgrounds have been described from several areas on the Bahama Bank. For example, there are well-documented hardgrounds from Yellow Bank (Taft et al. 1968) and the northern margin of Tongue of the Ocean (Palmer 1979) We recently discovered hardgrounds across a wide area in the southwestern section of the ooid shoals around the Tongue of the Ocean (Fig. 6). These locally extensive hardgrounds are formed by penecontemporaneous deposition of fibrous aragonite between sand grains (Fig. 6C–F). This same type of cementation is present in intertidal beachrock (for example, Gischler and Lomando 1997). Most hardgrounds on the Bahama bank have undergone some degree of early diagenetic alteration, after which the fibrous cement morphology is not easily distinguishable (Fig. 6D). This early diagenetic process further stabilizes the sediment. The cementation is usually

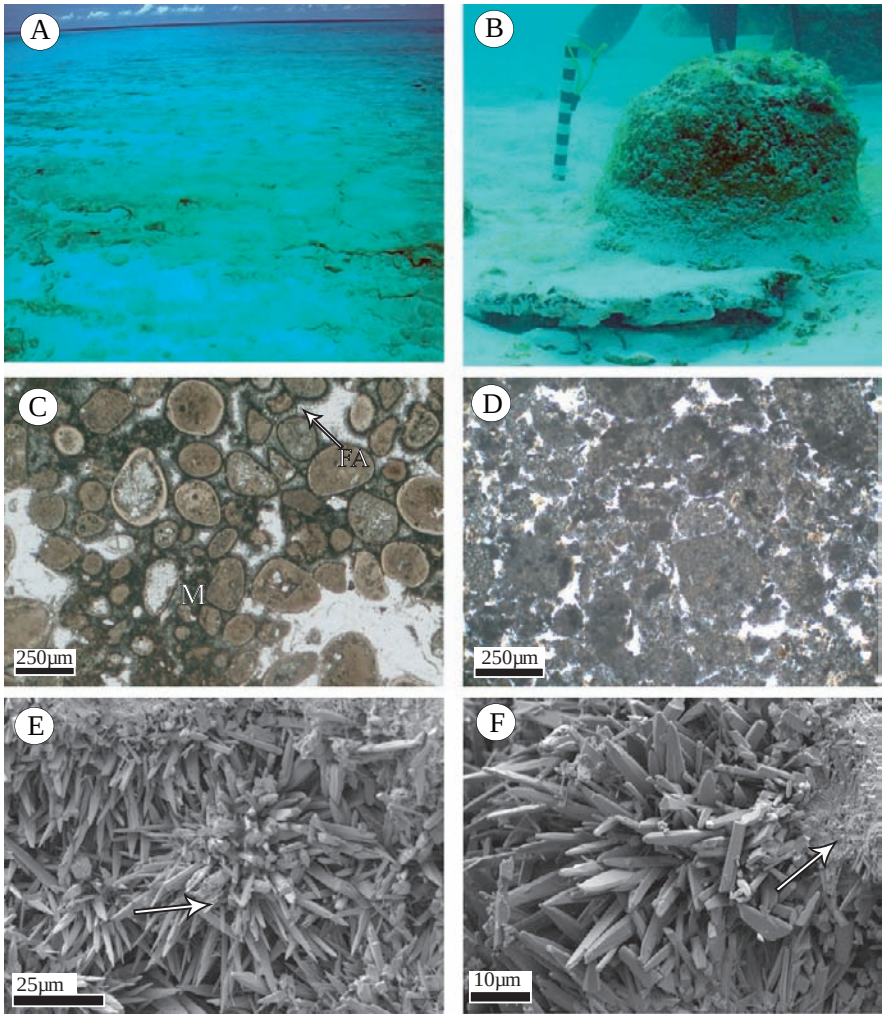

Fig. 6 Images of submarine hardgrounds, their microfabrics and microbialites. (**A**) View from the deck of our research vessel. R/V Tiburon three meters above the sea surface of a hardground pavement at ~2 m depth on an ooid sand shoal, Tongue of the Ocean (Fig. 4). The pavement extends for hundreds of meters, it cracks and breaks up to form intraclasts of varied sizes as seen in the foreground. (**B**). A small domal microbialite growing on a thin submarine hardground on an ooid sand shoal at a depth of ~2.5 m, Tongue of the Ocean (Fig. 4) Scale divisions 5 cm. (**C**) Examples of micritic (M) and fibrous aragonite (FA) as intergranular cements. Photomicrograph in plain polarized light. (**D**) Another fabric present in hardgrounds composed of peloids modified by early diagenetic recrystallization probably through a combination of local dissolution/reprecipitation and cyanobacterial boring. Grain boundaries are indistinct or jagged in the micritized areas. Photomicrograph in plain polarized light. (**E**) SEM image of spherulitic fibrous aragonite cement (arrow) that initiated from surrounding sand grains. (**F**) Higher magnification SEM image of fibrous aragonite cement growing on an initial micrite cement (arrow)

limited to layers of calcareous sand < 20 cm thick. These relatively thin layers of rock that are underlain by uncemented sand are mechanically unstable. They develop cracks, which in turn produce various sized interclasts (Fig. 6A). Multiple layers of hard-grounds are present in the Holocene sediments of eastern Great Bahama Bank (Palmer 1979). We have indicating that their formation is repeated. We have discovered several examples of stromatolites growing on submarine hardgrounds, including several stromatolites in the on shallow sand bars around the south end of the Tongue of the Ocean (Fig. 6B) and from the base of a giant stromatolite near Iguana Cay.

3.4 Interclasts and other Renewable Substrates

Shells of mollusks especially those of the large gastropod (*Strombus gigas*) litter many tidal channels and are large enough to provide stable substrate for small stromatolites (Fig. 7A). A shell that is the base of a small stromatolite (comparable to that of Fig. 7A) had a corrected ^{14}C age of 480±50 years (Dill et al. 1986). Clusters of cobble sized fragments of mollusks and corals intermixed with intraclasts, and locally enhanced by inter-particle cementation, can also provide stable substrates

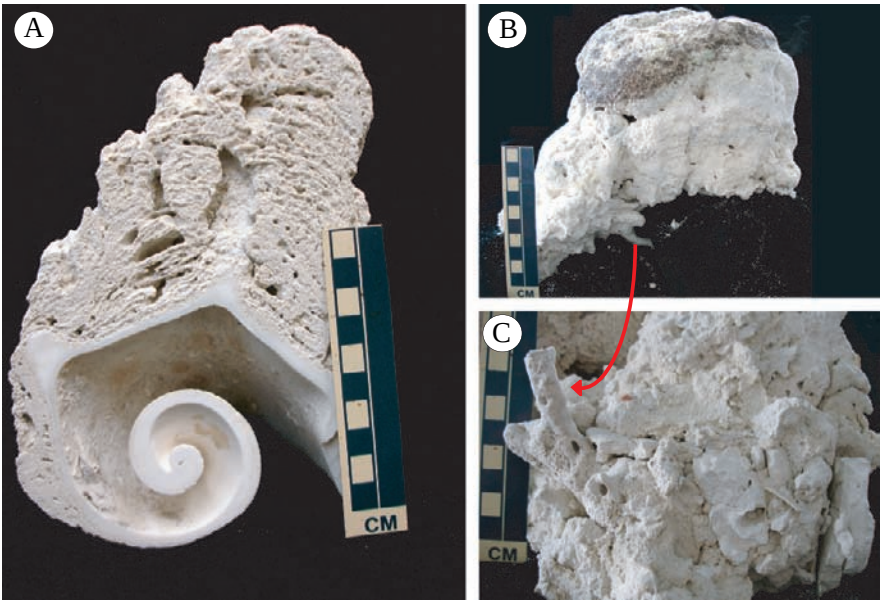

Fig. 7 Two examples of renewable substrates from Adderly Channel Depth range 5–7 m. (**A**) Cross section of a small stromatolite developed on a conch shell. (**B**) A small stromatolite on a conglomerate substrate. Scale divisions are 1 cm. (**C**) View of the underside of the specimen shown in B revealing that it is a composed of intraclasts of fine-grained sediment and metazoan debris

for microbialites (Fig. 7B and C). The variable degree of rounding of these clasts, their large grain sizes (> 5 cm), and their localized occurrence suggests they are storm deposits.

The substrates of intertidal occurrences of stromatolites appear to be quite different from the subtidal examples described above. On Stocking Island stromatolitic buildups of up to a meter thick grew on cemented branched coralline algae and vermetid gastropods that over lies Pleistocene limestone (Macintyre et al. 1996). The cements are magnesium-calcite and fibrous aragonite, indicating marine, rather than meteoric, deposition. At the Highborne Cay locality, the substrate of back reef stromatolites and "thrombolites" (Reid et al. 1999) consists of an unusual grain-free micrite composed largely of "filament moulds, 3–10 μm encased in spherulitic clusters of aragonite needles." (Reid et al. 1999). The substrates of both these two localities are products of penecontemporaneous cementation.

3.5 Firmgrounds

The firm-grounds that are renewable substrates for stromatolites in Adderly Channel are remarkable deposits (Fig. 8). Their occurrences and microstructure were thoroughly described and illustrated by Dill [1991], who termed them mud beds because of their softness and sticky feel. Dill [1991] and Shinn and co-authors (Shinn et al. 1993) reported that these laminated sediments are commonly about 10 cm thick and occur at depths of 4–8 m below sea level in the troughs between migrating sand waves (Fig. 8B) (Shinn et al. 1993). There they are underlain and overlain by ooid and/or peloid sand. These pure white sediments are soft but cohesive enough to break between the fingers with angular fractures. Intraclasts of the firmgrounds are abundant. Fragments of sea grass blades, wood, mangrove leaves, and palmetto fronds along with shells were commonly found within the laminations. The firmgrounds are composed of small argonite needles, which are often clumped together to form peloids around to 60 μm in diameter (Fig. 9B).

Dill [1991] proposed that these fine-grained laminated sediments containing terrestrially derived material were deposited during and following hurricanes when fine sediment suspended by storm waves settled from suspension. Confirmation of this interpretation came from a study of the deposits of Hurricane Andrew in 1992 (Shinn et al. 1993). This storm crossed the Joulters Cays, an area of ooid sands on northern Great Bahama Bank that has been studied extensively. There, soon after Hurricane Andrew, Shinn and co-authors (*ibid*) colleagues found firmgrounds and intraclasts of fine-grained sediment in tidal channels of ooid sands. The firmgrounds consisted of peloids 50–100 μm and some skeletal fragments sandwiched between uncemented ooid sand. These peloids, like those in Adderly Channel, consist of needle-shaped crystals of aragonite 1–3 μm (Fig. 9A). The use of mud in describing these sediments led to the interpretation that they accumulated by settling from suspension. The prevalence of laminated fine-sand

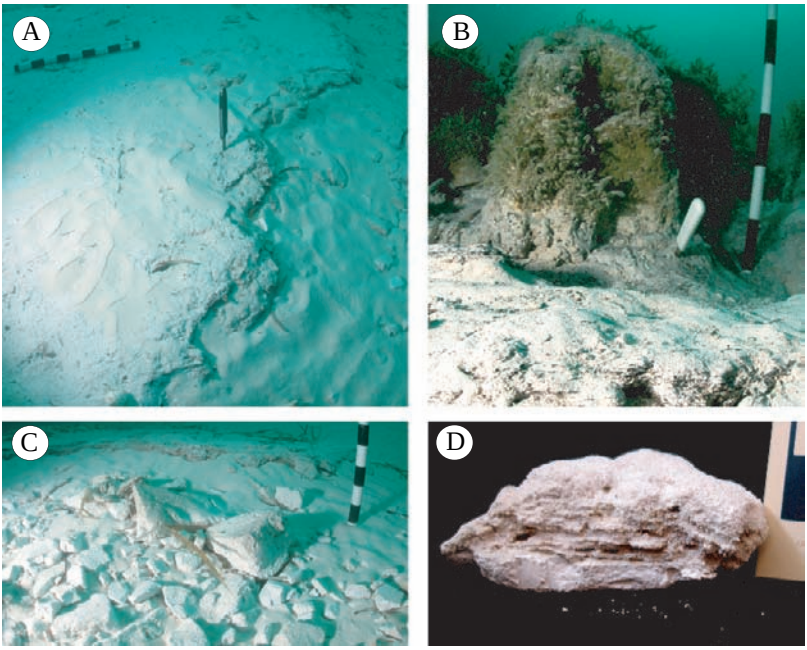

Fig. 8 Subtidal firm-ground substrates from Adderly Channel. (**A**) Example of an extensive layer of the firm-grounds, the "mud beds" of Dill [1991], from approximately six meters depth. Scale divisions 10 cm. Current erosion of the margin produces intraclasts as seen in **C**. (**B**) A small columnar stromatolite now covered with algae (*Batophora spp.*) that grew on a firmground like that in (a) exposed in the foreground. Scale division 10 cm, depth 7 m. (**C**) A local concentration of intraclasts produced by erosion shown in (**A**) depth 6 m. (**D**) A small stromatolite developed on a firmground like that in (Fig. 8A), depth 7 m; black scale bar 1 cm

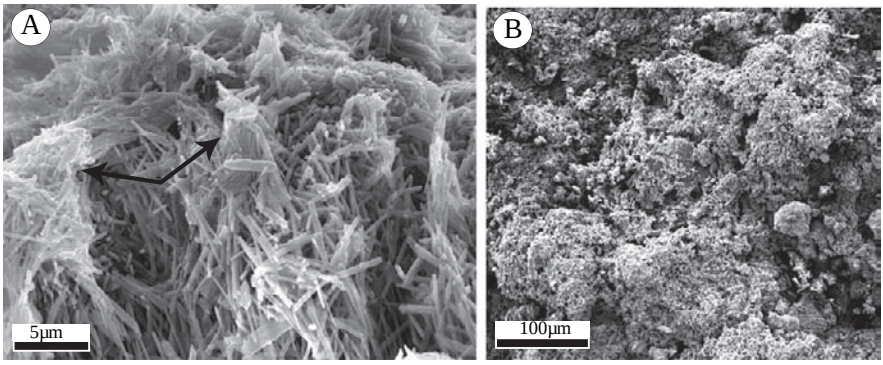

Fig. 9 Microstructure of the firmground substrate. (**A**) SEM image of fibrous aragonite from the firmground (Fig. 8A), (**B**) SEM image showing that the fibrous aragonite in Figure 8A occurs in semi-spherical clusters from 20 to 100 μm in diameter that are probably peloids

sized peloids, however, is more likely evidence that they are traction deposits in which soft but coherent peloids were sorted by bottom currents to produce the laminations.

Cementation and early diagenetic alteration of aragonite fibers increases the stability of the firmground sediment. When exposed to seawater the surfaces especially those of intraclasts "become encrusted with millimeter-thick, marine-carbonate cement"(Dill et al. 1986). We have found that this cement consists of intergrown aragonite fibers up to several microns long and 0.1 microns in diameter (Fig. 9A) oriented tangentially to the exposed surfaces. The aragonite fibers within the firmground are often fused together suggesting that penecontemporaneous recrystallization contributes to their coherence. Compaction dewatering may also have some affect on crystal morphology and packing. Together all these processes within the original firmground sediment lead to its coherence such that exposed surfaces are resistant to erosion, they can be the substrate for small columnar microbialites (Fig. 8B) and intraclasts can withstand movement by waves and currents (Fig. 8C).

3.6 Semi-Consolidated Mud Substrate

Two other types of renewable firm-ground substrates are noteworthy since they are likely common substrates for fossil microbialites. One occurs in submarine fine-grained sediments and develops automatically below the sediment-water interface. In most lime muds like those of Florida Bay and the Bahamas, the uppermost 15 cm grades from fluid mud to sediment with a yogurt like consistency to coherent sediment that although soft that fractures (Ginsburg and Lowenstam 1958). Strong wave action and significant bed load transport of shell fragments can scour the uppermost incoherent layer exposing the firm sediment as a potential substrate. The intraclasts of semi-coherent mud in Florida Bay and in northern Belize lagoons (RNG, personal observations) are evidence of this process.

3.7 Substrates in Peritidal Deposits

The contemporary peritidal deposits of Andros Island, which are intermittently exposed above sea level, contain both lithified substrates and firmgrounds (Figs. 10–11). Locally exposed sediments become cohesive through a combination of desiccation and microbial stabilization. One example of these peritidal firmgrounds forms on the natural levees of tidal channels (Fig. 10A and B (Hardie 1977). These levees receive fine-sand and silt sized peloids during flooding of spring tides or storms. In between these depositional events, the levees are exposed for 98 % of the year (Ginsburg et al. 1977) and develop desiccation cracks a few centimeters across and deep. At the same time cyanobacteria colonize the moist surfaces and develop a sediment-rich biofilm, coherent enough to be peeled away and to produce thin chip-like intraclasts (Fig. 10B) (Shinn et al. 1969).

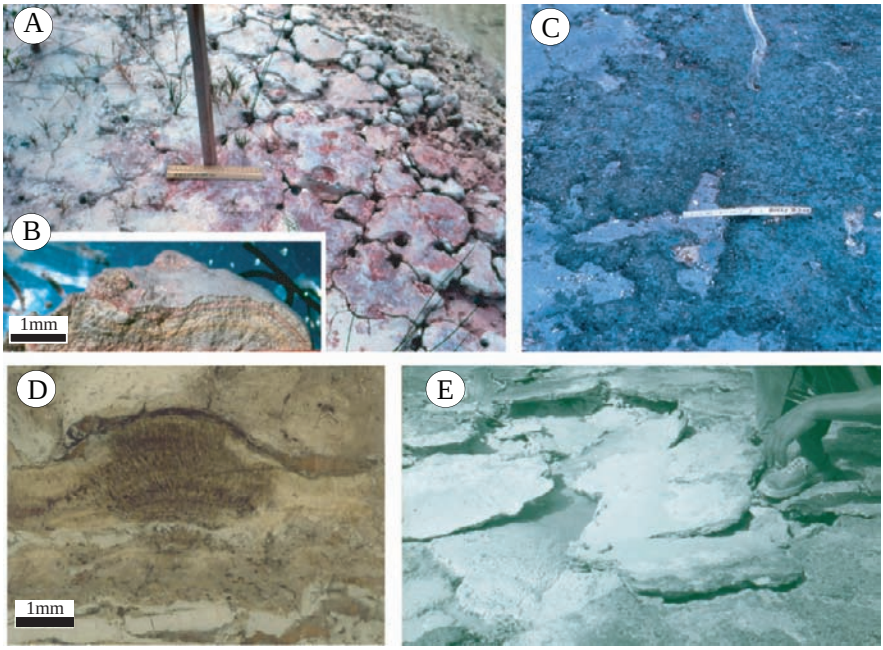

Fig. 10 Peritidal renewable substrates, northwest Andros Island, Bahamas. (**A**) View of the margin of a tidal channel showing firmgrounds of polygons produced by desiccation (See Hardie 1977). (**B**) Cross-section of a polygon in (**A**) showing the sediment-rich biofilm at the surface that contributes to the coherence of this fine-grained sediment. (**C**) A sediment rich microbial-mat with some cementation, likely induced by evaporation. These microbial mats are locally abundant on the surfaces of the Andros Island peritidal flats. (**D**) Stromatolitic structures on renewable peritidal crust from the fresh water marsh zone at Deep Creek. The light gray areas are formerly exposed and now cohesive surfaces. The darker gray and irregular areas consist of alternating laminations of the cyanobacteria *Scytonema spp.* and fine-grained carbonate sediment. Each of the radial filaments of *Scytonema* are coated by magnesium calcite (see Hardie 1977 for further details). (**E**) Large pieces of the well-cemented crust from one of several mostly exposed areas of the marine Three Creeks tidal flats of northwest Andros Island, Bahamas (described by Shinn et al., 1969 and Hardie 1977)

Thin well-cemented crusts develop on the surfaces of subaerially exposed sediments and are another lithified substrate on the peritidal deposits of Andros Island (Fig. 10E). There are similar crusts in the freshwater marshes of the Andros flats. These crusts are often covered by mushroom-like stromatolitic growths a few centimeters high that have radial and concentric internal structures composed largely of calcified filaments of the cyanobacteria *Sytonema* spp. (Fig. 10D). Each of the radial filaments of this alga are incased in carbonate Mg calcite (12–13 mol % Mg (Hardie 1977).

Intraclasts of the cemented crusts, especially those that occur as edgewise conglomerates (Fig. 11A) can also be substrates for stromatolites. The Upper Cambrian carbonates of Western Maryland are a well-documented example of stromatolites

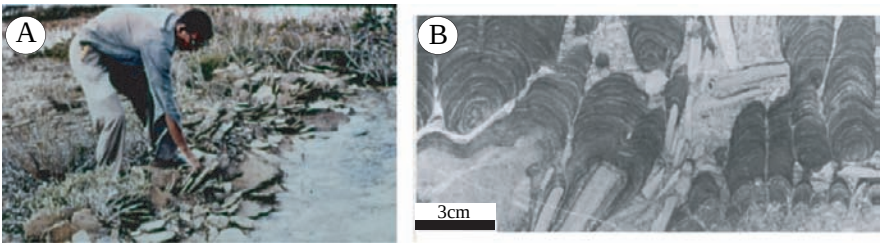

Fig. 11 (**A**) Edgewise conglomerate of platy intraclasts of the cemented crust. Breaking waves on a shoreline of Andros Island accumulated these book-like clusters. (**B**) Stromatolites growing on an edgewise conglomerate from peritdal sequences in Upper Cambrian of Maryland, offering an example of stroamtolite development upon substrates likely developed in a peritidal environment (photo Robert Demicco)

preferentially developing on clasts of cemented crusts (Demicco 1985). Due to the prevalence of firmgrounds and hardgrounds, when the surfaces of tidal flat deposits are flooded by a relative rise of sea level, there will be abundant substrates for a new generation of stromatolites.

4 Sediment Supply for Holocene Stromatolites

The prevalence of calcareous sands is a key element in the development of Holocene microbialites. The predominant grain types on Great Bahama Bank are peloids, well rounded ovoid or circular sand sized grains, and superficial ooids (Illing 1954), which are peloids thinly coated with concentric layers of aragonite in areas of persistent sand movement. The majority of peloids are likely fecal pellets of deposit-feeding invertebrate. Some peloids are also ooids, that have lost their concentric layering due to penecontemporaneous recrystallization or cyanobacteria microboring (Reid and MacIntyre 1998, 2000). The varying stages of this transformation can be observed in most thin sections of ooid sand.

The twice-daily tidal currents provide the peloid and ooid sand that is the building material for both the stromatolites and unlaminated microbiolites in Adderly Channel and elsewhere in the Exumas Island Chain. Ebb tidal currents, channeled by topography, transport peloids from the bankward side of Adderly Channel area to nourish the sand bar. In addition, some peloids are formed within the bar complex. Flood tidal currents produce bankward-migrating sand waves that deliver the sand to developing microbialites. The near continuous sand movement correlates with the formation of the oolitic coatings (Dill et al. 1986). It also limits colonization of microbialites by boring or encrusting metazoans and algae. A major decrease or cessation in the sediment flux results in the development of a algae-dominated benthic community (Dill et al. 1986). When stromatolites covered by an algal beard are sectioned they commonly reveal a horizon of bivalve and sponge borings along the margins (authors observations), suggesting that the eukaryotic community does not result in accretion. Only when there are regular high levels of sediment supply can uninterrupted growth of microbialites be maintained.

5 Discussion

5.1 Substrate Limitations

The consistent association of columnar Bahamian microbialites and with hard and firm surfaces in subtidal settings is convincing evidence that coherent substrates are necessary for the development of these microbial structures. At Adderly Channel, and in subtidal settings more generally, there may be substrate limitations due to high levels of bedload sediment and this sediment's frequent movement. Cyanobacteria readily colonize on most surfaces, including on uncemented sand and silt; however, the resulting stabilized surfaces do not appear to provide a suitable foundation for large columnar stromatolites. It is possible that such stabilized sediment surfaces could become submarine hardgrounds, but confirmation of this transformation will require much detailed sampling and high resolution dating.

Peritidal successions have more potential substrates than subtidal successions. However, colonization and accretion of sizeable stromatolites on those substrates requires a relative rise of sea level. The record of a transgression of peritidal deposits should show an upward progression from planar laminated substrates, to low relief arches succeeded by, distinct columnar stromatolites. A well-described fossil example of this succession is found in the cycles of stromatolites forming on peritidal laminates and conglomerates in the Proterozoic Atar Group in Mauritania (Bertrand Sarfati 1972)

In the Precambrian when there were no grazing or burrowing metazoans, benthic microbial communities would likely have been nearly ubiquitous on all surfaces. Even in the Cambrian, there is evidence for extensive benthic microbial mats (for example, Bailey et al. 2006). Given these circumstances, it is at first surprising that stromatolites in these strata often have a restricted distribution or are isolated to distinct horizons (for example, Bertrand Sarfati 1972; Demicco 1985). Although the anatomy of a carbonate platform is obviously complex and controlled by numerous factors, our examination of the Bahamian stromatolites prompts a simple explanation for the sporadic distribution of the stromatolites. In many platforms there is likely to be local substrate restriction in areas with a substantial mobile silt/sand sized detrital load, since our study of the Bahamian microbialites suggests that the formation of sizable stromatolites is dependent a firm foundation. Therefore, high amounts of detrital sediment may lead to a more heterogeneous distribution of bioherms and reefs. In areas where stromatolites are nearly ubiquitous—for example, the Paleoproterozoic Great Slave Lake carbonates (Hoffman 1974; Pope and Grotzinger 2003; Sami and James 1993) or Archean Steep Rock Group carbonates (Wilks and Nisbet 1985, 1988)—there is a small detrital load and abundant syndepositional cementation to provide widespread firm foundations.

5.2 Renewable Substrates and Stromatolite Initiation

The availability of renewable substrates allows for the repeated initiation of columnar stromatolites. In systems with low accommodation space (e.g. peritidal deposits)

all of the stromatolites will be isolated to distinct horizons because the accommodation space is almost instantaneously filled. In contrast, in subtidal settings, such as the Bahamian tidal channels, stromatolites can develop varying levels of synoptic relief. If continuously forming substrates are available, there is likely to be evidence for different ages of stromatolite initiation. This process is clearly visible in Addelry Channel in the Bahamas and in subtidal zone in the famous Western Australia Shark Bay modern stromatolite locality. In contrast, there is limited variation in synoptic relief in the peritidal and tidal stromatolites at Shark Bay (Fig. 2) or in the Bahamas. Variability in initiation patterns within a stromatolite horizon should be preserved in the rock record. Therefore, examination of the initiation patterns of ancient microbialites may offer a means to discern between subtidal and tidal/peritidal microbialite systems when diagnostic sedimentary features are lacking.

5.3 Early Diagenesis affects Later Growth

The Bahamian stromatolites fields are influenced by the interplay of diagenetic process and latter growth. The submarine hard-grounds and firm-grounds are extreme examples of how early diagenesis can transform unconsolidated sediment to hard and firm substrates. The early diagenetic recrystallization in the hard-grounds and in the surfaces of the firm-grounds appears to be largely driven by multiple stages of dissolution and reprecipitation, but cyanobacteria microboring is also undoubtedly also a contributor. Dissolution requires temporary undersaturation, which is related to the degradation of organics because Adderly Channel seawater is highly supersaturated with respect to calcite and aragonite. Analysis of sediment pore waters indicates there is widespread carbonate dissolution and reprecipitation on shelf sediments (Burdige and Hu 2005; Hu and Burdige 2007; Walter et al. 1993); this study and more extensive study of other localities (Macintyre et al. 2000; Reid et al. 1995; Reid et al. 1992; Reid et al. 2000) provides confirming petrographic evidence. Carbonate alteration in modern sediments has been linked with benthic sulfur cycling and aerobic respiration (Hu and Burdige 2007; Ku et al. 1999).

Uncertainty persists about the precise mechanism responsible for the widespread precipitation of carbonate as cement in the sediments of Great Bahama Bank. The relatively small amount of calcium carbonate that can be precipitated from a pore volume of seawater means that countless pore volumes are required to achieve significant cementation. The selective cementation around animal borings evidences the role of increased flow in cementation. The widespread occurrence of cements, ooids, lithification of fecal pellets (peloids) and possibly whitings, clouds of fine-grained carbonate sediment, testify to the pervasive non-skeletal precipitation. All of these processes are likely to some degree influenced by microbial processes. However, without detailed analyses of porewaters, and the isotope ratios of the cements it is difficult to gauge the degree to which microenvironments of carbonate precipitation were shifted from ambient seawater.

6 Conclusions

Even though cyanobacterial mats readily colonize almost any surface in the tidal channels, tidal bars, and shorelines of much of the Bahamas, stromatolite development appears to be contingent upon a stable substrate. Subtidal and peritidal environments on Great Bahama Bank provide a spectrum of these substrates for stromatolites that may be a guide for interpreting the origins of fossil substrates.

In shallow oceanic tidal channels to depths of at least 8 m of the Exuma Islands, large (up to 2 m tall) stromatolites develop preferentially on inherited and renewable substrates. The inherited substrates are well-cemented rock surfaces—Pleistocene limestone often veneered with paleosol or caliche-like crusts. The renewable substrates include submarine hardgrounds, firmgrounds, and conglomerates of skeletal debris and intraclasts. The firmgrounds and conglomerates, which are deposited during large storms, and are an example of rare events having a large effect on latter accretion.

The well-studied humid peritidal deposits of Andros Island offer examples of potential substrates. Hardgrounds a few cm thick develop on exposed surfaces. Coherence is caused by capillary evaporation aided cementation, stabilization from the microbial mats, and hardening through desiccation. The prevalence of firmgrounds and cemented crusts in peritidal environments makes them a likely foundation for development of stromatolites during a relative rise of sea level.

The penecontemporaneous cementation and early diagenetic recrystallization that produces submarine and subaerial hardgrounds and in places enhances the durability of firm grounds is a notable example of the feedback of early diagenesis on depositional processes.

Acknowledgments We are indebted to Eugene Shinn, Miriam Andres and Ian Macintyre for their penetrating and constructive reviews of the manuscript that much improved the final paper. We thank Mark Palmer and Henning Peters for assistance in the field work and for discussions that helped to develop interpretations. We appreciate Yildirim Dilek's encouragement and patience. Our successful field work was owing to the skill and diligence of Captain Tim Taylor and the crew of R/V Tiburon. We thank the Perry Marine Institute for use of their facilities and both the Ocean Research and Education Foundation and the Green Cay Foundation for funding. Permission to collect specimens came from the Fisheries Department, Government of the Bahamas.

References

Andres MS, Reid RP (2006) Growth morphologies of modem marine stromatolites: a case study from Highborne Cay, Bahamas. Sediment Geol 185:319–328

Andres MS, Sumner DY, Reid RP, Swart PK (2006) Isotopic fingerprints of microbial respiration in aragonite from Bahamian stromatolites. Geology 34:973–976

Arp G, Reimer A, Reitner J (1999) Calcification in cyanobacterial biofilms of alkaline salt lakes. Eur J Phycol 34:393–403

Arp G, Reimer A, Reitner J (2003) Microbialite formation in seawater of increased alkalinity, Satonda crater lake, Indonesia. J Sediment Res 73:105–127

Bailey JV, Corsetti FA, Bottjer DJ, Marenco KN (2006) Microbially-mediated environmental influences on metazoan colonization of matground ecosystems: evidence from the Lower Cambrian Harkless Formation. Palaios 21:215–226

Bertrand Sarfati J (1972) Paleoecologie de certains stromatolites en recifs des formations d precambrien superieur de groupe d' Atar (Mauritanie, Sahara occidental): creation d'especes nouvelles de ces recifs Palaeogeography, Palaeoclimatology, Palaeoecology 11:33–63

Black M (1933) The algal sediments of Andros Islands, Bahamas. R Soc Lond Philos Trans, B 222:165–192

Browne KM, Golubic S, Seong-Joo L (2000) Shallow marine microbial carbonate deposits, In: Riding R, Awramik SM (eds) Microbial sediments. Springer-Verlag Publishing, Berlin, pp 233–249

Burdige DJ, Hu XP (2005) Isotopic evidence for shallow-water carbonate dissolution and reprecipitation. Geochimica et Cosmochimica Acta 69:A130–A130

Demicco RV (1985) Platform and off-platform carbonates of the Upper Cambrian of western Maryland, USA. Sedimentology 32:1–22

Dill RF (1991) Subtidal Stromatolites, Ooids, and Crusted-Lime Muds at the Great Bahama Bank Margin. In: Osborne RH (ed) From Shoreline to Abyss, SEPM Special Publication: Tulsa, Society for Sedimentary Geology pp 147–171

Dill RF, Shinn EA, Jones AT, Kelly K, Steinen RP (1986) Giant Subtidal Stromatolites Forming in Normal Salinity Waters. Nature 324:55–58

Dravis JJ (1983) Hardened subtidal stromatolites, Bahamas. Science 219:385–386

Feldman M, McKenzie J (1998) Stromatolite-thrombolite associations in a modern environment, Lee Stocking Island, Bahamas. Palaios 13:201–212

Ginsburg RN, Hardie LA, Bricker OP, Garrett P, Wanless H (1977) Exposure index: a quantitative approach to defining position within the Tidal Zone. In: Hardie LA (ed) Sedimentation on the modern carbonate tidal flats of northwest Andros Island, bahamas, The John Hopkins University Press, Baltimore pp 7–12

Ginsburg RN, Lowenstam HA (1958) The Influence of Marine Bottom Communities on the Depositional Environment of Sediments. J Geol 66:310–318

Gischler E, Lomando AJ (1997) Holocene cemented beach deposits in Belize. Sediment Geol 110:277–297

Hardie LAE (1977) Sedimentation on the Modern Carbonate Tidal Flats of Northwest Andros Island, Bahamas. Studies in Geology 22, The John Hopkins University Press, Baltimore

Hoffman P (1974) Shallow and Deep-Water Stromatolites in Lower Proterozoic Platform-to-Basin Facies Change, Great-Slave-Lake, Canada. AAPG Bull 58:856–867

Hu XP, Burdige DJ (2007) Enriched stable carbon isotopes in the pore waters of carbonate sediments dominated by seagrasses: Evidence for coupled carbonate dissolution and reprecipitation. Geochimica et Cosmochimica Acta 71:129–144

Illing LV (1954) Bahamian Calcareous Sands. Am Assoc Pet Geol Bull 38:1–95

Ku TCW, Walter LM, Coleman ML, Blake RE, Martini AM (1999) Coupling between sulfur recycling and syndepositional carbonate dissolution: evidence from oxygen and sulfur isotope composition of pore water sulfate, South Florida Platform, USA. Geochimica et Cosmochimica Acta 63:2529–2546

Logan BW, (1961) Cryptozoon and Associate Stromatolites from the Recent, Shark Bay, Western-Australia: J Geol 69:517–529

Macintyre IG, Prufert-Bebout L, Reid RP (2000) The role of endolithic cyanobacteria in the formation of lithified laminae in Bahamian stromatolites. Sedimentology 47:915–921

Macintyre IG, Reid RP, Steneck RS (1996) Growth history of stromatolites in a Holocene fringing reef, Stocking Island, Bahamas. J Sediment Res 66:231–242

Monty CVL (1976) The Origin and Development of Cryptalgal Fabrics, In: Walter MR (ed) Stromatolites. Developments in Sedimentology Amsterdam Elsevier, pp 193–251

Palmer M (1979) Holocene Facies Geometry of the Leeward Bank Margin, Tongue of the Ocean, Bahamas, Unpublished Master's thesis, University of Miami, Miami pp 198

Papineau D, Walker JJ, Mojzsis SJ, Pace NR (2005) Composition and structure of microbial communities from stromatolites of Hamelin Pool in Shark Bay, Western Australia. Appl Environ Microbiol 71:4822–4832

Pierson BJ, Shinn EA (1983) Distribution and Preservation of Carbonate Cements in Pleistocene Limestones of Hogsty Reef Atoll, Southeast Bahamas. AAPG Bull 67:534–534

Playford PE, Cockbain AE (1976) Modern Algal Stromatolites at Hamelin Poor, a Hypersaline Barred Basin in Shark Bay, Western Australia, In: Walter MR (ed) Stromatolites: developments in sedimentology 20. Amsterdam, Elsevier, pp 389–413

Pope MC, Grotzinger JP (2003) Paleoproterozoic Stark Formation, Athapuscow Basin, Northwest Canada: Record of cratonic-scale salinity crisis. J Sediment Res 73:280–295

Reid RP, MacIntyre IG (1998) Carbonate recrystallization in shallow marine environments: a widespread diagenetic process forming micritized grains. J Sediment Res 68:928–946

Reid RP, MacIntyre IG (2000) Microboring versus recrystallization: further insight into the micritization process. J Sediment Res 70:24–28

Reid RP, Macintyre IG, Browne KM, Steneck RS, Miller T (1995) Modern Marine Stromatolites in the Exuma-Cays, Bahamas – Uncommonly Common. Facies 33:1–17

Reid RP, Macintyre IG, Post JE (1992) Micritized Skeletal Grains in Northern Belize Lagoon – a Major Source of Mg-Calcite Mud. J Sediment Petrol 62:145–156

Reid RP, Macintyre IG, Steneck RS (1999) A microbialite/algal ridge fringing reef complex, Highborne Cay, Bahamas. Atoll Res Bull 466:1–18

Reid RP, Visscher PT, Decho AW, Stolz JF, Bebout BM, Dupraz C, Macintyre IG, Paerl HW, Pinckney JL, Prufert-Bebout L, Steppe TF, DesMarais DJ (2000) The role of microbes in accretion, lamination, and early lithification of modern marine stromatolites. Nature 406:989–992

Sami TT, James NP (1993) Evolution of an Early Proterozoic Foreland Basin Carbonate Platform, Lower Pethei Group, Great Slave Lake, North-West Canada. Sedimentology 40:403–430

Semikhatov M, Gebelein MC, Cloud P Awramik S, Benmore W (1979) Stromatolite morphogenesis—progress and problems. Can J Earth Sci 19:922–1015

Shapiro RS, Aalto KR, Dill RF, Kenny R (1995) Stratigraphic Setting of a Subtidal Stromatolite Field, Iguana Cay, Exumas, Bahamas, In: Curran HA, White B (eds) Terrestrial and Shallow Marine Geology of the Bahamas and Bermuda, 300, Geological Society of America, Boulder pp 139–156

Shinn EA, Lloyd RM, Ginsburg RN (1969) Anatomy of a Modern Carbonate Tidal-flat, Andros Island, Bahamas. J Sediment Petrol 37:1202–1228

Shinn EA, Steinen RP, Dill RF, Major RP (1993) Lime-mud layers in high-energy tidal channels; a record of hurricane deposition. Geology 21:603–606

Taft WH, Arrington F, Haimovitz A, MacDonald M, Woolheater C (1968) Lithification of Modern Carbonate Sediments at Yellow Bank, Bahamas. Bull Mar Sci 18:762–828

Visscher PT, Reid RP, Bebout BM (2000) Microscale observations of sulfate reduction: correlation of microbial activity with lithified micritic laminae in modern marine stromatolites. Geology 28:919–922

Visscher PT, Reid RP, Bebout BM, Hoeft SE, Macintyre IG, Thompson JA (1998) Formation of lithified micritic laminae in modern marine stromatolites (Bahamas): the role of sulfur cycling. Am Mineral 83:1482–1493

Walter LM, Bischof SA, Patterson WP, Lyons TW (1993) Dissolution and Recrystallization in Modern Shelf Carbonates – Evidence from Pore-Water and Solid-Phase Chemistry. Philos Trans R Soc Lond A 344:27–36

Waterbury JB, Watson SW, Guillard RRL, Brand LE (1979) Widespread Occurrence of a Unicellular, Marine, Planktonic, Cyanobacterium. Nature 277:293–294

Wilks ME, Nisbet EG (1985) Archean Stromatolites from the Steep Rock Group, Northwestern Ontario, Canada. Can J Earth Sci 22:792–799

Wilks ME, Nisbet EG (1988) Stratigraphy of the Steep Rock Group, Northwest Ontario – a Major Archean Unconformity and Archean Stromatolites. Can J Earth Sci 25:370–391

Evaporite Microbial Films, Mats, Microbialites and Stromatolites

Robin L. Brigmon, Penny Morris and Garriet Smith

Abstract Evaporitic environments are found in a variety of depositional settings as early as the Archean. Depositional conditions, microbial communities and mineralogical compositions vary significantly as no two settings are identical. The common thread linking all of the settings is that evaporation exceeds precipitation, resulting in elevated concentrations of cations and anions that are higher than in oceanic systems. The Dead Sea and Storrs Lake are terrestrial examples of two diverse-modern evaporitic settings, as the former is below sea level and the latter is a coastal lake on an island in the Caribbean. Each system varies in water chemistry; the Dead Sea-dissolved ions originate from surface weathered materials, springs, and aquifers while the dissolved ion concentration in Storrs Lake is primarily derived from sea water. Consequently, some of the ions, e.g., Sr, Ba are found at significantly lower concentrations in Storrs Lake than in the Dead Sea. The origin of the dissolved ions are ultimately responsible for the pH of each system, the alkaline versus mildly the acidic. Each system exhibits unique biogeochemical properties as the extreme environments select certain microorganisms. Storrs Lake possesses significant biofilms and stromatolitic deposits; the alkalinity varies, depending on rainfall and storm, activity. The microbial community in Storrs Lake is much more diverse and active than those observed in the Dead Sea. The Dead Sea waters are mildly acidic, lack stromatolites, and possess a lower density of microbial populations. The general absence of microbial and biofilm fossilization is due to the depletion of HCO_3 and its slightly acidic pH.

1 Introduction

The existence of evaporitic environments can be inferred for as early as the Archean (Grozinger and Knoll 1999), but their depositional setting has varied over time. Some may have been lacustrine, or tidal flats or restricted marine, or possibly cave deposits, while others indicate playa settings (Buck 1980; Lowe 1983; Walter

R.L. Brigmon
Savannah River National Laboratory, Bldg. 999W Aiken, SC 29808, USA
e-mail: r03.brigmon@srnl.doe.gov

Y. Dilek et al. (eds.), *Links Between Geological Processes, Microbial Activities & Evolution of Life*, © All Rights Reserved 2008

1983; Olson 1984; Lindsay and Leven 1996; Muir 1987; Martini 1990; Pope and Grotzinger 2003). Each system is influenced by a different set of parameters and these differences can be reflected in the pH, ions in solution, organic and detrital sources.

Evaporitic environments, at least in geological terms, are transitional. However, sedimentary structures of organo-physico-chemical origin from these environments have been useful for historical classification (Eriksson et al. 2007). Changing climates can alter these environments and lead to their demise. For instance, the Dead Sea shoreline is dropping due to a variety of factors which are partly influenced by human activities (Yechieli et al. 1998). Storrs Lake, San Salvador Bahamas, could disappear if sea levels continue to rise due to global warming or potential nearby development and similar scenarios threaten the existence of other sites.

In this chapter we compare the microbiology and geochemistry of two diverse hypersaline systems, Storrs Lake in San Salvador, Bahamas, an island sea level lake and the Dead Sea, Israel, an inland evaporite basin. The objectives of this study are to (i) compare and contrast the fossilization of microbes and their organic products in environments that differ in salinity and substrate; (ii) use field methods combined with analytical techniques, electron microscopy (EM), and microbiological techniques for identification and characterization of microbial communities in environmental samples; (iii) discuss potential fossilization processes, identify probable microbial fossils, and the metallic ions association with fossilization; and (iv) document the role and importance of both biotic and abiotic processes for biofilm development in evaporite systems.

2 Background Information

2.1 Microbial Communities

Diverse microbial communities can develop within high salinity environments. The microbes are responsible for diverse biogeochemical and metabolic interactions that also alter any given environment (Krumbein et al. 2003). Temperature, community composition, and grazing by eukaryotes and water chemistry (particularly salinity) influence the rate of formation and lithification rates of these communities. Cyanobacteria are important in these saline environments due to their adaptation to desiccation and other stressors including ultraviolet light (UV) and nutrient limitations (Oren 1993).

These microbial communities, as determined by the substratum and environmental influences, can form simple structures that include the production of microbial films or biofilms, mats, microbialites, or complex stromatolites. A simple structure could be 1–5 μm in thickness and composed mostly of monoculture biofilms (Brigmon et al. 1995) or a stromatolite composed of a highly diverse, active microbial community (Farmer and Des Marais 1994). Although all of these structures

could be viewed as a continuum of size and complexity due to the interactions of microorganisms, environmental conditions, and organic products including extracellular polymers (ECPS) and inorganic substrates such as sand and dust (Fig. 1), certain characteristics define differences between the structural types. For example, biofilms are somewhat less complex and usually thinner, can form on living macrobiota and are more transient than other microbial consortial structures as those observed in cave vents (Brigmon et al. 1995). Abiotic processes including sediment deposition and physical/chemical precipitation can also be important in biofilm or mat formation (Fig. 1). These materials can serve as substrates for attachment, potential nutrient sources, as well as an ecological niche necessary for community development.

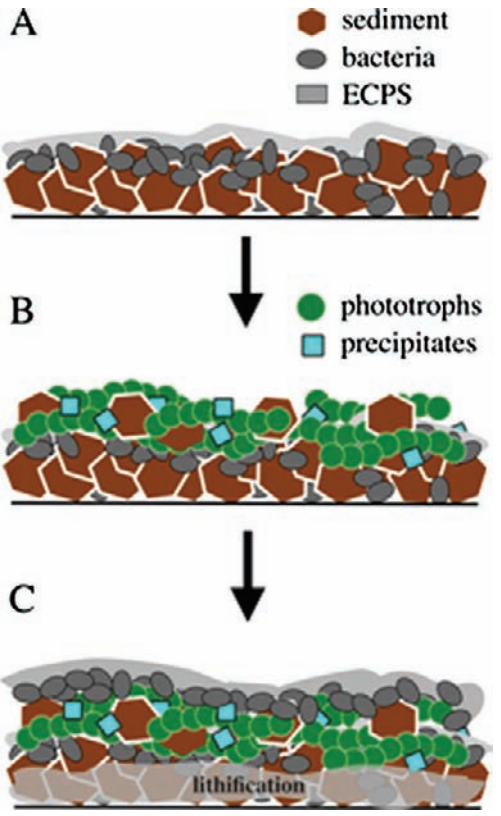

Fig. 1 A diagram illustrating the formation of biofilms because of the interactions of microorganisms, environmental conditions, and organic products, including extracellular polymers (ECPS) and inorganic substrates such as sand and dust. (**A**) Bacteria initially colonize the sediment or surface, and begin to produce ECPS. (**B**) Subsequent colonizers may include phototrophs including cyanobacteria near sunlight as well as mineral precipitates and other microorganisms. (**C**) Lithification occurs overtime through a combination of ECPS, microbial biofilm, and minerals interacting to create a hardened matrix

2.2 Biofilm

Biofilms exhibit a wide variation in complexity that is largely dependent on interactions among microorganisms, environmental conditions, and organic products including ECPS and inorganic substrates such as sand and dust (Fig. 1). Several classification systems have been developed to classify these unique microbial communities that result in structures (Eriksson et al. 2007). A formal system termed 'microbially induced sedimentary structures' (MISS) has been developed to classify the fossilization of biofilms (Noffke et al. 2001). For descriptive purposes, that variation can be categorized into three types, subaquatic, subaerial, and biodictyon (Krumbein et al. 2003).

Subaquatic biofilms are, as the name implies, biofilms constantly exposed to water. These aquatic biofilms, both marine and freshwater, demonstrate varying structural spatial and temporal heterogeneity. The marine microbial communities may form uniquely structured mucopolysaccharide layers in combination with other structures including corals for maintenance (Ritchie and Smith 2004). Marine biofilms can be highly diverse and may also contain Archaea (Wegley et al. 2002). Environmental changes such as tidal (marine) seasonal or episodic (storms) can drastically influence the biofilm structure, particularly when sedimentary deposition rates are altered. In carbonate rich water where sediment trapping, binding, and lithification occurs, these components are instrumental in forming stromatolites.

Subaerial biofilms are composed of 99% organic material with minimal amounts of water and can survive extreme environmental conditions such as evaporation or drought. The biofilms can cover rocks, minerals, sand, and other surfaces exposed to the atmosphere. Nutrient sources may include detritus, pollen, dust, animal (e.g. bird) waste, and runoff. Microorganisms in these films will often include phototrophic and nitrogen fixing species as well as chemoautotrophs. Subaerial biofilms can be observed in lichen communities, tidal mats, algal dominated systems, and covering rocks and other dry surfaces (Fig. 2). These biofilms are noted for their microbially produced melanins, cartenoids, mineral accumulation, metal precipitation, chlorophyll, and other metabolic byproducts that give them distinct pigmentation. Microbial activity in both sub-aquatic and sub-aerial biofilms can significantly increase the breakdown of silica in the amorphous, sub-crystalline, crystalline and granular forms of quartz (Brehm et al. 2005). This work by Brehm et al. (2005) emphasized weathering-enhancing processes that included effects of microorganisms and biofilms.

The term biodictyon comes from the Greek "bios" meaning "life" and "dictyon", meaning "net". These biofilms are characterized by living networks of mostly filamentous organisms imbedded in soil, sediment, or rock, which form mats. The networks create an ecological niche for trapping other microorganisms, minerals, sediments, water and nutrients as they percolate through the matrix. In certain conditions, including intertidal and mineral springs, the networks can generate ooids or calcispheres. The precipitation of ooids and calcispheres contribute to mat lithification (Dupraz and Visscher 2005). Higher organisms including bryozoans may

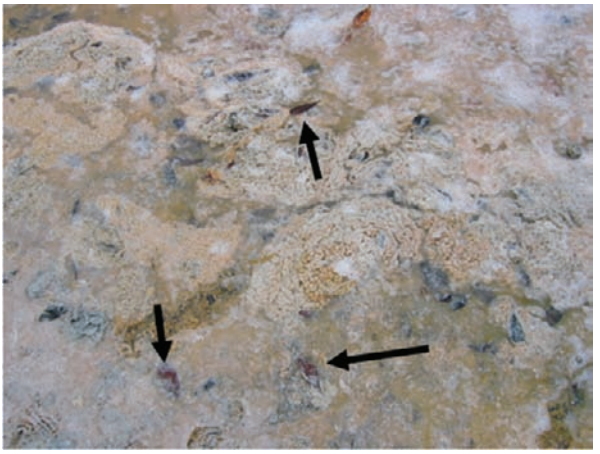

Fig. 2 *Rhizophora mangle* leaves being incorporated into biomats on the north end of Storrs Lake, Bahamas. Arrows pointing to leaves

depend on microorganisms in mats for mutual benefit as in hydrothermal systems (Morris et al. 2002). This interaction may include structural development in the bryozoans (Morris and Soule 2005).

2.3 Mats

Mats are multilayered, multidimensional matrixed microbial communities that incorporate detritus, minerals and associated geochemical materials including crystals (Krumbein et al. 2003). The interwoven patterns can form laminated or concentric structures. The pigments chlorophyll, phycocyanin and phycoerythrin are frequently detected by chromatographic and spectroscopic techniques. They can produce new minerals and in evaporite environments can influence the chemistry and associated microbial ecology (Gerdes et al. 1987; Noffke et al. 2001).

2.4 Microbialite

Microbialites are benthic microbial carbonate deposits that can vary in shape (e.g., columnar, sheet-like, branched, head shaped) depending on the microbial population, environment and the degree of lamination (Reid et al. 2003; Dupraz and Visscher 2005). Microbialite formation results from geochemical interactions combined with exopolymer-mediated calcification of cyanobacteria-dominated microbial mats. The stepwise biogeochemical interactions for microbialite formation occurring in a hypersaline lake (Eleuthera, Bahamas) has been described by Dupraz et al. (2004). Partial degradation of microbial produced ECPS by aerobic heterotrophs or UV fuels sulfate-reducing activity and increases alkalinity in mats, inducing $CaCO_3$

precipitation. As a result, the ECPS biofilm is calcified and serves as a substrate for physico-chemical precipitation of additional minerals from the alkaline lake water allowing build up of the microbialites.

2.5 Lithificatio

Lithfication is a microbialite characteristic and can vary from small scale nodules (mm) to larger structures including stromatolites (Krumbein et al. 2003). Microbialites are organosedimentary deposits that have accreted into structures as a result of benthic (prokaryotic and/or eukaryotic) communities or biofilms, trapping and binding detrital sediment in a polysaccharide matrix and/or becoming a niche for mineral precipitation (Burne and Moore 1987). The interaction of cyanobacteria with other bacteria has been shown to be critical in lithification. Experimental data have demonstrated that calcium carbonate precipitation only occurs on cyanobacterial filaments in the presence of active bacteria under specific geochemical conditions (Chafetz and Buczynski 1992). It was also found that dead cyanobacteria were coated with calcium carbonate by bacterial precipitation much more rapidly than live cyanobacteria.

2.6 Stromatolites

Stromatolites are produced by a combination of the accreted products from the dynamic interaction of microorganisms, microbial products including ECPS, and sediment (Decho 2000). Stromatolites have been defined as organosedimentary structures produced by sediment trapping, binding, and/or precipitation activity of microorganisms, primarily cyanobacteria (Awramik 1984). Certain cyanobacteria are known to precipitate, trap, and bind particles of calcium carbonate to form structures and to induce lithification (Chafetz and Buczynski 1992).

2.7 Storrs Lake Microbial Depositional Structures

Cyanobacteria have evolved different multiple strategies to adapt to environmental stresses including drying, high salinity, low nutrients, and UV light (Castenholz and Garcia-Pichel 2000). The adaptations include pigment production that protects cells from the deleterious effects of UV, desiccation and subsequent cell wall damage. Pigment production is particularly important in transient evaporite crust environments with wet and dry cycles. The cyanobacteria can dominate in hypersaline aquatic systems with limestone surfaces where they can be endolithic utilizing calcium carbonate that can lead to a permanent increase in travertine in stromatolites (Pentecost and Whitton 2000).

Cyanobacteria may also be the principal nitrogen fixers in a given ecosystem. Recent studies have demonstrated that epilithic cyanobacteria in Holocene beach

rock (Heron Island, Great Barrier Reef, Australia) are the main nitrogen fixers (Díez et al. 2007). These cyanobacteria have adapted to a wide range of environments, and their key metabolic activities including structure and function in similar hypersaline lakes is of great value to the maintenance of microbial-based ecosystems (Dupraz et al. 2004).

The diverse cyanobacteria is the major biofilm producer. The cyanobacteria community is composed predominantly of *Phormidium* as well as *Oscillatoria*, *Lyngbya* and *Spirulina* (Brigmon et al. 2006). The Storrs Lake cyanobacteria have been observed to be different from those examined at other San Salvador salinity sites as they have a higher proportion of phycobillin pigments (Brigmon et al. 2006). Below the photic zone Storrs Lake evaporite mats, the cyanobacteria are dead and are often fossilized, but the non-photosynthetic bacteria are dominant and demonstrate high metabolic activity (Brigmon et al. 2006).

The purple sulfur bacteria *Chromatium* spp. is dominant in the Storrs Lake reddish-pigmented layer biofilms commonly found on both the shoreline evaporite crusts and stromatolites. Sulfate reducing bacteria (SRBs) including *Desulfovibrio sp.* and the sulfur oxidizing bacteria, *Thiothrix* spp., are components of the stromatolite biofilms (Brigmon et al. 2006). SRBs function in the deeper or oxygen-limited layers of the biofilm where lithification may be occurring, whereas the sulfur oxidizers thrive at the oxygen interface near the water surface and obtaining energy from the hydrogen sulfide generated from the deeper anaerobic portions of the biomats (Brigmon et al. 1995).

2.8 Geology

2.8.1 Storrs Lake, San Salvador Island, Bahamas (Fig. 3)

The hypersaline Storrs Lake is located on the eastern side of San Salvador Island. It is 2.0 meters in depth, about 7.3 km long and 1.3 km to 50 m wide, with well developed stromatolites located a few hundred yards from the sea. The lake contains islands which support a diversity of plants including mangroves and sedges (*Carex*). Water is supplied from conduits within the bedrock, which includes the fossil reef, and from seepage through Holocene sand, allowing limited exchange with the ocean (Davis and Johnson 1990). Additional water sources are rainfall and tropical storms that carry ocean water shore and deposit it in Storrs and other San Salvador Island coastal lakes. The island, sediment deposition, and its ecosystem are influenced by hurricanes (Yannarell et al. 2007). Fluctuations in Storrs Lake water chemistry have been observed to vary in a 20 cm range (Zabielski and Neumann 1990). The water salinities vary from $70\,g\,L^{-1}$ to $100\,g\,L^{-1}$ and the pH varies between 8 and 9, depending on rainfall and storm activity.

Few plants or animals have been observed in or out of the lake along the littoral zone other than the microbial mats, associated stromatolites, microbialites, except the mangrove *Rhizophora* sp. and some sedge (*Carex*) that rim the lake. Microbial mats bordering the lake vary in size and thickness depending on weather conditions. These mats contain *Rhizophora* leaves which are assimilated into the mats (Fig. 2).

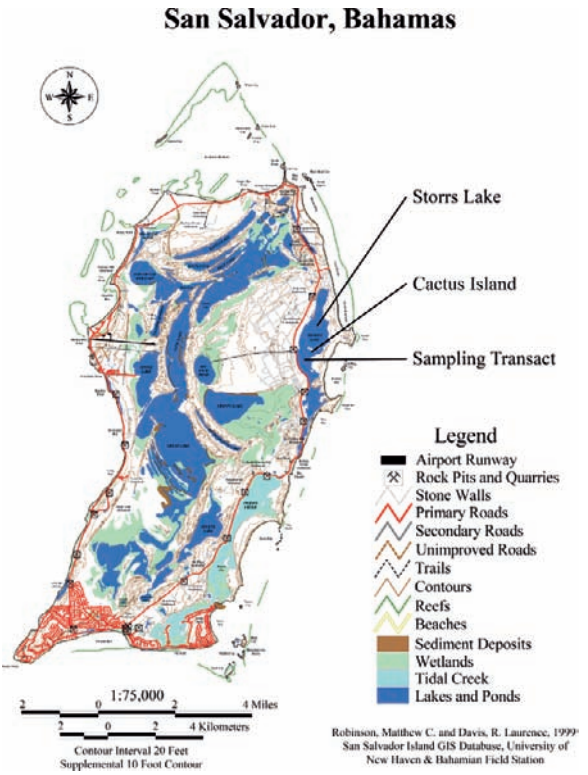

Fig. 3 Storrs Lake (Inset) is on the east side of San Salvador, Bahamas. The sampling transect is shown between the west side of Storrs Lake and Cactus Island

Organisms living in the water column include cyanobacteria, bacteria, diatoms, ostracods, and infrequent gastropods. Most likely halophilic Archaea species could be found in hypersaline Storrs Lake but were not measured here. The current chemical and detrital sedimentary deposits within the lake are usually less than one meter thick and are composed of finely laminated organic-rich carbonate mud and evaporite similar to Salt Pond that is adjacent to Storrs Lake (Yannarell et al. 2007). The nitrogen-fixing microbial community in Salt Pond has been shown to change spatially with seasonal salinity variations (Yannarell et al. 2006). The mineralogy of these sediments includes argonite, gypsum, and algal derived high-magnesium calcite in the form of clay-sized and sand-sized particles as well as a variety of stromatolitic structures (Zabielski and Neumann 1990).

During the Pleistocene, large portions of the island were covered by carbonate reefs at levels that were above today's sea levels (Teeter 1995). According to Teeter, the lakes are floored by Pleistocene carbonate bedrock covered by approximately 2 meters of unconsolidated Holocene sediments. Storrs Lake has been directly connected with the ocean, and the paleosalinity history has been reconstructed from MgO content of ostracod carapaces (Teeter 1995). The geology of

San Salvador includes three major rock types: eolanites, beachrock, and reefrock (Davis and Johnson 1990). The eolanites are most evident in carbonate dune ridges and are found throughout the island including the subsurface. The beachrock consists mostly of cemented shell fragments and ooliths and can be seen covering other rocks on the beaches. Reefrock is made up of fossilized reefs, including various corals, sponges, and cyanobacteria. The reported fossil reefs are found near the current island shoreline, including Storrs Lake. Stromatolites in Storrs Lake have been estimated to range in age of 2310 ± 70 yrs., growing at the rate of 16 cm/1000 years (Elliott 1994). Storrs Lake is probably as old as, if not older than the earliest dated modern stromatolites. Surveys of the various San Salvador lakes have demonstrated the existence of a diverse water chemistry, with some having salinities up to $300\,g\,L^{-1}$ (Teeter 1995).

2.8.2 Dead Sea Israel (Fig. 4)

The Dead Sea, a nonmarine evaporite basin, 400 m below sea level with an average pH of 6.3, and salinity of $229.9\,g\,L^{-1}$, is located on the northern branch of the African-Levant Rift Systems (Fig. 4). The rift system, according to one model, was formed by a series of strike slip faults, initially forming approximately 2 million years ago (Csato et al. 1997). Over geologic time the rift was occupied by a series of lakes; their existence was controlled by both tectonic activity and climate. Today the remaining lakes are the Sea of Galilee (Lake Kinneret) and the Dead Sea. The precursor of the Dead Sea was another hypersaline body of water, Lake Lisan (Yechieli et al. 1998). The Dead Sea receives its waters from the Jordan River system, runoff from wadis (the Arabic term for seasonal streams) during the winter months, limited rainwater, and from surrounding aquifers both subterraneous and through springs (Ehrlich and Zapkin 1985; Yechieli et al. 1996; Friedman 1998). The detrital and dissolved mineral materials deposited in the Dead Sea are from windblown materials and rock products ranging in age from Triassic to Quaternary and include gypsum, alkali basalt, chert, conglomerate, sandstone, limestone, clay, sand, sandstone, mudstone, marl, chalk, and dolostone (Sneh et al. 1998). Input from a variety of aquatic systems as well as weathering of these rock materials have contributed to the overall composition of in the Dead Sea.

During the 20th century the water level dropped and in 1979, after 300 years, the meromictic stratification with an anoxic water mass below 40 m was altered (Herut et al. 1997). Today, the Dead Sea experiences mostly annual stratification or a holometric regime (Lensky et al. 2005; Gavrieli et al. 2006). The drop in water, at least in part, is a result of increased fresh water diversion along the Jordan River system. Fresh water diversion may not entirely account for the drop in water level, as the balances of evaporation rate and subsurface water flow are not well understood (Lensky et al. 2005). Due to the drop in surface levels, the Dead Sea was separated into a northern and a southern basin in the 1960's (Steinhorn 1997). The northern basin is $\sim$324 m deep while the southern basin is shallower, with a maximum depth of 8 meters (Nissenbaum 1975; Steinhorn 1997). The southern basin is divided into evaporation pans for salt and potash production (Anati 1997; Hall 1997; Steinhorn

Fig. 4 Dead Sea, Israel. The arrows and numbers indicate the north and south basin sampling sites

1997). The residual end brines are depleted in potassium, sodium and are enriched in magnesium and chloride; these brines are subsequently pumped back into the Dead Sea. The effects are increased halite precipitation and salinity (Garvrieli 1997). The Dead Sea is expected to reach equilibrium but not to dry up, as the unique brine that would be left (Mg, Na, Ca, and Cl) and the low surface area to volume ratio would reduce the evaporation rate (Yechieli et al. 1998).

3 Methods and Materials

The collecting and processing methods described below for this project follow procedures that have been described by a number of authors (D'Amelio et al. 1989; Thomas-Keprta et al. 1998; Morris et al. 2003; Fratesi et al. 2004; Brigmon et al. 2006).

3.1 Storrs Lake

Stromatolites, biofilms, and water samples were collected from Storrs Lake, from the west shore of the lake to the east side of Cactus Island (Fig. 3). The coordinates and description of the sampling sites are listed in Table 1. The stromatolites, at all sampling points, had a cauliflower-type appearance, and varied in diameter from 10 cm-1.5 m. The microbial mats covering the stromatolites in the water column were 0.5 m thick in some places. Samples were collected with either 15 or 50 ml sterile polycarbonate tube (Fisher Scientific Fairlawn, NJ). Stromatolites were sampled by using the 50 cc sterile tubes to core a 2–3 cm long and 2 cm wide segment from the stromatolites at Sites 1, 2, and 7. The carbonate material was soft and easily obtained. Samples of microbial mats were obtained with either the 15 or 50 ml tubes. Some biofilms were sampled by scraping the edge of the tube on the film to limit perturbation of the stromatolites and liquid samples were collected by sterile 3 ml syringe. Select samples were kept on ice and returned to the US within 48 hours for microbial analysis. Samples for microscopy and total microbial densities were fixed in the field with ten percent formalin (Fisher Scientific, Fairlawn,

Table 1 Site descriptions from Storrs Lake, San Salvador Island

Site	Coordinates	Description
1	N 24.0549 W 74.45348	Storrs Lake western shore
2	N 24.0590 W 74.45247	20 m from shore
3	N 24.05901 W 74.45211	Past stromatolite mantle
4	N 24.05811 W 74.45132	Beginning of stromatolitic ridge between Cactus Island and shore
5	N 24.5893 W 74.4506	Middle of stromatolitic ridge
6	N 24.05957 W 74.45019	10 m from Cactus Island
7	N 24.06025 W 74.44879	Shore of Cactus Island
8	N 24.06038 W 74.44738	Western shore of Cactus Island
9	N 24.05973 W 74.44651	Northern shore of Cactus Island
10	N 24.06018 W 74.44373	Eastern shore (ocean side) of Cactus Island
11	N 24.05943 W 74.44016	Southern shore of Cactus Island
12	N 24.05973 W 74.44783	20 m from Eastern shore of Cactus Island (ocean side)

NJ). Temperature was measured in the field with a thermometer, dissolved oxygen concentration, nitrate, nitrite, and hydrogen sulfides were determined with field test kits (Chemetrics, Calverton, VA). Salinity was measured with a refractometer and pH with a battery-powered test meter (Fisher Scientific). A geochemical water survey of a 1000 m transect through Storrs Lake was conducted from the western shore to the eastern point of Cactus Island in July, 2001. Nitrate, nitrite, dissolved oxygen, temperature, pH, and salinity measurements were taken at 12 sampling sites with location coordinates determined by GPS (Garmin Model GPS 76). The high salinity of the water required dilution with deionized water to be examined with a refractometer. Measurements were taken with water samples obtained from a depth of 0.25 m. Storrs Lake had a maximum depth, 2.0 m during this sampling event.

Three water samples were collected and brought back from Sites 3 (water column) and 5 (stromatolite ridge) on ice for laboratory analysis by ion chromatography (IC). Chloride, sodium, lithium, manganese, calcium, nitrite, nitrate, phosphate, and sulfate concentrations from Storrs Lake were measured with a Dionex DX500 ion chromatograph equipped with a conductivity detector, and a 250-mm Dionex IonPac AS14 Analytical column (4-mm ID, 16-μm bead; Dionex Corp., Sunnyvale, CA), operated at ambient temperatures. A 3.5 mM sodium carbonate/1 mM sodium bicarbonate buffer solution was used as the eluent (1.2 mL/min) for the IC. Water samples were diluted 100X in deionized water, vortexed for 1 minute, then centrifuged for 5 min at 2500 rpm to prepare for the IC.

Total microbial population densities in the stromatolite samples obtained from Cores at Sites 1, 2, and 7 were determined by the Acridine Orange Direct Count (AODC) technique (Brigmon and De Ridder 1998). Discrete samples were collected aseptically from formalin fixed stromatolite cores, mixed with filter sterilized FA Buffer by Difco Inc. (Detroit, MI), and vortexed for 4 min. The resulting dilutions were filtered through Nucleopore, polycarbonate 0.2 μm membranes, and all microorganisms (prokaryotes, cyanobacteria, Archaea, fungi) were counted using epifluorescent microscopy (Axioskop, Carl Zeiss Inc., Thornwood, NY). Dry weights were determined, and microbial density results were reported in cells/gram dry weight (GDW).

Aerobic heterotrophic plate counts provide an estimate of the total number of viable aerobic and facultative bacteria in the stromatolites. Plates were prepared with fresh field samples at the Bahamas Field Station Laboratory to determine colony forming units (CFUs). Briefly, fresh 5 gm aliquots of stromatolites from Storrs Lake were weighed, ground, and aseptically mixed with 45 mL 0.2 μm filter–sterilized sea water, vortexed for 4 min, and plated on non-selective media glycerol artificial seawater agar (GASW) within hours after collection (Smith and Hayasaka 1982). Five dilutions were made in sterile seawater to determine microbial densities. Each dilution was plated in triplicate and the cultures were incubated at 37° C and CFUs determined after 7 days on a Leica Quebec Darkfield Colony Counter. Dry weights were determined on the stromatolite material tested; density determinations are reported in CFU/GDW.

Table 2 Summary data of Dead Sea (Israel) water and substrate survey. The Ein Gedi site is located in the northern basin and the other sites are in the southern basin

Site	Name	Coordinates	Water temp.	Description sediment sample	Depth of collection	Water sample*
1	Ein Gedi	31°27′09″N 35°23′57″E	31° C	sand, evaporites, primarily halite	.61 m	yes
2	Ein Boqeq (by Gardens Hotel)	31°11′48″N 35°21′45″E	32° C	sand mixed with silt	.61 m	yes
3	Ein Boqeq, 183 m. north of site 2		33° C	gravel mixed with sand, silt	.61 m	yes
4	Ein Boqeq, 805 m. north of site 2		30° C	silt	.13 m	yes
5	Hamme Zohar	31°10′12″N 35°22′02E	33.5° C	gravel and sand	.61 m	yes
6	Mt Sedom	31°05′23″N 35°23′35E		sand, silt with halite	surface sample	no
7	Mt Sedom	31°03′50″N 35°23′43″E		sand, silt with halite	surface sample	no

*all water collected approximately .1524 m below the surface.

3.2 Dead Sea

The samples were collected from seven sites on the western shoreline which included one site at Ein Gedi, three at Ein Boqeq, one at Hamme Zohar, and two at Mt. Sedom. Site coordinates, collected sedimentary materials, water temperature and collecting depths are listed in Table 2. The coordinates were determined with GPS (Magellan Model 2500T). Sterile 50 ml tubes (Fisher Scientific, Fairlawn, NJ) with screw caps were used to collect the materials and water samples. With the exception of the Ein Gedi halite, all samples were immediately preserved in five percent formalin (Fisher Scientific, Fairlawn, NJ). Halite samples were dissolved to the following: Halite dissolves in farmalin and, in order to preserve the relationship of the microbes to their substrates, were kept in sterile plastic bags without preservation. Water samples were collected at each collecting site and analyzed later for salinity, pH and chemical composition. Chemical analysis was done by S. Grasby, Canadian Geological Survey. Carlton C. Allen, NASA Johnson Space Center used a Scintag X-ray powder diffractometer (XRD) for mineral identification.

3.3 Electron Microscopy Analysis of Storrs Lake and the Dead Sea Samples

All preserved samples were initially analyzed with a Philips XL30 environmental electron microscope (ESEM) and were subsequently critically point dried, platinum coated for 15s and analyzed with a JEOL 6340F field emission scanning

electron microscope (FE-SEM) equipped with a light element electron dispersive X-ray spectrometry system (EDS). Carbonate and evaporite materials are subject to charging by the FE-SEM electron beam and can either destroy or alter thin biofilms and other organic features. The problem can be ameliorated by reducing the kV and adjusting the working distance. The kV for this study, depending on the materials, was varied from 3 kV to 10 kV with working distances varying from 4–6mm.

4 Results

4.1 Storrs Lake

4.1.1 Microbial Analysis

Storrs Lake microbialites are represented by biotically-formed stromatolites, microscopically observed as crystals, mineralized filaments, diatom tests, and other microorganisms. Stromatolites are most evident in the shallower areas of Storrs Lake but in this study were observed across the sampling transect. Samples for electron microscopy were taken from the stromatolite ridge described in Table 1.

Filaments: Mineralized filaments were composed of cyanobacteria and were common in the stromatolite biofilm samples. The forms include both continuous and segmented filaments (Figs. 5, 6, 7, and 8). In Figs. 5, 6, and 7, the fossilized cyanobacteria filaments with precipitated calcium carbonate are evident in the stromatolite samples. The fossilized filaments were observed to range in length from

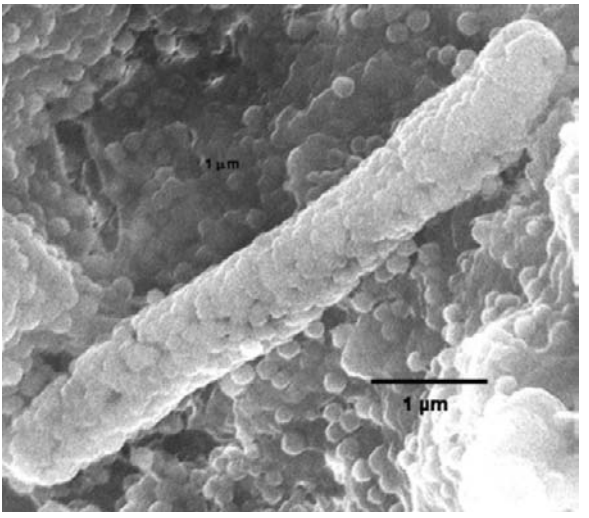

Fig. 5 FE-SEM images of intact mineralized filaments composed of cyanobacteria, which are common in the Storrs Lake stromatolites (Storrs Lake, San Salvador Island). *Arrows* indicate small ooid shaped mineral precipitates

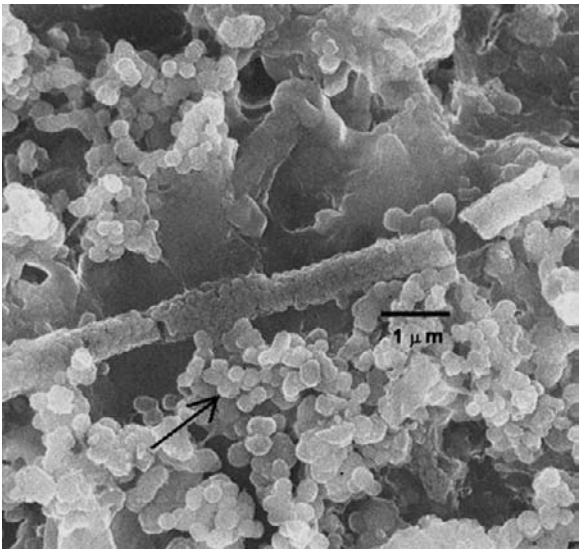

Fig. 6 FE-SEM images of segmented mineralized filaments with fossilized biofilms and smallest spheres (Storrs Lake, San Salvador Island)

approximately ten microns to several dozen microns forming a support matrix. Broken mineralized forms indicate that the mineralization was initially limited to external "mold" processes with the cellular material now degraded (Fig. 7). The thickness of the mineralization surrounding the filament is up to a micron, at most. Some of the filaments shown in Fig. 8 do not display the extent of mineralization

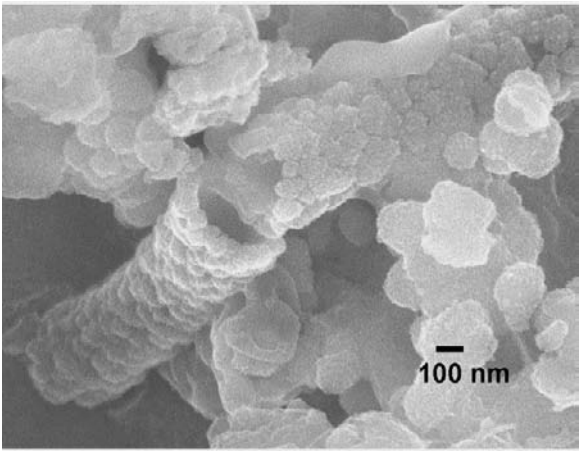

Fig. 7 FE-SEM images of broken fossilized filaments (Storrs Lake, San Salvador Island) that are similar to those in Fig. 5. The filament is hollow indicating that initial mineralization formed an external mold with small ooid shaped mineral deposits

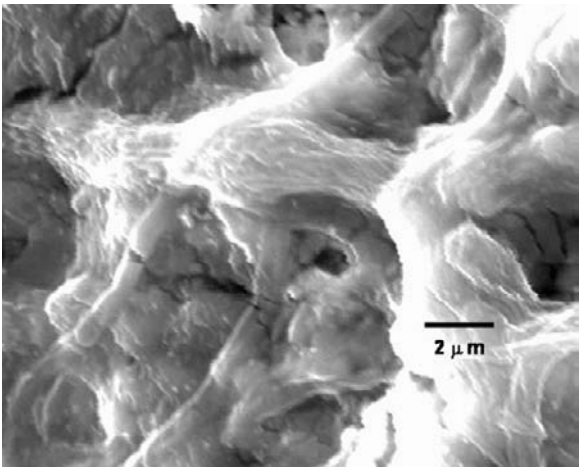

Fig. 8 FE-SEM images of cyanobacteria-like fossilized filaments also appearing as structural elements in biofilm formation covering stromatolites (Storrs Lake, San Salvador Island). The filaments are layered and intertwined and are indicative of microbial network building activities

and evidence of ECPS, indicating that they are most likely from layers on the exterior of the stromatolite biofilm. These mineralized formations were found to be associated with all microbial life in the stromatolites from various cyanobacteria, diatoms, spherical bacteria. Some filamentous fungi were observed in Storrs Lake biofilms but were not specifically identified. Fungi are known to have an impact on geological processes including stromatolite formation due to their ability to provide physical structure, aggregate particles, and to increase reactive areas (Sterflinger 2000).

Spheres: Spherical forms were observed throughout the samples and were found to vary in size. The largest spheres observed averaged 5.3μm in diameter, were relatively uncommon, and ranged from a smooth to rough texture (Fig. 9). Medium-sized spheres were commonly observed throughout the samples, usually appearing in clusters from 2–8μm, were associated with biofilm, averaged 2.0 μm and ranged from a smooth to rough texture (Fig. 10). The smallest spheres were imbedded in biofilm, usually associated with larger microbial features, apparently forming two distinct populations, the larger averaged 0.55 μm in diameter (Fig. 11) and the smallest were. The smaller 0.13 μm spheres were most likely produced abiotically, but the 0.55μm spheres may have been produced either biotically or abiotically.

Rod-Shaped: Rod-shaped or somewhat dumbell-shaped structures range in size from approximately 1.0–3.0 μm and were often associated with crystals within the biofilm matrix (Figs. 12A,B). Some were characterized by small-scale, coarse-grained roughness and often flattened in shape when attached to surfaces (Fig. 12B). Similar mat communities entrapping “dumbell-shaped” crystals of aragonite have been observed in Asta Springs at Yellow State National Park, Wyoming, USA

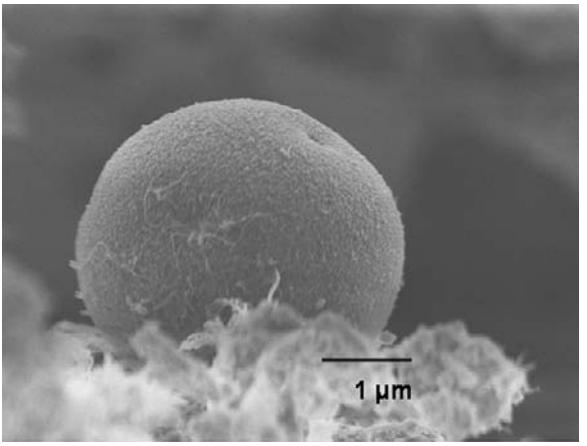

Fig. 9 FE-SEM images of an example of the largest spherical structures with sizes averaging 5.3 µm diameter and ranging from a smooth to a rough texture (Storrs Lake, San Salvador Island)

(Farmer and Des Marais 1994). The shorter rods may represent SRB as they were frequently associated with calcium sulfate crystals (Fig. 12B).

Diatoms: Diatoms were also observed as integral portions of the biofilm structure (Figs. 13A,B). Fig. 13A demonstrates a relatively intact diatom being incorporated into the biofilm. Rod-shaped bacteria are observed covering the diatom both in clumps as well as single cells, indicating colonization. In Fig. 13B a partially degraded diatom test is observed within the biofilm structure. Intact diatoms identified

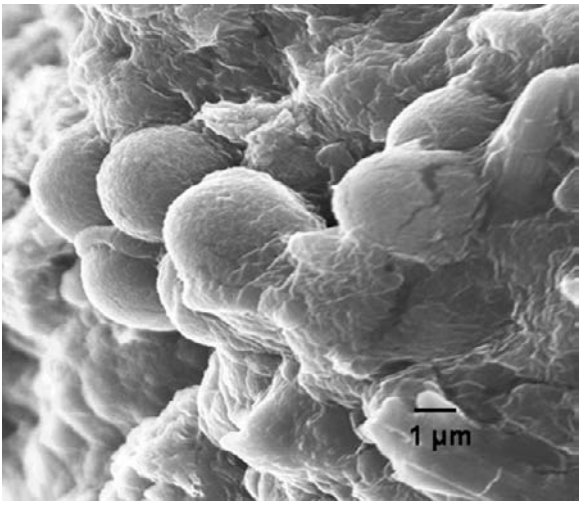

Fig. 10 FE-SEM images of medium sized spheres averaging 2.0 µ commonly appearing in clusters from 2 to 8, frequently associated with biofilm, and ranging from a smooth to a rough texture (Storrs Lake, San Salvador Island)

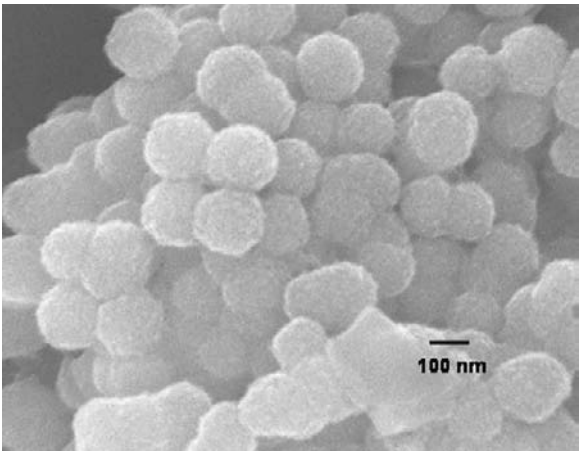

Fig. 11 FE-SEM images of the smallest spheres imbedded in biofilms; they occur in clusters and commonly associated with larger microbial features. The spheres form two distinct population sizes averaging 0.55 μm (imaged in this figure) and 0.13 μm (Storrs Lake, San Salvador Island)

in the samples included mainly *Pinnularia* with some *Navicula* and *Achnanthes* species. Again, the active bacteria attached both to the diatom as well as surrounding it with ECPS, thus indicating the ongoing nature of the biofilm building process.

Biofilms: Biofilms were found to consist of organic materials (bacteria, including cyanobacteria, fungi, diatoms) and inorganic (sand, limestone) materials enmeshed

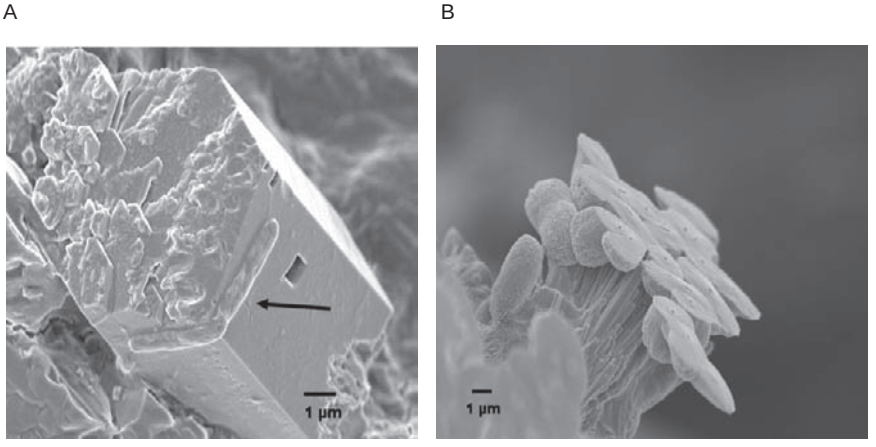

Fig. 12 (**A**) Storrs Lake, San Salvador Island, FE-SEM images. The arrow indicates a rod-shaped bacterium attached to the surface of a calcium sulfate crystal and associated with biofilms matrix. Other microbial examples were found, ranging in size from approximately 1.0–3.0 μm and commonly associated with crystals within the biofilm matrix. (**B**) Shorter rods locally appearing as rough textured dumbbells, were also observed, commonly associated with calcium sulfate crystals and likely representing sulfate reducing microbes

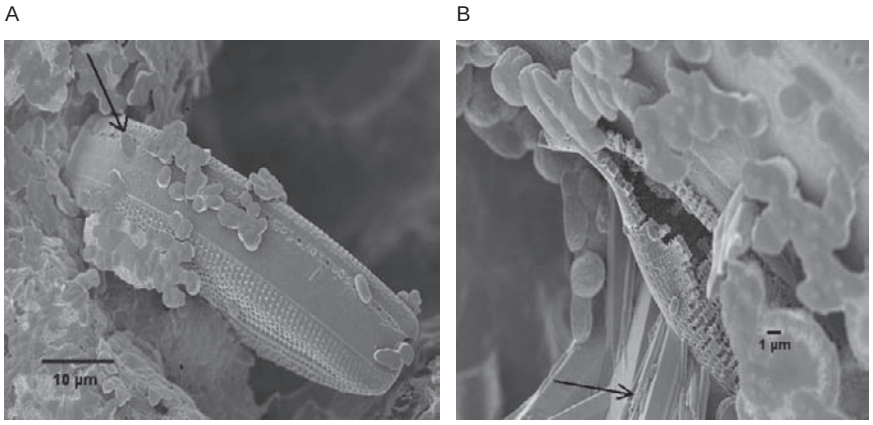

Fig. 13 Storrs Lake, San Salvador Island, FE-SEM images. Diatoms formed integral portions of the biofilm structure. (**A**) A relatively intact diatom being incorporated into the biofilm and partially covered by bacteria similar to those imaged in Fig. 12B (*arrow*). (**B**) A partially degraded diatom test observed in the biofilm structure and similar to Fig. 13A; there are also bacteria similar to Fig. 12 B and calcium sulfate crystals (*arrows*)

within the mat structure. Archaea species may have been observed in EM, but other tests would be necessary to discern them from other prokaryotes (Oren 1993). Close examination with the FE-SEM indicates that binding is due to microbially produced polysaccharide ECPS or "slime" (Figs. 14A,B). Examples of the binding can be seen in Fig. 14A, a fossilized cyanobacteria filament attached to mineralized sand and rock grains. In Fig. 14B, ECPS cross-links crystals several µm apart.

Microbial Densities: Total microbial densities (live, dead, aerobic, and anaerobic) in the stromatolites varied from 2.48×10^{10} cells/gdw in the Site 1 sample to 1.58×10^{10}k cells/gdw in the sample from Site 2 (Fig. 15). These density

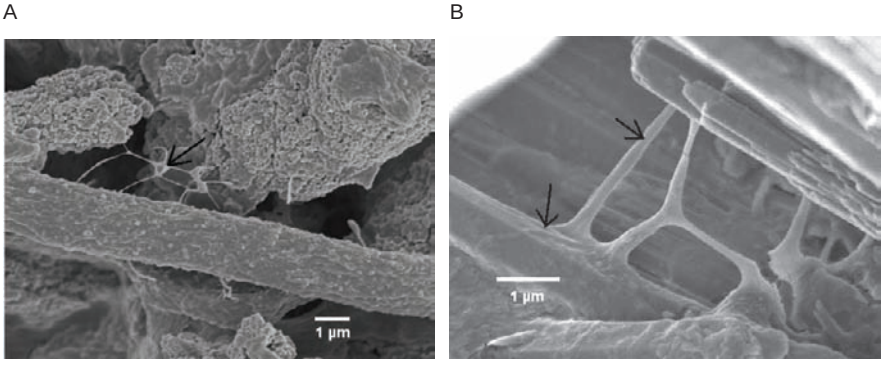

Fig. 14 Storrs Lake, San Salvador Island, FE-SEM images. (**A**) A fossilized cyanobacterial filament held to sand and rock grains by biofilms (ECPS). Arrow indicates cross-linked biofilm. (**B**) Higher magnification of Fig. 14A, arrow indicating the ECPS binding calcium sulfate crystals

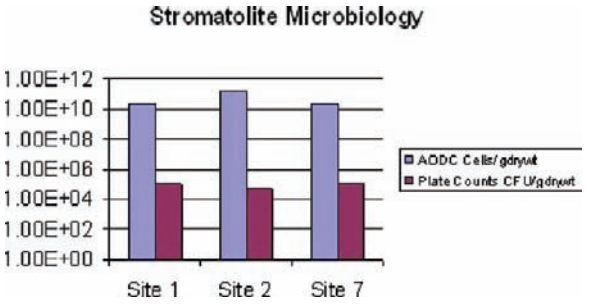

Fig. 15 Total and viable aerobic microbial densities in stromatolite samples from Storrs Lake, San Salvador Island

determinations included all algae, fungi, cyanobacteria, and bacteria, and were made from stromatolite material that was fixed in the field to preserve the sample integrity. The aerobic and/or facultative microbial densities or live microorganisms in the stromatolite cores ranged from 4.75×10^4 CFUs/gdw in Site 2 up to 9.46×10^5 CFUs/gdw in Site 1 (Fig. 15). While individual bacteria species were not identified from the viable cultures, many diverse morphological colony types and pigmented type variations were observed growing on the GASW medium.

4.1.2 Geochemical Gradient

Table 1 describes the Storrs Lake water sampling sites as to their GPS coordinates and physical characteristics. Table 3 contains all the field data that were taken during the survey. The sampling transect range of the coordinates is from the west shore of Storrs Lake (N 24.0549 W 74.45348) to the far end of Cactus Island (N 24.05943 W 74.44016). The results of the nitrate tests for all sampling sites were consistently

Table 3 Summary data of August 9, 2001, real time water chemistry survey in Storrs Lake, San Salvador Island

Site	Coordinates	N (ppm)	DO (ppm)	T (° C)	pH	Salinity (ppt)
1	N 24.0549 W 74.45348	nd**	6	39	8.24	68
2	N 24.0590 W 74.45247	nd	7	38.25	8.3	66
3	N 24.05901 W 74.45211	nd	7	37.8	8.36	66
4	N 24.05811 W 74.45132	nd	8	35	8.48	72
5	N 24.5893 W 74.4506	nd	8	36	8.51	74
6	N 24.05957 W 74.45019	nd	9	35	8.63	75
7	N 24.06025 W 74.44879	nd	not meas*	36.5	9	74
8	N 24.06038 W 74.44738	nd	not meas	37.5	8.9	75
9	N 24.05973 W 74.44651	nd	not meas	36	8.74	73
10	N 24.06018 W 74.44373	nd	not meas	32.5	8.72	77
11	N 24.05943 W 74.44016	nd	not meas	35.5	8.52	76
12	N 24.05973 W 74.44783	nd	not meas	39.5	8.97	82

*not meas=not measured.
**nd=not detected.

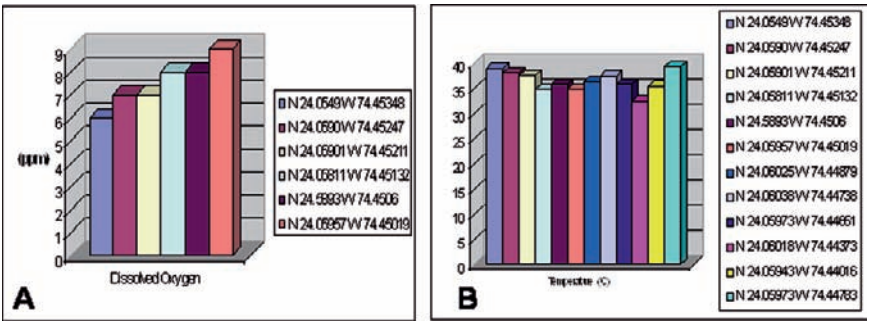

Fig. 16 (**A**) Dissolved oxygen concentrations in the water column, and (**B**) Temperature changes from the shoreline across the lake to Cactus Island

below the detection limit (1 ppm). Dissolved oxygen (DO) levels in the tests ranged from 6 ppm to 9 ppm with a mean of 7.5 ppm (Table 3). There was a gradient of increasing DO concentrations from the Storrs Lake western shore to the middle of the lake (Fig. 16A). The DO variation was most likely due to the higher density of biomats closer to the shorelines (Fig. 3). Water temperature ranged from 32.5° C to 39.5° C with a mean of 36.6° C (Fig. 16B). The lake temperatures peaked (39–39.5° C) at the first and last sampling sites close to the shorelines were also likely to the insulating effect of the biomats. The lake depths varied from 1 m to 2 m over the sampling transect.

The water pH ranged from 8.24 to 9 with a sampling mean of 8.36 (Table 2). There was a pH gradient higher near the island (pH 8.97) that decreased to 8.2 by the western shore (Fig. 17A). The pH showed an interesting profile being highest at Site 7 where the water was deepest (around 2 m) and then again elevated by Cactus Island (Site 12) (Fig. 17A). The salinity ranged from 66 g L^{-1} to 82 g L^{-1} with a mean of 73.2 g L^{-1} (Table 2). Salinity increased steadily as locations were sampled from west to east (Fig. 17B). Salinity followed the DO trend of gradually increasing throughout the sampling sites to the middle of Storrs Lake (Fig. 17B). Table 4 summarizes the statistical analysis of the water constituents as a function of location as shown from the survey. The positive correlations in Table 3 for the water chemistry demonstrate a significant trend of increasing dissolved oxygen (6–9 ppm), pH (8.2–9), and salinity water concentrations (66–82 g L^{-1}) across the transect moving west to east. No nitrate or nitrite was detected at any of the sampling sites with the field test kits. These findings were similar to previous geochemical analyses at Storrs Lake (Brigmon et al. 2006).

4.2 Dead Sea

With a salinity of 332.1 gL^{-1}, the Dead Sea (Fig. 4), with a salinity of 332.1gL^{-1} initially appears devoid of life, lacking the large, visual stromatolites and mats of Storrs Lake, Shark's Bay (Australia) or the tufa mounds of Mono Lake, California

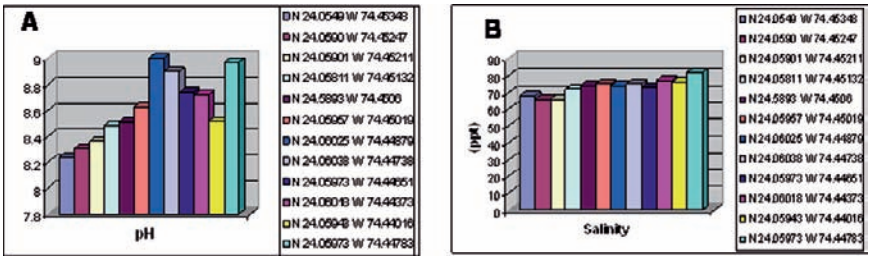

Fig. 17 (**A**) Sampling sites pH measurements, and (**B**) Salinity measurements across Storrs Lake, San Salvador Island

(Ehrlich and Zapkin 1985; Shearman 1998; Byrne et al. 2001; Brigmon et al. 2006). Microscopic and molecular data analyses indicate the existence of an abundant, albeit not homogeneous, halophilic species from the Dead Sea (Oren 1997). Many of the isolates belong to the domain Archaea, specifically Halobacteriacea (Oren 1988, 1993; Mack et al. 1993; Arahal et al. 2000), whereas the domain Bacteria is represented by gram-negative, moderate halophilic species, for example *Bacillus marismortui* (Oren 1988). Other microbial components include the green alga *Duniella*, halophilic ciliate and amoeboid protozoa, fungi and cyanobacteria (Elazari-Volcani 1943; Ehrlich and Zapkin 1985; Huval et al. 1995; Oren 1997). These microorganisms have been classified based on their environmental salt preference ranging from moderately halophilic species able to grow optimally between 0.5 and 2.5 m salt (Ventosa et al. 1998) to extremely halophilic up to 3.4 m and greater salt concentrations (Arahal et al. 2000).

4.2.1 Evaporite Minerals (FE-SEM Analysis)

Microorganisms associated with chloride mineral surfaces were limited to rod-shaped structures with filamentous, apical extensions (Fig. 18A). The microorganism and the chloride mineral were not stable in the FE-SEM electron beam and as a result were subject to charging and deterioration which can occur quickly during the imaging process. Fig. 18A is an example of the process as indicated by the unnatural wavy surface of the chloride mineral and the hole in one of the microbial filaments. Microbial fossilization is a cumulative process and begins with the precipitation of a limited number of $CaCO_3$ crystals on the surface of the extant

Table 4 Statistical analysis of real time ground water survey in Storrs Lake, San Salvador Island

Chemistry Parameter	mean (μ) $\pm$ standard deviation (σ)	Correlation (r)
Nitrate & Nitrite (ppm)	nd*	NA
Dissolved Oxygen (ppm)	7.5 ± 1.05	.9683
Temperature ($^\circ$ C)	36.55 ± 1.98	$-.2892$
pH	8.36 ± 0.899	.7425
Salinity (ppt)	73.17 ± 4.67	.8859

*nd=not detected.

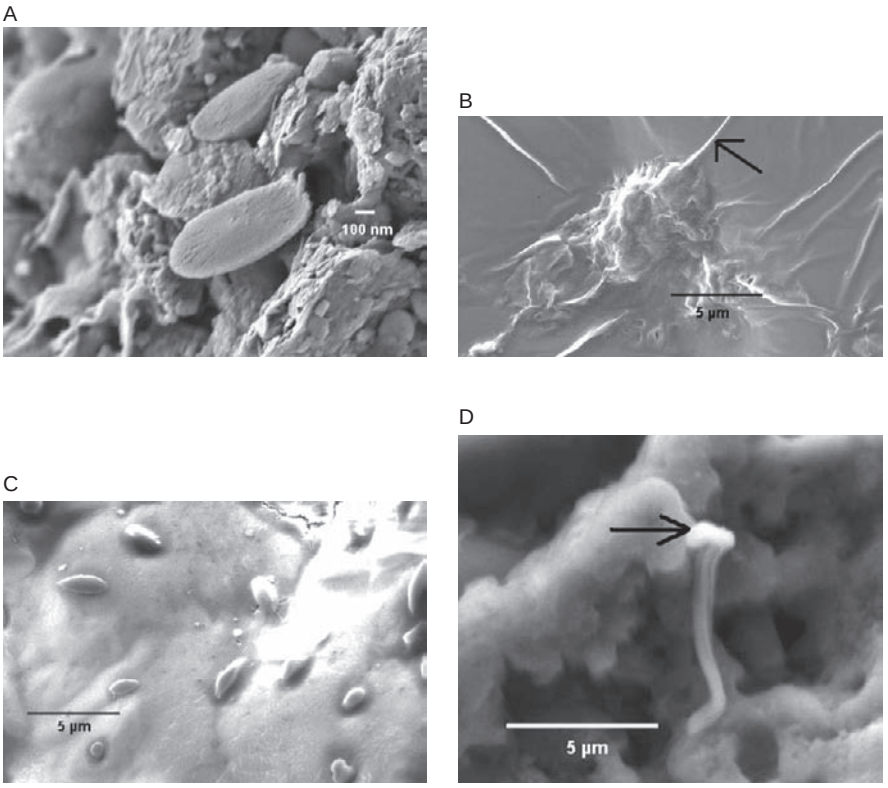

Fig. 18 FE-SEM images (Dead Sea, Israel) of (**A**) Halotolerant microorganisms associated with chloride mineral surfaces limited to rod-shaped structures with filamentous, apical extensions. (**B**) Wrinkled biofilms (labeled with *arrows*) extending outward from a fossilized microbe, and (**C**) Sand sized orthoclase and quartz fragments with rice-grain shaped potential microbes or fossilized remains. (**D**) ESEM images of filamentous microorganism with hammer-like extension (*arrow*) that appears to be attached to detrital filaments

organism with subsequent deposits that enclose the microbe and limited adjacent areas (Figs. 18A,B). Thin biofilms extend outward from the microbe as indicated by folding on the surface that formed during critical point drying (Fig. 18B). Gypsum deposits were small, usually in the 5–7 μm range, and associated with a chloride mineral. No evidence of microbial remains was found incrusting on the mineral.

4.2.2 Putative Microbes Associated with Sand-Sized Orthoclase and Quartz, Silts, Clays (FE-SEM Analysis)

Sand sized orthoclase and quartz fragments were anomalous as to the potential identification of microbes, biofilms or fossilized remains. Rice-grain shaped deposits that were in the 2–5 μm size range for microbes were found on these

detrital fragments, but there was no evidence of biofilms or other microbial remains (Fig. 18C). EDS spectra indicated low to nonexistent levels of carbon or other chemical signals of biotic remains such as potassium.

4.2.3 *Microbes Associated with Silts and Clays* (ESEM and FE-SEM Analysis)

Materials that were preserved in formalin in the field were brought back to the laboratory and observed with an environmental scanning electron microscope. This method of analysis proved to be very productive as a wide array of unfossilized microbes and thin or poorly preserved biofilms were detected. Some microbes were elongated with a hammer-like extension that appeared to be attached to detrital fragments (Figs. 18D, 19A). Others were elongated, appearing to bend around fragments, and some were rod shaped (Figs. 19B,C,D). The bacillus or rod shaped varied from those with relatively straight walls to those with more- or -less rounded rods (Figs. 19C,D). The bacillus-shaped microbe in Fig. 19D (Mt. Sedom) appeared to have substantial amounts of fossilized ECPS materials surrounding it. Some of the Mt. Sedom observed morphologies may represent the modern population, but some could have been weathered and transported from the surrounding geological deposits in a manner similar to the fossil coccoliths that were found in association with silts and clays (not shown). Figs. 19A and C demonstrate different morphologies typically observed in the Dead Sea samples attached to substrate. Fig. 19A represents filamentous-shaped microbes encased in a thin biofilm, whereas Fig. 19C depicts rod-shaped microorganisms.

All of the Dead Sea samples analyzed have lower microbial densities and apparently lower species diversity (Figs. 10, 12B, 18A,B,C,D). While some biofilms were observed (Fig. 18B), they were generally monolayered or only a few μm in thickness.

4.2.4 Mineralogy

The XRD analysis of the sedimentary materials from Ein Gedi included evaporites, primarily halite, sand-sized orthoclase and quartz sediments. Samples from Ein Boqeq and Mt. Sedom were primarily composed of silts and clays with lesser amounts of evaporites. EDS analysis indicates calcium sulfate (SEM visual analysis indicates gypsum), halite, magnesium chloride, potassium chloride and various silts and clays. In addition to these minerals, other investigators have reported magnesium bromide, carnallite, and calcium chlorite (Nissenbaum 1975; Ehrlich 1985; Zak 1997).

4.2.5 Water Chemistry

A comparison of the water chemistry analysis for the Dead Sea and Storrs Lake are summarized in Table 5.

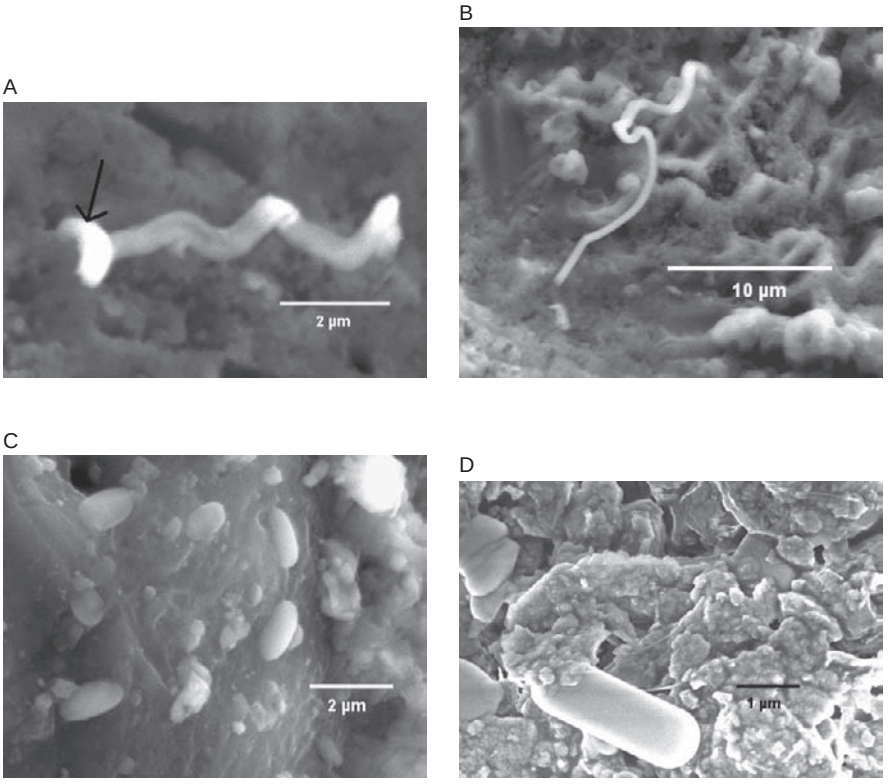

Fig. 19 Dead Sea, Israel. ESEM images. (**A**) Higher magnification of Fig. 18D. Filamentous microorganism with hammer-like extension (*arrow*), attached to detrital fragments. (**B**) Elongated filament bending around fragments and rocks. (**C**) Bacillus or rod shaped structures, inhabiting the surfaces of silts and clays. (**D**) Bacillus or rod-shaped, but with relatively straight walls in comparison with Fig. 19C. Substantial amounts of EPS materials are observed

4.2.6 Storrs Lake

The water chemistry for Storrs Lake varied, depending on whether the samples were obtained adjacent to the stromatolites or were obtained from the open areas of the lake (Table 5). The levels of ions near the stromatolites in descending order of dominance are Cl, Na, SO_4, F, Mn, Ca, and K. The following were not detected: Li, Fe, NO_2, NO_3, and PO_4. In the open waters their levels, in descending order of dominance, are Cl, Na, Ca, SO_4, and Mn. The following were not detected: K, Li, Fe, NO_2, NO_3, and PO_4. Most of these dissolved components represent major seawater components with the exception of Mn, Li, and F.

4.2.7 Dead Sea

The northern basin ions are represented in descending order by Mg, Ca, Cl, Na, K, Sr, HCO_3, SO_4, Si, Mn, and Li (Table 5). The following were not detected Fe, Ba, and NO_3. The southern basin ions, in descending order, were K, Mg, Na, Cl,

Table 5 Comparison of anion and cation concentrations, pH and average temperatures at select Storrs Lake and the Dead Sea locations

Measurements		Location			
		Dead Sea		Storrs Lake	
Chemical	Parameter	Dead Sea-Evaporite Ponds (N=4)	Dead Sea-Ein Gedi (N=1)	Storrs Lake-Stromatolites (N=3)	Storrs Lake Water (N=3)
	Na	23327	21010	25300	6670
	Ca	19017	23930	1230	5330
	K	8351.3	8351.3	640	nd
CATIONS	Mg	45280	45280	not meas.**	not meas.
($Mg\ L^{-1}$)	Mn	23.21	23.21	1500	433
	Li	8.69	8.69	nd	nd
	Fe	nd*	nd	nd	nd
	Ba	nd	nd	not meas.	not meas.
	Sr	299.7	364.6	not meas.	not meas.
	Si	nd	52.16	not meas.	not meas.
	Cl	222133	235150	52300	17700
	SO_4	464.9	195.6	5670	2300
ANIONS	HCO_3	300.47	344.5	not meas.	not meas.
($Mg\ L^{-1}$)	NO_2	not meas.	not meas.	nd	nd
	NO_3	nd	nd	nd	nd
	Fl	not meas.	not meas.	3440	nd
	PO_4	not meas.	not meas.	nd	nd
Temperature	(C)	31.5	32	36.3	36.8
	pH	6.3	6.3	8.8	8.4

nd* = not detected.
not meas** = not measured.

Ca, SO_4, HCO_3, Sr, Mn, and Li. The following were not detected: Fe, Ba, Si, and NO_3. Nitrite (NO_2) was not measured for the Dead Sea samples. The levels of the ions were similar in both basins with the exception of SO_4, which was higher in the southern basin and Sr, which was higher in the northern basin.

The dissolved ions, originating from surface-weathered materials, springs, and aquifers, are more diversified in the Dead Sea because of the long geological time encompassed in its formation. Storrs Lake's dissolved ion concentration is primarily derived from sea water and not products of geological processes over millions of years. Consequently, some of the ions (Sr, Ba) are found at significantly lower concentrations than in the Dead Sea. The origin of the dissolved ions are ultimately responsible for the pH of each system, both alkaline and mildly acidic.

5 Discussion

5.1 Nitrogen

Storrs Lake: Primary production and the conversion of N_2 to NH_3 (N_2 fixation) by certain cyanobacteria and eubacteria are important metabolic indicators of the potential contribution of microbial mats to carbon and nitrogen budgets of intertidal communities. From the data shown here it is evident that nitrogen is extremely limited in Storrs Lake (Table 5). N_2 fixation helps circumvent chronic N-limitation in oligotrophic marine systems. This process may meet mat and community N demands or serve as a supplemental (rather than exclusive) source of "new" nitrogen for mat growth. The large cyanobacterial component in this system no doubt plays a major role in nitrogen fixation. In either case, the environmental factors regulating N_2 fixation may subsequently control other mat activities including fixation, primary production, and growth of stromatolites.

Dead Sea: NO_3 (Table 5) was not detected and NO_2 was not measured in any of the samples. Previous researchers have measured N and the conclusion is that biological processes have minimal impact on the nitrogen cycles (Stiller and Nissenbaum 1999). Historically, the levels of N, particularly in the form of ammonia, increased after the 1979 water overturn. For example, in 1960, the recorded levels of N in the form of ammonia was $5.9\,mg\,L^{-1}$, but increased in 1991 to $8.9\,mg\,L^{-1}$. The ammonia sources were diffusion from bottom sediments and, potentially, production in oxygenated water by mineralization.

5.2 Strontium

Storrs Lake: Strontium levels were not measured in this work. Previous studies on San Salvador have demonstrated that strontium concentrations are elevated in comparison to open marine systems, but are not as concentrated as in the Dead Sea (Swart et al. 1987). The primary reason is the origin of the waters and the influence of heavy rain and tropical storms due to the proximity of the ocean (Fig. 3).

Dead Sea: Strontium levels are elevated in comparison to Storrs Lake and may have had several sources, including the Sedom lagoon, a Pliocene marine evaporite environment that formed the Sedom Formation. The Sedom Formation is exposed at Mt. Sedom (Table 2). Adjacent to the Sedom lagoon was a Cretaceous limestone and its weathered products provided additional strontium. An alternative source would have been dolomitization of the initial $CaCO_3$ in the Sedom lagoon (Gavrieli and Stein 2006). The earlier depositional sequences contributed to the water chemistry of the Dead Sea's hypersaline Pleistocene precursor, Lake Lisan. Thus, the strontium, as well as the elevated concentration of other ions, represents the evolution of a sea-level evaporite lagoon to an evaporite environment below sea-level.

5.3 Mineralization

We know that biological activity influences the geological processes of mineral precipitation and stromatolite building. The heterogeneity and temporal impacts of environmental influences make predictions and all encompassing explanations difficult, as biofilms associated with modern marine stromatolites are subjected to constantly changing environmental conditions resulting from tidal, seasonal, diurnal, and depositional events. For instance, the presence of mats or biofilms and organic substrates can provide favorable sites for the nucleations of crystals and contribute directly to biofilm structure (Farmer and Des Marais 1994).

Storrs Lake: The process of biofilm formation with biogeochemical interactions is demonstrated in Storrs Lake samples as crystals are covered with bacteria in Figs. 12A and B, Fig. 14 shows the exopolysaccharide produced by microorganisms and their role in binding inorganic materials including crystals. In hypersaline conditions this biological activity can lead to laminated deposition of minerals and associated microorganisms. For karst or carbonate waters and sediment, the cumulative interaction of microorganisms and geochemical conditions in the right environment can result in stromatolite formation (Eriksson et al. 2007).

Dead Sea: There is a paucity of microbially-mediated mineralization and biofilm development (Figs. 18, 19). A mildly acidic pH and low carbonate levels to the following: A mildly acidic pH and deplete HCO_3 (Table 5). Microbial diversity is restricted to obligate halophilic tolerant groups with periodic blooms of other groups such as the one-celled green alga *Dunaliella* after seasonal rains and runoffs from the wadis have diluted the surface waters (Nissenbaum 1975; Oren 1997). Under these conditions microbial groups commonly found in Storrs Lake such as cyanobacteria and fungi are restricted in their development. The halophilic groups produce relatively thin ECPS (Figs. 18A,B, 19C,D).

5.4 Environmental Influence

Storrs Lake: Evaporation exceeds precipitation, except during the rainy or storm seasons (Davis and Johnson 1990; Yannarell et al. 2007). Seasonal fluctuations result in large transitions in the water chemistry and microbial activity. Tropical storms (e.g., hurricanes) can have an even more dramatic effect on microbial activity due to changes in substrate, sediment, and water chemistry (Yannarell et al. 2007). The impact of hurricane disturbance and recovery on microbial community structure and ecosystem functions were studied in another San Salvador hypersaline lagoon, Salt Pond, which is close to Storrs Lake (Yannarell et al. 2007). This environmental microbiology study demonstrated the effects of hurricane related sand deposition on microbial nitrogen fixation rates. The rates were higher in mats re-colonizing sand depositional sites than those re-colonizing sand eroded sites. Microbial population recovery rates were favorably influenced at sites with high diversity, which structurally contributed to the rapid recovery of the disturbed ecosystem.

The living ecology in Storrs Lake is limited to a microbial community of mats, and no other animals were observed in this work. The microbial mats consisting of bacteria and algae along the shore varied in color from purple to green-brown, and featured a black bottom layer. There were a few dead fish and crabs along the shoreline, and seagulls were observed congregating on some of the stromatolites protruding from the lake as well as the island where they were nesting. The air around Storrs Lake was heavy with a sulfur smell. This sulfur odor was especially evident when wading through the lake as the sediments were stirred up. The lake's bottom consisted of areas of stromatolite growth and thick dark anoxic material, with a consistency of swamp sediments up to 1 meter in depth. An expanding landfill with trash, old vehicles, and other debris several hundred yards northwest of Storrs Lake could be a threat, due to leachate groundwater contamination. Recent, anthropogenic activity on San Salvador indicates that the future of Storrs Lake could be in danger from proposed coastal development (Don Gerace, Personal Communication).

Dead Sea: The Dead Sea is different from sea level evaporite systems similar to Storrs Lake and most nonmarine evaporite systems such as Mono Lake, California and the Great Salt Lake, Utah. For example, the pH level in the upper water mass is slightly acidic, 6.3, rather than basic, and the dominant ions are chlorine and magnesium for both the northern and southern basins (Nissenbaum 1975; Ehrlich and Zapkin 1985; Domagalski et al., 1989; MacIntyre et al. 1999). The Dead Sea water levels have dropped over 20 m since the 1950s (Gavrieli et al. 2006; Lyakhovsky and Gertman 2006). The drop in water levels is accompanied by a gradual increase in salinity and as the sulfate and bicarbonate are depleted, precipitation of aragonite and gypsum is decreased (Nissenbaum 1975; Gavrieli et al. 2006; Lyakhovsky and Gertman 2006). These events have been responsible for the increased halite precipitation (Gavrieli 1997). The changes in mineral precipitation may in part be due to the evaporation ponds in the southern basin (Gavrieli et al. 2006; Lyakhovsky and Gertman 2006). Nitrate levels have increased but are still low, as the area is arid and lacks significant numbers of cars, and there are no coal-burning industries (Berner and Berner 1996; Stiller and Nissenbaum 1999).

5.5 Hydrologic Systems

Storrs Lake: The hydrologic system on San Salvador has been documented by Davis and Johnson (1990). As is typical of karst areas, there are no surface water streams. Potential reasons for the trends demonstrated here are not certain as the water flow patterns can vary. Various vents feeding the water supply were noted on the north end of the Lake. Smaller vents were observed on Cactus Island. Another factor is tidal influence indirectly through subsurface seeps (Teeter 1995). These seeps may change with fluctuations in sediment deposition due to storm events. One possibility is when rain falls, water flows in towards the middle of the lake, making the hydrogen gradient stronger (pH) in the middle than on the

banks. This is evident in its hypersaline nature. The ocean side was higher in salinity, suggesting that this could be due to weathering of atmospheric salt deposition. The potential of biogeochemical interactions influencing the water chemistry due to the thick biofilm evident throughout the lake is also an alternative reason.

Dead Sea: The lake is roughly rectangular in shape with no outlet and is separated into a northern and southern basin. The northern basin is 400 m in depth and the southern basin is shallower, varying from 6 m to 8 m. The only fresh water source is the Jordan River and limited seasonal rain waters. The Dead Sea is dominated by a variety of salts, most of which emanate from springs in and around the lake (Nissenbaum 1975; Lensky et al. 2005). Many of the salts and the high levels of strontium are a result of meteoritic water circulating through residual depositional brines beginning with the Sedom Lagoon (Lensky et al. 2005).

5.6 Biofilms Mats, Stromatolites

Microbial film formation is dependent upon different factors for growth and metabolism. Marine biofilms form on a variety of biotic and abiotic surfaces. In intertidal systems these can be quite extensive (Decho 2000). Development of marine biofilms on abiotic surfaces begins with the attachment of microbes to surfaces and the secretion of ECPS (Decho 2000; Kawaguchi and Decho 2002). Cell to cell signals influence both community profiles and metabolic activities within the polymeric matrix (Davies et al. 1998). These can develop into mats with the addition of photoautotrophs to the community, which then can stimulate the precipitation or trapping of sediment.

The evolution from biofilms to mats to stromatolites is closely linked to water chemistry and the absence of invertebrate herbivores. Stromatolites are found in many different regions of the world and in a variety of habitats, including hypersaline environments. All of the stromatolites have a similar microbial ecology, including phototrophic microorganisms and photosynthetic microbial mats combined with fossilization (Reid et al. 2003). In alkaline hypersaline conditions both cyanobacteria and algae enable $CaCO_3$ precipitation, thus encouraging extensive microbialite structures.

Examples of modern stromatolites growing in a normal, tropical-marine, intertidal environment have been described from Stocking Island, Bahamas (Pickney et al. 1995). At this site, the activities of herbivores are restricted by the physical environment (i.e., tidal currents and shifting channel sands). The stromatolites described by Pickney et al. 1995 appear to be actively growing due to the association with microbial mats covering the stromatolite surface, an important discovery that explains the ecophysiological properties controlling stromatolite formation. As the organic mass ages and older components die, new growth of cyanobacteria and microbes ensure their continued existence with the open ocean conditions.

Storrs Lake: Hypersalinity, which can over time limit invertebrate grazing biofilms, selects for certain microorganisms (Elliott 1994). The stromatolites at Storrs Lake have been estimated to be around 2500 years old (Zabielski and Neumann 1990). These San Salvador stromatolites are similar in age to those on Stocking Island, Bahamas.

Total microbial densities in the Storrs Lake stromatolites were as high as 1.58×10^{10} cells/gdw in Site 2 and live microorganisms up to in 9.46×10^5 CFUs/gdw in Site 1 (Fig. 16), demonstrating high aerobic metabolic activity. While these plates were grown on GASW medium utilizing artificial seawater at 37° C, the resultant densities do not represent all viable bacteria present. Certain bacteria that could not grow in these conditions include obligate anaerobic or extreme halophilic microorganisms (Oren 1993). In addition, the salt requirement and tolerance of many bacteria vary according to other growth conditions including temperature and medium composition (Ventosa et al. 1998). A majority of environmental bacteria are often nonculturable when using one medium in any given location. The geochemical gradient observed in this study could yield a related gradient in microbial speciation due to the different available nutrients.

Symbiotic sulfur oxidizing bacteria including *Thiothrix* spp. forms laminated mats around detrital particles and builds nodules in the hindgut caecum of marine spatangoids (De Ridder and Brigmon 2003). Anaerobic conditions and hence the mutualism prevail in these small microbialites because *Thiothrix* spp bacteria remove sulfide. It is thought that the symbiosis provides a detoxifying effect with nutritional consequences to the echinoid (Brigmon and De Ridder 1998). Sulfur nodules (i.e., a nucleus wrapped by a layered microbial mat) are structurally similar to oncoids, a type of biolaminated particle in sedimentary structures (Visscher et al. 1998). No other algal types including green algae or red algae were observed in the stromatolite samples. This could have been to due their low densities, nutrient deficiencies (e.g. lack of nitrogen), or the high salinity.

Marine Systems: Corals form a similar biofilm, except much of the polymeric material is produced by mucus cells in the coral polyp (Harvell et al. 2007). The microbial community develops within the surface mucopolysaccharide layer, but does not appear to adhere to the epidermal cells (Ritchie 2006). Microbial cell-to-cell communication occurs by the production of homoserine lactones in marine systems to maintain biofilm structure (Johnson 2005). The microbial community profile is determined, in part, by the production of antibiotics and other allelopathic compounds (Ritchie 2006), and by carbon source availability. Distinct differences in biofilm species composition appear to be structural and functional. For example, in contrast to biofilms formed on microbialites and stromatolites, establishment of significant numbers of cyanobacteria only seems to occur on corals during black-band disease (Weil et al. 2006).

Dead Sea: The Dead Sea lacks obvious stromatolites, microbialites or biofilms, and cursory investigation did not produce any evidence of microbially induced calcium carbonate precipitation in the form of stromatolites. Microscopic investigations negate the visual finding, as there are a number of microbes present that are adapted to aquatic saline environments (Nissenbaum 1975; Oren and Anati 1996; Oren 1997).

Biofilm development was observed to be minimal in the Dead Sea samples. This was in contrast to Storrs Lake, which produces thick, viscous biofilms as well as stromatolites. The stromatolites in Storrs Lake are similar to those described in Stouts Lake (San Salvador, Bahamas) with active microbial mats (Elliott 1992). The Dead Sea biofilms were primarily detected with an environmental scanning electron microscope, and in contrast to Storrs Lake there was minimal fossilization (Figs. 19A,B,C and 21B). Fossilization in the biofilms and microbes is being controlled by the depletion of HCO_3 and the slightly acidic pH.

5.7 Nutrient Systems

Studies of the nutrient distribution, particularly carbon and nitrogen, within ecosystems can provide useful insights into the structure and function of those ecosystems. While N-fixation was not measured in Storrs Lake, the extreme N limitation in the system as demonstrated by both field (Test Kits) and laboratory techniques (IC) makes it apparent that this analysis needs to be addressed. A walk down of the surrounding area combined with the IC data (Tables 3 and 4) demonstrates that local sources of nitrogen are negligible. While not measured in this study, the uptake of dissolved organic carbon (DIC) from the water column is essential for photosynthesizing microbial mats as those at Storrs Lake. DIC that comes in contact with the biofilms are either fixed into organic matter abiotically or biotically, or diffused out to the water (Des Marais and Canfield 1994).

In a closed evaporite system like Storrs Lake the movement of DIC would not be as dynamic as in an open water system. Studies that compare extreme environments such as evaporite systems will enable us to better analyze the data, as it appears in comparing Storrs Lake and the Dead Sea that visual identification of organic activity can be difficult. Microscopic analysis, if they are directed towards stromatolitic or microbialite remains, can also fail, since life may be sparse and the chemistry may limit fossilization.

Biofilms can form under a wide range of conditions including extreme environments. Acidic streams from mines may contain metal-containing leachate including iron, sulfur, and arsenic that select for certain microorganisms. These materials have been shown to be accumulated as ferric arsenate and arsenate-sulphate precipitates in rapidly growing bacteria-made microbialite structures (Leblanc et al. 1996). The ongoing development of bacterial biofilms alternating with sand deposition, drying, and erosive cycles results in the formation of As-rich ferruginous accretions. These laminated and dome-shaped bacterial structures are similar to those of stromatolites but lack the abundance of cyanobacteria. This incorporation of minerals and metals into biofilms layered with sand and sediment is similar to those processes in natural systems (Krumbein 1978). Biofilms as well as microbialites and stromatolites are organosedimentary structures that can grow in a wide range of environments, where water temperature, nutrients, geology, and pH vary widely. While they are most often observed in neutral and alkaline waters, stromatolites can form in acid-sulfate

springs and geyser systems including geothermal areas in New Zealand (Jones et al. 2000) and the United Sates (Farmer and Des Marais 1994). As might be expected, the growth and development of stromatolites from acidic thermal waters compared with those from neutral and alkali waters have been found to be microbiologically and geochemically distinct (Jones et al. 2000).

While biofilms of varying quality and quantity can be observed worldwide, stromatolites are only seen in places where environmental conditions are conducive to growth and development of these unique structures. The formation of stromatolites, which are basically laminated microbial mats constructed from layers of filamentous and other microorganisms, requires certain environmental conditions. These conditions include the geochemistry, temperatures, water flow, depth, and microbiology similar to those found at Storrs Lake. Storrs Lake, due to its proximity to the ocean, shallower depth, and environmental factors is more dynamic in terms of spatial and temporal changes that have an obvious impact on the geomicrobiology of the site. Microbial diversity and densities were observed to be much greater in Storrs Lake compared to samples from the Dead Sea. The Dead Sea microorganisms, although in lower densities and apparent diversity, were observed to be actively attached to abiotic substrates.

Recent research on the microbiology of hypersaline systems (Yannarell et al. 2007) will likely provide valuable information in a number of fields. Much of the interest in microbiology of hypersaline systems is limited due to problems with isolation of organisms from environmental samples (Brigmon et al. 1994). Here, we extensively employed electron microscopy to allow direct examination of samples from those sites. Both culture and microscopy techniques have demonstrated an extremely active microbial community in Storrs Lake's stromatolites. However, the methods used to determine aerobic and heterotrophic microbial densities here were performed with GASW medium made with artificial seawater. Some extreme halophilic species may not grow at this salinity, and therefore this method may have underestimated the actual population.

6 Conclusions

In this review we have discussed and compared microbiology and geochemistry from two distinct hypersaline environments, Storrs Lake (San Salvador, Bahamas) and the Dead Sea (Israel). We have described the development of microbialites from biofilms to microbial mats, to more complex structures like stromatolites in Storrs Lake. We conclude that the Dead Sea has a very different, but limited, microbial ecology and point out the importance of biofilm establishment due to biotic and abiotic processes in evaporite systems. This ecological range does show the diversity and adaptability of microorganisms to their extreme environments, as well as highly dependent nature of the microbiology of these evaporite systems on the geology and other key, associated environmental influences. The development of stromatolites in Storrs Lake was related to oxygen, water flow, pH, and associated geochemistry

for the evaporite system. The characteristics of hypersaline microbialites in the Bahamas were compared with those in the Dead Sea.

We have observed unique interactions between geochemical (e.g. crystals) and possible microbiological activity. Future work on identifying specific microbial processes involved (e.g. redox coupled reactions) is needed to understand the function of those interactions in extreme geochemical environments. Here, we have shown how the diversity of the geological settings and microbial communities rise to unique ecosystems and structures. The incorporation of diatom tests adds to the strength and structure of the stromatolite biofilms. Bacterial products including ECPS were shown cross-linking various crystal types and fossilized bacteria to "cement" the structure together.

Biofilms are also excellent environments for stabilization of fossilized filaments, diatoms, and inorganic detritus. These conclusions are supported by other research indicating the importance of microbial –substrate interactions due to precipitation of carbonate "cement" as recently described in other tropical environments (Díez et al. 2007). Cyanobacteria in Storrs Lake make up most of the evaporite crust, as well as the fossilized material below and some other functions including UV-resistant pigments. These microbially produced pigments in evaporite most likely allow these resilient microorganisms to survive under a wide range of conditions. The interaction of an extremely active bacterial population with cyanobacteria evident here most likely accelerates calcium carbonate precipitation and fossilizations as documented in microbial mats in other sites studied by Chafetz and Buczynski (1992). We hypothesize that the nitrogen limitation is made up by the nitrogen fixing cyanobacteria and associated mat bacteria in the Storrs Lake biofilms.

Acknowledgments We would like to thank Dr. Donald T. Gerace, Chief Executive Officer, and Vincent Voegeli, Executive Director of the Gerace Research Center, San Salvador, Bahamas, for their support. We thank Christopher Berry and Victoria Stewart of the Savannah River National Laboratory for their analytical support. L. Hulse and Mayra Nelman, NASA-Johnson Space Center for Scanning and Environmental Electron Microscope access, Dr. Carlton C. Allen, NASA-Johnson Space Center for XRD analysis, Monica Byrne for many of the Storrs Lake images, coccoid measurements, Dawn Smith for field support at the Dead Sea, and Dr. S. Grasby, Canadian Geological Survey, Calgary for the Dead Sea water analysis. This paper was prepared in connection with work done under a subcontract to Contract No. DE-AC09-76SR00001 with the U.S. Dept. of Energy. The investigation of P. Morris was supported by NASA Astrobiology grant NAG9-1113, NAG9-1114. G. Smith was supported by NSF grant 0516347 and The World Bank Global Environmental Fund to the Coral Disease Working Group.

References

Anati DA (1997) The hydrography of a hypersaline lake. In: Niemi TM, Ben Avraham Z, Gat JR (eds) Oxford monographs on geology and geophysics 36. Oxford Press, London, pp 89–103

Arahal DR, Gutierrez MC, Volcani BE, Ventosa A (2000) Taxonomic analysis of extremely Halophilic Archaea isolated from 56-years-old Dead Sea brine samples. Systematic and Appl Microbiol 23:376–385

Awramik SM (1984) Ancient stromatolites and microbial mats. In: Cohen Y, Castenholz RW, Halvoroson HO (eds) Microbial mats: Stromatolites.. Alan R. Liss Inc., NY, pp 1–22

Berner EK, Berner RA (1996) Global environment: water, air and geochemical cycles. Prentice Hall, New Jersey, 376p

Brehm U, Gorbushina A, Mottershead D (2005) The role of microorganisms and biofilms in the breakdown and dissolution of quartz and glass. Paleogeography, palaeoclimatology, Paleoecology 219: 117–129

Brigmon RL, De Ridder C (1998) Symbiotic relationship of *Thiothrix* spp. with Echinoderms. Appl Environ Microbiol 64:3491–3495

Brigmon RL, Martin HW, Morris T, Zam S, Bitton G (1995) Biogeochemical Ecology of *Thiothrix* spp. in underwater Limestone Caves, Geomicrobiol J 12:141–159

Brigmon RL, Smith GW, Morris PA, Byrne M, McKay DS (2006) Microbial Ecology in Modern Stromatolites from San Salvador, Bahamas. In: Davis RL, Gamble DW (eds) Proceedings of the 12th Symposium on the Geology of the Bahamas and Other Carbonate Regions. Bahamian Field Station, San Salvador, Bahamas, pp 20–31

Buck SG (1980) Stromatolite and ooid deposits within the fluvial and lacustrine sediments of the Precambrian Ventersdorp Supergroup of South Africa. Precambrian Res 12:311–330

Burne RV, Moore LS (1987) Microbialites: organosedimentary deposits of benthic microbial communities. PALAIOS 3:241–254

Byrne M, Morris PA, Wentworth SJ, Brigmon RL, McKay DS (2001) Microbial biota from fractured stromatolite and biofilm samples: biomarkers from a hypersaline lake. Annual Meeting Geology Society of America, November 1–10, 2001, Boston, Massachusetts, p 452

Castenholz RW, Garcia-Pichel F (2000) Cyanobacterial responses to UV-radiation. In: Whitton BA, Potts M (eds) The Ecology of Cyanobacteria: their diversity in time & space. Kluwer, London, pp 591–611

Chafetz HS, Buczynski C (1992) Bacterially induced lithification of microbial mats. PALAIOS 7:277–293

Csato IC, Kendall CStC, Nairn AEM, Baum GR (1997) Sequence stratigraphic interpretations in the southern Dead Sea basin, Israel. Geol Soc Am Bull 108:1485–1501

Davies DG, Parsek MR, Pearson JP, Iglewski BH, Costerton JW, Greenberg EP (1998) The involvement of cell-to-cell signals in the development of a bacterial biofilm. Science 280:295–298

D'Amelio E, Cohen Y, Des Marais DV (1989) Comparative functional ultrastructure of two hypersaline submerged cyanobacterial mats: Guerrero Negro, Baja California Sur, Mexico, and Solar Lake, Sinai, and Egypt. In: Cohen Y, Rosenberg E (eds) Microbial mats: physiological ecology of benthic microbial communities American Society for Microbiology, pp 97–113

Davis RL, Johnson CR (1990) The Karst Hydrology of San Salvador Island, Bahamas. In: Mylroie J.E. (ed.) Proceedings of the 4th Symposium on the Geology of the Bahamas. Bahamian Field Station, San Salvador, Bahamas, pp 118–136

Decho AW (2000) Microbial biofilms in intertidal systems: an overview. Continental Shelf Res 20:1257–1273

De Ridder C, Brigmon RL (2003) "Farming" of microbial mats in the hindgut of echinoids. In: Krumbein WE, Paterson DM, Zavarzin GA (eds) Fossil and recent biofilms a natural history of life on Earth. Kluwer, The Netherlands, pp 217–225

Des Marais DJ, Canfield SE (1994) The carbon isotope biogeochemistry of microbial mats. In: Stal LJ, Caumette P (eds) Microbial mats. NATO ASI Series, Vol. G 35., Springer-Verlag, Berlin Heidelberg, pp 289–298

Díez B, Bauer K, Bergman B (2007) Epilithic cyanobacterial communities of a marine tropical beach rock (Heron Island, Great Barrier Reef): diversity and diazotrophy. Appl Environ. Microbiol. 73:3656–3668

Domagalski JL, Orem WH, Eugster HP (1989) Organic geochemistry and brine composition in Great Salt Lake, Mono, and Walker Lakes. Geochemica et Cosmochimica Acta 53:2857–2872

Dupraz C, Visscher PT (2005) Microbial lithification in marine stromatolites and hypersaline mats. Trends in Microbiol 13:429–436

Dupraz C, Visscher PT, Baumgartner LK, Reid RP (2004) Microbe–mineral interactions: early carbonate precipitation in a hypersaline lake (Eleuthera Island, Bahamas). Sedimentology 51:745–765

Elliott WM (1994) Stromatolites of the Bahamas. In: The 26th meeting of the association of marine laboratories of the Caribbean. Bahamian Field Station, San Salvador, Bahamas, pp 33–39

Elliott WM (1992) Stromatolites of Stouts Lake, San Salvador Island. Bahamas. In: Proceedings of the fourth symposium on the natural history of the bahamas. Bahamian Field Station, San Salvador, Bahamas, pp 49–58

Ehrlich HL, Zapkin MA (1985) Manganese-rich layers in calcareous deposits long the western shore of the Dead Sea may have a bacterial origin. Geomicrobiol. J. 4:207–221

Elazari-Volcani B (1943) Bacteria in the bottom sediments of the Dead Sea. Nature 152:274–275

Eriksson PG, Schieber J, Bouougri E, Gerdes G, Porada H, Banerjee S, Bose PK, Sarkar S (2007) Classification of structures left by microbial mats in their host environments. In: Schieber J, Bose PK, Eriksson PG, Banerjee S, Sarkar S, Altermann W, Catuneau O (eds) Atlas of microbial mats features within the clastic rock record. Elsevier

Farmer JD, Des Marais DJ (1994) Biological versus inorganic processes in stromatolite morphogenesis: observations from mineralizing sedimentary systems. In: Stal LJ, Caumette P (eds) Microbial mats. NATO ASI Series, Vol. G 35. Springer-Verlag, Berlin, Heidelberg, pp 61–68

Fratesi SE, Lynch FL, Kirkland BL, Brown LR (2004) Effects of SEM preparation techniques on the appearance of bacteria and biofilms in the Carter Sandstone. J Sedimentary Res 74:858–867

Friedman GM (1998) Temperature and salinity effects on ^{18}O fractionation for rapidly precipitated carbonates: laboratory experiments with alkaline lake water-perspective. Episodes 21:97–98

Gavrieli, I (1997) Halite deposition in the Dead Sea: 1960–1993. In: Niemi TM, Ben-Avraham Z (eds) The Dead Sea—The lake and its setting. Oxford Press, London

Gavrieli I, Stein M (2006) On the origin and fate of the brines in the Dead Sea basin. In: Enzel Y, Agnon A, Stein M (eds) New Frontiers in Dead Sea Paleoenvironmental Research. Geological Society of American Special Paper 401. pp 183–194

Gavrieli I, Lensky N, Dvorkin Y, Lyakhovsky V, Gertman I (2006) A multi-component chemistry-based model for the Dead Sea: modifications of the 1D Princeton Oceanographic Model. Geol Survey of Israel, Report GSI/24/2006

Gerdes G, Krumbein WE, Reineck HE (1987) Mellum. Portrait einer Insel. Kramer, Frankfurt, 344p

Grozinger JP, Knoll AH (1999) Stromatolites in Precambrain carbonates: Evolutionary mile posts or environmental dipsticks? Ann Rev Earth Planet Sci. 27:313–358

Hall JK (1997) Topography and bathymetry of the Dead Sea depression. In: Niemi TM, Ben Avraham Z, Gat JR (eds) Oxford monographs on geology and geophysics 36. Oxford Press, London, pp 11–21

Harvell D, Jordan-Dahlgren E, Merkel S, Rosenberg E, Raymundo L, Smith G, Weil E, Willis B (2007) Coral disease, environmental drivers, and the balance between coral and microbial associates. Oceanography 20:60–79

Herut B, Gavrieli I, Halicz L (1997) Sources and distribution of trace and minor elements in the western Dead Sea surface sediments. Appl Geochem 12:497–505

Huval JH, Latta R, Wallace R, Kushner DJ, Vreeland RH (1995) Description of two new species of *Halomonas*: *Halomonas israelensis* sp. nov., *Halomonas anadensis* sp. nov. Can J Microbiol 41:1124–1131

Johnson C (2005) Characterization of a coral-associated microbial community: the microbial ecology of *Pseudopterogorgia Americana*. MS Thesis, Marine Biomedicine and Environmental Science Department, Medical University of South Carolina, Charleston SC, USA

Jones B, Renaut RW, Rosen MR (2000) Stromatolites forming in acidic hot-spring waters, North Island, New Zealand. PALAIOS 15:450–475

Kawaguchi T, Decho AW (2002) In situ microspatial imaging using two-photon and confocal laser scanning microscopy of bacteria and extracellular polymeric secretions (EPS) within marine stromatolites. Mar Biotechnol 4:127–131

Krumbein WE (1978). Algal mats and their lithification. In: Krumbein WE (ed) Environmental biogeochemistry and geomicrobiology. Volume 1: The aquatic environment. Ann Arbor Science, MI, pp 209–225

Krumbein WE, Brehm U, Gerdes G, Gorbushina AA, Levit G, Palinka KA (2003) Biofilm, biodicton, biomat microbialites, oolites, stromatolites, geophysiology, global mechanism, parahistology. In: Krumbein WE, Paterson DM, Zavarzin GA (eds) Fossil and recent biofilms: a natural history of life on Earth. Kluwer, London, pp 1–27

Leblanc M, Achard B, Othman DB, Luck JM, Betrand-Sarfati J, Personné JCh (1996) Accumulation of arsenic from acidic mine waters by ferrunginous bacterial accretions (Stromatolites). Appl. Geochem 11:541–554

Lensky NG, Dovrkin Y, Lyakhovsky V (2005) Water, salt and energy balances of the Dead Sea. Water Resour Res 41:1–13

Lindsay JF, Leven JH (1996) Evolution of a Neoproterozoic to Paleozoic intracratonic setting, Officer Basin, South Australia. Basin Res 8:403–424

Lowe DR (1983) Restricted shallow water sedimentation of early Archean stromatolitic and evaporitic strata of the Strelley Pool chert, Pilbara Block, Western Australia. Precambrian Res 19:239–283

Mack EE, Mandelco L, Woese CR, Madigan MT (1993) *Rhodospirillum sodomense*, sp.l, nov., a Dead Sea *Rhodospirillum* species. Arch Microbiol. 160:363–371

MacIntyre S, Flynn KM, Jellison R, Romer JR (1999) Boundary mixing and nutrient fluxes in Mono Lake, California. Limnology and Oceanography 44:512–529

Martini JEJ (1990) An early Proterozoic playa in the Pretoria Group, Transvaal, South Africa. Precambrian Res 46:341–351

Morris PA, von Bitter P, Schenk P, Wentworth SJ (2002) Interactions of bryozoans and microbes in chemosynthetic hydrothermal vent system: Big Cove Formation (Lower Codroy Group, Lower Carboniferous, Middle Visean) Port au Port Peninsula, western Newfoundland, Canada. In: Wyse Jackson P, Buttler CJ, Spencer Jones ME (eds) Bryozoan Studies 2001.Balkima Press, The Netherlands, pp 221–228

Morris PA, Wentworth SJ, Nelman M, Byrne M, Longazo T, Galindo C, McKay D, Sams C (2003) Modern microbial fossilization processes as signatures for interpreting ancient terrestrial and extraterrestrial microbial forms. Lunar and Planetary Science Conference XXXIV, Abstract 1909, Houston, TX

Morris PA, Soule DF (2005) The potential role of microbial activity and mineralization in exoskeletal development in Microporellidae. In: Moyano H, Cancino JM, Wyse Jackson, PN (eds) Bryozoan Studies. Balkima Publishers, Leiden, London, New York, Philadelphia, Singapore, ISBN 0415372933, pp 181–186

Muir MD (1987) Facies models for Australian Precambrian evaporites. In: Peryt TM (ed) Evaporite basins, Lecture Notes in Earth Sciences 13. Springer-Verlag, Berlin, pp 5–21

Nissenbaum A (1975) The microbiology and biogeochemistry of the Dead Sea. Microbial Ecol 2:139–161

Noffke N, Gerdes G, Klenke T, Krumbein WE (2001) Microbially inducted structures – a new category within the classification of primary structures. J Sedimentary Res 71: 650–656

Olson RA (1984) Genesis of paleokarst and strata-bound zinc-lead-sulfide deposits in a Proterozoic dolostone, northern Baffin Island, Canada. Econ Geol 79:1056–1033

Oren A (1988) The microbial ecology of the Dead Sea. Adv Microb Ecol 10:193–229

Oren A (1993) Ecology of extremely halophilic micro-organisms. In: Vreeland RH, Hochstein LI (eds) The Biology of Halophilic Bacteria. CRC Press, Boca Raton, FL, pp 25–53

Oren A (1997) Microbiological studies of the Dead Sea: 1892–1992. In: Niemi TM, Ben Avraham Z, Gat JR (eds) Oxford monographs on geology and geophysics 36. Oxford Press, London, pp 205–216

Oren A, Anati DA (1996) Termination of the Dead Sea 1991–1995 stratification: biological and physical evidence. Israel J Earth Sci 45:81–88

Pentecost A, Whitton BA (2000) Limestones. In: Whitton BA, Potts, M (eds) The ecology of cyanobacteria: their diversity in time & space. Kluwer, London, pp 257–279

Pickney J, Paerl HW, Reid RP, Bebout B (1995) Exophysiology of stromatolitic microbial mats, stocking Island, Exuma Cays, Bahamas. Microb Ecol 29:19–37

Pope MC, Grotzinger JP (2003) Paleoproterozoic stark formation, Athapuscow Basin, Northwest Canada: record of cratonic-scale salinity crisis. J Sedim Res 73:280–295

Reid RP, Dupraz CD, Visscher PT, Sumner DY (2003) Microbial processes forming marine stromatolites. In: Krumbein WE, Paterson DM, Zavarzin GA (eds) Fossil and recent biofilms–a natural history of life on earth. Kluwer Academic Publishers, Dordrecht, Netherlands, pp 103–118

Ritchie KB (2006) Regulation of microbial populations by coral surface mucus and mucus-associated bacteria. Mar Ecol Prog Ser 322:1–14

Ritchie KB, Smith GW (2004) Microbial communities of coral surface mucopolysaccharide layers. In: Rosenberg E, Loya Y (eds) Coral health and disease. Springer-Verlag, Berlin, Germany, pp 259–263

Robinson MC, Davis LR (1999) San Salvador GIS database. University of New Haven and the Bahamian Field Station

Shearman D (1998) The Mono Lake tufas and ikaite columns of Ikka Fjord, Greenland. Geoscientist 8:4–5

Smith G, Hayasaka SS (1982) Nitrogenase activity of bacteria associated with *Halodule wrightii* roots. Appl Environ Microbiol43:1244–1248

Sneh A, Bartov Y, Weissbrodt T, Rosensaft M (1998) Geology map of Israel, 1:200000, 4 sheets. Israeli Geological Survey

Steinhorn I (1997) Evaporation estimate for the Dead Sea: essential considerations. In: Niemi TM, Ben-Avraham Z, Gat JR (eds) The Dead Sea, the Lake and its setting. Oxford monographs on geology and geophysics 36. Oxford Press, London, pp 122–132

Sterflinger K (2000) Fungi as geologic agents. Geomicrobiol J 17:97–124

Stiller M, Nissenbaum A (1999) Geochemical investigation of phosphorus and nitrogen in the hypersaline Dead Sea. Geochimica et Cosmochimica Acta 63:3467–3475

Swart PK, Ruiz J, Holmes CW (1987) Use of strontium isotopes to constrain the timing and mode of dolomitization of upper Cenozoic sediments in a core from San Salvador, Bahamas. Geology 15:262–265

Teeter JW (1995) Holocene saline Lake History, San Salvador Island, Bahamas. In: Curran HA, White B (eds) Terrestrial and shallow marine geology of the Bahamas and Bermuda. Boulder, CO. Geological Society of America, Special Paper 300

Thomas-Keprta K, McKay DS, Wentworth SJ, Taunton AE, Stevens TO, Allen CC, Gibson EK, Romanek CS (1998) Bacterial mineralization patterns in basaltic aquifers: implications for possible life in Mars meteorite ALH84001. *Geology* 26:1031–1035

Ventosa A, Nieto J, Oren, A (1998) Biology of moderately halophilic aerobic bacteria. Microbiol Mol Biol Rev 62:504–544

Visscher PT, Reid RP, Bebout BM, Hoeft SE, Macintyre IG, Thompson JA (1998) Formation of lithified micritic laminae in modern marine stromatolites (Bahamas): the role sulfur cycling. Am Min 83:1482–1493

Walter MR (1983) Archean stromatolites: evidence of earth's earliest benthos. In: Schopf JW (ed) Earth's earliest biosphere: its origin and evolution. Princeton University Press, New Jersey, pp 187–213

Wegley L, Yu Y, Breitbart M, Casas V, Kline DI, Rohwer F (2002) Coral-associated Archaea. Mar Ecol Prog Ser 273:89–96

Weil E, Smith G, Gil-Agudelo D (2006) Status and progress in coral reefs disease research. Dis Aquat Organ 69:1–7

Yannarell AC, Steppe TF, Paerl HW (2006) Genetic variance in the composition of two functional groups (Diazotrophs and Cyanobacteria) from a hypersaline microbial mat. Appl Environ Microbiol 72:1207–1217

Yannarell AC, Steppe TF, Paerl HW (2007) Disturbance and recovery of microbial community structure and function following Hurricane Frances. Environ Microbiol 9:576–583.

Yechieli Y, Gavrieli I, Berkowitz B, Ronen D (1998) Will the Dead Sea die? Geology 2:755–758

Yechieli Y, Ronen D, Kaufman A (1996) The source and age of groundwater brines in the Dead Sea area, as deduced from ^{36} Cl and ^{14} C. Geochimica et Cosmochimica Acta 60:1909–1916

Zabielski VP, Neumann C (1990) Field guide to Storrs Lake, San Salvador, Bahamas. In: 5th Symposium on the geology of the Bahamas Bahamian, Field Station, San Salvador, Bahamas, pp 49–57

Zak, I (1997) Evolution of the Dead Sea brines. In: Niemi TM, Ben-Avraham Z, Gat JR (eds) Oxford monographs on geology and geophysics 36. Oxford Press, London, pp 133–144

Microbial Life in Extreme Environments: Linking Geological and Microbiological Processes

Hailiang Dong

Abstract The last decade has seen extraordinary growth of Geomicrobiology, the interdisciplinary field between Geology and Microbiology. Microorganisms have been studied in numerous extreme environments on Earth, ranging from crystalline rocks from the deep subsurface, hypersaline lakes, to dry deserts and deep-ocean hydrothermal vent systems. This chapter reviews several active research frontiers in Geomicrobiology that demonstrate the importance of linking geological and microbiological processes in such studies: deep continental subsurface microbiology, microbial ecology in saline lakes, microbial formation of dolomite, geomicrobiology in dry deserts, fossil DNA and its use in paleoenvironmental reconstruction, and microbial weathering of oceanic crust. The author has no intention to provide a comprehensive review of all areas of Geomicrobiology, as this daunting task deserves a dedicated book on its own.

1 Introduction

The last decade has seen extraordinary growth of Geomicrobiology, the interdisciplinary field between Geology and Microbiology. Microorganisms have been studied in numerous extreme environments on Earth, ranging from crystalline rocks in the deep subsurface, hypersaline lakes on the Tibetan Plateau, to dry deserts in Atacama, Chile and Antarctic, and hydrothermal vent systems in deep oceans. Even signatures of possible ancient life on Mars and other planets are being revealed. In Geomicrobiology, scientists with diverse expertise work together to study how life on this planet interact with geological media (water, minerals, rocks, gases), and how life may have originated and evolved over billions of years.

Since the publication of an important paper "Life in extreme environments" in 2001 by Rothschild and Mancinelli (2001), this field continues to explode as evidenced by many recent books (Banfield et al. 2005; Bull 2004; Castello and Rogers 2005; Fredrickson and Fletcher 2001; Gerday and Glansdorff 2007; Konhauser

H. Dong
Department of Geology, Miami University, Oxford, OH, 45056, USA
e-mail: dongh@muohio.edu

Y. Dilek et al. (eds.), *Links Between Geological Processes, Microbial Activities & Evolution of Life*, © Springer Science+Business Media B.V. 2008

2006; Wilcock et al. 2004) and numerous review papers. Because of the diversity of the topics and rapid developments in this area, it is nearly impossible to write a comprehensive review chapter. Below is a review of some recent advances in certain selected areas. The paper is focused on prokaryotes (Bacteria and Archaea), as the scientific literature on eukaryotic microorganisms is relatively scarce. I hope that this review will promote more focused research in Geomicrobiology, and encourage collaboration among geologists, geochemists, soil scientists, microbiologists, and environmental engineers.

2 Continental Deep-Subsurface Research

Dark life, those microorganisms that exist in the subsurface independent of sunlight, comprises more than 50% of all biomass on Earth, yet many questions remain unanswered. For example, what is the lower limit of the biosphere? What is the energy source for dark life? How does subsurface life evolve in isolation from photosynthesis?

In addition to answering the above questions, investigations of geomicrobiological processes in the continental deep subsurface are driven by a number of theoretical and practical motivations. The theoretical reasons include our curiosity of the origins of life and possible presence of life in the deep subsurface of other planets such as Mars. Because of extreme conditions on the surface of early Earth (for example, intensive UV radiation), life processes on Earth surface would not be possible. It is speculated that life may have originated in the subsurface. Thus, studies of how life survive and function in the modern subsurface may shed some light on the origination of life on early Earth. Likewise, Martian surface conditions are not suitable for life, but life may potentially exist in the subsurface. On the practical ground, microorganisms isolated from the deep subsurface often contain unique assets, and they are ideal for environmental bioremediation, microbially enhanced oil recovery, and biotechnology and bioenergy applications.

The extreme conditions of the deep continental subsurface are typically represented by anaerobic environments, high (>13) or low pH (<1), high temperature ($\sim 120^{\circ}$ C) and pressure, high radiation (from decay of radioactive elements such as K, U, and Th), and high salinity (Rothschild and Mancinelli 2001). These extreme conditions are encountered either through deep drilling or establishment of underground laboratories. Worldwide only a few boleholes have been drilled with various depths. A few example include the Taylorsville Basin in Virginia (~ 3 km below land surface, bls) (Onstott et al. 1998), Cerro Negro drilling in NW New Mexico (200–300 m bls) (Fredrickson et al. 1997), and Chinese Continental Scientific Deep (CCSD) drilling project (5200 m bls) (Zhang et al. 2005; Zhang et al. 2006a). In the CCSD drilling, continuous cores were retrieved from the land surface down to 5200 m. Profiles of porosity, permeability, fluid and gas composition, rock types and structurally weak shear zones are established at high spatial resolution scales (meters). Despite the crystalline nature of the high pressure metamorphic rocks at the CCSD site, there is sufficient pore space to allow microorganisms to

live within them. Gas and fluid anomalies exist at certain depth intervals, and these are potential sites for harboring novel microorganisms. The CCSD site is ideal for addressing important questions such as: what is the bottom limit of the biosphere? Dai et al. (unpublished data) used multiple approaches to define this limit, including DAPI (4′,6-diamidino-2-phenylindole) counts, quantitative PCR (qPCR), phospholipid fatty acid analysis (PLFA), and hydrogenase activity. All these results appear to suggest that ∼4200 m is the lower limit of the biosphere at this site, which corresponds to ∼120° C in temperature.

Deep underground laboratories provide a more direct way to study the deep subsurface biosphere. Although many underground laboratories have been developed worldwide to study particle physics and astrophysics, engineering, and rock mechanics, their utility for biological investigations is a relatively new concept. The Deep Biosphere Laboratory (DBL) at Göteborg University, Sweden, is one of the best and it has been in operation since 1987. The DBL is situated at 450 m depth in the Äspö igneous rock, and various boreholes have explored depths to 1700 m (Pedersen 2001). The research activities of the DBL comprise both basic and applied research about life in various deep geological underground formations. The basic research focuses on biomass, diversity, activity and distribution of subsurface microorganisms, and on the interaction between microbes and metals, especially radionuclides. The applied aspect of the DBL lies at the microbiology of high level nuclear fuel waste disposal and on microbial degradation of hydrocarbon contaminants.

The underground gold mine in South Africa is another well-studied site, where extensive geomicrobiological investigations have been made in the past 8 years. The mine tunnels extend to depths of ∼5 km. Conditions in the mines approach the limits for life (high temperature, salinity, and ambient radiation; low availability of nutrients, energy sources, and water) and novel “extremophiles” are isolated from these environments (DeFlaun et al. 2007; Kieft et al. 2005; Takai et al. 2001; Trimarco et al. 2006). One example is *Geobacillus thermoleovorans* GE-7 that is isolated from pH 8.0, 50° C water from a dripping fracture near the top of an exploration tunnel at 3.2 km depth (DeFlaun et al. 2007). This aerobic, thermophilic, chemoorganotroph shows a strong resistance to gamma radiation (Fig. 1A), and this resistance may be related to its thick cell wall (Fig. 1B).

Readers are directed to recent review papers for comprehensive coverage on deep continental subsurface microbiology (Amend and Teske 2005; Fredrickson and Balkwill 2006; Kieft and Phelps 1997; Parkes and Wellsbury 2004; Pedersen 1997; Pedersen 2000). In light of some most recent developments, I focus on two specific aspects in this review: novel metabolic functions and energy sources.

2.1 Some Metabolic Functions of Continental Subsurface Microorganisms

Because of the unique geochemical, hydrological, and geological conditions of the deep subsurface, microorganisms that inhabit these environments are expected to be

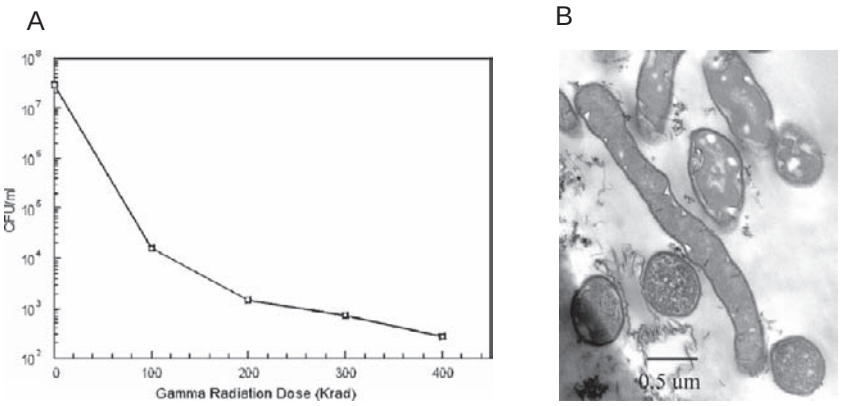

Fig. 1 (**A**) Radiation resistance of Ge-7. After exposure to 400 krad of gamm radiation, 0.001% GE-7 cells survived and were culturable. After DeFlaun et al. (DeFlaun et al. 2007); (**B**) Transmission electron micrograph of GE-7 cells stained with ruthenium red showing thick cell wall which may be related to its strong resistance to gamma radiation

different from surface organisms in their metabolic traits. However, our understanding of these organisms and their metabolic functions is hampered by the difficulty of cultivation. This difficulty is due to multiple reasons, among which our inability to duplicate the subsurface conditions in the laboratory and their slow growth rates are the major ones. Nonetheless, our current knowledge based on culture-independent approach, limited success in cultivation, and isotope geochemistry, and environmental metagenomics, suggests that the subsurface microorganisms are often anaerobic and thermophilic chemolithotrophs that are distinctly different from surface organisms. Specific characteristics of subsurface microorganisms depend on local geological and geochemical conditions. There are generally three categories of continental subsurface environments: subsurface aquifers and/or hydrothermal waters; sedimentary basins/oil reservoirs, and crystalline metamorphic/igneous rocks. Below is a summary of several major metabolic processes that occur in these environments.

2.1.1 Metal Reduction by Thermophilic Microorganisms

Metal reduction by thermophilic organisms is of great interest for a number of reasons. First, metal reduction by thermophilic organisms could have been an important process on early Earth (Vargas et al. 1998). Second, metal-microbe interaction is relevant as we search for life on other planets. For example, magnetite, a possible product of microbial reduction of iron, may be used as a biomarker for extraterrestrial life (Nealson et al. 2002). Third, metal reduction by thermophilic organisms is intimately connected to human life, such as bioremediation of heavy metals and radionuclides in abandoned nuclear facilities and landfill sites.

Thermophilic metal reducers are virtually present in all possible habitats, ranging from sedimentary basins (oil reservoirs) and terrestrial hydrothermal waters to deep subsurface crystalline rocks. They are widely distributed in 15 bacterial and

4 archaeal genera, and most of which are only capable of reducing Fe(III) in either aqueous or chelated form, with a few being able to reduce Fe(III) in crystalline iron oxides (Slobodkin 2005). Magnetite and siderite are usual products depending on specific environmental conditions. Heterotrophy is a dominant metabolic pathway for metal reducers with a few organisms capable of autotrophic growth. Interested readers are directed to a recent review paper (Slobodkin 2005). Most recently, a new anaerobic, thermophilic, facultatively chemolithoautotrophic bacterium is isolated from terrestrial hydrothermal springs that is capable of dissimilatory Fe(III) reduction (Zavarzina et al. 2007). *Thermincola ferriacetica* (Isolate Z-0001) is able to grow chemolithoautotrophically with molecular hydrogen as the only energy substrate, Fe(III) as electron acceptor and CO_2 as the carbon source (Zavarzina et al. 2007). Strain Z-0001T is the first thermophilic bacterium capable of both dissimilatory iron reduction and the anaerobic growth on CO coupled with hydrogen formation.

One interesting feature with certain thermophilic, acidophilic metal reducers is the ability to conserve energy from both Fe(III) reduction and Fe(II) oxidation under different conditions (*Acidimicrobium ferrooxidans*, *Sulfobacillus thermosulfidooxidans*, *Sulfobacillus acidophilus*) (Bridge and Johnson 1998). These organisms are capable of iron redox cycling when they are grown in batch cultures. Zhang et al. (2007) recently observed iron cycling with a neutrophilic thermophile (Fig. 2). Initially, it was thought that iron redox cycling was carried out by a mixed culture, however, iron cycling persisted after multiple transfers and isolation. The reduction of Fe(III) in iron oxides and clay minerals and oxidation of Fe(II) in iron sulfides operated at different pH conditions, with slightly acidic pH favoring Fe(III) reduction, and alkaline pH favoring Fe(II) oxidation. Lactate served as an electron donor during Fe(III) reduction and acetate was believed to be the electron acceptor during Fe(II) oxidation. Acetate as a possible electron acceptor is consistent with a previous observation that acetate is necessary to oxidize Fe(II) (Kappler and Newman 2004). Molecular analysis identified a single organism (*Thermoanaerobacter ethanolicus*) that may be responsible for both Fe(III) reduction and Fe(II) oxidation. However, further work is necessary to confirm these data.

2.1.2 Organic Carbon Degradation by Heterotrophic and Fermentative Organisms

In petroleum reservoirs or groundwater aquifers within sedimentary rocks, because of availability of abundant organic matter, subsurface organisms are generally characterized by organotrophic thermophiles/hyperthermophiles. Magot et al. (2004) and Van Hamme et al. (2003) reviewed the current state of knowledge of microorganisms from petroleum reservoirs, including mesophilic and thermophilic sulfate-reducing bacteria (SRB), methanogens, mesophilic and thermophilic fermentative bacteria, and iron-reducing bacteria. Many of these organisms can degrade sedimentary organic carbon (Krumholz et al. 1997; McMahon and Chapelle 1991) and oil components as energy and carbon sources. Among major groups of organisms identified (*Thermoanaerobacter*, *Thermodesulfovibrio*, *Thermotoga*,

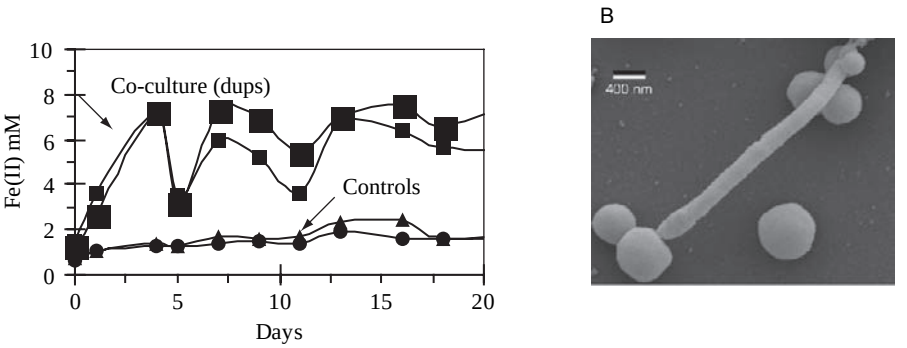

Fig. 2 Left: 0.5 N HCl extractable Fe(II) with time showing Fe reduction-oxidation cycles in clay mineral nontronite (23.4% structural Fe(III)) inoculated with a co-culture (mixture of rods and cocci) at pH 9.5. The no-cell controls do not show significant change in Fe(II) concentration. **Right**: SEM image showing a close association between rod-shaped and coccus-shaped cells. The scale bar is 400 nm. From Zhang et al. (2007)

Thermococcus, *Methanothermobacter*, *Methanococcus*, and *Methanobacterium* (Nazina et al. 2000; Orphan et al. 2000), SRB and methanogenic archaea are abundant. Thermophilic SRB are mainly various species of *Desulfotomaculum*, *Thermodesulforhabdus*, and *Desulfacinum* (Amend and Teske 2005).

In petroleum reservoirs, abundant organic compounds provide growth substrates for these heterotrophic sulfate reducers. In a recent study, Cai et al. (2007) reported that SRB are capable of coupling U(VI) reduction with oxidation of petroleum compounds with implication for a microbial role in uranium ore deposit formation in the Shashadetai deposit, the northern Ordos basin, NW China.

In sedimentary basins without petroleum reservoir, microorganisms, which live in highly-permeable sandstones, actually depend on organic materials from adjacent shales for growth (Krumholz et al. 1999; Krumholz et al. 1997). The interface between aquifer (high permeability) and aquitard (low permeability) appears to be the most important location for a number of important biogeochemical reactions including sulfate reduction (McMahon 2001). More recently, several thermophilic and hyperthermophilic SRB have been isolated, mainly in hydrothermal springs (Kaksonen et al. 2006; Kaksonen et al. 2007; Thevenieau et al. 2007). Because of more oligotrophic nature in these springs, SRB are typically capable of autotrophic growth with H_2 as an electron donor and CO_2 as a carbon source.

2.1.3 Sulfur Oxidation

In geothermal vents, solfataras, and hot springs, reduced sulfur compounds may be more important electron donors than organic carbon compounds. These environments often contain high concentrations of inorganic compounds such as CO_2, SO_2, N_2, CO, H_2, nitrate, and various metal oxides and sulfides (H_2S). As a result, the primary production of biomass is energized by chemolithoautotrophic redox reactions of these inorganic compounds. Synthesized biomass may be oxidized by

heterotrophic organisms. Among chemolithoautotrophs, oxidizers of sulfur compounds coupled with reduction of nitrate and oxygen are commonly isolated (Aragno 1992; France et al. 2006; Skirnisdottir et al. 2001), as elemental sulfur and sulfur compounds can serve as both electron acceptors and donors and are used by a number of microorganisms for growth.

The pathways and biochemistry of thermophilic, sulfur-oxidizing prokaryotes have been recently reviewed (Friedrich et al. 2005; Kletzin et al. 2004). Most archaeal sulfur oxidizers are aerobic or facultatively anaerobic, chemolithoautotrophic, thermoacidophilic, with *Acidianus ambivalens*, *A. infernos*, and *A. brierleyi* from the *Sulfolobales* order of the *Crenarchaeota* kingdom as representative organisms. Some of the *Sulfolobales* are facultative anaerobes growing either by hydrogen oxidation with S_0 as electron acceptor, forming H_2S, or by S_0 oxidation with oxygen, forming sulfuric acid. In the sulfur-oxidizing organisms, the cytoplasmic sulfur oxygenase reductase (SOR) catalyzes the conversion of sulfur in the presence of O_2 to give sulfite, thiosulfate and hydrogen sulfide as products (Friedrich et al. 2005).

Because geothermal fields are commonly rich in inorganic reduced sulfur compounds and, therefore, they are particularly suited for thermophilic sulfur-oxidizing bacteria (Aragno 1992; Ehrlich 2005; Friedrich 1998). However, relatively few thermophilic sulfur-oxidizing bacterial species have been isolated. Aragno (1992) divides sulfur-oxidizing thermophiles in the domain *Bacteria* into four main categories according to their metabolism. The first group contains hydrogen- and sulfur-oxidizing bacteria. Among this group are obligate chemolithoautotrophic bacteria in the *Aquifex-Hydrogenobacter* group and the spore-forming facultative chemolithoautotroph *Bacillus schlegelii*. The second group contains two *Thermothrix* species, strictly thermophilic sulfur oxidizers. The third category includes moderately thermophilic, acidophilic *Thiobacillus*-like bacteria. The fourth category includes moderately thermophilic, strongly acidophilic sulfur- and iron-oxidizing bacteria (Aragno 1992). Chemolithoautotrophic sulfur bacteria are diverse and are either alkaliphilic (Banciu et al. 2005; Sorokin et al. 2003), neutrophilic, or acidophilic (Friedrich 1998; Kelly et al. 1997; Lueders et al. 2001).

2.2 Energy Sources

The extent of deep continental subsurface microbial life is ultimately controlled by whether sufficient energy exists to sustain a minimal metabolism. Chemolithotrophic communities depend on geochemical energies for growth. H_2 is the most abundant source (Chapelle et al. 2002; Pedersen 2001; Stevens and McKinley 1995) and a variety of organisms can use H_2, including nitrate reducers, Mn (III) and Fe(III) reducers, sulfate reducers, and methanogens. A substantial amount of energy is generated when H_2 oxidation is coupled with these various electron acceptors (Amend and Teske 2005). The high diffusivity of H_2 makes it readily available to microorganisms in confined pore spaces in the deep subsurface.

There are multiple mechanisms for production of H_2 in the deep subsurface. The first two pathways are thermal decomposition and fermentation of organic

matter, respectively (Chapelle 2000). The third pathway is via reactions between ultramafic/mafic rocks and fluids, a process called serpentinization. Interest in studying the serpentinization process has been increasing in the recent years. This process can produce strongly reducing condition and high H_2 concentration. The H_2, CH_4, and other reduced compounds generated during this process may represent a substantial and widespread source of chemical energy for carbon fixation by autotrophic microbial communities in both surface and subsurface environments (Alt and Shanks 1998; Chapelle et al. 2002; Charlou et al. 2002; Charlou et al. 1998; Kelley et al. 2001; Kelley et al. 2005; Nealson et al. 2005; Sleep et al. 2004; Stevens and McKinley 1995). Because such ecosystems exist with no input from the sun, they could represent a significant source of primary biomass production in the subsurface. Such communities may be modern analogs of ancient communities that were present on the early Earth or existed on Mars and Europa (Fisk and Giovannoni 1999; Holm and Andersson 1998; McCollom et al. 1999; Shock 1997; Sleep et al. 2004; Zolotov and Shock 2004). Because of abundance of both H_2 and CO_2 during the serpentinization process, methanogens are usually the dominant organisms in the community (Chapelle et al. 2002; Stevens and McKinley 1995; Takai et al. 2004).

The strongly reducing conditions developed during the serpentinization process also favor abiotic synthesis of methane and other organic compounds from the reduction of CO_2, suggesting that serpentinites and the fluids discharging from them may be enriched in abiotically synthesized organic compounds (Abrajano et al. 1990; Berndt et al. 1996; Charlou and Donval 1993; Charlou et al. 2002; Charlou et al. 1998; Holm and Andersson 1998; Holm and Charlou 2001; Horita and Berndt 1999; McCollom and Seewald 2001; McCollom and Seewald 2003; McCollom and Seewald 2006; Shock and Schulte 1998). These organic compounds provide additional chemical energy for microorganisms in subsurface and hydrothermal environments, and may have been a primary source of prebiotic compounds during the early evolution of life (Holm and Andersson 1998; Russell 2003; Russell et al. 1998; Shock 1990; Shock and Schulte 1998). A variety of heterotrophic organisms could depend on abiotically synthesized organic compounds.

A few recent studies have strongly demonstrated the fourth pathway for H_2 generation in the continental subsurface, i.e., radiolytic H_2 production. In this pathway, H_2 is produced by radiolytic dissociation of H_2O during radioactive decay of U, Th, and K in the host rocks (Lin et al. 2005). This radiolytic H_2 is consumed by methanogens and abiotic hydrocarbon synthesis. Lin et al. (2005) demonstrated that this abiotic source of H_2 is sufficient to account for high concentrations of H_2 and to sustain the lithoautotrophic communities detected in fracture water of the deep mines of South Africa (Lin et al. 2007). Analysis of gases in crystalline igneous rocks from South Africa and Canada (Heidelberg et al. 2004; Lollar et al. 2006) has shown that these gases are composed predominantly of H_2 and CH_4 with some fractions of light hydrocarbons. The isotopic and chemical composition appears to suggest that they are a mixture of abiotic hydrocarbons and biotic CH_4 produced from methanogenic microbes utilizing the radiolytic H_2. In such settings, radiolytic H_2 may be the predominant source powering the deep subsurface microbial communities (Lin et al. 2005; Lin et al. 2007).

3 Saline Environments

Saline environments are globally distributed on Earth (Oren 2002b) and they are considered extreme environments for microbial life (Oren 1999). Although the oceans are the largest saline water bodies, hypersaline environments are generally defined as those containing salt concentrations in excess of sea water (3.5% total dissolved salts). A variety of hapersaline environments have been surveyed for microbial diversity such as the Great Salt Lake in Utah, the Great Salt Plains of Oklahoma, the Dead Sea, the Mediterranean Sea, the Solar Lake in Sinai, Egypt, Antarctic hypersaline lakes, deep-sea brine sediments, and various salterns (salt-recovering ponds) (DasSarma and Arora 2001). Hypersaline lakes fall into two categories: thalassohaline and athalassohaline. Thalassohaline lakes are those that originated by evaporation of seawater with Na^+ and Cl^- as the dominant ions. An example is the Great Salt lake in the Western United States. Athalassohaline lakes are derived from evaporation of freshwater that have ionic compositions different from that of sea water. Examples include soda lakes that contain high concentrations of carbonate and bicarbonate and an alkaline pH, but are depleted in Mg^{2+} and Ca^{2+}. The Dead Sea is an example, and it is slightly alkaline with higher concentrations of Mg^{2+} and Ca^{2+} than Na^+ and K^+.

Tibet is Earth's largest and highest plateau, and is often referred to as the roof of the world. Occupying an area of 2.3 million km^2 and rising 4000 m above sea level (Zheng and Yao 2004), it is one of the most sensitive areas to global climate change. The Tibetan Plateau is a unique place in the world that has developed thousands of lakes, most of which are saline or hypersaline (Fig. 3). As a result of uplift of the plateau from intercontinental convergence between India and the Asia continent tens of millions of years ago, atmospheric circulation underwent repeated vertical and horizontal changes. These climatic changes caused variations

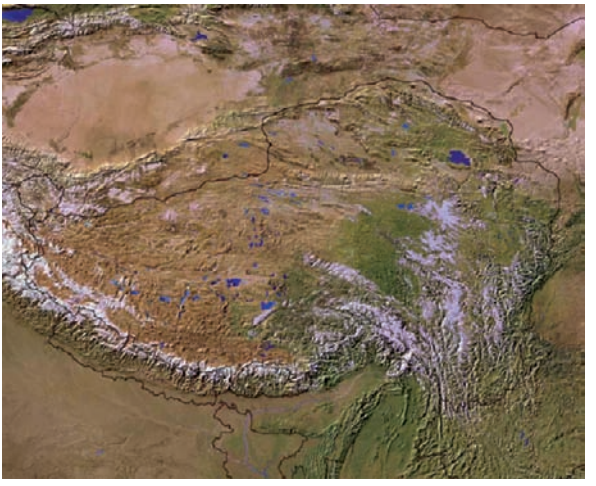

Fig. 3 Topography of the Tibetan Plateau and distribution of lakes (*in blue*). The largest one is Qinghai Lake, with the longest dimension of 106 km (lake area 4635 km^2)

in salinity of waters in the lake basins, the nature of sediments deposited, and the formation of numerous glacial lakes and the general evolution of lake basins (Zheng 1995). The total lake area is 4.5×10^4 km^2. The ages of the lakes are on the order of 2–8 millions (Zheng and Yao 2004; Zheng 1995). Available data suggest that some lakes have developed high salinity over a time scale of a few tens of thousands of years, mostly because of prolonged arid climate (Liu et al. 2007a; Liu et al. 2007b; Shen et al. 2005). Because the Tibetan lakes are at various stages of evolution (evaporation), they possess multiple environmental gradients such as salinity (from 0.1 to 426.3 g/L) and pH (5.4–9.8). Lake water chemistry are dominated by cations Na^+, K^+, Ca^{2+}, and Mg^{2+}, and anions Cl^-, SO_4^{2-}, CO_3^{2-}, and HCO_3^-. Boron concentrations (B_2O_3) can reach as high as 8000 mg/L and boron is mined in certain places.

Microbiological investigations have been made in various saline lakes for multiple reasons. First, biotechnological applications of halophilic microorganisms were recognized and employed even centuries ago, with a recently renewed interest (Oren 2002a). Potential exists to find novel applications with more in-depth research. Second, because of the presence of salt deposits and saline environments on Mars (Gendrin et al. 2005; Langevin et al. 2005; Squyres et al. 2004), studies of microbial diversity in terrestrial saline environments may shed light on the forms of extinct and/or extant life on Mars (Mancinelli et al. 2004). Third, primordial life on Earth might have started in hypersaline environments (Dundas 1998; Knauth 1998), thus research on microbial survivability and adaptation in saline environments bears relevance to our understanding of the early evolution of the biosphere on Earth.

Halotolerant and halophiles thrive in saline and hypersaline environments and include both prokaryotes and eukaryotes (DasSarma and Arora 2001). Among halophilic microorganisms are found a variety of heterotrophic and methanogenic archaea; photosynthetic, lithotrophic, and heterotrophic bacteria; and photosynthetic and heterotrophic eukaryotes. Previous studies have shown that the taxonomic diversity of microbial populations in terrestrial saline and hypersaline environments is low (DasSarma and Arora 2001; Oren 2001) and that, in general, microbial diversity decreases with increased salinity (Jiang et al. 2007b; Oren 2002a).

Halophilic microorganisms occur in a variety of shapes, sizes, and colors. Their surface tends to be rough with abundant appendages (flagella etc.) (Fig. 4). Some halophiles are extremely resistant to UV and gamma-radiation, such as *Halobacterium NRC-1* (Baliga et al. 2004; Kottemann et al. 2005), although the halophilic nature is not necessarily linked to the UV/gamma radiation resistance. It is interesting to note that halophiles isolated from the Tibetan lakes show extreme stress resistance (Jiang et al. 2006), including UV and gamma radiation (Fig. 5) and antibiotics (Jiang et al. unpublished data). It is not yet clear if the elevation of the Tibetan lakes preferentially select UV and gamma radiation resistant organisms.

A few books are dedicated to the ecology and biogeochemistry of halotolerant and halophilic microorganisms (Kushner 1993; Oren 1999; Ventosa 2004; Vreeland and Hochstein 1993). Here I review a few important topics in this area.

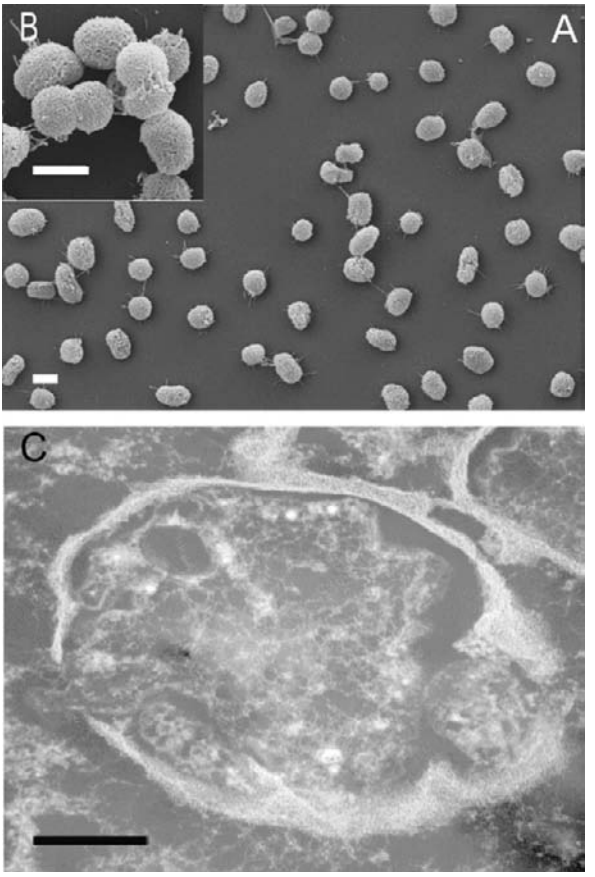

Fig. 4 **A** and **B**: Secondary electron image of a halophilic archaeal isolate 15N. The scale bar is 2 μm; **C**: Transmission electron image showing thick cell wall of this Gram-positive archaeon

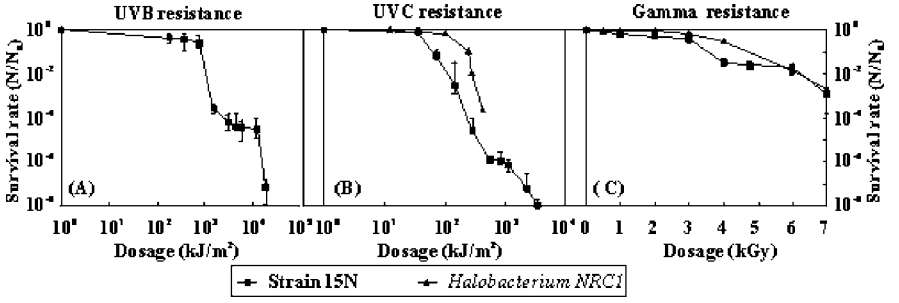

Fig. 5 Comparison of survival rate between 15N (*solid squares*) and *Halobacterium* NRC-1 (*solid triangles*) following ultraviolet light and gamma radiation. (**A**) UVB (312 nm) radiation. (**B**) UVC (254 nm) radiation. (**C**) ^{60}Co gamma radiation. N = number of viable cells after radiation; No = the initial number of viable cells in unradiated sample; Error bars represent standard errors from duplicate experiments. From Jiang et al. (unpublished data)

3.1 Effect of Salinity on Microbial Composition

Previous studies have shown that the taxonomic diversity of microbial populations in saline and hypersaline environments is low (Benlloch et al. 2002; DasSarma and Arora 2001; Oren 2001), consistent with general ecological principles that more extreme environments are inhabited by less diverse communities (Frontier 1985). In saline environments, microbial composition is primarily controlled by salinity (Oren 2002a; Wu et al. 2006). Wu et al. (2006) studied bacterioplankton (free-living) community composition along a salinity gradient of high-mountain lakes located on the Tibetan Plateau, China and reported succession of proteobacterial groups as a function of salinity. With increasing salinity, the relative abundance of the *Alphaproteobacteria* and the *Gammaproteobacteria* increases, but the *Betaproteobacteria* decreases. This observation is consistent with many other studies on inland waters (Bockelmann et al. 2000; Brummer et al. 2000; Glockner et al. 1999), dynamic saline systems such as estuaries (Bouvier and del Giorgio 2002; Cottrell and Kirchman 2003; Crump et al. 1999; del Giorgio and Bouvier 2002; Henriques et al. 2006; Kirchman et al. 2005; Zhang et al. 2006b) and costal solar salterns (Benlloch et al. 2002). Henriques et al. (Henriques et al. 2006) examined successions of multiple groups of bacteria and reported dominance of the *Alphaproteobacteria* and *Gammaproteobacteria* in the marine-brackish section of the Ria de Aveiro estuary (Portugal) and the *Betaproteobacteria*, the *Deltaproteobacteria* and the *Epsilonproteobacteria* in the freshwater section of the estuary. The reasons for such succession have been suggested to be related to cell inactivation/death due to dynamic hydrological conditions such as mixing of riverine and estuarine waters (Bouvier and del Giorgio 2002), but observed successions in stable water bodies appear to suggest that dynamic mixing is not necessarily a pre-condition (Wu et al. 2006). Other studies have shown different succession patterns with increased salinity. For example, Langenheder et al. (2003) showed that the *Alpha-* and *Betaproteobacteria*, and *Gammaproteobacteria* were more abundant under freshwater conditions. Bernhard et al. (2005) analyzed bacterioplankton community structure in Tillamook Bay, Oregon and its tributaries to evaluate phylogenetic variability and its relation to changes in environmental conditions along an esturine gradient. The authors observed that the *Gammaproteobacteria* and *Betaproteobacteria* and members of the *Bacteroidetes* dominated in freshwater samples, while the *Alphaproteobacteria*, *Cyanobacteria* and chloroplast genes dominated in marine samples. When bacteria are attached to solid particles, such successions are generally not observed (Jiang et al. 2007b; Selje and Simon 2003). Indeed, particle-attached and free-living bacterial community composition is fundamentally different (Acinas et al. 1999; Crump et al. 1999; DeLong et al. 1993; Phillips et al. 1999; Schweitzer et al. 2001).

3.2 Strategy of Microbial Adaptation to High Salinity

With increasing salinity, bacterial abundance decreases, but archaeal abundance increases (Jiang et al. 2007b). Most halophilic bacteria can only live at moderate

salinity up to 2.5 M salt concentrations (Ventosa et al. 1998), but halophilic archaea can survive up to salt saturation. Because of their different requirements for salt, halophilic bacteria and archaea tend to occupy different salinity niches with the former being dominant at low salinity and the latter being dominant at high salinity (Oren 1993). However, most halophilic species exist and function within a range of salinity. Within this range, adaptation to increase in salinity is achieved in different ways. The first (and the most important) one involves the accumulation of organic compatible solutes within cytoplasm without the need for change of intracellular proteins (thus called compatible). This mechanism, referred to as "organic-osmolyte strategy", is widespread among the domain *Bacteria* and *Eukarya* and some methanogenic *Archaea*. The major solutes are the amino acid derivatives glycine-betaine and ectoine (Galinski and Truper 1994). The genes encoding the enzymes for biosynthesis of these solutes have been isolated and sequenced. The second adaptation mechanism is the intracellular accumulation of high concentration of K^+. This strategy, referred to as "salt-in-cytoplasm strategy", requires extensive adaptation of the intracellular enzymatic machinery and therefore energetically expensive. This mechanism is used by a minority of the known halophiles, including *Halobacteriales* of the domain *Archaea* and *Haloanaerobiales* of the domain *Bacteria*.

3.3 Metabolic Processes in Saline Environments

There are a variety of metabolic processes in saline environments (Oren 2001). Here we summarize some recent advances in a few examples.

3.3.1 Ammonia Oxidation

Ammonia-oxidizing bacteria (AOB) are chemolithoautotrophs that use ammonia as the sole energy source and carbon dioxide as the carbon source. AOB catalyze the "nitrification process" ($NH_3 \rightarrow NO_2^- \rightarrow NO_3^-$), which has a key position in natural nitrogen cycling. Ammonia oxidation takes place either aerobically or anaerobically. Different AOB tend to occupy different environmental niches and respond to environmental changes (ammonium concentration, pH, redox state, and salinity) in a different way (Prosser and Embley 2002). In estuary and coastal environments, AOB respond to freshwater-marine salinity gradient and nitrogen inputs (among others) through changes in community composition and abundance (Francis et al. 2003; Freitag et al. 2006; Urakawa et al. 2006).

Energetic considerations suggest that aerobic autotrophic ammonia oxidation is not a favorable process in highly saline environments, because nitrifying bacteria gain little energy from oxidation of ammonium and nitrite, and a large fraction of generated energy has to be used to produce NADPH required for autotrophic CO_2 reduction (Oren 2001). Oren (2001) estimated that ammonia oxidation can exist at salinity up to ~16%. This consideration appears to explain the salt tolerance of AOB in pure cultures (0.6–11% salt with *Nitrosococcus halophilus* being the

most halophilic at 11% salt) (Koops et al. 2004) and in the saline Mono Lake in California (8.8% salinity, pH 9.8, ammonia concentration 0–30 μmol/L) (Joye et al. 1999; Ward et al. 2000). Using molecular techniques, AOB have been detected in various saline environments including some that have higher salinity than 16%, such as saline lakes in Antarctic and Greenland (salinity up to 10 times seawater) (Voytek et al. 1999), saline and alkaline lakes in Mongolia (up to 6 % salinity and pH 10) (Sorokin and Kuenen 2005), Negev desert soils (nitrification at 2.3 % salinity) (Nejidat 2005), salt saltern (up to 22% salinity) (Benlloch et al. 2002), and estuaries (Francis et al. 2003; Freitag et al. 2006). The members of the *Gammaproteobacteria* (*Nitrosococcus*) appear to be present only in saline lakes (Ward and O'Mullan 2005).

Recent molecular studies have discovered that ammonia oxidation can also be carried out by nonthermophilic crenarchaeota (Beman and Francis 2006; Francis 2007; Francis et al. 2005; Konneke et al. 2005; Mincer et al. 2007; Nicol and Schleper 2006; Park et al. 2006; Schleper et al. 2005; Treusch et al. 2005; Venter et al. 2004). A marine chemolithoautotrophic strain was isolated from a sea aquarium that uses ammonia as a sole energy source (Konneke et al. 2005). Archaeal ammonia oxidation has been shown to be an important process in a wide variety of natural environments including oceans (Coolen et al. 2007a; Francis et al. 2005; Mincer et al. 2007; Wuchter et al. 2006), marine and freshwater sediments (Beman and Francis 2006; Francis et al. 2005), soils (He et al. 2007; Leininger et al. 2006), and wastewater treatment bioreactors (Park et al. 2006). Further studies have shown that ammonia oxidizing archaea (AOA) are more abundant than their bacterial counterparts in certain soils (Leininger et al. 2006) and oceans (Mincer et al. 2007; Wuchter et al. 2006). These studies are largely based on quantitative polymerase chain reaction (qPCR) of *amoA*, a gene encoding the alpha-subunit of ammonia monooxygenase (the enzyme responsible for catalyzing the rate-limiting step in ammonia oxidation).

These exciting new discoveries have challenged the accepted view of microorganisms involved in the global nitrogen cycle, and have created ample opportunities for future research (Francis 2007; Nicol and Schleper 2006). Are AOA more abundant than AOB in other environments (such as lakes)? Are AOA more active than AOB (i.e., RNA-based approach)? How do AOA and AOB differentially respond to environmental changes, such as salinity, ammonia concentration and pH? How do AOA and AOB each contribute to the overall nitrification rate under different environmental conditions? The freshwater and saline lakes on the Titeban Plateau, NW China, are ideal for answering these important questions: (1) These lakes represent pristine environments, where perturbations from human activities have been minimal, allowing a focused study of natural (not anthropogenic) ammonia oxidation processes; (2) These lakes possess multiple environmental gradients such as salinity (from 0.1 to 426.3 g/L), pH (5.4–9.8), and ammonium concentration (a range but typically at <1 μM), allowing studies of environmental impacts on aerobic nitrifiers; (3) High elevation, dry climate, and closed basins of the lakes allow development of stable microbial communities and metabolic functions so that the effects of environmental conditions on the AOA/AOB community structure and functions can be discerned (Dong et al. 2006).

3.3.2 Chemolithotrophic Oxidation of Sulfur Compounds

Although chemolithoautotrophic sulfur-oxidizing bacteria (SOB) have been well studied in acidic (Madigan et al. 2004; Pronk et al. 1990) and neutral environments (Robertson and Kuenen 1999), the presence of this group in saline environments is not well understood. In the last decade, Sorokin and his co-workers have isolated a number of haloalkaliphilic SOB functioning at pH > 9.5 and inhabiting various saline soda lakes (sodium carbonate/bicarbonate instead of NaCl) of varying salinity, mostly in Central Asia (Sorokin and Kuenen 2005). These authors described three new genera in the *Gammaproteobacteria*: *Thioalkalimicrobium*, *Thioalkalivibrio*, and *Thioalkaspira*. Many species within these genera have an optimal pH of 9–10 and can tolerate a total NaCl concentration of up to 4.5 M. They are capable of autotrophically oxidize a number of sulfur compounds such as thiosulfate, sulfide, polysulfide, elemental sulfur, and sulfite. While most of these species are obligately aerobic, some can oxidize these compounds under microaerophilic and denitrifying conditions. The same authors, also using cultivation-based methods, have isolated a high diversity of moderately and extremely halophilic chemolithoautotrophic SOB in various hypersaline, but neutral-pH habitats, including four new genera and representatives of *Halothiobacillus* and *Thiomicrospira* (Sorokin et al. 2006a; Sorokin et al. 2006b). The highest NaCl concentration that some of species can tolerate is 5 M. Despite these recent advances in isolation and characterization of SOB, quantitative understanding of the importance of these organisms in the overall sulfur cycle is still lacking, especially in saline environments. Future studies should focus on measurements of rates of sulfur oxidation by various SOB species under in-situ conditions.

3.3.3 Sulfate Reduction

Sulfate-reducing bacteria (SRB) have been shown to use organic solutes (trehalose and glycine betaine) to provide osmotic balance in saline environments (Welsh et al. 1996). This is energetically expensive. In contrast to this demand, little energy is released when acetate is used as electron donor to couple with sulfate reduction (Oren 2001). When H_2 and lactate are used as electron donors, more energy is released (Oren 2001). This consideration explains why most SRB have an optimal salinity of no higher than 100 g/L, although the upper limit may be much higher (Belyakova et al. 2006; Jakobsen et al. 2006). In general, sulfate-reducing rate is inversely correlated with salinity (Brambilla et al. 2001; Kerkar and Bharathi 2007; Sorensen et al. 2005). A recent study reported that sulfate-reducing acitivity is optimal between a salinity of 6–12%. At 25% salinity when salt saturation begins, sulfate-reducing activity does not stop but becomes retarded untill 35%, after which it is almost negligible (Kerkar and Bharathi 2007).

4 Biogenic Formation of Dolomite

Dolomite, with a chemical composition of $[CaMg(CO_3)_2]$ and an ordered structure, is an important mineral both economically and scientifically. The physical and

chemical properties of dolomite rocks in sedimentary basins determine the size and quality of oil reservoirs. Dolomite formation plays an important role in global carbon cycling. Sequestration of the atmospheric CO_2 into dolomite may have partially contributed to gradual cooling of the Earth to the extent that life became possible. Dolomite may contain valuable information about the evolutionary history of the Earth.

Despite the economic and scientific importance of dolomite, the mechanism of its formation remains enigmatic. The well known "dolomite problem" can be stated: dolomite rock is one of the most common sedimentary materials, yet efforts to synthesize dolomite in the laboratory under simulated conditions (i.e., low temperature and pressure) have largely failed (Land 1998). Dolomite formation is thermodynamically favorable, but kinetically slow, i.e., there exists a kinetic energy barrier in its formation (Krauskopf and Bird 1995).

Dolomite can form via the following three pathways:

Table 1 Possible pathways for dolomite formation

Mechanism	Reaction	Ca	Mg	Sr	Mg/Ca	Sr/Ca	Case study
Replacive	$CaCO_3 + Mg^{2+} + 2HCO_3^- \rightarrow CaMg(CO_3)_2 + CO_2 + H_2O$	—	↓	↑	↓	↑	(Baker and Burns 1985)
Replacive	$2CaCO_3 + Mg^{2+} \rightarrow CaMg(CO_3)_2 + Ca^{2+}$	↑	↓	↑	↓	↑	(Kastner et al. 1990)
Primary	$Ca^{2+} + Mg^{2+} + 4HCO_3^- \rightarrow CaMg(CO_3)_2 + 2CO_2 + 2H_2O$	↓	↓	↓	↑	↑	(Wright and Wacey 2005)

After (Rodriguez et al. 2000).

↑= increases in aqueous concentration, ↓= decreases in concentration. — = no change in concentration.

The relative decrease or increase in Ca and Mg is obvious from the reactions. Sr substitutes for Ca more easily than Mg. Thus, Sr is released to solution when calcite is replaced by dolomite (reaction 1 & 2).

Geological observations (i.e., poor preservation of fossils, the coarseness of grains, cavities, and pore spaces) indicate that many dolomite rocks form via replacement of pre-existing calcite (Reaction 1 and 2) over a long time under conditions of high salinity and pH, a low Ca/Mg ratio, and an elevated temperature (Krauskopf and Bird 1995). Dolomite can also form via primary precipitation from aqueous solution (Reaction 3), especially for those dolomites that are associated with saline evaporite deposits (Vasconcelos and McKenzie 1997; Wright 1999; Wright and Oren 2005; Wright and Wacey 2005) and methane-bearing sediments and gas hydrates on ocean floor (Baker and Burns 1985; Cavagna et al. 1999; Pierre and Rouchy 2004; Rodriguez et al. 2000; Sassen et al. 2004). However, neither the replacement nor direct precipitation mechanism has been rigorously demonstrated in the laboratory at low temperatures in the absence of microbial activity.

The recent discovery of microbially mediated dolomite formation in culture experiments with sulfate reducing bacteria (SRB) suggests that bacteria can overcome the kinetic energy barrier to dolomite formation by increasing pH and carbonate alkalinity (Vasconcelos et al. 1995; Warthman et al. 2000) and by removing sulfate, a known inhibitor to homogeneous nucleation of dolomite in solution (Baker and

Kastner 1981). SRB may be important in mediating dolomite precipitation in nature, such as modern saline lakes and lagoons (Vasconcelos and McKenzie 1997; Wright 1999; Wright and Oren 2005; Wright and Wacey 2005). Among these, dolomites in the distal ephemeral lakes of the Coorong Region of South Australia are probably the best studied example. The role of SRB in dolomite precipitation in these lakes has been demonstrated with a combination of mineralogical, geochemical, isotopic, and microbial studies in both laboratory and in the field (Wacey et al. 2007; Wright 1999; Wright and Wacey 2005; Wright and Wacey 2007). One halophilic SRB that can promote dolomite precipitation has recently been isolated from a hypersaline coastal lagoon, Lagoa Vermelha, Rio de Janeiro, Brazil (Warthmann et al. 2005). Some halophilic bacteria can precipitate dolomite even in the presence of sulfate (Sanchez-Roman et al. 2005) and they may account for primary precipitation of dolomite in modern hypersaline environments. Methanogens may also be important in mediating dolomite precipitation (Roberts et al. 2004). These results collectively suggest that SRB, halophiles, and methanogens all play an important role in dolomite formation, especially in saline environments.

Gas hydrate and methane-seep deposits in deep oceans are the largest potential fossil fuel reservoir on Earth, and they play an important role in regulating global carbon cycle. Formation of dolomite in these environments is globally significant, both in modern (Aloisi et al. 2000; Formolo et al. 2004; Greinert et al. 2001; Kulm and Suess 1990; Roberts and Aharon 1994; Rodriguez et al. 2000; Sample and Reid 1998; Sassen et al. 2004; Stakes et al. 1999; vonRad et al. 1996) and ancient (Cavagna et al. 1999; Jorgensen 1992; Peckmann et al. 2001; Peckmann and Thiel 2004; Peckmann et al. 1999; Pierre and Rouchy 2004; Terzi et al. 1994) methane seeps and gas hydrate deposits. Multiple studies have published negative $\delta^{13}C$ values of authigenic dolomite associated with these deposits (Aloisi et al. 2000; Campbell et al. 2002; Greinert et al. 2001; Peckmann et al. 2001; Pierre and Rouchy 2004; Roberts and Aharon 1994; Sample and Reid 1998; Sassen et al. 2004; Stakes et al. 1999), implying that dolomite may be formed by microbial oxidation of methane or organic matter coupled with sulfate reduction (Mazzullo 2000). A recent study shows that dolomite formation in organic-rich marine sediments is controlled in part by competition between anaerobic methane oxidation and methanogenesis, which controls the speciation of dissolved CO_2. Anaerobic methane oxidation (AMO) increases the concentration of CO_3^{2-} through sulfate reduction, favoring dolomite formation, while methanogenesis increases the pCO_2 of the pore waters, inhibiting dolomite formation (Moore et al. 2004). However, a direct link between a microbial function and dolomite formation pathways has not been established for important carbon reservoirs such as gas hydrate and methane seep deposits. Moreover, dolomite formation under the in-situ conditions of gas hydrate deposits (i.e., in-situ pressure, temperature and water chemistry) has not been attempted.

5 Dry Deserts

Deserts are defined as areas that receive an average annual precipitation of less than 250 mm. Deserts and arid lands cover approximately one-third of the Earth's total

land surface, making them important ecosystems worldwide. Extreme deserts are found in both temperate and polar regions, such as Chile (Atacama Desert), the US (Mojave Desert), Antarctica, the Arctic and western China (e.g. Tibet, Taklimakan Desert).

Photosynthetic cyanobacteria are the primary inhabitants in these environments (Wynn-Williams 2000). These primary producers typically live a few millimeters below the surface of translucent rocks, such as quartz (Schlesinger et al. 2003; Warren-Rhodes et al. 2007; Warren-Rhodes et al. 2006), sandstone pebbles (Wynn-Williams 2000); halite (Wierzchos et al. 2006), and gypsum (Dong et al. 2007) (Fig. 6). This micro-habitat is apparently achieved as a result of balance between a sufficient supply of CO_2, N_2 and light to allow photosynthesis and N_2 fixation on one hand (Rothschild et al. 1994) and protection from intolerable levels of irradiation, high temperature, and arid surface condition (Cockell et al. 2005) on the other. Even 1 mm of rock matrix could provide sufficient shielding effect of UV-radiation (Cockell et al. 2005) to allow photosynthesis to proceed. Douglas and Yang (2002) found different types of cyanobacteria colonizing gypsum, bassanite ($2CaSO_4 \cdot (H_2O)$), and halite in distinct layers of color in an evaporite deposit from Death Valley, California, USA. From top down, the color changes from uncolonized, to orange-brown, to blue-green, and finally purple. This color change reflects different cyanobacterial community composition and suggests that different phototrophic communities may have different demand for water moisture and tolerance of UV radiation.

The distribution of cyanobacterial communities in desert pavements is not uniform, but instead in patches (Warren-Rhodes et al. 2007). The inter-site (from one desert site to another) differences in cyanobacterial spatial distribution pattern (e.g. mean inter-patch distance) are linked with mean annual precipitation and temperature, whereas patchiness within sites is correlated with local geology (greater colonization frequency of large rocks) and biology (dispersal during rainfall). On the continental scale, geographic isolation appears to be more important in controlling spatial distribution patterns of desert microorganisms.

Fig. 6 A green layer of colonized cyanobacteria in gypsic crust from Atacama Desert. The colonization depth is optimized for photosynthesis. Adopted from Dong et al. (2007)

Heterotrophic bacteria also occur widely in desert environments and their abundances appear to be related to mean annual precipitation. In the hyperarid core region of the Atacama Desert, the heterotrophic community preferably inhabits the soil subsurface (25–30 cm in depth) (Dress et al. 2006), rather than more hostile surface (Navarro-Gonzalez et al. 2003). The heterotrophic community composition is mainly composed of *Alphaproteobacteria*, *Actinobacteria*, *Flexibacteria*, *Firmicutes*, *Gemmatimonadetes*, *Planctomycetes*, and *Thermus/Deinococcus* (Chanal et al. 2006; de la Torre et al. 2003; Dress et al. 2006; Nagy et al. 2005; Navarro-Gonzalez et al. 2003). Metabolic functions of these groups in such environments remain largely speculative. Some members of *Alphaproteobacteria* may be potentially capable of aerobic anoxygenic photosynthesis (de la Torre et al. 2003).

Deserts have been proposed to be a good analog for Mars, because these two environments share many common characteristics. Among these are presence of sulfate deposits (Aubrey et al. 2006; Cooper and Mustard 2002; Dong et al. 2007; Gendrin et al. 2005; Hughes and Lawley 2003; Langevin et al. 2005; Squyres et al. 2004), low levels of refractory organic material, low number of detectable bacteria, and equal oxidation of L and D amino acids (Wierzchos et al. 2006). Organic materials may be preserved for geologically long periods in sulfate minerals (Aubrey et al. 2006). Indeed, salt deposits (halite and possibly sulfate) are one of the four possible life habitats on Mars as predicted by a radiative transfer model (Cockell and Raven 2004), and microbial life and their signatures in such deposits may be remotely detected by non-destructive spectroscopy methods, even when microbes colonize a few mm below the rock surface (Edwards et al. 2005). In addition microorganisms from desert environments have typically been adapted to extreme desiccation (Billi et al. 2000) and radiation (Rainey et al. 2005), two prevalent conditions on Mars and possibly other planets. When these organisms colonize the subsurface of rocks, their ability to resist radiation and desiccation is significantly enhanced (Cockell et al. 2005), apparently due to the shielding effect from rock matrix.

6 Fossil Microbial DNA in Ancient Sedimentary Rocks

Recent developments in molecular microbiology in the last decade have allowed us to investigate the abundance, distribution, and identity of microorganisms in various extreme environments (Barns et al. 1996; DeLong 1992; Giovannoni et al. 1990; Hugenholtz et al. 1998; Pace 1997; Takai and Horikoshi 1999). These new techniques have been used to not only study microorganisms in modern environments, but also in ancient rocks, i.e., fossil microbial DNA in ancient rocks. Studies have shown a great promise in reconstructing paleo microbial communities and paleoenvironmental conditions through investigations of fossil DNA and molecular biomarkers preserved in sediments and sedimentary rocks (Brocks et al. 2005; Coolen et al. 2004a; Coolen and Overmann 1998; Coolen and Overmann 2007). Coolen and his colleagues, as well as others, have recently demonstrated

that DNA can survive in organic carbon-rich anoxic and sulfidic sediments of stratified basins (Coolen et al. 2004a; Coolen et al. 2006a; Coolen et al. 2004b; Coolen and Overmann 1998; Coolen and Overmann 2007; Coolen et al. 2007b; D'Andrea et al. 2006). Measurable quantities of DNA buried within the Holocene sediments were as well preserved as the carotenoids of the sulfur bacteria (Coolen et al. 2006b; Coolen and Overmann 1998). The same level of preservation was observed between up to 9400-year-old DNA and recalcitrant alkenones of haptophytes in Ace Lake (Antarctica) (Coolen et al. 2004b) and in the Black Sea (Coolen et al. 2006a).

In parallel to Coolean and his colleagues, a group in Japan explored the concept of fossil DNA and its utility. Inagaki et al. (2001) studied microbial community of an oceanic subseafloor core sample of the Pleistocene age (1410 cm long, ~2–2.5 Ma) recovered from the West Philippine Basin at a depth of 5719 m. The authors reported the discovery of vertically shifted community structures of archaea. Beneath a surface community of ubiquitous deep-sea archaea, an unusual archaeal community consisting of extremophilic archaea, such as extreme halophiles and hyperthermophiles, was present. These organisms were interpreted to be microbial relicts of more than 2 million years old. The discovery of an unusual archaeal community in this core sample, inconsistent with the deep-sea environment, was inferred to reflect past terrestrial volcanic and submarine hydrothermal activities surrounding the West Philippine Basin.

In 2005, Inagaki et al. (2005) proposed the concept of "Paleome" for the first time: "the use of preserved DNA and/or microbes to interpret the past". The authors successfully extracted and amplified DNA from a core sample of black shale of the Cretaceous age (100 Ma) collected from Serre des Castets, near Marseilles, France. The authors used fluorescene particulate tracer beads (0.5 μm) during the coring and attempted to cultivate bacteria from the core material. No fluorescent particles were detected inside the core at depths greater than 2 mm. No viable cells were detected in the inner core samples, whereas abundant viable cells were detected in the drilling fluid and outer core material. The authors concluded that the cores were contamination free, and the microorganisms observed were indigenous.

The DNA sequences from the Cretaceous rocks were most similar to those commonly found in deep-sea sedimentary environments, which prevailed during the deposition of the black shales, but different from those commonly found in the modern terrestrial environment of the drill core (Inagaki et al. 2005). Moreover, the inferred aerobic/anaerobic habitats, based on relatedness of the detected DNA sequences to cultivated microorganisms, were consistent with the inferred paleoenvironmental conditions. In particular, a number of 16S rRNA gene clones of oceanic sulfate-reducing bacteria within the *Deltaproteobacteria* predominated at the oceanic anoxic event (OAE) layer of the Cretaceous black shale, but the number of clones of sulfate-reducing bacteria dramatically diminished in the sediment layers above and below the OAE layer. Instead, extant deep-sea genera predominated in these layers, including some psychrophilic and piezophilic members. Based on this correlation, the authors proposed the idea of "fossil DNA". The detected DNA

sequences were inferred to represent the relics of fossil microbial communities, not the modern microorganisms living within the black shale.

If proved to be genuine, this discovery has significant implications for the following three reasons:

1. Fossil DNA in the black shales can be used to understand microbial community structure, growth habitats, and their roles in global elemental cycling during the Cretaceous.
2. Because of global distribution of black shales and abundant information that they contain, fossil DNA within these rocks can be used to reconstruct global environments during the Cretaceous.
3. Fossil DNA provides an effective means to study biological evolution. Evolution of various processes throughout geological time, such as elemental cycling, chemical composition of the oceans, the atmosphere, and the crust, diversification of metabolism, and origins of multicellular organisms, is all intimately correlated with microbial evolution.

Despite the fact that the concept "Paleome" is supported by strong evidence, it is faced with many challenges and issues. The most important issue to be addressed is whether or not DNA can be preserved for such a long time (~100 Ma). Although previous studies have shown that dormant bacteria and archaea have been detected or cultivated within fluid inclusions of ancient halite crystals of 112–250 Ma in age (Fish et al. 2002; Kminek et al. 2003; Vreeland et al. 2007; Vreeland et al. 2000), Inagaki et al. (2005) are the first to detect DNA (not live microbes) in ancient, low-salinity black shales. Unlike DNA molecules, living microbes have mechanisms to repair damaged DNA, so the concept of ancient living microorganisms may be more acceptable than ancient DNA molecules. However, the topic of whether or not live organisms cultivated from brine fluid inclusions are indigenous is even debatable (Hazen and Roedder 2001; Powers et al. 2001), although recent accumulative evidence appears to support the indigenous nature of these organisms in ancient halite crystals (Vreeland et al. 2007).

In natural environments, aqueous solution, oxidizing environment, and radiation can all damage isolated DNA (outside living microbes) (Kminek et al. 2003; Lindahl 1993). Laboratory experiments have shown that under conditions of water availability and moderate temperature, DNA can not be preserved for more than a few thousands of years (Lindahl 1993). Similar to this result, in lake sediments of up to 11,000 years, the DNA abundance of phototrophic microorganisms decreases by six orders of magnitudes (Coolen and Overmann 1998). However, DNA preservation is favorable under low temperature and high salinity (ionic strength) conditions, especially under conditions of dry, anoxic, and clay-rich environments. Recent studies have shown that clay minerals can stabilize adsorbed DNA molecules (Ciaravella et al. 2004; Scappini et al. 2004). Inagaki et al. (2005) believe that the relatively dry, anoxic and clay-rich environments within their black shale are favorable factors to preserve ancient DNA molecules for as long as 100 Ma (Cretaceous).

In addition to the issue of DNA preservation, many other issues remain, commented on by Hoehler on the Inagaki et al. (2005) paper (Hoehler 2005): (1) Does the

age of the black shale represent the detected microorganisms? (2) When did the microorganisms enter the black shale to become isolated from the outside world? (3) When did the detected microorganisms stop metabolic activity to become fossils? Available evidence suggests that metabolic activity can exist long after sedimentation, ranging from hundreds of thousands of years to millions of years (D'Hondt et al. 2004; Parkes et al. 1994). Thus, ancient rocks may not necessarily contain ancient DNA. If not all microorganisms stopped metabolic activity and became preserved when the rock formed, but a small fraction of the population remained active, then the preserved (and detected) DNA does not represent the microbial community at the time of rock formation, and cannot be used to infer the paleoenvironmental conditions. These issues are important to study microbial evolution in a geological context, but they were not addressed in that study (Inagaki et al. 2005). Lack of archaeal DNA in the black shale (Inagaki et al. 2005) is another important issue to be resolved, because in general, archaea should be abundant in marine environments (Kuypers et al. 2001; Kuypers et al. 2002; Sinninghe Damsté and Coolen 2006).

In 2006, Sinninghe Damsté and Coolen (2006) published a comment paper and pointed out a few weaknesses of the original Inagaki et al. paper (2005). The main criticisms are reflected in three aspects:

1. The Inagaki et al. (2005) study lacks biomarker work. Although not specific individual microbial species, molecular biomarkers can be used to infer microbial functional groups in ancient rocks, because these compounds can be preserved in rocks much longer than DNA molecules (Brocks et al. 2005). A few studies (Kuypers et al. 2001; Kuypers et al. 2002; Tsikos et al. 2004) have detected archaeal lipid biomarkers in similar black shales to those studied by Inagaki et al. (2005), which is inconsistent with the lack of fossil archaeal DNA as reported by Inagaki et al. (2005). This inconsistency raises the possibility of DNA contamination in the Inagaki et al. study (Sinninghe Damsté and Coolen 2006). However, archaeal DNA may be degraded easier than bacterial DNA (Inagaki and Nealson, 2006), as evidenced in modern sediments (MacGregor et al. 1997; MacGregor et al. 2001). Thus, this issue remains to be resolved.
2. Sinninghe Damsté and Coolen (2006) believes that molecular clock rate of the rRNA gene in diatoms is 1% per 14 million years (Damste et al. 2004). With this molecular clock rate, it is expected that fossil DNA sequences of 112 million years should be 8% different from those of modern organisms. The DNA sequences detected by Inagaki et al. (2005) are closely related to those of modern organisms. However, the molecular clock rate is not well determined and this inference may not be quantitative.
3. If the sulfate-reducing bacteria are related to methane emissions in deep-sea cold seeps, then the $\delta^{13}C$ of lipid compounds should be very negative, because the lipid compounds should have been derived from biogenic methane ($\delta^{13}C = -80\%$) (Sinninghe Damsté and Coolen 2006). However, Inagaki et al. (2005) did not measure carbon isotopes of lipid compounds.

The debate of the concept “Paleome” will likely continue in the foreseeable future. The only way to validate this concept is through further testing. Fortunately, more opportunities have become available for such tests. For example, the Songliao Basin in the Northeastern China (near the Daqing oil field, Helongjiang Province, China) hosts a terrestrial record of Cretaceous black shales as thick as 5000 m (Chen 1987; Chen and Chang 1994). One unique feature in this sedimentary record is the alternation of black and red beds, presumably reflecting alternating reducing and oxidizing conditions during the Cretaceous time (Haskin et al. 2005). These rock formations have not been heated to more than 100° C, and they are ideal for microbiologi-

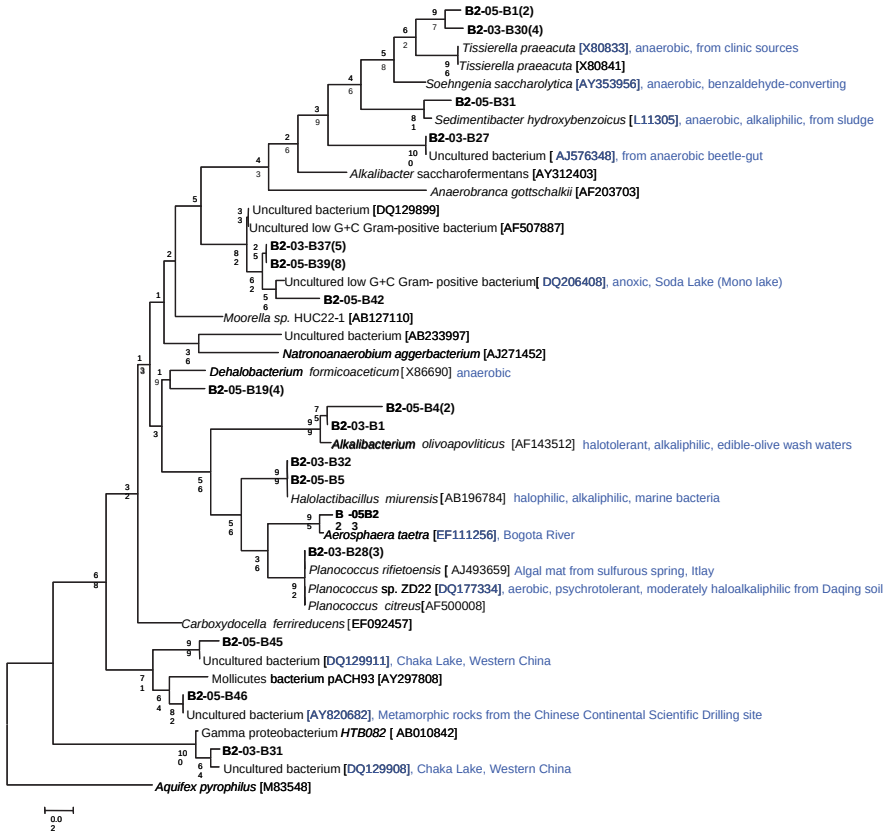

Fig. 7 Neighbor-joining tree (partial sequences, ∼600 bp) showing the phylogenetic relationships of bacterial 16S rRNA gene sequences cloned from two shale samples from the Songliao Basin, NW China to closely related sequences from the GenBank database. One representative clone type within each operational taxonomic unit (OUT) is shown, and the number of clones within each OTU is shown in the parenthesis. If there is only one clone sequence within a given OTU, the number “1” is omitted. Clone sequences from this study are coded as follows for the example of B2-05-B42: bacterial 16S rRNA gene clone number 42 from sample B2-05. Scale bars indicate the Jukes-Cantor distances. Bootstrap values of >50% (for 1000 iterations) are shown. *Aquifex pyrophilius* is used as the outgroup

cal work. Furthermore, abundant information on paleoclimate, paleogeography, and paleoenvironment is available, based on which microbial data can be interpreted.

Our preliminary data on the Songliao basin samples appear to support the "Paleome" concept. Employing the tracers and aseptic techniques during the coring, the extent of contamination was minimized. The innermost portions of two core samples, B2-03, a black mudstone from 1117 m depth, and B2-05, a red mudstone from 1215 m depth, were analyzed for mineralogy, geochemistry and microbiology. The salinity is low (0.1%), and pH is alkaline (~10). Similar to the findings of Inagaki et al. (2005), no archaeal DNA was extracted or amplified. Despite the fact that it is a terrestrial basin today, bacterial 16S rRNA gene sequences are closely related to those in GenBank that are previously recovered from aqueous environments, such as lakes and oceans (Fig. 7). The Songliao basin was a lake during the Cretaceous time, suggesting that the fossil DNA may have reflected the ancient environmental conditions of the basin. However, more data are necessary to confirm these initial findings.

7 Ocean Geomicrobiology

Oceans cover more than two thirds of the Earth's surface and they are full of life. Geomicrobiological processes in the global oceans have received increased interests in the last decade, as exemplified by many excellent research papers and books (Edwards et al. 2005; Teske 2006; Wilcock et al. 2004). Considering the rapid pace of the recent developments in this area, it is nearly impossible to write a comprehensive review. Below I touch five aspects: biomass abundance, diversity, some important metabolic functions, carbon sources, and the impacts of subsurface microorganisms on geological processes. We discuss these aspects in three representative environments of oceans: "normal" deep-sea sediments, gas hydrate deposits, and hydrothermal vents.

7.1 Biomass Abundance and Distribution

Microbial biomass generally decreases with increasing depth in deep-sea sediments, from 1.4 to $4 \times 10^9/cm^3$ at the surface sediment to $2.76 \times 10^6/cm^3$ at the average ocean sediment depth (500 m) (Parkes et al. 2000). However, prokaryotic populations have been detected in sediments as deep as 800 m below the seafloor (mbsf) by both intact cells and intact membrane lipids. The total prokaryotic biomass in marine subsurface has been estimated to be 50–80% of Earth's total prokaryotic biomass $\{4–6 \times 10^{30}$ cells, (Whitman et al. 1998)$\}$. The living prokaryotic biomass is estimated at 1.3×10^{29} cells. Bacterial populations and activity can increase near geochemical hotspots in deeper sediment layers, such as brine incursion or the presence of thermogenic methane (Parkes et al. 2000). Temperature, age, and porosity appear to be three factors responsible for decreased biomass with sediment depth.

Ancient sediments contain less biodegradable organic matter and are less likely to support microbial growth. One exception is gas hydrate deposits in deep sediments, where low molecular weight fatty acids are produced by thermogenic and biogenic processes. In such settings, biomass tends to be high.

7.2 Microbial Diversity

The known diversity on Earth includes approximately 6000 species of prokaryotes (http://www.bacterio.cict.fr/number.html), based on cultivated species (Pedros-Alio 2006). The unknown diversity is currently explored by using molecular microbiology techniques. Estimated bacterial diversity in the oceans is a few thousand taxa (Hagstrom et al. 2002), and more recently, many new bacterial taxa are being submitted to GenBank each year (Pommier et al. 2005). Because of the insufficient nature of clone library based estimates of microbial diversity, the actual diversity is probably much higher.

Microbial communities of deep marine sediments harbor members of distinct, uncultured archaeal and bacterial lineages (Teske 2006). There are 9 groups of the *Archaea*, as reviewed by Teske (2006). Among these, the Marine Benthic Group B *Archaea* (MBG-B) show a cosmopolitan occurrence pattern in a wide spectrum of marine sediments, surficial as well as subsurface, and normal marine sediments as well as hydrothermal vents. The second major group is the Marine Group I, which is abundant in both water column and subsurface sediments. This group may be facultatively autotrophic or of broad metabolic diversity. An autotrophic aerobic ammonia oxidizer, *Nitrosopumilus maritimus*, belongs to this group (Konneke et al. 2005). Unlike MBG-B and MGI, *Archaea* of the Marine Benthic Groups A and D are not abundant in deep-sea sediments. A few other groups occur in both marine and terrestrial subsurface, such as the MCG (Misscellaneous Crenarchaeotal Group), the SAGMEG (South African Gold Mine Euryarchaeotal Group), and the TMEG (Terrestrial Miscellaneous Euryarchaeotal Group) (Jiang et al. 2007a). Inagaki et al. (2006) reported the dominance of deep-sea archaeal group (DSAG) in gas hydrate-bearing sediments, which appears to be absent in the gas hydrate free sediments. The *Proteobacteria*, the candidate division JS-1 (Newberry et al. 2004), and the Chloroflexi division are three groups of the domain *Bacteria* identified in normal marine sediments by molecular methods. Cultivation yields a somewhat different picture: the *Firmicutes* (specifically *Bacillus* and *Thermosediminibacter*) and the *Actinobacteria*, a range of *Alphaproteobacteria* (*Rhizobium radiobacter*) and *Gammaproteobacteria* (genera *Photobacterium*, *Vibrio*, *Shewanella*, and *Halomonas*), and a novel member of the *Bacteroidetes* phylum are commonly recovered (Teske 2006).

In contrast to normal marine sediments, thermophilic and hyperthermophilic archaea and bacteria dominate deep-sea hydrothermal environments (Miroshnichenko and Bonch-Osmolovskaya 2006). *Archaea* are represented by thermophilic, lithotrophic methanogens (*Methanococcales* and *Methanopyrales*);

hyperthermophilic sulfate- and thiosulfate-reducing *Archaeoglobales*; hyperthermophilic, lithoautotrophic *Pyrolobus fumarii*; and thermophilic, organotrophic *Thermococcales*, *Pyrodictium*, and *Staphylothermus*. Recently, a few novel archaeal isolates have been obtained, including hyperthermophilic, lithotrophic, sulfur-respiring *Ignicoccus pacificus* of the family *Desulfurococcaceae* of the *Crenarchaeota* kingdom; hyperthermophilic, ferric iron reducing *Geoglobus ahangari* and *Geogemma barossii*; hyperthermophilic methanogens of the genera *Methanothermococcus*, *Methanocaldococcus*, and *Methanotorris*; and hyperthermophilic organotrophic species within the order *Thermococcales*. Molecular surveys and cultivations have revealed the following bacterial diversity: the order *Aquificales*; the subclass *Epsilonproteobacteria*; the order *Thermotogales*; the families *Thermodesulfobacteriaceae*, *Deferribacteraceae*, and *Thermaceae*; the family *Geobacteraceae*; *Firmicutes*; and a novel phylum represented by the genus *Calditrix*. Most isolates within these orders and families are obligate or facultative lithotrophs, oxidizing molecular hydrogen in the course of different types of anaerobic respiration or microaerobic growth (Miroshnichenko and Bonch-Osmolovskaya 2006).

7.3 Metabolic Functions

Large sulfate and methane gradients are typically observed in normal marine subsurface sediments (D'Hondt et al. 2004; D'Hondt et al. 2002) and are usually assumed to be caused by vertically stratified sulfate reducers and methanogens. Sulfate-reducers are expected to dominate in the sulfate-containing upper sediment layers; methanogenic archaea are expected in the methane-rich deeper sediment layers; and sulfate-dependent, methanotrophic consortia analogous to those found at gas hydrate deposits and hydrothermal sediments (Boetius et al. 2000; Hinrichs and Boetius 2002; Hinrichs et al. 1999; Michaelis et al. 2002; Orphan et al. 2001; Teske et al. 2003; Teske et al. 2002) are expected to dominate the sulfate-methane transition zone. However, functional gene surveys do not detect abundant dissimilatory sulfate reductase (dsrAB) and methyl-coenzyme M reductase (mcrA). One possible explanation is that sulfate reducers and methanogens may be minor components in the overall community. Low rates of methanogenesis and sulfate reduction may be sufficient to maintain the observed sulfate and methane profiles (D'Hondt et al. 2004), or some uncultivated prokaryotes may be sulfate-reducers and methanogens (Teske 2006).

Knowledge of metabolic functions in hydrothermal sediments is limited, largely because of the difficulty of obtaining isolates in this environment. Among the domain *Archaea*, three main functions have been identified: reduction of elemental sulfur with oxidation of H_2 (by *Ignicoccus pacificus*), iron reduction, and methanogenesis (Miroshnichenko and Bonch-Osmolovskaya 2006). Among the domain *Bacteria*, identified metabolic functions include organotrophy (thermophilic and piezophilic representatives within the order *Thermotogales*, representatives within the family *Thermaceae* and *Firmicutes*) (Reysenbach 2001a); lithoautotrophy {i.e.,

Aquificales using H_2, S^0, S_2^- or $S_2O_3^{2-}$ as energy sources and O_2, NO_3^-, or S^0 as electron acceptors (Reysenbach 2001b); representatives of the subgroup A of the *Epsilonproteobacteria*}; sulfate-reduction (representatives within the *Thermodesulfobacteriaceae* family); iron reduction (within the order *Deferribacterales* and the family *Geobacteraceae* within the subclass *Deltaproteobacteria*); and H_2 oxidation coupled with reduction of elemental sulfur and nitrate (representatives of the *Epsilonproteobacteria*).

In gas hydrate deposits, main metabolic functions are sulfate reduction coupled with oxidation of methane and/or hydrocarbons (Joye et al. 2004; Nauhaus et al. 2002; Orphan et al. 2001; Teske et al. 2003; Thomsen et al. 2001; Valentine and Reeburgh 2000). Methane is either microbial or abiotic in origin and it migrates upward from deep sediments, where it meets sulfate that diffuses downward from seawater. When methane and sulfate meets at the transition, steep gradients of methane and sulfate develop, where sulfate-reducing bacteria and methane oxidizing archaea work together to form a coupled reaction (Valentine and Reeburgh 2000). A few studies have shown that the rate of sulfate reduction generally exceeds the rate of anaerobic oxidation of methane and the two processes are loosely coupled, suggesting that the majority of sulfate reduction is likely fueled by the oxidation of other organic matter (Formolo et al. 2004; Joye et al. 2004). Increased alkalinity from oxidation of methane and other organic matter results in formation of authigenic carbonates (Moore et al. 2004; Sassen et al. 2004).

7.4 Carbon Sources Fuelling Marine Subsurface Microorganisms

On the Earth's surface (both terrestrial and ocean surfaces), within the water column, and in marine sediments, essentially all life forms rely either directly or indirectly on the energy supplied by the sun and incorporated into biomass by photosynthetic organisms. In marine subsurface, microorganisms essentially depend on "dark energy", reduced chemical species (including H_2) derived from the oceanic crust, as a main energy source. Using chemical energy, lithoautotrophic organisms are alive and well (Teske 2005). Using catalysed reporter deposition-fluorescence in situ hybridization (CARD-FISH), Schippers et al. (2005) identified that a fraction of the sub-seafloor prokaryotes ($\sim$4%) is alive, even in very old (10 million yr) and deep ($>$400 m) sediments. All detectable living cells belong to the *Bacteria* and have turnover times of 0.25–22 yr, comparable to surface sediments. This raises a question of energy source in the deep marine subsurface. Unlike organic-rich continental shelf sediments and gas hydrate deposits, carbon sources in deep-sea sediments are usually limited. For lithoautotrophic organisms, carbon sources are abundant, in the form of CO, CO_2, and CH_4. For heterotrophic organisms, organic matter is scarce and it is not clear what possible organic carbon substrate is. While it is known that fluids from 3.5-Ma oceanic crust are capable of supporting microbial growth (Cowen et al. 2003), including nitrate reducers, thermophilic sulfate reducers, and thermophilic fermentative heterotrophs, whether or not abiotically produced

carbon substrates can be used by microbes was not demonstrated until recently. Horsfield et al. (2006) demonstrated that abiotically driven degradation products of buried marine sedimentary organic matter can provide substrates for microbial activity in deep sediments at convergent continental margins and possibly in other deep-sea sedimentary environments. This study is highly significant in showing that refractory organic matter can be important sources of carbon for marine subsurface microorganisms.

7.5 The Impacts of Subsurface Microorganisms on Geological Processes

Microorganisms at and beneath the ocean floor play an important role in rock/glass alteration (Fisk et al. 1998; Furnes and Staudigel 1999; Staudigel et al. 2006), chemical and isotopic exchange between the oceanic crust and the sea water (Furnes et al. 2001), and biogeochemical cycles of C, Fe, S and other elements (Edwards et al. 2005; Fisk et al. 1998). The prominent role of microorganisms in weathering of basalt and glass has been demonstrated in both laboratory culture study (Bach and Edwards 2003; Staudigel et al. 1995; Staudigel et al. 1998; Thorseth et al. 1995a; Wu et al. 2007) and in-situ incubation experiments (Bach and Edwards 2003). In these studies, Fe- and Mn-oxidizing lithoautotrophs obtained from deep-sea environments have been demonstrated to be capable of growth on basalt glass as the sole source of energy and they are found to enhance the rate of basalt dissolution by up to an order of magnitude (Edwards et al. 2004; Templeton et al. 2005). In these processes, they derive energy from oxidation of sulfides, methane, ferrous iron and manganese, and H_2, reduction of ferric iron, sulfate, and CO_2, and respiration and fermentation of organic matter.

Some unique textures result when microorganisms weather basaltic glass in the oceanic crust, such as tubular structures (Fisk et al. 1998; Thorseth et al. 1995b). These textures are typically accompanied by characteristic enrichments of certain elements and depletion of others as well as isotope variations (Banerjee et al. 2006; Fisk et al. 2003; Furnes et al. 2001; Storrie-Lombardi and Fisk 2004; Thorseth et al. 2003; Thorseth et al. 1995b). Taken together, these features have been used as biosignatures to determine biogenicity of ancient rock records on early Earth and Mars (Fisk et al. 2006; Furnes et al. 2005; Furnes et al. 2004; McLoughlin et al. 2007). However, cautions have to be exercised not to over-interpret the importance of these textural and geochemical evidence, unless other supporting evidence, such as nucleaic acids and lipid biomarkers, is presented.

Acknowledgments Dong's former PhD students, Gengxin Zhang and Hongchen Jiang, provided Figure 2, 4, & 5. This work was supported by grants from National Science Foundation (EAR-0345307) and U.S. Department of Energy (DE-FG02-07ER64369) to HD. The author is grateful to Nicola McLoughlin and Tamas Torok for their comments which improved the quality of the manuscript.

References

Abrajano TA, Sturchio NC, Kennedy BM, Lyon GL, Muehlenbachs K, Bohlke JK (1990) Geochemistry of reduced gas related to serpentinization of the Zambales ophiolite, Philippines. App Geochem 5:625–630

Acinas SG, Anton J, Rodriguez-Valera F (1999) Diversity of free-living and attached bacteria in offshore western Mediterranean waters as depicted by analysis of genes encoding 16S rRNA. Appl Environ Microbiol 65:514–522

Aloisi G, Pierre C, Rouchy JM, Foucher JP, Woodside J, Party MS (2000) Methane-related authigenic carbonates of eastern Mediterranean Sea mud volcanoes and their possible relation to gas hydrate destabilisation. Earth Planet Sci Lett 184:321–338

Alt JC, Shanks WCI (1998) Sulfur in serpentinized oceanic peridotites: Serpentinization processes and microbial sulfate reduction. J Geophys Res 103:9917–9929

Amend JP, Teske A (2005) Expanding frontiers in deep subsurface microbiology. Palaeogeog Palaeoclimat Palaeoecol 219:131–155

Aragno M (1992) Aerobic, chemolithoautotrophic, thermophilic bacteria. In Kristjansson JK (ed) Thermophilic bacteria, CRC Press, Boca Raton, pp 77–103

Aubrey A, Cleaves HJ, Chalmers JH, Skelley AM, Mathies RA, Grunthaner FJ, Ehrenfreund P, Bada JL (2006) Sulfate minerals and organic compounds on Mars. Geology 34:357–360

Bach W, Edwards KJ (2003) Iron and sulfide oxidation within the basaltic ocean crust: implications for chemolithoautotrophic microbial biomass production. Geochim Cosmochim Acta 67: 3871–3887

Baker PA, Burns SJ (1985) The occurrence and formation of dolomite in organic-rich continental margin sediments. Am Assoc Pet Geol Bull 69:1917–1930

Baker PA, Kastner M (1981) Constraints on the formation of sedimentary dolomite. Science 213:214–216

Baliga NS, Bjork SJ, Bonneau R, Pan M, Iloanusi C, Kottemann MCH, Hood L, DiRuggiero J (2004) Systems level insights into the stress response to UV radiation in the halophilic archaeon Halobacterium NRC-1. Genome Res 14:1025–1035

Banciu H, Sorokin DY, Rijpstra WIC, Damste JSS, Galinski EA, Takalchi S, Muyzer G, Kuenen JG (2005) Fatty acid, compatible solute and pigment composition of obligately chemolithoautotrophic alkaliphilic sulfur-oxidizing bacteria from soda lakes. FEMS Microbiol Lett 243: 181–187

Banerjee NR, Furnes H, Muehlenbachs K, Staudigel H, de Wit M (2006) Preservation of similar to 3.4–3.5 Ga microbial biomarkers in pillow lavas and hyaloclastites from the Barberton Greenstone Belt, South Africa. Earth Planet Sci Lett 241:707–722

Banfield JF, Cervini-Silva J, Nealson KM (2005) Molecular geomicrobiology. The Mineralogical Society of America, Chantilly, VA, 294p

Barns SM, Delwiche CF, Palmer JD, Pace NR (1996) Perspectives on archaeal diversity, thermophily, and monophyly from environmental rDNA sequences. Proc Natl Acad Sci USA 17:9188–9193

Belyakova EV, Rozanova EP, Borzenkov IA, Tourova TP, Pusheva MA, Lysenko AM, Kolganova TV (2006) The new facultatively chemolithoautotrophic, moderately halophilic, sulfate-reducing bacterium Desulfovermiculus halophilus gen. nov., sp nov., isolated from an oil field. Microbiology 75:161–171

Beman JM, Francis CA (2006) Diversity of ammonia-oxidizing archaea and bacteria in the sediments of a hypernutrified subtropical estuary: Bahia del Tobari, Mexico. Appl Environ Microbiol 72:7767–7777

Benlloch S, Lopez-Lopez A, Casamayor EO, Ovreas L, Goddard V, Daae FL, Smerdon G, Massana R, Joint I, Thingstad F, Pedros-Alio C, Rodriguez-Valera F (2002) Prokaryotic genetic diversity throughout the salinity gradient of a coastal solar saltern. Environ Microbiol 4:349–360

Berndt ME, Allen DE, Seyfried WE (1996) Reduction of CO2 during serpentinization of olivine at 300°C and 500 bar. Geology 24:351–354

Bernhard AE, Colbert D, McManus J, Field KG (2005) Microbial community dynamics based on 16S rRNA gene profiles in a Pacific Northwest estuary and its tributaries. FEMS Microbiol Ecol 52:115–128

Billi D, Friedmann EI, Hofer KG, Caiola MG, Ocampo-Friedmann R (2000) Ionizing-radiation resistance in the desiccation-tolerant cyanobacterium Chroococcidiopsis. Appl Environ Microbiol 66:1489–1492

Bockelmann U, Manz W, Neu TR, Szewzyk U (2000) Characterization of the mcirobial community of lotic organic aggregates ('river snow') in the Elbe River of Germany by cultivation and molecular methods. FEMS Microbiol Ecol 33:157–170

Boetius A, Ravenschlag K, Schubert CJ, Rickert D, Widdel F, Gieseke A, Amann R, Jorgensen BB, Witte U, Pfannkuche O (2000) A marine microbial consortium apparently mediating anaerobic oxidation of methane. Nature 407:623–626

Bouvier TC, del Giorgio PA (2002) Compositional changes in free-living bacterial communities along a salinity gradient in two temperate estuaries. Limnol Ocean 47:453–470

Brambilla E, Hippe H, Hagelstein A, Tindall BJ, Stackbrandt E (2001) 16S diversity of cultured and uncultured prokaryotes of a mat sample from Lake Fryxell, McMurdo Dry Valleys, Antarctica. Extremephiles 5:23–33

Bridge TAM, Johnson DB (1998) Reduction of soluble iron and reductive dissolution of ferric iron-containing minerals by moderately thermophilic iron-oxidizing bacteria. Appl Environ Microbiol 64:2181–2186

Brocks JJ, Love GD, Summons RE, Knoll AH, Logan GA, Bowden SA (2005) Biomarker evidence for green and purple sulphur bacteria in a stratified Palaeoproterozoic sea. Nature 437:866–870

Brummer IHM, Fehr W, Wagner-Dobler I (2000) Biofilm community structure in polluted rivers: abundance of dominant phylogenetic groups over a complete annual cycle. Appl Environ Microbiol 66:3078–3082

Bull AT (2004) Microbial diversity and bioprospecting. ASM press, Washington DC, 496pp

Cai CF, Dong H, Li H, Xiao X, Ou G (2007) Mineralogical and geochemical evidence for coupled bacterial uranium mineralization and hydrocarbon oxidation in the Shashagetai deposit, NW China. Chem Geol 236:167–179

Campbell KA, Farmer JD, Des Marais D (2002) Ancient hydrocarbon seeps from the Mesozoic convergent margin of California: carbonate geochemistry, fluids and palaeoenvironments. Geofluids 2:63–94

Castello JD, Rogers SO (2005) Life in ancient ice. Princeton University Press, Princeton, NJ, 307pp

Cavagna S, Clari P, Martire L (1999) The role of bacteria in the formation of cold seep carbonates: geological evidnece from Monferrato (Tertiary, NW Italy). Sediment Geol 126:253–270

Chanal A, Chapon V, Benzerara K, Barakat M, Christen R, Achouak W, Barras F, Heulin T (2006) The desert of Tataouine: an extreme environment that hosts a wide diversity of microorganisms and radiotolerant bacteria. Environ Microbiol 8:514–525

Chapelle FH (2000) Ground-water microbiology and geochemistry. John Wiley & Sons, Inc., New York

Chapelle FH, O'Neill K, Bradley PM, Methe BA, Ciufo SA, Knobel LL, Lovley DR (2002) A hydrogen-based subsurface microbial community dominated by methanogens. Nature 415:312–315

Charlou JL, Donval JP (1993) Hydrothermal methane venting between 12°N and 26°N along the Mid-Atlantic Ridge. J Geophys Res 98:9625–9642

Charlou JL, Donval JP, Fouquet Y, Jean-Baptiste P, Holm N (2002) Geochemistry of high H2 and CH4 vent fluids issuing from ultramafic rocks at the Rainbow hydrothermal field (36o 14'N, MAR). Chem Geol 191:345–359

Charlou JL, Fouquet Y, Bougault H, Donval JP, Etoubleau J, Jean-Baptiste P, Dapoigny A, Appriou P, Rona PA (1998) Intense CH4 plumes generated by serpentinization of ultramafic rocks at the intersection of the 15°20'N fracture zone and the Mid-Atlantic Ridge. Geochim Coschim Acta 62:2323–2333

Chen PJ (1987) Cretaceous paleogeography of China. Palaeogeog Palaeoclimat Palaeoecol 59: 49–56

Chen PJ, Chang ZL (1994) Nonmarine Cretaceous stratigraphy of eastern China. Cretaceous Res 5:245–257

Ciaravella A, Scappini F, Franchi M, Cecchi-Pestellini C, Barbera M, Candia R, Gallori E, Micela G (2004) Role of clays in protecting adsorbed DNA against X-ray radiation. Inter J Astrobiol 3:31–35

Cockell CS, Raven JA (2004) Zones of photosynthetic potential on Mars and the early Earth. ICARUS 169:300–310

Cockell CS, Schuerger AC, Billi D, Friedmann EI, Panitz C (2005) Effects of a simulated martian UV flux on the cyanobacterium, Chroococcidiopsis sp 029. Astrobiology 5:127–140

Coolen MJK, Hopmans EC, Rijpstra WIC, Muyzer G, Schouten S, Volkman JK, Sinninghe-Damste JS (2004a) Evolution of the methane cycle in Ace Lake (Antarctica) during the Holocene: response of methanogens and methanotrophs to environmental change. Org Geochem 35: 1151–1167

Coolen MJL, Abbas B, van Bleijswijk J, Hopmans EC, Kuypers MMM, Wakeham SG, Damste JSS (2007a) Putative ammonia-oxidizing Crenarchaeota in suboxic waters of the Black Sea: a basin-wide ecological study using 16S ribosomal and functional genes and membrane lipids. Environ Microbiol 9:1001–1016

Coolen MJL, Boere A, Abbas B, Baas M, Wakeham SG, Sinninghe Damsté JS (2006a) Fossil DNA derived from alkenone-biosynthesizing haptophytes and other algae in Holocene sediment from the Black Sea. Paleoocean 21, PA1005-doi:10.1029/2005PA001188.

Coolen MJL, Muyzer G, Rijpstra WIC, Schouten S, Volkman JK, Sinninghe Damsté JS (2004b) Combined DNA and lipid analyses of sediments reveal changes in Holocene haptophyte and diatom populations in an Antarctic lake. Earth Planet Sci Lett 223:225–239

Coolen MJL, Muyzer G, Schouten S, Volkman JK, Sinninghe Damsté JS (2006b) Sulfur and methane cycling during the Holocene in Ace Lake (Antarctica) revealed by lipid and DNA stratigraphy. In Neretin LN (ed) Past and present marine water column anoxia, NATO science series: IV-Earth and environmental sciences. Springer, Dordrecht, pp 41–65

Coolen MJL, Overmann J (1998) Analysis of subfossil molecular remains of purple sulfur bacteria in a lake sediment. Appl Environ Microbiol 64:4513–4521

Coolen MJL, Overmann J (2007) 217 000-year-old DNA sequences of green sulfur bacteria in Mediterranean sapropels and their implications for the reconstruction of the paleoenvironment. Environ Microbiol 9:238–249

Coolen MJL, Volkman JK, Abbas B, Muyzer G, Schouten S, Damste JSS (2007b) Identification of organic matter sources in sulfidic late Holocene Antarctic fjord sediments from fossil rDNA sequence analysis. Paleoocean 22, Art. No. PA2211

Cooper CD, Mustard JF (2002) Spectroscopy of loose and cemented sulphate-bearing soils: implications for duricrust on Mars. ICARUS 158:42–55

Cottrell MT, Kirchman DL (2003) Contribution of major bacterial groups to bacterial biomass production (thymidine and leucine incorporation) in the Delaware estuary. Limnol Ocean 48: 168–178

Cowen JP, Giovannoni SJ, Kenig F, Johnson HP, Butterfield D, Rappe MS, Hutnak M, Lam P (2003) Fluids from aging ocean crust that support microbial life. Science 299:120–123

Crump BC, Armbrust EV, Baross JA (1999) Phylogenetic analysis of particle-attached and free-living bacterial communities in the Columbia river, its estuary, and the adjacent coastal ocean. Appl Environ Microbiol 65:3192–3204

D'Andrea WJ, Lage M, Martiny JBH, Laatsch AD, Amaral-Zettler LA, Sogin ML, Huang Y (2006) Alkenone producers inferred from well-preserved 18S rDNA in Greenland lake sediments. J Geophys Res 111, G0313: doi:10.1029/2005JG000121

D'Hondt S, Jorgensen BB, Miller DJ, Batzke A, Blake R, Cragg BA, Cypionka H, Dickens GR, Ferdelman T, Hinrichs KU, Holm NG, Mitterer R, Spivack A, Wang GZ, Bekins B, Engelen B, Ford K, Gettemy G, Rutherford SD, Sass H, Skilbeck CG, Aiello IW, Guerin G, House C,

Inagaki F, Meister P, Naehr T, Niitsuma S, Parkes RJ, Schippers A, Smith DC, Teske A, Wiegel J, Padilla CN, Acosta JLS (2004) Distributions of microbial activities in deep subseafloor sediments. Science 306:2216–2221

D'Hondt S, Jørgensen BB, Miller DJ, Batzke A, Blake R, Cragg BA, Cypionka H, Dickens GR, Ferdelman T, Hinrichs K-U, Holm NG, Mitterer R, Spivack A, Wang G, Bekins B, Engelen B, Ford K, Gettemy G, Rutherford SD, Sass H, Skilbeck CG, Aiello IW, Gu'erin G, House C, Inagaki F, Meister P, Naehr T, Niitsuma S, Parkes RJ, Chippers A, Smith DC, Teske A, Wiegel J, Padilla CN, Acosta JLS (2004) Distributions of microbial activities in deep subseafloor sediments. Science 306:2216–2221

D'Hondt S, Rutherford S, Spivack AJ (2002) Metabolic activity of subsurface life in deep–sea sediments. Science 295:2067–2070

Damste JSS, Muyzer G, Abbas B, Rampen SW, Masse G, Allard WG, Belt ST, Robert JM, Rowland SJ, Moldowan JM, Barbanti SM, Fago FJ, Denisevich P, Dahl J, Trindade LAF, Schouten S (2004) The rise of the rhizosolenid diatoms. Science 304:584–587

DasSarma S, Arora P (2001) Halophiles. Encyclopedia of life Sciences, 2001. Nature Publishing Group, pp 1–9

DeFlaun MF, Fredrickson JK, Dong H, Pfiffner SM, Onstott TC, Balkwill DL, Streger SH, Stackebrandt E, Knoessen S, van Heerden E (2007) Isolation and characterization of a Geobacillus thermoleovorans species from an ultra-deep South African gold mine. Syst App Microbiol 30:152–164

de la Torre JR, Goebel BM, Friedmann EI, Pace NR (2003) Microbial diversity of cryptoendolithic communities from the McMurdo Dry Valleys, Antarctica. Appl Environ Microbiol 69: 3858–3867

del Giorgio PA, Bouvier TC (2002) Linking the physiologic and phylogenetic successions in free-living bacterial communities along an estuarine salinity gradient. Limnol Ocean 47:471–486

DeLong EF (1992) Archaea in coastal marine environments. Proc Nat Acad Sci 89:5685–5689

DeLong EF, Franks DG, Alldredge AL (1993) Phylogenetic diversity of aggregate-attached vs. free-living marine bacterial assemblages. Limnol Ocean 38:924–934

Dong H, Rech JA, Jiang H, Sun H, Buck BJ (2007) Endolithic cyanobacteria in soil gypsum: Occurrences in Atacama (Chile), Mojave (United States), and Al-Jafr Basin (Jordan) deserts. J Geophys Res-Biogeosci 112, doi:10.1029/2006JG000385

Dong H, Zhang G, Jiang H, Yu B, Chapman LR, Lucas CR, Fields MW (2006) Microbial diversity in sediments of saline Qinghai Lake: Linking geochemical controls to microbial diversity. Microb Ecol 51:65–82

Douglas S, Yang HX (2002) Mineral biosignatures in evaporites: presence of rosickyite in an endoevaporitic microbial community from Death Valley, California. Geology 30:1075–1078

Drees KP, Neilson JW, Betancourt JL, Quade J, Henderson DA, Pryor BM, Maier RM (2006) Bacterial diversity in the hyper-arid core of the Atacama desert, Chile. Appl Environ Microbiol 72:7902–7908

Dundas I (1998) Was the environment for primoridal life hypersaline? Extremophiles 2:,375–377

Edwards HGM, Villar SEJ, Parnell J, Cockell CS, Lee P (2005) Raman spectroscopic analysis of cyanobacterial gypsum halotrophs and relevance for sulfate deposits on Mars. Analyst 130:917–923

Edwards K, Bach W, McCollom T, Rogers D (2004) Neutrophilic iron-oxidizing bacteria in the ocean: their habitats, diversity, and roles in mineral deposition, rock alteration, and biomass production in the deep-sea. Geomicrobiol J 21:393–404

Ehrlich HL (2005) Geomicrobiology. Marcel Dekker. Inc, New York

Fisk MR, Giovannoni SJ (1999) Sources of nutrients and energy for a deep biosphere on Mars. J Geophys Res 104:11805–11815

Fisk MR, Giovannoni SJ, Thorseth IH (1998) Alteration of oceanic volcanic glass: textural evidence of microbial activity. Science 281:978–980

Fisk MR, Popa R, Mason OU, Storrie-Lombardi MC, Vicenzi EP (2006) Iron-magnesium silicate bioweathering on Earth (and Mars?) Astrobiology 6:48–68

Fish SA, Shepherd TJ, McGenity TJ, Grant WD (2002) Recovery of 16S ribosomal RNA gene fragments from ancient halite. Nature 417:432–436

Fisk MR, Storrie-Lombardi MC, Douglas S, Popa R, McDonald G, Di Meo-Savoie C (2003) Evidence of biological activity in Hawaiian subsurface basalts. Geochem Geophys Geosys 4:Art. No. 1103

Formolo MJ, Lyons TW, Zhang CL, Kelley C, Sassen R, Horita J, Cole DR (2004) Quantifying carbon sources in the formation of authigenic carbonates at gas hydrate sites in the Gulf of Mexico. Chem Geol 205:253–264

Franca L, Rainey FA, Nobre MF, Costa MS (2006) Tepidicella xavieri gen. nov., sp nov., a betaproteobacterium isolated from a hot spring runoff. Inter J Syst Evol Microbiol 56:907–912

Francis CA (2007) New processes and players in the nitrogen cycle: the microbial ecology of anaerobic and archaeal ammonia oxidation. ISME J 1

Francis CA, O'Mullan GD, Ward BB (2003) Diversity of ammonia monooxygenase (amoA) genes across environmental gradients in Chesapeake Bay sediments. Geobiology 1:129–140

Francis CA, Roberts KJ, Beman JM, Santoro AE, Oakley BB (2005) Ubiquity and diversity of ammonia-oxidizing archaea in water columns and sediments of the ocean. Proc Nat Acad Sci 102:14683–14688

Fredrickson JK, Balkwill DL (2006) Geomicrobial processes and biodiversity in the deep terrestrial subsurface. Geomicrobiol J 23:345–356

Fredrickson JK, Fletcher M (2001) Subsurface microbiology and biogeochemistry. Wiley-Liss, Inc., New York

Fredrickson JK, McKinley JP, Bjornstad BN, Long PE, Ringelberg DB, White DC, Krumholz LR, Suflita JM, Colwell FS, Lehman RM, Phelps TJ, Onstott TC (1997) Pore-size constraints on the activity and survival of subsurface bacteria in a late Cretaceous shale-sandstone sequence, Northwestern New Mexico. Geomicrobiol J 14:183–202

Freitag TE, Chang L, Prosser JI (2006) Changes in the community structure and activity of betaproteobacterial ammonia-oxidizing sediment bacteria along a freshwater-marine gradient. Environ Microbiol 8:684–696

Friedrich CG (1998) Physiology and genetics of sulfur-oxidizing bacteria. Adv Microb Physiol 39:235–289

Friedrich CG, Bardischewsky F, Rother D, Quentmeier A, Fischer J (2005) Prokaryotic sulfur oxidation. Curr Opin Microbiol 8:253–259

Frontier S (1985) Diversity and structure in aquatic ecosystems. Ocean Mar

Furnes H, Banerjee NR, Muehlenbachs K, Kontinen A (2005) Preservation of biosignatures in metaglassy volcanic rocks from the Jormua ophiolite complex. Finland Precam Res 136: 125–137

Furnes H, Banerjee NR, Muehlenbachs K, Staudigel H, de Wit M (2004) Early life recorded in archean pillow lavas. Science 304:578–581

Furnes H, Muehlenbachs K, Torsvik T, Thorseth IH, Tumyr O (2001) Microbial fractionation of carbon isotopes in altered basaltic glass from the Atlantic Ocean, Lau Basin and Costa Rica Rift. Chem Geol 173:313–330

Furnes H, Staudigel H (1999) Biological mediation in ocean crust alteration: how deep is the deep biosphere? Earth Planet Sci Lett 166:97–103

Galinski EA, Truper HG (1994) Microbial behavior in salt-stressed ecosystems. FEMS Microbiol Rev 15:95–108

Gendrin A, Mangold N, Bibring JP, Langevin Y, Gondet B, Poulet F, Bonello G, Quantin C, Mustard J, Arvidson R, LeMouelic S (2005) Suffates in martian layered terrains: the OMEGA/Mars Express view. Science 307:1587–1591

Gerday C, Glansdorff N (2007) Physiology and biogeochemistry of extremophiles. ASM Press, Washington DC, 450pp

Giovannoni SJ, Britschgi TB, Moyer CL, Field FG (1990) Genetic diversity of Sargasso Sea bacterioplankton. Nature 345:60–65

Glockner FO, Fuchs BM, Amann R (1999) Bacterioplankton compositions of lakes and oceans: a first comparison based on fluorescence in situ hybridization Appl Environ Microbiol 65:3721–3726

Greinert J, Bohrmann G, Suess E (2001) Gas hydrate associated carbonates and methane venting at Hydrate Ridge: classification, distribution, and origin of authigenic carbonates. In: Paull CK, Dillon WP (eds) Natural gas hydrates: occurrence, distribution and detection, 124. Geophysical Monograph, American Geophysical Union, Washington, D.C, pp 99–113

Hagstrom A, Pommier T, Rohwer F, Simu K, Stolte W, Svensson D, Zweifel UL (2002) Use of 16S Ribosomal DNA for Delineation of Marine Bacterioplankton Species. Appl Environ Microbiol 68:3628–3633

Haskin LA, Wang A, Jolliff BL, McSween HY, Clark BC, Des Marais DJ, McLennan SM, Tosca NJ, Hurowitz JA, Farmer JD, Yen A, Squyres SW, Arvidson RE, Klingelhofer G, Schroder C, de Souza PA, Ming DW, Gellert R, Zipfel J, Bruckner J, Bell JF, Herkenhoff K, Christensen PR, Ruff S, Blaney D, Gorevan S, Cabrol NA, Crumpler L, Grant J, Soderblom L (2005) Water alteration of rocks and soils on Mars at the Spirit rover site in Gusev crater. Nature 436:66–69

Hazen RM, Roedder E (2001) How old are bacteria from the Permian age? Nature 411:155

He JZ, Shen JP, Zhang LM, Zhu YG, Zheng YM, Xu MG, Di HJ (2007) Quantitative analyses of the abundance and composition of ammonia-oxidizing bacteria and ammonia-oxidizing archaea of a Chinese upland red soil under long-term fertilization practices. Environ Microbiol, doi:10.1111/j.1462-2920.2007.01358.x

Heidelberg JF, Seshadri R, Haveman SA, Hemme CL, Paulsen IT, Kolonay JF, Eisen JA, Ward N, Methe B, Brinkac LM, Daugherty SC, Deboy RT, Dodson RJ, Durkin AS, Madupu R, Nelson WC, Sullivan SA, Fouts D, Haft DH, Selengut J, Peterson JD, Davidsen TM, Zafar N, Zhou LW, Radune D, Dimitrov G, Hance M, Tran K, Khouri H, Gill J, Utterback TR, Feldblyum TV, Wall JD, Voordouw G, Fraser CM (2004) The genome sequence of the anaerobic, sulfate-reducing bacterium Desulfovibrio vulgaris Hildenborough. Nat Biotechnol 22:554–559

Henriques IS, Alves A, Tacao M, Almeida A, Cunha A, Correia A (2006) Seasonal and spatial variability of free-living bacterial community composition along an estuarine gradient (Ria de Aveiro, Portugal) Est Coast Shelf Sci 68:139–148

Hinrichs K-U, Boetius A (2002) The anaerobic oxidation of methane: new insights in microbial ecology and biogeochemistry. In: Wefer G, Billett D, Hebbeln D, Jorgensen BB, Schluter M (eds) Ocean Marine systems. Springer-Verlag, Berlin-Heidelberg, pp 457–477

Hinrichs KU, Hayes JM, Sylva SP, Brewer PG, DeLong EF (1999) Methane-consuming archaebacteria in marine sediments. Nature 398:802–805

Hoehler TM (2005) Cretaceous park? A commentary on microbial paleomics. Astrobiology 5: 95–99

Holm NG, Andersson EM (1998) Hydrothermal systems. In: Brack A (ed) The molecular origins of life. Cambridge University Press, Cambridge, UK, pp 86–99

Holm NG, Charlou J-L (2001) Initial indications of abiotic formation of hydrocarbons in the Rainbow ultramafic hydrothermal system, Mid-Atlantic Ridge. Earth Planet Sci Lett 191:1–8

Horita J, Berndt ME (1999) Abiogenic methane formation and isotopic fractionation under hydrothermal conditions. Science 285:1055–1057

Horsfield B, Schenk HJ, Zink K, Ondrak R, Dieckmann V, Kallmeyer J, Mangelsdorf K, di Primlo R, Wilkes H, Parkes RJ, Fry J, Cragg BA (2006) Living microbial ecosystems within the active zone of catagenesis: Implications for feeding the deep biosphere. Earth Planet Sci Lett 246: 55–69

Hugenholtz P, Goebel BM, Pace NR (1998) Impact of culture-independent studies on the emerging phylogenetic view of bacterial diversity. J Bacteriol 180:4765–4774

Hughes KA, Lawley B (2003) A novel Antarctic microbial endolithic community within gypsum crusts. Environ Microbiol 5:555–565

Inagaki F, Nealson KH (2006) Molecular signals from ancient materials: challenges to deep-biosphere and paleoenvironmental research- A response to the comments of Sinninghe Damste and Coolen. Astrobiology 6:303–307

Inagaki F, Nunoura T, Nakagawa S, Teske A, Lever M, Lauer A, Suzuki M, Takai K, Delwiche M, Colwell FS, Nealson KH, Horikoshi K, D'Hondt S, Jorgensen BB (2006) Biogeographical distribution and diversity of microbes in methane hydrate-bearing deep marine sediments on the Pacific Ocean Margin. Proc Natl Acad Sci USA 103:2815–2820

Inagaki F, Okada H, Tsapin AI, Nealson KH (2005) The Paleome: a sedimentary genetic record of past microbial communities. Astrobiology 5:141–153

Inagaki F, Takai K, Komatsu T, Kanamatsu K, Fujioka K, Horikoshi K (2001) Archaeology of Archaea: Geomicrobiological record of Pleistocene thermal events concealed in a deep-sea subseafloor environment. Extremophiles 5:385–392

Jakobsen TF, Kjeldsen KU, Ingvorsen K (2006) Desulfohalobium utahense sp nov., a moderately halophilic, sulfate-reducing bacterium isolated from Great Salt Lake. Inter J Sys Evol Microbiol 56:2063–2069

Jiang H, Dong H, Ji S, Ye Y, Wu N (2007a) Microbial diversity in the deep marine sediments from the Qiongdongnan basin in South China Sea. Geomicrobiol J 24:505–517

Jiang H, Dong H, Zhang G, Yu B, Chapman LR, Fields MW (2006) Microbial diversity in water and sediment of Lake Chaka: an athalassohaline hypersaline lake in Northwestern China. Appl Environ Microbiol 72:3832–3845

Jiang HC, Dong HL, Yu BS, Liu XQ, Li YL, Ji SS, Zhang CLL (2007b) Microbial response to salinity change in Lake Chaka, a hypersaline lake on Tibetan plateau. Environ Microbiol 9:2603–2621

Jorgensen NO (1992) Methane-derived carbonate cementation of Holocene marine sediments from Kattegat, Denmark. Cont Shelf Res 12:1209–1218

Joye SB, Boetius A, Orcutt BN, Montoya JP, Schulz HN, Erickson MJ, Lugo SK (2004) The anaerobic oxidation of methane and sulfate reduction in sediments from Gulf of Mexico cold seeps. Chem Geol 205:219–238

Joye SB, Connell TL, Miller LG, Oremland RS, Jellison RS (1999) Oxidation of ammonia and methane in an alkaline, saline lake. Limnol Ocean 44:178–188

Kaksonen AH, Spring S, Schumann P, Kroppenstedt RM, Puhakka JA (2006) Desulfotomaculum thermosubterraneum sp nov., a thermophilic sulfate-reducer isolated from an underground mine located in a geothermally active area. Inter J Sys Evol Microbiol 56:2603–2608

Kaksonen AH, Spring S, Schumann P, Kroppenstedt RM, Puhakka JA (2007) Desulfolvirgula thermocuniculi gen. nov., sp nov., a thermophilic sulfate-reducer isolated from a geothermal underground mine in Japan. Inter J Syst Evol Microbiol 57:98–102

Kappler A, Newman DK (2004) Formation of Fe(III)-minerals by Fe(II)-oxidizing photoautotrophic bacteria. Geochim Coschim Acta 68:1217–1226

Kastner M, Elderfield H, Martin JB, Suess E, Kvenvolden KA, Garrison RE. (1990) Diagenesis and interstitial-water chemistry at the Peruvian continental margin-major constituents and strontium isotopes. In: Suess E, von Huene R (eds) Proceedings of ocean drilling program, scientific results, 112. Ocean Drilling Program, College Station, TX, pp 413–440

Kelley DS, Karson JA, Blackman DK, Fruh-Green GL, Butterfield DA, Lilley MD, Olson EJ, Schrenk MO, Roe KK, Lebon GT, Rivizzigno P (2001) An off-axis hydrothermal vent field near the Mid-Atlantic Ridge at 30 degrees N. Nature 412:145–149

Kelley DS, Karson JA, Fruh-Green GL, Yoerger DR, Shank TM, Butterfield DA, Hayes JM, Schrenk MO, Olson EJ, Proskurowski G, Jakuba M, Bradley A, Larson B, Ludwig K, Glickson D, Buckman K, Bradley AS, Brazelton WJ, Roe K, Elend MJ, Delacour A, Bernasconi SM, Lilley MD, Baross JA, Summons RT, Sylva SP (2005) A serpentinite-hosted ecosystem: The lost city hydrothermal field. Science 307:1428–1434

Kelly DP, Shergill JK, Lu W-P, Wood AP (1997) Oxidativemetabolism of inorganic sulfur compounds by bacteria. Antonie van Leeuwenhoek 71:95–107

Kerkar S, Bharathi PAL (2007) Stimulation of sulfate-reducing activity at salt-saturation in the salterns of Ribandar, Goa, India. Geomicrobiol J 24:101–110

Kieft TL, McCuddy SM, Onstott TC, Davidson M, Lin LH, Mislowack B, Pratt L, Boice E, Lollar BS, Lippmann-Pipke J, Pfiffner SM, Phelps TJ, Gihring T, Moser D, Heerden A (2005)

Geochemically generated, energy-rich substrates and indigenous microorganisms in deep, ancient groundwater. Geomicrobiol J 22:325–335
Kieft TL, Phelps TJ (1997) Life in the slow lane. In: Amy PS, Haldeman DL (eds) The microbiology of the terrestrial subsurface. CRC Press, Boca Raton, FL, pp 137–164
Kirchman DL, Dittel AI, Malmstrom RR, Cottrell MT (2005) Biogeography of major bacterial groups in the Delaware Estuary. Limnol Ocean 50:1697–1706
Kletzin A, Urich T, Muller F, Bandeiras TM, Gomes CM (2004) Dissimilatory oxidation and reduction of elemental sulfur in thermophilic archaea. J Bioenerg Biomemb 36:77–91
Kminek G, Bada JL, Pogliano K, Ward JF (2003) Radiation-dependent limit for the viability of bacterial spores in halite fluid inclusions and on Mars. Radiat Res 159:722–729
Knauth LP (1998) Salinity history of the Earth's early ocean. Nature 395:554–555
Konhauser K (2006) Introduction to geomicrobiology. Blackwell Publishing, Oxford, UK.
Konneke M, Bernhard AE, de la Torre JR, Walker CB, Waterbury JB, Stahl DA (2005) Isolation of an autotrophic ammonia-oxidizing marine archaeon. Nature 437:543–546
Koops HP, Purkhold U, Pommerening-Roser A, Timmermann G, Wagner M (2004) The lithoautotrophic ammonia-oxidizing bacteria. The Prokaryotes: an evolving electronic resource for the microbiological community.
Kottemann MCH, Kish A, Iloanusi C, Bjork S, DiRuggiero J (2005) Physiological responses of the halophilic archaeon Halobacterium sp strain NRC1 to desiccation and gamma irradiation. Extremephiles 9:219–227
Krauskopf KB, Bird DK (1995) Introduction to geochemistry. McGraw-Hill, New York.
Krumholz LR, Harris SH, Tay ST, Suflita JM (1999) Characterization of two subsurface H-2-utilizing bacteria, Desulfomicrobium hypogeium sp nov and Acetobacterium psammolithicum sp nov., and their ecological roles. Appl Environ Microbiol 65:2300–2306
Krumholz LR, McKinley JP, Ulrich FA, Suflita JM (1997) Confined subsurface microbial communities in Cretaceous rock. Nature 386:64–66
Kulm LD, Suess E (1990) Relationship between carbonate deposits and fluid venting: Oregon accretionary prism. J Geophys Res 95:8899–8915
Kushner DJ (1993) Growth and nutrition of halophilic bacteria. In: Vreeland RH, Hochstein LI (eds) The biology of halophilic bacteria. CRC Press, Boca Raton, pp 87–103
Kuypers MMM, Blokker P, Erbacher J, Kinkel H, Pancost RD, Schouten S, Sinninghe Damsté JS (2001) Massive expansion of marine archaea during a mid-Cretaceous oceanic anoxic event. Science 293:92–94
Kuypers MMM, Blokker P, Hopmans EC, Kinkel H, Pancost RD, Schouten S, Sinninghe Damsté JS (2002) Archaeal remains dominate marine organic matter from the early Albian Oceanic Anoxic Event 1b. Palaeogeog Palaeoclimat Palaeoecol 185:211–234
Land LS (1998) Failure to precipitate dolomite at 25°C from dilute solutions despite 1000-fold oversaturation after 32 years. Aquatic Geochem 4:361–368
Langenheder S, Kisand V, Wikner J, Tranvik LJ (2003) Salinity as a structuring factor for the composition and performance of bacterioplankton degrading riverine DOC. FEMS Microbiol Ecol 45:189–202
Langevin Y, Poulet F, Bibring JP, Gondet B (2005) Sulfates in the north polar region of Mars detected by OMEGA/Mars express. Science 307:1584–1586
Leininger S, Urich T, Schloter M, Schwark L, Qi J, Nicol GW, Prosser JI, Schuster SC, Schleper C (2006) Archaea predominate among ammonia-oxidizing prokaryotes in soils. Nature 442: 806–809
Lin LH, Hall J, Lippmann-Pipke J, Ward JA, Lollar BS, DeFlaun M, Rothmel R, Moser DP, Gihring TM, Mislowack B, Onstott TC (2005) Radiolytic H-2 in continental crust: Nuclear power for deep subsurface microbial communities. Geochem Geophys Geosyst 6:Q07003
Lin LH, Wang PL, Rumble D, Lippmann-Pipke J, Boice E, Pratt LM, Lollar BS, Brodie EL, Hazen TC, Andersen GL, DeSantis TZ, Moser DP, Kershaw D, Onstott TC (2007) Long-term sustainability of a high-energy, low-diversity crustal biome. Science 314:479–482
Lindahl T (1993) Instability and decay of the primary structure of DNA. Nature 362:709–715

Liu XQ, Dong H, Rech JA, Shen J, Wang SM, Wang YB, Yang B (2007a) Evolution of Chaka Salt Lake in NW China in response to climatic change during the latest Pleistocene-Holocene. Quat Sci Rev, In revision.

Liu XQ, Ni P, Dong HL, Wang TG (2007b) Homogenization temperature and its significance for primary fluid inclusion in halite formed in Chaka salt lake, Qardam basin. Acta Petrologica Sinica 23:113–116

Lollar BS, Lacrampe-Couloume G, Slater G, Ward JA, Moser DP, Gihring TM, Lin LH, Onstott TC (2006) Unravelling abiogenic and biogenic sources of methane in the Earth's deep subsurface. Chem Geol 226:328–339

Lueders T, Chin KJ, Conrad R, Friedrich M (2001) Molecular analyses of methyl-coenzyme M reductase alpha-subunit (mcrA) genes in rice field soil and enrichment cultures reveal the methanogenic phenotype of a novel archaeal lineage. Environ Microbiol 3:194–204

MacGregor BJ, Moser DP, Alm EW, Nealson KH, Stahl DA (1997) Crenarchaeota in Lake Michigan Sediment. Appl Environ Microbiol 63:1178–1181

MacGregor BJ, Moser DP, Baker BJ, Alm EW, Maurer M, Nealson KH, Stahl DA (2001) Seasonal and spatial variability in Lake Michigan sediment small-subunit rRNA concentrations. Appl Environ Microbiol 67:3908–3922

Madigan MT, Martinko JM, Parker J (2004) Brock biology of microorganisms. Prentice Hall, Upper Saddle River, NJ

Magot M, Basso O, Tardy-Jacquenod C, Caumette P (2004) Desulfovibrio bastinii sp. nov. and Desulfovibrio gracilis sp. nov., moderately halophilic, sulfate-reducing bacteria isolated from deep subsurface oilfield water. Inter J Sys Evol Microbiol 54:1693–1697

Mancinelli RL, Fahlen TF, Landheim R, Klovstad MR (2004) Brines and evaporites: analogs for Martian life. Adv Space Res 33:1244–1246

Mazzullo SJ (2000) Organogenic Dolomitization in peritidal to deep-sea sediments. J. Sediment Res 70:10–23

McCollom TM, Ritter G, Simoneit BRT (1999) Lipid synthesis under hydrothermal conditions by Fischer-Tropsch-type reactions. Orig Life Evol Bipsph 29:153–166

McCollom TM, Seewald JS (2001) A reassessment of the potential for reduction of dissolved CO2 to hydrocarbons during serpentinization of olivine. Geochim Coschim Acta 65: 3769–3778

McCollom TM, Seewald JS (2003) Experimental constraints on the hydrothermal reactivity of organic acids and acid anions: I. Formic acid and formate. Geochim Coschim Acta 67: 3625–3644

McCollom TM, Seewald JS (2006) Carbon isotope composition of organic compounds produced by abiotic synthesis under hydrothermal conditions. Earth Planet Sci Lett 243:74–84

McLoughlin N, Brasier MD, Wacey D, Green OR, Perry RS (2007) On biogenicity criteria for endolithic microborings on early earth and beyond. Astrobiology 7:10–26

McMahon PB (2001) Aquifer/aquitard interfaces: mixing zones that enhance biogeochemical reactions. Hydrogeol J 9:34–43

McMahon PB, Chapelle FH (1991) Microbial production of organic acids in aquitard sediments and its role in aquifer geochemistry. Nature 349:233–235

Michaelis W, Seifert R, Nauhaus K, Treude T, Thiel V, Blumenberg M, Knittel K, Gieseke A, Peterknecht K, Pape T, Boetius A, Amann R, Jørgensen BB, Widdel F, Peckmann J, Pimenov NV, Gulin MB (2002) Microbial reefs in the Black Sea fueled by anaerobic oxidation of methane. Science 297:1013–1015

Mincer TJ, Church MJ, Taylor LT, Preston C, Kar DM, DeLong EF (2007) Quantitative distribution of presumptive archaeal and bacterial nitrifiers in Monterey Bay and the North Pacific Subtropical Gyre. Environ Microbiol 9:1162–1175

Miroshnichenko ML, Bonch-Osmolovskaya EA (2006) Recent developments in the thermophilic microbiology of deep-sea hydrothermal vents. Extremophiles 10:85–96

Moore TS, Murray RW, Kurtz AC, Schrag DP (2004) Anaerobic methane oxidation and the formation of dolomite. Earth Planet Sci Lett 229:141–154

Nagy ML, Pe'rez A, Garcia-Pichel F (2005) The prokaryotic diversity of biological soil crusts in the Sonoran Desert (Organ Pipe Cactus National Monument, AZ). FEMS Microbiol Ecol 54:233–245

Nauhaus K, Boetius A, Kruger M, Widdel F (2002) In vitro demonstration of anaerobic oxidation of methane coupled to sulphate reduction in sediment from a marine gas hydrate area. Environ Microbiol 4:296–305

Navarro-Gonzalez R, Rainey FA, Molina P, Bagaley DR, Hollen BJ, de la Rosa J, Small AM, Quinn RC, Grunthaner FJ, Caceres L, Gomez-Silva B, McKay CP (2003) Mars-like soils in the Atacama Desert, Chile, and the dry limit of microbial life. Science 302:1018–1021

Nazina TN, Kosareva IM, Davidov AS, Tourova TP, Novikova EV, Khafizov RR, Poltaraus AB (2000) Physicochemical and microbiological characteristics of groundwater from observation wells of a deep radioactive liquid waste repository. Microbiol 69:89–95

Nealson KH, Belz A, McKee B (2002) Breathing metals as a way of life: geobiology in action. Antonie van Leeuwenhoek 81:215–222

Nealson KH, Inagaki F, Takai K (2005) Hydrogen-driven subsurface lithoautotrophic microbial ecosystems (SLiMEs): do they exist and why should we care? Trends Microbiol 13:405–410

Nejidat A (2005) Nitrification and occurrence of salt-tolerant nitrifying bacteria in the Negev desert soils. 2005, 52:21–29

Newberry CJ, Webster G, Cragg BA, Parkes RJ, Weightman AJ, Fry JC (2004) Diversity of prokaryotes and methanogenesis in deep subsurface sediments from the Nankai Trough, Ocean Drilling Program Leg 190. Environ Microbiol 6:274–287

Nicol GW, Schleper C (2006) Ammonia-oxidising Crenarchaeota: important players in the nitrogen cycle? Trends Microbiol 14:207–212

Onstott TC, Phelps TJ, Colwell FS, Ringelberg D, White DC, Boone DR, McKinley JP, Stevens TO, Long PE, Balkwill DL, Griffin WT, Kieft T (1998) Observations pertaining to the origin and ecology of microorganisms recovered from the deep subsurface of Taylorsville Basin, Virginia. Geomicrobiology 15:353–385

Oren A (1993) Ecology of extremely halophilic microorganisms. In: Vreeland RH, Hochstein LI (eds) The biology of halophilic bacteria. CRC Press, Boca Raton, FL, pp 25–53

Oren A (1999) Microbiology and biogeochemistry of hypersaline environments. CRC Press, New York

Oren A (2001) The bioenergetic basis for the decrease in metabolic diversity at increasing salt concentrations: implications for the functioning of salt lake ecosystems. Hydrobiologia 466:61–72

Oren A (2002a) Diversity of halophilic microorganisms: environments, phylogeny, physiology, and applications. J Ind Microbiol Biotech 28:56–63

Oren A (2002b) Halophilic microorganisms and their environments. Kluwer Academic, Dordrecht; Boston, 575pp

Orphan VJ, House CH, Hinrichs KU, McKeegan KD, DeLong EF (2001) Methane-consuming archaea revealed by directly coupled isotopic and phylogenetic analysis. Science 293:484–487

Orphan VJ, Taylor LT, Hafenbradl D, Delong EF (2000) Culture-dependent and culture-independent characterization of microbial assemblages associated with high-temperature petroleum reservoirs. Appl Environ Microbiol 66:700–711

Pace NR (1997) A molecular view of microbial diversity and the biosphere. Science 276:734–740

Park HD, Wells GF, Bae H, Criddle CS, Francis CA (2006) Occurrence of ammonia-oxidizing archaea in wastewater treatment plant bioreactors. Appl Environ Microbiol 72:5643–5647

Parkes RJ, Cragg BA, Bale SJ, Getliff JM, Goodman K, Rochelle PA, Fry JC, Weightman AJ, Harvey SM (1994) Deep bacterial biosphere in Pacific Ocean sediments. Nature 371:410–413

Parkes RJ, Cragg BA, Wellsbury P (2000) Recent studied on bacterial population and processes in subseafloor sediments: a review. Hydrogeol J 8:11–28

Parkes RJ, Wellsbury P (2004) Deep biospheres. In: Bull AT (ed) Microbial diversity and bioprospecting. ASM Press, Washington, DC, pp 120–129

Peckmann J, Gischler E, Oschmann W, Reitner J (2001) An early carboniferous seep community and hydrocarbon-derived carbonates from the Harz Mountains, Germany. Geology 29: 271–274
Peckmann J, Thiel V (2004) Carbon cycling at ancient methane-seeps. Chem Geol 205:443–467
Peckmann J, Thiel V, Michaelis W, Clari P, Gaillard C, Martire L, Reitner J (1999) Cold seep deposits of Beauvoisin (Oxfordian; southeastern France) and Marmorito (Miocene; norther Itlay): microbially induced authigenic carbonates. Inter J Earth Sci 88:60–75
Pedersen K (1997) Microbial life in deep granitic rock. FEMS Microbiol Rev 20:399–414
Pedersen K (2000) Exploration of deep intraterrestrial microbial life: current perspectives. FEMS Microbiol Lett 185:9–16
Pedersen K (2001) Diversity and activity of microorganisms in deep igneous rock aquifers of the fennoscandian shield. In: Frederick JF, Fletcher M (eds) Subsurface microgeobiology and biogeochemistry. Wiley-Liss, New York, pp 97–139
Pedros-Alio C (2006) Marine microbial diversity: can it be determined? Trends Microbiol 14: 257–263
Phillips CJ, Smith Z, Embley TM, Prosser JI (1999) Phylogenetic differences between particle-associated and planktonic ammonia-oxidizing bacteria of the beta subdivision of the class Proteobacteria in the northwestern Mediterranean Sea. Appl Environ Microbiol 65:779–786
Pierre C, Rouchy JM (2004) Isotopic compositions of diagenetic dolomites in the Tortonian marls of the western Mediterranean margins: evidence of the past gas hydrate formation and dissociation. Chem Geol 205:469–484
Pommier T, Pinhassi J, Hagstrom A (2005) Biogeographic analysis of ribosomal RNA clusters from marine bacterioplankton. Aquat Microb Ecol 41:79–89
Powers DW, vreeland RH, Rosenzweig WD (2001) How old are bacteria from the Permian age? Reply. Nature 411:155–156
Pronk JT, Meulenberg R, Hazeu W, Bos P, Kuenen JG (1990) Oxidation of reduced inorganic sulfur-compounds by acidophilic Thiobacilli. FEMS Microbiol Rev 75:293–306
Prosser JI, Embley TM (2002) Cultivation-based and molecular approaches to characterisation of terrestrial and aquatic nitrifiers. Antonie van Leeuwenhoek 81:165–179
Rainey FA, Ray K, Ferreira M, Gatz BZ, Nobre MF, Bagaley D, Rash BA, Park MJ, Earl AM, Shank NC (2005) Extensive diversity of ionizing-radiation-resistant bacteria recovered from a Sonoran Desert Soil and Description of Nine New Species of the Genus Deinococcus obtained from a single soil sample. Appl Environ Microbiol 71:5225–5235
Reysenbach A-L (2001a) Thermotogales. In: Boone DR, Garrity, GMe (eds) Bergey's Manual of systematic bacteriology, 1. Springer, Berlin Heidelberg New York, pp 396–387
Reysenbach AL (2001b) Aquificales. In: Boone DR, Garrity GMe (eds) Bergey's manual of systematic bacteriology, 1. Springer, Berlin Heidelberg New York, pp 369–387
Roberts HH, Aharon P (1994) Hydrocarbon-derived carbonate buildups of the northern Gulf-of-Mexico continental slope – a review of submersible investigations. Geo-Mar Lett 14:135–148
Roberts JA, Bennett PC, Gonzalez LA, Macpherson GL, Milliken KL (2004) Microbial precipitation of dolomite in methanogenic groundwater. Geology 32:277–280
Robertson LA, Kuenen JG (1999) The colorless sulfur bacteria, 1999. Springer-Verlag
Rodriguez NM, Paull CK, Borowski WS (2000) Zonation of authigenic carbonates within gas-hydrate bearing sedimentary sections on the Blake Ridge: offshore southeastern North America. In: Paull CK, Matsumoto R, Wallace PJ, Dillon WP (eds) Proceedings of Ocean Drilling program, scientific research, 164, pp 301–312
Rothschild LJ, Giver LJ, White MR, Mancinelli RL (1994) Metabolic-activity of microorganisms in evaporites. J. Phycol 30:431–438
Rothschild LJ, Mancinelli RL (2001) Life in extreme environments. Nature 409:1092–1101
Russell MJ (2003) The importance of being alkaline. Science 302:580–581
Russell MJ, Daia DE, Hall AJ (1998) The emergence of life from FeS bubbles at alkaline hot springs in an acid ocean. In: Wiegel J, Adams MWW (ed) Thermophiles: the keys to molecular evolution and the origin of life? Taylor & Francis, pp 77–126

Sample JC, Reid MR (1998) Contrasting hydrogeologic regimes along strike-slip and thrust faults in the Oregon convergent margin: evidence from the chemistry of syntectonic carbonate cements and veins. GSA Bull 110:48–59

Sanchez-Roman M, McKenzie JA, Vasconcelos C, Rivadeneyra M (2005) Bacterially induced dolomite formation in the presence of sulfate ions under Aerobic conditions. 2005 AGU Fall meeting, San Francisco

Sassen R, Roberts HH, Carney R, Milkov AV, DeFreitas DA, Lanoil B, Zhang CL (2004) Free hydrocarbon gas, gas hydrate, and authigenic minerals in chemosynthetic communities of the northern Gulf of Mexico continental slope: relation to microbial processes. Chem Geol 205:195–217

Scappini F, Casedi F, Zamboni R, Franchi M, Gallori E, Monti S (2004) Protective effect of clay minerals on adsorbed nucleic acid against UV radiation: possible role in the origin of life. Inter J Astrobiol 3:17–19

Schippers A, Neretin LN, Kallmeyer J, Ferdelman TG, Cragg BA, Parkes RJ, Jorgensen BB (2005) Prokaryotic cells of the deep sub-seafloor biosphere identified as living bacteria. Nature 433:861–864

Schleper C, Jurgens G, Jonuscheit M (2005) Genomic studies of uncultivated archaea. Nat Rev Microbiol 3:479–488

Schlesinger WH, Pippen JS, Wallenstein MD, Hofmockel KS, Klepeis DM, Mahall BE (2003) Community composition and photosynthesis by photoautotrophs under quartz pebbles, southern Mojave Desert. Ecology 84:3222–3231

Schweitzer B, Huber I, Amann R, Ludwig W, Simon M (2001) alpha- and beta-Proteobacteria control the consumption and release of amino acids on lake snow aggregates. Appl Environ Microbiol 67:632–645

Selje N, Simon M (2003) Composition and dynamics of particle-associated and free-living bacterial communities in the Weser estuary, Germany. Aquat Microb Ecol 30:221–237

Shen J, Liu XQ, Wang SM, Matsumoto R (2005) Palaeoclimatic changes in the Qinghai Lake area during the last 18,000 years. Quat Int 136:131–140

Shock EL (1990) Geochemical constraints on the origin of organic compounds in hydrothermal systems. Origins of life and evolution of the bipsphere, 20:331–367

Shock EL (1997) High-temperature life without photosynthesis as a model for mars. J Geophys Res 102:23687–23694

Shock EL, Schulte MD (1998) Organic synthesis during fluid mixing in hydrothermal systems. J Geophys Res 103:28513–28517

Sinninghe Damsté JS, Coolen MJL (2006) Fossil DNA in Cretaceous black shales: myth or reality. Astrobiology 6:299–302

Skirnisdottir S, Hreggvidsson GO, Holst O, Kristjansson JK (2001) Isolation and characterization of a mixotrophic sulfur-oxidizing Thermus scotoductus. Extremephiles 5:45–51

Sleep NH, Meibom A, Fridriksson T, Coleman RG, Bird DK (2004) H2-rich fluids from serpentinization: Geochemical and biotic implications. Proc Natl Acad Sci USA 101:12818–12823

Slobodkin AI (2005) Thermophilic microbial metal reduction. Microbiol 74:501–504

Sorensen KB, Canfield DE, Teske AP, Oren A (2005) Community composition of a hypersaline endoevaporitic microbial mat. Appl Environ Microbiol 71:7352–7365

Sorokin DY, Antipov AN, Kuenen JG (2003) Complete denitrification in coculture of obligately chemolithoautotrophic haloalkaliphilic sulfur-oxidizing bacteria from a hypersaline soda lake. Arch Microbiol 180:127–133

Sorokin DY, Kuenen JG (2005) Chemolithotrophic halo alkaliphiles from soda lakes. FEMS Microbiol Ecol 52:287–295

Sorokin DY, Tourova TP, Kolganova TV, Spiridonova EM, Berg IA, Muyzer G (2006a) Thiomicrospira halophila sp nov., a moderately halophilic, obligately chemolithoautotrophic, sulfur-oxidizing bacterium from hypersaline lakes. Inter J Sys Evol Microbiol 56:2375–2380

Sorokin DY, Tourova TP, Lysenko AM, Muyzer G (2006b) Diversity of culturable halophilic sulfur-oxidizing bacteria in hypersaline habitats. Microbiology 152:3013–3023

Squyres SW, Grotzinger JP, Arvidson RE, Bell JF, Calvin W, Christensen PR, Clark BC, Crisp JA, Farrand WH, Herkenhoff KE, Johnson JR, Klingelhofer G, Knoll AH, McLennan SM, McSween HY, Morris RV, Rice JW, Rieder R, Soderblom LA (2004) In situ evidence for an ancient aqueous environment at Meridiani Planum, Mars. Science 306:1709–1714

Stakes DS, Orange D, Paduan JB, Salamy KA, Maher N (1999) Cold-seeps and authigenic carbonate formation in Monterey Bay, California. Mar Geol 159:93–109

Staudigel H, Chastain RA, Yayanos A, Bourcier W (1995) Biologically mediated dissolution of glass. Chem Geol 126:147–154

Staudigel H, Furnes H, Banerjee NR, Dilek Y, Muehlenbachs K (2006) Microbes and volcanoes: a tale of the oceans, ophiolites, and greenstone belts. GSA Today 16:4–10

Staudigel H, Yayanos A, Chastain RA, Davies G, Verdurmen EA, Schiffman P, Bourcier R, De Baar H (1998) Biologically mediated dissolution of volcanic glass in seawater. Earth Planet Sci Lett 164:233–244

Stevens TO, McKinley JP (1995) Lithoautotrophic microbial ecosystems in deep basalt aquifers. Science 270:450–454

Storrie-Lombardi MC, Fisk MR (2004) Elemental abundance distributions in suboceanic basalt glass: evidence of biogenic alteration. Geochem Geophys Geosys 5:Art. No. Q10005

Takai K, Gamo T, Tsunogai U, Nakayama N, Hirayama H, Nealson KH, Horikoshi K (2004) Geochemical and microbiological evidence for a hydrogen-based, hyperthermophilic subsurface lithoautotrophic microbial ecosystem (HyperSLiME) beneath an active deep-sea hydrothermal field. Extremophiles 8:269–282

Takai K, Horikoshi K (1999) Genetic diversity of archaea in deep-sea hydrothermal vent environments. Genetics 152: 1285–1297

Takai K, Moser DP, Onstott TC, Spoelstra N, Pfiffner SM, Dohnalkova A, Fredrickson JK (2001) *Alkaliphilus transvaalensis* gen. nov., sp. nov., an extremely alkaliphilic bacterium isolated from a deep South African gold mine. Inter J Sys Evol Microbiol 51:1245–1256

Templeton AS, Staudigel H, Tebo BM (2005) Diverse Mn(II)-oxidizing bacteria isolated from submarine basalts at Loihi Seamount. Geomicrobiol J 22:127–139

Terzi C, Aharon P, Lucchi FR, Vai GB (1994) Petrography and stable-isotope aspects of cold vent activity imprinted on Miocene age calcari-a-lucina from Tuscan and Romagna Apennines, Italy. Geo-Mar Lett 14:177–184

Teske A, Dhillon A, Sogin ML (2003) Genomic markers of ancient anaerobic microbial pathways: sulfate reduction, methanogenesis, and methane oxidation. Biol Bull 204:186–191

Teske A, Hinrichs K-U, Edgcomb V, Gomez AdV, Kysela D, Sylva SP, Sogin ML, Jannasch HW (2002) Microbial diversity of hydrothermal sediments in the Guaymas Basin: evidence for anaerobic methanotrophic communities. Appl Environ Microbiol 68:1994–2007

Teske AP (2005) The deep subsurface biosphere is alive and well. Trends Microbiol 13:402–404

Teske AP (2006) Microbial communities of deep marine subsurface sediments: Molecular and cultivation surveys. Geomicrobiol J 23:357–368

Thevenieau F, Fardeau ML, Ollivier B, Joulian C, Baena S (2007) Desulfomicrobium thermophilum sp nov., a novel thermophilic sulphate-reducing bacterium isolated from a terrestrial hot spring in Colombia. Extremophiles 11:295–303

Thomsen TR, Finster K, Ramsing NB (2001) Biogeochemical and molecular signatures of anaerobic methane oxidation in a marine sediment. Appl Environ Microbiol 67:1646–1656

Thorseth IH, Furnes H, Tumyr O (1995a) Textural and chemical effects of bacterial activity on basaltic glass: an experimental approach. Chem Geol 119:139–160

Thorseth IH, Pedersen RB, Christie DM (2003) Microbial alteration of 0-30-Ma seafloor and sub-seafloor basaltic glasses from the Australian Antarctic Discordance. Earth Planet Sci Lett 215:237–247

Thorseth IH, Torsvik T, Furnes H, Muehlenbachs K (1995b) Microbes play an important role in the alteration of oceanic crust. Chem Geol 126:137–146

Treusch AH, Leininger S, Kletzin A, Schuster SC, Klenk HP, Schleper C (2005) Novel genes for nitrite reductase and Amo-related proteins indicate a role of uncultivated mesophilic crenarchaeota in nitrogen cycling. Environ Microbiol 7:1985–1995

Trimarco E, Balkwill D, Davidson M, Onstott TC (2006) In situ enrichment of a diverse community of bacteria from a 4–5 km deep fault zone in South Africa. Geomicrobiol J 23:463–473

Tsikos H, Karakitsios V, van Breugel Y, Walsworth-Bell B, Petrizzo MR, Bombardiere L, Sinninghe Damsté JS, Schouten S, Erba E, Premoli Silva I, Farrimond, P, Tyson, RV, Jenkyns HC (2004) Organic-carbon deposition in the Cretaceous of the Ionian Basin, NW-Greece: the Paquier Event (OAE 1b) re-visited. Geol Mag 141:401–416

Urakawa H, Kurata S, Fujiwara T, Kuroiwa D, Maki H, Kawabata S, Hiwatari T, Ando H, Kawai T, Watanabe M, Kohata K (2006) Characterization and quantification of ammonia-oxidizing bacteria in eutrophic coastal marine sediments using polyphasic molecular approaches and immunofluorescence staining. Environ Microbiol 8:787–803

Valentine DL, Reeburgh WS (2000) New perspectives on anaerobic methane oxidation. Environ Microbiol 2:477–484

Van Hamme JD, Singh A, Ward OP (2003) Recent advances in petroleum microbiology. Microbiol Mol Biol Rev 67:503–549

Vargas M, Kashefi K, Blunt-Harris EL, Lovley DR (1998) Microbiological evidence for Fe(III) reduction on early Earth. Nature 395:65–67

Vasconcelos C, McKenzie JA (1997) Microbial mediation of modern dolomite precipitation and diagenesis under anoxic conditions (Lagoa Vermelha, Rio de Janeiro, Brazil). J. Sediment Res 67:378–390

Vasconcelos C, McKenzie JA, Bernasconi S, Grujic D, Tien AJ (1995) Microbial mediation as a possible mechanism for natural dolomite formation at low temperature. Nature 377:220–222

Venter JC, Remington K, Heidelberg JF, Halpern AL, Rusch D, Eisen JA, Wu DY, Paulsen I, Nelson KE, Nelson W, Fouts DE, Levy S, Knap AH, Lomas MW, Nealson K, White O, Peterson J, Hoffman J, Parsons R, Baden-Tillson H, Pfannkoch C, Rogers YH, Smith HO (2004) Environmental genome shotgun sequencing of the Sargasso Sea. Science 304:66–74

Ventosa A (2004) Halophilic microorganisms. Springer, Berlin, New York, 349pp

Ventosa A, Nieto JJ, Oren A (1998) Biology of moderately halophilic aerobic bacteria. Microbiol Mol Biol Rev 62:504–544

vonRad U, Rosch H, Berner U, Geyh M, Marchig V, Schulz H (1996) Authigenic carbonates derived from oxidized methane vented from the Makran accretionary prism off Pakistan. Mar Geol 136:55–77

Voytek MA, Priscu JC, Ward BB (1999) The distribution and relative abundance of ammonia-oxidizing bacteria in lakes of the McMurdo Dry Valley, Antarctica. Hydrobiologia 401: 113–130

Vreeland RH, Hochstein LI (1993) The biology of halophilic bacteria. CRC Press, Boca Raton, FL, pp 25–53

Vreeland RH, Jones J, Monson A, Rosenzweig WD, Lowenstein TK, Timofeeff M, Satterfield C, Cho BC, Park JS, Wallace A, Grant WD (2007) Isolation of live Cretaceous (121–112 million years old) halophilic Archaea from primary salt crystals. Geomicrobiol J 24:275–282

Vreeland RH, Rosenzweig WD, Powers DW (2000) Isolation of a 250 million-year-old halotolerant bacterium from a primary salt crystal. Nature 407:897–900

Wacey D, Wright DT, Boyce AJ (2007) A stable isotope study of microbial dolomite formation in the Coorong Region, South Australia. Chem Geol 244:155–174

Ward BB, Martino DP, Diaz MC, Joye SB (2000) Analysis of ammonia-oxidizing bacteria from hypersaline Mono Lake, California, on the basis of 16S rRNA sequences. Appl Environ Microbiol 66:2873–2881

Ward BB, O'Mullan GD (2005) Community level analysis: Genetic and biogeochemical approaches to investigate community composiiton and function in aerobic ammonia oxidation. Methods Enzymol 397:397–413

Warren-Rhodes KA, Rhodes KL, Boyle L, Pointing SB, Chen Y, Liu SJ, Zhou PJ, McKay CP (2007) Cyanobacterial ecologyacross environmental gradients and spatial scales in China's hot and cold deserts. FEMS Microbiol Ecol 61:470–482

Warren-Rhodes KA, Rhodes KL, Pointing SB, WEwing S, Lacap DC, Gomez-Silva B, Amundson R, Friedmann EI, McKay CP (2006) Hypolithic cyanobacteria, dry limit of photosynthetic and microbial community ecology in the hyperarid Atacama Desert. Microb Ecol 52:389–398

Warthmann R, van Lith Y, Vasconcelos C, McKenzie JA, Karpoff AM (2000) Bacterially induced dolomite precipitation in anoxic culture experiments. Geology 28:1091–1094

Warthmann R, Vasconcelos C, Sass H, McKenzie JA (2005) *Desulfovibrio brasiliensis* sp. nov., a moderate halophilic sulfate-reducing bacterium from Lagoa Vermelha (Brazil) mediating dolomite formation. Extremephiles 9:255–261

Welsh DT, Lindsay YE, Caumette P, Herbert RA, Hannan J (1996) Identification of trehalose and glycine betaine as compatible solutes in the moderately halophilic sulfate reducing bacterium Desulfovibrio halophilus. FEMS Microbiol Lett 140:203–207

Whitman WB, Coleman DC, Wiebe WJ (1998) Prokaryotes: the unseen majority. Proc Natl Acad Sci U S A 95:6578–6583

Wierzchos J, Ascaso C, McKay CP (2006) Endolithic cyanobacteria in halite rocks from the hyperarid core of the Atacama desert. Astrobiology 6:415–422

Wilcock WSD, Delong EF, Kelley DS, Baross JA, Cary SC (2004) The Subseafloor Biosphere at Mid-Ocean Ridges. American Geophysical Union, Washington, DC.

Wright D (1999) The role of sulphate-reducing bacteria and cyanobacteria in dolomite formation in distal ephemeral lakes of the Coorong region, South Australia. Sed Geol 126:147–157

Wright DT, Oren A (2005) Nonphotosynthetic bacteria and the formation of carbonates and evaporites through time. Geomicrobiol J 22:27–53

Wright DT, Wacey D (2005) Precipitation of dolomite using sulphate-reducing bacteria from the Coorong Region, South Australia: significance and implications. Sedimentology 52:987–1008

Wright DT, Wacey D (2007) Precipitation of dolomite using sulphate reducing bacteria from the Coorong Region, South Australia: significance and implications. Sedimentology 52

Wu LL, Jacobson AD, Chen HC, Hausner M (2007) Characterization of elemental release during microbe-basalt interactions at T=28 degrees C,. Geochimica et Cosmochimica Acta 71:2224–2239

Wu QL, Zwart G, Schauer M, Kamst-van Agterveld MP, Hahn MW (2006) Bacterioplankton community composition along a salinity gradient of sixteen high-mountain lakes located on the Tibetan Plateau, China. Appl Environ Microbiol 72:5478–5485

Wuchter C, Abbas B, Coolen MJL, Herfort L, van Bleijswijk J, Timmers P, Strous M, Teira E, Herndl GJ, Middelburg JJ, Schouten S, Damste JSS (2006) Archaeal nitrification in the ocean. Proc Natl Acad Sci U S A 103:12317–12322

Wynn-Williams DD (2000) Cyanobacteria in deserts-life at the limit? In: Whitton BA, Potts M(eds) The ecology of cyanobacteria-their diversity in time and space. Kluwer Academic Publishers, Dordrecht, The Netherlands, pp 341–366

Zavarzina DG, Sokolova TG, Tourova TP, Chernyh NA, Kostrikina NA, Bonch-Osmolovskaya EA (2007) *Thermincola ferriacetica* sp nov., a new anaerobic, thermophilic, facultatively chemolithoautotrophic bacterium capable of dissimilatory Fe(III) reduction. Extremophiles 11:1–7

Zhang G, Dong H, Jiang H, Xu Z, Eberl D (2006) Unique microbial community in drilling fluid from Chinese Continental Scientific Deep Drilling. Geomicrobiological Journal, 23:1–16

Zhang G, Dong H, Jiang H, Xu Z, Eberl D (2006a) Unique microbial community in drilling fluid from Chinese Continental Scientific Deep Drilling. Geomicrobiol J 23:499–514

Zhang GX, Dong HL, Jiang HC, Kukkadapu RK, Kim JW, Eberl DD, Xu ZQ (2007) Evidence for Microbially-Mediated Iron Redox Cycling in the Deep Subsurface. Appl Environ Microbiol In submission

Zhang Y, Jiao NZ, Cottrell MT, Kirchman DL (2006b) Contribution of major bacterial groups to bacterial biomass production along a salinity gradient in the South China Sea. Aquat Microb Ecol 43:233–241

Zheng D, Yao TD (2004) Uplifting of Tibetan Plateau with its environmental effects. Science Press, Beijing, China

Zheng MP (1995) An introduction to saline lakes on the Qinghai-Tibet Plateau. Kluwer Academic Publishers, Dordrecht, The Netherlands, 294pp
Zolotov MY, Shock EL (2004) A model for low-temperature biogeochemistry of sulfur, carbon, and iron on Europa. J. Geophy Res -Planets 109:E06003

Marine Methane Biogeochemistry of the Black Sea: A Review

Thomas Pape, Martin Blumenberg, Richard Seifert, Gerhard Bohrmann and Walter Michaelis

Abstract Both the anaerobic and the aerobic oxidation of methane are fundamental microbial processes with far reaching influences on global element cycles and, consequently, on the physico-chemical nature of the hydro- and atmosphere. These processes lead to substantial removal of the radiatively active gas methane and are powerful factors in controlling the composition of ecosystems and the distribution of authigenic deposits at methane-rich sites. For instance, the sulfate-dependent anaerobic oxidation of methane (AOM) mediated by methanotrophic Archaea and sulfate-reducing Bacteria yields hydrogen sulfide and bicarbonate ions, which subsequently react with ions derived from pore waters and the water column to form sulfidic and carbonaceous minerals. The aerobic oxidation of methane, performed by obligate aerobic Bacteria particularly effective at oxic-anoxic boundaries, leads to the generation of carbon dioxide, which is a less radiative gas than methane but has higher residence times in the atmosphere.

The geochemical characteristics of the contemporary Black Sea promote processes associated with the conversion of methane and are considered to resemble those of the Paleo/Mesoproterozoic global ocean. Geochemical and molecular microbiological considerations support the idea that the microbes involved in the AOM emerged before the Archaean – Proterozoic transition, and became more important in the Paleoproterozoic, when oceanic deep waters are thought to contain high amounts of methane and adequate amounts of sulfate. With the rise of atmospheric oxygen in the Paleo/Mesoproterozoic, substantial parts of the global ocean became oxygenated, which promoted the spreading of aerobic methanotrophs. Since then, biogeochemical remnants, like fossil seep deposits or lipid biomarkers strongly depleted in ^{13}C, demonstrate the relevance of methanotrophy in Earth history.

Methane in the contemporary Black Sea is mainly sourced from sedimentary gas reservoirs at emission sites like cold seeps and mud volcanoes. Detailed seismic and hydroacoustic investigations at deep-water cold seep areas on the Ukrainian shelf (northwestern Black Sea), the continental slope off Georgia (southeastern Black

T. Pape
Research Center Ocean Margins, University of Bremen, Klagenfurter Strasse, D-28334 Bremen, Germany
e-mail: tpape@uni-bremen.de

Y. Dilek et al. (eds.), *Links Between Geological Processes, Microbial Activities & Evolution of Life*, © Springer Science+Business Media B.V. 2008

Sea) and at mud volcanoes located in the Sorokin Trough (northern Black Sea) provided insights into their subsurface structures, fluid migration pathways, and extents of gas plumes in the water column. This review considers recent studies on sources and migration pathways of methane, and its fate in the sediments in the water column of the Black Sea with special emphasis on the anaerobic and aerobic microbial methane consumption.

1 Introduction

Since the onset of life strong chemical feedbacks arose between biosphere and geosphere. Because methane apparently was an abundant constituent of the Early Earth's atmo- and hydrosphere (Pavlov et al. 2003; Kasting 2005) the metabolisms of recent methane-consuming microorganisms might mirror feasibilities established by the earliest forms of life. Though considerable progress could be achieved during the last 30 years in elucidating geochemical and microbial methane dynamics, many aspects of microbial methanogenesis and methanotrophy are still under debate.

1.1 Methane Generation and Migration in Marine Environments

Beside abiotic formations of hydrocarbons in hydrothermally affected systems and crystalline rocks, methane is generated by the activity of methanogenic Archaea ('biogenic' methane) and by thermocatalytic degradation ('thermogenic' methane) of organic matter. Biogenic methane is mainly produced either by CO_2 reduction with hydrogen (chemical reaction I)

$$CO_2 + 4\,H_2 \rightarrow CH_4 + 2\,H_2O \qquad \text{(I)}$$

or by acetate fermentation (reaction II)

$$CH_3COO^- + H_2O \rightarrow CH_4 + HCO_3^- \qquad \text{(II)}$$

Moreover, a variety of methylated compounds like methanol or methylamines serve as substrate for microbial methanogenesis (Balch et al. 1979), but this process appears to be of minor quantitative relevance for the global methane budget compared to methane production from CO_2 reduction or acetate splitting.

In addition to microbial methane from shallow sediments and the water column, methane is supplied from underlying sediments forced by sediment compaction, tectonic compression or a combination of both mechanisms. In case the concentration of dissolved methane in pore fluids exceeds its solubility, the excess of methane either forms free gas or, under appropriate physico-chemical conditions, gas hydrates (Bohrmann and Torres 2006; Sloan and Koh 2007). Hence, sedimentary methane is transported either by fluid migration or diffusion of dissolved gas, or as free gas, which is released into the water column at cold seeps and mud volcanoes.

Furthermore, it is well known, that substantial amounts of methane can be adsorbed to mineral surfaces and protected against microbial degradation (Brekke et al. 1997; Knies et al. 2004).

The relative partitioning of methane into its major sedimentary reservoirs (dissolved in interstitial waters, as free gas, adsorbed to mineral surfaces, bound in gas hydrates) during its rise to the seafloor is crucial for an assessment of the methane bioavailability and calculations of methane budgets and fluxes. However, the response of sedimentary methane pools to environmental changes is highly dynamic and quantitative estimations are adapted from few investigations only. For example, high amounts of methane are sequestered in the lattices of gas hydrates (Buffett 2000; Bohrmann and Torres 2006; Sloan and Koh 2007). The formation of these ice-like clathrates is mainly governed by the local pressure-temperature regime, which confines their occurrences to a certain depths range, as well as by the supply of the guest molecules (mainly methane) and water. In case ambient conditions drop out of the gas hydrate stability zone (GHSZ) due to environmental changes, gas hydrates decompose rapidly and may provide large quantities of free gas for seepage from the seafloor (Kvenvolden 1988). Substantiated by their highly dynamic physico-chemical nature, sediment destabilizations on continental margins (Mienert et al. 1998, 2005) and past global climate variations (Dickens et al. 1995, Haq 1998; Clennell et al. 1999; Dickens, 2001, 2003) were related to extensive dissociation of gas hydrates. A decrease in $\delta^{13}C$ of carbonates and organic matter by $-2.5‰$ across the Paleocene/Eocene thermal maximum (ca. 55.5 Myr) was attributed to extensive release of ^{13}C-depleted carbon from decomposing gas hydrates. The negative excursion in $\delta^{13}C$ was accompanied by a significant increase in global surface and deep ocean temperatures by about 4–6° C and by a shoaling of the lysocline depth by up to 400 m (Kennett and Stott 1991; Tripati and Elderfield 2005). These scenarios are of major concern for modern atmosphere properties, since the methane flux generated by present-day anthropogenic activity is of similar magnitude to that calculated to have caused such considerable changes in the past (Dickens et al. 1997).

1.2 Methanotrophy in Marine Environments

In marine settings, methane consumption is performed by phylogenetically diverse microorganisms under oxic and under anoxic conditions.

1.2.1 The Aerobic Oxidation of Methane

In oxygenated marine environments, methane oxidation is performed by obligate aerobic Bacteria, preferentially thriving at oxic-anoxic boundaries where methane and oxygen often co-occur. Using molecular oxygen, methane is sequentially oxidized to carbon dioxide according to the following carbon pathway

$$CH_4 \rightarrow CH_3OH \rightarrow HCHO \rightarrow HCOOH \rightarrow CO_2$$

Aerobic methanotrophs are found among bacterial groups belonging to the gamma- (type I, type X methanotrophs) or the alpha- (type II) proteobacteria (Hanson and Hanson 1996). Type I methanotrophs comprise genera like *Methylobacter*, *Methylococcus*, and *Methylomonas*, while among type II methanotrophs *Methylosinus* and *Methylocystis* are found.

1.2.2 The Anaerobic Oxidation of Methane

The anaerobic oxidation of methane (AOM) was uncovered as a geochemical key process within anoxic, methane-rich and sulfate-bearing marine sediments (Barnes and Goldberg 1976; Reeburgh 1976) and is believed to be a much more effective biological sink for methane than the aerobic methane oxidation (Reeburgh 1996, 2007). Supported by geochemical and molecular biological findings, the sulfate-dependent AOM (net chemical reaction V) is considered to be mediated by a consortium of methanotrophic Archaea and sulfate-reducing Bacteria (Hoehler et al. 1994; Hinrichs et al. 1999; Boetius et al. 2000; Michaelis et al. 2002; Nauhaus et al. 2002) according to the proposed equations (III) and (IV):

$$CH_4 + 2\,H_2O \rightarrow CO_2 + 4\,H_2 \qquad \text{(III)}$$

$$SO_4{}^{2-} + 4\,H_2 + H^+ \rightarrow HS^- + 4\,H_2O \qquad \text{(IV)}$$

$$CH_4 + SO_4{}^{2-} \rightarrow HCO_3{}^- + HS^- + H_2O \qquad \text{(V)}$$

As such, the process of AOM includes CO_2-based methanogenesis in reverse. AOM-driven sulfate reduction and archaeal methanogenesis have thought to be spatial mutually exclusive for a long time. However, several methodological approaches point to a conjoint operation of both processes in the marine environments (Pimenov et al. 1997; Hoehler et al. 2000; Inagaki et al. 2004; Krüger et al. 2005). Moreover, there is evidence that some Archaea can be involved in both, AOM and methanogenesis (Krüger et al. 2003; Hallam et al. 2004; Orcutt et al. 2005; Seifert et al. 2006), but their metabolic capabilities and physiologies are still poorly understood.

It is well established by now that the sulfate-dependent AOM is driven by at least three anaerobic methanotrophic archaeal clades (ANME-1 to ANME-3) related to the orders *Methanosarcinales*, or *Methanococcoides* and *Methanolobus*, frequently observed in physical and physiological coupling to sulfate-reducing proteobacteria (SRB) of the *Desulfosarcina/Desulfococcus* group (Hinrichs et al. 1999, 2000; Boetius et al. 2000; Orphan et al. 2001, 2002; Hinrichs and Boetius 2002; Blumenberg et al. 2004; Knittel et al. 2005) or the *Desulfobulbus* group (Niemann et al. 2006; Lösekann et al. 2007). Even though the co-occurrence of multiple phylotypes is known, characteristic population structures, including the prevalence of a certain ANME group, were found at several AOM sites (Hinrichs et al. 1999;

Boetius et al. 2000; Orphan et al. 2001, 2002; Michaelis et al. 2002; Teske et al. 2002; Blumenberg et al. 2004; Niemann et al. 2006).

1.3 Chemical Indicators for Methanotrophy in Marine Ecosystems

Due to concomitant bicarbonate release, precipitates of authigenic carbonates are commonly found at ancient and contemporary sites of sulfate-dependent AOM (Ritger et al. 1987). Depending on the signature of the stable C-isotopes of the methane consumed and the kinetic C-isotope fractionation during its conversion, AOM-related carbonates are commonly characterized by extreme depletions in ^{13}C. Furthermore, biochemical remnants of AOM-performing microorganisms, like shells of seep-associated metazoa and lipid biomarkers, are incorporated to some degree into the carbonate matrix (Peckmann and Thiel 2004; Campbell 2006). Commonly, a suite of archaeal and bacterial lipids strongly depleted in ^{13}C are related to AOM consortia (e.g. Elvert et al. 1999; Hinrichs et al. 2000; Pancost et al. 2001; Pancost and Sinninghe Damsté 2003; Peckmann and Thiel 2004) and, moreover, the distribution patterns of these lipids allows for a differentiation between the ANME consortia (Blumenberg et al. 2004; Niemann et al. 2006).

It is generally believed that authigenic carbonates might persist through geological times and that the organic matter entrapped is protected against diagenetic transformation to a large extent (Peckmann and Thiel 2004). Hence, authigenic carbonates bear an excellent historical record of (sub)recent and fossil AOM settings. Further, they affect the ocean-atmosphere carbon transfer, since they are in principle terminal sinks of methane.

2 The Black Sea

The Black Sea basin represents an extraordinary area for studies of recent processes related to the cycling of methane-derived carbon. It comprises the world's largest anoxic and sulfidic marine water body and the largest surface water reservoir of dissolved methane being more than 96 Tg (Reeburgh et al. 1991).

2.1 Geologic Setting and Geochemical Characteristics

The Black Sea is a Cretaceous-Palaeogene back-arc basin (Starostenko et al. 2004), which is separated into a western and an eastern sub-basin by the Andrusov Ridge (Fig. 1). Deepening of the basins existed since the latest Eocene to recent times (Nikishin et al. 2003). Currently, both basins are covered with 12–16 km thick organic-rich sediments, which, inferred from seismic studies, represent up to five stratigraphic units from the Upper Cretaceous to the Pliocene-Quarternary (Jones and Gagnon 1994; Nikishin et al. 2003; Starostenko et al. 2004). With respect to

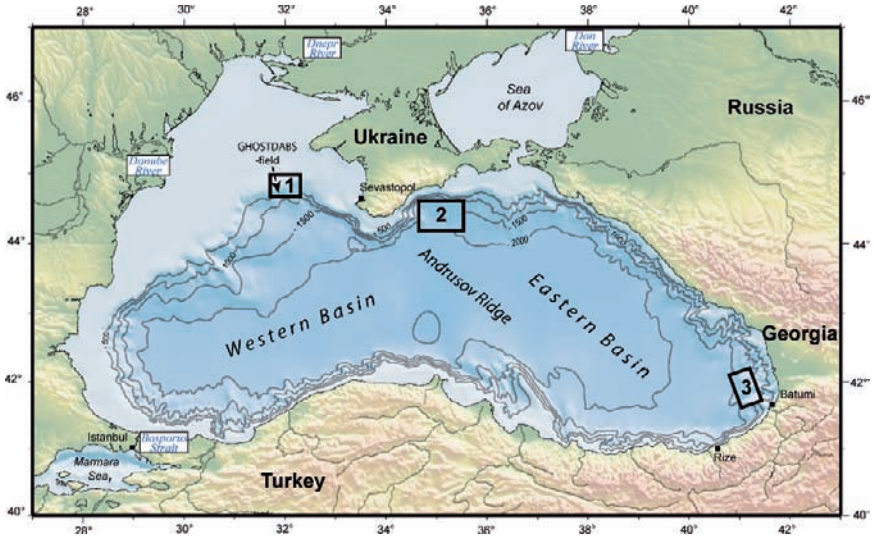

Fig. 1 Bathymetric map of the Black Sea indicating areas discussed in the paper located on the Ukrainian shelf (1), in the Sorokin Trough (2), and on the Georgian shelf and continental slope (3). Study area (1) covers the GHOSTDABS-field. Major tributaries are the Danube, the Dnepr and the Dnestr rivers as well as the Don river through the Sea of Azov. Water outflow from the Black Sea is restricted to the Bosporus Strait

recent oil and gas supply, the Late Oligocene – Lower Miocene Maikopian complex, which is composed of organic rich clay sediments of 4–5 km thickness, is of major interest.

The Black Sea was a freshwater lake during the last glaciation, and more marine conditions were caused by the intrusion of high saline Mediterranean waters through the Bosporus Strait, which is considered to have started at about 9.4 kyrs B.P. (Ross et al. 1970; Jones and Gagnon 1994; Ryan et al. 1997). The contemporary Black Sea is a semi-closed basin with its sole drainage through the Bosporus Strait into the Mediterranean. Freshwater supply is sustained by river run-off of the Danube, Dnepr, Don (via the Sea of Azov) and several minor tributaries (Murray and Yakushev 2006). As a consequence of constant water column stratification due to strong salinity and density gradients, the present-day ventilation of deeper water masses (maximum depth about 2200 m) is restricted, leading to a permanently anoxic zone that has evolved in the deeper Black Sea basin during the last 8000 years (Lamy et al. 2006). Today, the oxic-anoxic transition zone is positioned at varying water depths between 80 and 140 m (Özsoy and Ünlüata 1997; Murray and Yakushev 2006). Methane concentrations $> 15\mu M$ have been measured in depths below 1000 m (Fig. 2). Sulfate is present at concentrations sufficient to sustain the sulfate-dependent AOM in euxinic waters and within the sulfate-methane transition zone at 2–4 m sediment depths (Weber et al. 2001; Jørgensen et al. 2004). As indicated by sulphide concentration profiles and distributions of bacterial lipid

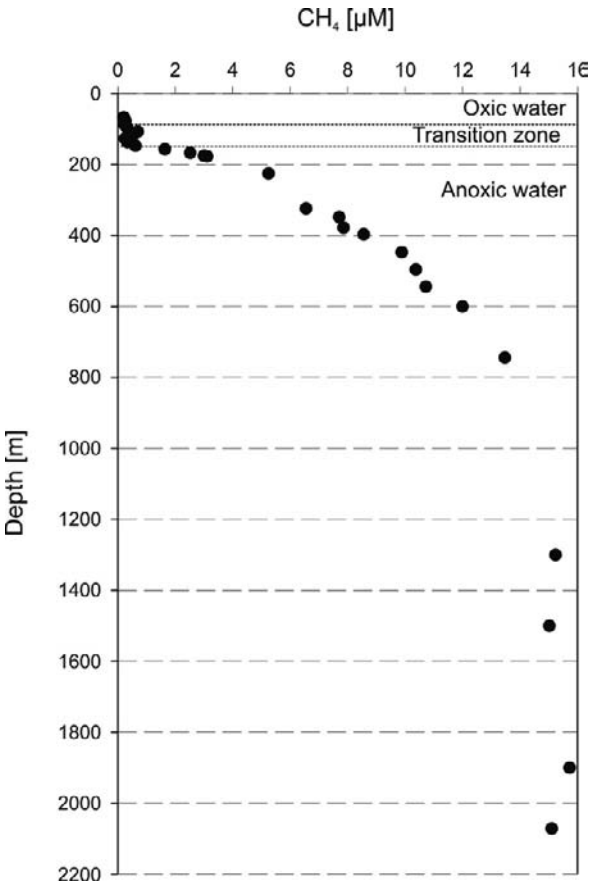

Fig. 2 Combined depth distributions of dissolved methane compiled from several stations located on the Ukrainian shelf and in the central western Black Sea basin. The general position of the oxic-anoxic transition zone separating the oxic and the anoxic water bodies is illustrated

biomarkers, sulfate reduction also occurs in the oxic-anoxic transition zone (Murray and Yakushev 2006; Wakeham et al. 2007).

2.2 Gas Generation, Migration Pathways and Emission Sites

Due to its rapid subsidence, the Black Sea sedimentary basin is characterized by sediment deformations, which create pathways for ascending fluids and hydrocarbons. Several areas of pronounced gas seepage und mud volcanic activity were examined by means of seismic profiling and hydroacoustic measurements in recent years. These investigations provided insights into subsurface structures, fluid migration pathways, spatial distributions of sedimentary gas and shallow gas hydrate

accumulations, and extents of gas plumes in the water column. Gas bubble flares, indicating intense gas discharge into the water column, were documented for instance in the central Black Sea (Ivanov et al. 1996; Limonov et al. 1997; Shnukov et al. 2004), on the Bulgarian, Romanian, and Ukrainian shelf and slope (Egorov et al. 1998; Ivanov et al. 1998; Luth et al. 1999; Naudts et al. 2006; Artemov et al. 2007), in the Sorokin Trough southeast of the Crimean Peninsula, (Greinert et al. 2006) and on the slopes offshore Georgia and Turkey (Sahling et al. 2004; Klaucke et al. 2006; Bohrmann et al. 2007) within a large water depth range. These gas bubble streams could generally be attributed to cold gas seep structures or mud volcanoes.

Given the appropriate pressure-temperature conditions, gas hydrates often occur spatially related to such gas accumulations. Adapted from its physico-chemical conditions, the upper boundary of the GHSZ for pure methane in the Black Sea was calculated to be situated around 700 m water depths (Bohrmann et al. 2003). Since the early findings by Yefremova and Zhizhchenko (1974), shallow gas hydrate occurrences were inferred from geophysical surveys or proven by recovery from several places in the Black Sea. By means of acoustic measurements, gas hydrate accumulations are indicated by a 'bottom simulating reflector' (BSR), which marks the thermobaric base of the GHSZ. So far BSR-like structures are only reported from restricted areas, like in the northwestern Black Sea west of the Dnepr canyon (Lüdmann et al. 2004; Zillmer et al. 2005), offshore Georgia in the southeastern Black Sea (Akhmetzhanov et al. 2007; Bohrmann et al. 2007), and in the southwestern Black Sea off Turkey (Sahling et al. 2004). For the Danube deep-sea fan on the Romanian slope, Popescu et al. (2006) reported the detection of multiple bottom-simulating reflections, which the authors interpret as former positions of the base of the GHSZ. In some cases, however, Black Sea gas hydrate occurrences became evident although no BSR was found. An example is the Sorokin Trough, where gas hydrates were recovered (Ivanov et al. 1998; Blinova et al. 2003; Bohrmann et al. 2003; Aloisi et al. 2004) and 'bright spots' in the seismic record might indicate accumulations of gas hydrates and free gas at flanks of diapiric structures (Bouriak and Akhmetjanov 1998; Krastel et al. 2003), despite the apparent absence of a BSR.

For some sites located in the GHSZ, vigorous gas discharge into the water column and the co-occurrence of shallow-buried gas hydrates were documented. For example, temporary formations of huge gas plumes (Greinert et al. 2006) and wide distributions of gas hydrate pieces in sediments (Aloisi et al. 2004) were observed at the Dvurechenskii mud volcano (DMV) located in the Sorokin Trough in about 2000 m water depths. Consequently, a shift of the local thermodynamic conditions towards the boundaries of the GHSZ was proposed due to the ascent of warm and saline fluids in the centre of the structure, where gas bubbles escaped the seafloor (Fig. 3; Bohrmann et al. 2003; Aloisi et al. 2004). These findings underline the sensitivity of shallow-buried gas hydrates to changes of the environmental setting and are of great relevance for the still uncertain estimates of methane fluxes from decomposing gas hydrates.

Specifically within the UNESCO-IOC 'Training-trough-Research'-programme and joint German and European research projects ('GHOSTDABS' 'METRO', 'CRIMEA') geological settings, and geochemical and microbiological aspects at

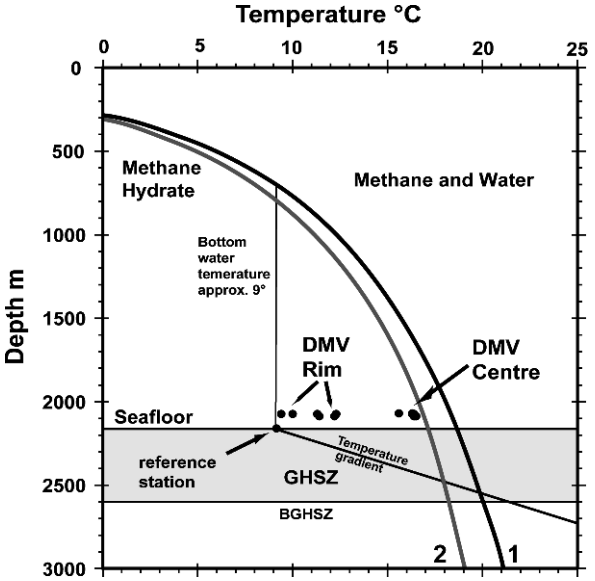

Fig. 3 Hydrate stability field calculated for pure methane and Black Sea water chlorinity of 355 mM (1) and elevated pore water chlorinity of 900 mM (2) in sediments from the Dvurechenskii mud volcano (DMV) (modified from Bohrmann et al. 2003). At the centre of the DMV thermodynamic conditions are close to the boundaries of the hydrate stability field. A location outside of mud volcano structures at the Sorokin Trough was taken as reference station. GHSZ = Gas hydrate stability zone; BGHSZ = Base of GHSZ

cold seeps in the northwestern and southeastern Black Sea as well as at mud volcanoes in the Sorokin Trough were explored (see Fig. 1 for study areas). During several cruises, remotely operated vehicles and a submersible were deployed, which allowed for comprehensive visual inspections and detailed sampling of seep-associated sediments and authigenic carbonates, biological material, and discharged gases at selected locations.

2.2.1 Mud Volcanoes

A number of mud volcano structures are known from deep waters (1000–2000 m) in the central Black Sea (Ivanov et al. 1996; Limonov et al. 1997; Gaynanov et al. 1998), and in the Sorokin Trough (Bohrmann et al. 2003; Krastel et al. 2003; Greinert et al. 2006). In contrast to the majority of Black Sea cold seeps investigated so far, the mud volcanoes are often characterized by strong bathymetric reliefs due to the expulsion of fluid mud and mud breccia (Limonov et al. 1997).

In recent years, mud volcanoes of the Sorokin Trough (Fig. 1; area 2) came into the focus of intense research. It is believed that fluid migration in the Sorokin Trough is facilitated by mud diapirism within the general compressional tectonic regime. Due to mobilization of the deeply buried (6–10 km in the western basin; Nikishin et al. 2003) clay-rich Maikopian formation, mud diapirs and diapric ridges

are formed in the overlying sediments (Krastel et al. 2003). Faults created in these sediments serve as potential fluid migration pathways. Accordingly, degradation of organic matter from the Maikopian series is considered to form the principal gas source for mud volcanoes in the Sorokin Trough. This assumption was supported by the seismic prove of deep-rooted mud diapirism and the direct observation of Maikopian fragments in expelled mud breccia (Ivanov et al. 1998).

The Dvurechenskii mud volcano (DMV, 44°17′N; 34°59′E) is one of the intensely studied out of a suite of mud volcanoes located in the Sorokin Trough in depths of approx. 2000 m (Fig. 4). During recent years the DMV came into the focus of intense research with respect to subsurface structures (Krastel et al. 2003), compositions and extends of ascending fluids and gases (Bohrmann et al. 2003; Aloisi et al. 2004; Wallmann et al. 2006), as well as the presence of gas hydrates and carbonate precipitates (Blinova et al. 2003; Bohrmann et al. 2003). Morphologically, the DMV is an oval structure of about 1000 m in seabed diameter characterized by a flat top. As illustrated by seismic profiling, it is most probably located on a fault zone on top of a diapiric structure of ascending Maikopian clay (Krastel et al. 2003). Deduced from the subsurface structures and the chemical characteristics of gases in the porewaters, gas generation for some Sorokin Trough mud volcanoes was attributed to thermocatalytic organic matter degradation (Mazzini et al. 2004; Stadnitskaia et al. 2005). For instance, $\delta^{13}C$ values of about −56‰ for methane (relative to the V-PDB standard as for all $\delta^{13}C$ values herein) and relatively high concentrations of higher methane homologues were found in deposits of the Kazakov mud volcano, which is closely located to the DMV. For several other Sorokin Trough mud volcanoes, including the DMV, strong depletions in ^{13}C (up to −70.4‰) of methane

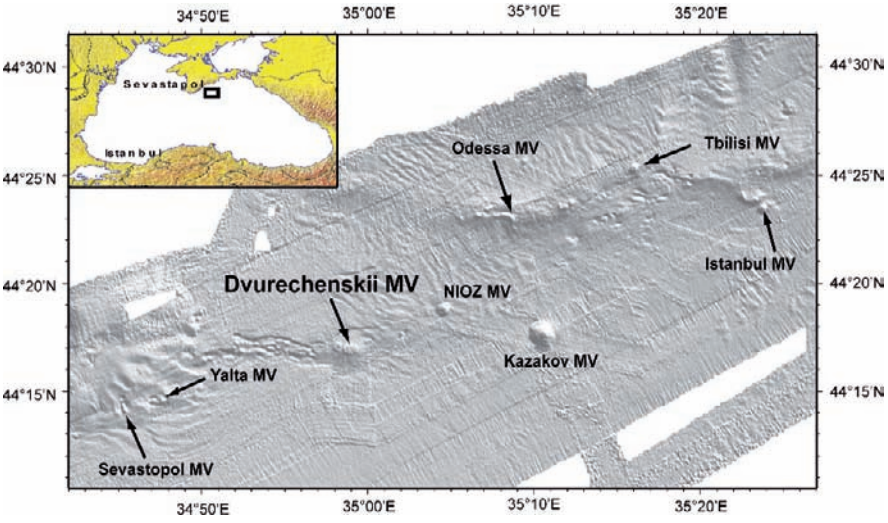

Fig. 4 Bathymetric map of the central Sorokin Trough southeast of the Crimean Peninsula (modified from Bohrmann et al. 2003). Locations of major mud volcanoes (MV) including the Dvurechenskii MV are shown

in surface sediments were interpreted as significant admixture of biogenic methane (Blinova et al. 2003; Mazzini et al. 2004). Consequently, Blinova et al. (2003) assume biodegradation of hydrocarbons accumulated in deep sediment layers below the DMV to release ^{13}C-depleted methane.

As indicated by pore water geochemical modelling for the DMV, about 80% of the methane transported with ascending fluids during periods of quiescent dewatering is consumed by AOM within the surface sediments (Wallmann et al. 2006). However, periods of high activity causing vigorous gas seepage were also recognized and Egorov et al. (2003) reported a vertical extension of a gas bubble plume released from the DMV of up to 1300 m. Strong fluctuations in the gas emissions as observed by Greinert et al. (2006), complicate accurate long-term calculations of the total gas discharge from the DMV.

2.2.2 Cold Seeps

Cold seeps and decomposing gas hydrates are considered to contribute the majority (86–91% of all sources) of the entire Black Sea methane reservoir (Kessler et al. 2006). Numerous cold seeps were well documented on the Ukrainian shelf and slope around the Dnepr paleo-delta area during earlier studies (Polikarpov et al. 1992; Egorov et al. 1998; Luth et al. 1999). Naudts et al. (2006) and Artemov et al. (2007) detected more than 2200 gas seeps between 66 and 825 m water depth by means of echosounding (Fig. 5). Most of these seeps are located above 725 m water depth, which coincides with the upper boundary of the GHSZ calculated for the formation of pure methane hydrate in the Black Sea. Thus, the authors suggested that in deeper parts of the survey area gas hydrates form and prevent major gas seepage into the water column.

A shallow-water seep area (GHOSTDABS-field; 44°46′N; 31°59′E) in the Dnepr paleo-delta, which is characterized by intense bubble discharge and a high density of methane-related microbial mats, was investigated during several cruises (Egorov et al. 1998; Luth et al. 1999; Michaelis et al. 2002). Methane (>95%) is the major volatile escaping from the GHOSTDABS-field seafloor, and, indicated by its stable isotope composition ($\delta^{13}C = -62.4$ to $-68.3‰$; $\delta^{2}H = -245$ to $-255‰$ V-SMOW [unpublished data]), is predominantly sourced by microbial methanogenesis (Michaelis et al. 2002). By its position on a morphological ridge, the area is protected from sediment slumping, which is common along the shelves and continental slopes. Seepage throughout an extended time period promoted long-term biomass accumulation through AOM-performing microbial mats. At many sites of effusive gas discharge, the mats formed tower-like structures which extend up to about 4 m from the seafloor and consist of cm- to dm-thick biomass with a skeleton of authigenic cavernous carbonates (Fig. 6). Benthic and sub-seafloor methanotrophic microbial mats have also been reported in the eastern Black Sea off Russia and Georgia (Akhmetzhanov et al. 2007; Bahr et al. 2008), but only in the GHOSTDABS-field they were recognized to establish seep-related towers of several meters in height, so far (Fig. 6).

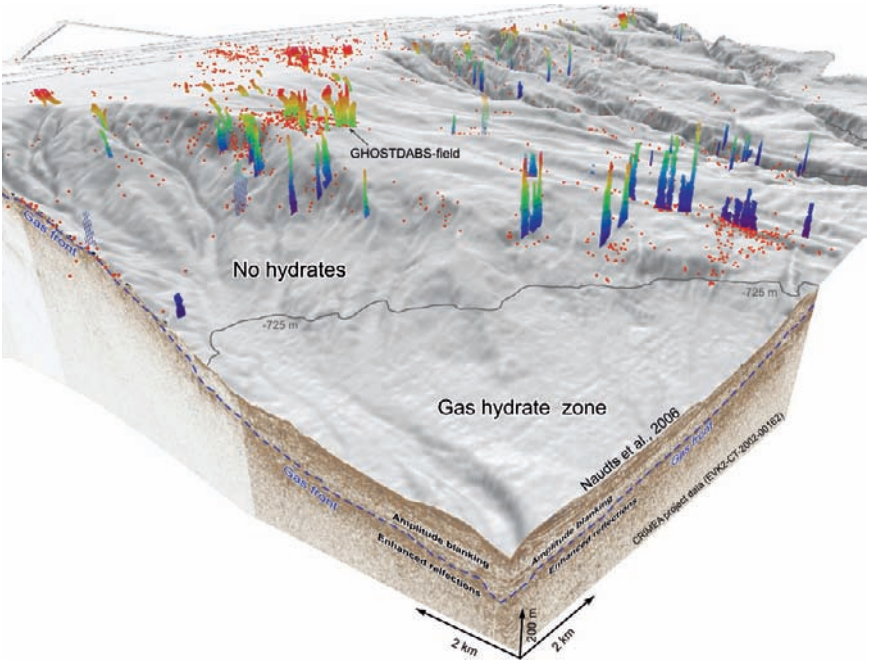

Fig. 5 View from SW on a bathymetry map of a part of the Ukrainian shelf and upper continental slope (adapted from Naudts et al. 2006). The position of the GHOSTDABS-field is indicated. Seep locations are depicted as red dots and some seeps are shown as 3D flares. Seeps predominate above the gas hydrate stability zone, delineated by the 725 m contour line. Reprinted with permission from Marine Geology (Naudts et al., Marine Geology 227, 177–199). Copyright (2007) Elsevier B.V.

Deep-water cold seeps were also discovered on the continental slope offshore Georgia, southeastern Black Sea (Fig. 1; area 3; Akhmetzhanov et al. 2007). Gas flares in the water column and several individual seafloor gas emission sites were detected by hydroacoustic measurements, video observations, sidescan sonar mapping and seismic profiling (Klaucke et al. 2006). The seeps are located in water depths between 850 and 1200 m on the tops and flanks of ridge structures. A prominent seep site, the Batumi seep area (41°58'N and 41°17'E; approx. 850 m water depth), is characterized by a high number of gas flares (Fig. 7).

Like for the mud volcanoes in the Sorokin Trough, the Maikopian series is considered as a probable source for hydrocarbons emanating from cold seeps offshore Georgia (Klaucke et al. 2006; Akhmetzhanov et al. 2007). In the eastern Black Sea the Maikopian has been deformed into a number of ridges due to tectonic loading (Tugolesov et al. 1985). Seismic profiling showed that seepages at the Batumi seep area are related to fluid migration along faults and fractures caused by the diapiric uplift (Akhmetzhanov et al. 2007). Low-molecular-weight hydrocarbons in shallow sediments at the Batumi seep area were strongly dominated by methane (> 99.9%;

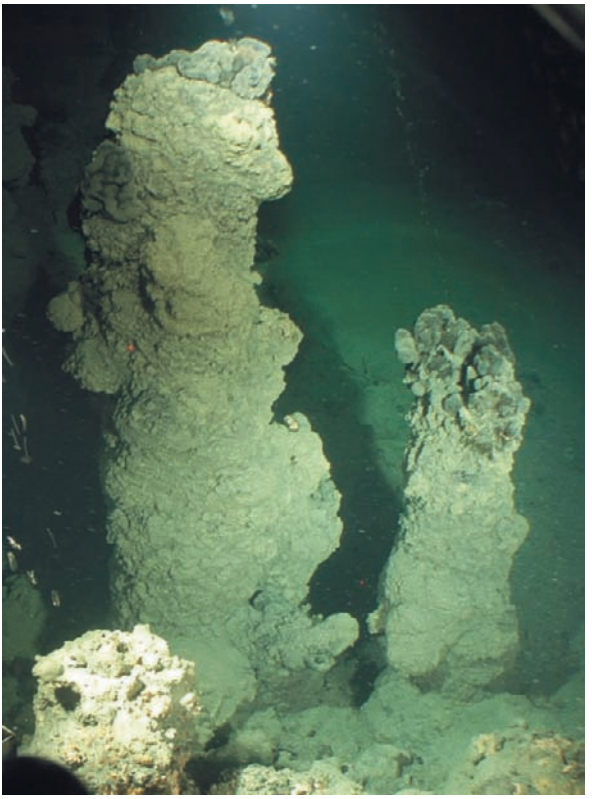

Fig. 6 View from inside of a submersible on tower-like structures growing in anoxic waters (230 m water depth) of the Black Sea on the Ukrainian shelf. The tower-like bioherms are up to 4 m in height, constructed by massive microbial mats and internally stabilized by carbonate precipitates. For position of the study area refer to Fig. 1, area (1)

Bohrmann et al. 2007) indicative of gases predominantly of microbial origin. In addition, oil seeps, where oil is associated to fluid and gas seepage, were reported from the Georgian continental slope west off Batumi (Akhmetzhanov et al. 2007, Bohrmann et al. 2007) and the Eastern Black Sea at the Turkish shelf and slope off Rize (Kruglyakova et al. 2004). Consistently, relative enrichments of higher methane homologues point to significant admixtures of gases from deeper sources at oil seeps, close to the Batumi seep area (Bohrmann et al. 2007; Heeschen et al. 2007).

Contrary to shallow-water cold seeps in the northwestern Black Sea, where gas streams were found to percolate huge microbial formed towers, at the Batumi seep area the gas mostly seeped from holes perforating the seafloor. Microbial mats attached to carbonate pieces and randomly distributed carbonaceous pinnacles of cm- to dm-height erecting from the seafloor were also recognized in this area (Bohrmann et al. 2007).

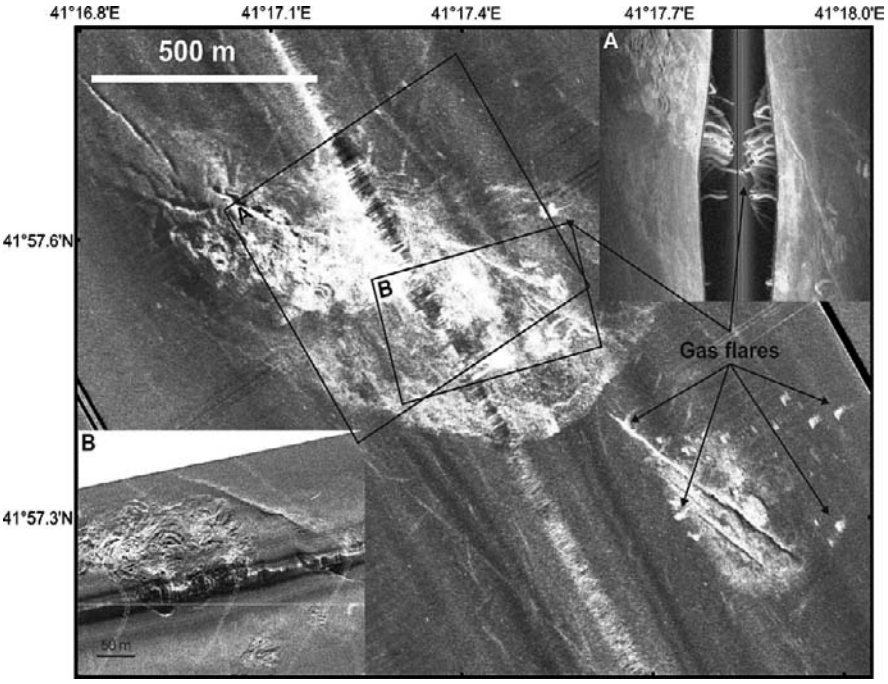

Fig. 7 Mosaic of sidescan sonar data obtained with a deep-towed chirp sidescan sonar system (DTS-1) illustrating the deep-water Batumi seep area offshore Georgia in about 850 m water depth (taken from Klaucke et al. 2005, EOS transactions, 86). High backscatter is shown as light tones. (**A**) Unprocessed 75-kHz sidescan sonar data indicating several acoustic anomalies in the water column (gas flares). (**B**) Sonograph of 410 kHz sidescan sonar data possibly showing fluidized upper sediments around individual gas seeps

3 Microbial Processes Affecting Methane Turnover in the Black Sea

3.1 Methanogenesis

In addition to main methane release from underlying reservoirs and decomposing gas hydrates, the Black Sea water column methane budget is as well maintained by microbial methanogenesis in shelf and slope sediments (Kessler et al. 2006) and to a much lesser extent in the euxinic water body (Ivanov et al. 2002).

3.1.1 Methanogenesis in Shallow Sediments

Methane production is the terminal step in organic matter degradation, hence, methanogenesis rates are in principle affected by the availability of organic matter at a given location. Sedimentary methanogenesis was estimated to contribute between 8.9 and 13.9% of the total Black Sea methane reservoir (Kessler et al. 2006). For

surface sediments on the Ukrainian shelf, Krüger et al. (2005) calculated potential methanogenesis rates (0.005–0.01 μmol methane $g_{dw}^{-1}d^{-1}$) which might be an order of magnitude lower than potential methanotrophy rates (0.02–0.04 μmol methane $g_{dw}^{-1}d^{-1}$). Thus, the authors state that microbial methanogenesis primarily takes place in deeper, sulfate-depleted sediment horizons. However, phylogenetic affiliations of methanogens in shallow Black Sea sediments are poorly constraint so far, to the best of our knowledge.

3.1.2 Methanogenesis in the Water Column

It is common view that water column microbial methane production in the Black Sea plays only a minor role (Pimenov et al. 2000; Reeburgh 2007). Microbial methanogenesis is thermodynamically unfavoured compared to sulfate reduction, and methanogenic Archaea and SRB often compete for the same substrate (in the case of CO_2 reduction for available hydrogen). Hence, biological methane generation was generally considered to be restricted to anoxic environments where sulfate is close to zero (Martens and Berner 1974).

Minor contributions to the Black Sea water column methane reservoir might be derived from methanogens thriving in anoxic waters, which do not compete with sulfate reducers for substrates (Balch et al. 1979), and from the guts and fecal pellets of zooplankton in the suboxic zone. Microbial methanogenesis in zooplanktonic guts is indicated by increasing methane concentrations, accompanied by a relative ^{12}C-enrichment observed in the upper, oxygenated water column of the Black Sea (density σ_T of 15.2; Fig. 8, left). Using ^{14}C-bicarbonate as tracer, Pimenov and Neretin (2006) observed methanogenesis in a depth interval which was also characterized by sulfate-reduction. The phylogenetic classification of water column methanogens is not well investigated so far, but affiliates of the orders *Methanobacteriales* and *Methanosarcinales* might be responsible for water column methanogenesis (Vetriani et al. 2003). Interestingly, recent studies revealed the co-occurrence of sulfate reduction and methanogenesis on a very small scale most likely due to different substrates used by both microbial groups (Seifert et al. 2006). However, water column methanogenesis does not contribute more than 1% to the entire methane reservoir (Kessler et al. 2006).

3.2 Methanotrophy

Effective methane dissolution and oxidation mechanisms proceeding in upper sediment layers and the water column result in less than 2% of methane annually supplied to the Black Sea basin escaping into the atmosphere (Reeburgh et al. 1991; Kessler et al. 2006). In conclusion, more than 98% of the total Black Sea methane reservoir is converted by the AOM in euxinic waters and effective methanotrophy was also reported for the suboxic water column (Reeburgh et al. 1991, 2006; Gal'chenko et al. 2004; Kessler et al. 2006).

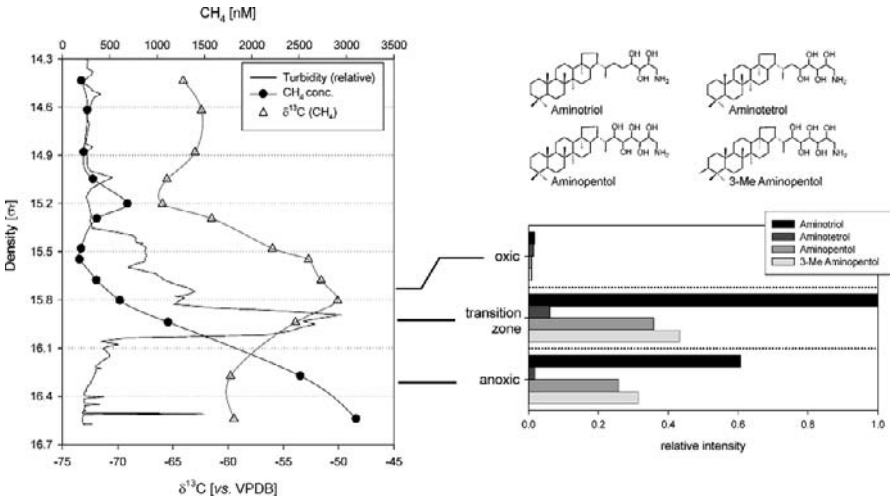

Fig. 8 Methanotrophic activity and microorganisms at the chemocline of the Black Sea at about 100 m water depth (modified after Blumenberg et al. 2007).
Left: Concentrations, carbon stable isotope ratios of methane, and turbidity in the water column in close vicinity to the GHOSTDABS-field plotted against density (σ_T). Depth intervals according to Konovalov and Murray (2001): Average depths for σ_T values of 14.4 and 16.5 are 50 m and 186 m, respectively. The turbidity maximum indicates the water depth with suboxic conditions (oxic-anoxic transition zone) that overlies the anoxic sulfidic zone (according to Eremeeva and Degterev 1993).
Right: Chemical structures of amino-group bearing bacteriohopanepolyols (BHPs) indicative of methanotrophic Bacteria, and their distributions and relative amounts in particulate material retrieved by filtering water samples taken above, within, and below the oxic-anoxic transition zone. Relative concentrations were calculated from responses of compound specific fragment losses during LC-MS-MS collision experiments and were normalised to the most abundant BHP (aminotriol in particulate matter retrieved from the transition zone)

Despite this effective filter for uprising methane, hydroacoustic flare imaging and geochemical studies demonstrated that some part of gas reaches the seawater-atmosphere boundary. For an individual high-density seepage area in the deep northwestern Black Sea (Artemov et al. 2007) calculated that less than 2% of gas bubbles discharged from the seafloor reaches the atmosphere. Based on modelling the sea-atmosphere methane exchange in the Dnepr paleo-delta area and the Sorokin Trough, fluxes above a relatively shallow cold seep (90 m depth) were estimated to be 5 times higher than for open Black Sea waters (Schmale et al. 2005). The authors suggested that only methane ejected close to the sea surface can escape methane oxidation and enter the atmosphere.

3.2.1 Aerobic Methanotrophy in the Suboxic Water Column

The aerobic methanotrophy (MO) in oxygenated waters of the Black Sea is quantitatively only of minor relevance (e.g. Reeburgh et al. 1991), when compared to AOM

in anoxic settings. Kessler et al. (2006) estimated rates of methane consumption in the upper 100 m of the water column to be 0.36 nM yr^{-1} whereas in the underlying waters methane is consumed with 0.6 μM yr^{-1}. With respect to MO, the oxic-anoxic transition zone, where methane and various electron acceptors including oxygen co-occur in high amounts, is most relevant (Saydam et al. 1993; Pimenov et al. 2000; Ivanov et al. 2002). In this depth interval a steep gradient in methane concentration and $\delta^{13}C$ profiles (Fig. 8, left) indicates that methane consuming microorganisms significantly reduce the amount of dissolved methane. Although they represent only a minor constituent of the bacterial population (about 4% of bacterial cells in the suboxic water column; Schubert et al. 2006a), methanotrophic Bacteria accumulate in the oxic-anoxic transition zone (Gal'chenko et al. 1988; Schubert et al. 2006a). By use of immunofluorescence techniques it was observed that the type I and type II aerobic methanotrophs *Methylobacter*, *Methylococcus*, *Methylomonas*, *Methylocystis*, and *Methylosinus*, are the prevailing MO mediating genera in suboxic waters (Gal'chenko et al. 1988).

For a water column station close to the GHOSTDABS-field on the Ukrainian shelf, Blumenberg et al. (2007) traced vertical distributions of phylogenetically diverse aerobic methanotrophic Bacteria. The authors analyzed intact bacteriohopanepolyols (BHPs), of which some are indicative of specific bacterial lineages (e.g. Talbot et al. 2001). Strong enrichments of BHPs demonstrated accumulations of aerobic methanotrophs in the oxic-anoxic transition zone compared to over- and underlying water layers (Fig. 8, right). Moreover, the occurrence of specific BHPs suggests type I (γ-proteobacteria) rather than type II (α-proteobacteria) methanotrophs as dominant methane consuming Bacteria (Blumenberg et al. 2007). This is in line with recent microbiological studies, which showed a high density of γ-proteobacteria of the Methylococcaceae (type I methanotrophs) in this depth interval (Schubert et al. 2006a). Consequently, the results argue for the activity of aerobic rather than anaerobic methanotrophs effecting strong ^{13}C-enrichments of methane as observed for this water column depth range (Fig. 8, left; Blumenberg et al. 2007). Consistent with these findings, the presence of BHPs characteristic for methanotrophic Bacteria was also recently published from the central Black Sea water column (Wakeham et al. 2007).

3.2.2 Anaerobic Methanotrophy in Anoxic Settings

The most effective sink of methane in the Black Sea is the anaerobic oxidation of methane (AOM) in anoxic sediments and the euxinic water column (Kessler et al. 2006). The process of AOM was thoroughly studied in the shallow water cold seep area of the GHOSTDABS-field in the northwestern Black Sea (Fig. 1; area 1). This location is characterized by a high density of microbial mats constructing tower-like bioherms, which are internally stabilized by carbonate precipitates (see Fig. 6). Strong depletions in ^{13}C of both, bulk microbial biomass ($\delta^{13}C = -72.2‰$) and of carbonate ($\delta^{13}C = -25.5$ to $-32.2‰$), indicate a major portion of carbon to originate from the uptake of methane (Michaelis et al. 2002). Considering a relatively low energy yield provided by the process of AOM (Hoehler et al. 1994),

a relatively low growth rate of the indigenous methanotrophic consortia and in consequence, geochemical and –morphological conditions having remained stable for a long time period, have to be assumed for that area. However, the upper age limit of the microbial tower-like structures is given by the limnic-marine transition of the Black Sea and the subsequent development of a permanent anoxic water body about 8.0 kyr ago (Lamy et al. 2006).

Evidenced by molecular biological approaches, the massive microbial mats mainly consist of consortia of densely aggregated Archaea (ANME-1 cluster) and SRB of the *Desulfosarcina/Desulfococcus*-group (Michaelis et al. 2002). Later studies uncovered that in addition to the ANME-1 dominated mats, ANME-2 associations are also present in specific parts of the bioherms (Blumenberg et al. 2004; Treude et al. 2007). By means of lipid biomarker distributions and molecular microbiological techniques (fluorescence in situ hybridization and transmission electron microscopy), ANME-2 were observed to prevail in black gas-filled globules growing on top of the structures (Blumenberg et al. 2004). This approach additionally led to the identification of ANME-specific patterns of archaeal and bacterial lipid biomarkers strongly depleted in ^{13}C (Fig. 9). It was found that ANME-1 Archaea are the exclusive producers of individual tetraether lipid-derived C_{40} isoprenoids ($\delta^{13}C$ down to $-91‰$), whereas members of the ANME-2 cluster contain, for instance, high concentrations of *sn*-2-hydroxyarchaeol ($\delta^{13}C$ down to $-102‰$; Blumenberg et al. 2004). In addition, ANME-1 associated Bacteria were observed to contain mainly ether-bound lipids (i.e. dialkyl glycerol diethers), whereas Bacteria associated to ANME-2 appear to synthesize specific fatty acids (e.g. hexadec-11-enoic acid; data not shown). Remarkably, although both bacterial associates belong to the *Desulfosarcina/Desulfococcus*-group, they show pronounced differences in their lipid biomarker inventories (Fig. 9).

The vertical distributions and phylogenetic affiliations of AOM-mediating microorganisms living in Black Sea waters were followed in recent years by molecular biological and lipid biomarker approaches. Lipids diagnostic for AOM-performing microorganisms were well distributed in the euxinic water body (Schouten et al. 2001; Wakeham et al. 2003; Schubert et al. 2006a; Wakeham et al. 2007). It was observed that ANME-1 (below 600 m water depth) and ANME-2 (above 600 m) related lineages preferentially occur in certain depth ranges (Vetriani et al. 2003; Durisch-Kaiser et al. 2005; Schubert et al. 2006a, b). In contrast, affiliates of the ANME-3 group were not reported from the Black Sea so far, to the best of our knowledge. An accumulation of ANME-1 communities in deeper waters is in accordance with previous findings of Wakeham et al. (2003), who reported the presence of tetraether lipid-derived C_{40} isoprenoids ($\delta^{13}C$ down to $-67‰$) in suspended particulate matter of the euxinic zone below 700 m water depths. However, AOM-specific biomarkers from euxinic waters were not significantly incorporated into sinking particles. Thus, the authors concluded that sediments may not always record AOM in the overlying water column.

The occurrence of massive AOM-derived pure biomass in the GHOSTDABS-field facilitated studies on metabolic and biosynthetic capabilities of the AOM-associated prokaryotes in vitro. For instance, long-term feeding experiments with

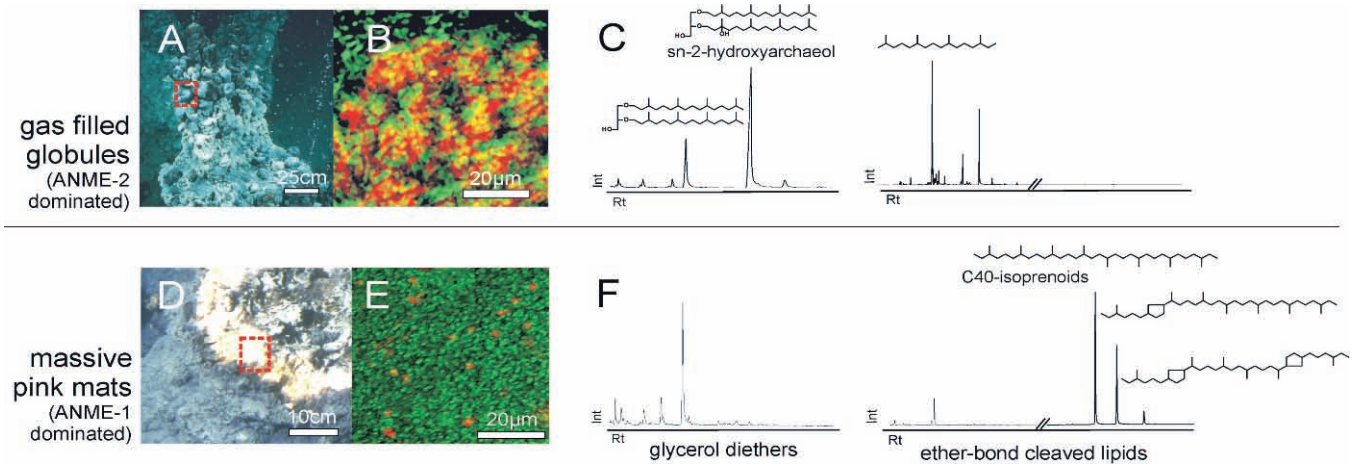

Fig. 9 Images of a tower-like structure combined with results from molecular microbiological and lipid biomarker investigations (modified after Blumenberg et al. 2004).
(**A**), Predominating black parts of the gas- and water-filled globules at the top of the towers (ANME-2 dominated consortium). (**D**), Part of a broken microbial structure with the massive pink-orange predominating mat (ANME-1 dominated). The inner part of the bioherms consists of gray-greenish porous carbonate. (**B** and **E**), Images obtained by fluorescence in situ hybridization on thin sections using group-specific oligonucleotide probes. (**B**), ANME-2-dominated mat (probes: EelMS932 (ANME-2), fluorescence green; *Desulfosarcina/Desulfococcus*-group DSS658cy3, fluorescence red) and (**E**), ANME-1 dominated mat (probes: ANME-1 fluorescence green; *Desulfosarcina/Desulfococcus*-Group DSS658cy3, fluorescence red). Note the lesser abundance of SRB in the ANME-1 association compared to the ANME-2 association. Scale bars indicate different microscopic magnifications

^{13}C-labeled methane revealed significant enrichments in ^{13}C (~10‰) for the bulk microbial mat after 12 months (Blumenberg et al. 2005). Remarkably, general higher ^{13}C-accumulations in the bacterial compared to the archaeal lipid components as well as strong differences in the ^{13}C-incorporation into individual archaeal and bacterial cell membrane lipids were found. The variations in the ^{13}C-incorporation into cell lipids were interpreted as indications for different anabolic rates as well as different responses of the phylogenetically diverse methanotrophic communities to the experimental conditions adjusted (ANME-1 associations appear to prefer low methane partial pressure habitats; Blumenberg et al. 2005; Nauhaus et al. 2005). In a subsequent experiment, another mat subsample was incubated over a period of 242 days and concentrations and stable C-isotopes of isotopically *non*-labelled methane were traced to gain information on the turnover of methane carbon. During this approach a decrease in concentration, accompanied by a relative enrichment of ^{12}C of the residual methane (Fig. 10, left; Seifert et al. 2006) was measured. These results indicate that in contrast to the classical view of microbial transformation processes, the mats performed both, sulfate-dependent methane oxidation and methanogenesis. Calculations of the turnover rates for methane oxidation and methane production gave a ratio of about 2:1 (Fig. 10, right). Thus, parallel investigations of concentrations of methane and its stable C-isotope signatures uncovered variable methane dynamics of these mats, which question previous rate calculations based on methane concentration changes only.

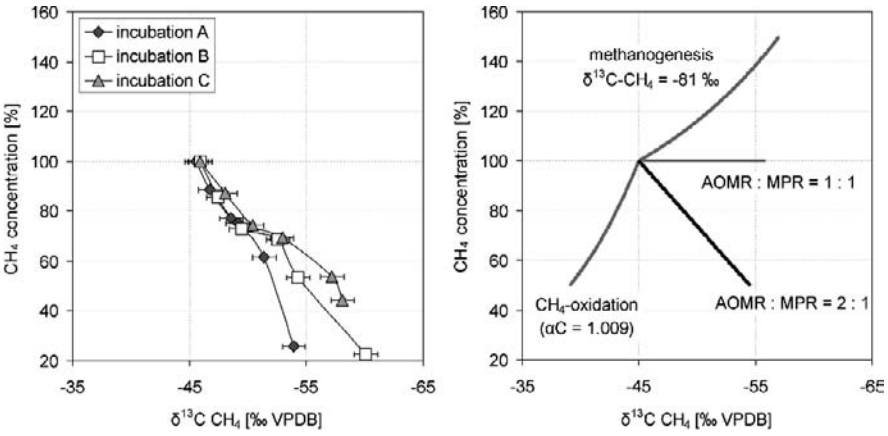

Fig. 10 *Left*: Measured changes of the concentration and isotopic composition of methane during 242 days of incubation of a microbial mat.
Right: Modelled shifts of the concentration and isotopic composition of methane in a closed system during methane oxidation, methane production, and both processes taking place concurrently. Initial conditions chosen are a CH_4-concentration of 100% and a δ^{13}C-CH_4 of −45‰ (alike the δ^{13}C of the CH_4 used for the incubation experiments). AOMR = Rate of anaerobic CH_4-oxidation; MPR = Rate of CH_4-production. Note that the observed variations are very well mirrored by the curve calculated for a concurrent presence of CH_4-oxidation and CH_4-production with a AOMR:MPR of 2:1 (*black curve in the right figure*). Reprinted with permission from Organic Geochemistry (Seifert et al., Organic Geochemistry 37, 1411–1419). Copyright (2007) Elsevier B.V.

3.3 Authigenic Carbonates in the Black Sea

In recent years, a number of studies dealt with the formation mechanisms, morphologies, chemistry, and petrography of methane-derived authigenic calcium carbonates recovered from cold seeps and mud volcanoes in the Black Sea, as well as the phylogenetic compositions of associated microbial populations (Peckmann et al. 2001; Thiel et al. 2001; Lein et al. 2002; Michaelis et al. 2002; Blinova et al. 2003; Bohrmann et al. 2003; Mazzini et al. 2004; Sahling et al. 2004; Pape et al. 2005; Pimenov and Ivanova 2005; Reitner et al. 2005a, b; Stadnitskaia et al. 2005; Bahr et al. 2008). Although considered to result from the AOM in general, as inferred from ^{13}C-depletions of the carbonate, a variety of morphologies including slabs, crusts, massive blocks, and towers, imply different geochemical settings at the carbonate precipitation sites, like in different sediment layers, at the sediment – seawater boundary or in the water column (Peckmann et al. 2001; Michaelis et al. 2002; Mazzini et al. 2004). Accordingly, $\delta^{13}C\text{-}_{Carbonate}$ values ranging from −8.5 to −46.9‰ for a suite of carbonates sampled in the northern and central Black Sea suggest that variable portions of carbon derived from AOM, oxidation of organic matter, and from sea water bicarbonate are incorporated into the carbonate matrix (Mazzini et al. 2004).

Site-specific geochemical characteristics, like chemical compositions of ascending fluids, methane flux rates, sulfate availability, and sediment structure lead to variations in the carbonate mineralogy basically comprising high portions of Mg-calcite or aragonite (Peckmann et al. 2001; Mazzini et al. 2004; Bahr et al. 2008). Carbonate cemented deposits of consolidated hemipelagic sedimentary units and mud breccia are frequently reported (Peckmann et al. 2001; Mazzini et al. 2004). However, the suppression of Mg incorporation into the calcite matrix at the presence of sulfate, as well as a preferential precipitation of aragonite over calcite at high sulfate concentrations is well established (Burton 1993; Kralj et al. 2004). Bahr et al. (2008) observed strong discrepancies with respect to Mg contents between different mineralogical facies constructing a massive authigenic carbonate piece retrieved from the Dolgovskoy Mound in the deep northeastern Black Sea. The authors concluded that these differences might be correlated to spatially or timely different environmental conditions affecting carbonate precipitation. Thus, carbonate mineralogy might be used to characterize sulfate availabilities at carbonate formation sites. Reitner et al. (2005b) suggested that the mineralogy of authigenic carbonates is affected by the phylogenetic affiliation of the AOM consortia involved in the precipitation, since in laboratory studies ANME-1 populations were found to have lower methane turnover rates than the ANME-2 communities (Nauhaus et al. 2005). Consequently, high methane turnover rates as performed by ANME-2 consortia are considered to result in low sulfate concentrations in interstitial waters and may favour Mg-calcite versus aragonite precipitaiton.

Distribution patterns and signatures of stable C-isotopes of specific lipid biomakers incorporated in Black Sea carbonates were analyzed to obtain insights into the composition of microbial communities involved in carbonate precipitation and, consequently, into the respective environmental settings. $\delta^{13}C$ values of carbonate-associated lipids attributed to AOM-mediating Archaea and Bacteria were generally

lower than −70‰ (Thiel et al. 2001; Michaelis et al. 2002; Stadnitskaia et al. 2003, 2005). These ratios of stable C-isotopes indicate that methane was the major carbon source for the microorganisms involved in carbonate precipitation, since they reflected those of methane in surrounding sediments.

Pape et al. (2005) found similar lipid biomarker patterns for a carbonate crust associated to an intense seepage site in the GHOSTDABS-field (230 m) and for a carbonate retrieved from the deep northwestern Black Sea (about 1555 m depth). The lipid inventory of both carbonates, including high abundances of strongly ^{13}C depleted ($\delta^{13}C$ between −82.8 and −101.1‰) compounds like dialkyl glycerol diethers, archaeol, and *sn*-2-hydroxyarchaeol, implied the prevalence of ANME-2 consortia (Blumenberg et al. 2004). Accordingly, these observations were interpreted as indicators for comparably high microbial methane turnover rates at these individual shallow-water and deep-water sites. For several carbonate pieces sampled at mud volcanoes located in the Sorokin Trough, Stadnitskaia et al. (2005) determined the prevalence of ANME-1 Archaea by use of 16S rRNA gene sequences and lipid biomarker data. Members of the ANME-1 group were also found to prevail in three different facies constructing a massive carbonate block retrieved from the deep northeastern Black Sea (Bahr et al. 2008). These observations indicate that fossil carbonates offer potential information on the geochemical (relative methane flux, formation depths) and biological (affiliation of microbial communities) characteristics at AOM sites during their precipitation.

3.4 The Black Sea – A Recent Analogue of Methane-Rich Ancient Oceans

It is generally accepted that the Neoarchaean-Paleoproterozoic ocean geochemistry is complied with the requirements of microbial methane consumption and that both, aerobic as well as anaerobic methanotrophy emerged in early stages of the biological evolution (Battistuzzi et al. 2004). Although some aspects on the compositions of the Early Earth's hydro- and atmosphere are speculative, several findings suggest that the Neoarchaean (2.8–2.5 Gyr ago) ocean was essentially devoid of molecular oxygen and poor in sulfate, but contained significant concentrations of methane provided by methanogens (Canfield et al. 2000; Catling et al. 2001; Habicht et al. 2002; Pavlov et al. 2003; Kasting 2005) and potentially by hydrothermal activity (Horita and Berndt 1999; Touret 2003). Microbial methanogenesis was assumingly based on CO_2-reduction through H_2, which both were released by terrestrial volcanism and introduced to the waters of the early ocean via diffusion through the atmosphere-seawater-boundary (Kasting et al. 2001), by submarine hydrothermalism, and by the alteration of mafic rocks.

The oceanic sulfate concentration is considered to have gradually increased subsequent to the initial atmospheric oxygenation, which induced continental weathering of sulphur-containing minerals (Canfield et al. 2000; Farquhar et al. 2000; Habicht et al. 2002). Photosynthetic release of molecular oxygen most probably commenced in the course of the Meso/Neoarchaean (3.2–2.5 Gyr) and amounts of atmospheric

oxygen and oceanic sulfate were already present in the Paleoproterozoic (Canfield 1998; Kasting et al. 2001; Holland 2002; Kaufman and Xiao 2003; Kah et al. 2004; Kopp et al. 2005; Baudouin-Cornu and Thomas 2007). However, some geochemical indicators (e.g. accumulation rates of organic carbon, trends in sulfate and sulphide concentrations, density of iron sulphide precipitates, trends in sulphur and molybdenum isotopes) signify oceanic oxygenation considerably lagging that of the atmosphere, and point to euxinic conditions persisting widely in deep waters until the Mesoproterozoic (Des Marais et al. 1992; Canfield 1998; Shen et al. 2002; Arnold et al. 2004; Holland 2006). In this context, the set of Neoarchaean organic matter (about 2.7 Gyr) strongly depleted in ^{13}C was recently suggested to mirror anaerobic methanotrophy (Hinrichs 2002) rather than aerobic methane consumption, as previously thought (Strauss and Moore 1992; Hayes 1994; Rye and Holland 2000).

The geochemical situation of the early Proterozoic global ocean might be assumed as having been quite similar to that of the modern deeper Black Sea with the absence of oxygen, and methane and sulfate concentrations sufficient to facilitate sulfate-dependent AOM. With the rise in oxygen, aerobic methanotrophy became more important in the Proterozoic ocean, while AOM-performing prokaryotes were pushed back into remaining anoxic, methane-rich niches present only within the sediments for most marine areas. Genome sequence-based estimations of divergence times for major microbial phyla quite well support the geochemically-substantiated assumptions on the evolution of methanotrophy. Battistuzzi et al. (2004) proposed the Mesoarchaean as date of origin of anaerobic methanotrophic Archaea (after 3.1 Gyr), while aerobic methanotrophic Bacteria (2.8–2.5 Gyr) would have evolved later in the Neoarchaean. Consequently, aerobic and anaerobic methanotrophy appear to be an effective and widespread processes promoting carbon cyling since Proterozoic times.

Petrological, biological and organic geochemical remnants in methane-seep associated deposits, like authigenic carbonates, fossilized seep metazoans and microbial lipid biomarkers prove the relevance of anaerobic and aerobic methanotrophy until modern times (Peckmann and Thiel 2004; Birgel et al. 2006; Campbell 2006). Authigenic carbonates have been found at numerous locations covering a time span from Recent to Palaeozoic (Peckmann and Thiel 2004). In contrast, the composition of fossil methanotrophic communities mediating carbonate precipitation has only poorly investigated to the best of our knowledge. For Black Sea methanotrophs, where aerobic and anaerobic methanotrophs occur in many places in high cell density, detailed insights into their population structures and physiological capabilities were gained in recent years. These findings will help to identify and evaluate the impact of methanotrophy on fossil ecosystems. For instance, processes related to the probable chronologically successive emergence of anaerobic and aerobic methanotrophs and their specific impact on methane budgets might be well studied in the stratified Black Sea waters.

Acknowledgments The manuscript benefited greatly from the very careful and detailed reviews of M. Torres, I. Klaucke, and V. Thiel. We thank A. Bahr for his suggestions on an earlier version of the manuscript.

This is publication no. GEOTECH - 287 of the R&D-Programme GEOTECHNOLOGIEN funded by the German Ministry of Education and Research (BMBF) and German Research Foundation (DFG), project METRO (Methane and methane hydrates within the Black Sea: Structural analyses, quantification and impact of a dynamic methane reservoir; grant 03G0604A). Financial support was also obtained from the DFG as part of the DFG-Research Center Ocean Margins (RCOM) of the University of Bremen and from the project Bl971/1-1. This is publication RCOM0527.

References

Akhmetzhanov AM, Ivanov MK, Kenyon NH, Mazzini A and Cruise participants (2007) Deep-water cold seeps, sedimentary environments and ecosystems of the Black and Tyrrhenian Seas and Gulf of Cadiz, IOC Technical Series No. 72. UNESCO, 99 pp

Aloisi G, Drews M, Wallmann K, Bohrmann G (2004) Fluid expulsion from the Dvurechenskii mud volcano (Black Sea): Part I. Fluid sources and relevance to Li, B, Sr, I and dissolved inorganic nitrogen cycles. Earth Planet Sci Lett 225:347–363

Arnold GL, Anbar AD, Barling J, Lyons TW (2004) Molybdenum isotope evidence for widespread anoxia in mid-proterozoic oceans. Science 304:87–90

Artemov YG, Egorov VN, Polikarpov GG, Gulin SB (2007) Methane emission to the hydro- and atmosphere by gas bubble streams in the Dnieper Paleo-delta, the Black Sea Marine. Ecol J 6:5–26

Bahr A, Pape T, Bohrmann G, Mazzini A, Haeckel M, Reitz A, Ivanov M (2008) Authigenic carbonate precipitates from the NE Black Sea: a mineralogical, geochemical and lipid biomarker study. Int J Earth Sci, doi: 10.1029/2001GC000286 (in press)

Balch WE, Fox GE, Magrum LJ, Woese CR, Wolfe RS (1979) Methanogens: reevaluation of a unique biological group. Microbiol Mol Biol Rev 43:260–296

Barnes RO, Goldberg ED (1976) Methane production and consumption in anaerobic marine sediments. Geology 4:297–300

Battistuzzi AU, Feijao A, Hedges SB (2004) A genomic timescale of prokaryote evolution: insights into the origin of methanogenesis, phototrophy, and the colonization of land. BMC Evol Biol 4:44–59

Baudouin-Cornu P, Thomas D (2007) Evolutionary biology: oxygen at life's boundaries. Nature 445:35–36

Birgel D, Peckmann J, Klautzsch S, Thiel V, Reitner J (2006) Anaerobic and aerobic oxidation of methane at Late Cretaceous seeps in the Western Interior Seaway, USA. Geomicrobiol J 23:565–577

Blinova V, Ivanov MK, Bohrmann G (2003) Hydrocarbon gases in deposits from mud volcanoes in the Sorokin Trough, north-eastern Black Sea. Geo-Mar Lett 23:250–257

Blumenberg M, Seifert R, Reitner J, Pape T, Michaelis W (2004) Membrane lipid patterns typify distinct anaerobic methanotrophic consortia. Proc Natl Acad Sci U S A 101:11111–11116

Blumenberg M, Seifert R, Nauhaus K, Pape T, Michaelis W (2005) *In vitro* study of lipid biosynthesis in an anaerobically methane oxidizing microbial mat. Appl Environ Microbiol 71:4345–4351

Blumenberg M, Seifert R, Michaelis W (2007) Aerobic methanotrophy in the oxic-anoxic transition zone of the Black Sea water column. Org Geochem 38:84–91

Boetius A, Ravenschlag K, Schubert CJ, Rickert D, Widdel F, Gieseke A, Amann R, Jørgensen BB, Witte U, Pfannkuche O (2000) A marine microbial consortium apparently mediating anaerobic oxidation of methane. Nature 407:623–626

Bohrmann G, Ivanov M, Foucher J-P, Spiess V, Bialas J, Greinert J, Weinrebe W, Abegg F, Aloisi G, Artemov Y, Blinova V, Drews M, Heidersdorf F, Krabbenhöft A, Klaucke I, Krastel S, Leder T, Polikarpov I, Saburova M, Schmale O, Seifert R, Volkonskaya A, Zillmer M (2003) Mud

volcanoes and gas hydrates in the Black Sea: new data from Dvurechenskii and Odessa mud volcanoes. Geo-Mar Lett 23:239–249

Bohrmann G, Pape T, and Cruise participants (2007) Report and preliminary results of R/V METEOR Cruise M72/3, Istanbul – Trabzon – Istanbul, 17 March–23 April, 2007. Marine gas hydrates of the Eastern Black Sea, Berichte, Fachbereich Geowissenschaften, Universität Bremen, No. 261, Bremen, 176pp

Bohrmann G, Torres ME (2006) Gas hydrates in marine sediments. In: Schulz HD, Zabel M (eds) Marine geochemistry, 2nd edn. Springer, Heidelberg, pp 481–512

Bouriak SV, Akhmetjanov AM (1998) Origin of gas hydrate accumulations on the continental slope of the Crimea from geophysical studies. In: Henriet J-P, Mienert J (eds) Gas hydrates: relevance to world margin stability and climate change, Geological Society, London, special publication 137, pp 215–222

Brekke T, Lonne O, Ohm SE (1997) Light hydrocarbon gases in shallow sediments in the northern North Sea. Mar Geol 137:81–108

Buffett BA (2000) Clathrate hydrates. Annu Rev Earth Planet Sci 28:477–507

Burton EA (1993) Controls on marine carbonate cement mineralogy: review and reassessment. Chem Geol 105:163–179

Campbell KA (2006) Hydrocarbon seep and hydrothermal vent paleoenvironments and paleontology: past developments and future research directions. Palaeogeog Palaeoclimat Palaeoecol 232:362–407

Canfield DE (1998) A new model for Proterozoic ocean chemistry. Nature 396:450–453

Canfield DE, Habicht KS, Thamdrup B (2000) The Archaean sulfur cycle and the early history of atmospheric oxygen. Science 288:658–661

Catling DC, Zahnle KJ, McKay C (2001) Biogenic methane, hydrogen escape, and the irreversible oxidation of early earth. Science 293:839–843

Clennell MB, Hovland M, Booth JS, Henry P, Winters WJ (1999) Formation of natural gas hydrates in marine sediments 1. Conceptual model of gas hydrate growth conditioned by host sediment properties. J Geophys Res 104:22985–23003

Des Marais DJ, Strauss H, Summons RE, Hayes JM (1992) Carbon isotope evidence for the stepwise oxidation of the Proterozoic environment. Nature 359:605–609

Dickens G (2001) On the fate of past gas: what happens to methane released from a bacterially mediated gas hydrate capacitor? Geochem Geophys Geosyst (G^3) 2. doi:10.1029/2000GC00013

Dickens GR (2003) Rethinking the global carbon cycle with a large, dynamic and microbially mediated gas hydrate capacitor. Earth Planet Sci Lett 213:169–183

Dickens GR, O'Neil JR, Rea DK, Owen RM (1995) Dissociation of oceanic methane hydrate as a cause of the carbon isotope excursion at the end of the Paleocene. Paleoceanography 10:965–971

Dickens GR, Castillo MM, Walker JCG (1997) A blast of gas in the latest Paleocene: simulating first-order effects of massive dissociation of oceanic methane hydrate. Geology 25:259–262

Durisch-Kaiser E, Klauser L, Wehrli B, Schubert C (2005) Evidence of intense archaeal and bacterial methanotrophic activity in the Black Sea water column. Appl Environ Microbiol 71:8099–8106

Egorov VN, Luth U, Luth C, Gulin MB (1998) Gas seeps in the submarine Dnieper Canyon, Black Sea: acoustic, video and trawl data. In: Luth U, Luth C, Thiel H (eds) Methane gas seep explorations in the Black Sea (MEGASEEBS), Project Report Reihe E. University of Hamburg. Berichte des Zentrums für Meeres- und Klimaforschung, pp 11–21

Egorov VN, Polikarpov GG, Gulin SB, Artemov YG, Stokozov NA, Kostova SK (2003) Modern conception about forming-casting and ecological role of methane gas seeps from bottom of the Black Sea. Mar Ecol J 2:5–26

Elvert M, Suess E, Whiticar MJ (1999) Anaerobic methane oxidation associated with marine gas hydrates. Superlight C-isotopes from saturated and unsaturated C_{20} and C_{25} irregular isoprenoids. Naturwissenschaften 86:295–300

Eremeeva LV, Degterev AK (1993) On the problem of a turbid layer occurring near the upper boundary of the hydrogen sulphide zone in the Black Sea. Phys Oceanogr 4:169–172

Farquhar J, Bao H, Thiemens M (2000) Atmospheric influence of earth's earliest sulfur cycle. Science 289:756–758

Gal'chenko VF, Abranochkina FN, Bezrukova LV, Sokolova EN, Ivanov MV (1988) Species composition of the aerobic methanotrophic microflora of the Black Sea. Mikrobiologiya 57:305–311

Gal'chenko VF, Lein AY, Ivanov MV (2004) Rates of microbial production and oxidation of methane in the bottom sediments and water column of the Black Sea. Microbiology 73:224–236

Gaynanov VG, Bouriak SV, Ivanov MK (1998) Seismic evidence for gas accumulation related to the area of mud volcanism in the deep Black Sea. Geo-Mar Lett 18:139–145

Greinert J, Artemov Y, Egorov V, De Batist M, McGinnis D (2006) 1300-m-high rising bubbles from mud volcanoes at 2080 m in the Black Sea: hydroacoustic characteristics and temporal variability. Earth Planet Sci Lett 244:1–15

Habicht KS, Gade M, Thamdrup B, Berg P, Canfield DE (2002) Calibration of sulfate levels in the Archean ocean. Science 298:2372–2374

Hallam SJ, Putnam N, Preston CM, Detter JC, Rokhsar D, Richardson PM, DeLong EF (2004) Reverse methanogenesis: testing the hypothesis with environmental genomics. Science 305:1457–1462

Hanson RS, Hanson TE (1996) Methanotrophic bacteria. Microbiol Rev 60:439–471

Haq BU (1998) Natural gas hydrates: searching for the long-term climatic and slope-stability records. In: Henriet J-P, Mienert J (eds) Gas hydrates: relevance to world margin stability and climate change, Geological Society, London, special publication 137, pp 303–318

Hayes JM (1994) Global methanotrophy at the Archaean-Proterozoic transition. In: Bengtson S (ed) Early life on Earth, Nobel Symposium No. 84, Columbia University Press, pp 220–236

Heeschen KU, Haeckel M, Hohnberg H-J, Abegg F, Bohrmann G (2007) Pressure coring at gas hydrate-bearing sites in the eastern Black Sea off Georgia. Geophys Res Abstr 9:03078

Hinrichs K-U (2002) Microbial fixation of methane carbon at 2.7 Ga: was an anaerobic mechanism possible? Geochem Geophys Geosyst (G^3) 3. doi:10.1029/2001GC000286

Hinrichs K-U, Boetius A (2002) The anaerobic oxidation of methane: new insights in microbial ecology and biogeochemistry. In: Wefer G, Billet D, Hebbeln D, Jørgensen BB, Schlüter M, van Weering TCE (eds) Ocean margin systems, Springer-Verlag, Heidelberg, pp 457–477

Hinrichs K-U, Hayes JM, Sylva SP, Brewer PG, DeLong EF (1999) Methane-consuming archaebacteria in marine sediments. Nature 398:802–805

Hinrichs K-U, Summons RE, Orphan VJ, Sylva SP, Hayes JM (2000) Molecular and isotopic analysis of anaerobic methane-oxidizing communities in marine sediments. Org Geochem 31:1685–1701

Hoehler TM, Alperin MJ, Albert DB, Martens CS (1994) Field and laboratory studies of methane oxidation in an anoxic marine sediment: evidence for a methanogen-sulfate reducer consortium. Global Biogeochem Cycles 8:451–463

Hoehler TM, Borowski WS, Alperin MJ, Rodriguez NM, Paull CR (2000) Model, stable isotope, and radiotracer characterization of anaerobic methane oxidation in gas hydrate-bearing sediments of the Blake Ridge. In: Paull CK, Matsumoto R, Wallace PJ, Dillon WP (eds) Proceedings of the Ocean Drilling Program, Scientific Results, 164, Ocean Drilling Program, pp 79–85

Holland HD (2002) Volcanic gases, black smokers, and the great oxidation event. Geochim Cosmochim Acta 66:3811–3826

Holland HD (2006) The oxygenation of the atmosphere and oceans. Philos Trans R Soc Lond B Biol Sci 361:903–915

Horita J, Berndt ME (1999) Abiogenic methane formation and isotopic fractionation under hydrothermal conditions. Science 285:1055–1057

Inagaki F, Tsunogai U, Suzuki M, Kosaka A, Machiyama H, Takai K, Nunoura T, Nealson KH, Horikoshi K (2004) Characterization of C_1-metabolizing prokaryotic communities in methane seep habitats at the Kuroshima Knoll, Southern Ryukyu Arc, by analyzing *pmoA*, *mmoX*, *mxaF*, *mcrA*, and 16S rRNA genes. Appl Environ Microbiol 70:7445–7455

Ivanov MK, Limonov AF, van Weering TCE (1996) Comparative characteristics of the Black Sea and Mediterranean Ridge mud volcanoes. Mar Geol 132:253–271

Ivanov MK, Limonov AF, Woodside JM (1998) Extensive deep fluid flux through the sea floor on the Crimean continental margin (Black Sea). In: Henriet J-P, Mienert J (eds) Gas hydrates: relevance to world margin stability and climate change, Geological Society, London, special publication 137, pp 195–213

Ivanov MV, Pimenov NV, Rusanov II, Lein AY (2002) Microbial processes of the methane cycle at the North-western shelf of the Black Sea. Estuar Coast Shelf Sci 54:589–599

Jones GA, Gagnon AR (1994) Radiocarbon chronology of Black Sea sediments. Deep Sea Res Part I Oceanogr Res Pap 41:531–557

Jørgensen BB, Böttcher ME, Lüschen H, Neretin LN, Volkov II (2004) Anaerobic methane oxidation and a deep H_2S sink generate isotopically heavy sulfides in Black Sea sediments. Geochimica et Cosmochimica Acta 68:2095–2118

Kah LC, Lyons TW, Frank TD (2004) Low marine sulphate and protracted oxygenation of the Proterozoic biosphere. Nature 431:834–838

Kasting JF (2001) The rise of atmospheric oxygen. Science 293:819–820

Kasting JF (2005) Methane and climate during the Precambrian era. Precambrian Res 137:119–129

Kasting JF, Pavlov AA, Siefert JL (2001) A coupled ecosystem-climate model for predicting the methane concentration in the Archean atmosphere. Orig Life Evol Biosph 31:271–285

Kaufman AJ, Xiao S (2003) High CO_2 levels in the Proterozoic atmosphere estimated from analyses of individual microfossils. Nature 425:279–282

Kennett JP, Stott LD (1991) Abrupt deep-sea warming, palaeoceanographic changes and benthic extinctions at the end of the Palaeocene. Nature 353:225–229

Kessler JD, Reeburgh WS, Southon J, Seifert R, Michaelis W, Tyler SC (2006) Basin-wide estimates of the input of methane from seeps and clathrates to the Black Sea. Earth Planet Sci Lett 243:366–375

Klaucke I, Sahling H, Bürk D, Weinrebe W, Bohrmann G (2005) Mapping deep-water gas emissions with sidescan sonar. EOS Trans 86:341–352

Klaucke I, Sahling H, Weinrebe W, Blinova V, Bürk D, Lursmanashvili N, Bohrmann G (2006) Acoustic investigation of cold seeps offshore Georgia, Eastern Black Sea. Mar Geol 231:51–67

Knies J, Damm E, Gutt J, Mann U, Pinturier L (2004) Near-surface hydrocarbon anomalies in shelf sediments off Spitsbergen: evidences for past seepages. Geochem Geophys Geosyst (G^3) 5. doi:10.1029/2003GC000687

Knittel K, Lösekann T, Boetius A, Kort R, Amann R (2005) Diversity and distribution of methanotrophic Archaea (ANME) at cold seeps. Appl Environ Microbiol 71:467–479

Konovalov SK, Murray JW (2001) Variations in the chemistry of the Black Sea on a time scale of decades (1960–1995). J Mar Syst 31:217–243

Kopp RE, Kirschvink JL, Hilburn IA, Nash CZ (2005) The Paleoproterozoic snowball Earth: a climate disaster triggered by the evolution of oxygenic photosynthesis. Proc Natl Acad Sci U S A 102:11131–11136

Kralj D, Kontrec J, Brecevic L, Falini G, Nöthig-Laslo V (2004) Effect of inorganic anions on the morphology and structure of magnesium calcite. Chem Eur J 10:1647–1656

Krastel S, Spiess V, Ivanov M, Weinrebe W, Bohrmann G, Shashkin P, Heidersdorf F (2003) Acoustic investigations of mud volcanoes in the Sorokin Trough, Black Sea. Geo-Mar Lett 23:230–238

Krüger M, Meyerdierks A, Glöckner FO, Amann R, Widdel F, Kube M, Reinhardt R, Kahnt J, Böcher R, Thauer RK, Shima S (2003) A conspicious nickel protein in microbial mats that oxidize methane anaerobically. Nature 426:878–881

Krüger M, Treude T, Wolters H, Nauhaus K, Boetius A (2005) Microbial methane turnover in different marine habitats. Palaeogeog Palaeoclimatol Palaeoecol 227:6–17

Kruglyakova RP, Byakov YA, Kruglyakova MV, Chalenko LA, Shevtsova NT (2004) Natural oil and gas seeps on the Black Sea floor. Geo-Mar Lett 24:150–162

Kvenvolden KA (1988) Methane hydrate – a major reservoir of carbon in the shallow geosphere? Chem Geol 71:41–51

Lamy F, Arz HW, Bond GC, Bahr A, Pätzold J (2006) Multicentennial-scale hydrological changes in the Black Sea and northern Red Sea during the Holocene and the Arctic/North Atlantic Oscillation. Paleoceanography 21. doi:10.1029/2005PA001184

Lein AY, Ivanov MV, Pimenov NV, Gulin MB (2002) Geochemical characteristics of the carbonate constructions formed during microbial oxidation of methane under anaerobic conditions. Microbiology 70:78–90

Limonov AF, Van Weering TCE, Kenyon NH, Ivanov MK, Meisner LB (1997) Seabed morphology and gas venting in the Black Sea mudvolcano area: observations with the MAK-1 deep-tow sidescan sonar and bottom profiler. Mar Geol 137:121–136

Lösekann T, Knittel K, Nadalig T, Fuchs B, Niemann H, Boetius A, Amann R (2007) Diversity and abundance of aerobic and anaerobic methane oxidizers at the Haakon Mosby Mud Volcano, Barents Sea. Appl Environ Microbiol 73:3348–3362

Lüdmann T, Wong HK, Kondering P, Zillmer M, Petersen J, Flüh E (2004) Heat flow and quantity of methane deduced from a gas hydrate field in the vicinity of the Dnieper Canyon, northwestern Black Sea. Geo-Mar Lett 24:182–193

Luth C, Luth U, Gebruk A, Thiel H (1999) Methane gas seeps along the oxic/anoxic gradient in the Black Sea: manifestations, biogenic sediment compounds and preliminary results on benthic ecology. Mar Ecol 20:221–249

Martens CS, Berner RA (1974) Methane production in the interstitial waters of sulfate-depleted marine sediments. Science 185:1167–1169

Mazzini A, Ivanov MK, Parnell A, Stadnitskaia A, Cronin BT, Poludetkina E, Mazurenko L, Van Weering TCE (2004) Methane-related authigenic carbonates from the Black Sea: geochemical characterisation and relation to seeping fluids. Mar Geol 212:153–181

Michaelis W, Seifert R, Nauhaus K, Treude T, Thiel V, Blumenberg M, Knittel K, Gieseke A, Peterknecht K, Pape T, Boetius A, Amann R, Jørgensen BB, Widdel F, Peckmann J, Pimenov NV, Gulin MB (2002) Microbial reefs in the Black Sea fueled by anaerobic oxidation of methane. Science 297:1013–1015

Mienert J, Posewang J, Baumann M (1998) Gas hydrates along the northeastern Atlantic margin: possible hydrate-bound margin instabilities and possible release of methane. In: Henriet J-P, Mienert J (eds) Gas hydrates: relevance to world margin stability and climate change, Geological Society, London, special publication 137, pp 275–291

Mienert J, Vanneste M, Bünz S, Andreassen K, Haflidason H, Sejrup HP (2005) Ocean warming and gas hydrate stability on the mid-Norwegian margin at the Storegga Slide. Mar Petrol Geol 22:233–244

Murray JW, Yakushev E (2006) The suboxic transition zone in the Black Sea. In: Neretin LN (ed) Past and present water column anoxia, Springer, Dordrecht, pp 105–138

Naudts L, Greinert J, Artemov Y, Staelens P, Poort J, Van Rensbergen P, De Batist M (2006) Geological and morphological setting of 2778 methane seeps in the Dnepr paleo-delta, northwestern Black Sea. Mar Geol 227:177–199

Nauhaus K, Boetius A, Krüger M, Widdel F (2002) *In vitro* demonstration of anaerobic oxidation of methane coupled to sulphate reduction in sediment from a marine gas hydrate area. Environ Microbiol 4:296–305

Nauhaus K, Treude T, Boetius A, Krüger M (2005) Environmental regulation of the anaerobic oxidation of methane: comparison of ANME-I and ANME-II-communities. Environ Microbiol 7:98–106

Niemann H, Lösekann T, De Beer D, Elvert M, Nadalig T, Knittel K, Amann R, Sauter EJ, Schlüter M, Klages M, Foucher JP, Boetius A (2006) Novel microbial communities of the Haakon Mosby mud volcano and their role as a methane sink. Nature 443:854–858

Nikishin AM, Korotaev MV, Ershov AV, Brunet M-F (2003) The Black Sea basin: tectonic history and Neogene-Quaternary rapid subsidence modelling. Sediment Geol 156:149–168

Orcutt B, Boetius A, Elvert M, Samarkin V, Joye SB (2005) Molecular biogeochemistry of sulfate reduction, methanogenesis and the anaerobic oxidation of methane at Gulf of Mexico cold seeps. Geochim Cosmochim Acta 69:4267–4281

Orphan VJ, House CH, Hinrichs K-U, McKeegan KD, DeLong EF (2001) Methane-consuming Archaea revealed by directly coupled isotopic and phylogenetic analysis. Science 293:484–487

Orphan VJ, House CH, Hinrichs K-U, McKeegan KD, DeLong EF (2002) Multiple archaeal groups mediate methane oxidation in anoxic cold seep sediments. Proc Natl Acad Sci U S A 99:7663–7668

Özsoy E, Ünlüata Ü (1997) Oceanography of the Black Sea: a review of some recent results. Earth Sci Rev 42:231–272

Pancost RD, Bouloubassi I, Aloisi G, Sinninghe Damsté JS, the Medinaut Shipboard Scientific Party (2001) Three series of non-isoprenoidal dialkyl glycerol diethers in cold-seep carbonate crusts. Org Geochem 32:695–707

Pancost RD, Sinninghe Damsté JS (2003) Carbon isotopic composition of prokaryotic lipids as tracers of carbon cycling in diverse settings. Chem Geol 195:29–58

Pape T, Blumenberg M, Seifert R, Egorov VN, Gulin SB, Michaelis W (2005) Lipid geochemistry of methane-seep-related Black Sea carbonates. Palaeogeogr Palaeoclimatol Palaeoecol 227:31–47

Pavlov AA, Hurtgen MT, Kasting JF, Arthur MA (2003) Methane-rich Proterozoic atmosphere? Geology 31:87–90

Peckmann J, Thiel V (2004) Carbon cycling at ancient methane-seeps. Chem Geol 205:443–467

Peckmann J, Reimer A, Luth U, Luth C, Hansen BT, Heinicke C, Hoefs J, Reitner J (2001) Methane-derived carbonates and authigenic pyrite from the northwestern Black Sea. Mar Geol 177:129–150

Pimenov NV, Ivanova AE (2005) Anaerobic methane oxidation and sulfate reduction in bacterial mats on coral-like carbonate structures in the Black Sea. Microbiology 74:362–370

Pimenov NV, Neretin LN (2006) Composition and activities of microbial communities involved in carbon, sulfur, nitrogen and manganese cycling in the oxic/anoxic interface of the Black Sea. In: Neretin LN (ed) Past and present water column anoxia, Springer, Dordrecht, pp 501–221

Pimenov NV, Rusanov II, Poglazova MN, Mityushina LL, Sorokin DY, Khmelenina VN, Trotsenko YA (1997) Bacterial mats on coral-like structures at methane seeps in the Black Sea. Microbiology 66:354–360

Pimenov NV, Rusanov II, Yusupov SK, Fridrich J, Lein AY, Wehrli B, Ivanov MV (2000) Microbial processes at the aerobic-anaerobic interface in the deep-water zone of the Black Sea. Microbiology 69:436–448

Polikarpov GG, Egorov VN, Gulin SB, Gulin MB, Stokozov NA (1992) Gas seeps from the Black Sea bottom – a new object of molismology. In: Polikarpov GG (ed) Molismology of the Black Sea, Naukova Dumka, Kiev, Ukraine, pp 10–28 (in Russian)

Popescu I, De Batist M, Lericolais G, Nouze H, Poort J, Panin N, Versteeg W, Gillet H (2006) Multiple bottom-simulating reflections in the Black Sea: potential proxies of past climate conditions. Mar Geol 227:163–176

Reeburgh WS (1976) Methane consumption in Cariaco Trench waters and sediments. Earth Planet Sci Lett 28:337–344

Reeburgh WS (1996) "Soft spots" in the global methane budget. In: Lidstrom ME, Tabita FR (eds) Microbial growth on C_1 compounds, Kluwer Academic Publishers, Dordrecht, pp 334–342

Reeburgh WS (2007) Oceanic methane biogeochemistry. Chem Rev 107:486–513

Reeburgh WS, Ward BB, Whalen SC, Sandbeck KA, Kilpatrick KA, Kerkhof LJ (1991) Black Sea methane geochemistry. Deep Sea Res 38:S1189–S1210

Reeburgh WS, Tyler SC, Carroll J (2006) Stable carbon and hydrogen isotope measurements on Black Sea water-column methane. Deep Sea Res Part II Top Stud Oceanogr 53:1893–1900

Reitner J, Peckmann J, Blumenberg M, Michaelis W, Reimer A, Thiel V (2005a) Concretionary methane-seep carbonates and associated microbial communities in Black Sea sediments. Palaeogeogr Palaeoclimatol Palaeoecol 227:18–30

Reitner J, Peckmann J, Reimer A, Schumann G, Thiel V (2005b) Methane-derived carbonate build-ups and associated microbial communities at cold seeps on the lower Crimean shelf (Black Sea). Facies 51:66–79

Ritger S, Carson B, Suess E (1987) Methane-derived authigenic carbonates formed by subduction-induced pore-water expulsion along the Oregon/Washington margin. Geol Soc Am Bull 98:147–156

Ross DA, Degens ET, MacIlvaine J (1970) Black Sea: recent sedimentary history. Science 170:163–165

Ryan WBF, Pitmann III WC, Major CO, Shimkus K, Moskalenko V, Jones GA, Dimitrov P, Gorür N, Sakinç M, Yüce H (1997) An abrupt drowning of the Black Sea shelf. Mar Geol 138:119–126

Rye R, Holland HD (2000) Life associated with a 2.76 Ga ephemeral pond?: Evidence from Mount Roe #2 paleosol. Geology 28:483–486

Sahling H, and Cruise participants (2004) Report and preliminary results of R/V Poseidon cruise P317/4, Istanbul – Istanbul, 16 October–4 November 2004. Berichte aus dem Fachbereich Geowissenschaften der Universität Bremen, No. 235, Bremen, 92 pp

Saydam C, Tugrul S, Basturk O, Oguz T (1993) Identification of the oxic/anoxic interface by isopycnal surfaces in the black sea. Deep Sea Res Part I Oceanogr Res Pap 40:1405–1412

Schmale O, Greinert J, Rehder G (2005) Methane emission from high-intensity marine gas seeps in the Black Sea into the atmosphere. Geophys Res Lett 32. doi:10.1029/2004GL021138

Schouten S, Wakeham SG, Sinninghe Damsté JS (2001) Evidence for anaerobic methane oxidation by archaea in euxinic waters of the Black Sea. Org Geochem 32:1277–1281

Schubert CJ, Coolen MJL, Neretin LN, Schippers A, Abbas B, Durisch-Kaiser E, Wehrli B, Hopmans EC, Sinninghe Damsté JS, Wakeham S, Kuypers MMM (2006a) Aerobic and anaerobic methanotrophs in the Black Sea water column. Environ Microbiol 8:1844–1856

Schubert CJ, Durisch-Kaier E, Klauser L, Vazquez F, Wehrli B, Holzner C, Kipfer R, Schmale O, Greinert J, Kuypers MMM (2006b) Recent studies on sources and sinks of methane in the Black Sea. In: Neretin LN (ed) Past and present water column anoxia, Springer, Dordrecht, pp 419–441

Seifert R, Nauhaus K, Blumenberg M, Krüger M, Michaelis W (2006) Methane dynamics in a microbial community of the Black Sea traced by stable carbon isotopes *in vitro*. Org Geochem 37:1411–1419

Shen Y, Canfield DE, Knoll AH (2002) Middle proterozoic ocean chemistry: evidence from the McArthur Basin, Northern Australia. Am J Sci 302:81–109

Shnukov EF, Lein AY, Egorov VN, Kleshenko SA, Gulin SB, Artemov YG, Arslanov HA, Kutnyi VA, Logvina EA (2004) Discovery in the Black Sea of deep-water biogenic buildups. Dopovidi Natsional'noi Akademii Nauk Ukraini 1:118–122 (in Russian)

Sloan ED, Koh CA (2007) Clathrate hydrates of natural gases. CRC Press. 752 pp

Stadnitskaia A, Baas M, Ivanov MK, van Weering TCE, Sinninghe Damsté JS (2003) Novel archaeal macrocyclic diether core membrane lipids in a methane-derived carbonate crust from a mud volcano in the Sorokin Trough, NE Black Sea. Archaea 1:1–9

Stadnitskaia A, Muyzer G, Abbas B, Coolen MJL, Hopmans EC, Baas M, Van Weering TCE, Ivanov MK, Poludetkina E, Sinninghe Damsté JS (2005) Biomarker and 16S rDNA evidence for anaerobic oxidation of methane and related carbonate precipitation in deep-sea mud volcanoes of the Sorokin Trough, Black Sea. Mar Geol 217:67–96

Starostenko V, Buryanov V, Makarenko I, Rusakov O, Stephenson R, Nikishin A, Georgiev G, Gerasimov M, Dimitriu R, Legostaeva O (2004) Topography of the crust-mantle boundary beneath the Black Sea Basin. Tectonophysics 381:211–233

Strauss H, Moore T (1992) Abundances and isotopic composition of carbon and sulfur species in whole rock and kerogen samples. In: Schopf JW, Klein C (eds) The proterozoic biosphere, Cambridge University Press, Cambridge, pp 709–789

Talbot M, Watson DF, Murrell JC, Carter JF, Farrimond P (2001) Analysis of intact bacteriohopanepolyols from methanotrophic bacteria by reversed-phase high-performance liquid chromatography-atmopheric pressure chemical ionisation mass spectrometry. J Chromatogr A 921:175–185

Teske A, Hinrichs K-U, Edgcomb V, De Vera Gomez A, Kysela D, Sylva SP, Sogin ML, Jannasch HW (2002) Microbial diversity of hydrothermal sediments in the Guaymas Basin: evidence for anaerobic methanotrophic communities. Appl Environ Microbiol 68:1994–2007

Thiel V, Peckmann J, Richnow HH, Luth U, Reitner J, Michaelis W (2001) Molecular signals for anaerobic methane oxidation in Black Sea seep carbonates and a microbial mat. Mar Chem 73:97–112

Touret JLR (2003) Remnants of early Archaean hydrothermal methane and brines in pillow-breccia from the Isua Greenstone Belt, West Greenland. Precambrian Res 126:219–233

Treude T, Orphan V, Knittel K, Gieseke A, House CH, Boetius A (2007) Consumption of methane and CO_2 by methanotrophic microbial mats from gas seeps of the anoxic Black Sea. Appl Environ Microbiol 73:2271–2283

Tripati A, Elderfield H (2005) Deep-sea temperature and circulation changes at the Paleocene-Eocene Thermal Maximum. Science 308:1894–1898

Tugolesov DA, Gorshkov AS, Meysner LB, Soloviov VV, Khakhalev EM, Akilova YV, Akentieva GP, Gabidulina TI, Kolomeytseva SA, Kochneva TY, Pereturina IG, Plashihina IN (1985) Tectonics of the Mesozoic Sediments of the Black Sea Basin, Moscow, 215 pp (in Russian)

Vetriani C, Tran HV, Kerkhof LJ (2003) Fingerprinting microbial assemblages from the oxic/anoxic chemocline of the Black Sea. Appl Environ Microbiol 69:6481–6488

Wakeham SG, Lewis CM, Hopmans EC, Schouten S, Sinninghe Damsté JS (2003) Archaea mediate anaerobic oxidation of methane in deep euxinic waters of the Black Sea. Geochim Cosmochim Acta 67:1359–1374

Wakeham SG, Amann R, Freeman KH, Hopmans E, Jørgensen BB, Putnam IF, Schouten S, Sinninghe Damsté JS, Talbot HM, Woebken D (2007) Microbial ecology of the stratified water column of the Black Sea as revealed by a comprehensive biomarker study. Org Geochem 38:2070–2097

Wallmann K, Drews M, Aloisi G, Bohrmann G (2006) Methane discharge into the Black Sea and the global ocean via fluid flow through submarine mud volcanoes. Earth Planet Sci Lett 248:544–559

Weber A, Riess W, Wenzhoefer F, Jørgensen BB (2001) Sulfate reduction in Black Sea sediments: in situ and laboratory radiotracer measurements from the shelf to 2000 m depth. Deep Sea Res Part I Oceanogr Res Pap 48:2073–2096

Yefremova AG, Zhizhchenko BP (1974) Occurrence of crystal hydrates of gases in the sediments of modern marine basins. Doklady Akademii Nauk, SSSR Earth Science Section 214:219–220

Zillmer M, Flueh ER, Petersen J (2005) Seismic investigation of a bottom simulating reflector and quantification of gas hydrate in the Black Sea. Geophys J Int 161:662–678

From Volcanic Winter to Snowball Earth: An Alternative Explanation for Neoproterozoic Biosphere Stress

Robert J. Stern, D. Avigad, N. Miller and M. Beyth

Abstract The ~450 million years of Neoproterozoic time (1000–542 Ma) was a remarkable episode of change in the Earth system and the biosphere. Here we develop and explore the hypothesis that explosive volcanism was at least partly responsible for Neoproterozoic climate change, synopsized as the "Volcanic winter to snowball Earth" (VW2SE) hypothesis. We review how climate cools as a result of sulfuric acid aerosols injected into the stratosphere by violent volcanic eruptions. A protracted increase in explosive volcanism could disrupt Earth's radiative balance by continuously injecting sulfur aerosols into the stratosphere, causing cooling that could lead to glaciation. This mechanism would be especially effective when acting in concert with other agents for cooling. We show that the global Neoproterozoic magmatic flux was intense, so that explosive volcanism episodicly had a major effect on climate. Neoproterozoic volcanism and glacial activity happened about the same times in the Cryogenian and Ediacaran periods with no glaciation and reduced igneous activity in the Tonian Period. Glaciation followed soon after igneous activity increased as the supercontinent Rodinia broke apart, suggesting a causal relationship. The tectonic setting of climate-controlling explosive volcanism changed systematically over the Neoproterozoic supercontinent cycle, from extension-related early to arc-related late. Marinoan (~635 Ma) glaciation in particular corresponds to a peak time of subduction-related igneous activity in the Arabian-Nubian Shield and the East African Orogen. Isotopic chemostratigraphies are generally consistent with VW2SE hypothesis. These observations cumulatively support the VW2SE hypothesis as a viable explanation for what solid Earth processes caused Neoproterozoic climate oscillations.

R.J. Stern
Geosciences Dept.,
U Texas at Dallas, Richardson TX 75083-0688 USA
e-mail: rjstern@utdallas.edu

Y. Dilek et al. (eds.), *Links Between Geological Processes, Microbial Activities & Evolution of Life*, © Springer Science+Business Media B.V. 2008

1 Introduction

The ~450 Myr –long Neoproterozoic Era is subdivided into three periods: Tonian (1000–850 Ma), Cryogenian (850–635 Ma) and Ediacaran (635–542 Ma; Fig. 1). The first two periods are associated with microscopic biota of low complexity, but the Ediacaran Period yielded macroscopic, soft-bodied, complex metazoans. These typically were centimeters to decimeters in greatest dimension, with some giants more than a meter long. Ediacaran fossils include discs, fronds, and segmented shapes that are similar in some ways to modern animals, accompanied by fossils unlike anything seen in Phanerozoic assemblages (Narbonne 2005). By the beginning of Cambrian time all major animal phyla were established.

We are starting to delineate the Neoproterozoic record of life, and how lifeforms of increasing complexity and size evolved over this time. The rate of biological diversification was affected by changes in the physical world, including oceanic and atmospheric composition (especially rising oxygen contents; Knoll 2003), climate and tectonics. These variables interacted in ways that are still being discovered. The nexus of these Earth system changes is showcased by the controversial Snowball Earth hypothesis, which seeks to explain climate change, especially for the Cryogenian (Allen 2006; http://www.snowballearth.org/). There were several Neoproterozoic ice ages (Fig. 1), and these events give the name "Cryogenian" (greek for "birth of ice") to middle Neoproterozoic time, although more limited glaciation also occurred in the Ediacaran Period. Some scientists think that extreme biosphere stress caused by Neoproterozoic climate change stimulated biological change leading to the development of metazoa (Hoffman 1999). Others conclude that Neoproterozoic biosphere stress due to Neoproterozoic ice ages was more subtle (Corsetti et al. 2006) or that glacial extremes did not preclude photosynthesis and therefore were not analogous to the hard snowball model originally proposed by Hoffman et al. (1998).

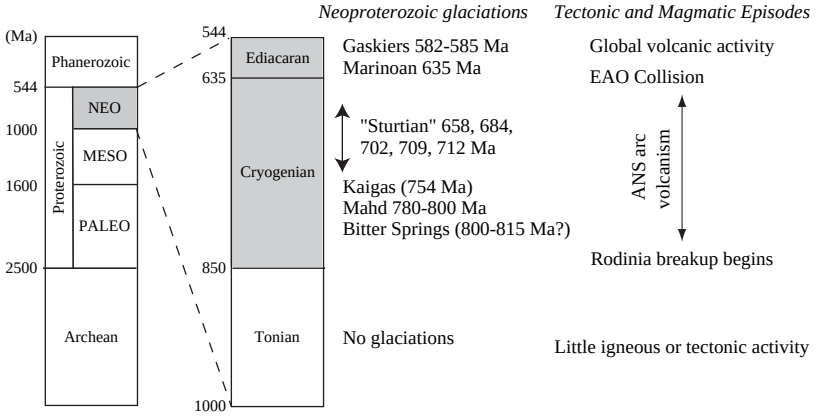

Fig. 1 Neoproterozoic time (*left*) showing the timing of glacial episodes (*center*) and timing of magmatism. Not that Tonian period has little igneous activity and no glaciation, and that glacial episodes overlap times of maximum igneous activity

The chronology of Neoproterozoic glacial episodes is still being revised as new radiometric ages are obtained. Evidence for climate change comes from direct and indirect indicators. The most direct evidence of Cryogenian glaciation is lithostratigraphic: tillites, with clear genetic indications of glacial derivation (e.g., striated or faceted clasts, dropstones), and less diagnostic diamictites, which are often considered glaciogenic. The oldest Neoproterozoic glacial deposits probably were small in extent, poorly preserved, and thus difficult to find, but the oldest may be the ~780 Ma Mahd adh Dhab tillites of Saudi Arabia (Stern et al. 2006). Another candidate for first Neoproterozoic glaciation is represented by the ~800 Ma Bitter Springs negative $\delta^{13}C$ anomaly, but the age and inferred glaciation are poorly constrained, as discussed below. With these possible exceptions, the ~754 Ma Kaigas glacial episode (Hoffmann et al. 2006) is the oldest certain Neoproterozoic glaciation.

Indirect indicators of Neoproterozoic climate change are preserved in carbonate sediments. Tillites may be abruptly overlain by distinctive carbonate successions (cap carbonates) and are typically preceded by pronounced decrease of seawater $\delta^{13}C$ (as proxied by marine carbonates). Although the specific origin of these negative $\delta^{13}C$ excursions is controversial, their common association with glacial deposits suggests an effective way to correlate carbonate units deposited in association with Neoproterozoic ice ages (Knoll et al. 1986). Yet correlation on the basis of negative $\delta^{13}C$ anomalies can be ambiguous (i.e., cf. Halverson et al. 2005 vs. in press) and a robust $\delta^{13}C$ (and $^{87}Sr/^{86}Sr$) global chemostratigraphy remains to be constructed, particularly for early Cryogenian time (Melezhik et al. 2001). Halverson et al. (in press) propose that the ~800 Ma age inferred for the Bitter Springs negative $\delta^{13}C$ anomaly in Australia correlates with similar pre-Sturtian excursions in Svalbard and NW Canada. However, none of the latter excursions are obviously associated with glaciogenic strata, and alternative correlations with pre-Sturtian excursions demonstrably younger than the Bitter Springs anomaly are possible (Miller et al., in prep.).

Until recently the Sturtian was thought to be a global episode of glaciation but these deposits range in age from ~712 Ma to ~650 Ma (Allen et al. 2002; Lund et al. 2003; Kendall et al. 2006; Fanning 2006). Only the ~635 Ma Marinoan episode still appears to have been global and long lasting (Bodiselitsch et al. 2005). The last clear Neoproterozoic glaciation occurred ~580 Ma, known as the Gaskiers or Varanger glaciation (Bowring et al. 2003). This is also about the time of the "main erosional phase" of the Arabian-Nubian Shield (Garfunkel 1999), possibly due to continental glaciation (Stern et al. 2006).

It is not surprising that our understanding of Neoproterozoic biogeological events and Earth system interactions is changing rapidly, as an international and interdisciplinary group of researchers find new pieces of the Neoproterozoic climate change puzzle. Although far removed in time from modern concerns about global warming, the stratigraphic record of these Neoproterozoic events demonstrates the "limits of global change" (Hoffman and Schrag 2002). This global search for new perspectives is one of the most interdisciplinary and international geoscientific efforts underway. It is to be expected that such an inquiry into deep time spawns controversy. The scope and significance of this controversy encourages exploration of both the broad fabric of the Neoproterozoic solid Earth-climate-life system as

well as detailed examination of individual disciplinary threads. This essay follows one of these threads, namely the hypothesis that explosive volcanic activity was an important cause of Neoproterozoic climate change.

What caused Neoproterozoic ice ages is a central controversy, because we cannot pretend to understand Neoproterozoic global change if we do not understand what caused it. The sun was fainter in the Neoproterozoic than today (Tajika 2003), but this was not the principal trigger because the Sun was significantly fainter earlier in Earth history, with modest climatic effects. The oldest known glaciation is recorded by glaciogenic diamictites of the ~2.9 Ga Pongola Supergroup, and glaciation also occurred ~2.2–2.5 Ga (Kirschvink et al. 2000). There is no evidence for glaciation for the next 1.5 billion years prior to the oldest Neoproterozoic glaciations. The distribution of landmasses may also have been important. Hoffman et al. (1998) suggested that the relatively close dispersal of continents about the equator greatly enhanced continental weathering. By this scheme, carbon was buried in continental margin sediments, thereby drawing down atmospheric CO_2 and cooling climate. This ultimately led to a runaway increase in planetary albedo as glaciation spread to low latitudes, culminating in global glaciation and stopping the hydrologic cycle. This "hard snowball" interpretation has been increasingly challenged as more is learned about the number and intensity of Neoproterozoic ice ages and as we better understand the range and controls of greenhouse gas feedbacks (e.g., Hyde et al. 2000). Some researchers support the hypothesis that cooling resulted mainly from weathering-related carbon burial and CO_2 fixation (Schrag et al. 2002; Donnadieu et al. 2004), perhaps stimulated by increased clay formation (Kennedy et al. 2006). Other mechanisms include the loss of a once more significant atmospheric methane component (a much more effective greenhouse gas compared to CO_2) due to rising oxygen contents (Schrag et al. 2002), and Earth's passage through an intergalactic cloud (Pavlov et al. 2005).

It is remarkable in this wide-ranging discussion that explosive volcanism has not been explicitly considered as a possible cause, because this is known to affect climate on many timescales (Robock 2000), and has been suggested as a way to counteract modern "global warming" (Crutzen 2006). The fact that this possible mechanism has not been considered motivates this essay. The argument is empirical, progressing from the well-documented and modern to the speculative and ancient. We begin by reviewing the cause of volcanically-induced cooling, then examine evidence from three Holocene and Pleistocene eruptions (Pinatubo, Tambora, and Toba). We then discuss whether or not a prolonged increase in explosive volcanism could affect climate sufficiently to trigger an ice age, using Pleistocene glaciation of the N. Hemisphere as an analog. We document prolific global igneous activity during the Neoproterozoic, and link this to the scale of explosive volcanism. We note that there was elevated igneous activity during the part of Neoproterozoic time that witnessed glaciation and that explosive volcanism could have been an important cause. We conclude that explosive volcanism is a viable explanation for Neoproterozoic climate change and propose a mixed acronym for the hypothesis: VW2SE (volcanic winter to snowball Earth). It is our hope that the VW2SE hypothesis broadens discussions about the causes of Neoproterozoic climate change and about how solid Earth processes affect climate and life.

2 Explosive Volcanism and Atmospheric Cooling

Benjamin Franklin was perhaps first to note that climate was affected by intense volcanism, linking a severe winter in Europe during 1783–1784 to the euption of Laki, Iceland (Franklin 1784). Almost 200 years elapsed before the idea was resurrected by Lamb (1970), who developed the Dust-Veil Index to quantify the cooling effects of volcanic ash in the atmosphere. The idea of volcanically-induced cooling was further developed by Kennett and Thunnell (1977), who inferred that volcanic pulses at 0–2, 5, 10, and 14–16 Ma caused cooler climate. It is now widely accepted that explosive eruptions of sufficient magnitude – especially Plinian eruptions – can cause cooler climate (Robock 2004). This linkage led to development of the "Volcanic Winter" concept (Rampino et al. 1988), which focusses on short-term (1–3 years) climate cooling caused by explosive volcanism.

Explosive volcanism mainly affects climate by injecting sulfur dioxide (SO_2) into the stratosphere. Volcanic ash is also injected but this settles quickly out of the atmosphere and so causes little cooling; in contrast, sulfur aerosols can remain suspended for a year or more. A globe-encircling volcanic cloud forms in several weeks as the SO_2 is converted in the lower stratosphere (18–25 km) to frozen particles of sulfuric acid (H_2SO_4), 0.1–1 mm in diameter. Cooling of the troposphere and Earth surface results because these microdroplets reflect a significant fraction of incoming solar radiation back into space. The geographic extent of cooling resulting from volcanic aerosols depends on eruption latitude and stratospheric winds, with equatorial eruptions having the greatest effect (Self 2006)

Because S aerosols disrupt Earth's radiative balance, the short-term effect of explosive volcanism is usually cooling of the Earth's surface and troposphere. The historical relationship between injection of sulfur into the stratosphere by explosive volcanism and cooling is so strong that Sigurdsson (1990) proposed the following empirical relationship between a volcano's sulfur yield (M_S) and the ensuing maximum surface temperature anomaly, ΔT:

$$\Delta T = -5.9 \times 10^{-5} \times M_S^{0.31}.(M_S \text{ in grams}) \quad (1)$$

This relationship has been reconsidered by Blake (2003), who found that the mass of emitted SO_2 is 0.1–1 % of magma mass, with a best fit mass for SO_2:

$$\text{Megatons } SO_2 = 1.77(\text{mass of magma in gigatons})^{0.64} \quad (2)$$

Blake (2003) also concluded that the volcanic SO_2 is effectively converted into stratospheric aerosols when the ratio of eruption plume height to tropopause height is greater than $\sim$1.5. Blake (2003) also noted that of the stratospheric eruption clouds in the period 1400–1994, those <5 Gt magma appear to have had insignificant effects on Northern Hemisphere summer temperature whereas data for eruptions of >10 Gt magma suggest a mean cooling of $\sim 0.35^\circ$ C.

Figure 2 shows various volcanic inputs to the atmosphere, emphasizing interactions and fates for various volcanic inputs and their impacts on Earth's radiative heat balance (after McCormick et al. 1995; Robock 2000). Apart from the formation of

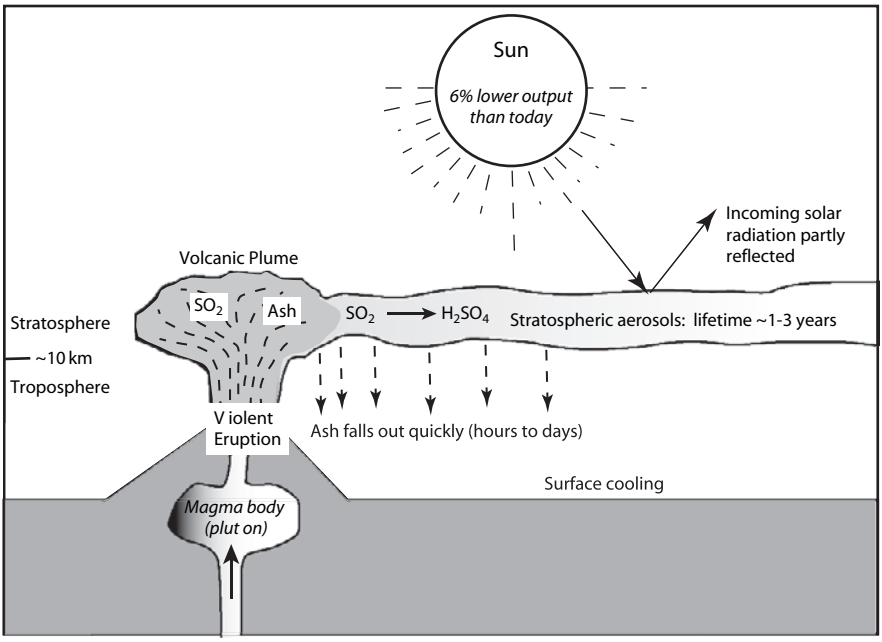

Fig. 2 Schematic diagram showing how explosive volcanism leads to climate cooling through the formation of sulphuric acid aerosols in the stratosphere. Figure is greatly simplified after Self (2006) and Robock (2000)

sulfuric acid aerosols, however, the influence of volcanic eruptions on atmospheric chemistry has not been explored in detail. Chlorine (and HCl in gaseous or aerosol form) may also be injected and this is likely to be detrimental to stratospheric ozone, but its specific climatic effects are unknown (Tabazadeh and Turco 1993; Robock 2000). Water and carbon dioxide are also injected into the atmosphere, but CO_2 in particular has warming effects that operates on a longer timescales than stratospheric cooling.

To better illustrate how explosive volcanism affects climate, three examples are presented. In this discussion we refer to the Volcanic Explosivity Index (VEI) of Newhall and Self (1982) to indicate the relative intensity of an explosive eruption. The VEI is a semi-quantitative logarithmic scale (0–8), based on a combination of erupted tephra volume and eruption plume height.

2.1 Pinatubo 1991

This eruption was relatively modest (VEI = 5–6) but is the largest to have occurred since remote sensing satellites began measuring global atmospheric sulfur and temperature. Along with petrologic investigations of eruptive products, these coupled observations provided a remarkably complete example of how one explosive eruption affected climate. Until there is a comparable or larger eruption that can

be studied, testing whether or not explosive volcanism could have triggered Neoproterozoic glaciations largely requires scaling up from understanding the Pinatubo eruption.

Pinatubo's volcanic ash and lavas were unusually rich in sulfur with bulk contents of 1500–2400 ppm, and even contained anhydrite phenocrysts. Satellite-measured sulfur levels were orders of magnitude higher than that expected from simple degassing of the involved melt volume (Keppler 1999). The eruption appears to have been triggered by injection of S-rich, oxidized basalt into dacitic magma (De Hoog et al. 2004). In this scenario, the magma mixture released a S-rich fluid (possibly extracted as exsolved hydrous fluids) that may have collected at the top of the magma reservoir, and this provided the SO_2 injected into the atmosphere.

The eruption, and its effect on the stratosphere, were monitored by two important satellite systems; the Total Ozone Mapping Spectrometer (TOMS) and the Stratospheric Aerosol and Gas Experiment II (SAGE II). TOMS provided daily sulfur dioxide and ozone concentrations, and showed that Pinatubo injected a total of $\sim$20 million tons of sulfur into the atmosphere (Bluth et al. 1992). SAGE II measured the stratospheric optical depth (D) through the atmospheric limb at sunrise and sunset. Knowing D, the vertical transmittance of the solar radiation through the atmosphere was calculated (higher D equals smaller transmittance). In general, non-transmitted solar radiation is either absorbed by the stratospheric gases and aerosols or is scattered back into space. It is through this mechanism that explosive eruptions reduce incoming solar radiation to Earth's troposphere and surface. TOMS and SAGE II thus measured Pinatubo-related volcanic ash as well as the sulfuric acid aerosols. Before Pinatubo erupted, D was globally low, $\sim 10^{-3}$. Forty days following the eruption, an aerosol cloud completely encircled the globe in a narrow zone, with maximum D $\sim 10^{-1}$, about two orders of magnitude higher than D before the eruption. Twenty months after the eruption, the aerosol cloud was dispersed globally, with D lowered to between 10^{-2} and 10^{-1}.

Global cooling caused by Pinatubo's S in the stratosphere lasted for years. Surface air temperatures over Northern Hemisphere continents were lower than normal by up to 2° C in the summer of 1992 and warmer than normal by up to 3° C in the winters of 1991–1992 and 1992–1993. Global warming may have been retarded for several years after the Pinatubo eruption because of the cooling effects of its volcanic aerosols (Robock 2000).

2.2 Eighteen Hundred and Froze to Death: Tambora 1815–1816

The greatest volcanic impact on climate in historical time resulted from the eruption of Mount Tambora in Indonesia. The April 1815 explosive eruption was one of the largest in the last 10,000 years (Rampino et al. 1988). The eruption ejected $\sim$100 km^3 of pyroclastic trachyandesite (VEI$\sim$7), forming a caldera $\sim$7 km across and reducing the summit by 1400 m. The rapid eruption rate and the area of ash dispersal suggest that the eruption column may have reached 50 km, well into the stratosphere. An estimated 60 million tonnes of sulfur rose into the stratosphere.

Within 3 months unusual optical effects due to the volcanic cloud were observed. Spectacular sunsets and twilights were observed in England in the summer of 1815. In the spring and summer of 1816 a persistent "dry fog" was observed in the northeastern USA. Rampino et al. (1988) conclude that the haze must have been located above the troposphere, since neither surface winds nor rain dispersed it and because the total lunar eclipse of 9–10 June was extremely dark. In New York, the Sun dimmed enough that sunspots were visible to the naked eye. Some of the painter J.M.W. Turner's work, characterized by vivid orange and red skies, captured the unusual appearance of the atmosphere during this period (Oppenheimer 2003). This great climate-affecting eruption may have inspired Byron to write "Darkness", a portion of which may have attempted to capture the mood spawned by the eruption:

I had a dream, which was not all a dream.
The bright sun was extinguish'd, and the stars
Did wander darkling in the eternal space,
Rayless, and pathless, and the icy earth
Swung blind and blackening in the moonless air;
Morn came and went – and came, and brought no day,
And men forgot their passions in the dread
Of this their desolation; and all hearts
Were chill'd into a selfish prayer for light

Extract from Darkness by Lord Byron 1816

It is generally accepted that the Tambora eruption caused a brief but intense episode of cooling as a result of injecting massive quantities of sulfur into the stratosphere (Self 2006). 1816 became known as the "Year without a Summer" because of the impact on North American and European weather. Harvests were poor in the Northern Hemisphere and livestock suffered. Post (1977) characterized 1816–1819 the last great subsistence crisis to affect the Western world; 1816–1817 witnessed the worst famine in over a century. He used grain prices as a proxy for harvest outcomes through the second half of the 1810s. Prices doubled between 1815 and 1817, indicating that harvests were deficient over much of the Northern Hemisphere. This is a good indication that climatic effects associated with the Tambora eruption severely stressed the biosphere.

2.3 Toba, 74 Ka

The greatest eruption known from the past 110,000 years was at Toba, Sumatra 74 ± 2 Ka ago (Oppenheimer 2002), with VEI$\sim$8 (Zielinski et al. 1996), $\sim$3500 times greater than Tambora 1815. Not surprisingly for such an ancient eruption, estimates of the sulphur yield vary by two orders of magnitude (35–3300 million tonnes; Oppenheimer 2002). Greenland Ice Sheet Project 2 (GISP2) cores nevertheless provide indirect evidence of the importance of eruptive sulfur fluxes over the

last 110 Ka, with sulfate spikes observed at 69.4, 71, 72, and 73.6 Ka (Zielinski et al. 1996). Using the latest GISP2 chronology, the 71 Ka anomaly is dated to 70 ± 5 Ka (Oppenheimer 2002). This anomaly, thought to be due to the Toba eruption, is the largest sulfate anomaly in the entire GISP2 record.

Numerical modeling of the Toba eruption indicates that the residence time of stratospheric SO_2 was two to three times longer than the observed effects of Pinatubo, requiring 5–6 years to return to normal levels (Bekki et al. 1996).

The increased atmospheric opacity caused by the eruption should have strongly cooled Earth's surface and troposphere. It might have produced a volcanic winter followed by a few years when surface-temperatures decreased by 3–5° C, inferred from equation [1]. The eruption occurred during the oxygen isotope stage 5a-4 transition, close to the beginning of the last glacial period (Wisconsin glaciation, ~70,000–10,000 years ago), thus the Toba eruption may have either triggered this glaciation, or accelerated a shift to glacial conditions already underway (Rampino and Self 1992). It has also been suggested, based on genetic RNA "clocks", that cooling caused by the Toba eruption triggered an environmental catastrophe that almost extinguished the human race (Ambrose 1998).

The paleoclimatic effects of Toba are still being investigated, with alternate interpretations regarding timing, the amount of sulfur injected into the atmosphere, the degree of cooling, and the possibility that the GISP2 sulfur spike was caused by another eruption. Oppenheimer (2002) summarizes this controversy.

3 Can Episodes of Increased Explosive Volcanism Cause Ice Ages?

The Pinatubo and Tambora examples demonstrate that individual volcanic events can cool the Earth's surface for periods of a few years, and the Toba example suggests that a single large eruption can have a greater effect. It is also recognized that several sequential eruptions can cool climate over longer intervals, up to decades (Zielinski 2000). The next temporal scale that needs to be considered is whether protracted explosive volcanism could force enough cooling to trigger an ice age. This question was answered in the affirmative by Pollock et al. (1976), but very little published work on the subject has followed. Explosive volcanism would have to be sufficiently intense and persistent to cause cooling leading to a significant increase in the annual cryosphere (the proportion of Earth's surface covered by sea ice, snowfields and glaciers). This in turn could have tipped the radiative heat balance to a runaway ice-albedo feedback, a climate instability in which the absorption of surface radiation over open-ocean regions does not balance heat loss from ice-covered regions reflected to space, thereby accelerating cooling and ice growth (Hoffman and Schrag 2002). Runaway ice-albedo feedback is recognized as a key aspect of Neoproterozoic glaciation, regardless of what initially caused cooling.

Increased explosive volcanism may have catalyzed extensive N. Hemisphere glaciation during the Late Pliocene. The beginning of the widespread N. Hemisphere

"ice age" ~2.65 Ma ago is often explained as the result of closing the isthmus of Panama, drastically changing Atlantic ocean circulation or uplift of the Tibetan Plateau, but these events probably occurred too early to be the exclusive mechanism (Prueher and Rea 2001). The change from a precession-dominated orbital regime to an obliquity-dominated orbital regime may also have contributed to N. Hemisphere glaciation (Maslin et al. 1998). In contrast, Prueher and Rea (1998, 2001) suggested that N. Hemisphere glaciation was at least partly caused by a major increase in explosive volcanic activity. This idea derives from empirical observations that ash layers and glacigenic deposits in ODP Leg 145 cores coincide.

A rapid increase in Late Pliocene glacial erosion and sedimentation by ice-rafting is inferred from ODP Leg 145 cores. Evidence of deposition by ice-rafting is suggested by sand-sized or larger material on the deep sea floor that is not volcanic ash, mixed with pelagic sediments, and deposited too far from continental margins to have been transported by downslope processes (Prueher and Rea 2001). Ice-rafted debris first appeared in the North Pacific in the latest Miocene or earliest Pliocene, indicating that some glaciers around the N. Pacific reached sea level by that time, but there is little evidence of ice-rafted debris during middle Pliocene time. The resurgence of Late Pliocene ice-rafted sediments coincides with an order-of-magnitude increase in the frequency and thickness of volcanic ash layers. ODP Leg 145 shipboard scientists noted that the first ash layers always occurred just below the first dropstones, suggesting that the enhanced volcanic activity just preceded the onset of full-scale Northern Hemisphere glaciation (Prueher and Rea 2001). Magnetic susceptibility measurements of ODP Leg 145 cores indicate that the change from pre-glacial pelagic diatom ooze to glacial-age clay-rich ooze happened within a few thousand years, an interval seemingly too rapid for tectonic or orbital forcing but consistent for a sudden increase in explosive volcanism (Prueher and Rea 1998, 2001).

Prueher and Rea (2001) suggested the following scenario: the Northern Hemisphere had been cooling slowly since ~3.5 Ma. A million years of slow cooling brought it to the threshold of continental ice sheet formation, and a sudden upsurge in explosive volcanism provided the final impetus for rapid ice buildup. "The combination of widespread volcanism at climatically sensitive latitudes of 50–60°N, the natural sensitivity of the Arctic to volcanic forcing, and the coeval insolation minimum brought on full scale Northern Hemisphere glaciation quite rapidly, within the 2000 or 3000 years indicated by the sediments of the North Pacific" (Prueher and Rea 2001; p. 228).

4 Evidence that Explosive Volcanism Caused Neoproterozoic Ice Ages

The preceding discussion indicates that increased explosive volcanism can disrupt Earth's radiative balance by repeatedly injecting sulfur aerosols into the stratosphere, thereby fostering cooling that, in extreme cases, could lead to glaciation.

Explosive volcanism need not be the sole cause of cooling, but would be especially effective when coincident with other agents of cooling, such as depletion of a prior greenhouse gas source such as methane, position of continents, orbital forcing, or intergalactic dust. Explosive volcanism could also have stimulated cooling by feedbacks related to atmospheric CO_2 drawdown. Such mechanisms for cooling climate have been considered by many other researchers, but here we focus on the possibility that explosive volcanism was primarily responsible or contributed significantly. Explosive volcanism could also serve to help decrease atmospheric CO_2. Ash dispersal fertilizes the oceans by greatly increasing the supply of nutrients (i.e., P and Fe: Anbar and Knoll 2002). This would have spurred photosynthetic marine life, leading to reduced atmospheric CO_2. Abundant ash and associated lava flows on land also stimulates chemical weathering, further drawing down atmospheric CO_2 (Goddéris et al. 2003). Of course, igneous activity also adds a lot of atmospheric CO_2 which warms climate although this acts over longer time periods and could be overridden in the short term by volcanic winter effects and in the long term by weathering and fertilization.

Numerical global climate models have yet to address VW2SE, so the following discussion is qualitative and empirical. Discussion builds on the conclusion that the VW2SE hypothesis is broadly viable, and considers four related fundamental queries: How important was Neoproterozoic explosive volcanism? How did explosive volcanism intensity vary throughout the Neoproterozoic supercontinent cycle? How did the timing of peak explosive volcanism correspond with glacial episodes? Is the hypothesis consistent with Sr, C, and O isotopic chemostratigraphy?

4.1 On the Importance of Neoproterozoic Explosive Volcanism

We need a quantitative assessment of how vigorous was Neoproterozoic explosive volcanism – especially compared to Mesoproterozoic and Paleozoic time - in order to test the VW2SE hypothesis. We know of no such assessment, so an indirect and qualitative assessment is developed here. Primary focus is naturally on direct evidence of explosive volcanism of great geographic extent, especially beds of airfall tuff, but this flux has not been quantified. Neoproterozoic ash beds are important targets for geochronology, especially where interbedded with carbonates (Condon et al. 2005; Hoffmann et al. 2004, 2006; Halverson et al. 2005). Because direct evidence for explosive volcanism (highly weatherable or chemically labile tuffs and pyroclastic rocks) are often obliterated by erosion, deformation, metamorphism, or in the case of VW2SE mixed with glacial deposits, we use the global distribution of Neoproterozoic igneous rocks as proxy for explosive volcanism. Plutonic rocks may not always form below explosive volcanoes, but they often do, especially if these magmas are rich in water and silica (Lipman 2007). White et al. (2006) conclude that the ratio of intrusives emplaced to extrusives erupted (I/E) ranges widely but shows no systematic variation with tectonic setting. They further suggest that an I/E $\sim$5, with considerable uncertainty, applies to a wide range of magmatic compositions and tectonic settings.

This suggests that the intensity of Neoproterozoic explosive volcanism can be inferred from relative volumes of Neoproterozoic intrusions, comprising both juvenile continental crust that formed and of older crust that was remelted during Neoproterozoic time. The area of such crust is controversial. For example, Condie (1998, 2000) infers modest Neoproterozoic crustal growth and igneous activity, whereas other estimates indicate that the Neoproterozoic was an important time of crustal growth (Reymer and Schubert 1984; Goodwin 1991; Rogers et al. 1995; Trompette 2000). Some of this disagreement may reflect a bias towards well-studied areas of N. America, Europe, and Australia. However, the greatest tracts of Neoproterozoic igneous rocks are in more poorly studied regions, especially Africa, South America, and Asia. Another complexity is common overprinting of Neoproterozoic crust in Eurasia and N. America by Phanerozoic orogens, such that even in well-studied European basement exposures it is difficult to determine how much was originally Neoproterozoic crust; all that can be stated with certainty is that much of it was. Finally, Neoproterozoic crust is often preferentially exploited by younger rifts and orogenic belts, thus complicating estimates of original distribution and abundance. Rifts related to the breakup of Gondwana preferentially exploited Neoproterozoic orogens, and much of this crust is now buried beneath subsiding passive margins. Orogenic reworking of these leading edges tectonically mixes Neoproterozoic and Phanerozoic terranes and the nonfossiliferous nature of the Neoproterozoic elements makes them difficult to recognize. This problem is particularly large for the Neoproterozoic of Eurasia, but the problem is diminishing as especially U-Pb zircon ion probe dating of this basement advances.

Disagreement about the abundance of Neoproterozoic igneous rocks also reflects different approaches: for example Condie (1998; Fig. 5) focuses on juvenile crust and subdivides Earth history in a way that neglects most of Neoproterozoic time, whereas Goodwin (1991) considers Precambrian time within four specific intervals (Early, Middle, and Late Proterozoic and Archean), and estimates areas of continental crust that formed during each time. Figure 3 presents our view of the global abundance of Neoproterozoic crust, based on a literature survey that is explained elsewhere (Stern and Stewart, in press). Comparing Goodwin's estimates or Fig. 3 to that of Condie (1998; Fig. 5) results in a very different impression about the importance of Neoproterozoic igneous activity. The contrast is especially striking for Africa, where Condie (1998; Fig. 5) shows minor Neoproterozoic crust compared with Fig. 3 and Goodwin's (1991) estimate that ~51 % of the continent consists of Neoproterozoic crust.

Disagreement about the area of Neoproterozoic crust discussed above emphasizes the challenges involved in quantifying igneous activity. This is further complicated because multiple ages are reported for tracts of continental crust, including isotopic "mantle extraction" model ages, zircon crystallization ages, and thermochronologies. These different ages provide different insights about how continental crust formed and was thermally reworked; correspondingly, what is meant by the age of a crustal tract must therefore be defined for each compilation. Progress in understanding crustal growth and how this may have affected exterior Earth subsystems (e.g., hydrosphere, climate, etc.) requires a GIS database for global crust,

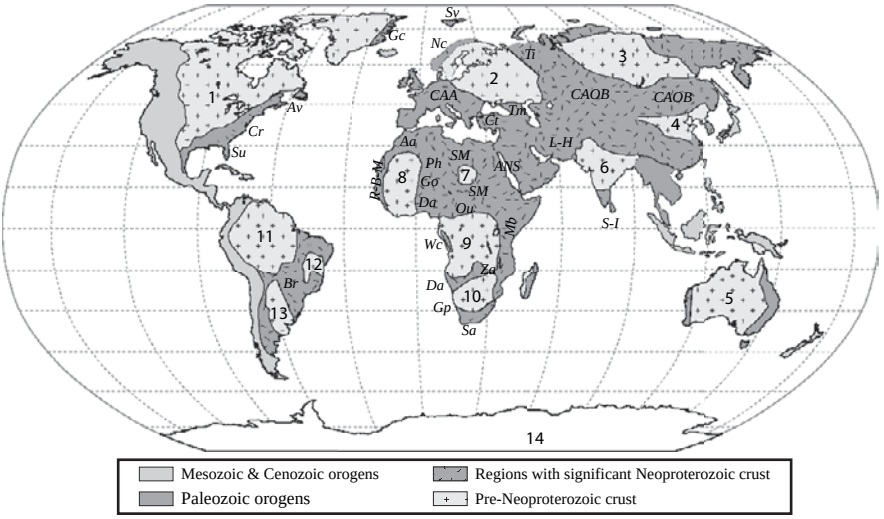

Fig. 3 Neoproterozoic crust worldwide (modified by Stern (in press), after Ernst et al. (2007)). Numbers correspond to pre-Neoproterozoic cratons: 1 = North American-Greenland craton; 2 = Baltic-East European craton; 3 = Siberian craton; 4 = N. China craton; 5 = Australia craton; 6 = Indian craton; 7 = Uweinat; 8 = West African craton; 9 = Congo craton; 10 = S. African craton; 11 = Amazon craton; 12 = Sao Francisco craton; 13 = Rio de la Plata craton; 14 = E. Antarctic craton. Italicized abbreviations are Neoproterozoic terranes (clockwise from North America: *Su* = Suwanee; *Cr* = Carolinia; *Av* = Avalonia; *Gc* = Greenland Caledonides; *Sv* = Svalbaard; *Nc* = Norwegian Caledonides; *CAA* = Cadomian, Avalonian, and Amorican; *Ct* = Cadomian of Turkey; *Tm* = Trans-caucusian massif; *Ti* = Timanides; *CAOB* = Central Asian Orogenic Belt; *L-H* = Lut and Helmut blocks; *S-I* = Southern India and Sri Lanka; *ANS* = Arabian-Nubian Shield; *Mb* = Mozambique Belt; *SM* = Saharan Metacraton; *Ou* = Oubangides; *Za* = Zambezi Belt; *Sa* = Saldanian; *Gp* = Gariep Belt; *Da* = Damaran; *Wc* = West Congo; *Dh* = Dahomides; *Go* = Gourma; *Ph* = Pharusian Belt; *Aa* = Anti-atlas; *R-B-M* = Rokelides, Bassalides, and Mauretides; *Br* = Brasiliano belts)

which does not yet exist but which would be invaluable for a wide range of fundamental geoscientific queries, including the question of Neoproterozoic igneous activity and explosive volcanism. Such a GIS will require a concerted international effort to build, update, and maintain and is far beyond the scope of this essay.

Absent such a global crustal GIS, we must nevertheless attempt to objectively estimate the volume of Neoproterozoic crust. Estimates available for this survey broadly support a concensus view that volumes of Neoproterozoic crust production were large. For example, Goodwin (1991) estimated that ~17 % of the present continental crust formed or was thermally reworked during Neoproterozoic time. Similarly, Maruyama and Liou (1998) suggested that perhaps 20 % of the area of all orogenic belts formed between 0.7 and 0.6 Ga. On a more regional scale, Reymer and Schubert (1984) concluded that 80 % of the entire Phanerozoic growth rates was required to generate the Neoproterozoic Arabian-Nubian Shield alone, although this estimate has been revised considerably (Stern 1994).

Table 1 Global Inventory of Neoproterozoic Crust

Continent	area (10^6 km^2)	% of continental area	Areal % Neoproterozoic	Neoproterozoic area (10^6Km^2)
Africa	30.37	20.36	50.60	15.37
N. America	24.49	16.42	1.60	0.39
S. America	17.84	11.96	14.90	2.66
Antarctica	13.72	9.20	8.30	1.14
Asia	43.81	29.38	9.10	3.99
Australia + NewGuin	8.5	5.70	2.80	0.24
Europe	10.4	6.97	8.40	0.87
Eurasia	52.21	35.01		
total	149.13	100		24.65

(From Table 5-1 of Goodwin, 1991)

Figure 3 shows where a significant part of the continental crust is Neoproterozoic, for all of the continents. Table 1, modified from Goodwin (1991), is to our knowledge the only areal estimate of Neoproterozoic crust. Although this estimate considers only exposed continental areas, and thus excludes perhaps an additional ~30 % of continental crust in submarine shelval areas (Cogley 1984), we use these areas to infer minimal volumes of Neoproterozoic crust production and, derivatively, as a general proxy for Neoproterozoic igneous activity likely to have been associated with explosive volcanism.

It is beyond the scope of this essay to consider in any greater detail the nature of Neoproterozoic igneous activity preserved on the continents. The interested reader is encouraged to read Stern (in press) for a more detailed overview of Neoproterozoic crustal growth.

4.2 Neoproterozoic Igneous Activity and the Supercontinent Cycle

Modern plate tectonic processes form and rejuvenate continental crust largely by igneous activity within the context of a supercontinent cycle, and similar processes operated in Neoproterozoic time (Murphy and Nance 2003). The Neoproterozoic witnessed the breakup of the supercontinent Rodinia and the reassembly of its fragments into a new supercontinent, known as Greater Gondwana or Pannotia, by the end of the era. Rodinia remained intact during the Tonian period (*tonos* is Greek for tension or stretching) and the first 150 Ma of Neoproterozoic time witnessed little igneous activity. In contrast, the Cryogenian period – when Rodinia broke up beginning ~830 Ma ago (Li et al. 1999; Torsvik 2003) – experienced intense magmatic activity. Early Cryogenian igneous rocks related to Rodinia breakup are well preserved in western N. America, China, Australia, and Siberia, leading to the inference that some of these were adjacent crustal tracts prior to early Cryogenian rifting (Burret and Berry 2000; Sears and Price 2003; Wang and Li 2003). Rodinia fragmentation required formation of new subduction zones, and Cryogenian magmatism reflected the increasing vigor of volcanic activity at rifts, volcanic rifted

margins, and island arcs. Breakup continued throughout the rest of Neoproterozoic time. Completion of the Neoproterozoic supercontinent cycle during Ediacaran time was associated with orogenic collapse and the start of a new cycle of rifting.

Progression from breakup of Rodinia to assembly of Greater Gondwana represents a ~300 Ma long supercontinent cycle (Nance et al. 1988), over which time the efficacy of divergent- and convergent-margin volcanism to inject S into the stratosphere and thus affect climate would have evolved (Fig. 4). Fragmentation of Rodinia was protracted and continued throughout the rest of Neoproterozoic time (Hoffman 1999; Goodge et al. 2002; Lund et al. 2003). Increased igneous activity was an inevitable result of Rodinia breakup, both in and around the widening rifts and at new subduction zones and island arcs that formed to allow the rifts to widen into oceans. Explosive volcanism is associated with both convergent and divergent plate boundaries (Mason et al. 2004), but eruptions must be subaerial or nearly so

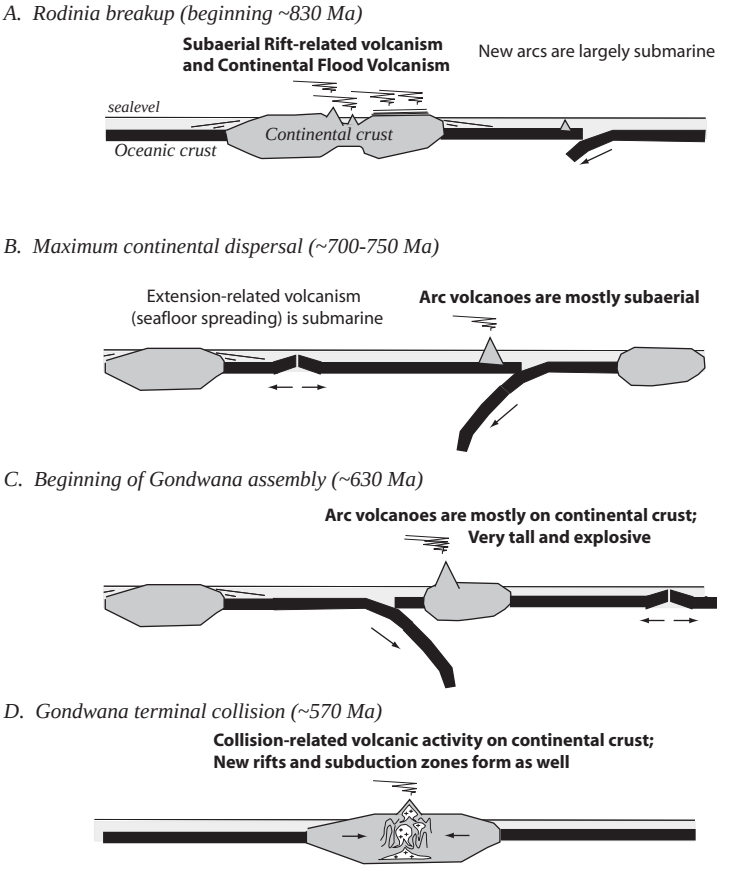

Fig. 4 Progressions in volcanic activity during the Neoproterozoic supercontinent cycle, greatly simplified. Figure is greatly simplified after Stern (in press). Important styles of volcanism for controlling climate are shown in bold letters

for volcanic plumes to rise into the stratosphere. Over the Neoproterozoic supercontinent cycle, explosive volcanism would at first have been dominated by rifts, with arcs and collision-related igneous activity becoming progresively more important. This progression can be inferred because maturing rifts tend to subside below sealevel as rifting progresses to seafloor spreading whereas arc volcanoes and the crust on which they are built become increasingly emergent (subaerial). Continental rifting volcanism could inject SO_4 into the stratosphere, but the extent to which this could cause cooling is controversial (see different views of Wignall 2001 and Self et al. 2005). Convergent margin igneous activity is likely to become increasingly subaerial over the Neoproterozoic supercontinent cycle, as submarine and barely emergent island arc volcanoes are replaced by continental Andean-type arc volcanoes. Arc volcanoes, near sealevel when they formed at the start of the cycle, would have been dominated by low-K tholeiitic and medium-K calc-alkaline magmas. Because of their relatively low explosivity, injection of S into the stratosphere is less likely, thus these volcanoes would have modest effects on climate. Submarine volcanoes could not inject S into the stratosphere in any case, and emergent arc volcanoes would have been relatively low, further making it difficult to inject S into the stratosphere. The effect of arc volcanism on climate should progressively increase over the supercontinent cycle, as juvenile arcs coalesced to produce thicker crust, and arc volcanoes became taller and erupted more fractionated and thus explosive magmas. In summary, extension-related volcanism would have been a more important agent of climate change in early Cryogenian time whereas arc volcanism should have become more important in the late Cryogenian and Ediacaran periods (Fig. 4). This progression may be part of the reason why the first significant Neoproterozoic glaciations followed a few tens of millions of years after Rodinia began to break up ~830 Ma.

The Ediacaran period witnessed significant glaciation and igneous activity at diverse tectonic settings, reflecting magmatic activity associated with collision and post-orogenic collapse. Such a transition is observed in the Arabian-Nubian Shield at ~600Ma, when convergent margin magmatism was replaced by post-tectonic or anorogenic magmatism (e.g., Beyth et al. 1994); a similar transition is inferred for Neoproterozoic crust of eastern North America and western Europe (Nance et al., in press). The end-Neoproterozoic supercontinent started to breakup almost immediately, with transtension and rifting on its northern and western margins (Nance et al., in press) along with formation of new subduction zones with Andean-type arcs along its southern margins (Terra Australis Orogen of Cawood 2005).

4.3 Synchroneity of Neoproterozoic Glaciation and Igneous Activity

Indirect support for the VW2SE hypothesis comes from the overlapping ages of igneous activity and glaciation, and from the observation that both are missing from the 150 Ma long Tonian record (Fig. 1). We agree with the conclusion of Fairchild

and Kennedy (2007, in press): "The most plausible root causes for long-term change in the surface Earth System are deep-earth processes and biological innovation . . ." Other resesearchers have also inferred a causal relationship between Neoproterozoic tectonics and magmatism on the one hand and glaciation on the other. Hoffman et al. (1998) concluded that cooling began about the time of Rodinia breakup ∼830 Ma, and inferred a link between breakup and cooling. Widespread igneous activity began globally about this time, especially in China, Africa, and western N. American. Flood basalt volcanism related to Rodinia breakup, forming especially the Laurentian magmatic province at ∼780Ma, was inferred by Goddéris et al. (2003) to have caused climate cooling, due to decreased atmospheric CO_2 resulting from accelerated weathering of basalt. Donnadieu et al. (2004) also linked cooling to reduced atmospheric CO_2 caused by Rodinia breakup, but emphasized the role of increased runoff. Further support for the idea that vigorous tectonic movements are associated with glaciation is found in the distribution of Neoproterozoic Banded Iron Formation (BIF) – one of the hallmarks of the Snowball Earth Hypothesis. Young (2003) noted that Neoproterozoic BIFs were generally deposited in tectonically active (rift) settings. Most Neoproterozoic BIFs are broadly Sturtian (700 ± 30 Ma), recording an important episode of tectonic and perhaps seafloor hydrothermal activity. The observation that Neoproterozoic glacial sediments were deposited during times of strong tectonic movements is consistent with the VW2SE hypothesis.

Below we consider a very interesting line of evidence in support of the VW2SE hypothesis: the similar timing of Marinoan glaciation and peak igneous activity in the Arabian-Nubian Shield (ANS) and East African Orogen (EAO). Among the Neoproterozoic glacial episodes, the comparatively well-studied ∼635 Ma Marinoan glaciation displays evidence that best supports a truly global glaciation (Allen 2006). Thus, if the VW2SE hypothesis has any merit, evidence for it should be apparent in association with the Marinoan glaciation. Figure 5 compares the timing of major Neoproterozoic glaciations with igneous rock ages in the ANS (Fig. 5A) and the entire EAO (Fig. 5B,C). We recognize that the EAO (including the ANS) preserves only a fraction, perhaps 30 %, of total global Neoproterozoic igneous activity, that geochronologic results are partly biased toward datable units (zircon-bearing or high Rb-Sr plutonic rocks), and that the relationship between age distributions of dominantly plutonic rocks and the record of explosive volcanism is not resolved. Nevertheless, taken at face value, the comparison suggests that Marinoan glaciation closely corresponded to a time of peak igneous activity in the EAO and ANS, providing specific if coincidental support for the VW2SE hypothesis.

Detrital zircon U-Pb SHRIMP ages from Cambrian and Ordovician strata deposited on various segments of the Arabian-Nubian Shield (N. Ethiopia, southern Israel) provide an additional perspective on the timing of igneous activity along the EAO. A preponderance of the detrital zircon ages are concentrated at 650–600 Ma (Avigad et al. 2003, 2007; Kolodner et al. 2006) strengthening the notion that Marinoan glaciation coalesced with intense igneous activity along the EAO.

In addition to evidence of near-equatorial glaciation at sea level (Sohl et al. 1999), the global extent inferred for the Marinoan glaciation is supported by identical ages retrieved from ash beds associated with Neoproterozoic glacigenic sediments in

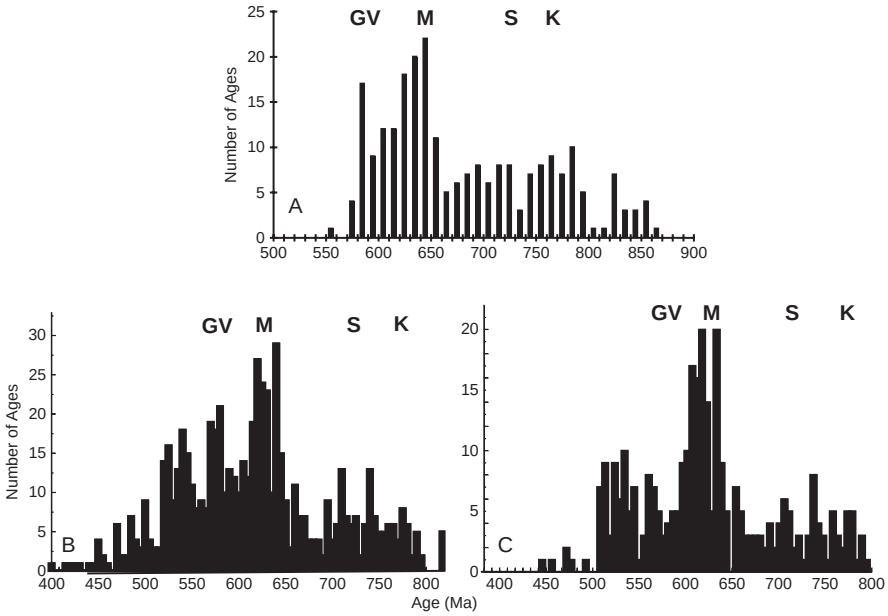

Fig. 5 Relationship between Neoproterozoic glaciations and igneous activity in the Arabian-Nubian Shield. (**A**) Robust radiometric ages of the ANS (Johnson and Kattan 2007). (**B**) Ages for East Africa and Madagascar (n = 695; Meert 2003). (**C**) Eastern Africa and Madagascar, zircon ages only (Meert 2003). Bold letters signify major Neoproterozoic glaciations: KM = Kaigan-Mahd (∼ 780 − 750 Ma); S = Sturtian (∼ 680 − 750 Ma); M = Marinoan (635 Ma); GV = Gaskiers/Varager (580 Ma)

Namibia and China (ash bed at top of Nantuo tillite in south China is 635.2 ± 0.6 Ma (Condon et al. 2005); ash bed in Ghaub dropstone beds in Namibia is 635.5 ± 1.2 Ma (Hoffmann et al. 2004); the Marinoan Flinders Range glaciogenic sequence has not been similarly constrained by high precision dating. We do not know if these geographically disparate ash beds were derived from the same eruption or from the ANS, but these results demonstrate that explosive volcanism and glaciation were then intimately associated and nearly synchronous (if not coeval) on a widespread (if not global) scale. Regardless, the strong correlation between peak Neoproterozoic magmatic activity in the ANS-EAO and ∼635 Ma ashes associated with geographically disparate Marinoan glacial deposits currently forms a strong argument for further considering the VW2SE hypothesis.

A secondary peak in the ANS and EAO igneous rock record at ∼580 Ma could similarly indicate an episode of increased explosive volcanism that was coincident with the Gaskiers/Varanger glaciation. We also note that there are no clear peaks in the histograms that correspond to the times of pre-Marinoan glacial episodes (Mahd, Kaigas, and Sturtian). This may partly reflect the under-representation of older Neoproterozoic igneous rocks on these histograms. This in turn suggests that tests of this hypothesis should focus initially on the Marinoan glaciation. Some potentially

corroborating studies already exist. For example, Bodiselitsch et al. (2005) found Ir anomalies at the base of post-Marinoan cap carbonates from the Eastern Congo craton. Although attributed to an extraterrestrial origin, Ir anomalies could also result from enhanced volcanism at 635Ma. Ir has been found in airborne particulates from Kilauea eruptions (Zoller et al. 1983) and in ashes of the British Tertiary province (Elliot et al. 1992; Schmitz and Asaro 1996). Furthermore, Bodiselitsch et al. (2005) also found very high element/Al ratios of Th, Ta, Hf, K, and Ti, consistent with inclusion of a silicic or Hawaiian-like volcanic component.

4.4 Isotopic Constraints

Sr, C, and S isotopes provide environmental constraints. The $^{87}Sr/^{86}Sr$ record of marine carbonate sediments, which proxy for seawater, reveal an ocean with sources of Sr that changed from dominantly oceanic ~800 Ma to dominantly continental ~600 Ma (Walter et al. 2000; Melezhik et al. 2001; Halverson et al., in press). It must be noted that, although low seawater $^{87}Sr/^{86}Sr$ indicates mantle activity, it does not proxy for explosive volcanism because major, climate-affecting eruptions may involve remelted older crust at Andean-type margins and continental collision zones. Such magmas will have elevated $^{87}Sr/^{86}Sr$, so that increased igneous activity and explosive volcanism could in different circumstances act to raise or lower seawater $^{87}Sr/^{86}Sr$. For this reason, Sr isotopic data provides a relativley weak test of the VW2SE hypothesis.

Carbon isotopes provide a better test of the VW2SE hypothesis. It is well known that Neoproterozoic glacial episodes are associated with negative $\delta^{13}C$ excursions, which often begin before the glacial episode itself and endure after glacial recovery, as recorded in cap carbonate successions (Halverson et al. 2002, 2005). Negative $\delta^{13}C$ excursions are variously explained (e.g., large scale methane release, collapse of biosphere, etc.), but it is also possible that these $\delta^{13}C$ excursions at least partly reflect increased addition of mantle CO_2 ($\delta^{13}C \sim -6$ ‰), released by volcanic activity. Estimates of C flux from the solid Earth suggests that inputs from arc volcanoes today are about twice that from mid-ocean ridges and that hot spot contributions are insignificant (Sano and Williams 1996), although major flood basalt eruptions introduce massive amounts of CO_2 (Wignall 2001). Volcanic inputs will have variously negative $\delta^{13}C$ (~ -1 to -10‰), in the range appropriate for the negative $\delta^{13}C$ excursions. Of course the addition of large amounts of CO_2 should warm climate, not cool it, unless sufficient SO_4 was also injected into the stratosphere to overcome the greenhouse warming effect of volcanic CO_2 until Earth's ice-covered surface was extensive enough and planetary albedo low enough for runaway cooling. This would have been most likely when explosive, S-rich arc volcanism was important, as would be expected during the middle of the Neoproterozoic supercontinent during the Cryogenian Period. Arc volcanism would have been less important at the beginning and end of the Neoproterozoic cycle, thus the ~800 Ma Bitter Springs and ~ 600–540 Ma Shuram anomaly (Halverson et al. 2005; Le Guerroué et al. 2006)

may have been associated with subordinate arc volcanism, stratospheric sulfur, and climate cooling.

Sulfur isotopic compositions of Neoproterozoic sedimentary rocks may provide a key test for the VW2SE hypothesis. Mantle inputs should have $\delta^{34}S \sim 0‰$ (Holser et al. 1988) but the effect of significant inputs of such sulfur on the composition of sedimentary sulfate and sulfide is not clear. This is because coexisting sulfide and sulfate strongly fractionate sulfur isotopes, given by $\Delta^{34}S$ ($= \delta^{34}S_{sulfate} - \delta^{34}S_{sulfide}$), the difference for the Phanerozoic being $>46‰$ (Canfield and Teske 1996). The $\delta^{34}S$ for pyrite decreases by several tens per mil during Sturtian and Marinoan glaciations; the $\delta^{34}S$ sulfate record is less complete but significant $\delta^{34}S$ decreases are also suggested by the compilation of Hurtgen et al. (2005) and is expected from equilibrium with coexisting sulfides (Hurtgen et al. 2005).

Could the large negative excursions observed for $\delta^{34}S$ during glacial episodes be due to magmatic inputs of S? Variations in $\delta^{34}S$ for sedimentary sulfate and sulfide are generally explained as a change in the balance between removal of sulfur from seawater as sulfide vs. sulfate (Hurtgen et al. 2002). This variable is significant because ^{32}S is preferentially removed by sulfide burial. Positive $\delta^{34}S$ excursions thus reflect a greater ratio of sulfide to sulfate burial, whereas negative excursions result when a greater fraction of total sulfur is buried as sulfate. Neoproterozoic negative $\delta^{34}S$ excursions could reflect increased sulfate burial, but it is difficult to imagine why more sulfate – which is most commonly found in evaporates – would be preferentially deposited during the cold climate of a glaciation; furthermore, some models for Neoproterozoic glacial episodes predict oceanic anoxia, which should result in much more sulfide than sulfate deposition (Hurtgen et al. 2002). However, it is by no means agreed that the oceans during Neoproterozoic glacial episodes were anoxic. Using the S isotopic chemostratigraphy of Neoproterozoic rocks to test the VW2SE hypothesis is thus difficult because we do not yet understand what effect increased volcanic S would have on the marine S cycle. Hurtgen et al. (2002) suggested $\delta^{34}S$ inputs from rivers are $\sim 6‰$ but this is poorly constrained. What would volcanic arc input be? Bulk Earth and MORB-like $\delta^{34}S \sim 0‰$ or like modern arc volcanics, which range widely: 0 to $+10‰$ (De Hoog et al. 2001). In summary we conclude that although the S isotope system was greatly disrupted about the time of Neoproterozoic glaciations, there is not currently a sufficient basis to interpret the cause of variations, including the possibility of a VW2SE hypothesis.

5 Conclusions

The hypothesis that explosive volcanism was at least partly responsible for Neoproterozoic climate change is viable if not proven. The mechanism of cooling by sulfuric acid aerosols in the stratosphere is well-established from studies of recent volcanic eruptions. It is possible – as demonstrated by recent analogs – that a persistent episode of plinian eruptions alone could cause ice ages. A qualitative inventory of Neoproterozoic igneous rocks shows that these are very abundant, so

that the derivative Neoproterozoic explosive magmatic flux could have seriously impacted climate. The general timing of Neoproterozoic volcanism and glacial activity correspond, with no glaciation and reduced igneous activity in the Tonian era. Glaciation followed soon after increased igneous activity began as Rodinia broke apart. The Marinoan (~635 Ma) glaciation in particular corresponds to a peak time of igneous activity in the Arabian-Nubian Shield and the East African Orogen. Explosive volcanism need not be the sole cause of cooling, and would be especially effective when happening in concert with other agents of cooling, such as lowered atmospheric CO_2 due to enhanced weathering, methane oxidation, latitudinal position and configuration of continents, orbital forcing, intergalactic dust, etc. These observations indicate that the hypothesis that some if not all of the Neoproterozoic ice ages were at least partly caused by increased explosive volcanism warrants further testing.

Acknowledgments This research was supported by USA-Israel Binational Science Foundation grant 2002337 and NSF grant EAR-0509486. We especially thank S. Self for helping us understand the climate effects of explosive volcanism and J. Alt for comments about S isotopes. the GSA Pardee Symposium convenors for the invitation to participate in the session, which greatly stimulated our thinking about this problem. We appreciate the critical comments of R. M. Mitterer, K. Muehlenbachs, and M. De Wit. This is UTD Geosciences contribution # 1121.

References

Allen PA (2006) Snowball Earth on trial. EOS 87 45:495–496

Allen PA, Bowring SA, Leather J, Brasier M, Cozzi A, Grotzinger JP, McCarron G, Amthor J (2002) Chronology of Neoproterozoic glaciations: new insights from Oman. 16th International Sedimentological Congress, Johannesburg, International Association of Sedimentologists, pp 7–8 (abs)

Ambrose SH (1998) Late Pleistocene human population bottlenecks, volcanic winter, and differentiation of modern humans. J Hum Evol 34:623–651

Anbar AD, Knoll AH (2002) Proterozoic Ocean Chemistry and Evolution: A Bioinorganic Bridge? Science 297:1137–1142

Avigad D, Kolodner K, McWilliams M, Persing H, Weissbrod T (2003) Origin of northern Gondwana Cambrian sandstone revealed by detrital zircon SHRIMP dating. Geology 31: 227–230

Avigad D, Stern RJ, Beyth M, Miller N, McWilliams MO (2007) Detrital zircon geochronology of Cryogenian diamictites and Lower Paleozoic sandstone in Ethiopia (Tigrai): age constraints on Neoproterozoic glaciation and crustal evolution of the southern Arabian-Nubian Shield. Precambrian Res 154:88–106

Bekki S, Pyle JA, Zhong W, Toumi R, Haigh JD, Pyle DM (1996) The role of microphysical and chemical processes in prolonging the climate forcing of the Toba eruption. Geophys Res Lett 23:2669–2672

Beyth M, Stern RJ, Altherr R, Kröner A (1994) The Late Precambrian Timna Igneous Complex, southern Israel: evidence for comagmatic-type sanukitoid monzodiorite and alkali granite magma. Lithos 31:103–124

Blake S (2003) Part IV: Atmospheric, climatic and environmental impacts of volcanic emissions. Correlations between eruption magnitude, SO_2 yield, and surface cooling. In: Oppenheimer C, Pyle DM, Barclay J (eds) Volcanic Degassing, Geological Society, London, Special Publication 213, pp 371–380

Bluth GJS, Doiron SD, Schnetzler SC, Krueger AJ, Walter LS (1992) Global tracking of the SO clouds from the June 1991 Mount Pinatubo eruptions. Geophys Res Lett 19:151

Bodiselitsch B, Koeberl C, Master S, Reimold WU (2005) Estimating duration and intensity of Neoproterozoic snowball glaciations from Ir Anomalies. Science 308(5719):239–242

Bowring SA, Myrow PM, Landing E, Ramezani J, Grotzinger J (2003) Geochronological constraints on terminal Neoproterozoic events and the rise of metazoans. Geophys Res 5:13219 (abs)

Burret C, Berry R (2000) Proterozoic Australia-Western United States (AUSWUS) fit between Laurentia and Australia. Geology 28:103–106

Canfield DE, Teske A (1996) Late Proterozoic rise in atmosphere oxygen concentration inferred from phylogenetic and sulfhur-isotope studies. Nature 382:127–132

Cawood PA (2005) Terra Australis Orogen: Rodinia breakup and development of the Pacific and Iapetus margins of Gondwana during the Neoproterozoic and Paleozoic. Earth-Sci Rev 69:249–279

Cogley JG (1984) Continental margins and the extent and number of continents. Rev Geophys Space Phys 22:101–122

Condie KC (1998) Episodic continental growth and supercontinents: a mantle avalanche connection? Earth Planet Sci Lett 163:97–108

Condie KC (2000) Episodic continental growth models: afterthoughts and extensions. Tectonophysics 322:153–162

Condon D, Zhu M, Bowring S, Wang W, Yang A, Jin Y (2005) U-Pb ages from the Neoproterozoic Doushantuo Formation, China, Science 308:95–98

Corsetti FA, Olcott AN, Bakermans C (2006) The biotic response to Neoproterozoic snowball Earth. Palaeogeogr Palaeoclimatol Palaeoecol 232:114–130

Crutzen PJ (2006) Albedo enhancement by stratospheric sulfur injections: a contribution to resolve a policy dilemma? Clim Change 77:211–219

De Hoog JCM, Hattori KH, Hoblitt RP (2004) Oxidized sulfer-rich mafic magma at Mount Pinatubo, Philippines. Contrib Mineral Petrol 146:750–761

De Hoog JCM, Talor BE, van Bergen MJ (2001) Sulfur isotope systematices of basaltic lavas from Indonesia: Implications for the sulfur cycle in subduction zones. Earth Planet Sci Lett 189:237–252

Donnadieu Y, Goddéris Y, Ramstein G, Nédelec A, Meert, J (2004) A 'snowball Earth' climate triggered by continental break-up through changes in runoff. Nature 428:303–306

Elliot WC, Aronson JL, Millard HT Jr (1992) Iridium content of basaltic tuffs and enclosing black shales of the balder formation, North Sea. Geochim Cosmochim Acta 56:2955–2961

Ernst WG, Hacker BR, Liou JG (2007) Petrotectonics of ultrahigh-pressure crustal and upper mantle rocks-implications for Phanerozoic collisional orogens. In: Sears J, Harms T, Evenchick C (eds) Whence the mountains? Inquiries into the evolution of orogenic systems: a volume in honor of Raymond A. Price, Geological Society of America, Special Paper No. 433, 27–49

Fairchild IJ, Kennedy MJ (2007) Neoproterozoic glaciation in the Earth system. J Geol Soc London 164:895–921

Fanning CM (2006) Constraints on the timing of the Sturtian glaciation from southern Australia; i.e., for the true Sturtian, Geological Society of America Abstracts with Programs 38:115 (abs)

Franklin B (1784) Meteorological imaginations and conjectures. Memoirs of the Literary and Philosophical Society of Manchester 2:357–361

Garfunkel Z (1999) History and paleogeography during the Pan-African orogen to stable platform transition: reappraisal of the evidence from the Elat area and the northern Arabian-Nubian Shield. Isr J Earth Sci 48:135–157

Goddéris Y, Donnadieu Y, Nédélec A, Dupré B, Dessert C, Grard A, Ramstein G, François LM (2003) The Sturtian 'snowball' glaciation: fire and ice. Earth Planet Sci Lett 211:1–12

Goodge J, Myrow P, Williams IS, Bowring SA (2002) Age and provenance of the Beardmore group, Antarctica: constraints on Rodinia Supercontinent breakup. J Geol 110:393–406

Goodwin AM (1991) Precambrian geology: the dynamic evolution of the continental crust. Academic Press, London, 666pp

Halverson GP, Dudas F, Maloof AC, Bowring SA (2007) Evolution of the $^{87}Sr/^{86}Sr$ composition of Neoproterozoic seawater. Palaeogeogr Palaeoclimatol Palaeoecol 256:103–129
Halverson GP, Hoffman P, Schrag D (2002) A major perturbation of the carbon cycle before the Ghaub glaciation (Neoproterozoic) in Namibia: prelude to snowball Earth? Geochem Geophys Geosyst 3(6). doi:10.1029/2001GC000244
Halverson GP, Hoffman PF, Schrag DP, Maloof AC, Rice AHN (2005) Toward a Neoproterozoic composite carbon-isotope record. Geol Soc Am Bull 117:1181–1207
Hoffman PF (1999) The break-up of Rodinia, birth of Gondwana, true polar wander and the snowball Earth. J Afr Earth Sci 28:17–33
Hoffman PF, Kaufman AJ, Halverson GP, Schrag DP (1998) A Neoproterozoic snowball Earth. Science 281:1342–1346
Hoffmann K-H, Condon DJ, Bowring SA, Crowley JL (2004) U-Pb zircon date from the Neoproterozoic Ghaub Formation, Namibia: constraints on Marinoan glaciation. Geology 32:817–820
Hoffmann K-H, Condon DJ, Bowring SA, Prave AR, Fallick A (2006) Lithostratigraphic, carbon ($\delta^{13}C$) isotope and U-Pb zircon age constraints on early Neoproterozoic (ca. 755 Ma) glaciation in the Gariep Belt, southern Namibia. Snowball Earth Conference,, 2006, Ascona, Switzerland p 51 (abs), 16–21 July 2006
Hoffman PF, Schrag DP (2002) The snowball Earth hypothesis: testing the limits of global change. Terra Nova 14:129–155
Holser WT, Schidlowski M, McKenzie FT, Maynard JB (1988) Geochemical cycles of carbon and sulfur, In: Gregor CB, Garrels RM, McKenzie FT, Maynard JB (eds) Chemical cycles in the evolution of the Earth, Wiley, New York, pp 105–173
Hurtgen MT, Arthur MT, Suits NS, Kaufman AJ (2002) The sulfur isotopic composition of Neoproterozoic seawater sulfate: implications for a snowball Earth? Earth Planet Sci Lett 203:413–429
Hurtgen MT, Arthur MT, Halverson GP (2005) Neoproterozoic sulfur isotopes, the evolution of microbial sulfur species, and the burial efficiency of sulfide as sedimentary pyrite. Geology 33:41–44
Hyde WT, Crowley TJ, Baum SK, Peltier WR (2000) Neoproterozoic 'snowball Earth' simulations with a coupled climate/ice-sheet model. Nature 405:425–429
Johnson PR, Kattan FH (2007) Geochronologic dataset for Precambrian rocks in the Arabian Peninsula: a catalog of U-Pb, Rb-Sr, Ar-Ar, and Sm-Nd ages, Saudi Arabian Deputy Ministry for Mineral Resources Open-File Report USGS-OF-2007-3, 40pp
Kendall BS, Creaser RA, Selby D (2006) Re-Os geochronology of postglacial black shales in Australia: constraints on the timing of the 'Sturtian' glaciation. Geology 34:729–732
Kennedy M, Drosser M, Mayer LM, Pevear D, Mrofka D (2006) Late precambrian oxygenation; inception of the clay mineral factory. Science 311:1446–1449
Kennett JP, Thunnell RC (1977) Global increase in Quaternary explosive volcanic eruptions. Science 187:1231–1234
Keppler H (1999) Experimental evidence for the source of excess sulfur in explosive volcanic eruptions. Science 284:1652–1654
Kirschvink JL, Gaidos EJ, Bertani LE, Beukes NJ, Gutzmer J, Maepa LN, Steinberger RE (2000) Paleoproterozoic snowball Earth: extreme climatic and geochemical global change and its biological consequences. Proc Natl Acad Sci 97:1400–1405
Knoll AH (2003) Life on a young planet; The first three billion year of evolution on Earth, Princeton University Press, Princeton/Oxford, 277pp
Knoll AH, Hayes JM, Kaufman AJ, Swett K, Labert IB (1986) Secular variation in carbon isotope ratios from upper Proterozoic successions of Svalbard and East Greenland. Nature 321:832–838
Kolodner K, Avigad D, McWilliams M, Wooden JL, Weissbrod T, Feinstein S (2006) Provenance of north Gondwana Cambrian-Ordovician sandstone: U-Pb SHRIMP dating of detrital zircons from Israel and Jordan. Geol Mag 143:367–391
Lamb HH (1970) Volcanic dust in the atmosphere; with a chronology and assessment of its meteorological significance. Philos Trans R Soc Lond A 266:425–533
Le Guerroué E, Allen PA, Cozzi A, Etienne JL, Fanning M (2006) 50 Myr recovery from the largest negative $\delta^{13}C$ excursion in the Ediacaran ocean. Terra Nova 18:147–153

Li ZX, Li XH, Kinny PD, Wan J (1999) The breakup of Rodinia: did it start with a mantle plume beneath South China? Earth Planet Sci Lett 173:171–181
Lipman PW (2007) Incremental assembly and prolonged consolidation of Cordilleran magma chambers: evidence from the Southern Rocky Mountain volcanic field. Geospheres 3:42–70
Lund K, Aleinkoff JA, Evans KV, Fanning CM (2003) SHRIMP U-Pb geochronology of Neoproterozoic Windermere Supergroup, central Idaho: implications for rifting of western Laurentia and synchroneity of Sturtian glacial deposits. Geol Soc Am Bull 115:349–372
Maruyama S, Liou JG (1998) Initiation of ultrahigh-pressure metamorphism and its significance on the Proterozoic-Phanerozoic boundary. IslArc 7:6–35
Maslin MA, Li XS, Loutre M-F, Berger A (1998) The contribution of orbital forcing to the progressive intensification of Northern Hemisphere glaciation. Quaternary Sci Rev 17:411–426
Mason BG, Pyle DM, Oppenheimer C (2004) The size and frequency of the largest explosive eruptions on Earth. B Volcanol 66:735–748
McCormick MP, Thomason LW, Trepte CR (1995) Atmospheric effects of the Mt. Pinatubo eruption. Nature 373:399–404. doi:10.1038/373399a0
Meert JG (2003) A synopsis of events related to the assembly of eastern Gondwana. Tectonophysics 362:1–40
Melezhik VA, Gorokhov IM, Kuznetsov AB, Fallick AE (2001) Chemostratigraphy of Neoproterozoic carbonates: implications for 'blind dating'. Terra Nova 13:1–11
Murphy JB and Nance RD (2003) Do supercontinents turn inside-in or inside-out? Int Geol Rev 47:591–619
Nance D, Worsley TR, Moody JR (1988) The supercontinent cycle. Sci Am 259(1):72
Nance RD, Murphy RD, Strachan RA, Keppie JD, Gutiérez-Alonson G, Fernández-Suárez J, Quesada C, Linnemann U, D'Lemos R, Pisarevsky SA (in press) Neoproterozoic-early Palaeozoic tectonostratigraphy and palaeogeography of the peri-Gondwanan terranes: Amazonian versus West African connections. In: Nasser, E Liégeois, J-P (eds) The boundaries of the West African craton, Geological Society of London Special Publication
Narbonne GM (2005) The Ediacara Biota: Neoproterozoic origin of animals and their ecosystems. Annu Rev Earth Planet Sci 33:421–442
Newhall CG, Self S (1982) The volcanic explosivity index (VEI): an estimate of explosive magnitude for historical volcanism. J Geophys Res 87:1231–1238
Oppenheimer C (2002) Limited global change due to the largest known Quaternary eruption, Toba~74 kyr BP? Quaternary Sci Rev 21:1593–1609
Oppenheimer C (2003) Climatic, environmental and human consequences of the largest known historic eruption: Tambora volcano (Indonesia) 1815. Prog Phys Geog 27:230–259
Pavlov AA, Toon OB, Pavlov AK, Bally J, Pollard D (2005) Passing through a giant molecular cloud: "Snowball" glaciations produced by interstellar dust. Geophys Res Lett 32:L03705, doi:10.1029/2004GL021890
Pollock JB, Toon OB, Sagan C, Summers A, Balwin B, van Camp W (1976) Volcanic explosions and climate change: a theoretical assessment. J Geophys Res 81:1071–1083
Post JD (1977) The last great subsistence crisis in the Western World. Johns Hopkins University Press, Baltimore, MD, 240pp
Prueher LM, Rea DK (1998) Rapid onset of glacial conditions in the subarctic North Pacific at 2.67 Ma: clues to causality. Geology 26:1027–1030
Prueher LM, Rea DK (2001) Volcanic triggering of late Pliocene glaciation: evidence from the volcanic glass and ice-rafted debris to the North Pacific Ocean. Palaeogeogr Palaeoclimatol Palaeoecol 173:215–230
Rampino MR, Self S (1992) Volcanic winter and accelerated glaciation following the Toba supereruption. Nature 359:50–52
Rampino MR, Self S, Stothers RB (1988) Volcanic winters. Annu Rev Earth Planet Sci 16:73–99
Reymer A, Schubert G (1984) Phanerozoic addition rates to the continental crust and crustal growth. Tectonics 3:63–77
Robock A (2000) Volcanic eruptions and climate. Rev Geophy 38:191–219

Robock A (2004) Climatic impact of volcanic emissions. In: Sparks RSJ, Hawkesworth CJ, The state of the planet: frontiers and challenges in geophysics, Geophysical Monograph Series, American Geophysical Union, Washington, DC 150:125–134
Rogers JJW, Unrug R, Sultan M (1995) Tectonic assembly of Gondwana. J Geodynamics 19:1–34
Sano Y, Williams SN (1996) Fluxes of mantle and subducted carbon along convergent plate boundaries. Geophys Res Lett 23:2749–2752
Schmitz B, Asaro F (1996) Iridium geochemistry of volcanic ash layers from early Eocene rifting of the northeastern North Atlantic and some other Phanerozoic events. Geol Soc Am Bull 115:349–372
Schrag DP, Berner RA, Hoffman PF, Halverson GP (2002) On the initiation of a snowball Earth. Geochem Geophy Geosyst 3(6):1036. doi:10.1029/2001GC000219
Sears JW, Price RA (2003) Tightening the Siberian connection to western Laurentia. Geol Soc Am Bull 115:943–953
Self S (2006) The effects and consequences of very large explosive volcanic eruptions. Phil Trans R Soc A 364:2073–2097
Self S, Thordarson T, Widdowson M (2005) Gas fluxes from flood basalt eruptions. Elements 1:283–287
Sigurdsson H (1990) Evidence of volcanic loading of the atmosphere and climate response. Palaeogeogr Palaeoclimatol Palaeoecol 89:277–289
Sohl LE, Christie-Blick N, Kent DV (1999) Paleomagnetic polarity reversals in Marinoan (ca. 600 Ma) glacial deposits of Australia: implications for the duration of low-latitude glaciation in Neoproterozoic time. Geol Soc Am Bull 111:1120–1139
Stern RJ (1994) Arc assembly and continental collision in the Neoproterozoic East African Orogen: implications for the consolidation of Gondwanaland. Annu Rev Earth Planet Sci 22:319–335
Stern RJ, Avigad D, Miller NR, Beyth M (2006) Geological Society of Africa Presidential Review, No. 10: evidence for the snowball Earth hypothesis in the Arabian-Nubian Shield and East African Orogen. J Afr Earth Sci 44:1–20
Stern RJ (in press) Neoproterozoic crustal growth: The solid Earth system during a critical episode of Earth history. Gondwana Research doi: 10.1016/j.gr. 2007.08.006
Tabazadeh A, Turco RP (1993) Stratospheric chlorine injection by volcanic eruptions: HCl scavenging and implications for ozone. Science 260:1082–1084
Tajika E (2003) Faint young Sun and the carbon cycle: implication for the Proterozoic global glaciations. Earth Planet Sci Lett 214:443–453
Torsvik T (2003) The Rodinia jigsaw puzzle. Science 300:1379–1381
Trompette R (2000) Gondwana evolution; its assembly at around 600 Ma. C R Acad Sci Paris, Sci de la Terre et des Planets 330:305–315
Walter MR, Veevers JJ, Calver CR, Gorjan P, Hill AC (2000) Dating the 840–544 Ma Neoproterozoic interval by isotopes of strontium, carbon and sulfur in seawater, and some interpretative models. Precambrian Res 100:371–433
Wang J, Li Z-X (2003) History of Neoproterozoic rift basins in South China: Implications for Rodinia break-up 122:141–158
White SM, Crips JA, Spera FJ (2006) Long-term volumetric eruption rates and magma budgets. Geochem Geophys Geosyst 7(3). doi:10.1029/2005GC001002
Wignall PB (2001) Large igneous provinces and mass extinctions. Earth-Sci Rev 53:1–33
Young GM (2003) Stratigraphic and tectonic settings of Proterozoic glaciogenic rocks and banded iron-formations: relevance to the snowball Earth debate. J Afr Earth Sci 35:451–466
Zielinski GA (2000) Use of paleo-records in determining variability within the volcanism-climate system. Quaternary Sci Rev 19:417–438
Zielinski GA, Mayewski PA, Meeker LD, Whitlow S, Twickler MS, Taylor K (1996) Potential atmospheric impact of the Toba mega-eruption ~71,000 years ago. Geophys Res Lett 23:837–840
Zoller WH, Parrington JR, Kotra JMP (1983) Iridium Enrichment in Airborne Particles from Kilauea Volcano: January 1983. Science 222:1118–1121

Index

Note: Italics page numbers indicate figures and/or tables.

A

Achnanthes, 214
Acidianus ambivalens, *A. brierleyi*, and *A. infernos*, 243
Acidimicrobium ferrooxidans, 241
Actinobacteria, 255, 261
Adderly Channel (Bahamas), *180–182*
  stromatolitic substrates, 183, 188
Aerobic methanotrophs, 296–297
Alphaproteobacteria, 143, *144*, 248, 255, 261, 297
Alteration zones, *99–100*
Ambient inclusion trails, *123*, *125–129*
  in Biwabik Iron Formation, 114, *116*
  on brachiopod shell, *118*
  characteristics of, 113–114, *115*, *124*
  in Doushantou Formation, *117*
  in Fortescue Group, *116*
  in Gunflint Iron Formation, 114, *116*
  in Ironwood Iron Formation, 114
  localities of, *120*
  in Middle Devonian fish scales, 126, 128, *129*, 130
  model for formation of, *130*
  laboratory experiments for, 132–133
  recognition by Auto-Montage, 119, 122, *123*
  in Soltanieh Formation, *118*
  taphonomic preservation of, 130–132
  in Warrawoona Group, 114, *116*, 119
Ammonia oxidation, 249–250, 261
Amphibolite facies metamorphism and carbon isotopes, *48*
Anaerobic methane oxidation (AMO), 253, 284
Anaerobic oxidation of methane (AOM), 144–145, 151, 281, 291, 297, 301, 303
Analytical differences, 160
Andros Island, 179, 188, *189–190*, 193
  location of, *181*
Apex Chert (Pilbara Supergroup), ambient inclusion trails, *124*, *125*
Aquifer-aquitard interface, 242
Aquifex-Hydrogenobacter group, 243
Aquificales, 262–263
Arabian-Nubian Shield, Neoproterozoic glaciations and magmatism in, *330*
Aragonite, deposition of, 186, 188
Aragonite cementation, *184*, *187*, 188
Archaea, *247*
  anaerobic methane-oxidizing (ANME), 151, *163*, 165–166, 298, *299*, 300–302
  community composition, *153*, 159
  cultivation techniques for, 169–170
  Dead Sea, 218
  diversity of, 146–152, 168
  groups of, 261
  halophilic species, 204
  limited diversity being cultured, 160
  metabolism, 7, 262
  and methane hydrates, *153*
  methanogenic, 10, 242, 249, 261
  and nucleic acid analysis, 8, 136
  phylogenetic tree of, *137*, *147*, *149*
Archaeoglobales, 262
Archaeoglobus fulgidus, *167*, 168
Atacama Desert, cyanobacteria from, *254*
Atlantic Ocean floor, carbon isotopes, *54*
Authigenic minerals, *5*, 301–302
Auto-Montage images, ambient inclusion trails, *123*

B

Bacillus, 261
Bacillus marismortui, 218

Bacillus schlegelii, 243
Bacillus-shaped structures, *221*
Bacteria
  from Arctic seafloor, 10
  colonies of, *141*, *215*
  community composition, *153*, 159
  cultivation techniques for, 169–170
  diversity of, 138–146, 168
  halophilic, 249
  JS1, *137*, 139, 141, 261
  limited diversity being cultured, 160
  metabolism, 262
  and methane hydrates, *153*
  methanotrophic, *296*
  and nucleic acid analysis, 8, 136
  oxidation and methanogenesis, *55*
  phylogenetic tree of, *137*
  shown by nucleic acid analyses, 9
  sulfate-reducing, *214*
  sulfur-oxidizing thermophiles, 243
  within surface pits, 4
Bacteriohopanepolyols (BHPs), *296*, 297
Bacteroidetes, 248, 261
Bahamian microbialite substrates, *182*
Bahamian stromatolites, 179–180, *181*, 182–193
Barberton greenstone belt, 28–29
  age of, *56*
  age of bioalteration, 6
  carbon isotopes, *47–48*, *54*
  images of bioalteration, *38–39*, *44*
  pillow lavas, *28*
  stratigraphic section, *27*
Batophora spp., *187*
Batumi seep, 292–293, *294*
Benthic community, and cyanobacteria, 178
Betaproteobacteria, 248
Bioalteration
  in Archean seafloor, *58*
  biochemical mechanisms of, 4, 264
  BSE images of, *5*, *42–43*
  and celadonite, *50*
  chemical signatures of, *5*, 6, 264
  comparison between ancient and modern, 58–61
  distribution of textures with depth, *50*
  and early life, 53–57, 60
  epifluorescence images of, *9*
  experimental, 11
  documented occurrences of, *12*
  modern and ancient, 2, 33–39
  nucleic acid associated with, 8
  vs. palagonitization, 3, *104*
  and porosity and permeability, *50*
  and pyrite, *50*
  significance as a biomarker, 49–59
  syngenicity with rock, 6
  tectonic control of, 52–53, 60
  textures, 4, *5*, *9*, *34–35*, *38*
  X-ray maps of, *42–43*
  See also Microstructures
Biofilm, *85*, *189*, 198–201
  and coral, 227
  formation of, 188, *199*, 226
  fossilized, *211*
  globules concentrated in, *91*
  from Storrs Lake, 214–215
Biogenicity of microstructures, 97, 101–102
Biogeochemistry, 281–303
Bioherms, *293*, 297–298, *299*
Biomarkers, 49, 97, 169, 240, 255, 258, 264, 298, *299*
Biomass abundance and distribution, 260–261
Bitter Springs Formation, *314*, 315, 331
Biwabik Iron Formation, 114, *116*
Black, Maurice, 179
Black Sea, 285–294
  analogue of ancient oceans, 302–303
  bioherms in, *293*, 297–298, *299*
  cold seeps in, 291–294, *292*
  dissolved methane in, *287*
  gas seeps, 287–288
  geology and geochemistry, 285–287
  map of, *286*
  methanotrophic activity in, *296*
  microbial processes in, 294–304
  mud volcanoes, 288–291
  plot of hydrate stability field, *289*
  and Proterozoic global ocean, 281
Bock Cay (Bahamas), *180–181*
Brachiopod shell, with ambient inclusion trail, *118*
Bryozoans, and biofilm, 200–201
Byron, Lord, "Darkness," 320

C

Cactus Island (Bahamas), *204*, *217*
Calditrhrix, 262
Carbon dioxide reduction, 264, 282, 302
Carbon isotope signatures, 45–49, 331
  in Black Sea bioherms, 297–298
  in carbonates, 7, *8*, *46–48*, 301
  of individual cells, 169
  in lipids, 285, 300–302
  in mantle carbon dioxide, 8
  in methane, 290–291, *296*

Neoproterozoic, 315
in pillow lavas, 8, *54*
Carbon of photosynthetic origin, and Archaea, 169
Carbon sources for microbes, 263–264
Carbonate precipitation, due to microbial metabolism, 178
Cascadia Margin, 138, 141, 145, 147–148, 150
Catalyzed reporter deposition-fluorescence in situ hybridization (CARD-FISH), 136, 169, 263
Cerro Negro, New Mexico, 238
Chemical signatures
of alteration, *5*, 6–7, 264, 285
of methanotrophy, 285
Chemical structures of bacteriohopanepolyols (BHPs), *296*
Chemolithoautotrophs, 10–11, 70, 241–243, 249–251, 262–263
Chinese Continental Scientific Deep (CCSD) drilling project, 238–239
Chloroflexi, 138–139, *140*, 146, 261
Chromatium spp., 203
Circulation obviation retrofit kits (CORKs), 154
Climate cooling
and Neoproterozoic volcanic activity, 316, 322–323, *330*, 332–333
and sulfur aerosols, 317, *318*, 319–322, 428
Coast Range ophiolite, 20, *23*
Cold seeps of Black Sea, 291–294
Composition
of alteration zones, *99–100*
of communities, *153*, 154, 159, 178
of minerals, *81*
Conglomerate, edgewise, *190*
Continental deep-subsurface research, 238–244
Corsica, 22–23
age of ophiolitic rocks, *56*
carbon isotopes, *47–48*
map of, *24*
Costa Rica Rift, *14*
bioaltered samples, 8, *9*
carbon isotopes, *54*
Cratons, map of, *325*
Crenarchaeota, 148, 243, 250, 262
from Arctic seafloor, 10
phylogenetic tree of, *149*
Cultured isolates, 159–161
Cyanobacteria, *210*, *212*, *215*, 218, 248
forming depositional structures, 202–203
as main builder of stromatolites, 178–179
nitrogen-fixing, 223, 230
photosynthetic, *254*
Scytonema spp., *189*
and surface colonization, 188, 193

D

Dark life, 238
Dead Sea (Israel)
biofilm, *219*, 228
environmental influences, 225
filamentous structures, *219*, *221*
geology of, 205–206
halotolerant microorganisms, *219*
hydrologic systems, 226
methods and materials, 209–210
microbes present in, 227
microbially mediated mineralization, 224
nitrogen, 223
nutrients in, 228–229
satellite photograph of, *206*
strontium, 223
water and substrate survey, *209*
water properties, 217–218, *222*
Deep Biosphere Laboratory (DBL), 239
Deep-sea archaeal group (DSAG), *146–147*, 148, 154, 261
Deferribacteraceae, 262
Deltaproteobacteria, 136, 144, *145*, 146, 151, 248, 256, 263
Denaturing gradient gel electrophoresis (DGGE), 138
Desulfacinum, 242
Desulfobulbus, 284
Desulfosarcina/*Desulfococcus*, 284, 298, *299*
Desulfovibrio sp., 203
Desulfurococcaceae, 262
Detroit Seamount, age of, *77*
Diagenesis and stromatolite growth, 192
Diatoms, from Storrs Lake, 213–214, *215*
Dipterus valenciennesi, *128*
Dissimilatory sulfite reductase alpha and beta subunit (*dsrAB*), 161–162, 168, 262
Distribution of microbes, 138, 154
DNA, fossil, 255–260
DNA analyses, 8–9, 166–168, 264
DNA preservation, 257
Dolomite formation, 7, 251, *252*, 253
Doushantou Formation, *117*, 119
Dry desert environments, 253–254
Duniella, 218
Dvurechenskii mud volcano, 288, *289–290*

E
Eastern Mediterranean Sea sapropel, 148
Emperor Seamounts, 76–97, *77*
Energy dispersive spectrometry (EDS) data, *81*, *85*
Energy sources for microbes, 104–106, 170, 243–244, 263
Environmental influences, 224–225
Environmental scanning electron microscopy (ESEM) of globular structures, *94*
Epsilonproteobacteria, 248, 262–263
Europa, possible life on, 244
Evaporite minerals, 218–220
Evaporitic environments, depositional setting in, 197–198
Evolution of life
  in ancient oceans, 302–303
  and saline environments, 246
  and timeline of ophiolites and greenstone belts, *56*
Experimental microbe feeding, 299–300
Explosive volcanism
  and atmospheric cooling, 317–321
  and ice ages, 321–323
  Neoproterozoic, 323–326
Extracellular polymeric secretions (ECPS), *199*, *221*, 230
Extreme environments and life, 237–238
"Extremophiles," 239
Exuma Islands (Bahamas), *180–182*, 193

F
Fermentation, 241–242, 264, 282
Filamentous structures
  of cyanobacteria, *210*, *212*
  with iron oxyhydroxides, *88*
  from Storrs Lake, 210–212
  on surfaces, 88–90
  in volcanic rocks, 83–84, *85*, 86, 88
  See also Ambient inclusion trails
Firmgrounds as stromatolitic substrates, 186, *187*, 188, *189*
Firmicutes, 255, 261–262
Flexibacteria, 255
Fluid inclusions, containing microbes, 257
Fluorescent-in-situ-hybridization secondary-ion-mass-spectroscopy (FISH-SIMS), 169
Fortescue Group, *116*
  See also Pilbara Supergroup
Fossil DNA, 255–260
Franciscan Complex, 20–22
  age of, *56*
  carbon isotopes, *47–48*
  map of, *23*
  Nacasio Reservoir pillow lavas, *18*
Functional gene approach, 160, 161–164
Fungi, cryptoendolithic, 11

G
Gallionella, 10
Gammaproteobacteria, 141, *142*, 143, 248–250, 261, 297
Gas hydrates, 252, 260–263, 282–283, 287–288
Gemmatimonadetes, 255
GenBank database, *137*, *163*, 166, *259*, 260–261
Gene-based analyses, history of, 159
Genomic approaches, 166–168
Geobacillus thermoleovorans, 239, *240*
Geobacteraceae, 262
Geochemistry, 40–45, *86*, 264
  in ancient oceans, 302–303
  energy sources for microbes, 104–106, 243–244, 263
  formation of carbonate, 301–302
  formation of palagonite, 75–76
  palagonitization vs. bioalteration, *5*, 6
  Storrs Lake, *216*
Geogemma barossii, 262
Geoglobus ahangari, 262
Geologic processes and microbes, 264
GHOSTDABS-field, 291, *292*, 298, 302
Glaciations and magmatism, Neoproterozoic, *314*
Globular microstructures, *91*
  environmental scanning electron microscope (ESEM) images, *94*
  gas-filled, *299*
  on surfaces, 88–90
  in volcanic glass, *85*
  in zeolite cavities, 93–94
Gondwana, 324, 326, *327*
Granular texture, 4–5
  and carbon lining, 6
Green non-sulfur bacteria (GNS), *see* Chloroflexi
Greenstone belts, 25–33, 58
  bioalteration textures in, 36, 38–39
  carbon isotopes in carbonate associated with pillow lavas, *46*
  geochemistry, 44–45
  importance of geochemical fingerprinting, 7
  and microbial activity, 2
Guaymas Basin, 148, 162, 164–165

Gulf of Mexico, 138
Gunflint Iron Formation, 114, *116*

H
Haloanaerobiales, 249
Halobacteriacea, 218
Halobacteriales, 249
Halobacterium NRC-1, 246
  survival rate after radiation, *247*
Halomonas, 261
Halophilic archaeal isolate 15N, *247*
Hardgrounds and stromatolites, 183–185
Heterotrophs, 10–11, 160, 241–242
Highborne Cay (Bahamas), *181*, 186
Hole CY-1 (Cyprus), *16*
Holes (DSDP, ODP)
  396B, *13*, *34*, *42*, *50*
  407, *13*, *50*
  409, *13*, *50*
  410A, *13*, *50*
  411, *13*
  417D, *13*, *50*
  418A, *13*, *34*, *50*
  479, 7
  504B, *14*, *50*
  648B, *13*
  834B, *14*, *50*
  896A, *9*, *14*, *34*, *50*
  1173, *153*, 164
  1176, 138, *153*
  1203, 76, *77–78*, *81*, *85*, *87–88*, *98*
  1204, 76, *77*, *79*, *81*, *85*, *87–88*, *91*, *94*, *98*
  1205, 76, *77*, *79*, *85*, *87*
  1206, 76, *77*, *80–81*, *85*, *87*, *89–93*, *97*
  1225, *153*
  1227, 138, 148, *153*, 162, 169
  1228, 162
  1229, 136, 138, 148, *153*, 162, 164, 166, *167*, 168–169
  1230, *153*, 164–165, 169
  1244, *153*
  1245, 148
  1251, 148, *153*
Hyaloclastites
  and biomass on Archean seafloor, *58*
  and carbon isotopes, 8
  photomicrographs of bioalteration, *38*
  Solund-Stavfjord ophiolite, *18*
Hydrate stability field, calculated for Black Sea, *289*
Hydrogen generation, 243–244
  and ridge structure and spreading rate, *54–55*
Hydrogen isotope signature, 291
Hydrogen-consuming reactions, 10, 262–264
Hydrologic systems, 225–226
Hyphomonas sp., 10

I
Ignicoccus pacificus, 262
Iguana Cay (Bahamas), *181*, 183
In-situ oceanic crust, age of, *56*
Iron-metabolizing bacteria, 10
Ironwood Iron Formation, 114
Isua supracrustal belt, 26–27
  age of, *56*
  carbon isotopes, *47–48*
  pillow lavas, *28*
Izu-Ogasawara Arc, 148

J
Jack Hills zircons, age of, *56*
Japan Trench, 139
Japanese epithermal gold mine, 148
Jormua ophiolite, 24–25
  age of, *56*
  carbon isotopes, *47–48*, *54*
  map of, *26*
  stratigraphic section, *16*

K
Kangaroo Caves (Pilbara Supergroup), ambient inclusion trails, *124–125*
Kizildag ophiolite, 16–17
  age of, *56*
  carbon isotopes, *47–48*
  map of, *21*
  pillow lavas, *17*
  stratigraphic section, *16*
Koko Seamount, age of, *77*
Kuroshima Knoll, 147

L
Lau Basin lithologic section, *14*
Lakes and dolomite formation, 253
Lee Stocking Island (Bahamas), *182*
Lithification of microbialite, 202
Lyngbya, 203

M
Mahd adh Dhab tillites, 315
Maikopian formation, 286, 289–290, 292
Maps
  Bahamian microbialite substrates, *182*
  Bahamian stromatolites, *181*
  Barberton greenstone belt, *29*
  Black Sea mud volcanoes, *290*

Maps (*cont.*)
Coast Range ophiolite, *23*
Corsica, *24*
cratons, *325*
Franciscan Complex, *23*
Jormua ophiolite, *26*
Kizildag ophiolite, *21*
Mirdita ophiolite, *22*
Neoproterozoic crust, *325*
Nicasio Reservoir (California), *23*
North China craton, *31*
Pechenga greenstone belt, *32*
Pilbara region (Western Australia), *30*
San Salvador Island (Bahamas), *204*
Solund-Stavfjord ophiolite, *25*
Troodos ophiolite, *20*
Ukrainian shelf, *292*
Ward Creek (California), *23*
Marine group I, phylogenetic tree of, *152*
Marinoan glaciation, 313–315, 329–333
Marinobacter sp., 10
Mars and life, 238, 244, 246, 255, 264
Meiji Seamount, age of, *77*
Mesophilic methanogens, 150, 160
and methane hydrates, 151
Metabolic functions, 262
Metabolic functions of continental subsurface microbes, 239–243
Metagenome of subsurface sediment, 166, *167*, 168
Metagenomics, methods of, 166
Metal reduction by thermophiles, 240–241
Metamorphic mineral age, and bioalteration, 6
Methane
in Black Sea, 281–282
carbon isotope ratios, 7, *296*, *300*
concentration of, *167*, *296*, *300*
dissolved, *287*
generation and migration, 282–283
Methane cycle, and Archaea, 146, 150–151
Methane hydrates, and archaeal and bacterial communities, *153*, 154
Methane-sulfate interfaces, 136, 165–166, 263
Methanobacteriales, *163*
Methanobacterium, 242
Methanobrevibacter, 162, 164
Methanocaldococcus, 262
Methanocaldococcus jannaschii, *167*
Methanococcales, *163*, 168, 261
Methanococcoides, 284
Methanococcus, 242
Methanoculleus marisnigri, *167*
Methanogenesis, 161
in ancient oceans, 302
and dolomite formation, 253
effect on carbon isotopes, 7–8
genes, 162–167
and oxidation, 263–264, 281, 283–284
rates, 295
in sediments, 294–295
in water column, 295–297
Methanogens
lineages, *163*
in marine sediments, 164–166
pathways, 166, *167*
Methanolobus, 284
Methanomicrobiales, *163*, 165, 168
Methanopyrales, 261
Methanosaeta, 164
Methanosaetaceae, *163*
Methanosarcina, 164, 168
Methanosarcinales, *163*, 165, 284
Methanospirillum hungatei, *167*
Methanothermobacter, *167*, 242
Methanothermococcus, 262
Methanotorris, 262
Methanotrophic activity, in Black Sea, 295, *296*
Methods, 77–78, 80, 82–83, 207–210
Methyl-coenzyme M reductase alpha subunit (*mcrA*), 161–162, *163*, 164–166, 168, 262
Methylene-5,6,7,8-tetrahydromethanopterin dehydrogenase, *167*
Methylobacter, 284, 297
Methylococcus, 284, 297
Methylocystis, 284, 297
Methylomonas, 284, 297
Methylosinus, 284, 297
Micrite cementation, *184*
Microbe impact on geologic processes, 264
Microbes associated with mineral fragments, 219–220
Microbes at glass-alteration interface, 9
Microbial activity, recorded in ancient rocks, 2
Microbial alteration of volcanic glass over time, 1–2
Microbial cells, shown by scanning electron microscopy (SEM), 9
Microbial communities, structures formed by, 198–199
Microbial densities
in ocean sediments, 135
in Storrs Lake, 215, *216*, 227

Microbial diversity, 136, 154, 159, 261–262
archaeal, 146–152, 168
bacteria, 138–146, 168
Microbial mats, *189*, 198–199, 201, *293*, 297, *299*
and carbon isotope signatures, *300*
formation of, 226
Microbial metabolic type, and carbon isotopes, 7
Microbial niches, 71–73
Microbial seafloor life, proposed studies of, 152–153
Microbialite, 178, *180*, *184*, 188, 201–202
See also Stromatolites
Microbially induced sedimentary structures (MISS), 200
Microbially mediated mineralization, 224
Microbially produced polysaccharide (ECPS), *215*
Microbiological constraints, 10–11
Micro-FISH experiments, 169
Microfossils in seafloor basalt, 69
Microstructures
element mapping of, *86*
filamentous, *86–87*, *92–93*, *98*, *211–212*, *219*, *221*
globular, *91*
spherical, *213–214*
tubular, *132*
tunnel type, *84*, *86*
Mineral compositions, *81*, 220
Mirdita ophiolite, 17–19
age of, *56*
carbon isotopes, *47–48*, *54*
map of, *22*
photomicrographs of bioalteration, *37*
pillow lavas, *17*
stratigraphic section, *16*
Miscellaneous Crenarchaeotic group (MCG), 148, *149*, 150, 154, 261
Model of ambient inclusion trail formation, *130*
Moorella thermoacetica, 168
Mud volcanoes of Black Sea, 289–291
Multiple strand displacement amplification (MDA), 168

N

Nankai Trough, 138–139, 147–148, 150, 162, 164
NanoSIMS ion images of ambient inclusion trails, *128*
Nano-sized organisms, 7
Navicula, 214
Neighbor-joining tree, *see* Phylogenetic tree
Neoproterozoic climate change, reasons for, 316, 322–323, 332–333
Neoproterozoic crust, 324–326
Neoproterozoic glaciations and magmatism, *314*, 315, 328–329, *330*, 331
Neoproterozoic volcanic activity, *327*
Nintoku Seamount, age of, *77*
Nitrogen, 223
Nitrosococcus halophilus, 249–250
Nitrosopumilus maritimus, 261
Nontronite, Fe redox cycles in, *242*
North China craton, pillow lavas, *28*
Nucleic acid analyses, 8–9, 264
Nutrients
and bioalteration, 40, 105–106
and microbial cultivation, 170, 227
phosphorus in glass, 10, 41
reduced chemical species, 263
in Storrs Lake and Dead Sea, 228–229

O

Obsidian Pool hot spring, 139
Ocean crust, 32–33
as a bioreactor, 51–52, 60
carbon isotopes, *46*
geochemistry, 41–42
images of bioalteration, *9*, *34–35*, *42*
lithological logs, *13–14*
microbes in hydrothermal vent waters, 70
microbial colonization of, 102–108
modern, 12–15, 33–36
oldest in situ, 2
tectonic control of bioalteration in, 52–53
Ocean geomicrobiology, 260–264
Oceanic anoxic event (OAE) layer, and sulfate-reducing bacteria, 256
Oceanic biosphere, mapping, 49–51, 60
Ojin Seamount, age of, *77*
Ontong Java Plateau
bioalteration in glass from, 9–10
carbon isotopes, *54*
photomicrographs of bioalteration, *35*
Ophiolites, 15–25
ages and stratigraphy, *16*
bioalteration textures in, 36–37
carbon isotopes, *46*
geochemical fingerprinting, 7
geochemistry, 42–43
and microbial activity, 2
Organic carbon, 169, 241–242

"Organicosmolyte strategy," 249
Oscillatoria, 203
Oxidation and methanogenesis, effect on carbon isotopes, 7–8
Oxidation of Fe and Mn, 10–11, 73, 264
Oxygen in water, Cactus Island, *217*

P
Palagonitization vs. bioalteration, 3–4, 70, *104*
  alteration zones, 94, 96–97
  chemical signatures of, *5*, 6
  formation of palagonite, 74–76
  petrography of palagonite, 73–74
"Paleome," 256–257, 259–260
Pechenga greenstone belt, 32–33
  age of, *56*
  carbon isotopes, *47–48*
  pillow lavas, *28*
  stratigraphic section, *27*
Permeability and porosity, and bioalteration, *50*
Peru Margin, 136, 138, 141, 145, 147–148, 150, 161–166, *167*, 169
Petroleum, and microbes, 241–242
Phillipsite, *85*
  and microbial encrustations, 73
  and microstructures, *91–93*
Phormidium, 203
Phosphorus in glass as nutrient, 10, 41
Photobacterium, 261
Photosynthesis by cyanobacteria, and carbonate precipitation, 178
Photosynthetic origin of organic carbon, and Archaea, 169
Phylogenetic groups, of seafloor microbes, 10
Phylogenetic tree, *163*
  Alphaproteobacteria, *144*
  Archaea and Bacteria, *137*
  bacterial gene sequences, *259*
  Chloroflexi, *140*
  deep-sea archaeal group (DSAG), *147*
  Deltaproteobacteria, *145*
  Gammaproteobacteria, *142*
  marine group I, *152*
  miscellaneous Crenarchaeotic group (MCG), *149*
Piezophilic bacteria, 256, 262
Pilbara Supergroup, 30–31
  age of, *56*
  age of bioalteration, 6
  ambient inclusion trails in, 119, 122, *123–126*
  carbon isotopes, *47–48*
  images of bioalteration, *38*, *44*
  map of, *120–121*
  pillow lavas, *28*
  stratigraphic section, *27*
Pillow lavas
  Barberton greenstone belt, *28*
  and biomass on Archean seafloor, *58*
  carbon isotopes in associated carbonate, *8*, *46*
  Corsica, *19*
  Isua supracrustal belt, *28*
  Jormua ophiolite, *18*
  Kizildag ophiolite, *17*
  and microbial activity, 2
  Mirdita ophiolite, *17*
  Nicasio Reservoir, California, *17*
  North China craton, *28*
  Pechenga greenstone belt, *28*
  Pilbara Supergroup, *28*
  Solund-Stavfjord ophiolite, *18*
  Troodos ophiolite, *17*
  Ward Creek, California, *19*
Pinatubo (1991), 318–319
Pinnularia, 214
Planctomycetes, 255
Polymerase chain reaction (PCR), 136, 160–162, 168
  DNA amplification using, 166
Porosity and bioalteration, *50*
Proteobacteria, 141, 261
Psychrophilic bacteria, 160, 256
Pyrodictium, 262
Pyrolobus fumarii, 262

Q
Qinghai Lake, *245*

R
Radiolytic hydrogen as energy source, 244
Raman spectra, *39*, *96*, *97*
"Rare Biosphere," 169
Redox-driven niche colonization, 105–106
Rhizobium radiobacter, 261
Rhizophora mangle leaves, *201*
Ridge structure, and hydrogen generation, *54–55*
Rodinia breakup, 313, 326–329, 333
Rod-shaped microstructures, 212–213, *214*

S
Saline environments, 245–246, 248–251
"Salt-in-cytoplasm strategy," 249
Sample logs for sites, *78–80*

San Salvador Island (Bahamas), *181*
See also Storrs Lake, Bahamas
Scanning electron microscopy (SEM), and microbial cells, 9
Scytonema spp., *189*
Sea of Okhotsk, 141, 145, 147–150
bacterial colonies in sediment core from, 138, *141*
Seawater circulation, 7
Secondary ion mass spectra, filamentous structure, *90*
Seeps, in Black Sea, *292*, *294*
Serpentinization and energy generation, 244
Shark Bay stromatolites, *179*
Shewanella, 261
Soltanieh Formation, *118*
Solund-Stavfjord ophiolite, 23–24
age of, *56*
carbon isotopes, *47–48*, *54*
map of, *25*
photomicrographs of bioalteration, *37*
stratigraphic section, *16*
Songliao Basin, NW China, bacterial gene sequences, *259*, 260
Sorokin Trough
and gas hydrates, 288
mud volcanoes, 282, *289–290*, 302
South African gold mine, 239
South African Gold Mine Euryarchaeotic Group (SAGMEG), 148, 150, 261
Spheres, from Storrs Lake, 212, *213–214*
Spirulina, 203
Spreading rate, and hydrogen generation, *54–55*
Staphylothermus, 262
Stocking Island (Bahamas), and stromatolites, 226–227
Storrs Lake, Bahamas
bacteria on crystals, *214*
diatom in biofilm, *215*
environmental influences, 224–225
filamentous structures, *210–212*
fossilized cyanobacteria, *215*
geology of, 203–205
hydrologic systems, 225–226
location of, *204*
methods and materials, 207–210
microbial densities, *216*, 227
microbial depositional structures, 202–203
microbially mediated mineralization, 224
nitrogen, 223
nutrients in, 228–229
pH and salinity measurements, *218*
and *Rhizophora mangle* leaves, *201*
site descriptions, *207*
spherical microstructures, 212, *213–214*
and stromatolites, 227–228
strontium, 223
water properties, *216–218*, *222*
Stratigraphic section
Barberton greenstone belt, *27*
Jormua ophiolite, *16*
Kizildag ophiolite, *16*
lithological logs of ocean crust, *13–14*
Mirdita ophiolite, *16*
Pechenga greenstone belt, *27*
Pilbara Supergroup, *27*
Solund-Stavfjord ophiolite, *16*
Troodos ophiolite, *16*
Strelley Pool sandstone
ambient inclusion trails from, *123*, *126–128*, 131
characteristics of ambient inclusion trails, *124*
map of, *121*
modern contamination of ambient inclusion trails in, *132*
See also Pilbara Supergroup
Stromatolites
Bahamian, 179–193
definition of, 177
and diagenetic processes, 192
diverse morphologies, *180*
on firmground substrates, *187*, 193
formation of, 178–179, 193, 198–199, 202, 226
geologic occurrence of, 177–178
on hardground substrates, 193
history of study of, 179
on inherited substrates, 183, 193
maps of, *181–182*
microbialite on hardground, *184*
Pethei Group, *178*
on renewable substrates, 183, *185*, 186, *189*, 191–193
sediment supply for Holocene, 190
Shark Bay, *179*
Storrs Lake, 227
substrate limitations for, 191
in Upper Cambrian rocks of Maryland, 189, *190*
Strombus gigas, 185
Strontium, 223, 331
Subaerial exposure of Pleistocene limestone, as inherited stromatolitic substrate, 183
Substrates, of stromatolites, 183–190

Suiko Seamount, age of, *77*
Sulfate reduction, and carbonate precipitation, 178
Sulfate-methane transition zone, 136, 165–166, 263
Sulfate-reducing microbes, *214–215*, 241–242, 251, 262–264, 284
Sulfate-reduction genes, 162, 168
Sulfobacillus acidophilus and *S. thermosulfidooxidans*, 241
Sulfolobales, 243
Sulfur aerosols and cooling, 317–322, 328
Sulfur isotope signatures, 331–332
Sulfur oxidation, 242–243, 251, 264
Sulfur-metabolizing bacteria, 10
Supercontinent cycle, and Neoproterozoic igneous activity, 326–328
Surface-area changes, 5
Syndepositional substrates for stromatolites, 183, 185–186
Syngenicity, bioalteration and rock age, 6

T
Tambora (1815–1816), 319–320
Taylorsville Basin, Virginia, 238
Terrestrial miscellaneous Euryarchaeotal group (TMEG), 261
Thermaceae, 262
Thermincola ferriacetica, 241
Thermoanaerobacter ethanolicus, 241
Thermococcales, 262
Thermococcus, 242
Thermodesulfobacteriaceae, 262–263
Thermodesulforhabdus, 242
Thermodesulfovibrio, 241
Thermophiles
  and deep-sea hydrothermal environments, 256, 261–262
  Fe reduction-oxidation cycles in, *242*
  from gold mine, 148, 262
  metal reduction by, 240–241
  molecular H and carbon dioxide metabolism, 10
  sulfur oxidizing, 242–243, 263
Thermosediminibacter, 261
Thermothrix, 243
Thermotoga, 241
Thermotogales, 262
Thermus/Deinococcus, 255
Thiobacillus-like bacteria, 243
Thiothrix spp., 203, 227
Tibetan Plateau, lakes of, *245*, 250
Time of flight secondary ion mass spectrometry (ToF-SIMS) image, filamentous structure, *89*
Timeline, ophiolites and greenstone belts, *56*
Toba (74 Ka), 320–321
Tongue of the Ocean, *181*, 183, 185
Troodos ophiolite, 15–16
  age of, *56*
  carbon isotopes, *47–48*, *54*
  drill hole CY-1, *16*
  images of bioalteration, *43*
  map of, *20*
  photomicrographs of bioalteration, *37*
  pillow lavas, *17*
  stratigraphic section, *16*
Tubular texture, 4–5, 264
  and carbon lining, 6
  See also Ambient inclusion trails
Tunnel structures, in volcanic glass, 83, *85*
Turbidity at Black Sea chemocline, *296*

V
Vibrio, 261
Volcanic glass
  changed surface area due to bioalteration vs. abiotic alteration, 5
  experimental dissolution of, 11
  limited age range of, 7
  and microhabitats, 70–71
  tunnels in, 83
"Volcanic winter to snowball Earth" (VW2SE), 313, 316, 323, 328–332
Volcanism and climate cooling, *318*, *327*

W
Warrawoona Group, 114, *116*, 119
  See also Pilbara Supergroup
Water properties, *216–218*, 221, *222*
Wutai Group, 31–32
  age of, *56*
  carbon isotopes in carbonate associated with pillow lavas, *47*

X
X-ray maps, 6

Y
Yellowstone National Park, 139, 213
Yonaguni Knoll, 148

Z
Zeolite-greenschist facies metamorphism and carbon isotopes, *48*